cGMP Pathways as Novel Molecular Targets in the Brain for Fast Auditory Processing and Cognitive Function

Dissertation
der Mathematisch-Naturwissenschaftlichen Fakultät
der Eberhard Karls Universität Tübingen
zur Erlangung des Grades eines
Doktors der Naturwissenschaften
(Dr. rer. nat.)

Vorgelegt von
Philine Silja Marchetta
aus Tettnang

Tübingen
2022

Gedruckt mit Genehmigung der Mathematisch-Naturwissenschaftlichen Fakultät der Eberhard Karls Universität Tübingen.

Tag der mündlichen Qualifikation:	22.07.2022
Dekan:	Prof. Dr. Thilo Stehle
1. Berichterstatterin:	Prof. Dr. Marlies Knipper
2. Berichterstatter:	Prof. Dr. Peter Ruth
3. Berichterstatterin:	Prof. Dr. Kerstin Schwabe

Nicht-Sehen trennt den Menschen von den Dingen.
Nicht-Hören trennt den Menschen vom Menschen.
Immanuel Kant

Contents

Abbreviations

ABR	auditory brainstem response
Arc	activity-regulated cytoskeleton-associated protein
AC	auditory cortex
ACTH	adrenocorticotrope hormone
AF	afferent fibers
ANF	auditory nerve fiber
ANP	atrial natriuretic peptide
ASD	autism spectrum disorder
ASR	acoustic startle response
ASSR	auditory steady-state response
AT	acoustic trauma
BDNF	brain derived neurotrophic factor
BK	big potassium
BLEV	BDNF-Live-Exon-Visualization
BNP	B-type natriuretic peptide
BOLD	blood oxygenation level dependent
CA	cornu amonis
CaMKIIα	Ca^{2+}/calmodulin-dependent protein kinase IIα
cGKI	cGMP-dependent protein kinase I
cGMP	cyclic guanosine monophosphate
cKO	conditional KO
CNS	central nervous system
CN	cochlear nucleus
CNP	C-type natriuretic petide
CORT	corticosterone
CRH	corticotropin-releasing hormone
DAB	3,3'-diaminobenzidine (DAB)
DG	dentate gyrus
DCN	dorsal CN
DPOAE	distortion product otoacoustic emission
EC	entorhinal cortex
EF	efferent fiber
EW	embryonal week
fEPSP	field excitatory postsynaptic potential
GC	glucocorticoid
GABA	γ-aminobutyric acid
GR	glucocorticoid receptor
GTP	guanosine-5'-triphosphate
HPA-axis	hypothalamus-pituitary-adrenal axis

IC	inferior colliculus
IHC	inner hair cell
IN	interneuron
I/O	input/output
KCC2	potassium chloride cotransporter 2
KCNQ4	KQT member 4
KO	knockout
LOC	lateral olivocochlear
LTD	long-term depression
LTP	long-term potentiation
MGB	medial geniculate body
MR	mineralocorticoid receptor
nNOS	neuronal NO synthases
NO	nitric oxide
OHC	outer hair cell
P	postnatal day
Pax	paired box protein
PAR	poly (ADP-ribose)
PARP	PAR polymerase
PDE	phosphodiesterase
pGC	particulate guanylate cyclase
PPF	prepulse facilitation
PPI	prepulse inhibition
PST	permanent threshold shift
PV	parvalbumine
PVN	paraventricular nucleus
Sat	satellite cell
SC	Schaffer's collateral
sGC	soluble guanylate cyclase
SGN	spiral ganglion neuron
SO	stratum oriens
SOC	superior olivary complex
SP	stratum pyramidale
SPL	sound pressure level
SR	spontaneous firing rate
StR	stratum radiatum
TMX	tamoxifen
VCN	ventral CN

Summary

Second-messenger cascades play important roles in controlling development, adaptive plasticity, metabolic supply, and protective processes in nearly every organ across the lifespan. Cyclic guanosine monophosphate (cGMP) signaling as the second messenger of the cGMP/cGKI cascade is involved in many developmental and maintenance steps of cell growth and survival. Thus, it also plays an important role in sensory systems, such as the auditory system, which has been the focus of the research presented in this thesis. Components of the cGMP cascade have been found to be involved in protection or recovery of auditory sensory structures after damage, such as loud traumatic overexposure, to maintain threshold sensitivity (Jaumann et al., 2012). However, our hearing enables us to perform far more complex sensory functions than just perceiving sounds: in order to use speech, a fast information processing is required to follow complex auditory signals in rapid succession. These signals moreover have to be amplified through attention and learning dependent processes. The key signature that may link this gained hearing acuity with central cognitive processes has remained elusive. In the present study we could demonstrate that the absence of brain-derived neurotrophic factor (BDNF) in Pax2-lineage descendants in Bdnf^{Pax2}KO mice caused fast auditory processing deficits despite maintained basic hearing function. It was suggested that Pax2-positive GABAergic precursor cells migrate in a BDNF-dependent manner to hindbrain regions to contact, among others, auditory nerves and auditory brainstem regions. We found here that as a result, in Bdnf^{Pax2}KO mice, a dysbalance of excitation and inhibition was observed in the auditory cortex and hippocampus. This dysbalance was accompanied by reduced hippocampal synaptic scaling and deficits in learning and social behavior, which, taken together, constitutes an immature-like, autistic phenotype (Eckert, Marchetta et al., 2021). Regarding the influence of cGMP generators on memory and cognition (Delhaye and Bardoni, 2021), studies now are in progress to test the influence of cGMP stimulators in Bdnf^{Pax2}KO mice. A possible key role of BDNF was also suggested for age-dependent hearing deficits and speech discrimination problems. Age-dependent speech discrimination problems are suggested to be linked with auditory nerve fiber loss (cochlear synaptopathy). In our research group it was shown previously that animals with cochlear synaptopathy could prevent e.g., age-dependent temporal discrimination loss if they were still able to centrally compensate (Möhrle et al., 2016). Aged animals that could not centrally compensate lost temporal coding ability (Möhrle et al., 2016). In the present study, it was shown that prolonged auditory nerve latency was associated with cochlear synaptopathy of a distinct auditory nerve fiber type, the loss of which may be critical for central compensation and temporal coding. When this fast driving force is attenuated, hippocampal synaptic scaling is hampered. Moreover, as a result the recruitment of BDNF in capillaries and nerve terminals of the hippocampus - possibly reflecting coupling and remodelling of neuronal activity to vascular metabolic supply - is reduced (Marchetta, Savitska, et al., 2020). In line with vascular metabolic supply being strongly influenced by cGMP signaling (Duchemin et al., 2012), we indeed could observe a significant positive influence of phosphodiesterase (PDE) 9 inhibitors on animals with an age- and stress-induced loss of central compensation (Savitska, ..., Marchetta et al., under revision). We could up to now conclude that BDNF in inhibitory brainstem neurons is critical for fast auditory processing and that fast auditory processing is in turn required for the recruitment of BDNF in frontal brain regions, influencing central adaptation and cognition in a cGMP-sensitive process (Marchetta, Savitska, et al., 2020, Eckert, Marchetta et al., 2021, Savitska, ..., Marchetta et al., under revision). We next asked for key signatures that might bridge BDNF-dependent frontal brain plasticity responses with peripheral fast auditory processing. Activation of stress receptors is

hypothesized to be needed for memory-dependent plasticity changes. To investigate the role of stress receptors on hearing, particularly on the auditory periphery, mineralo- and glucocorticoid receptors (MR and GR) were deleted in adult mice through a tamoxifen induced CaMKIIαCre-lox system. CaMKIIα is mainly expressed in the forebrain, including the hippocampus. In accordance, MRGR cKO exhibited a deletion of MR and GR in frontal brain regions, as shown for the hippocampus, but not in the cochlea (Marchetta et al., 2022). Interestingly, we could demonstrate that central (limbic) MR and GR can influence peripheral fast auditory processing with a positive impact on auditory nerve discharge rate through MR and a negative impact of auditory nerve synchrony through GR (Marchetta et al., 2022). This suggests that stress receptors may bridge peripheral with central auditory processing (Marchetta et al., 2022). Here again the central role of cGMP generators for the observed plasticity changes became evident. As part of a future outcome of this study, altered sGC and GC-A expression pattern in frontal brain regions in MR and GR cKO mice (Calis, ..., Marchetta et al., in preparation) may underscore a new key role of cGMP generators, particularly of GC-A during BDNF- and stress-related auditory adaptation processes (Calis, ..., Marchetta et al., in preparation). Aiming to get insights into a potential protective role of GC-A for central auditory processing, global GC-A deficient mice were analyzed and shown to display impaired outer hair cell function already in young animals and developed a greater vulnerability of inner hair cells to noise- and age-dependent hearing loss, including central auditory processing deficits (Marchetta, Möhrle, et al., 2020). Thus, the stimulation of GC-A signaling may have the potential to protect the auditory system from hearing loss. In conclusion, we would like to introduce cGMP-generators, particularly GC-A, as potential new drug targets to intervene in auditory processing deficits that may also stimulate auditory attention and learning-dependent amplification processes.

Zusammenfassung

Second-Messenger spielen in fast allen Organen über die gesamten Lebensspanne eine wichtige Rolle bei der Steuerung von Entwicklung, Plastizität, Stoffwechselversorgung und Schutzmechanismen. Zyklisches Guanosinmonophosphat (cGMP) als second messenger der cGMP/cGKI-Kaskade ist an vielen Entwicklungs- und Erhaltungsschritten von Zellwachstum und -überleben beteiligt. Daher spielt cGMP auch eine wichtige Rolle in sensorischen Systemen, wie dem auditorischen System, das hier im Rahmen der vorgestellten Arbeit untersucht wird. Es wurde gezeigt, dass Komponenten der cGMP-Kaskade am Schutz oder der Wiederherstellung auditorischer Strukturen nach einer Schädigung, wie nach lauter traumatischer Überbelastung, beteiligt sind, um die Schwellenempfindlichkeit zu erhalten (Jaumann et al., 2012). Unser Gehör ermöglicht uns jedoch weitaus komplexere sensorische Funktionen als nur die Wahrnehmung von Geräuschen: um komplexe auditorische Signale wie Sprache detektieren zu können, ist eine schnelle Informationsverarbeitung erforderlich. Auditorischen Signale werden dabei zudem mittels aufmerksamkeits- und lernabhängiger Prozesse verstärkt. Der Mechanismus, der diese gesteigerte Hörschärfe mit zentralen kognitiven Prozessen verbinden könnte, ist bislang nicht bekannt. In der vorliegenden Studie konnten wir zeigen, dass das Fehlen des neurotrophen Faktors (BDNF) in Pax2-positiven Vorläuferzellen von Bdnf^{Pax2}KO Mäusen trotz intakter Grundhörfunktion zu Defiziten bei der schnellen Hörverarbeitung führt. Es wurde vermutet, dass Pax2-positive GABAerge Vorläuferzellen in einer BDNF-abhängigen Weise in Regionen des Hinterhirns wie Hörnerv und auditorischer Hirnstamm wandern. Wir haben festgestellt, dass in Bdnf^{Pax2}KO-Mäusen ein Ungleichgewicht zwischen Erregung und Hemmung im auditorischen Kortex und im Hippokampus herrscht. Diese Dysbalance ging mit einer reduzierten synaptischen Plastizität im Hippokampus und mit Defiziten im Lern- und Sozialverhalten einher, was sich in einem unreifen, autistischen Phänotyp äußerte (Eckert, Marchetta et al., 2021). Auf Grundlagen dieser Erkenntnis werden derzeit Studien durchgeführt, um in Bdnf^{Pax2}KO-Mäusen den Einfluss von cGMP-Stimulatoren zu testen, die nachweislich Gedächtnis und Kognition beeinflussen können (Delhaye and Bardoni, 2021). Eine mögliche Schlüsselrolle von BDNF wurde außerdem für altersabhängige Hördefizite und Sprachdiskriminierungsprobleme angedacht. Es wird vermutet, dass letztere mit dem Verlust von Hörnervfasern (kochleäre Synaptopathie) zusammenhängen. In unserer Forschungsgruppe wurde zuvor gezeigt, dass Tiere mit kochleärer Synaptopathie z.B. altersabhängige temporale Hörverluste verhindern konnten, wenn sie noch in der Lage waren, diese zentral zu kompensieren (Möhrle et al., 2016). Alte Tiere, die nicht zentral kompensieren konnten, wiesen eine reduzierte zeitliche Auflösung des Hörvermögens auf (Möhrle et al., 2016). Hier konnte gezeigt werden, dass eine verlängerte Latenzzeit des Hörnervs mit der kochleären Synaptopathie eines bestimmten Hörnerven-Fasertyps einhergeht, dessen Verlust für die zentrale Kompensation und die zeitliche Kodierung entscheidend sein könnte. Wenn diese schnelle Antriebskraft abgeschwächt ist, wird die synaptische Plastizität im Hippokampus beeinträchtigt. Außerdem wird dadurch die Rekrutierung von BDNF in den Kapillaren und Nervenendigungen des Hippokampus reduziert, was möglicherweise die Kopplung neuronaler Aktivität an die vaskuläre Stoffwechselversorgung widerspiegelt (Marchetta, Savitska, et al., 2020). Im Einklang mit der Tatsache, dass die vaskuläre Stoffwechselversorgung stark von cGMP beeinflusst wird (Duchemin et al., 2012), konnten wir tatsächlich einen positiven Einfluss von Phosphodiesterase (PDE) 9-Hemmern auf Tiere mit einem alters- und stressbedingten Verlust der zentralen Kompensation beobachten (Savitska, ..., Marchetta et al., in Revision). Wir konnten bisher schlussfolgern, dass BDNF in inhibitorischen Hirnstammneuronen für die schnelle Hörverarbeitung entscheidend ist und dass die schnelle

Hörprozessierung wiederum für die Rekrutierung von BDNF in frontalen Hirnregionen erforderlich ist, was die zentrale Anpassung und Kognition in einem cGMP-abhängigen Prozess beeinflusst (Marchetta, Savitska, et al., 2020, Eckert, Marchetta et al., 2021, Savitska, ..., Marchetta et al., in Revision). Als Nächstes suchten wir nach einem Baustein, der BDNF-abhängige Plastizitätsreaktionen im Frontalhirn mit der peripheren schnellen Hörverarbeitung verbinden könnte. Es wird angenommen, dass die Aktivierung von Stressrezeptoren für gedächtnisabhängige Plastizitätsänderungen erforderlich ist. Um die Rolle der Stressrezeptoren beim Hören, insbesondere in der auditorischen Peripherie, zu untersuchen, wurden Mineral- und Glukokortikoidrezeptoren (MR und GR) in erwachsenen Mäusen durch ein Tamoxifen-induziertes CaMKIIαCre-lox-System ausgeschaltet. CaMKIIα wird hauptsächlich im Vorderhirn, einschließlich Hippokampus, exprimiert. Dementsprechend zeigten MRGR cKO eine Deletion von MR und GR in frontalen Hirnregionen, wie im Hippokampus gezeigt, aber nicht in der Kochlea (Marchetta et al., 2022). Interessanterweise konnten wir zeigen, dass zentrale (limbische) MR und GR die periphere schnelle Hörverarbeitung beeinflussen können, wobei MR einen positiven Einfluss auf die Entladungsrate des Hörnervs und GR einen negativen Einfluss auf die Synchronizität der Hörnervfasern hat (Marchetta et al., 2022). Dies deutet darauf hin, dass Stressrezeptoren eine Brücke zwischen peripherer und zentraler auditorischer Verarbeitung schlagen können (Marchetta et al., 2022). Auch hier wurde die zentrale Rolle der cGMP-Generatoren für die beobachteten Plastizitätsänderungen deutlich. Wie Ergebnisses weiterführender Studien zeigten, sind veränderte sGC- und GC-A-Expressionsmuster im Frontalhirn von MR- und GR-cKO-Mäusen zu finden (Calis, ..., Marchetta et al., in Vorbereitung), was eine neue Schlüsselrolle von cGMP-Generatoren, insbesondere von GC-A, während BDNF- und stressbedingter auditorischer Anpassungsprozesse bedeuten könnte (Calis, ..., Marchetta et al., in Vorbereitung). Mit dem Ziel, Einblicke in eine mögliche protektive Rolle von GC-A für die zentrale auditorische Verarbeitung zu erhalten, wurden Mäuse mit globaler GC-A-Defizienz analysiert und es zeigte sich bereits bei jungen Tieren eine beeinträchtigte Funktion der äußeren Haarzellen, sowie eine größere Anfälligkeit der inneren Haarzellen für lärm- und altersabhängigen Hörverlust, einschließlich Defizite bei der zentralen auditorischen Verarbeitung (Marchetta, Möhrle, et al., 2020). Die Stimulation der GC-A Kaskade könnte daher das Potenzial haben, das auditorische System vor Hörverlust zu schützen. Zusammenfassend stellen wir cGMP-Generatoren, insbesondere GC-A, als potenzielle pharmakologische Zielstrukturen vor, die bei Defiziten in der auditorischen Verarbeitung eingreifen und auch die auditorische Aufmerksamkeit und lernabhängige Verstärkungsprozesse verbessern könnten.

List of Publications in the Thesis

Accepted Papers

Eckert P*, Marchetta P*, Manthey MK*, Walter MH, Jovanovic S, Savitska D, Singer W, Jacob MH, Rüttiger L, Schimmang T, Milenkovic I, Pilz PKD, Knipper M. (2021): Deletion of BDNF in Pax2 Lineage-Derived Interneuron Precursors in the Hindbrain Hampers the Proportion of Excitation/Inhibition, Learning, and Behavior. Front Mol Neurosci.

Marchetta P*, Savitska D*, Kübler A, Asola G, Manthey M, Möhrle D, Schimmang T, Rüttiger L, Knipper M, Singer W. (2020): Age-Dependent Auditory Processing Deficits after Cochlear Synaptopathy Depend on Auditory Nerve Latency and the Ability of the Brain to Recruit LTP/BDNF. Brain Sci.

Marchetta P, Eckert P, Lukowski R, Ruth P, Singer W, Rüttiger L, Knipper M. (2022): Loss of central mineralocorticoid or glucocorticoid receptors impacts auditory nerve processing in the cochlea. iScience

Marchetta P*, Möhrle D*, Eckert P, Reimann K, Wolter S, Tolone A, Lang I, Wolters M, Feil R, Engel J, Paquet-Durand F, Kuhn M, Knipper M, Rüttiger L. (2020): Guanylyl Cyclase A/cGMP Signaling Slows Hidden, Age- and Acoustic Trauma-Induced Hearing Loss. Front Aging Neurosci.

*Equal Contribution

1 Introduction

The average life span of humans increases, and thereby also the average age of the world's population. One consequence of increasing age is the growing number of people suffering from hearing loss. Today about 466 million people worldwide are affected by disabling hearing loss and this number is expected to double by 2050 (Wilson et al., 2017). Not only in the elderly population, but already in childhood hearing loss appears with a high prevalence (Moore et al., 2020). This high prevalence is of considerable importance, as it has recently been discovered that hearing loss is a remarkable risk factor for the development of Alzheimer's disease (Chern and Golub, 2019; Lin et al., 2011; Livingston et al., 2017; Wilson et al., 2019), which however can be prevented, when the hearing impairment is treated (Montero-Odasso et al., 2020).

Despite the high prevalence of hearing impairment, it is often not measurable in a typical audiometric observation, as thresholds are often not affected but the patients have difficulties to understand speech in a noisy environment (Füllgrabe and Moore, 2014). The reason for this hidden hearing loss was suggested to lie in cochlear synaptopathy, which is the loss of cochlear nerve synapses (Kobel et al., 2017; M. C. Liberman and Kujawa, 2017). One key signature that is crucial for proper speech understanding is the high temporal resolution for auditory stimuli (Benasich et al., 2002). To fully distinguish complex auditory stimuli such as speech, it is necessary for the auditory system to perceive rapid (i.e., in the order of ms) modulations (Poldrack et al., 2001), which has to develop by the maturation of fast temporal auditory processing abilities (Benasich et al., 2002; Tallal, 1980). This gives a strong hint that hearing function, especially fast auditory processing and cognition are linked. Also, in children impaired fast temporal auditory processing was shown to causally contribute to cognitive skills underlying speech (Foss-Feig, Adkinson, et al., 2017). Further in neurodevelopmental disorders such as autism spectrum disorder (ASD), the development of proper temporal auditory processing can be impaired, which leads to reduced speech understanding (Brock et al., 2002).

1.1 The auditory system

1.1.1 The ascending auditory pathway

The organ that detects auditory stimuli and transfers them into neuronal information is the cochlea and is, along with the vestibular organ located in the inner ear (Fettiplace, 2011). The coiled cochlea is organized tonotopically with higher frequencies being represented in the base and lower frequencies in the apex (Von Bekesy and Wever, 1960). Of the sensory cells - called hair cells - three rows of outer hair cells (OHC) and one row of inner hair cells (IHC) are found in the organ of Corti, all embedded in supporting cells (Figure 1A). Shearing movements between the tectorial- and the basilar membrane are required for the generation of receptor potentials in the hair cells. It is known that IHC and OHC act in different ways. While IHC are the primary receptor cells, OHC actively produce non-linear electromotility after changes of the membrane potential and are therefore important for changes in the sound pressure level (SPL) and amplification (Fettiplace, 2011; M. Malmierca and Merchan, 2004). The information from the sensory cells is transferred to the brain by two types of spiral ganglion neurons (SGN), type I and type II afferent auditory nerve fibers (ANF). In addition, efferent neurons project from the brainstem (mostly the superior olivary complex; SOC) to or near IHC within the auditory nerve. For the afferent fibers, type I ANF are those that innervate IHC; they are thickly myelinated and represent 90-95 % of all afferent fibers. Type II ANF that innervate OHC make up the remaining 5-10 % of all afferent fibers and have only a thin myelination (Heil and Peterson, 2015). IHC transmit the acoustic information via several ribbon synapses (Glowatzki and Fuchs, 2002), which contain a readily releasable pool of glutamate vesicles and thereby mediate synchronous and temporal precise synaptic transmission (Moser et al., 2006; Nouvian et al., 2006). At the postsynapse the type I ANF can be classified in more detail (Figure 1B) into those with high spontaneous firing rates (high-SR) and low detection thresholds ($>$ 18 spikes/s, 60 % of type I ANF) and those with low- and medium spontaneous firing rates (low- and medium-SR) with higher detection thresholds and wider dynamic range ($<$ 0.5 to 18 spikes/s, 40 % of type I ANF). Both in combination are essential for detecting sound in a dynamic SPL range and precise processing of temporal auditory stimuli (Buran et al., 2010; Kiang, 1965; Knipper et al., 2013; M. C. Liberman, 1978; Rüttiger et al., 2017; Sachs and Abbas, 1974).

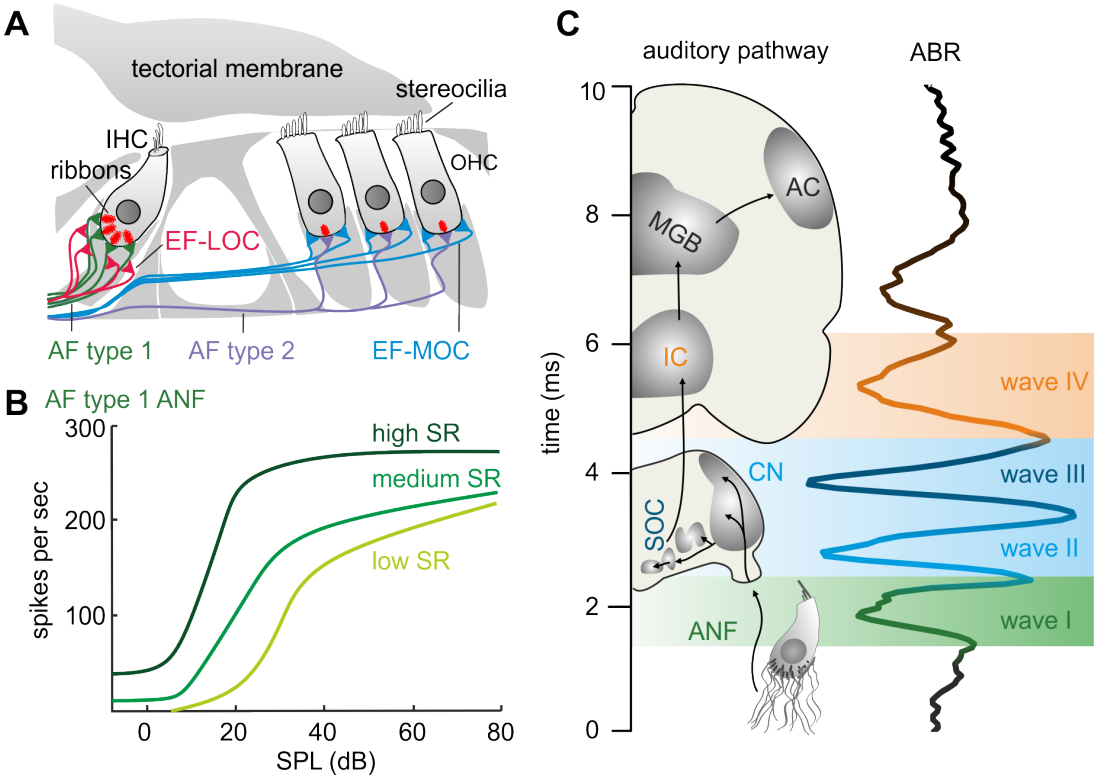

Figure 1: The ascending auditory pathway. (A) The organ of Corti contains one row of inner hair cells (IHC) and three rows of outer hair cells (OHC). The tips of the stereocilia on the apical part of OHC contact the tectorial membrane. The ribbon structured presynapses contain vesicles that can release transmitters (red). Afferent fibers (AF) can be subdivided into AF type I (95 %), which have contact with IHC (green), and AF type II (5 %), which have contact with OHC (purple). Efferent fibers (EF-LOC; pink) project from the lateral part of the superior olivary complex in the auditory brainstem and contact AF type I in an axo-dendritic manner. OHC have direct efferent fiber feedback (EF-MOC; blue) from the medial part of the superior olivary complex. Adapted from Figure 1 in Knipper et al., 2013). (B) AF type I auditory nerve fibers (ANF) can be subdivided in three groups, depending on their spontaneous firing rate (SR) and their threshold characteristics. In cats, ANF with a high-SR (dark green) have a low theshold and ANF with medium- (middle green) or low-SR (bright green) are sensitive to higher SPL and have a larger dynamic response range. Adapted from Figure 8B in Young, 2012. (C) Auditory stimuli are processed along the auditory pathway and can be measured by auditory brainstem responses (ABR). Each of the peaks in the measured signal reflects the summed activity in an area of the ascending auditory pathway during acoustic stimulation. In mice, wave I (green) represents the activity of the ANF, wave II (bright blue) the cochlear nucleus (CN), wave III (blue) the superior olivary complex (SOC), and wave IV (orange) the lateral lemniscus and inferior colliculus (IC). Adapted from Figure 1E in Marchetta et al., 2022.

SGN are located in the Rosenthal's spiral canal, inside the cochlear middle axis, the bony modiolus (Carricondo and Romero-Gomez, 2019). The acoustic portion of the audiovestibular nerve - the VIIIth cranial nerve - is formed by the axons of all afferent neurons (De No, 1933), which project to the cochlear nucleus (CN; Carricondo and Romero-Gomez, 2019). The CN contains a dorsal (DCN) and a ventral (VCN) part. The

VCN projects via the superior olivary complex (SOC) and the lateral lemiscus to the inferior colliculus (IC). From there, the auditory information is transferred to the medial geniculate body (MGB) of the thalamus, and the auditory cortex (AC) (Coleman and Clerici, 1987; M. Malmierca and Merchan, 2004; M. Malmierca et al., 1997).
If the hearing function should be analyzed, the auditory-evoked activity can be measured by auditory brainstem responses (ABR). The wave-shaped averaged signal reflects the summed activity of nuclei along the ascending auditory pathway (Rüttiger et al., 2017, Figure 1C).

1.1.2 Hearing and cognitive function

The hippocampus, being part of the limbic system, is also involved in the processing of auditory stimuli and strong interactions between the hippocampus and the auditory system have been described. The hippocampus is an integration centre in the brain and is well known for its role in memory and spatial learning (Hernandez-Mercado and Zepeda, 2021) but is also involved in responses to stress (Szeszko et al., 2018) and regulation of emotions (Ghasemi et al., 2021). The anatomic structures of the hippocampus contain the dentate gyrus (DG), the four regions of the cornu ammonis (CA1 to CA4) and the subiculum (Rao et al., 2022). The Schaffer's collaterals (SC) are projecting fibers from CA3 to CA1 and are highly associated with memory and learning (Kullmann, 2011; Steward and Scoville, 1976; Witter, 2012).
Sensory input from the neocortex reaches the hippocampus via the entorhinal cortex (EC). In the perforant pathway, afferent fibers from the EC project to the stratum lacunosum-moleculare and contact the dendrites of the pyramidal cells of the hippocampus (Ginsberg et al., 2010; Schultz and Engelhardt, 2014). In addition a direct projection between the AC and the CA1 region of the hippocampus is described (Cenquizca and Swanson, 2007).
The hippocampus is involved in episodic memory (Nyhus and Curran, 2010), which is an important feature for the recognition of sound (O'Keefe and Nadel, 1978; Sakurai, 1990), discrimination of acoustic stimuli (Itskov et al., 2012; Vinnik et al., 2012), and also in the context of auditory fear conditioning (Moita et al., 2003; O'Keefe and Nadel, 1978). It contributes to the processing of acoustically complex stimuli such as speech or music (Davis and Johnsrude, 2003) and is involved in a process that is called sensory gating that describes a neural filter mechanism in which evoked responses of redundant information, as e.g. repeated auditory stimuli, are reduced (Bickford-Wimer et al., 1990).

Age-related hearing loss, which is often sensorineural hearing loss due to aging, is also related to a decreased performance in the Morris water maze and hippocampal synapse degeneration in mice (Beckmann et al., 2020; Yu et al., 2011). Sensorineural hearing loss is caused by any kind of hearing loss due to combined dysfunction of the cochlea and the auditory nerve (Zahnert, 2011). In addition, after an acoustic trauma (AT), hippocampus-related functions, such as spatial learning and memory (Cui et al., 2009; Cui et al., 2012; Liu et al., 2016; Uran et al., 2010; Y. Zhang et al., 2021; Zheng et al., 2014), neurogenesis (Cui et al., 2009; Cui et al., 2012; L. Zhang et al., 2019, 2021), and long-term potentiation (LTP; L. Zhang et al., 2021) were reduced. For proper cognitive function and (social) behavior, a balance between cortical cellular excitation and inhibition is crucial (Yizhar et al., 2011). A dysbalance between this cortical excitation and inhibition was observed after AT in the hippocampus by changes of neurotransmission (Cui et al., 2009; Cui et al., 2012; L. Zhang et al., 2019, 2021). All these studies indicate that hearing loss can lead to hippocampal malfunction.

However, the hippocampus is not only involved in damaging consequences of AT, but also in the positive effects of acoustic stimulation on cognitive function. For different species, enriching sound, such as music, leads to an increase in gene expression of genes that play a role in several brain functions, as for example neurogenesis, learning, and memory in adults (Chaudhury et al., 2013) or during early development (Oikkonen et al., 2016). Also, the neural connectivity between memory-associated brain areas could be improved after acoustic stimulation (Chaudhury et al., 2013). In addition, short non-traumatic mild acoustic exposure could enhance auditory function, memory performance, and LTP in adult mice (Matt et al., 2018). In conclusion, enriching sound exposure was shown to stimulate memory-linked brain function.

1.1.3 Top-down signaling in the auditory pathway

Being surrounded by a complex, variable, and noisy acoustic environment, listening subjects require a strategy to extract meaningful information (Bregman, 1994). One famous example of such an auditory scene analysis is the so-called cocktail party effect, where the listener segregates the voice of one specific speaker from background noise (Cherry, 1953). During this auditory scene analysis, important sound streams are filtered from multiple overlapping sources, which is called auditory streaming (Rankin and Rinzel, 2022). The exact mechanisms of auditory streaming are not clear yet, but it is known that auditory

attention is required (Rankin and Rinzel, 2022). Attention is a cognitive process that influences all stages of auditory processing, beginning in the AC and ending in the inner ear (Collet et al., 1994; Galbraith et al., 2003; Lukas, 1980; Picton and Hillyard, 1974; Rinne et al., 2008). Therefore, for auditory attention, corticofugal signaling - top-down signaling from the central nervous system (CNS) to the auditory periphery - is essential. The corticofugal projections reach from the AC to the MGB, the IC, and the CN (Terreros and Delano, 2015). Corticofugal efferent signaling also modulates learning-induced plasticity in both, animals (Bajo et al., 2010; Gao and Suga, 2000) and humans (Chandrasekaran and Kraus, 2010; Kraus and White-Schwoch, 2015; Musacchia et al., 2007). Therefore, also the hippocampus is directly involved in auditory top-down signaling, as it is connected with the septum, amygdala, striatum and cingulate cortex (G.-D. Chen et al., 2014; Vinogradova, 1975; H. Zhang et al., 2011). All of them are responsive to acoustic stimuli, some even in a tonotopically organised manner (Bordi and LeDoux, 1992; G.-D. Chen et al., 2012). As the hippocampus is also involved in endocrine systems, such as the stress axis (E. De Kloet et al., 2018), which also influences hearing function (Canlon et al., 2007; Singer, Kasini, et al., 2018), indirect top-down signaling via vascular distribution of hormones to the auditory periphery could also be expected.

1.2 Development of the hearing sense

1.2.1 Hearing onset and critical period for the auditory system

The auditory system with all its complexity needs time to develop. In humans, the development of the hearing sense starts in the embryo already in the 27th week of pregnancy (Figure 2). In contrast, in many rodents the onset of hearing occurs quite late after birth, around postnatal day (P) 10 in mice (de Villers-Sidani et al., 2007). The hearing function is not completely matured after the onset of hearing. Instead, it is subsequently shaped during a critical period. In humans, this critical period ranges from birth up to the age of 2-3 years (Sharma et al., 2016), while the critical period of a mouse starts at P10 and lasts to P14 (de Villers-Sidani et al., 2007). During the critical period, the maturation of subcortical and cortical sensory areas is promoted, which is necessary to adapt the auditory system to very specific acoustic settings of each individual's environment (Persic et al., 2020). During this step, a tonotopic map develops that is needed for frequency tuning (Sanes and Woolley, 2011; Werker and Hensch, 2015). Also, features such as fast auditory processing, tuning bandwidth, binaural hearing, and perception of modulated amplitudes

and frequencies are built (Caras and Sanes, 2015; Insanally et al., 2009; Nakahara et al., 2004; Polley et al., 2013). On account of this optimization, language acquisition, phoneme identification, and the development of a musical aptitude is possible in humans (Penhune, 2011; Werker and Hensch, 2015; Zhao and Kuhl, 2016.

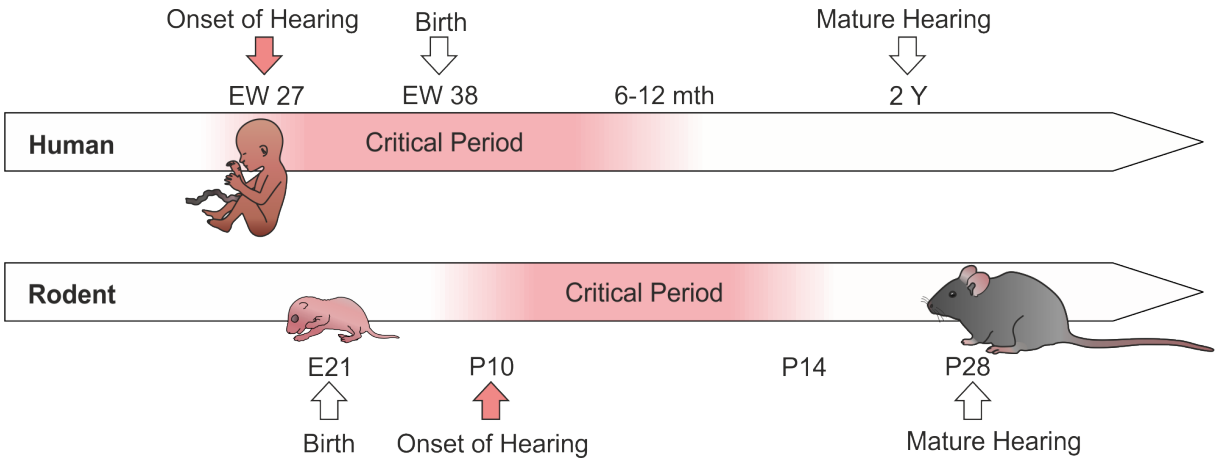

Figure 2: Development of the auditory sense. In humans, the onset of hearing occurs during pregnancy around the embryonic week (EW) 27. Afterwards the critical period (red) for hearing experience starts that lasts up to one year after birth. The maturation of the auditory sense is complete by the age of two years. In rodents, the onset of hearing is after birth around postnatal day (P) 10 with the critical period until about P14. The hearing is mature at 28 days after birth. Adapted from Figure 1 in Knipper et al., 2020.

The importance of proper development of the auditory function is highlighted by the fact that developmental hearing loss, which is the sensory impairment with the highest prevalence in children, has a large impact on deficits in both perception and cognition, which includes delayed language acquisition (Davidson et al., 2019; Moeller et al., 2007; Nicholas and Geers, 2006; Svirsky et al., 2004). Even if the hearing thresholds return to a normal level after a transient developmental hearing loss (as e.g. after middle ear infections), auditory behavioral deficits can remain (Asbjørnsen et al., 2005; Pillsbury et al., 1991; Sanes, 2016; Whitton and Polley, 2011). It is assumed that inhibitory synapse function at the level of both brainstem and cortex plays a role for behavioral deficits after developmental hearing loss, even if the hearing loss was only transient (Sanes, 2013), and that peripheral auditory processing deficits in early childhood can have long-lasting effects in higher order auditory functions, such as speech understanding and auditory attention (Haapala et al., 2015; Haapala et al., 2014).

This critical period in the maturation of the auditory sense has an importance for the starting time point for cochlear implants in infants with hearing loss. It was shown that the outcome of a cochlea implant - in terms of not only hearing function but also develop-

ment of language (Kral and Sharma, 2012; Nicholas and Geers, 2006) and cognitive skills - was better the earlier the surgery was performed in congenitally deaf children (Gordon et al., 2022; Kay-Rivest et al., 2022).

Interestingly, in parallel to the onset and maturation of hearing, the hemodynamic response of the brain develops. Earlier than P11 in rodents, which is before the onset of hearing, brain activation is not yet associated with increasing cerebral blood flow, resulting in an absent or negative blood oxygenation level dependent (BOLD) signal (Colonnese et al., 2008; Iadecola, 2017; Kozberg et al., 2013). Within three weeks after birth, neural activity leads to faster and more intense hemodynamic responses, measurable by BOLD fMRI (Colonnese et al., 2008; Iadecola, 2017) and linked to an increase in vascular density, increased synaptogenesis, and sensitivity towards vasoactive stimuli (Colonnese et al., 2008; Engl et al., 2017; Goyal et al., 2014; Iadecola, 2017; Nehlig et al., 1989).

Further, in a time frame similar to the maturation of the auditory sense, hippocampal LTP gradually matures in rodents (Ostrovskaya et al., 2020). Thereby, the maturation of the hearing sense, the hemodynamic response, and the hippocampal LTP are three mechanisms that develop in parallel and may even be functionally linked.

1.2.2 Balanced excitation and inhibition in auditory circuits

Long before the onset of hearing (at embryonal day 17.5), spontaneous action potentials from IHC can be recorded in mice cochlea (Marcotti et al., 2003). For chickens (Jones et al., 2001), but also for different mammals, such as cats (Jones et al., 2007) and rats (Tritsch and Bergles, 2010), the auditory nerve exhibits a comparable spontaneous bursting pattern in neonates before the onset of hearing, suggesting that this phenomenon may be common across animal classes (Figure 3A). This spontaneous periphery-driven activity, along with the later sensory-evoked activity, is necessary for a proper development of the central auditory system and corticogenesis to ensure processes such as neurogenesis, migration, and differentiation of neurons and network formation (Kilb et al., 2011). Before the onset of hearing the developing brain is hyperexcitable. The reason for this is that neurons which release γ-aminobutyric acid (GABA) and are later in life inhibitory, are excitatory at this time point. The factor that determines the either inhibitory or excitatory effects of GABA is the chloride gradient along the the plasma membrane. Early in development, the chloride gradient is preferentially shifted to a chloride efflux and depolarization of the neuron and changes later on for GABA to become inhibitory (Ben-Ari,

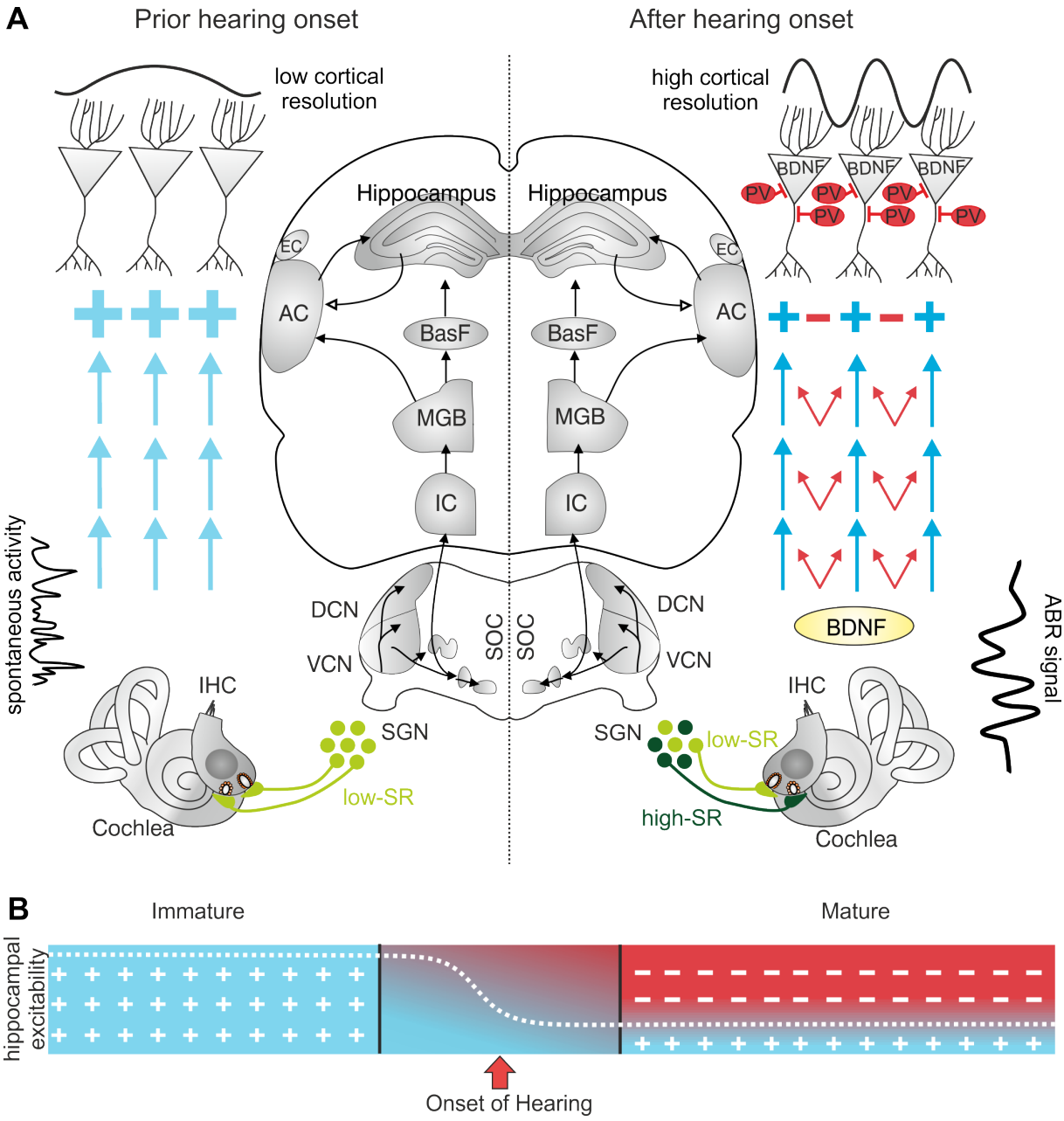

Figure 3: Inhibitory neuronal circuits in the auditory system before and after hearing onset. (A, left) In the immature auditory system, low-SR ANF(bright green) are already firing, but only in a spontaneous manner. At this time, GABAergic neurons in the ascending auditory pathway are still excitatory, and excitation is dominant over inhibition (blue +). This leads to a low cortical resolution and unspecific capacity for sensory stimuli. (A, right) With the onset of hearing, high-SR ANF (dark green) develop, making fast auditory processing possible. They promote BDNF upregulation in the cochlea (yellow) and probably also in other parts of the auditory pathway. In parallel, a switch of GABA from depolarizing to hyperpolarizing occurs (Löhrke et al., 2005). BDNF can regulate the formation of parvalbumin (PV) inhibitory interneuron (IN) contacts with cortical pyramidal neurons to sharpen the receptive fields and increase the cortical resolution. (B) Before the onset of hearing (immature), the hippocampus is hyper-excitable (blue area, +). With the beginning of sensory experience during the critical period, GABA becomes inhibitory, and the spontaneous baseline excitability of the hippocampus is lowered, which is necessary to enable synaptic scaling in the mature state. BasF = basal Forebrain; EC = entorhinal cortex. Adapted from Figure 1 in Knipper et al., 2021.

2002; Marin and Rubenstein, 2001). For the the auditory system it was shown that this excitatory-to-inhibitory switch occurs after hearing onset in a region-specific way (Friauf et al., 2011; Kandler and Friauf, 1995) and is hypothesized to be dependent on sensory experience (Figure 3B; Shibata et al., 2004).

In this process of maturation, brain derived neurotrophic factor (BDNF) possibly plays a role, as it promotes the expression of potassium chloride cotransporter 2 (KCC2; Wardle and Poo, 2003) that is required for the excitatory-to-inhibitory switch (De Koninck, 2007). In the immature rodent cochlea, BDNF is expressed in both IHC and OHC (Wiechers et al., 1999). During early postnatal development at P4, a tonotopic organisation of BDNF mRNA was observed in the cochlea, with the highest expression in apical and medial turns (Wiechers et al., 1999). By time BDNF is downregulated in IHC and OHC and upregulated in SGN - which remains until adulthood - where BDNF can be found in a tonotopic gradient with highest expression in regions of the cochlea that encodes higher frequencies (Adamson et al., 2002; Schimmang et al., 2003; Sobkowicz et al., 2002). According to constitutive BDNF knockout (KO) mouse models, BDNF is necessary for the recruitment of afferent type II fibers to OHC in the high frequency region of the cochlea during early postnatal development (Schimmang et al., 2003) and for the survival of vestibular neurons (Ernfors et al., 1994). As shown by electron microscopy, BDNF is also expressed in inner border- and phalangeal cells that support and surround the IHC (Sobkowicz et al., 2002). However, the role of BDNF in the cochlea is still not completely explored, especially as global BDNF KO mice die prior to onset of hearing (Ernfors et al., 1994; Fritzsch et al., 2004).

In the ascending auditory pathway BDNF additionally plays a crucial role in the development of the auditory function. In the AC, BDNF is involved in the process of long-lasting inhibitory potentiation after the first sensory auditory experience (Xu et al., 2010). Here, BDNF and inhibitory fast-spiking parvalbumin (PV)-positive interneurons (IN) in combination contribute to the sharpening of receptive fields (Figure 3A; Hong et al., 2008; Jiao et al., 2011). Entire networks are formed in fronto-striatal areas that are involved in attention-driven amplification processes. Thereby, the proper integration of inhibitory PV-positive GABAergic IN networks in the cortex is required for improved fast auditory perception and memory-linked processes (Irvine, 2018a; Knipper et al., 2020; Kraus and White-Schwoch, 2015; Weinberger, 2015) and the dysfunction of PV-IN is linked with various neurodevelopmental disorders (Ferguson and Gao, 2018; Marin, 2012).

1.3 Influence of stress perception on hearing

After the proper maturation of the auditory system, the hearing function is not fixed along the life span. Instead, it is modifiable and also vulnerable to damage. For instance, the auditory system can be disturbed by loud noise (Matt et al., 2018) and, among other factors, chronic stress also negatively influences tinnitus symptoms (Mazurek et al., 2015). On the other hand, the hearing function can be temporally changed by e.g., auditory attention and neural amplification processes (Matt et al., 2018), and acute stress can be protective to the hearing function after AT (Canlon et al., 2011; Meltser and Canlon, 2011; Y. Wang and Liberman, 2002). Modulations of the auditory system in both directions can be elicited by different levels of stress.

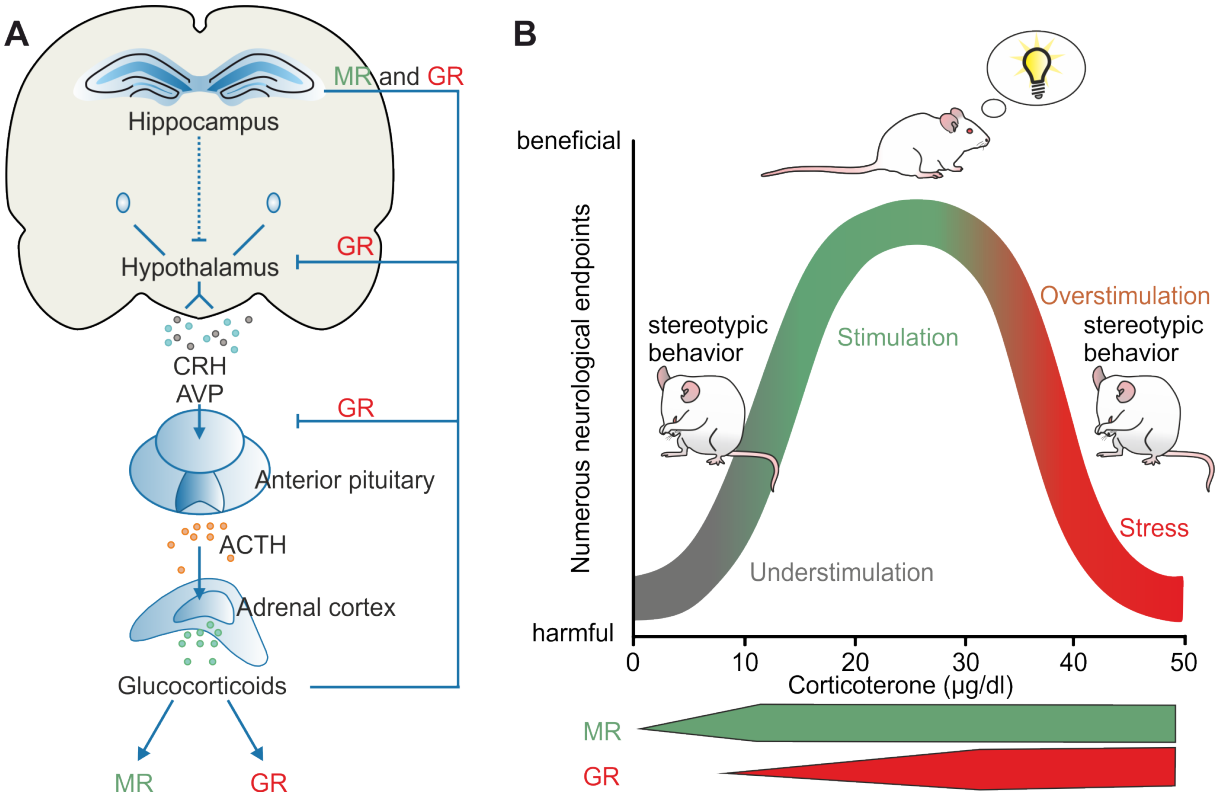

Figure 4: Stress hormone release and effects bodily effects. (A) Schematic illustration of the HPA-axis shows a connection between the hippocampus and the hypothalamus, going to the anterior pituitary, ending with the glucocorticoid (GC) release in the adrenal cortex. GC bind to mineralo- (MR) and glucocorticoid receptors (GR), which give feedback to the HPA-axis at different levels. Adapted from Figure 1 in Schloesser et al., 2012. (B) Inverted U-shaped curve of the effect of stress on the body. Both, understimulation and overstimulation in the stress system are negative, but a moderate stress level is advantageous. The onset of the stress response and mild stress is associated with MR (green) and chronic stress, with GR (red). Adapted from Figure 1 in Sapolsky, 2015.

In general, the perception of stress leads to several physiological processes with the aim of adapting to ongoing changes in the environment and thereby promotes the survival

of the organism (E. R. De Kloet et al., 2005; Sapolsky et al., 2000), mediated by the glucocorticoid (GC) concentration in the blood (E. R. De Kloet et al., 2005). The GC release is driven by the hypothalamic-pituitary-adrenal axis (HPA-axis), which is named by the anatomical structures that are mainly involved in this stress response (Herman and Cullinan, 1997). The hippocampus (Figure 4A) regulates the endocrine system by the modulation of the paraventricular nucleus (PVN) of the hypothalamus. The PVN releases corticotrophin-releasing hormone (CRH) and arginine-vasopressin, both are transported via the portal vessel system to the pituitary gland, where it activates the synthesis of pro-opiomelanocortin that is processed to adrenocorticotrophic hormone (ACTH), which is released. This finally leads to the secretion of GC from the adrenal glands into the blood circuit. The main GC are cortisol in humans and corticosterone (CORT) in rodents (Herman and Cullinan, 1997; Joels and de Kloet, 1994). GC are necessary for the development of organs and tissue, the modulation of inflammation and the control of behavior and neuronal functions, e.g., during the stress response. In association with stress, they also trigger memory storage in preparation for future stressful events (Canlon et al., 2007; E. R. De Kloet et al., 2005). The level of the GC is controlled by neuronal and hormonal mechanisms, which contain a negative feedback action to the hypothalamus and the pituitary gland. This regulation is important for the GC balance (E. R. De Kloet et al., 2005; Joels and de Kloet, 1994). While understimulation is depriving for the brain, the chronic exposure to high stress levels is also harmful, so a beneficial level of stimulation lays in the middle (Figure 4B, Sapolsky et al., 2000).

It is known that the body has two types of receptors that bind the released GC - mineralocorticoid receptors (MR) and glucocorticoid receptors (GR) - which are expressed in the whole body with different characteristics in binding affinity and expression density (E. R. De Kloet et al., 2005). MR additionally bind the very similarly structured, less concentrated mineralocorticoids, such as aldosterone, which are not involved in the stress response but are instead responsible for the sodium retention in the kidney (Joels and de Kloet, 1994). MR are highly affine to GC but have a relatively low capacity, which makes them very active during the onset of stress. GR, on the other hand, have only a tenth of the affinity to GC compared to MR but a much higher capacity, which is why GR is active only under strong or chronic stress conditions (E. R. De Kloet et al., 1999; Sapolsky, 2015). Both are nuclear receptors and are transcription factors that regulate gene expression (Joels and de Kloet, 1994). High amounts of MR and GR are co-expressed in the neurons of limbic structures (E. R. De Kloet et al., 2005). The hippocampus contains

both MR and GR. Most of the other brain areas contain almost exclusively GR (E. R. De Kloet et al., 1999). In the auditory periphery, GR is expressed with a higher density in the inner ear than in vestibular regions. In the cochlea, GR are located in the SGN and also with lower density in the stria vascularis and the organ of Corti, specifically in IHC and OHC (Curtis and Rarey, 1995; W.-J. ten Cate et al., 1993; W. J. ten Cate et al., 1992). MR are also expressed in the cochlea, where they play a role in the maintenance of ion balance. They are expressed in the stria vascularis and also in IHC, OHC, spiral limbus, and SGN (Erichsen et al., 2001; Kil and Kalinec, 2013; Yao and Rarey, 1996).
GR are known to play a crucial role in memory consolidation and therefore long-term adaptation to stressful situations (E. R. De Kloet et al., 1999). MR are important for the onset and regulation of the HPA-axis. In the CNS, they play also an important role for the autonomic outflow and blood pressure response of a stressful event. Further, MR are crucial for selective attention and reaction to novel situations (Joels and de Kloet, 2017). Because of this two-receptor stress response system, one could describe GC as a double-edged sword that coordinates the brain and behavior because the HPA-axis is controlled by MR and the memory storage of the experience is induced by GR (Joels and de Kloet, 2017).
The differential effects of stress on the auditory function has been shown (Basappa et al., 2012; Canlon et al., 2011; Mazurek et al., 2015; Meltser and Canlon, 2011; Singer, Kasini, et al., 2018; Y. Wang and Liberman, 2002), but the exact role of physiological activation of MR and GR in the forebrain for peripheral auditory function is unclear.

1.4 The role of cGMP on hearing

As the prevalence of hearing impairment is very high and the link between hearing loss and cognitive impairment has been shown (Livingston et al., 2017), there is an urgent need to find ways to overcome hearing impairments. Although devices to assist or replace cochlear function exist (i.e., hearing aids, cochlear implants), there are currently many limitations; for example sensorineural hearing loss can poorly be corrected by the amplification of sound alone (Lesica, 2018). Extensive research is ongoing but until now no gene replacement treatment to treat sensorineural hearing loss (Omichi et al., 2019) and no potent pharmacological treatment to prevent or restore hearing function during age or in response to daily noise exposure is approved (Hammill, 2017; Omichi et al., 2019).
One possible pharmaceutical target is the second messenger cyclic guanosine monophos-

phate (cGMP; for review see Marchetta et al., 2021). The presence of cGMP was already described in the cochlea long ago (Guth and Stockwell, 1977), including detailed knowledge about the expression pattern of cGMP and up- and downstream players (for review see Fitzakerley and Trachte, 2018). It is also expressed in the CNS, where it plays a role in memory and cognitive function (Argyrousi et al., 2020; Fedele and Ricciarelli, 2021; Taoro-Gonzalez et al., 2022). cGMP modulates several different actions in the body, ranging from, e.g., platelet aggregation and blood pressure to neurotransmission and sexual arousal. It is synthesized by soluble (sGC) and membrane-bound particulate (pGC) guanylyl cyclases (Figure 5). sGC are activated by their ligand nitric oxide (NO), while pGC are activated by peptide ligands. Apart from five other pGC, GC-A and GC-B are the most extensivly-researched guanylyl cyclases. GC-A binds atrial (ANP), and B-type (BNP) natriuretic peptides, whereas GC-B binds C-type natriuretic peptides (CNP; Friebe and Koesling, 2003; Kemp-Harper and Feil, 2008; Kleppisch and Feil, 2009; Kuhn, 2009; Potter, 2011; Schulz, 2005).

Recently, a protective role of cGMP/cGMP-dependent protein kinase I (cGKI) signaling cascade on hearing function was described in a rat model exposed to AT. The treatment of a cGMP-hydrolyzing phosphodiesterase (PDE) 5 inhibitor was shown to prevent noise-induced hearing loss when injected 120 min before AT and then nine times in 12-h intervals (Jaumann et al., 2012). As the cGMP cascade seems to be a potential target for otoprotection, the upstream mechanism (the cGMP-producing component) that is responsible for this effect was searched for. When the role of sGC for hearing function was analyzed specifically, neither sGC1 nor sGC2 deletion had an influence on OHC functionality, measured with distortion product otoacoustic emissions (DPOAE) and ABR threshold analyses (Möhrle et al., 2017). In fact, the dampening sound of AT was even less harmful for the auditory function of both sGC1 and sGC2 KO mice. However, a crucial role for the protection from synaptopathy after AT could be described, when animals were treated phamacolgically with a sGC stimulator (Möhrle et al., 2017). It is known that AT increases neuronal NO synthases (nNOS) expression in neurons of the CN and SGN (Coomber et al., 2014), perhaps providing a direct link between the NO production after AT and protection of IHC.

For GC-B a role in the development of sensory axon T-branching (bifurcation) of ANF was described (Schmidt et al., 2007). The global inactivation of GC-B revealed an important role of GC-B on temporal auditory processing, such as delayed late ABR waves and diminished responses to amplitude modulated stimuli. GC-B KO also showed reduced

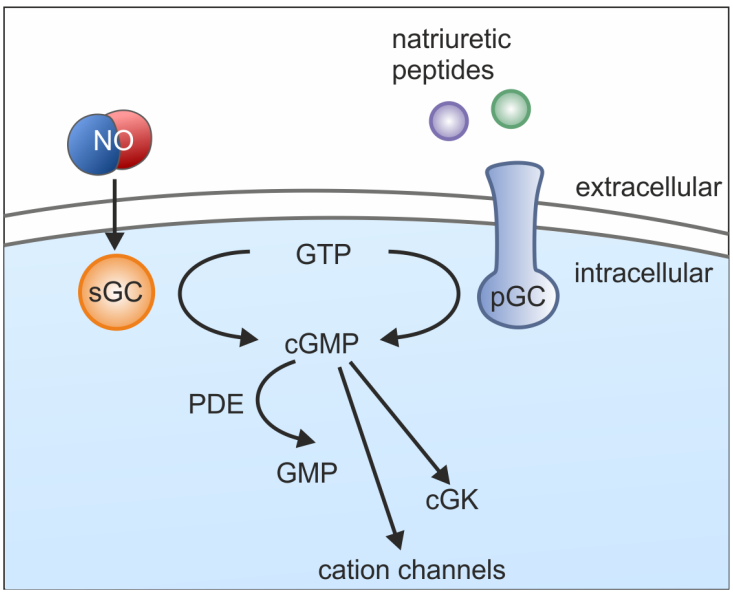

Figure 5: Schematic view of cGMP signaling. Activation of soluble guanylyl cyclases (sGC) by nitric oxide (NO) and particulate guanylyl cyclases (pGC). Cyclic guanosine monophosphate (cGMP) is synthesized from guanosine-5'-triphosphate (GTP) by sGC or pGC. cGMP can activate cGMP-dependent protein kinases (cGK) or cation channels and thereby plays a crucial role in many organs. cGMP is degraded by phosphodiesterases (PDE). Adapted from Figure 1 in Kemp-Harper and Feil, 2008.

efferent cholinergic feedback to IHC and OHC and weaker temporal precision of auditory processing measured with acoustic startle reaction (ASR) (Wolter et al., 2018) in mice. GC-A was described to be expressed in the inner ear, but the effects on peripheral auditory function remained unclear (Fitzakerley and Trachte, 2018; Krause et al., 1997). As both, sGC and GC-B were shown to modulate the auditory function very differently but could not explain the protective effects that were observed after the PDE5 inhibitor treatment, it was hypothesized that GC-A could be the missing link that explains the otoprotective function of PDE5 inhibitors.

2 Objectives

The main objective of this study was to investigate the bidirectional link between peripheral (fast) auditory function and central cognitive response mechanisms, how this link can be modulated, and the main factors that influence this bidirectional link. Different mouse models were used to investigate the consequences of reduced auditory nerve input due to an age-related or developmental phenotype on cognitive function. Further, genetic manipulations in the forebrain were performed to study top-down effects on the auditory periphery.

In detail, the specific influence of BDNF in the auditory periphery in $Bdnf^{Pax2}KO$ mice, which have deficits in fast auditory processing, on higher brain function was of interest (Chapter 3.1). The aim was to understand, how the maturation of fast auditory processing (high-SR ANF) would influence DCN signaling, the shaping of PV-IN in the AC and hippocampus, the hippocampal LTP, memory task performance (multiple T-maze), and social behavior in a Crawley's 3-chamber sociability test (Eckert et al., 2021).

Next, the auditory and cognitive function of aged BLEV reporter mice that show a transcription of activity-dependent Bdnf-exon-IV and -VI on the ability to centrally compensate was analyzed. It was hypothesized that the maintenance of fast auditory processing (high-SR ANF activity) is required for central compensation mechanisms to balance peripheral hearing loss, for hippocampal memory-related processes (LTP) and for neurovascular coupling in central brain areas (Chapter 3.2; Marchetta, Savitska, et al., 2020).

How central stress hormone receptors MR and GR that were deleted in adult mice under the promoter of CaMKIIα are influencing the auditory periphery via a top-down loop, was investigated by measuring basic and temporal auditory processing and performing immunohistochemistry to analyze IHC pre- and postsynaptic integrity and correlating each individual animal's hearing function with the stress levels (Chapter 3.3; Marchetta et al., 2022).

Finally, searching for a potential pharmaceutical target to overcome sensorineural hearing loss, the potential role of GC-A within the auditory function was analyzed (Chapter 3.4). The expression of GC-A and its ligands ANP and BNP was shown in the cochlea. The peripheral hearing function of global GC-A KO mice was analyzed by measuring ABR and DPOAE during the "normal situation" but also when the hearing system had to adapt during aging or after AT (Marchetta, Möhrle, et al., 2020).

3 Results

3.1 Part 1: Effects of BDNF deletion in GABAergic precursor cells before hearing onset on development of fast auditory processing, cognition and behavior

The results and figures described in the following section refer to Eckert, Marchetta et al., 2021, "Deletion of BDNF in Pax2 Lineage-Derived Interneuron Precursors in the Hindbrain Hampers the Proportion of Excitation/Inhibition, Learning, and Behavior." Frontiers in Molecular Neuroscience. 2021, which is attached in the appendix 6.1. Data that are not included in Eckert, Marchetta et al., 2021 are shown as additional figures.

For the implementation of fast auditory processing in the AC and memory related areas, the maturation of the inhibitory PV-IN network is crucial. A failure of this network is linked with neurodevelopmental disorders such as ASD (for review see Marin, 2012). The precursor cells for those GABAergic IN in the cortex are paired box protein (Pax) 6 positive and derive from the subpallium (Guo and Anton, 2014). In contrast Pax2 positive GABAergic IN precursor cells derive from the third ventricle and migrate due to BDNF to hindbrain regions, such as the auditory periphery (Maricich and Herrup, 1999; Nornes et al., 1990; Rowitch et al., 1999). The role of Pax2 positive cells for higher brain function and brain neurodevelopment is unclear. However, it was shown that mice with a loss of BDNF in Pax2 positive cells ($Bdnf^{Pax2}KO$) have a circling phenotype and difficulties in precise, supra-threshold auditory processing, while thresholds remained intact (Chumak et al., 2016; Zuccotti et al., 2012). Here, the role of BDNF in Pax2 positive cells in the development of fast auditory processing, expression of excitatory and inhibitory markers in the CNS, hippocampal function, memory and social behavior is investigated.

3.1.1 BDNF is present in Pax2-lineage descendants in brainstem and hypothalamic regions but not in cortical and hippocampal regions

To localize the exact deletion pattern of BDNF in $Bdnf^{Pax2}KO$ mice, Pax2-Cre mice were crossed with a $Rosa^{TdTomato}$ reporter mouse (Madisen et al., 2010). The offspring mice showed endogenous red fluorescence in all cells that express Pax2. Additionally, brain sections and cochlear whole-mounts were labeled with a staining of Bdnf mRNA and PV protein at different age during maturation. Bdnf mRNA was expressed in GABAergic IN,

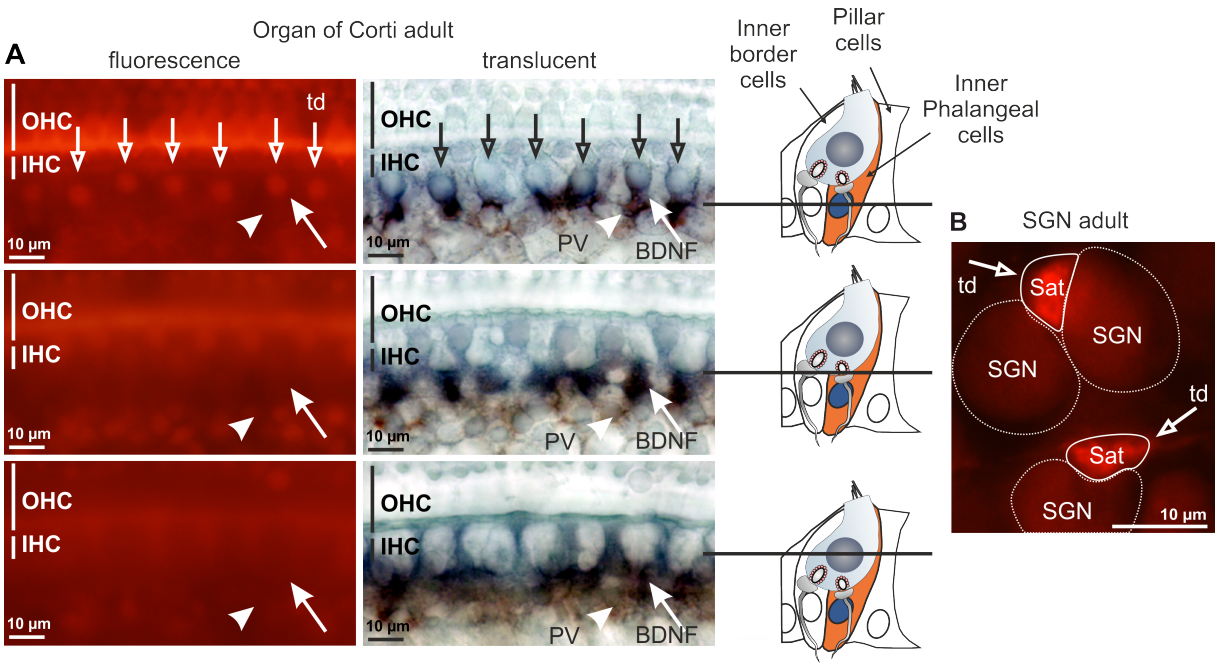

Figure 6: BDNF expression in the cochlea of Pax2-CRE-Rosa^{TdTomato} reporter mice. (A) Adult Pax2-CRE-Rosa^{TdTomato} reporter mice showed at the lower focus level Pax2+ cells (open arrows; top panels) in the basal turn, with co-localization of Bdnf mRNA (closed arrows; dark blue) and PV (arrowhead; brown) below the IHC seen in the upper focus level. The focus level is shown (black bar right panels). (B) Pax2-CRE-Rosa^{TdTomato} reporter mice showed Pax2+ cells (open arrows) in the satellite cells (Sat), but not the SGN.

derived from Pax2-lineage descendants, in non-neuronal cells of the cochlea, such as inner phalangeal supporting cells (Figure 1A) and satellite cells (Figure 1B). From P10 on, a time point that is around the onset of the critical period for hearing function, but also the beginning of the development of PV-IN networks and their integration into fronto-striatal circuits (Kimura and Itami, 2019), an overlap of Bdnf mRNA and Pax2-Cre activity was seen in neurons of the auditory brainstem and midbrain (DCN and IC), but not in frontal brain regions, such as hypothalamus, hippocampus and cortex (Figure 1 in Eckert, Marchetta et al., 2021).

3.1.2 BDNF deletion in Pax2-lineage descendants led to reduced fine-grained auditory function

The hearing function of Bdnf^{Pax2}KO mice was analyzed by recording click-, noise- and pure tone stimuli evoked ABR. While the thresholds of Bdnf^{Pax2}KO mice were only slightly elevated, as already shown in previous studies (Chumak et al., 2016; Zuccotti et al., 2012), the supra-threshold amplitude of ABR wave I was reduced in Bdnf^{Pax2}KO mice compared to controls (Suppl. Figure 2 in Eckert, Marchetta et al., 2021).

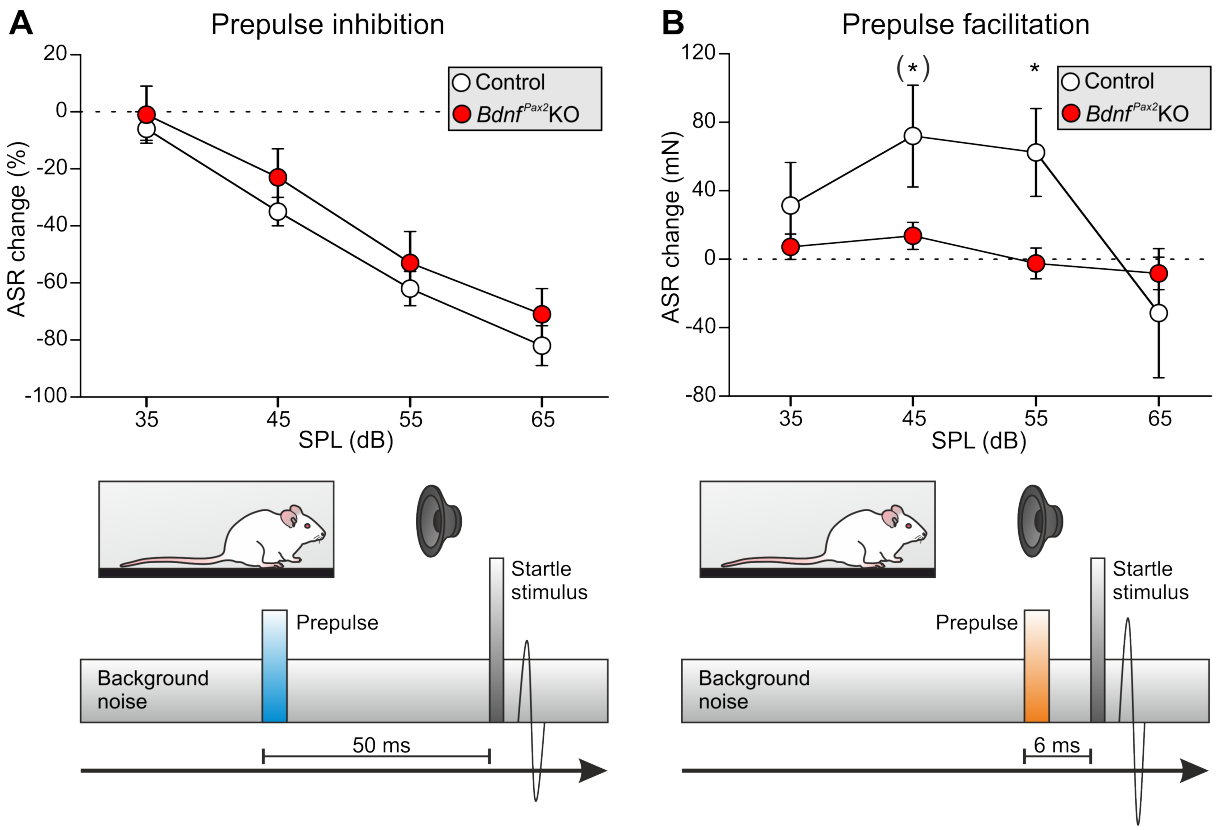

Figure 7: Acoustic startle response (ASR) in Bdnf^{Pax2}KO mice. (A) Modulation of ASR by prepulse inhibition was not altered in Bdnf^{Pax2}KO, while (B) prepulse facilitation was reduced compared to controls.

Response of first order projecting neurons of the auditory input were recorded in the DCN, by placing the electrodes in the fusiform/pyramidal neurons that receive excitatory input from the auditory nerve at the basal dendrites and that are modulated by inhibitory GABAergic vertical cells, contacting the soma. With acoustic stimulation, the response threshold was higher for Bdnf^{Pax2}KO mice, the frequency tuning (measured by the quality factor Q10) was less sharp, and the dynamic range was reduced compared to controls. Bdnf^{Pax2}KO mice had a normal maximal firing rate but the spontaneous firing rate was increased. Within high-frequency-, but not low-frequency sidebands the inhibitory strength was reduced in Bdnf^{Pax2}KO mice. Further, the action-potential firing rate ratio between excitatory and non-inhibitory areas was reduced in Bdnf^{Pax2}KO mice, indicating reduced tonic inhibitory strength (Figure 7, Eckert, Marchetta et al., 2021). Analyzing supra-threshold ABR wave IV, a reduced amplitude and prolonged latency was observed in Bdnf^{Pax2}KO mice, suggesting that Bdnf^{Pax2}KO mice might suffer from temporal auditory processing deficits. In addition, phase-locked responses to amplitude modulated stimuli were analyzed by measuring auditory steady-state responses (ASSR). The temporal resolution was decreased in Bdnf^{Pax2}KO mice at modulation depths higher

than 10 %, seen by higher thresholds and smaller signals, as well as a reduced growth function when measuring with increasing stimulus intensities. For the latter, the effects were most prominent at low SPL, indicating temporal auditory processing deficits close to the level of hearing threshold (Suppl. Figure 2, Eckert, Marchetta et al., 2021).

A	PPI	repeated measurements ANOVA	SPL: F(2,28)=68.9; Genotype: F(2,28)=0.14 p = 0.869	
B	PPF	repeated measurements ANOVA	Interaction: F(1.86, 26.00) = 4.19 p=0.029	WT vs. KO @45 dB SPL P<0.1 @55 dB SPL P<0.5
	WT: n = 7, KO: n = 9 mice			

Table 1: Statistics related to Figure 7

To investigate whether these reductions coincided with temporal discrimination deficits as observed in animals and children with fast auditory processing deficits (Fitch et al., 2013), the ASR were measured. The use of prepulses and the modulation of lead times between prepulse and startle stimuli can provide insight into central temporal resolution deficits. Prepulses for prepulse inhibition (PPI) and prepulse facilitation (PPF) were given before the startle stimulus, with 50 ms and 6 ms lead time, respectively. Bdnf^{Pax2}KO mice had a normal PPI with a decreased ASR (Figure 7A). However, PPF was nearly absent (Figure 7B) in Bdnf^{Pax2}KO mice, which indicates a profound deficit in the detection of short time-interval stimuli in Bdnf^{Pax2}KO mice.

3.1.3 Bdnf^{Pax2}KO mice exhibit altered excitation and inhibition in the AC and hippocampus

Impairment of another set of GABAergic IN precursors, that are Pax6-positive is linked with a failed formation of fast-spiking PV-IN network and neurodevelopmental disorders. Up to now the function of Pax2-positive GABAergic IN precursors on PV-IN in the forebrain is unclear. It was of interest, how the deletion of Bdnf in Pax2-positive GABAergic hindbrain neurons would affect the inhibitory IN network in the hippocampus and cortical areas. Therefore, the expression of PV, but also activity-regulated cytoskeleton-associated protein (Arc), a marker for excitatory neurons (Bramhall et al., 2015; Tzingounis and

Nicoll, 2006) was analyzed. Counting the number of PV-positive somata in the AC layer II/IV and the hippocampus, no differences between controls and Bdnf^{Pax2}KO mice were observed, confirming that the GABAergic IN reached their final destination in the hippocampus and cortical regions.

Next, the arborization of PV-IN synapses was analyzed by calculating the overall integrated density of PV protein labelling, which was reduced in Bdnf^{Pax2}KO mice in the hippocampal CA1 and CA3 region and the AC. In contrast, mRNA of the excitatory marker Arc was increased in similar regions of the same slices, when observing them during double-method immunohistochemistry staining and in situ hybridization mRNA detection. Also, Arc protein was elevated in a second experimental subset of the double-method in the hippocampal regions CA1 and CA3 and the AC. In the same brain sections, no difference of Bdnf mRNA was observed, leading to the conclusion that Bdnf^{Pax2}KO mice have altered excitation and inhibition balance, although the number of PV-IN, as well as the Bdnf mRNA level, were not changed (Figure 2 in Eckert, Marchetta et al., 2021).

The disturbed excitation/inhibition balance in Bdnf^{Pax2}KO mice might be related to an immature phenotype. To prove this, hippocampal brain slices of Bdnf^{Pax2}KO mice and controls at different ages were stained: at the age of P6-P10, which is before the onset of hearing (De Koninck, 2007), at P14, which is at the end of the critical period for the development of the hearing sense (De Koninck, 2007) and in adult animals. In juveniles (P6-P10) the integrated density of PV staining was remarkably low in both groups of genotype, in hippocampal CA1 and CA3 regions. At P14 the level of PV increased in both areas of interest in controls, while it remained low in Bdnf^{Pax2}KO mice, which was also the case for adult animals, indicating that Bdnf^{Pax2}KO mice actually showed an immature level of PV. However, the changes in PV-IN network formation were not found in the somatosensory cortex and the cerebellum (Figure 3 in Eckert, Marchetta et al., 2021), indicating that the observed immature phenotype is specifically associated with the hearing sensory modality and is not a common feature of all sensory cortices.

3.1.4 Bdnf^{Pax2}KOs exhibit elevated LTP and reduced LTD

To proof if a disbalance of excitatory and inhibitory proteins is mirrored in impaired memory function, in vitro recordings of hippocampal brain slices were performed. When stimulated with a tetanic high frequency stimulus to induce LTP, the field excitatory

postsynaptic potential (fEPSP) increased for controls, but it increased much more in Bdnf^{Pax2}KO mice within the 60 min of recording. To proof if this phenotype of hippocampal function is also immature-like, LTP of pre-hearing control pups (P6-P10) was measured. The fEPSP levels of adult Bdnf^{Pax2}KO mice were comparable to those of the P6-P10 control pups, suggesting that Bdnf^{Pax2}KO mice remain at an overexcitation immature stage of hippocampal synaptic plasticity, possibly due to insufficient maturation of PV-IN to tonically inhibit the pyramidal neurons.

In addition, the weakening of synapses by long-term depression (LTD) for synaptic homeostasis was induced by slower stimulation (1 Hz, 15 min). While in controls the signal went back to the baseline level after LTP, the fEPSP of Bdnf^{Pax2}KOs was not different from the high level after LTP stimulation, indicating that the re-scaling of excitatory synapses was impaired maybe because of abnormal high levels of Arc and the reduced activity maturation state of PV-IN of Bdnf^{Pax2}KO mice. To link the memory function with sensory experience, the animals were shortly exposed to a non-traumatic enriching sound. It was shown before that sound enrichment does not only improve auditory function, but also increases LTP and memory formation even two weeks after exposure (Matt et al., 2018). For controls this LTP adjustment could be described, but for fEPSP signals of sound enriched Bdnf^{Pax2}KO mice no difference was seen in comparison with sham exposed animals, as both of them showed increased LTP compared with controls and no further increase of the fEPSP signal was possible (Figure 4, Eckert, Marchetta et al., 2021). Although differences in postsynaptic plasticity were observed, the presynaptic function was not altered in Bdnf^{Pax2}KO mice, as no differences could be observed when measuring input-out (I/O) function at different stimulation levels or paired-pulse facilitation (Suppl. Figure 1, Eckert, Marchetta et al., 2021).

3.1.5 Bdnf^{Pax2}KOs exhibit diminished learning, reduced exploratory activity, and enhanced anxiety

To link the elevated Arc levels and altered hippocampal synaptic plasticity of Bdnf^{Pax2}KO mice with learning behavior, a multiple T-maze paradigm was used. The mice had to find the way in a maze with seven decision points with the final goal to reach their mouse house on top of a platform. The analysis included the count of errors at the decision points during the training. Bdnf^{Pax2}KO mice made more errors at the beginning of the training but also at time points that should reflect either short-term or long-term memory

consolidation. The worse memory performance could, however, not be linked with the circling phenotype of Bdnf^{Pax2}KO mice (Figure 5, Eckert, Marchetta et al., 2021).
To test the social behavior, a three-chamber "Crawley's Sociability" task (Silverman et al., 2010) was performed. The sniffing time of the experimental mice towards either the stranger or the empty cage was monitored. Controls preferred to interact with the stranger compared with the empty cage. Different from this, Bdnf^{Pax2}KO mice did not show a preference, although the latency for the first entry to each chamber was not different from controls, giving evidence that the reduced social interaction in Bdnf^{Pax2}KO was not an artefact related to locomotor problems. Additionally, the exploration behavior was reduced in Bdnf^{Pax2}KO compared to controls, measured by fewer entries in both compartments. This could possibly be linked to an increased stress or anxiety response. In this context, other typical anxiety- and stress-triggered behavior patterns, namely freezing and self-grooming were increased in Bdnf^{Pax2}KO mice and also endogenous blood CORT level was increased. Again, no correlation between circling and sniffing contact, exploration of the chambers, freezing, self-grooming or CORT level could be found, respectively (Figure 6 in Eckert, Marchetta et al., 2021).

In conclusion, the results of Eckert, Marchetta et al., 2021 suggest that the loss of BDNF in Pax2-lineage descendants in hindbrain regions in Bdnf^{Pax2}KO mice may lead to a reduced tonic inhibition in the auditory periphery and thereby reduced fast auditory processing and fine-grained hearing function. This leads to impaired activity-driven recruitment of the GABAergic PV-IN network in AC and hippocampus. As a result Bdnf^{Pax2}KO mice observed shortfalls in adjustments of stimulus-induced hippocampal LTP/LTD, learning, and anxiety control, due to inability to perform synaptic scaling in the hippocampus.

3.2 Part 2: Role of peripheral temporal auditory processing in aged mice on cognitive function

The results and figures described in the following section refer to Marchetta, Savitska, et al., 2020, "Age-Dependent Auditory Processing Deficits after Cochlear Synaptopathy Depend on Auditory Nerve Latency and the Ability of the Brain to Recruit LTP/BDNF." Brain Sci. 2020, which is attached in the appendix 6.2.

Aging people often describe to have difficulties in speech understanding, although audiometric thresholds are normal. This hidden hearing loss was up to now directly linked to progressive cochlear synaptopathy, comparable to a phenotype observed in rodents due to the loss of afferent ANF. Especially the loss of low-SR ANF was thought to be responsible for hidden hearing loss, as they are the most vulnerable ANF class (Furman et al., 2013; Heinz and Young, 2004; Ruel et al., 2008). However, recently it was shown that reduced temporal auditory processing, measured by ASSR, was not necessarily a correlate of cochlear synaptopathy, if the reduced auditory input could be centrally compensated (Möhrle et al., 2016). As the high-SR ANF are responsible for fast auditory processing, it was hypothesized that in contrast to previous views the loss of high-SR ANF would be responsible for fast auditory processing deficits and failure of central compensation. In Marchetta, Savitska, et al., 2020, the hearing function of aged mice was measured with ABR and both, thresholds and supra-threshold waves were analyzed. The animals were then subdivided into animals with a high and a low ability to compensate the peripheral age-dependent hearing loss to reach a sufficient central temporal auditory processing and cognitive function. To study the temporal auditory processing, ASSR upon amplitude modulated sound stimuli were recorded. To evaluate the integrity of the IHC, the ribbon synapses were stained and counted. Hippocampal synaptic plasticity was tested in vitro by measuring fEPSPs and inducing LTP. Finally, the amount of activity-dependent Bdnf gene transcription was analyzed.

3.2.1 ABR thresholds and waves of middle-aged and old mice

The hearing function of young (2.9–6.6 months), middle-aged (9.4–14.3 months) and old (15.3–22.5 months) BDNF-Live-Exon-Visualization (BLEV) reporter mice (Singer, Manthey, et al., 2018) was analyzed by measuring ABR with lower- (click) and higher-frequency (noise) containing most relevant broadband stimuli, as well as pure tone fre-

quencies, covering the hearing range of mice. While middle-aged animals showed an increased threshold only for tones of frequencies at 22.6 kHz and higher, the hearing loss of old animals was already visible with the broadband click and noise and over the whole frequency spectrum of pure-tones (Figure 1 in Marchetta, Savitska, et al., 2020).
The degeneration of IHC and ANF (synaptopathy) was shown to be independent of OHC function (Kujawa and Liberman, 2009) and can be caused by age (P. Wu et al., 2019) or AT (Valero et al., 2017). The supra-threshold ABR wave I and IHC ribbon numbers were investigated, to analyze more specifically a potential synaptopathy. While the ABR wave I was reduced to the same amount in both, middle-aged and old mice, wave IV amplitude of middle-aged animals was less reduced compared to old animals, suggesting that middle-aged animals, in contrast to old animals could better compensate the peripheral hearing loss (reduced ABR wave I amplitude; reflecting cochlear synaptopathy) towards a higher central output activity (ABR wave IV amplitude). Young animals were shown to have a higher number of IHC ribbons than middle-aged and old animals. This was especially prominent for high-frequency cochlear regions (midbasal cochlear turn, i.e. $>$ 17 kHz). It was thereby shown that the number of IHC ribbons was decreased in middle-aged and old mice (Figure 2 in Marchetta, Savitska, et al., 2020).

3.2.2 Central compensation and temporal auditory processing following age-related reduced auditory nerve activity depend on the latency of the auditory nerve response

Both, middle-aged and old mice had reduced auditory nerve activity, which was in general compensated better by middle-aged animals. However, there was some variation between individual mice. It was questioned how well each mouse was able to centrally compensate a low peripheral ABR wave I processing to the processing of ABR wave IV, taking place in more centrally located areas of the auditory pathway. Therefore, ABR wave I and wave IV strength were calculated and correlated. The slope of the regression lines of all three groups of age was similar, meaning that the disproportional ABR wave IV amplification towards ABR wave I strength was not reduced over age. However, the y-axis intercept, indicating a general sensitivity for stimuli, and also reflecting ABR wave amplitudes I and IV growth function as shown before, decreases with age. This mirrors the in general smaller ABR wave amplitudes in aged animals.
For analysis of neural gain, the individual animal's ratio of wave I to wave IV was calculated and plotted against wave I amplitude strength. A regression line with a power

function was fitted to the data of all groups of age together. Young animals exhibited a flat regression curve with normal wave I amplitudes, while both, middle-aged and old animals had the reduced ABR wave I amplitudes, and showed a larger variety in the wave I to IV ratio. Therefore middle-aged and old mice were subdivided in animals with a small central neural gain (when the dots were located below the power line = low compensators) and animals with large, functional neural gain (when the dots were located above the power line = high compensators). In fact, high and low compensators could be found in both, middle-aged and old mice (Figure 3 in Marchetta, Savitska, et al., 2020).

3.2.3 Reduced temporal auditory processing is linked with lower hippocampal LTP and lower levels of hippocampal BDNF

Next, the hearing function of high vs. low compensators was studied. No difference was found in ABR wave I amplitude strength between high and low compensators. However, wave IV was more reduced in low compensators than in high compensators. This was due to the different levels of central compensation. Interestingly, high and low compensators differed also in the latency of ABR wave I. When compared to young mice, the latency was prolonged in low compensators, but not in high compensators. This result is of importance, because high-SR fibers with low thresholds have the shortest latency in comparison to fibers with low-SR fibers (Rhode and Smith, 1986) and these findings may be a hint that low compensators exhibit reduced activity of high-SR ANF. Not only wave I latency was prolonged in low compensators, but also the duration from ABR wave II to wave IV, when compared to young animals, indicating a delay of central transmission in low compensators. IHC ribbon numbers were more reduced in low compensators compared to high compensators, especially at high frequency regions. Here, low compensators exhibited a ribbon loss of $> 50\%$, which indicates at least a significant contribution of high-SR ANF, as they represent about 60% of all fibers (Buran et al., 2010). To investigate the central temporal integration of auditory stimuli, ASSR were measured. A reduction in the processing of these temporally complex stimuli could be observed in low compensators compared to high compensators, showing that low compensators may have difficulties in the temporal segregation resolution of complex, modulated stimuli, possibly due to a lack of high-SR ANF (Figure 4 in Marchetta, Savitska, et al., 2020). A link between high-SR ANF activity and memory-related functions was shown previously in

connection with sound exposure (Eckert et al., 2021). To find out if this link can also be shown for an age-related phenotype, hippocampal synaptic plasticity changes in fEPSPs were measured and LTP induced in high- and low compensators, with the hypothesis that low compensators would have reduced LTP due to the loss of high-SR ANF. Indeed, when comparing the mean from the last 10 min of the 60 min recording after high frequency stimulation the fEPSP was reduced in low compensators compared to high compensators (Figure 5 in Marchetta, Savitska, et al., 2020).

In previous studies, BLEV reporter mice were used to show the recruitment of activity-dependent Bdnf exon-IV and exon-VI transcripts in the hippocampus, as CFP and YFP were tagged to the translational sites of Bdnf exon-IV and -VI mRNA (Singer, Manthey, et al., 2018). The CFP and YFP expression could be correlated with central compensation mechanisms and hippocampal synaptic plasticity (Eckert, Marchetta et al., 2021). In the presented study the same reporter mouse line was used. CFP and YFP expression and co-staining with PV, to detect fast-spiking IN, was inspected with high resolution fluorescence stacks in the hippocampus. YFP Bdnf exon-VI transcripts, that were translated in nerve terminals, overlap or are in vicinity close to CFP Bdnf exon-IV transcripts, which are mainly expressed in capillaries (Singer, Manthey, et al., 2018). The integrated density of both, CFY and YFP fluorescence was reduced for low compensators in the CA3 region compared to high compensators, indicating a possible reduction of neurovascular coupling in the hippocampus as a consequence of reduced high-SR ANF activity. The level of PV was not different for both groups of aged animals, what however cannot exclude the presence of subtle changes in the inhibitory PV-IN network that might become apparent only when examined in a higher number of animals (Figure 6 in Marchetta, Savitska, et al., 2020).

Independently of age and the ABR wave I strength, a delayed auditory nerve response was related with a low central compensation. This led to reduced temporal coding and less LTP and hippocampal Bdnf transcripts in low compensators, indicating that it is not age-dependent cochlear synaptopathy per se, but rather reduced high-SR ANF activity, that is responsible for limited memory-dependent temporal auditory processing disorders such as impaired speech understanding in noise.

3.3 Part 3: Influence of chronic stress and attention on auditory nerve sensitivity and temporal processing

The results and figures described in the following section refer to Marchetta, Eckert et al., "Loss of central mineralocorticoid or glucocorticoid receptors impacts auditory nerve processing in the cochlea." iScience 2022, which is attached in the appendix 6.3. Data that are not included in Marchetta et al., 2022 are shown as additional figures.

Up to now, the mechanism that explains how central cognitive deficits and peripheral hearing loss are linked is not understood yet. What is known is that central hearing deficits also relate to impaired attention and executive function (B. R. Rutherford et al., 2018). Interestingly, both of them are also influenced by the exposure to chronic stress (Canlon et al., 2013; Panza et al., 2019; Perez-Valenzuela et al., 2019). In Marchetta et al., 2022 the influence of forebrain stress receptors (MR and GR) on peripheral auditory function, temporal auditory processing and IHC pre-/postsynapse integrity was analyzed.

3.3.1 Deletion of MR and GR in CaMKIIα expressing forebrain regions but not in the cochlea

To study effects of central stress responses on the auditory periphery, an appropriate mouse model was needed, in which the deletion of MR and GR was (i) tissue specific for limbic forebrain regions and (ii) inducible at a specific age (here in adult animals). Therefore a tamoxifen (TMX) inducible CreERT2-dependent deletion of MR and GR was performed under the promoter of Ca^{2+}/calmodulin-mediated protein kinase IIα (CaMKIIα, Erdmann et al., 2007). By crossing CaMKIIα-CreERT2 mice with the $Rosa^{tdTomato}$Cre-reporter strain (Madisen et al., 2010), red fluorescence, indicating Cre activiation, was only seen in Cre positive mice after TMX in the hippocampus, but not the cochlea. In conditional $MRGR^{CaMKII\alpha}$Cre KO (MRGR cKO) mice, TMX injection activated Cre, which led to deletion MR and GR in the forebrain of adult Cre positive animals, proven by antibody staining. MR and GR were not deleted in the cochlea (Suppl. Figure 1 in Marchetta et al., 2022).

3.3.2 MR and GR have a negative impact on the auditory nerve input via top-down signaling

The hearing of MRGR cKO was analyzed four weeks after TMX injection. Neither ABR thresholds (click-, noise-, or pure tone evoked), nor thresholds for eliciting DPOAE, nor thresholds for compound action potentials (CAP) of the auditory nerve, revealed differences between MRGR cKO and controls. However, when supra-threshold ABR wave I and IV were analyzed, input/output (I/O) functions of both waves were increased in MRGR cKO mice and the CAP latency of wave I, was reduced. These findings indicate a faster and elevated response in the auditory periphery of MRGR cKO, even if MR and GR were not deleted in the auditory nerve function but only in forebrain regions. The deletion of limbic MR and GR was not only affecting peripheral hearing, but also the ASSR that was increased in the absence of limbic MR and GR when measuring with different parameters of modulation depth, stimulus level and speed (Figure 1 in Marchetta et al., 2022). This suggests that the acute, combined central MR and GR deletion does not influence OHC function, but disinhibits peripheral and central temporal auditory responses. Accordingly, MR and GR activation during a stressful event most likely inhibits the auditory nerve response.

3.3.3 Differential effects of central MR and GR on auditory nerve discharge rate and synchronicity

The number of IHC ribbons, which influence auditory processing through defining ANF's discharge rate (Buran et al., 2010; Kujawa and Liberman, 2009) was analyzed in MRGR cKO mice. Related to the increased ABR wave I amplitude an increased or similar number of IHC ribbons was expected as they usually behave proportionally (Buran et al., 2010; Kujawa and Liberman, 2009). Surprisingly, the number of ribbons was reduced in MRGR cKO mice, especially for high-frequency cochlear regions.

As IHC ribbon number and ABR wave I amplitude did not match as expected, it was hypothesized that the phenotype of MRGR cKO could be the result of an overlap of complex individual effects of MR and GR in the forebrain. Therefore, single-deletion MR cKO and GR cKO mice were used to study IHC ribbon numbers. Indeed, MR cKO had - like MRGR cKO mice - a reduced number of IHC ribbons compared to controls. In contrast, the number of ribbons was not changed for GR cKO mice, indicating that the reduced number of ribbons in MRGR cKO may be predominantly caused by the deletion

of limbic MR (Figure 2, Marchetta et al., 2022).

This finding raised the question if also auditory function is different in MR cKO and GR cKO mice. Analyzing ABR and DPOAE thresholds, no effects of central MR or GR deletion was found (Suppl. Figure 2 in Marchetta et al., 2022), again supporting the hypothesis that central MR and GR are not influencing OHC functionality. But now, in MR cKO, the lower number of IHC ribbons was linked with a smaller amplitude of ABR wave I. In addition, CAP thresholds were increased and CAP latencies were prolonged. The dampening effect of central MR deletion on the auditory periphery was furthermore compensated in MR cKO mice in more central auditory processing areas, as responses of the IC (ABR wave IV) and ASSR with different stimulus settings were not different from those of control mice (Figure 3 in Marchetta et al., 2022). On the opposite, GR cKO mice, which did not show differences in the number of IHC ribbon synapses, had increased ABR wave amplitudes, reduced CAP thresholds and CAP latency and stronger responses to various amplitude modulated stimuli. While IHC ribbons were not affected, removal of central GR likely influenced the auditory periphery by changes in spike timing and a stronger synchronicity of ANF responses (Figure 4 in Marchetta et al., 2022), both necessary for the ability to follow amplitude-modulated stimuli (D. H. Johnson, 1980).

3.3.4 AT affects auditory nerve responses through limbic MR and GR

Next, the influence of combined MR and GR deletion on auditory processing following AT was investigated. A standard protocol of exposure to 120 dB SPL at 10 kHz for 40 min was used to generate a permanent threshold shift (PTS). 14 days following AT, the PTS was smaller in MRGR cKO, measured by ABR elicited with click- and noise-burst (Figure 8A) and pure tone auditory stimuli (Figure 8B), most pronounced at the best frequency hearing range around 11.3 kHz. However, the significant difference in ABR PTS was not reflected in OHC function identified by DPOAE thresholds (Figure 8C). This indicates that the deletion of limbic MR and GR positively influenced the vulnerability of neural auditory responses upon AT via a mechanism that does not depend on the OHC function. The functional correlate of the protective effect of combined MR and GR deletion on hearing thresholds after AT was found in a lower loss of ABR amplitude after AT, evident in averaged ABR wave I and IV amplitudes at stimulation levels between 40 and 90 dB SPL (Figure 8D and E). However, no differences in averaged ABR latency shifts at stimulation levels between 40 and 90 dB SPL after AT were observed for wave

I and IV of MRGR cKO and controls (Figure 8D and F). This unexpected result can be explained through the overlapping positive effect of MR on auditory-nerve responses and IHC ribbon numbers, and a negative effect of GR on auditory-nerve amplitude, latency, and synchronized neural responses to tones, as shown previously in studies performed in single MR cKO and GR cKO mice. In conclusion, the central deletion of both MR and GR significantly weakened the damaging effect of AT on neural auditory responses, without affecting OHC function. Central MR/GR activation clearly worsened auditory-nerve processing after AT. The overall negative effect was revealed as combined negative and positive effects of central GR and MR.

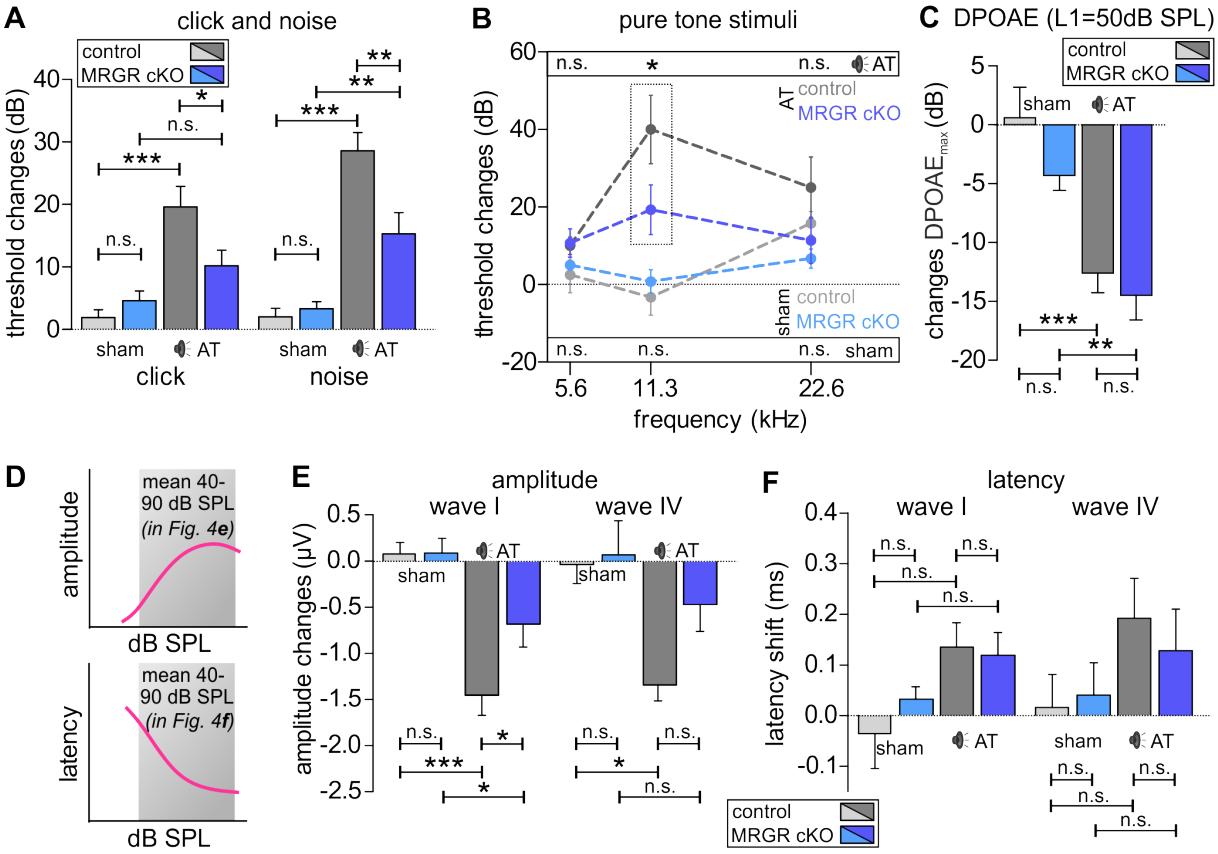

Figure 8: Hearing function is protected in MRGR cKO 14 days after acoustic trauma (AT). (A) 14 days after sham exposure, click- and noise-evoked ABR thresholds were not different, but less threshold loss was seen after AT in MRGR cKO mice compared to control mice. (B) No difference in pure tone ABR threshold between MRGR cKO and control mice after sham exposure, but less threshold increase after AT in MRGR cKO for 11 kHz stimuli. (C) Reduced maximal DPOAE responses after AT in MRGR cKO and control mice, but no difference between MRGR cKO and control mice after sham or AT. (D) The mean individual ear's amplitude and latency was calculated between 40 and 90 dB SPL for comparison of (E) amplitude and (F) latency changes. (E) After sham exposure, click-evoked ABR wave I and IV amplitudes changes did not differ, but less amplitude loss was seen 14 days after AT in MRGR cKO mice compared to control mice. (F) No difference in click-evoked latencies 14 days after sham or AT in MRGR cKO mice compared to control mice for ABR wave I and IV. Mean ± SEM.

A	click	1-way ANOVA	F(3,52)=11.23 p < 0.0001	WT sham vs. KO sham: p > 0.05 WT sham vs. WT AT: p < 0.001 KO sham vs. KO AT: p > 0.05 WT AT vs. KO AT: p < 0.05
	noise	1-way ANOVA	F(3,52)=23.14 p < 0.0001	WT sham vs. KO sham: p > 0.05 WT sham vs. WT AT: p < 0.001 KO sham vs. KO AT: p < 0.01 WT AT vs. KO AT: p < 0.01
	WT sham: n = 7/14, AT: n = 6/12, KO sham: n = 7/14, AT: n = 8/16 mice/ears			
B	f-ABR	2-way ANOVA	F(3,59)=11.70 p < 0.0001	p > 0.5 at 5.6 and 22. kHz p < 0.05 at 11.3 kHz
	WT sham: n = 6, AT: n = 6, KO sham: n = 5, AT: n = 7 ears/mice			
C	DPOAE	1-way ANOVA	F(3,28)=13.30 p < 0.0001	WT sham vs. KO sham: p > 0.05 WT sham vs. WT AT: p < 0.001 KO sham vs. KO AT: p < 0.01 WT AT vs. KO AT: p > 0.05
WT sham: n = 3/6, AT: n = 5/9, KO sham: n = 4/8, AT: n = 5/9 mice/ears				
E	wave I amplitude	1-way ANOVA	F(3,50)=13.33 p < 0.0001	WT sham vs. KO sham: p > 0.05 WT sham vs. WT AT: p < 0.001 KO sham vs. KO AT: p < 0.05 WT AT vs. KO AT: p < 0.05
	wave IV amplitude	1-way ANOVA	F(3,52)=4.749 p = 0.0053	WT sham vs. KO sham: p > 0.05 WT sham vs. WT AT: p < 0.05 KO sham vs. KO AT: p > 0.05 WT AT vs. KO AT: p > 0.05
WT sham: n = 7/14, AT: n = 6/12, KO sham: n = 7/14, AT: n = 8/16 mice/ears)				
F	wave I latency	1-way ANOVA	F(3,51)=2.554 p = 0.0656	
	wave IV latency	1-way ANOVA	F(3,52)=1.149 p = 0.3381	
WT sham: n = 7/14, AT: n = 6/12, KO sham: n = 7/14, AT: n = 8/16 mice/ears				

Table 2: Statistics related to Figure 8

3.3.5 Different blood CORT levels do not cause the differential effects on peripheral hearing in MR-, and GR- and MRGR cKO mice

It is known that interventions on the HPA-axis - such as the deletion of stress receptors in the forebrain - can have effects on the blood CORT level (Erdmann et al., 2007). Therefore, individual animal's basic stress level was analyzed by collecting blood under anesthesia and the CORT level of the plasma was investigated. While the CORT level was not different for MR cKO and control mice, GR cKO and MRGR cKO mice showed increased CORT levels. Interestingly, GR cKO and MRGR cKO mice also had increased ABR wave and ASSR amplitudes as well as reduced latency. However, if the individual CORT levels were correlated with maximal ABR wave amplitudes or latency, no significant regression was found for any of the experimental groups (Figure 5 in Marchetta et al., 2022). This leads to the conclusion that the elevation of the CORT level after GR deletion is most likely not the cause for the hearing phenotype in MRGR cKO and GR cKO mice.

In conclusion, central MR and GR activation have the potential to act positively and negatively on IHC synapses and auditory nerve synchrony. Thereby, the MR and GR signaling thus provides a novel auditory key signature on how peripheral hearing and central auditory processing and cognitive function are linked (Figure 6 in Marchetta et al., 2022).

3.4 Part 4: The role of cGMP/GC-A signaling on auditory function

The results and figures described in the following section refer to Marchetta, Möhrle, et al., 2020, "Guanylyl Cyclase A/cGMP Signaling Slows Hidden, Age- and Acoustic Trauma-Induced Hearing Loss." Frontiers in Aging Neuroscience. 2020, which is attached in the appendix 6.4.

In the inner ear, cGMP signaling has been described to facilitate otoprotection in rats after noise exposure on peripheral and central hearing function, what was observed through PDE5 inhibition (Jaumann et al., 2012). As PDE convert active cyclic nucleotide molecules cyclic AMP (cAMP) and cGMP to inactive 5'nucleotide forms, the blocking of PDE by PDE inhibitors leads to an increase of cGMP (Snyder and Vanover, 2017). Searching for an upstream target of the shown otoprotective cGMP signaling cascade, the effects of the most important guanylate cyclases on hearing function were analysed (for review see Marchetta et al., 2021). While sGC activity seems to be crucial for the continuing integrity of IHC and OHC (Möhrle et al., 2017) and GC-B for the development of axon branching and temporal auditory processing (Wolter et al., 2018), the effect of GC-A was not depicted, yet. Therefore, in the following series of experiments, the influence of GC-A on hearing and otoprotection was analyzed (Marchetta, Möhrle, et al., 2020), hopefully providing the upstream target for the observed PDE5 inhibitor effects on auditory function and vulnerability.

3.4.1 GC-A, ANP and BNP expression in cochlear cells

First, the expression pattern of GC-A and its ligands was described for the auditory periphery, by performing whole-mount dissections of the cochlea, stained for GC-A mRNA. In contrast to the expression pattern of GC-B and sGC (Marchetta et al., 2021), GC-A mRNA expression was found in OHC but not in IHC. In many, but not all SGN GC-A mRNA was expressed as well. Beside tissue staining, hair cells were dissected and isolated from adult mice for mRNA analyses by reverse transcription PCR. Again, GC-A mRNA was shown to be present in IHC and SGN but not OHC. Interestingly, GC-A's ligands ANP and BNP were expressed allover the analyzed cell types, i.e. IHC and OHC, as well as SGN (Figure 1 in Marchetta, Möhrle, et al., 2020).

3.4.2 GC-A KO mice exhibit early dysfunction of OHC but not IHC and ANF

As the expression of GC-A and its ligands ANP and BNP was confirmed in the cochlea, the functional effects of GC-A on hearing were analyzed. Click-, noise burst- and frequency specific pure tone-evoked ABR were measured in young mice (2-4 months) with a global genetic disruption of GC-A and littermate controls. No difference could be found between hearing thresholds of GC-A KO mice and controls for any stimulus (Figure 2 in Marchetta, Möhrle, et al., 2020).

For the specific analysis of electromotile OHC function, DPOAE were measured (Rüttiger et al., 2017). The DPOAE signals were observed at specific frequencies with f2 = 4-32 kHz and levels ranging from L2 = -10 to 65 dB SPL in GC-A KO and control mice. No difference was found in the DPOAE thresholds of young GC-A KO mice and controls. However, when the I/O growth functions at specific frequencies were analyzed, for low frequencies (f2 = 5.6 kHz) no difference between GC-A KO and control mice was observed, but the I/O functions were reduced in GC-A KO mice at higher frequencies (f2 = 11.3 kHz) being in the frequency spectrum in which mice have lowest perception thresholds (Markl and Ehret, 2009). When the staining of the membranous voltage-gated K^+-channel of the subfamily KQT member 4 (KCNQ4) together with the motor protein prestin was analyzed, the expression of KCNQ4 was reduced in basal cochlear turns (Figure 3 in Marchetta, Möhrle, et al., 2020). KCNQ4 plays an important role to maintain the resting potential and for the survival of OHC (Marcotti and Kros, 1999). The expression of the membrane-located protein prestin was unchanged.

Beside OHC function, the sensorineural auditory signaling was of interest. Therefore, from the sound-evoked ABR supra-threshold wave I and wave IV were examined. Both ABR waves were not similar in size in young GC-A KO mice when compared to controls, instead wave I was even slightly higher in KO animals, although this difference was not visible at the level of ABR wave IV anymore, indicating that the cochlear input either was centrally adapted or compensated (Figure 5 in Marchetta, Möhrle, et al., 2020).

In young animals, the deletion of GC-A was worsening OHC function, especially for high frequencies but neither affecting thresholds, nor IHC or ANF function.

3.4.3 GC-A deletion augments age-related synaptopathy and neuropathy but not loss of OHC function

Age very often goes hand in hand with age-related hearing loss, which is unfortunately linked with increased social isolation and the risk of developing dementia (Bowl and Dawson, 2019; Wilson et al., 2019). To investigate a possible connection between GC-A and age-related hearing loss, the hearing function of GC-A KO mice and controls was studied during the aging process in three groups of age. Beside the already observed young mice, middle-aged (7-12 months) and old animals (16-18 months) were now analyzed in terms of effects of age-related hearing loss in interaction with the presence or absence of GC-A. The background strain of GC-A control and mutant mice is the commonly used C57BL/6 strain, which has a mutation within the cadherin 23 gene, being involved in the stereociliar tip-links. Especially at higher frequencies, C57BL/6 mice develop progressing hearing loss with a loss of IHC and OHC, which makes them a suitable model to study age-related hearing loss (Kazmierczak et al., 2007; Noben-Trauth et al., 2003; Siemens et al., 2004). Therefore it was not surprising that all middle-aged and old mice showed increased ABR thresholds compared with young mice. In addition, middle-aged and old GC-A KO mice had even stronger increase of thresholds, with the strongest effects in the middle-age animals. The smaller difference in old animals can be explained by the already strong age-related haring loss in control mice, masking the differences between the genotypes (Figure 1 in Marchetta, Möhrle, et al., 2020).

When measuring DPOAE similar as for young animals no difference between GC-A KO mice and controls was observed in thresholds of middle-aged and old animals. Also similar as for young mice, no difference between the genotypes was found for the I/O function at a low frequency (f2 = 5.6 kHz) in middle-aged and old animals, but a reduction at a higher frequency (f2 = 11.3 kHz) was - as already shown in young animals - seen in middle-aged and old GC-A KO. The KCNQ4 staining, which was already reduced in young GC-A KO mice , was further reduced in basal cochlear turns in GC-A KO mice across all groups of age. The expression of the membrane-located protein prestin was reduced only in old GC-A KO mice, which is probably related to a degeneration of cell-membrane in old animals (Figure 3 in Marchetta, Möhrle, et al., 2020). Interestingly, the difference of DPOAE amplitudes between GC-A KO mice and controls maintained constant over age for 5.6 and 11.3 kHz (Figure 8 in Marchetta, Möhrle, et al., 2020), confirming that age-dependent hearing loss due to loss of OHC function is independent of GC-A signaling.

Synaptopathy can be found independently of OHC loss by changes of ABR supra-threshold responses and loss of IHC ribbon numbers, indicating for IHC synaptopathy and ANF neuropathy (Kujawa and Liberman, 2009), here analyzed in aging GC-A KO mice and controls. While ABR wave I and IV amplitudes were not reduced in young KO and control animals, the lack of GC-A led to a stronger loss of amplitude over the course of age-related hearing loss (Figure 5 in Marchetta, Möhrle, et al., 2020). In line with these findings, the number of midbasal and basal IHC ribbon synapses was reduced in middle-aged and old GC-A KO mice, when compared to age-matched controls (Figure 6 in Marchetta, Möhrle, et al., 2020). Also, the difference between GC-A KO mice and controls in terms of amplitude loss relative to young animals was increasing over age (Figure 8 in Marchetta, Möhrle, et al., 2020).

The deletion of GC-A did not additionally interfere with the loss of OHC function over age but apparently augmented the age-related synaptopathy and neuropathy in advanced age.

3.4.4 GC-A deletion augments AT-Induced synaptopathy and neuropathy but Not loss of OHC function

Beside the effect of age, the exposure to loud, traumatic sound can cause hair cell and sensory fiber degeneration and hearing loss. Young GC-A KO mice and controls were exposed to 40 min broadband noise (8-16 kHz) at 120 dB SPL. The ABR and DPOAE threshold shift between the pre- and seven days post-AT measurement were calculated. Neither for pure-tone frequency evoked ABR nor for DPOAE a different threshold shifts for the two genotypes could be observed.

For analysis of vulnerability of OHC seven days after AT, DPOAE I/O functions were measured and compared between young GC-A KO mice and controls. The I/O functions did not differ after AT between the genotypes at both measured frequencies of 5.6 and at 11.3 kHz (Figure 4 in Marchetta, Möhrle, et al., 2020). Indeed, control mice showed a greater loss of 2f1-f2 DPOAE amplitude, compared to GC-A KO mice (Suppl. Figure 1 in Marchetta, Möhrle, et al., 2020), very likely due to the fact that the growth function in higher frequencies was already reduced before AT and the relative loss is actually similar for both groups.

As an increased level of cGMP was shown to play an otoprotective role in the sensorineuronal components of auditory processing (Jaumann et al., 2012), the supra-threshold ABR

waves were analyzed in GC-A KO mice and controls, expecting a greater vulnerability for noise-induced sensorineural hearing loss in GC-A KO mice. Indeed, ABR wave I and IV amplitudes were more reduced seven days after AT in young and also middle-aged GC-A KO mice, compared to age-matched controls (Figure 5 in Marchetta, Möhrle, et al., 2020). Also the number of IHC ribbon synapses in midbasal and higher frequency cochlear turns was reduced seven days after AT in young GC-A KO mice, when compared to controls (Figure 6 in Marchetta, Möhrle, et al., 2020).
The lack of GC-A was not additionally worsening OHC function and thresholds after AT. Quite different, IHC and ANF were more vulnerable towards AT in the absence of GC-A.

3.4.5 GC-A mediated poly (ADP-ribose) polymerase (PARP) activity in the cochlea

The experiments of the presented studies provided evidence for a GC-A/cGMP-mediated otoprotective effect, although the mechanism of this protection is still not understood. Therefore, we studied poly (ADP-ribose) (PAR) polymers, products of PAR polymerase (PARP) activity (Paquet-Durand et al., 2007). These were shown to be enhanced in animals that were treated with a PDE5 inhibitor and thereby increased cGMP levels (Jaumann et al., 2012).
3,3'-diaminobenzidine (DAB) staining with a primary antibody against PAR was performed in cochlear sections of young GC-A control and KO mice, with and without AT. The PAR staining was quantified by "blinded" volunteers, judging which cell nuclei were stained more darkly. PAR was found in nuclei of IHC and OHC, Deiters' cells and SGN or satellite cells. Without AT, the PAR staining was judged less dark in OHC of midbasal and basal turns of GC-A KO, compared to controls. After AT the PAR staining intensity differences were less clear in OHC; PARP activity was only reduced in midbasal turns of GC-A KO mice. In basal turns, the PAPR activity was already reduced in controls and no difference could be observed in comparisons to GC-A KO mice. The PAR intensity for IHC was not different in midbasal turns in GC-A KO mice, compared to control mice before AT. After AT, in midbasal and basal turns the PAR staining was reduced in IHC and SGN of GC-A KO mice, compared to controls (Figure 7 in Marchetta, Möhrle, et al., 2020).
In summary, in the healthy hearing situation in young animals, GC-A is otoprotective for OHC, but independent of aging and AT. In contrast GC-A does not influence IHC/SGN function in young mice, but when they were challenged by age or AT exposure, GC-A

had a protective role for IHC and SGN.

4 Discussion

4.1 Part 1: BDNF in GABAergic Pax2-lineage descendants is crucial for the development of high-SR ANF activity

The results of Eckert, Marchetta et al., 2021 indicate that the expression of BDNF in GABAergic Pax2-lineage descendants is important for the development of a critical sub-

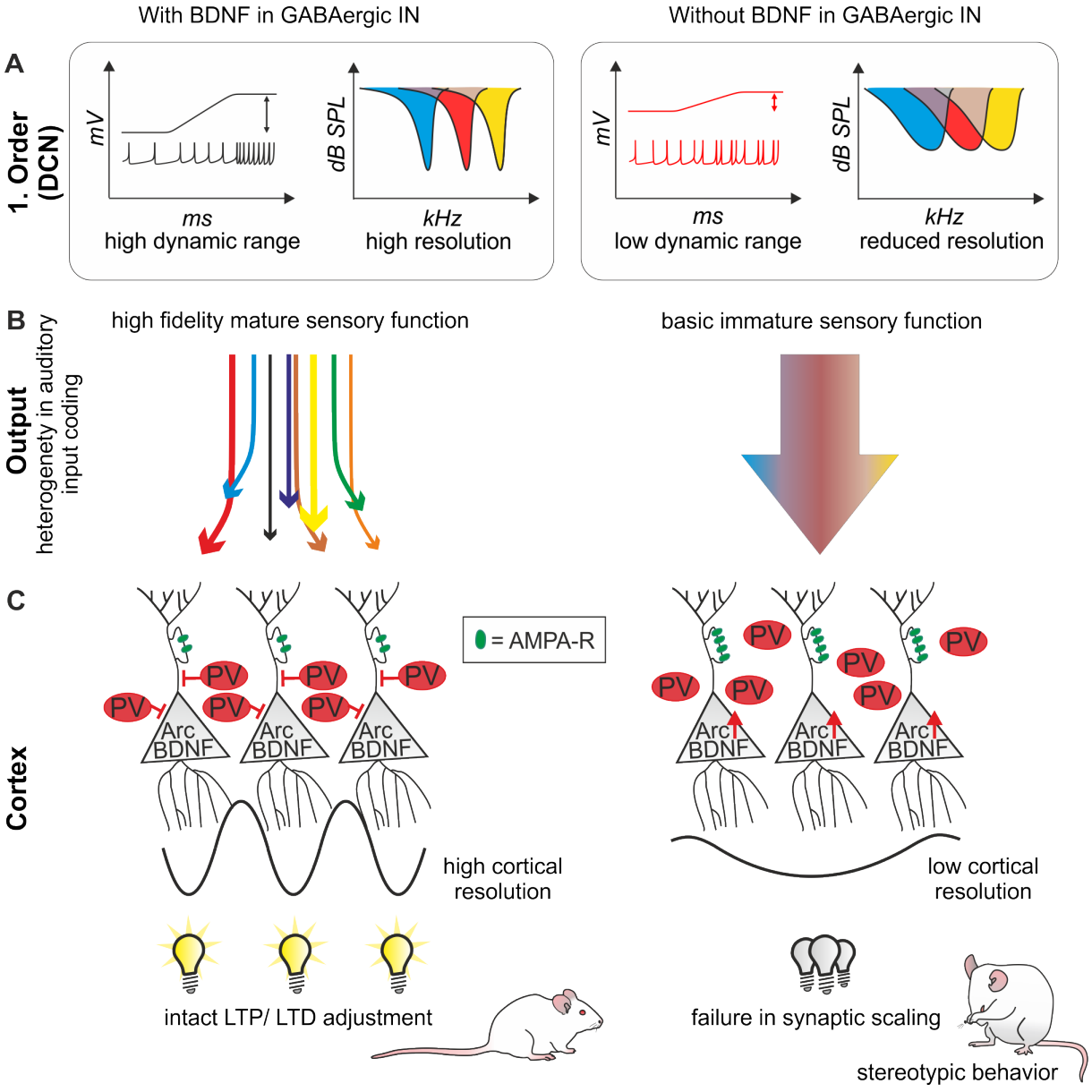

Figure 9: BDNF in GABAergic IN precursors shapes fast auditory processing and cognitive function. (A) Bdnf^{Pax2}KO mice (right column) have a reduced dynamic range and resolution of neuronal representation for auditory stimuli in the DCN in comparison to controls (left columns). (B) The auditory function develops only if BDNF is expressed in GABAergic IN precursors, (C) which leads to a failed PV-IN arborization in the AC and hippocampus, resulting in impaired synaptic scaling in LTP and LTD and stereotypic behavior of Bdnf^{Pax2}KO mice. AMPA-R = AMPA receptor. Adapted from Figure 8 in Eckert, Marchetta et al., 2021.

cortical basis for reduced internal noise levels and higher auditory-specific resolution (Figure 9A), which are a prerequisite for sensory maturation (Figure 9B), cortical resolution and stimulus-induced hippocampal LTP and LTD adjustment, social behavior, learning and anxiety control (Figure 9C).

4.1.1 BDNF expression in Pax2-lineage descendants in the auditory periphery

By the use of Pax2-CRE-Rosa^{tdTomato} reporter mice, the expression pattern of BDNF mRNA in Pax2-lineage descendants was confirmed in peripheral auditory areas, such as supporting cells in the cochlea, DCN, and IC, but also the cerebellum and hypothalamic regions, all regions in which the presence of Pax2 has been detected in previous studies (Fotaki et al., 2008; Maricich and Herrup, 1999; Nornes et al., 1990; Rowitch et al., 1999). It is still of a general debate whether BDNF is expressed directly in GABAergic IN precursors. Literature often claims an absence of BDNF in inhibitory IN (Andreska et al., 2014; Canals et al., 2001; Cohen-Cory et al., 2010); however, a few studies provided evidence for BDNF expression in GABAergic neurons, in either PV-IN of cortical regions, or IN-precursors in spinal-cord neurons (Z. J. Huang et al., 1999; Jungbluth et al., 1997; Tomas et al., 2020). Eckert, Marchetta et al., 2021 thus strongly supports the latter findings and suggests reconsidering the presence of BDNF expression in inhibitory GABAergic precursor cells. It remains necessary to clarify whether BDNF has a function within GABAergic IN, for instance in guidance supporting navigation along pre-formed vascular-networks (Li et al., 2016; Won et al., 2013). Since BDNF expression in phalangeal cells (Figure 6) may control synaptogenesis at IHC after hearing onset (Sobkowicz et al., 2002), its participation in the shaping of vesicle exocytosis at IHC synapses (Chumak et al., 2016) and the shaping of fast high-SR ANF responses through tonic inhibition of efferent fibers (Knipper et al., 2015; Knipper et al., 2020; Ruel et al., 2001) may be conceivable. Interestingly, PV expression was likely reduced in the inner phalangeal cells on the pillar side (Figure 6), i.e., the side, relative to the IHC, where the high-SR, low-threshold fibers connect (Taberner and Liberman, 2005). Thereby, it may be postulated that BDNF expressing Pax2-lineage descendants play a role at the part of the IHC that is required to code postsynaptic high-SR fiber processing (Jean et al., 2018).

4.1.2 Deletion of BDNF in peripheral GABAergic precursor cells leads to changes in balance of central excitation and inhibition

In the auditory periphery of Bdnf^{Pax2}KO mice, a normal basal hearing function was observed (Eckert, Marchetta et al., 2021, Chumak et al., 2016; Zuccotti et al., 2012). Also, normal encoding of amplitude-modulated tones at higher SPL was found in Bdnf^{Pax2}KO mice (Suppl. Figure 2D in Eckert, Marchetta et al., 2021), which requires intact low-SR ANF function (Bharadwaj et al., 2014). These low-SR ANF develop early after hearing onset (Glowatzki and Fuchs, 2002; Grant et al., 2010) and are most likely functional in Bdnf^{Pax2}KO mice. In contrast, high-SR ANF with low activation thresholds and shortest latency develop later after hearing onset (Bourien et al., 2014; Glowatzki and Fuchs, 2002; Grant et al., 2010; Heil et al., 2008; Meddis, 2006) and might be dysfunctional in Bdnf^{Pax2}KO mice. A hint for reduced high-SR ANF activity in Bdnf^{Pax2}KO mice is given by the reduced DCN input with wider bandwidth and reduced sideband inhibition but elevated spontaneous neuron activity, ending up with less inhibitory shaping of vertical cells (Spirou et al., 1999). Further, the loss of short lead time detection during PPF in ASR measurements in Bdnf^{Pax2}KO mice may be explained through diminished temporal auditory processing and thereby reduced high-SR ANF activity (Figure 7). The reduced levels of tonic inhibitory strength at the DCN in Bdnf^{Pax2}KO mice (Figure 4 in Eckert, Marchetta et al., 2021) may indeed reflect an initial stage of hyperexcitability, during which GABAergic neurons are still excitatory. For establishment of balanced excitation and inhibition in neuronal circuits, the migration of cortical IN is essential. These migrating IN change their response signal to GABA from a motogenic to a stop signal prior to synaptogenesis (Bortone and Polleux, 2009). The potassium-chloride co-transporter KCC2 thereby acts as the excitatory-to-inhibitory switch for GABA to become hyperpolarizing (Ben-Ari, 2002; Marin and Rubenstein, 2001), reducing Ca^{2+} influx and reducing the IN motility. One strong modulator of KCC2 activity is BDNF (De Koninck, 2007; Wardle and Poo, 2003), which is highly activity-driven (Wollet and Kim, 2022). Possibly the excitatory-to-inhibitory switch did not properly occur with the absence of BDNF in GABAergic precursor neurons.

It is further hypothesized that the maturation of tonic inhibition and thereby fast auditory processing is required for the formation of perisomatic and dendritic PV-IN. This inhibitory network arborization develops during the critical time period between P10 and P14 in controls and was shown to be reduced in the AC and hippocampus of Bdnf^{Pax2}KO

mice, although the number of PV-IN somata in adults was not changed (Figure 2,3 in Eckert, Marchetta et al., 2021,). This indicates that, although BDNF was deleted in Pax2-positive GABAergic IN precursors, the Pax6-positive GABAergic IN precursors properly migrated from subpallidal regions to the cortex or hippocampus (Marin and Rubenstein, 2001). During development, sensory input that results in neuronal activity during the critical, sensitive period is necessary for the migration of inhibitory IN in the cortex and for their integration in functional circuits (de Villers-Sidani et al., 2007; Lim et al., 2018). The latter is implemented by formation of perisomatic PV-IN networks in the cortex for which activity-dependent BDNF from pyramidal neurons is essential (Griffen and Maffei, 2014; Hong et al., 2008; Lim et al., 2018; Meis et al., 2019; Xu et al., 2010). Thereby, functional fast auditory processing should be considered as a critical subcortical process on which cognitive functions depend. Proper tonic inhibition is required for the integration of inhibitory IN networks in the hippocampus and AC. These inhibitory IN-networks enable neurons to become tuned to defined receptive fields, allow precise pattern segregation and shape temporal precision by feed-forward inhibition (Leutgeb et al., 2007; Pouille and Scanziani, 2001), and regulate plasticity in the cortex (Hensch, 2005).

The study of Eckert, Marchetta et al., 2021 shows once more how important critical or sensitive periods of brain development are. Even if it is known that brain plasticity is most prominent during this critical period and that neural circuits that define central auditory processing are shaped by early experience (Elbert et al., 1995; K. H. Kim et al., 1997; Pantev et al., 1998), the understanding of its molecular and neural basis and also the adaptation of therapies, such as drugs, hearing aids and other clinical therapies, is very minor. It is therefore worthwhile to postulate a role of fast auditory processing in the activation of promoters in the BDNF gene in pyramidal cortical neurons and continue studying this in a suitable animal model.

In humans, deficits in fast auditory processes impede initial language development and other higher-order processes, including social learning (Fitch et al., 1997; Fitch and Tallal, 2003; Rendall et al., 2017). Numerous causes of neurodevelopmental brain disorders, including ASD and schizophrenia, which are mainly associated with deficits in forebrain regions (Levitt et al., 2004; Lewis et al., 2005; Reim and Schmeisser, 2017), may also be related to altered sensory information processing due to deficient development of gating processes in lower brain regions, especially since failure to migrate and integrate GABAergic IN into functional circuits has been hypothesized to lead to neurodevelopmental disorders (for review see: Marin, 2012).

4.1.3 The dysbalance of excitation and inhibition in Bdnf^{Pax2}KO mice results in impaired executive function

In parallel with the impaired formation of PV-IN networks, the level of Arc was increased in the AC and hippocampus of Bdnf^{Pax2}KO mice, possibly due to reduced contacts of PV-IN with pyramidal neurons. Arc is expressed in excitatory neurons of the hippocampus and cortex, but in some areas it can be found also in GABAergic projection neurons (Gong et al., 2020; Vazdarjanova et al., 2006). The expression level of Arc is dependent on the stimulation intensity of the hippocampus (Bramham et al., 2008; Link et al., 1995; Vazdarjanova et al., 2006). A glutamatergic stimulation of projection neurons leads to a fast increase of Arc and a reduction of AMPA receptors in the postsynaptic membrane, which weakens the synaptic strength (Waung et al., 2008). As Arc levels are extremely high and saturated in Bdnf^{Pax2}KO mice because the hippocampal excitatory baseline was not down-scaled properly by the development of PV-IN, the high-frequency stimulation of the hippocampus (LTP) leads to elevated fEPSP, such as in an immature system (Figure 4 in Eckert, Marchetta et al., 2021). Also, the weakening of the synaptic strength with low-frequency stimulation (LTD) can not bring the level of fEPSP back to baseline, possibly due to the saturation of Arc, making it impossible for further elevations and thereby removal of postsynaptic AMPA receptors (Waung et al., 2008). The inflexibility of hippocampal synaptic scaling in Bdnf^{Pax2}KO mice shows that sound enrichment, which usually drives positive feedback circles for task-specific amplification processes (Irvine, 2018a; Matt et al., 2018), does not have the expected effects. As AMPA receptor trafficking is a prerequisite for cognitive functions such as discrimination of novelty (Waung et al., 2008), the dysfunctional AMPA receptor trafficking in Bdnf^{Pax2}KO mice could explain the deficits in the multiple T-maze (Figure 5 in Eckert, Marchetta et al., 2021). Further, the impaired social behavior, reduced exploratory movements, increased anxiety and stress behavior, increased motor activity, and stereotypic behavior could be consequences of dysfunctional AMPA receptor trafficking, as not only novelty discrimination, but also stress behavior is controlled by AMPA receptors (Derkach et al., 2007; Penrod et al., 2019; Roth et al., 2020).

Many of the described phenotypes of Bdnf^{Pax2}KO mice can be linked to those of ASD mouse models, such as reduced PV-IN networks (Pirone et al., 2018; Takano, 2015), elelvated Arc expression (Goel et al., 2018; Korb and Finkbeiner, 2011), increased hippocampal LTP (Mohn et al., 2014), increased CORT levels (Das et al., 2019), and im-

mature synapses (Hickman et al., 2015). Also for another autistic mouse model with a deficiency of adenomatis polyposis coli protein (J. M. Alexander et al., 2020; Hickman et al., 2015; Mohn et al., 2014), immature synapse development have been reported, as well as a reduced fine-grained hearing function with reduced dynamic range and impaired IHC ribbons at pillar sides have been described (Hickman et al., 2015), again indicating deficits in high-SR ANF.

Knowing that signaling by high-SR ANF seems to play a crucial role for the maturation of the auditory system, and cGMP is linked with proper high-SR signaling, a pharmaceutical treatment with for instance PDE inhibitors to increase the level of cGMP might help to overcome not only the hearing, but also the cognitive phenotypes of $Bdnf^{Pax2}KO$ mice. It is, however, questionable if this treatment will be effective in adult animals or if it needs to be applied during the critical period of hearing development.

4.2 Part 2: The latency of the auditory nerve processing influences fast auditory processing, hippocampal function and Bdnf transcription, independent of age

The study by Marchetta, Savitska, et al., 2020 described that, independent of age and the overall reduced auditory nerve amplitude itself, the delayed auditory nerve activity latency was linked to a low central gain and reduced temporal auditory resolution, LTP induction and hippocampal Bdnf transcription (Figure 10).

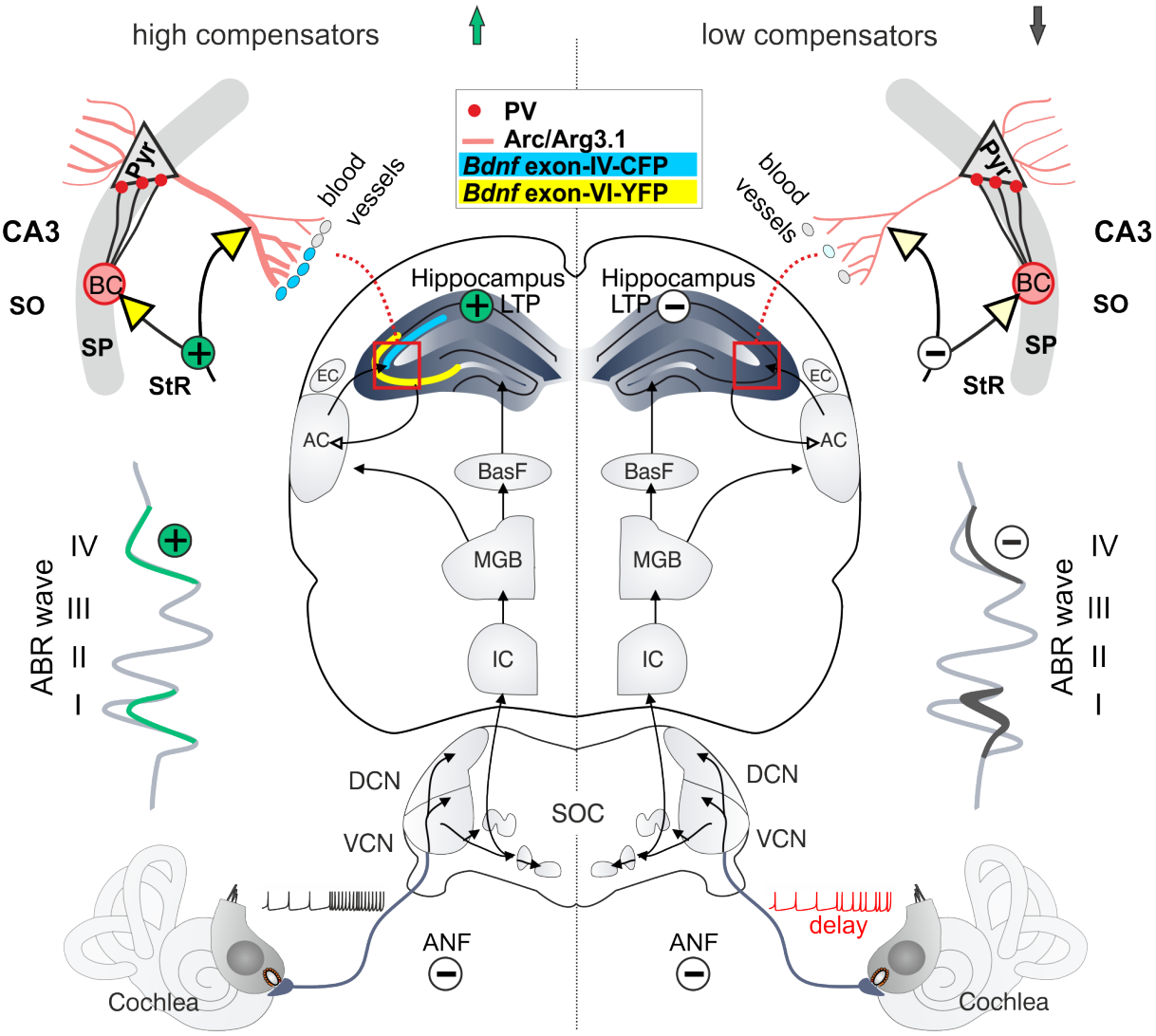

Figure 10: Abstract scheme of central compensation mechanisms in the auditory system. In aged animals, proper fast auditory processing was linked with a high compensation ability (left panel), with disproportionally increased ABR wave IV after reduced ABR wave I input, leading to higher hippocampal LTP and larger Bdnf exon-IV and exon-VI expression. In contrast, animals with reduced temporal auditory processing (prolonged latency) had low compensating capacities and therefore had also a reduction in ABR wave I and IV, LTP and Bdnf exon-IV and exon-VI expression. SO = stratum oriens; SP = stratum pyramidale; StR = stratum radiatum. Adapted from Figure 7 in Marchetta, Savitska, et al., 2020.

Thereby not age-dependent cochlear synaptopathy, but instead reduced fast auditory processing, which depends on high-SR ANF activity, may be responsible for impaired memory-dependent temporal auditory perception that is required for understanding speech in noise.

4.2.1 Short latency during age is needed for proper auditory function

Hearing loss is a big problem in the aging population. However, a huge challenge in the diagnosis and treatment is hidden hearing loss, defined as difficulties in understanding acoustic stimuli, such as speech in noisy, acoustically challenging environment but without measurable changes in audiometric thresholds (Frisina and Frisina, 1997; King and Stephens, 1992; Ouda et al., 2015; Saunders et al., 1992). This hidden hearing loss, even if not measurable with standard auditometry, was shown to be linked with cochlear synaptopathy (Kobel et al., 2017; M. C. Liberman and Kujawa, 2017). This sensorineural hearing loss causes poorer speech perception (Bramhall et al., 2015). The current opinion is that the loss of low-SR ANF during cochlear synaptopathy would cause deficits in fast auditory processing (Furman et al., 2013; Sergeyenko et al., 2013), as low-SR ANF become perceptible at supra-threshold levels and in acoustically difficult situations, e.g., with background noise (Bourien et al., 2014). Several studies find deficits in perception of acoustic stimuli in humans despite unchanged thresholds (Furman et al., 2013; King and Stephens, 1992; Saunders et al., 1992; Sergeyenko et al., 2013), for which the loss of low-SR ANF would provide an explanation model for hidden hearing loss, as detection with high-SR ANF that have low thresholds would be already saturated (Bharadwaj et al., 2014; Bourien et al., 2014; Parthasarathy and Kujawa, 2018). In addition, low-SR ANF are more vulnerable for noise damage or during aging (Bourien et al., 2014; Heinz and Young, 2004; Ruel et al., 2008). Despite these two strong hints that make it likely that low-SR ANF are responsible for hidden hearing loss and thereby deficits in fast auditory processing, an alternative hypothesis was described: Williamson et al. showed that mice of young and old age did not show differences in peripheral hearing thresholds, but rather fast auditory processing, measured by gap detection and ABR latency, was reduced in elder animals (Williamson et al., 2015), indicating that perhaps not low-SR, but instead high-SR ANF are responsible for hidden hearing loss, as they are linked with the shortest latency responses (Rhode and Smith, 1986). In the present study, low compensators had a prolonged latency of ABR wave I, which mirrors the activity of the auditory nerve, and

also a loss of IHC ribbon synapses in high frequency cochlear regions when compared with high compensators. The loss of IHC ribbons was more than 60% of the summed ribbon number. This, together with the prolonged latency indicates that also high-SR ANF must be affected (Yates, 1991). As a consequence of prolonged latency and reduced fast auditory processing, aged animals exhibited reduced central compensation (Figure 4 in Marchetta et al., 2021).

High-SR ANF mature after the onset of hearing and are necessary for the setting of an excitation and inhibition baseline by recruitment of PV-IN microcircuits to provide the possibility for auditory-specific stimulus induced contrast-amplification and central neural gain (Eckert, Marchetta et al., 2021; for review see Knipper et al., 2020). This central neural gain, here impaired in low compensators, may be linked to the (dys-)function of high-SR ANF activity.

Already before, an indirect prediction for the need of high-SR ANF for central compensation after synapthopathy was described in a computerized model: a specific amount of high-SR ANF remaining after AT would be crucial for an increase of auditory brainstem neurons' discharge rates that drive central compensation (Schaette and Kempter, 2009, 2012).

4.2.2 Short latency during age is needed for proper hippocampal function

Both, middle-aged and old mice showed not only a low capacity for central compensation when the auditory nerve latency was prolonged, but also lower hippocampal LTP and reduced activation of Bdnf transcripts in the hippocampus when compared with mice with normal latency and good compensation mechanisms. This means that along with reduced peripheral temporal auditory processing, changes can be found even in higher order brain areas, such as the hippocampus. This can be explained by the fact that the central compensation mechanism due to attention-driven contrast amplification also activates several regions in the fronto-striatal brain areas via auditory sound processing in the MGB (Irvine, 2018a; Kilgard et al., 2002; Kraus and White-Schwoch, 2015). Here, the basal forebrain plays a role in accentuation of auditory stimuli (Irvine, 2018b; Kilgard et al., 2002; Kraus and White-Schwoch, 2015); the inferior frontal gyrus helps to distinguish new or divergent signals from earlier ones (M. S. Malmierca et al., 2014; Schönwiesner et al., 2007); the hippocampus is crucial for the extraction of behaviorally relevant signals, adaptation of synaptic strength and thereby formation of memory stores (Irvine, 2018b;

Kraus and White-Schwoch, 2015; Weinberger, 2015). Finally, the prefrontal cortex is targeted for responses related to attention-driven plasticity (Irvine, 2018a; Viho et al., 2019). The link between central amplification processes and attention- and memory-circuits was shown following AT (e.g., Gröschel et al., 2014; Kaltenbach and Zhang, 2007; Matt et al., 2018; Salvi et al., 2000; Vogler et al., 2011), but it can be hypothesized that the similar mechanism and link occurs during central compensation of age-related sensorineural hearing loss (Marchetta et al., 2021; Möhrle et al., 2016). To enable central neural gain, the functionality of high-SR ANF is required, to provide a low baseline due to inhibitory PV-IN network microcircuits (for reviews see: Knipper et al., 2021; Knipper et al., 2020). Only with this low baseline is a central neural compensation or attention-triggered selective contrast-amplification possible (Dragicevic et al., 2019; Knipper et al., 2020; Miller and Buschman, 2013; Nunez and Malmierca, 2007; Wittekindt et al., 2014).

The driving force for central neural gain and contrast amplification after reduced peripheral input is a context-specific signal to ensure that the neuronal amplification specifically occurs in the frequency regions that were deprived (Matt et al., 2018). As a metric for context-specific stimulation, the recruitment of activity-dependent BDNF was visualized before (Matt et al., 2018; Singer, Manthey, et al., 2018). Here, elevated Bdfn exon-IV-CFP and -VI-YFP expression was observed in the auditory brainstem and the hippocampus after the exposure to acoustic enrichment (80 dB SPL, 40 min, 10 kHz). This elevation of CFP and YFP was described together with a neural amplification and increased hippocampal LTP (Matt et al., 2018). The stimulating effect of sound could not be seen in exposure conditions with a loud, traumatic sound of 120 dB SPL (40 min, 10 kHz) that led to a reduction of peripheral auditory input with a critical loss of high-SR ANF, and in consequence, no increase of hippocampal Bdfn exon-IV-CFP and -VI-YFP levels or LTP could be observed (Matt et al., 2018). In Marchetta et al., 2021, a reduction of peripheral auditory input, most likely with reduced high-SR ANF functionality, was correlated with reduced Bdfn exon-IV-CFP and -VI-YFP levels and LTP in the hippocampus of low compensators. When observing the Bdfn transcript level differences between high- and low compensators, the Bdfn exon-VI-YFP fluorescence was most prominently reduced in presynaptic nerve dendrites of low compensators (Figure 6 in Marchetta et al., 2021). BDNF is anterogradely transported to these mossy fiber nerve endings in an activity-dependent way (Dieni et al., 2012; Singer, Manthey, et al., 2018). The Bdnf exon-IV-CFP expression was mostly reduced in the capillary vessels that are found in the fissura hippocampalis (Figure 6 in Marchetta et al., 2021). In the capillary

vessels, the Bdnf exon-IV was localized in platelets (Singer, Manthey, et al., 2018), where it activates calcium channels (Chacon-Fernandez et al., 2016) to regulate the blood flow (Hillman, 2014). In conclusion, the reduced levels of neuron ending-associated Bdfn exon-VI-YFP fluorescence and of blood vessel-associated Bdnf exon-IV-CFP fluorescence may be a hint for reduced neurovascular coupling in low compensators. It was shown before that memory-deficits due to hypertension in old mice was correlated with low BDNF levels (Tucsek et al., 2017). Also, attention- and memory-linked amplification processes and their dysfunction can be linked to reduced circulation of blood flow in the aged system (Shi et al., 2016).

In Marchetta, Savitska, et al., 2020, the proper function of high-SR ANF in the aged system, was shown to be crucial for the normal auditory function, including fast auditory processing that is needed for the maintenance of cognitive function, along with physiological activity-dependant hippocampal BDNF expression and neurovascular coupling. The impaired function of high-SR ANF activity could thereby lead to cognitive decline and Alzheimer's disease.

4.3 Part 3: Differential effects of central MR or GR deletion on the auditory periphery

Stress activates the HPA-axis, and, as a consequence, the release of GC modulates sensory gating and central neuronal networks independently from peripheral sensory function (Basner et al., 2014; J. C. Johnson et al., 2021).

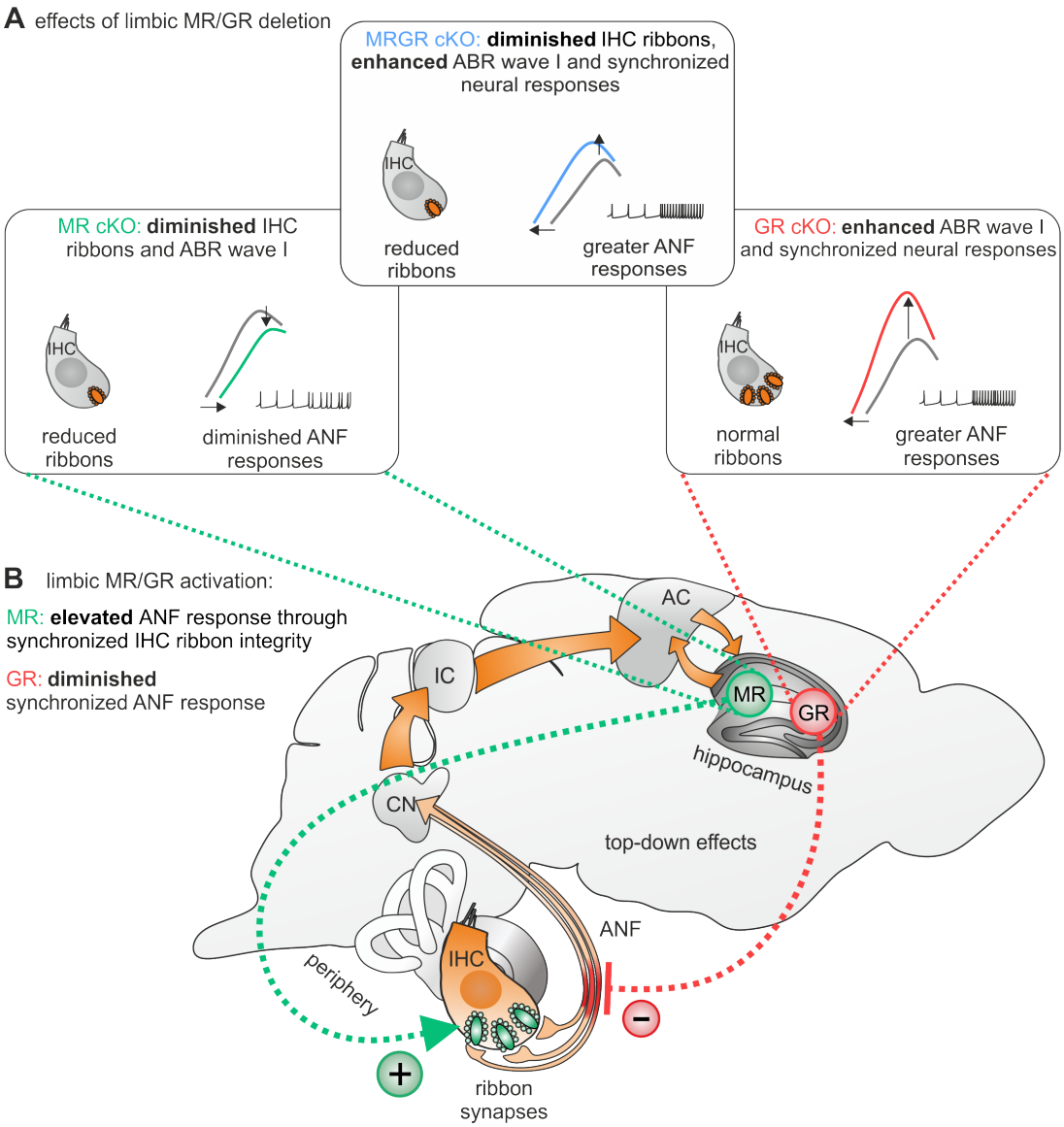

Figure 11: Effects of central MR/GR activation on the auditory periphery. (A) Central MR deletion leads to reduced IHC ribbon numbers and ABR wave I amplitude, while synchronization of ANF responses was not affected. Central GR deletion resulted in normal IHC ribbon numbers but increased ANF synchrony. MRGR double cKO showed a mixed phenotype with reduced IHC ribbon numbers and increased ANF responses. (B) The activation of central MR may contribute to discharge rate and IHC integrity, which is crucial for improved temporal auditory processing and ASSR. Central GR activation may inhibit the ANF synchrony and temporal auditory processing. Adapted from Figure 6 in Marchetta et al., 2022.

Mouse models with an adult-age deletion via TMX of the different stress receptors MR and/or GR in the adult CNS (CaMKIIα) were used, making it possible to report differential roles of central MR and GR on IHC synapse and ANF processing via a top-down mechanism (Figure 11A). The results of Marchetta et al., 2022 provide a model in which MR, associated with the acute stress response and GR, associated with chronic stress, can be seen as modulators processing and filtering at subcortical levels during auditory perception. Limbic MR and GR (Figure 11B) function thereby possibly influence speech comprehension and cognitive hearing function.

4.3.1 Specific deletion pattern of MR and GR after TMX injection

As MR and GR are essential for development and a global deletion of GR or MR leads to early death or dramatic diseased phenotype (Berger et al., 1998; Cole et al., 1995; Erdmann et al., 2007), adult mice with an acute deletion of MR and/or GR after TMX-inducible Cre activation were used (Berger et al., 2006; Erdmann et al., 2008). The deletion was performed under the promoter of CaMKIIα, which is expressed in glutamatergic neurons of the adult forebrain (Erdmann et al., 2008), but not the cochlea (Meese et al., 2017). It is important to note that MR and GR, which both bind GC (Mifsud and Reul, 2016), not only show different expression patterns (Reul and Kloet, 1985), they also differ in their binding affinity, as described before (Gomez-Sanchez and Gomez-Sanchez, 2014; Mifsud and Reul, 2016). But as the activation of both receptors - MR and GR - is linked to differential influences on peripheral auditory processing, non-redundant and rather counteracting functions could be described for effects on the auditory system, similar as for other circuit functions (E. R. De Kloet et al., 2000; McCann et al., 2021; Mifsud and Reul, 2016; Reul and Kloet, 1985).

MR not only binds GC, but also aldosterone (Gomez-Sanchez and Gomez-Sanchez, 2014). Aldosterone has influences on the endocochlear potential and thereby the hearing function (Bazard et al., 2020; Williamson et al., 2020). However, the endocochlear potential mainly drives the OHC transducer current, which would have been seen in DPOAE as well(Y. Wang et al., 2019). Indeed, the OHC function was not affected in MR cKO mice. Also, for aldosterone activation of MR, the inactivation of cortisol and CORT is required by 11beta-hydroxysteroid dehydrogenase type 2 (11β-HSD2; Gomez-Sanchez and Gomez-Sanchez, 2014). 11β-HSD2 could not be shown within immunoreactivity in inner-ear tissues (Terakado et al., 2011).

4.3.2 Differential impact of central MR and GR activation on the auditory periphery

The results of Marchetta et al., 2022 indicate that MR or GR activation in the hippocampus and forebrain is influencing the auditory periphery. Here, however, when deleting central MR and GR, no effect on OHC functionality could be observed, measured by DPOAE (Figure 1, Suppl. Figure 2 in Marchetta et al., 2022). This is in line with previous reports, describing stress effects on hearing function being independent of OHC (Singer, Kasini, et al., 2018). Instead, the hearing phenotype of MR, GR, and MRGR cKO mice was shown in the auditory periphery as low as at the level of IHC ribbon synapses (MR cKO; Figure 2 in Marchetta et al., 2022) or ANF fibers (GR cKO; Figure 4 in Marchetta et al., 2022) or both (MRGR cKO; Figure 1, 2 in Marchetta et al., 2022). Thereby a stress-dependent, top-down signaling mechanism from the forebrain to peripheral auditory areas could be confirmed within the study.

While leaving auditory thresholds intact, the simultaneous deletion of MR and GR in the forebrain led to increased early and late ABR waves, reduced CAP latency, and increased response to amplitude modulated stimuli (Figure 1 in Marchetta et al., 2022). CAP recordings in particular can give information about ANF function and distinct ANF type contribution, as they reflect the summed single-fiber action potentials (Earl and Chertoff, 2010; Rüttiger et al., 2017). In this way, changes in the CAP thresholds are due to altered functionality of high-SR ANF with low thresholds, as low SR-fibers do not contribute to CAP thresholds (Bourien et al., 2014) and high-SR ANF define perception thresholds and shortest latency (Heil et al., 2008; Meddis, 2006; Rhode and Smith, 1986).

At first, the reduced IHC ribbon number in MRGR cKO mice seemed to be contradicting to the enhanced and faster response of the auditory nerve. When suggesting a complex mixed phenotype in MRGR cKO mice that consists of two contrasting effects of single MR or GR deletion, this could be confirmed. MR cKO mice showed a reduced IHC ribbon numbers similar to MRGR cKO mice, while GR cKO mice had IHC ribbon numbers similar to controls. As MR cKO mice had reduced ABR wave I amplitude, prolonged CAP latency, and increased CAP thresholds, while the ASSR was not affected, a role of central MR on temporal resolution of ANF responses through modulation of IHC ribbon integrity can be concluded (Figure 6 in Marchetta et al., 2022). Interestingly, the ribbon loss was most prominent at the pillar side of IHC in both MR cKO and MRGR cKO mice (Suppl. Figure 2 in Marchetta et al., 2022). The pillar/modiolar spatial gradient in IHC ribbon synapses can give information about postsynaptic ANF characteristics re-

garding SR and threshold differences (M. C. Liberman and Oliver, 1984; M. Liberman, 1982; Merchan-Perez and Liberman, 1996. The predominantly reduced ribbon number at the pillar side in MR cKO mice leads to the assumption that MR activation in the limbic system can stimulate synaptic contacts to high-SR ANF with low thresholds that are located on the pillar side of IHC presynapses (M. C. Liberman and Oliver, 1984; M. Liberman, 1982; Merchan-Perez and Liberman, 1996).

In contrast, the number of IHC ribbons was not reduced in GR cKO mice (Figure 2 in Marchetta et al., 2022), and the ratio between pillar and modiolar ribbon synapses was not altered (Suppl. Figure 3 in Marchetta et al., 2022). Instead, the ABR waves I and IV were increased, CAP thresholds improved, CAP latencies shorter, and responses for amplitude modulated stimuli were greater in GR cKO mice compared with controls (Figure 4 in Marchetta et al., 2022). The observation of this GR cKO phenotype led to the conclusion that GR activation in the limbic system affects the auditory periphery in an inhibitory top-down manner by influencing the spike time synchrony. One factor that is influencing spike synchronization are voltage-gated calcium channels in IHC (Neef et al., 2009; Zidanic and Fuchs, 1995), which play a role in exocytosis and are, due to the high turnover, dependent on good metabolic supply (M. A. Rutherford et al., 2021; Wong et al., 2013; L.-G. Wu et al., 2014). It could be hypothesised that the activation of central GR could trigger this metabolic supply and support precise spike synchronization. As limbic GR deletion improved CAP latency and threshold, GR activation might also have effects on high-SR ANF that were shown to be the ANF influencing CAP thresholds (Bourien et al., 2014). This statement could be strengthened by previous experiments, showing a protective effect of antagonizing GR on the dynamic range after sound overexposure (Singer, Kasini, et al., 2018). The dynamic range of ANF is defined by the range of stimulus intensities in which an increasing discharge rate can be observed and is independent from presence or absence of synaptic ribbons (Buran et al., 2010).

4.3.3 Top-down influences of central stress receptors on the auditory periphery, independent of the CORT level

The results of Marchetta et al., 2022 show effects of central MR and GR activation in a differential manner. Looking for a possible mechanism, the levels of CORT in the blood were analyzed for individual mice (Figure 5 in Marchetta et al., 2022). Surprisingly no correlation between the hearing phenotype and the CORT level became evident for the

following reasons:

(i) False positive alterations of the blood CORT due to sex, circadian rhythm or anesthesia influences (Arnold and Langhans, 2010; Atkinson and Waddell, 1997) could be most likely excluded, as the group matching, timing and experimental condition for blood sample collection were identical for cKO and control mice.

(ii) As only for GR- and MRGR cKO mice changes in the blood CORT level were observed, but not for MR cKO mice, which nevertheless showed a top-down mediated hearing phenotype, at least the central activation of MR is unlikely to influence the auditory periphery in an CORT-independent way.

(iii) In previous studies it could be shown that high blood CORT levels are linked with smaller auditory nerve responses (Singer, Kasini, et al., 2018). In Marchetta et al., 2022, however, the highest CORT levels were observed in GR cKO mice, that in parallel showed larger and faster auditory nerve responses. Thereby CORT itself might not be responsible for the auditory phenotype in MR-, GR- and MRGR cKO mice.

(iv) Nevertheless, other stress-related hormonal modulators should be considered to influence and correlate with the auditory phenotypes. Here, CRH that is distributed throughout the CNS and HPA-axis and releases adrenocorticotropin (Richard and Lopez, 2013) could be involved in the observed top-down cascades. How exactly CRH could influence the AN signaling is still elusive but CRH was described to be involved in the development of IHC innervation (Graham and Vetter, 2011) and to modulate hearing sensitivity and noise vulnerability (Graham et al., 2011; Graham et al., 2010; Vetter, 2015). To describe a possible role of CRH on auditory nerve processing, its expression pattern and blood level should be analyzed in MR-, GR-, and MRGR cKO mice.

(v) As described before, beside the ascending auditory pathway also several descending circuits, called corticofugal feedbacks are known. One retrocochlear top-down mechanism is the olivocochlear efferent feedback signaling that is involved in selective attention (Lopez-Poveda, 2018). In LOC responses, which are part of the olivocochlear efferent system, the neurotransmitter dopamine plays a role as a modulator for tonic inhibition of CAP wave I amplitude and latency (Ruel et al., 2001). In conclusion, dopamine could be a possible modulator for the top-down mediated responses of central stress perception.

4.3.4 The differential roles of central MR and GR in auditory gating

In this study the finding that MR stimulation, linked with acute stress, supports the previously-stated idea that acute, low level stress is beneficial for the auditory function (Meltser and Canlon, 2011; Y. Wang and Liberman, 2002), such as acute stress in rodents, induced by restraint stress, which enhanced acoustically evoked responses in the AC (Ma et al., 2015) or low dosage of CORT that improved sound-induced responses even in the CA3 region of the hippocampus (Maxwell et al., 2006). Also the acute treatment with artificial GC, hydrocortisone, was shown to temporarily stimulate auditory evoked potentials in humans (Ashton et al., 2000; Born et al., 1988). Thereby, a crucial role of MR could be unraveled for auditory-related top-down signaling, possibly also involved in auditory neural circuits for e.g. selective attention, speech discrimination, or communication skills (Jauset-Berrocal and Soria-Urios, 2018; Micheyl et al., 2006; Schaffert et al., 2019; Sihvonen et al., 2017; Sinha et al., 2011). How important MR is for proper CNS function, can be seen as reduced or absent MR is associated with ASD (Cukier et al., 2020; Patel et al., 2016), which again, as previously described is linked to sensory deficits, such as fast auditory processing disorders (Foss-Feig, Schauder, et al., 2017, Eckert, Marchetta et al., 2021).

In contrast, high-level stress can lead to reduced auditory gating (Elling et al., 2011; Ma et al., 2017; Maxwell et al., 2006; Stevens et al., 2001; White et al., 2005). Also the induction of stress due to AT led to reduced auditory responsiveness (Matt et al., 2018; Ryan et al., 2016), as well as posttraumatic stress, or chronic stress (MacGregor et al., 2020; Mazurek et al., 2015; Turner et al., 2019. All the described effects can possibly be linked to central/limbic GR activation, leading to reduced spike-timing precision and synchronization in the auditory nerve. Tinnitus is described to be highly stress dependent (Boecking et al., 2021; Clifford et al., 2019; Elarbed et al., 2021; Park et al., 2020; Van Munster et al., 2020). Central GR activity may also be involved in the development and maintenance of tinnitus, that is known to be linked with chronic stress (Mazurek et al., 2015), as there is evidence that tinnitus is highly affected by reduced high-SR function (Knipper et al., 2013). On a clinical point of view, the hyperfunction of the pituitary glands due to a tumor could lead to the risk for hearing impairment in patients (Kuan et al., 2017), and the adrenal cortical insufficiency was shown to lower hearing thresholds and improve hearing sensitivity (Henkin et al., 1967), providing a strong evidence for the effects of HPA-axis activation on hearing function.

As there is evidence, that limbic/central MR and GR effect auditory processing via a top-down loop, they could also play a role in perceptual auditory object recognition. Thereby, a listener is able to put auditory attention to selective auditory streams, such as for example one specific voice in a crowd, or one instrument in the orchestra (Pressnitzer et al., 2008). This streaming or object recognition needs to match incoming auditory stimuli with other auditory information that is stored and that is memorized during this recognition process (Cope et al., 2015). The way of auditory perception in which central and peripheral auditory processing are linked is not yet understood (J. C. Johnson et al., 2021), but there is evidence that pre-cognitive subcortical processing is used (Antunes and Malmierca, 2021; Michie et al., 2016; Pérez-González and Malmierca, 2014) that could be on an early peripheral level as early as the cochlea (Pressnitzer et al., 2008). As MR activity is linked with attention (Cornelisse et al., 2011), the central MR stimulation could possibly be the missing link that connects central and peripheral auditory processing that is required for the streaming process.

As for several functions in the body, MR and GR act like the double edged sword that cause either positive and negative effects, depending on the concentration of GC, also for the pre-cognitive cochlear processing they could work in a differential manner with the potential to intervene with pharmacologic treatment to balance the auditory cognitive function.

4.4 Part 4: GC-A deletion has differential contribution to IHC and OHC survival in a healthy, aged, or injured system

GC-A and its ligands ANP and BNP could be identified in the cochlea, as described before (Fitzakerley and Trachte, 2018; Kemp-Harper and Feil, 2008; Kleppisch and Feil, 2009; Kuhn, 2003, 2009; Möhrle et al., 2017; Schulz, 2005; zum Gottesberge et al., 1991), with a specific GC-A expression in SGN and OHC, but not IHC (Figure 12A).

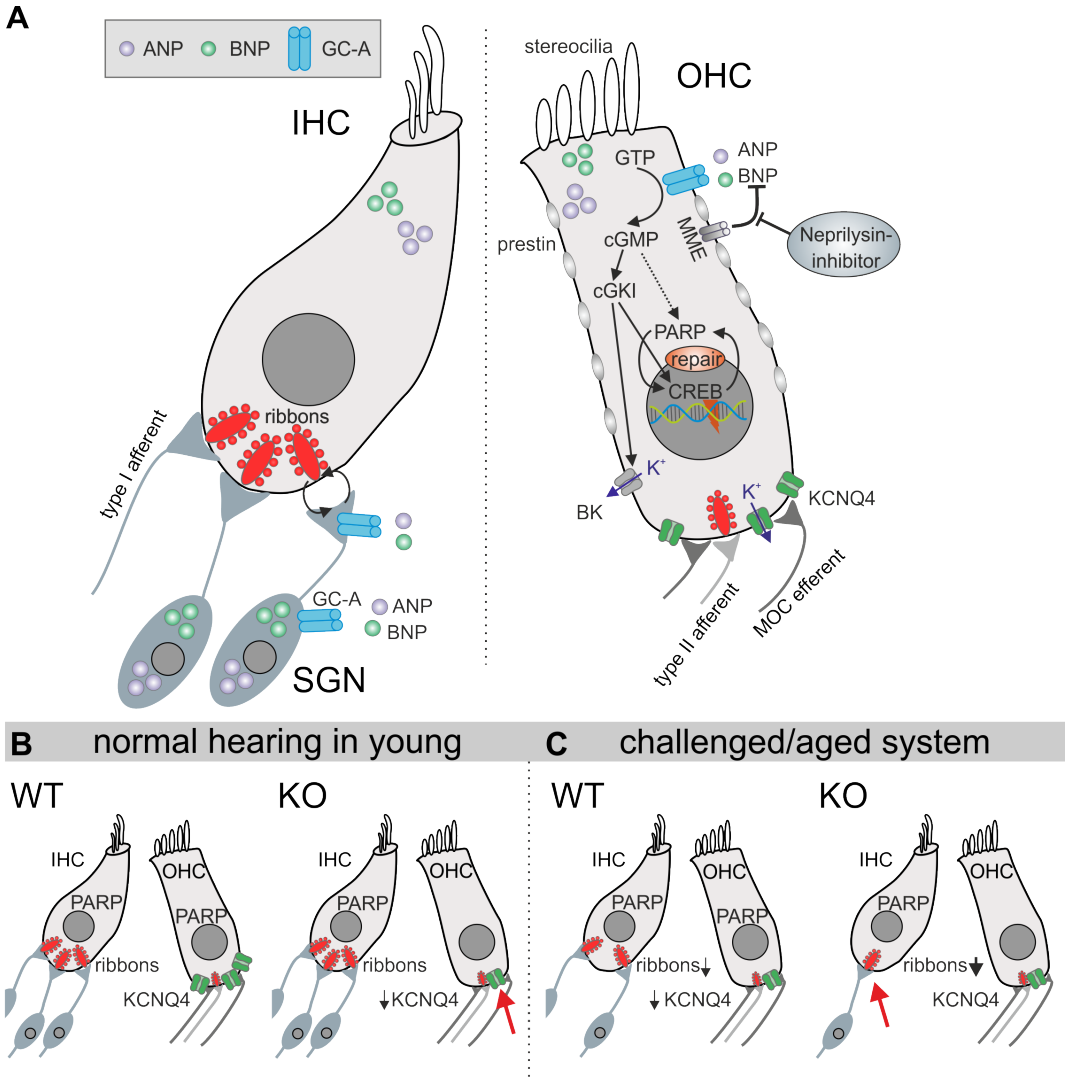

Figure 12: GC-A/cGMP expression and hypothesized signaling mechanisms in the organ of Corti. (A) GC-A (blue) is expressed in OHC and SGN, where it binds its ligands ANP and BNP. GC-A activation drives a cGMP dependent cascade that increases PARP. GC-A effects in IHC are caused by the pre- and postsynaptic extracellular communication via ANP and BNP. (B) In young GC-A KO OHC with KCNQ4 expression are impaired, while the IHC ribbon number is not reduced. (C) After challenging the auditory system (AT or age), the IHC ribbon number was more reduced in GC-A KO than in controls, while AT or age did not additionally reduce OHC function (adapted from Marchetta, Möhrle, et al., 2020, Figure 9).

Marchetta, Möhrle, et al., 2020 showed that the deletion of GC-A increases the vulnerability for hidden hearing loss and noise- and age-dependent hearing loss. The thresholds of aged GC-A KO increased, while OHC I/O functions were already reduced at high frequencies in young GC-A KO mice (Figure 12B). However, this OHC phenotype could not be additionally accentuated by AT ore age. In contrast, IHC ribbon synapse impairment and reduced ABR wave amplitudes developed in GC-A KO just over age or after AT, revealing differential mechanisms of GC-A on IHC and OHC function (Figure 12C).

4.4.1 Expression of GC-A and its ligands in the cochlea

In line with the literature, (Fitzakerley and Trachte, 2018; Kemp-Harper and Feil, 2008; Kleppisch and Feil, 2009; Kuhn, 2003, 2009; Möhrle et al., 2017; Schulz, 2005; zum Gottesberge et al., 1991) GC-A expression and expression of its ligand ANP and BNP could be confirmed in OHC and SGN. ANP and BNP, but not GC-A expression could be shown in IHC. The absence of GC-A in IHC, could indicate a paracrine or autocrine ANP- or BNP/GC-A signaling effect on either OHC or SGN, through which GC-A could indirectly influence IHC via retrograde signaling (Kujawa and Liberman, 2009) from postsynaptic SGN to IHC presynapses. This retrograde signaling could be involved in AT-induced damage of pre- and postsynapses of IHC, maybe including SGN signaling cascades (Sugawara et al., 2005; Wan et al., 2014).

4.4.2 GC-A KO mice exhibit reduced OHC function that is independent of AT and age

Although DPOAE and ABR thresholds, were not changed in young GC-A KO mice, the DPOAE growth functions, evoked with higher frequency stimuli (f2 = 11.3 kHz) were already reduced. Also, the expression of KCNQ4 was reduced in OHC's membranes of young GC-A KO mice. At rest, KCNQ4 is crucial for the maintenance of the major OHC K^+ current $I_{K,n}$ (Housley and Ashmore, 1992; Kharkovets et al., 2006; Marcotti and Kros, 1999). Reduced or dysfunctional KCNQ4 in OHC can lead to progressive hearing loss at higher frequencies, also during age-dependent or noise-induced hearing loss (Kharkovets et al., 2006; Peixoto Pinheiro et al., 2021; Van Eyken et al., 2006). KCNQ4 channels are dependent on the functionality of the big potassium (BK) channel (Rüttiger et al., 2004). As BK channels can be activated by cGMP/cGKI-induced phosphorylation (Kyle et al., 2013; Zhou et al., 2010), a link between KCNQ4 and contribution of GC-A on high frequency OHC function could be imagined. In addition, the treatment with the

PDE5 inhibitor vardenafil led to a protection of the noise-induced reduction of KCNQ4 OHC membrane expression at high frequency cochlear regions in a cGMP-dependent way (Jaumann et al., 2012). However, the reduction of OHC function and KCNQ4 expression have been show to be independent of age-related or noise-induced hearing loss (Figure 8 in Marchetta, Möhrle, et al., 2020), which indicates that beside the otoprotective mechanism of cGMP on KCNQ4 after AT, another otoprotective GC-A/cGMP/cGKI signaling cascade may be involved.

The global deletion of GC-A also led to a reduction of PAR in OHC. PARP activity plays a role in DNA repair and transcription activity and can be directly, or indirectly activated by cGMP via CREB (Y.-M. Kim et al., 1999; Paquet-Durand et al., 2007; Sahaboglu et al., 2010) and is linked with survival and anti-aging processes (Beneke and Bürkle, 2007). Thereby the activation of PARP, either directly via GC-A/cGMP, or in a CREB-dependent way could help to maintain OHC function.

4.4.3 GC-A KO mice exhibit stronger IHC synaptopathy and auditory neuropathy in response to AT and age

In contrast to the OHC function impairment due to GC-A deletion that was not further accentuated after challenging the auditory system such as aging or AT, the GC-A deletion led almost only under these challenged conditions to a phenotype in IHC and SGN (Figure 8 in Marchetta, Möhrle, et al., 2020). As GC-A expression was shown in SGN, but not IHC, the IHC phenotype is most likely linked with a disruption of the GC-A/cGMP/cGKI/PARP cascade in SGN. Here, the observed IHC ribbon synapse reduction might be related to deafferentation of SGN, what typically occurs in age-related or noise-induced hearing loss (Kujawa and Liberman, 2009; Pujol and Puel, 1999). When GC-A was deleted, the number of IHC ribbons declined and thereby also the ABR wave I response was reduced in GC-A KO mice. This indicates a synaptopathy in aged or overexposed animals. In young GC-A KO mice a reduction of IHC ribbons and of PAR staining in SGN and IHC was observed, although ABR wave I was not affected. How exactly PARP activity and IHC function and pre-/postsynaptic integrity are linked cannot be ultimately answered here and needs further studies.

IHC are sensitive for metabolic changes and thereby are involved in age-dependent and hidden hearing loss (Keithley, 2020). While the effects of GC-A deletion were seen predominantly in the integrity of the pre-/postsynaptic arrangement in the IHC from high

frequency cochlear turns after AT or in aged animals, a potential role of GC-A/cGMP signaling on energy consumption and metabolism in the auditory periphery may be considered.

4.4.4 cGMP signaling as a potential pharmaceutical target to treat auditory and cognitive impairment

In the study of Marchetta, Möhrle, et al., 2020, an otoprotective effect of the ANP/GC-A/cGMP/PKG signaling cascade could be shown. The GC-A mediated effects seem to be most promising for IHC synaptopathy and hidden hearing loss, as well as age-related and noise-induced hearing loss. The treatment with the ligand ANP would be promising, as it was already shown that ANP is, at least temporarily, beneficial for hearing thresholds when administered intravenously, which led to the hypothesis of a critical role of ANP on ANF in the cochlea (Yoon et al., 2015). Recently, a role of ANP was reported to promote neurite outgrowth and survival of SGN against excitotoxicity (Sun et al., 2021). It is still on debate, if the second ligand of GC-A, BNP, is expressed in the cochlea (Fitzakerley and Trachte, 2018; Marchetta, Möhrle, et al., 2020). However, there is the hint that the treatment with BNP or NT-proBNP could be promising for hearing restoration, as low levels of NT-proBNP in blood plasma of patients could be linked to hearing impairment (Ma et al., 2021). In the context of inflammation, BNP was also shown to increase the open probability of BK channels in dorsal root ganglia of spinal sensory neurons and to suppress membrane excitability to inhibit inflammatory pain (Li et al., 2016). Also in the inner ear excitotoxicity after AT was prevented by BK activation (Engel et al., 2006; Rüttiger et al., 2004) and it could be hypothesized that the BNP/GC-A/cGMP/PKG signaling cascade may be involved in this mechanism of otoprotection. To increase the level of natriuretic peptides (ANP and BNP), the degrading enzymes, such as the membrane metalloendopeptidase should be inhibited. It could be shown that membrane metalloendopeptidases are expressed in the inner ear (Fitzakerley and Trachte, 2018) and give thereby a potential target for pharmaceutical stimulation of the natriuretic petides/GC-A/cGMP/PKG cascade.

Not only for peripheral, but also for central auditory signaling and memory-linked processes GC-A could be an interesting target, since central GC-A is involved in neurogenesis (Muller et al., 2009) and angiogenesis (Kuhn, 2009), which both are crucial processes for proper memory function (Anacker and Hen, 2017) and for brain recovery (Xiong et al.,

2010).

In addition to stimulating the upstream GC-A/cGMP/PKG cascade, cGMP levels can also be increased by inhibiting the downstream cGMP-degrading PDE. Especially PDE9 inhibitors might be a potent candidate to counteract peripheral and central hearing impairments, as PDE9 is expressed in both, cochlea and AC (Figure 1 in Marchetta, Möhrle, et al., 2020). In the CNS PDE9a inhibitors, predominantly controlled by GC-A and not NO-GC (Harms et al., 2019; Lee et al., 2015), were shown to improve hippocampal function (Kroker et al., 2012; Prieto et al., 2017), and social behavior (M. Alexander et al., 2016). First evidence was given, that the treatment with PDE9a inhibitors could improve peripheral and central auditory processing (Savitska, ..., Marchetta et al., under revision) and auditory gating in a model of Huntington's disease (Nagy et al., 2015). In addition, PDE9a inhibitors can intervene HPA-axis balance (X.-F. Huang et al., 2018) and thereby could indirectly affect the described stress-associated auditory and cognitive function (Marchetta et al., 2022, Calis, ..., Marchetta et al., in preparation).

Beside the discussed effects of GC-A/cGMP signaling, the nNOS/NO/sGC/cGMP cascade is another cGMP cascade that is linked with auditory and cognitive function (Marchetta et al., 2021). The role of sGC/cGMP in learning and memory is well described (Bradley and Steinert, 2016; Fedele and Ricciarelli, 2021; Russwurm et al., 2013). NO, released from nNOS, modulates many physiological functions in the brain, as for instance neurogenesis, synaptic plasticity and is a critical short distance messenger for synaptic plasticity in learning and memory (Kourosh-Arami et al., 2020). NO was shown to be not only released from pyramidal neurons in the CNS, but also from inhibitory nNOS-positive GABAergic IN, which contact with parenchymal arterioles to regulate arteriolar diameters (Cauli et al., 2004; Kocharyan et al., 2008). Interestingly, the exposure of chronic stress led to reduced neurovascular coupling by reduced NO-release from GABAergic IN (Han et al., 2019). The effects of chronic stress on peripheral and central auditory processing and memory-linked functions, therefore need to be considered also in the context of reduced sGC activation (Calis, ..., Marchetta et al., in preparation).

Another, probably most important role attributed to cGMP signaling is vascular function (Feil et al., 2003; Kemp-Harper and Feil, 2008) and also in the brain it is involved in neurovascular coupling processes (Han et al., 2019; Olthof et al., 2019). Even more, the neurovascular coupling due to cGMP signaling was hypothesized to play a role in fast auditory processing (Knipper et al., 2020; Marchetta et al., 2021). As mentioned before, the maturation of the auditory system goes in parallel with the development of activity-

dependent hemodynamic responses and the maturation of hippocampal function. Also, in the rodent brain, the expression of GC-A and its ligands ANP and BNP increases at P7, shortly before the onset of hearing and reaches a maximum at around P28 (Muller et al., 2009), the end of the critical period for the auditory sense (De Koninck, 2007). It was hypothesized that the maturation of fast auditory processing, due to proper high-SR ANF signaling is not only linked with inhibitory PV-IN microcircuits, but also functionally linked with hemodynamic BOLD fMRI responses and the development of adult-like LTP (Knipper et al., 2021; Marchetta et al., 2021). Thereby cGMP would also be involved in the maturation of cortical fast-spiking PV-IN networks, that are crucial for feedforward and feedback inhibitory circuits (Cardin et al., 2009; G. Chen et al., 2017; Sohal et al., 2009).

4.5 Overall conclusion

The studies with selected transgenic mouse models gave insights into the bidirectional connection between the peripheral- and central auditory processing and cognition, all giving evidence that functional high-SR signaling is crucial for proper central auditory processing and memory acquisition (Figure 13A) and a lack of high-SR signaling might bring lower cortical resolution and impaired hippocampal function (Figure 13B).

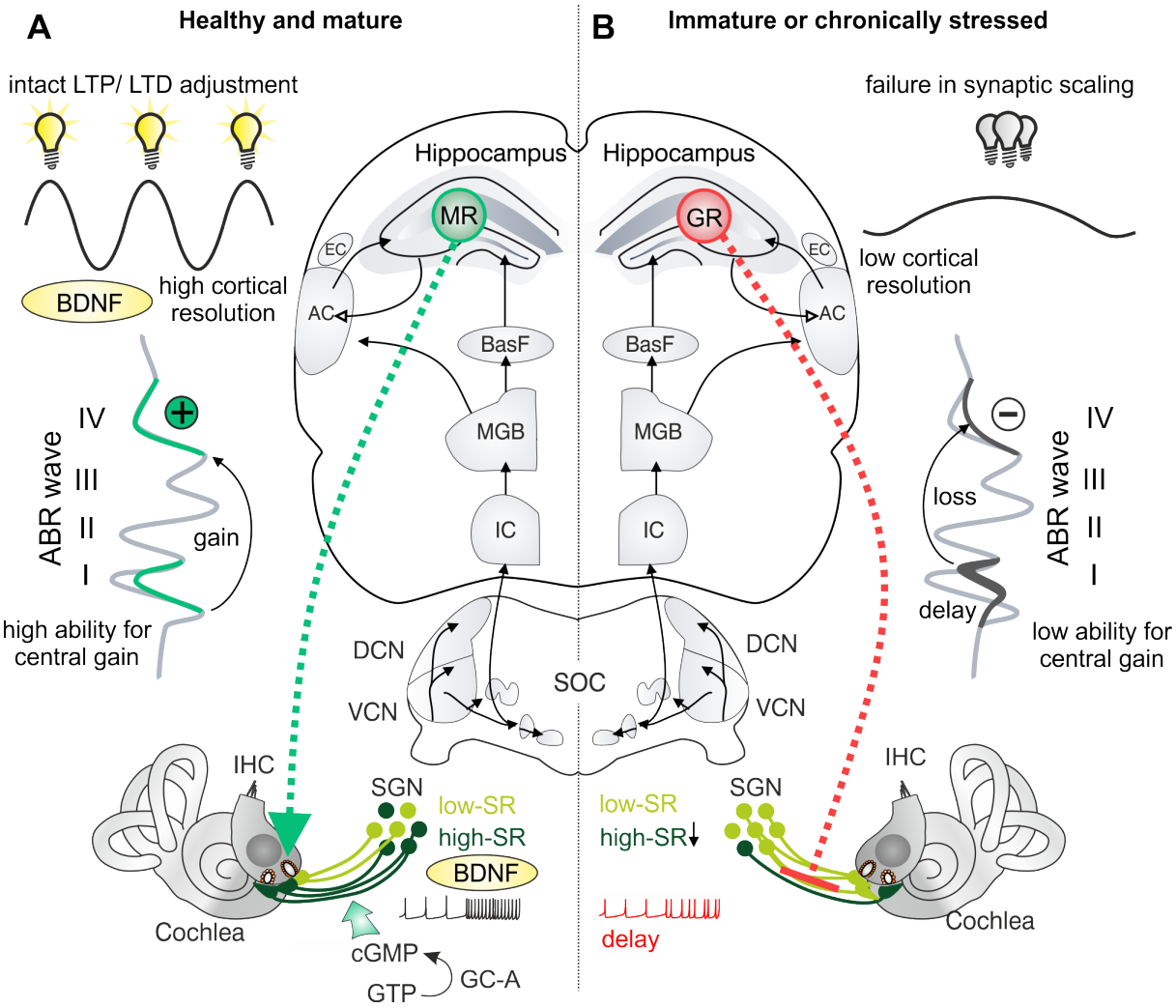

Figure 13: High-SR ANF signaling as a prerequisite for auditory receptive fields and stimulus-dependent memory consolidation. (A) Proper high-SR ANF function is needed for the development of tonic inhibition, the capacity for central neural gain, a high cortical resolution and intact hippocampal synaptic scaling. The activation of central MR triggers attention-linked processes that stimulate the discharge rate in IHC ribbons and thereby fast auditory processing in a top-down manner. Stimulating the GC-A/cGMP cascade possibly could be used as a potential pharmacological treatment to improve high-SR ANF function. (B) Reduced high-SR ANF leads to delayed latency, a lower capacity for central neural gain, a low cortical resolution and impaired hippocampal synaptic scaling. This could possibly be caused by the activation of central GR due to chronic stress, what affects the ANF in an inhibitory way via top-down signaling.

First, the specific role of BDNF in GABAergic precursor neurons for the development of fast auditory processing was analyzed. It was shown that possibly the missing high-SR ANF activity was the reason for the absence of tonic inhibition and the missing integration of inhibitory PV-IN in the hippocampus and AC, which lead to impaired executive function and an autistic-like phenotype (Eckert, Marchetta et al., 2021). But also in the mature system, the maintenance of high-SR ANF in the aged auditory system is crucial for temporal auditory processing, as a prolonged latency (indicating high-SR ANF loss) was the reason for reduced ASSR and a low compensation ability of ABR wave I but not aging per se or the level of cochlear synaptopathy itself. Even more, the reduced fast auditory processing was linked with weaker hippocampal LTP and reduced recruitment of Bdnf transcripts in the hippocampus. The latter indicates a reduced neurovascular coupling in animals with low compensating capacities (Marchetta, Savitska, et al., 2020). The forebrain can also influence the auditory periphery in a top-down manner. Interestingly, the analysis of induced, tissue-specific MR and/or GR deletion revealed that MR and GR show contrasting effects on either ANF activity and discharge rates (MR cKO), or on (high-SR ANF) spike timing and synchrony (GR cKO; Marchetta et al., 2022). Trying to overcome developmental, age dependent and stress related high-SR ANF shortfalls, a suitable candidate was found: GC-A was shown to play a protective role in hidden hearing loss, especially in the challenged (aged or noise-exposed) auditory system. Additionally, a second otoprotective role of GC-A was observed for OHC function, that already occurred in young GC-A KO but was independent of age or AT (Marchetta, Möhrle, et al., 2020). In conclusion, stimulating cGMP cascades could be promising for the prevention or restoration of hearing function during age or after traumatic noise exposure. But even more, the influence of cGMP stimulators could possibly improve memory and cognition in Bdnf^{Pax2}KO mice, it could support neurovascular coupling in aged animals with lost central compensation (Savitska, ..., Marchetta et al., under revision) and finally could intervene stress related auditory adaption processes (Calis, ..., Marchetta et al., in preparation). In this regard, cGMP generators are pharmaceutical targets worthy of further investigation with respect to their effects on auditory and cognitive functions.

References

Adamson, C. L., Reid, M. A., & Davis, R. L. (2002). Opposite actions of brain-derived neurotrophic factor and neurotrophin-3 on firing features and ion channel composition of murine spiral ganglion neurons. Journal of Neuroscience, 22(4), 1385–1396.

Alexander, J. M., Pirone, A., & Jacob, M. H. (2020). Excessive β-catenin in excitatory neurons results in reduced social and increased repetitive behaviors and altered expression of multiple genes linked to human autism. Frontiers in Synaptic Neuroscience, 12, 14.

Alexander, M., Gasperini, M., Tsai, P., Gibbs, D., Spinazzola, J., Marshall, J., Feyder, M., Pletcher, M., Chekler, E. P., Morris, C., et al. (2016). Reversal of neurobehavioral social deficits in dystrophic mice using inhibitors of phosphodiesterases pde5a and pde9a. Translational Psychiatry, 6(9), e901–e901.

Anacker, C., & Hen, R. (2017). Adult hippocampal neurogenesis and cognitive flexibility—linking memory and mood. Nature Reviews Neuroscience, 18(6), 335–346.

Andreska, T., Aufmkolk, S., Sauer, M., & Blum, R. (2014). High abundance of bdnf within glutamatergic presynapses of cultured hippocampal neurons. Frontiers in Cellular Neuroscience, 8, 107.

Antunes, F. M., & Malmierca, M. S. (2021). Corticothalamic pathways in auditory processing: Recent advances and insights from other sensory systems. Frontiers in Neural Circuits, 15.

Argyrousi, E. K., Heckman, P. R., & Prickaerts, J. (2020). Role of cyclic nucleotides and their downstream signaling cascades in memory function: Being at the right time at the right spot. Neuroscience & Biobehavioral Reviews, 113, 12–38.

Arnold, M., & Langhans, W. (2010). Effects of anesthesia and blood sampling techniques on plasma metabolites and corticosterone in the rat. Physiology & Behavior, 99(5), 592–598.

Asbjørnsen, A. E., Obrzut, J. E., Boliek, C. A., Myking, E., Holmefjord, A., Reisaeter, S., Klausen, O., & Møller, P. (2005). Impaired auditory attention skills following middle-ear infections. Child Neuropsychology, 11(2), 121–133.

Ashton, C. H., Lunn, B., Marsh, V. R., & Young, A. H. (2000). Subchronic hydrocortisone treatment alters auditory evoked potentials in normal subjects. Psychopharmacology, 152(1), 87–92.

Atkinson, H. C., & Waddell, B. J. (1997). Circadian variation in basal plasma corticosterone and adrenocorticotropin in the rat: Sexual dimorphism and changes across the estrous cycle. Endocrinology, 138(9), 3842–3848.

Bajo, V. M., Nodal, F. R., Moore, D. R., & King, A. J. (2010). The descending corticocollicular pathway mediates learning-induced auditory plasticity. Nature Neuroscience, 13(2), 253–260.

Basappa, J., Graham, C. E., Turcan, S., & Vetter, D. E. (2012). The cochlea as an independent neuroendocrine organ: Expression and possible roles of a local hypothalamic–pituitary–adrenal axis-equivalent signaling system. Hearing Research, 288(1-2), 3–18.

Basner, M., Babisch, W., Davis, A., Brink, M., Clark, C., Janssen, S., & Stansfeld, S. (2014). Auditory and non-auditory effects of noise on health. The Lancet, 383(9925), 1325–1332.

Bazard, P., Ding, B., Chittam, H. K., Zhu, X., Parks, T. A., Taylor-Clark, T. E., Bhethanabotla, V. R., Frisina, R. D., & Walton, J. P. (2020). Aldosterone up-regulates voltage-

gated potassium currents and nkcc1 protein membrane fractions. Scientific Reports, 10(1), 1–14.

Beckmann, D., Feldmann, M., Shchyglo, O., & Manahan-Vaughan, D. (2020). Hippocampal synaptic plasticity, spatial memory, and neurotransmitter receptor expression are profoundly altered by gradual loss of hearing ability. Cerebral Cortex, 30(8), 4581–4596.

Ben-Ari, Y. (2002). Excitatory actions of gaba during development: The nature of the nurture. Nature Reviews Neuroscience, 3(9), 728–739.

Benasich, A. A., Thomas, J. J., Choudhury, N., & Leppänen, P. H. (2002). The importance of rapid auditory processing abilities to early language development: Evidence from converging methodologies. Developmental Psychobiology: The Journal of the International Society for Developmental Psychobiology, 40(3), 278–292.

Beneke, S., & Bürkle, A. (2007). Poly (adp-ribosyl) ation in mammalian ageing. Nucleic Acids Research, 35(22), 7456–7465.

Berger, S., Bleich, M., Schmid, W., Cole, T. J., Peters, J., Watanabe, H., Kriz, W., Warth, R., Greger, R., & Schütz, G. (1998). Mineralocorticoid receptor knockout mice: Pathophysiology of na+ metabolism. Proceedings of the National Academy of Sciences, 95(16), 9424–9429.

Berger, S., Wolfer, D. P., Selbach, O., Alter, H., Erdmann, G., Reichardt, H. M., Chepkova, A. N., Welzl, H., Haas, H. L., Lipp, H.-P., et al. (2006). Loss of the limbic mineralocorticoid receptor impairs behavioral plasticity. Proceedings of the National Academy of Sciences, 103(1), 195–200.

Bharadwaj, H. M., Verhulst, S., Shaheen, L., Liberman, M. C., & Shinn-Cunningham, B. G. (2014). Cochlear neuropathy and the coding of supra-threshold sound. Frontiers in Systems Neuroscience, 8, 26.

Bickford-Wimer, P. C., Nagamoto, H., Johnson, R., Adler, L. E., Egan, M., Rose, G. M., & Freedman, R. (1990). Auditory sensory gating in hippocampal neurons: A model system in the rat. Biological Psychiatry, 27(2), 183–192.

Boecking, B., Rose, M., Brueggemann, P., & Mazurek, B. (2021). Two birds with one stone.–addressing depressive symptoms, emotional tension and worry improves tinnitus-related distress and affective pain perceptions in patients with chronic tinnitus. Plos O ne, 16(3), e0246747.

Bordi, F., & LeDoux, J. (1992). Sensory tuning beyond the sensory system: An initial analysis of auditory response properties of neurons in the lateral amygdaloid nucleus and overlying areas of the striatum. Journal of Neuroscience, 12(7), 2493–2503.

Born, J., Hitzler, V., Pietrowsky, R., Pauschinger, P., & Fehm, H. (1988). Influences of cortisol on auditory evoked potentials (aeps) and mood in humans. Neuropsychobiology, 20(3), 145–151.

Bortone, D., & Polleux, F. (2009). Kcc2 expression promotes the termination of cortical interneuron migration in a voltage-sensitive calcium-dependent manner. Neuron, 62(1), 53–71.

Bourien, J., Tang, Y., Batrel, C., Huet, A., Lenoir, M., Ladrech, S., Desmadryl, G., Nouvian, R., Puel, J.-L., & Wang, J. (2014). Contribution of auditory nerve fibers to compound action potential of the auditory nerve. Journal of Neurophysiology, 112(5), 1025–1039.

Bowl, M. R., & Dawson, S. J. (2019). Age-related hearing loss. Cold Spring Harbor perspectives in medicine, 9(8), a033217.

Bradley, S. A., & Steinert, J. R. (2016). Nitric oxide-mediated posttranslational modifications: Impacts at the synapse. Oxidative Medicine and Cellular Longevity, 2016.

Bramhall, N., Ong, B., Ko, J., & Parker, M. (2015). Speech perception ability in noise is correlated with auditory brainstem response wave i amplitude. Journal of the American Academy of Audiology, 26(05), 509–517.

Bramham, C. R., Worley, P. F., Moore, M. J., & Guzowski, J. F. (2008). The immediate early gene arc/arg3. 1: Regulation, mechanisms, and function. Journal of Neuroscience, 28(46), 11760–11767.

Bregman, A. S. (1994). Auditory scene analysis: The perceptual organization of sound. MIT press.

Brock, J., Brown, C. C., Boucher, J., & Rippon, G. (2002). The temporal binding deficit hypothesis of autism. Development and Psychopathology, 14(2), 209–224.

Buran, B. N., Strenzke, N., Neef, A., Gundelfinger, E. D., Moser, T., & Liberman, M. C. (2010). Onset coding is degraded in auditory nerve fibers from mutant mice lacking synaptic ribbons. Journal of Neuroscience, 30(22), 7587–7597.

Canals, J. M., Checa, N., Marco, S., Akerud, P., Michels, A., Perez-Navarro, E., Tolosa, E., Arenas, E., & Alberch, J. (2001). Expression of brain-derived neurotrophic factor in cortical neurons is regulated by striatal target area. Journal of Neuroscience, 21(1), 117–124.

Canlon, B., Meltser, I., & Hasson, D. (2011). The effects of acute and chronic stress on auditory function: Experimental and clinical studies. Proceedings of the International Symposium on Auditory and Audiological Research, 3, 1–9.

Canlon, B., Meltser, I., Johansson, P., & Tahera, Y. (2007). Glucocorticoid receptors modulate auditory sensitivity to acoustic trauma. Hearing Research, 226(1-2), 61–69.

Canlon, B., Theorell, T., & Hasson, D. (2013). Associations between stress and hearing problems in humans. Hearing Research, 295, 9–15.

Caras, M. L., & Sanes, D. H. (2015). Sustained perceptual deficits from transient sensory deprivation. Journal of Neuroscience, 35(30), 10831–10842.

Cardin, J. A., Carlen, M., Meletis, K., Knoblich, U., Zhang, F., Deisseroth, K., Tsai, L.-H., & Moore, C. I. (2009). Driving fast-spiking cells induces gamma rhythm and controls sensory responses. Nature, 459(7247), 663–667.

Carricondo, F., & Romero-Gomez, B. (2019). The cochlear spiral ganglion neurons: The auditory portion of the viii nerve. The Anatomical Record, 302(3), 463–471.

Cauli, B., Tong, X.-K., Rancillac, A., Serluca, N., Lambolez, B., Rossier, J., & Hamel, E. (2004). Cortical gaba interneurons in neurovascular coupling: Relays for subcortical vasoactive pathways. Journal of Neuroscience, 24(41), 8940–8949.

Cenquizca, L. A., & Swanson, L. W. (2007). Spatial organization of direct hippocampal field ca1 axonal projections to the rest of the cerebral cortex. Brain Research Reviews, 56(1), 1–26.

Chacon-Fernandez, P., Säuberli, K., Colzani, M., Moreau, T., Ghevaert, C., & Barde, Y.-A. (2016). Brain-derived neurotrophic factor in megakaryocytes. Journal of Biological Chemistry, 291(19), 9872–9881.

Chandrasekaran, B., & Kraus, N. (2010). The scalp-recorded brainstem response to speech: Neural origins and plasticity. Psychophysiology, 47(2), 236–246.

Chaudhury, S., Nag, T. C., Jain, S., & Wadhwa, S. (2013). Role of sound stimulation in reprogramming brain connectivity. Journal of Biosciences, 38(3), 605–614.

Chen, G., Zhang, Y., Li, X., Zhao, X., Ye, Q., Lin, Y., Tao, H. W., Rasch, M. J., & Zhang, X. (2017). Distinct inhibitory circuits orchestrate cortical beta and gamma band oscillations. Neuron, 96(6), 1403–1418.

Chen, G.-D., Manohar, S., & Salvi, R. (2012). Amygdala hyperactivity and tonotopic shift after salicylate exposure. Brain Research, 1485, 63–76.

Chen, G.-D., Radziwon, K. E., Kashanian, N., Manohar, S., & Salvi, R. (2014). Salicylate-induced auditory perceptual disorders and plastic changes in nonclassical auditory centers in rats. Neural Plasticity.

Chern, A., & Golub, J. S. (2019). Age-related hearing loss and dementia. Alzheimer Disease and Associated Disorders, 33(3), 285.

Cherry, C. (1953). The cocktail party effect. The Journal of the Acoustical Society of America, 25(5), 975–979.

Chumak, T., Rüttiger, L., Lee, S. C., Campanelli, D., Zuccotti, A., Singer, W., Popelar, J., Gutsche, K., Geisler, H.-S., Schraven, S. P., Jaumann, M., Panford-Walsh, R., Hu, J., Schimmang, T., Zimmermann, U., Syka, J., & Knipper, M. (2016). Bdnf in lower brain parts modifies auditory fiber activity to gain fidelity but increases the risk for generation of central noise after injury. Molecular Neurobiology, 53(8), 5607–5627.

Clifford, R. E., Baker, D., Risbrough, V. B., Huang, M., & Yurgil, K. A. (2019). Impact of tbi, ptsd, and hearing loss on tinnitus progression in a us marine cohort. Military Medicine, 184(11-12), 839–846.

Cohen-Cory, S., Kidane, A. H., Shirkey, N. J., & Marshak, S. (2010). Brain-derived neurotrophic factor and the development of structural neuronal connectivity. Developmental Neurobiology, 70(5), 271–288.

Cole, T. J., Blendy, J. A., Monaghan, A. P., Krieglstein, K., Schmid, W., Aguzzi, A., Fantuzzi, G., Hummler, E., Unsicker, K., & Schütz, G. (1995). Targeted disruption of the glucocorticoid receptor gene blocks adrenergic chromaffin cell development and severely retards lung maturation. Genes & Development, 9(13), 1608–1621.

Coleman, J. R., & Clerici, W. J. (1987). Sources of projections to subdivisions of the inferior colliculus in the rat. Journal of Comparative Neurology, 262(2), 215–226.

Collet, L., Bouchet, P., Pernier, J., et al. (1994). Auditory selective attention in the human cochlea. Brain Research, 633(1-2), 353–356.

Colonnese, M. T., Phillips, M. A., Constantine-Paton, M., Kaila, K., & Jasanoff, A. (2008). Development of hemodynamic responses and functional connectivity in rat somatosensory cortex. Nature Neuroscience, 11(1), 72–79.

Coomber, B., Berger, J. I., Kowalkowski, V. L., Shackleton, T. M., Palmer, A. R., & Wallace, M. N. (2014). Neural changes accompanying tinnitus following unilateral acoustic trauma in the guinea pig. European Journal of Neuroscience, 40(2), 2427–2441.

Cope, T. E., Baguley, D. M., & Griffiths, T. D. (2015). The functional anatomy of central auditory processing. Practical Neurology, 15(4), 302–308.

Cornelisse, S., Joëls, M., & Smeets, T. (2011). A randomized trial on mineralocorticoid receptor blockade in men: Effects on stress responses, selective attention, and memory. Neuropsychopharmacology, 36(13), 2720–2728.

Cui, B., Wu, M., & She, X. (2009). Effects of chronic noise exposure on spatial learning and memory of rats in relation to neurotransmitters and nmdar2b alteration in the hippocampus. Journal of Occupational Health, 0902160059–0902160059.

Cui, B., Wu, M., She, X., & Liu, H. (2012). Impulse noise exposure in rats causes cognitive deficits and changes in hippocampal neurotransmitter signaling and tau phosphorylation. Brain Research, 1427, 35–43.

Cukier, H. N., Griswold, A. J., Hofmann, N. K., Gomez, L., Whitehead, P. L., Abramson, R. K., Gilbert, J. R., Cuccaro, M. L., Dykxhoorn, D. M., & Pericak-Vance, M. A. (2020). Three brothers with autism carry a stop-gain mutation in the hpa-axis gene nr3c2. Autism Research, 13(4), 523–531.

Curtis, L. M., & Rarey, K. E. (1995). Effect of stress on cochlear glucocorticoid protein. ii. restraint. Hearing Research, 92(1-2), 120–125.

Das, I., Estevez, M. A., Sarkar, A. A., & Banerjee-Basu, S. (2019). A multifaceted approach for analyzing complex phenotypic data in rodent models of autism. Molecular Autism, 10(1), 1–15.

Davidson, L. S., Geers, A. E., Hale, S., Sommers, M. M., Brenner, C., & Spehar, B. (2019). Effects of early auditory deprivation on working memory and reasoning abilities in verbal and visuo-spatial domains for pediatric ci recipients. Ear and Hearing, 40(3), 517.

Davis, M. H., & Johnsrude, I. S. (2003). Hierarchical processing in spoken language comprehension. Journal of Neuroscience, 23(8), 3423–3431.

De Kloet, E. R., Joels, M., & Holsboer, F. (2005). Stress and the brain: From adaptation to disease. Nature Reviews Neuroscience, 6(6), 463–475.

De Kloet, E. R., Oitzl, M. S., & Joels, M. (1999). Stress and cognition: Are corticosteroids good or bad guys? Trends in Neurosciences, 22(10), 422–426.

De Kloet, E. R., Van Acker, S. A., Sibug, R. M., Oitzl, M. S., Meijer, O. C., Rahmouni, K., & De Jong, W. (2000). Brain mineralocorticoid receptors and centrally regulated functions. Kidney International, 57(4), 1329–1336.

De Kloet, E., Meijer, O. C., de Nicola, A. F., de Rijk, R. H., & Joëls, M. (2018). Importance of the brain corticosteroid receptor balance in metaplasticity, cognitive performance and neuro-inflammation. Frontiers in Neuroendocrinology, 49, 124–145.

De Koninck, Y. (2007). Altered chloride homeostasis in neurological disorders: A new target. Current Opinion in Pharmacology, 7(1), 93–99.

De No, L. (1933). Vestibulo-ocular reflex arc. Arch Neurol Psychiat, 30, 245–291.

Delhaye, S., & Bardoni, B. (2021). Role of phosphodiesterases in the pathophysiology of neurodevelopmental disorders. Molecular Psychiatry, 26(9), 4570–4582.

Derkach, V. A., Oh, M. C., Guire, E. S., & Soderling, T. R. (2007). Regulatory mechanisms of ampa receptors in synaptic plasticity. Nature Reviews Neuroscience, 8(2), 101–113.

de Villers-Sidani, E., Chang, E. F., Bao, S., & Merzenich, M. M. (2007). Critical period window for spectral tuning defined in the primary auditory cortex (a1) in the rat. Journal of Neuroscience, 27(1), 180–189.

Dieni, S., Matsumoto, T., Dekkers, M., Rauskolb, S., Ionescu, M. S., Deogracias, R., Gundelfinger, E. D., Kojima, M., Nestel, S., Frotscher, M., et al. (2012). Bdnf and its pro-peptide are stored in presynaptic dense core vesicles in brain neurons. Journal of Cell Biology, 196(6), 775–788.

Dragicevic, C. D., Marcenaro, B., Navarrete, M., Robles, L., & Delano, P. H. (2019). Oscillatory infrasonic modulation of the cochlear amplifier by selective attention. PLoS One, 14(1), e0208939.

Duchemin, S., Boily, M., Sadekova, N., & Girouard, H. (2012). The complex contribution of nos interneurons in the physiology of cerebrovascular regulation. Frontiers in Neural Circuits, 6, 51.

Earl, B. R., & Chertoff, M. E. (2010). Predicting auditory nerve survival using the compound action potential. Ear and Hearing, 31(1), 7–21.

Eckert, P., Marchetta, P., Manthey, M. K., Walter, M. H., Jovanovic, S., Savitska, D., Singer, W., Jacob, M. H., Rüttiger, L., Schimmang, T., Milenkovic, I., Pilz, P. K. D., & Knipper, M. (2021). Deletion of bdnf in pax2 lineage-derived interneuron precursors in the hindbrain hampers the proportion of excitation/inhibition, learning, and behavior. Frontiers in Molecular Neuroscience, 14, 39.

Elarbed, A., Fackrell, K., Baguley, D. M., & Hoare, D. J. (2021). Tinnitus and stress in adults: A scoping review. International Journal of Audiology, 60(3), 171–182.

Elbert, T., Pantev, C., Wienbruch, C., Rockstroh, B., & Taub, E. (1995). Increased cortical representation of the fingers of the left hand in string players. Science, 270(5234), 305–307.

Elling, L., Steinberg, C., Bröckelmann, A.-K., Dobel, C., Bölte, J., & Junghofer, M. (2011). Acute stress alters auditory selective attention in humans independent of hpa: A study of evoked potentials. PLoS One, 6(4), e18009.

Engel, J., Braig, C., Rüttiger, L., Kuhn, S., Zimmermann, U., Blin, N., Sausbier, M., Kalbacher, H., Münkner, S., Rohbock, K., Ruth, P., Winter, H., & Knipper, M. (2006). Two classes of outer hair cells along the tonotopic axis of the cochlea. Neuroscience, 143(3), 837–849.

Engl, E., Jolivet, R., Hall, C. N., & Attwell, D. (2017). Non-signalling energy use in the developing rat brain. Journal of Cerebral Blood Flow & Metabolism, 37(3), 951–966.

Erdmann, G., Schutz, G., & Berger, S. (2008). Loss of glucocorticoid receptor function in the pituitary results in early postnatal lethality. Endocrinology, 149(7), 3446–3451.

Erdmann, G., Schütz, G., & Berger, S. (2007). Inducible gene inactivation in neurons of the adult mouse forebrain. BMC Neuroscience, 8(1), 1–10.

Erichsen, S., Berger, S., Schmid, W., Stierna, P., & Hultcrantz, M. (2001). Na, k-atpase expression in the mouse cochlea is not dependent on the mineralocorticoid receptor. Hearing Research, 160(1-2), 37–46.

Ernfors, P., Lee, K.-F., & Jaenisch, R. (1994). Mice lacking brain-derived neurotrophic factor develop with sensory deficits. Nature, 368(6467), 147–150.

Fedele, E., & Ricciarelli, R. (2021). Memory enhancers for alzheimer's dementia: Focus on cgmp. Pharmaceuticals, 14(1), 61.

Feil, R., Lohmann, S. M., de Jonge, H., Walter, U., & Hofmann, F. (2003). Cyclic gmp-dependent protein kinases and the cardiovascular system: Insights from genetically modified mice. Circulation Research, 93(10), 907–916.

Ferguson, B. R., & Gao, W.-J. (2018). Pv interneurons: Critical regulators of e/i balance for prefrontal cortex-dependent behavior and psychiatric disorders. Frontiers in Neural Circuits, 12, 37.

Fettiplace, R. (2011). Hair cell transduction, tuning, and synaptic transmission in the mammalian cochlea. Comprehensive Physiology, 7(4), 1197–1227.

Fitch, R. H., Miller, S., & Tallal, P. (1997). Neurobiology of speech perception. Annual Review of Neuroscience, 20(1), 331–353.

Fitch, R. H., & Tallal, P. (2003). Neural mechanisms of language-based learning impairments: Insights from human populations and animal models. Behavioral and Cognitive Neuroscience Reviews, 2(3), 155–178.

Fitch, R. H., Alexander, M. L., & Threlkeld, S. W. (2013). Early neural disruption and auditory processing outcomes in rodent models: Implications for developmental language disability. Frontiers in Systems Neuroscience, 7, 58.

Fitzakerley, J. L., & Trachte, G. J. (2018). Genetics of guanylyl cyclase pathways in the cochlea and their influence on hearing. Physiological Genomics, 50(9), 780–806.

Foss-Feig, J. H., Adkinson, B. D., Ji, J. L., Yang, G., Srihari, V. H., McPartland, J. C., Krystal, J. H., Murray, J. D., & Anticevic, A. (2017). Searching for cross-diagnostic convergence: Neural mechanisms governing excitation and inhibition balance in schizophrenia and autism spectrum disorders. Biological Psychiatry, 81(10), 848–861.

Foss-Feig, J. H., Schauder, K. B., Key, A. P., Wallace, M. T., & Stone, W. L. (2017). Audition-specific temporal processing deficits associated with language function in children with autism spectrum disorder. Autism Research, 10(11), 1845–1856.

Fotaki, V., Price, D. J., & Mason, J. O. (2008). Newly identified patterns of pax2 expression in the developing mouse forebrain. BMC Developmental Biology, 8(1), 1–11.

Friauf, E., Rust, M. B., Schulenborg, T., & Hirtz, J. J. (2011). Chloride cotransporters, chloride homeostasis, and synaptic inhibition in the developing auditory system. Hearing Research, 279(1-2), 96–110.

Friebe, A., & Koesling, D. (2003). Regulation of nitric oxide-sensitive guanylyl cyclase. Circulation Research, 93(2), 96–105.

Frisina, D. R., & Frisina, R. D. (1997). Speech recognition in noise and presbycusis: Relations to possible neural mechanisms. Hearing Research, 106(1-2), 95–104.

Fritzsch, B., Tessarollo, L., Coppola, E., & Reichardt, L. F. (2004). Neurotrophins in the ear: Their roles in sensory neuron survival and fiber guidance. Progress in Brain Research, 146, 265–278.

Füllgrabe, C., & Moore, B. C. (2014). Effects of age and hearing loss on stream segregation based on interaural time differences. The Journal of the Acoustical Society of America, 136(2), EL185–EL191.

Furman, A. C., Kujawa, S. G., & Liberman, M. C. (2013). Noise-induced cochlear neuropathy is selective for fibers with low spontaneous rates. Journal of Neurophysiology, 110(3), 577–586.

Galbraith, G. C., Olfman, D. M., & Huffman, T. M. (2003). Selective attention affects human brain stem frequency-following response. Neuroreport, 14(5), 735–738.

Gao, E., & Suga, N. (2000). Experience-dependent plasticity in the auditory cortex and the inferior colliculus of bats: Role of the corticofugal system. Proceedings of the National Academy of Sciences, 97(14), 8081–8086.

Ghasemi, M., Navidhamidi, M., Rezaei, F., Azizikia, A., & Mehranfard, N. (2021). Anxiety and hippocampal neuronal activity: Relationship and potential mechanisms. Cognitive, Affective, & Behavioral Neuroscience, 1–19.

Ginsberg, S. D., Alldred, M. J., Counts, S. E., Cataldo, A. M., Neve, R. L., Jiang, Y., Wuu, J., Chao, M. V., Mufson, E. J., Nixon, R. A., et al. (2010). Microarray analysis of hippocampal ca1 neurons implicates early endosomal dysfunction during alzheimer's disease progression. Biological Psychiatry, 68(10), 885–893.

Glowatzki, E., & Fuchs, P. A. (2002). Transmitter release at the hair cell ribbon synapse. Nature Neuroscience, 5(2), 147–154.

Goel, A., Cantu, D. A., Guilfoyle, J., Chaudhari, G. R., Newadkar, A., Todisco, B., de Alba, D., Kourdougli, N., Schmitt, L. M., Pedapati, E., et al. (2018). Impaired perceptual learning in a mouse model of fragile x syndrome is mediated by parvalbumin neuron dysfunction and is reversible. Nature Neuroscience, 21(10), 1404–1411.

Gomez-Sanchez, E., & Gomez-Sanchez, C. E. (2014). The multifaceted mineralocorticoid receptor. Comprehensive Physiology, 4(3), 965.

Gong, W.-K., Ni, J., Yu, L.-F., Wang, L., & Huang, Z.-L. (2020). Temporal dynamics of arc/arg3. 1 expression in the dorsal striatum during acquisition and consolidation of a motor skill in mice. Neurobiology of Learning and Memory, 168, 107156.

Gordon, S. A., Waltzman, S. B., & Friedmann, D. R. (2022). Delayed cochlear implantation in congenitally deaf children—identifying barriers for targeted interventions. International Journal of Pediatric Otorhinolaryngology, 155, 111086.

Goyal, M. S., Hawrylycz, M., Miller, J. A., Snyder, A. Z., & Raichle, M. E. (2014). Aerobic glycolysis in the human brain is associated with development and neotenous gene expression. Cell Metabolism, 19(1), 49–57.

Graham, C. E., Basappa, J., Turcan, S., & Vetter, D. E. (2011). The cochlear crf signaling systems and their mechanisms of action in modulating cochlear sensitivity and protection against trauma. Molecular Neurobiology, 44(3), 383–406.

Graham, C. E., Basappa, J., & Vetter, D. E. (2010). A corticotropin-releasing factor system expressed in the cochlea modulates hearing sensitivity and protects against noise-induced hearing loss. Neurobiology of Disease, 38(2), 246–258.

Graham, C. E., & Vetter, D. E. (2011). The mouse cochlea expresses a local hypothalamic-pituitary-adrenal equivalent signaling system and requires corticotropin-releasing factor receptor 1 to establish normal hair cell innervation and cochlear sensitivity. Journal of Neuroscience, 31(4), 1267–1278.

Grant, L., Yi, E., & Glowatzki, E. (2010). Two modes of release shape the postsynaptic response at the inner hair cell ribbon synapse. Journal of Neuroscience, 30(12), 4210–4220.

Griffen, T. C., & Maffei, A. (2014). Gabaergic synapses: Their plasticity and role in sensory cortex. Frontiers in Cellular Neuroscience, 8, 91.

Gröschel, M., Ryll, J., Götze, R., Ernst, A., & Basta, D. (2014). Acute and long-term effects of noise exposure on the neuronal spontaneous activity in cochlear nucleus and inferior colliculus brain slices. BioMed Research International, 2014.

Guo, J., & Anton, E. (2014). Decision making during interneuron migration in the developing cerebral cortex. Trends in Cell Biology, 24(6), 342–351.

Guth, P., & Stockwell, M. (1977). Guanylate cyclase and cyclic guanosine monophosphate in the guinea-pig cochlea. Journal of Neurochemistry, 28(1), 263–265.

Haapala, S., Niemitalo-Haapola, E., Raappana, A., Kujala, T., Suominen, K., Jansson-Verkasalo, E., & Kujala, T. (2015). Long-term influence of recurrent acute otitis media on neural involuntary attention switching in 2-year-old children. Behavioral and Brain Functions, 12(1), 1–8.

Haapala, S., Niemitalo-Haapola, E., Raappana, A., Kujala, T., Suominen, K., Kujala, T., & Jansson-Verkasalo, E. (2014). Effects of recurrent acute otitis media on cortical speech-sound processing in 2-year old children. Ear and Hearing, 35(3), e75–e83.

Hammill, T. L. (2017). A review of the progress and pitfalls of fda policy process: Planning a pathway for pharmaceutical interventions for hearing loss development. Hearing Research, 349, 172–176.

Han, K., Min, J., Lee, M., Kang, B.-M., Park, T., Hahn, J., Yei, J., Lee, J., Woo, J., Lee, C. J., et al. (2019). Neurovascular coupling under chronic stress is modified by altered gabaergic interneuron activity. Journal of Neuroscience, 39(50), 10081–10095.

Harms, J. F., Menniti, F. S., & Schmidt, C. J. (2019). Phosphodiesterase 9a in brain regulates cgmp signaling independent of nitric-oxide. Frontiers in Neuroscience, 837.

Heil, P., Neubauer, H., Brown, M., & Irvine, D. R. (2008). Towards a unifying basis of auditory thresholds: Distributions of the first-spike latencies of auditory-nerve fibers. Hearing Research, 238(1-2), 25–38.

Heil, P., & Peterson, A. J. (2015). Basic response properties of auditory nerve fibers: A review. Cell and Tissue Research, 361(1), 129–158.

Heinz, M. G., & Young, E. D. (2004). Response growth with sound level in auditory-nerve fibers after noise-induced hearing loss. Journal of Neurophysiology, 91(2), 784–795.

Henkin, R. I., McGlone, R. E., Daly, R., Bartter, F. C., et al. (1967). Studies on auditory thresholds in normal man and in patients with adrenal cortical insufficiency: The role of adrenal cortical steroids. The Journal of Clinical Investigation, 46(3), 429–435.

Hensch, T. K. (2005). Critical period plasticity in local cortical circuits. Nature Reviews Neuroscience, 6(11), 877–888.

Herman, J. P., & Cullinan, W. E. (1997). Neurocircuitry of stress: Central control of the hypothalamo–pituitary–adrenocortical axis. Trends in Neurosciences, 20(2), 78–84.

Hernandez-Mercado, K., & Zepeda, A. (2021). Morris water maze and contextual fear conditioning tasks to evaluate cognitive functions associated with adult hippocampal neurogenesis. Frontiers in Neuroscience, 15.

Hickman, T. T., Liberman, M. C., & Jacob, M. H. (2015). Adenomatous polyposis coli protein deletion in efferent olivocochlear neurons perturbs afferent synaptic maturation and reduces the dynamic range of hearing. Journal of Neuroscience, 35(24), 9236–9245.

Hillman, E. M. (2014). Coupling mechanism and significance of the bold signal: A status report. Annual Review of Neuroscience, 37, 161–181.

Hong, E. J., McCord, A. E., & Greenberg, M. E. (2008). A biological function for the neuronal activity-dependent component of bdnf transcription in the development of cortical inhibition. Neuron, 60(4), 610–624.

Housley, G. D., & Ashmore, J. F. (1992). Ionic currents of outer hair cells isolated from the guinea-pig cochlea. The Journal of Physiology, 448(1), 73–98.

Huang, X.-F., Jiang, W.-T., Liu, L., Song, F.-C., Zhu, X., Shi, G.-L., Ding, S.-M., Ke, H.-M., Wang, W., O'Donnell, J. M., et al. (2018). A novel pde 9 inhibitor wyq-c36d ameliorates corticosterone-induced neurotoxicity and depression-like behaviors by cgmp-creb-related signaling. CNS Neuroscience & Therapeutics, 24(10), 889–896.

Huang, Z. J., Kirkwood, A., Pizzorusso, T., Porciatti, V., Morales, B., Bear, M. F., Maffei, L., & Tonegawa, S. (1999). Bdnf regulates the maturation of inhibition and the critical period of plasticity in mouse visual cortex. Cell, 98(6), 739–755.

Iadecola, C. (2017). The neurovascular unit coming of age: A journey through neurovascular coupling in health and disease. Neuron, 96(1), 17–42.

Insanally, M. N., Köver, H., Kim, H., & Bao, S. (2009). Feature-dependent sensitive periods in the development of complex sound representation. Journal of Neuroscience, 29(17), 5456–5462.

Irvine, D. R. (2018a). Auditory perceptual learning and changes in the conceptualization of auditory cortex. Hearing Research, 366, 3–16.

Irvine, D. R. (2018b). Plasticity in the auditory system. Hearing Research, 362, 61–73.

Itskov, P. M., Vinnik, E., Honey, C., Schnupp, J., & Diamond, M. E. (2012). Sound sensitivity of neurons in rat hippocampus during performance of a sound-guided task. Journal of Neurophysiology, 107(7), 1822–1834.

Jaumann, M., Dettling, J., Gubelt, M., Zimmermann, U., Gerling, A., Paquet-Durand, F., Feil, S., Wolpert, S., Franz, C., Varakina, K., Xiong, H., Brandt, N., Kuhn, S., Geisler, H.-S., Rohbock, K., Ruth, P., Schlossmann, J., Hütter, J., Sandner, P., ... Rüttiger, L. (2012). Cgmp-prkg1 signaling and pde5 inhibition shelter cochlear hair cells and hearing function. Nature Medicine, 18(2), 252–259.

Jauset-Berrocal, J. A., & Soria-Urios, G. (2018). Cognitive neurorehabilitation: The foundations and applications of neurologic music therapy. Revista de Neurologia, 67(8), 303–310.

Jean, P., de la Morena, D. L., Michanski, S., Tobón, L. M. J., Chakrabarti, R., Picher, M. M., Neef, J., Jung, S., Gültas, M., Maxeiner, S., et al. (2018). The synaptic

ribbon is critical for sound encoding at high rates and with temporal precision. eLife, 7, e29275.

Jiao, Y., Zhang, Z., Zhang, C., Wang, X., Sakata, K., Lu, B., & Sun, Q.-Q. (2011). A key mechanism underlying sensory experience-dependent maturation of neocortical gabaergic circuits in vivo. Proceedings of the National Academy of Sciences, 108(29), 12131–12136.

Joels, M., & de Kloet, E. R. (1994). Mineralocorticoid and glucocorticoid receptors in the brain. implications for ion permeability and transmitter systems. Progress in Neurobiology, 43(1), 1–36.

Joels, M., & de Kloet, E. R. (2017). 30 years of the mineralocorticoid receptor: The brain mineralocorticoid receptor: A saga in three episodes. Journal of Endocrinology, 234(1), T49–T66.

Johnson, D. H. (1980). The relationship between spike rate and synchrony in responses of auditory-nerve fibers to single tones. The Journal of the Acoustical Society of America, 68(4), 1115–1122.

Johnson, J. C., Marshall, C. R., Weil, R. S., Bamiou, D.-E., Hardy, C. J., & Warren, J. D. (2021). Hearing and dementia: From ears to brain. Brain, 144(2), 391–401.

Jones, T. A., Jones, S. M., & Paggett, K. C. (2001). Primordial rhythmic bursting in embryonic cochlear ganglion cells. Journal of Neuroscience, 21(20), 8129–8135.

Jones, T. A., Leake, P. A., Snyder, R. L., Stakhovskaya, O., & Bonham, B. (2007). Spontaneous discharge patterns in cochlear spiral ganglion cells before the onset of hearing in cats. Journal of Neurophysiology, 98(4), 1898–1908.

Jungbluth, S., Koentges, G., & Lumsden, A. (1997). Coordination of early neural tube development by bdnf/trkb. Development, 124(10), 1877–1885.

Kaltenbach, J. A., & Zhang, J. (2007). Intense sound-induced plasticity in the dorsal cochlear nucleus of rats: Evidence for cholinergic receptor upregulation. Hearing Research, 226(1-2), 232–243.

Kandler, K., & Friauf, E. (1995). Development of glycinergic and glutamatergic synaptic transmission in the auditory brainstem of perinatal rats. Journal of Neuroscience, 15(10), 6890–6904.

Kay-Rivest, E., McMenomey, S. O., Jethanamest, D., Roland Jr, J. T., Shapiro, W. H., Waltzman, S. B., & Friedmann, D. R. (2022). Cochlear implant outcomes in charge syndrome: Updated perspectives. Otology & Neurotology: Official Publication of the American Otological Society, American Neurotology Society [and] European Academy of Otology and Neurotology.

Kazmierczak, P., Sakaguchi, H., Tokita, J., Wilson-Kubalek, E. M., Milligan, R. A., Müller, U., & Kachar, B. (2007). Cadherin 23 and protocadherin 15 interact to form tip-link filaments in sensory hair cells. Nature, 449(7158), 87–91.

Keithley, E. M. (2020). Pathology and mechanisms of cochlear aging. Journal of Neuroscience Research, 98(9), 1674–1684.

Kemp-Harper, B., & Feil, R. (2008). Meeting report: Cgmp matters.

Kharkovets, T., Dedek, K., Maier, H., Schweizer, M., Khimich, D., Nouvian, R., Vardanyan, V., Leuwer, R., Moser, T., & Jentsch, T. J. (2006). Mice with altered kcnq4 k+ channels implicate sensory outer hair cells in human progressive deafness. The EMBO Journal, 25(3), 642–652.

Kiang, N. Y.-S. (1965). Stimulus coding in the auditory nerve and cochlear nucleus. Acta Oto-Laryngologica, 59(2-6), 186–200.

Kil, S.-H., & Kalinec, F. (2013). Expression and dexamethasone-induced nuclear translocation of glucocorticoid and mineralocorticoid receptors in guinea pig cochlear cells. Hearing Research, 299, 63–78.

Kilb, W., Kirischuk, S., & Luhmann, H. J. (2011). Electrical activity patterns and the functional maturation of the neocortex. European Journal of Neuroscience, 34(10), 1677–1686.

Kilgard, M. P., Pandya, P. K., Engineer, N. D., & Moucha, R. (2002). Cortical network reorganization guided by sensory input features. Biological Cybernetics, 87(5), 333–343.

Kim, K. H., Relkin, N. R., Lee, K.-M., & Hirsch, J. (1997). Distinct cortical areas associated with native and second languages. Nature, 388(6638), 171–174.

Kim, Y.-M., Chung, H.-T., Kim, S.-S., Han, J.-A., Yoo, Y.-M., Kim, K.-M., Lee, G.-H., Yun, H.-Y., Green, A., Li, J., et al. (1999). Nitric oxide protects pc12 cells from serum deprivation-induced apoptosis by cgmp-dependent inhibition of caspase signaling. Journal of Neuroscience, 19(16), 6740–6747.

Kimura, F., & Itami, C. (2019). A hypothetical model concerning how spike-timing-dependent plasticity contributes to neural circuit formation and initiation of the critical period in barrel cortex. Journal of Neuroscience, 39(20), 3784–3791.

King, K., & Stephens, D. (1992). Auditory and psychological factors in 'auditory disability with normal hearing'. Scandinavian Audiology, 21(2), 109–114.

Kleppisch, T., & Feil, R. (2009). Cgmp signalling in the mammalian brain: Role in synaptic plasticity and behaviour. cGMP: Generators, Effectors and Therapeutic Implications, 549–579.

Knipper, M., Panford-Walsh, R., Singer, W., Rüttiger, L., & Zimmermann, U. (2015). Specific synaptopathies diversify brain responses and hearing disorders: You lose the gain from early life. Cell and Tissue Research, 361(1), 77–93.

Knipper, M., Singer, W., Schwabe, K., Hagberg, G. E., Hegner, Y. L., Rüttiger, L., Braun, C., & Land, R. (2021). Disturbed balance of inhibitory signaling links hearing loss and cognition. Frontiers in Neural Circuits, 15.

Knipper, M., Van Dijk, P., Nunes, I., Rüttiger, L., & Zimmermann, U. (2013). Advances in the neurobiology of hearing disorders: Recent developments regarding the basis of tinnitus and hyperacusis. Progress in Neurobiology, 111, 17–33.

Knipper, M., Van Dijk, P., Schulze, H., Mazurek, B., Krauss, P., Scheper, V., Warnecke, A., Schlee, W., Schwabe, K., Singer, W., Braun, C., Delano, P. H., Fallgatter, A. J., Ehlis, A.-C., Searchfield, G. D., Munk, M. H. J., Baguley, D. M., & Rüttiger, L. (2020). The neural bases of tinnitus: Lessons from deafness and cochlear implants. Journal of Neuroscience, 40(38), 7190–7202.

Kobel, M., Le Prell, C. G., Liu, J., Hawks, J. W., & Bao, J. (2017). Noise-induced cochlear synaptopathy: Past findings and future studies. Hearing Research, 349, 148–154.

Kocharyan, A., Fernandes, P., Tong, X.-K., Vaucher, E., & Hamel, E. (2008). Specific subtypes of cortical gaba interneurons contribute to the neurovascular coupling response to basal forebrain stimulation. Journal of Cerebral Blood Flow & Metabolism, 28(2), 221–231.

Korb, E., & Finkbeiner, S. (2011). Arc in synaptic plasticity: From gene to behavior. Trends in Neurosciences, 34(11), 591–598.

Kourosh-Arami, M., Hosseini, N., Mohsenzadegan, M., Komaki, A., & Joghataei, M. T. (2020). Neurophysiologic implications of neuronal nitric oxide synthase. Reviews in the Neurosciences, 31(6), 617–636.

Kozberg, M. G., Chen, B. R., DeLeo, S. E., Bouchard, M. B., & Hillman, E. M. (2013). Resolving the transition from negative to positive blood oxygen level-dependent responses in the developing brain. Proceedings of the National Academy of Sciences, 110(11), 4380–4385.

Kral, A., & Sharma, A. (2012). Developmental neuroplasticity after cochlear implantation. Trends in Neurosciences, 35(2), 111–122.

Kraus, N., & White-Schwoch, T. (2015). Unraveling the biology of auditory learning: A cognitive–sensorimotor–reward framework. Trends in Cognitive Sciences, 19(11), 642–654.

Krause, G., zum Gottesberge, A. M. M., Wolfram, G., & Gerzer, R. (1997). Transcripts encoding three types of guanylyl-cyclase-coupled trans-membrane receptors in inner ear tissues of guinea pigs. Hearing Research, 110(1-2), 95–106.

Kroker, K. S., Rast, G., Giovannini, R., Marti, A., Dorner-Ciossek, C., & Rosenbrock, H. (2012). Inhibition of acetylcholinesterase and phosphodiesterase-9a has differential effects on hippocampal early and late ltp. Neuropharmacology, 62(5-6), 1964–1974.

Kuan, E. C., Peng, K. A., Suh, J. D., Bergsneider, M., & Wang, M. B. (2017). Otolaryngic manifestations of cushing disease. Ear, Nose & Throat Journal, 96(8), E28–E30.

Kuhn, M. (2003). Structure, regulation, and function of mammalian membrane guanylyl cyclase receptors, with a focus on guanylyl cyclase-a. Circulation Research, 93(8), 700–709.

Kuhn, M. (2009). Function and dysfunction of mammalian membrane guanylyl cyclase receptors: Lessons from genetic mouse models and implications for human diseases. cGMP: Generators, Effectors and Therapeutic Implications, 47–69.

Kujawa, S. G., & Liberman, M. C. (2009). Adding insult to injury: Cochlear nerve degeneration after "temporary" noise-induced hearing loss. Journal of Neuroscience, 29(45), 14077–14085.

Kullmann, D. M. (2011). Interneuron networks in the hippocampus. Current Opinion in Neurobiology, 21(5), 709–716.

Kyle, B. D., Hurst, S., Swayze, R. D., Sheng, J., & Braun, A. P. (2013). Specific phosphorylation sites underlie the stimulation of a large conductance, ca2+-activated k+ channel by cgmp-dependent protein kinase. The FASEB Journal, 27(5), 2027–2038.

Lee, D. I., Zhu, G., Sasaki, T., Cho, G.-S., Hamdani, N., Holewinski, R., Jo, S.-H., Danner, T., Zhang, M., Rainer, P. P., et al. (2015). Phosphodiesterase 9a controls nitric-oxide-independent cgmp and hypertrophic heart disease. Nature, 519(7544), 472–476.

Lesica, N. A. (2018). Why do hearing aids fail to restore normal auditory perception? Trends in Neurosciences, 41(4), 174–185.

Leutgeb, J. K., Leutgeb, S., Moser, M.-B., & Moser, E. I. (2007). Pattern separation in the dentate gyrus and ca3 of the hippocampus. Science, 315(5814), 961–966.

Levitt, P., Eagleson, K. L., & Powell, E. M. (2004). Regulation of neocortical interneuron development and the implications for neurodevelopmental disorders. Trends in Neurosciences, 27(7), 400–406.

Lewis, D. A., Hashimoto, T., & Volk, D. W. (2005). Cortical inhibitory neurons and schizophrenia. Nature Reviews Neuroscience, 6(4), 312–324.

Li, Z.-W., Wu, B., Ye, P., Tan, Z.-Y., & Ji, Y.-H. (2016). Brain natriuretic peptide suppresses pain induced by bmk i, a sodium channel-specific modulator, in rats. The Journal of Headache and Pain, 17(1), 1–15.

Liberman, M. C. (1978). Auditory-nerve response from cats raised in a low-noise chamber. The Journal of the Acoustical Society of America, 63(2), 442–455.

Liberman, M. C., & Kujawa, S. G. (2017). Cochlear synaptopathy in acquired sensorineural hearing loss: Manifestations and mechanisms. Hearing Research, 349, 138–147.

Liberman, M. C., & Oliver, M. E. (1984). Morphometry of intracellularly labeled neurons of the auditory nerve: Correlations with functional properties. Journal of Comparative Neurology, 223(2), 163–176.

Liberman, M. (1982). Single-neuron labeling in the cat auditory nerve. Science, 216(4551), 1239–1241.

Lim, L., Mi, D., Llorca, A., & Marin, O. (2018). Development and functional diversification of cortical interneurons. Neuron, 100(2), 294–313.

Lin, F. R., Metter, E. J., O'Brien, R. J., Resnick, S. M., Zonderman, A. B., & Ferrucci, L. (2011). Hearing loss and incident dementia. Archives of Neurology, 68(2), 214–220.

Link, W., Konietzko, U., Kauselmann, G., Krug, M., Schwanke, B., Frey, U., & Kuhl, D. (1995). Somatodendritic expression of an immediate early gene is regulated by synaptic activity. Proceedings of the National Academy of Sciences, 92(12), 5734–5738.

Liu, L., Shen, P., He, T., Chang, Y., Shi, L., Tao, S., Li, X., Xun, Q., Guo, X., Yu, Z., et al. (2016). Noise induced hearing loss impairs spatial learning/memory and hippocampal neurogenesis in mice. Scientific Reports, 6(1), 1–9.

Livingston, G., Sommerlad, A., Orgeta, V., Costafreda, S. G., Huntley, J., Ames, D., Ballard, C., Banerjee, S., Burns, A., Cohen-Mansfield, J., et al. (2017). Dementia prevention, intervention, and care. The Lancet, 390(10113), 2673–2734.

Löhrke, S., Srinivasan, G., Oberhofer, M., Doncheva, E., & Friauf, E. (2005). Shift from depolarizing to hyperpolarizing glycine action occurs at different perinatal ages in superior olivary complex nuclei. European Journal of Neuroscience, 22(11), 2708–2722.

Lopez-Poveda, E. A. (2018). Olivocochlear efferents in animals and humans: From anatomy to clinical relevance. Frontiers in Neurology, 9, 197.

Lukas, J. H. (1980). Human auditory attention: The olivocochlear bundle may function as a peripheral filter. Psychophysiology, 17(5), 444–452.

Ma, L., Zhang, J., Yang, P., Wang, E., & Qin, L. (2015). Acute restraint stress alters sound-evoked neural responses in the rat auditory cortex. Neuroscience, 290, 608–620.

Ma, L., Li, W., Li, S., Wang, X., & Qin, L. (2017). Effect of chronic restraint stress on inhibitory gating in the auditory cortex of rats. Stress, 20(3), 312–319.

Ma, L., Zhang, Y., Liu, P., Li, S., Li, Y., Ji, T., Zhang, L., & Chhetri, J. (2021). Plasma n-terminal pro-b-type natriuretic peptide is associated with intrinsic capacity decline in an older population. The journal of Nutrition, Health & Aging, 25(2), 271–277.

MacGregor, A. J., Joseph, A. R., Walker, G. J., & Dougherty, A. L. (2020). Co-occurrence of hearing loss and posttraumatic stress disorder among injured military personnel: A retrospective study. BMC Public Health, 20(1), 1–7.

Madisen, L., Zwingman, T. A., Sunkin, S. M., Oh, S. W., Zariwala, H. A., Gu, H., Ng, L. L., Palmiter, R. D., Hawrylycz, M. J., Jones, A. R., et al. (2010). A robust and high-throughput cre reporting and characterization system for the whole mouse brain. Nature Neuroscience, 13(1), 133–140.

Malmierca, M. S., Sanchez-Vives, M. V., Escera, C., & Bendixen, A. (2014). Neuronal adaptation, novelty detection and regularity encoding in audition. Frontiers in Systems Neuroscience, 8, 111.

Malmierca, M., & Merchan, M. (2004). The rat nervous system.

Malmierca, M., Rees, A., & Le Beau, F. (1997). Ascending projections to the medial geniculate body from physiologically identified loci in the inferior colliculus. Acoustical signal processing in the central auditory system (pp. 295–302). Springer.

Marchetta, P., Eckert, P., Lukowski, R., Ruth, P., Singer, W., Rüttiger, L., & Knipper, M. (2022). Loss of central mineralocorticoid or glucocorticoid receptors impacts auditory nerve processing in the cochlea. iScience, 103981.

Marchetta, P., Möhrle, D., Eckert, P., Reimann, K., Wolter, S., Tolone, A., Lang, I., Wolters, M., Feil, R., Engel, J., Engel, J., Paquet-Durand, F., Kuhn, M., Knipper, M., & Rüttiger, L. (2020). Guanylyl cyclase a/cgmp signaling slows hidden, age- and acoustic trauma-induced hearing loss. Frontiers in Aging Neuroscience, 12, 83.

Marchetta, P., Rüttiger, L., Hobbs, A. J., Singer, W., & Knipper, M. (2021). The role of cgmp signalling in auditory processing in health and disease. British Journal of Pharmacology.

Marchetta, P., Savitska, D., Kübler, A., Asola, G., Manthey, M., Möhrle, D., Schimmang, T., Rüttiger, L., Knipper, M., & Singer, W. (2020). Age-dependent auditory processing deficits after cochlear synaptopathy depend on auditory nerve latency and the ability of the brain to recruit ltp/bdnf. Brain Sciences, 10(10), 710.

Marcotti, W., Johnson, S. L., Holley, M. C., & Kros, C. J. (2003). Developmental changes in the expression of potassium currents of embryonic, neonatal and mature mouse inner hair cells. The Journal of Physiology, 548(2), 383–400.

Marcotti, W., & Kros, C. J. (1999). Developmental expression of the potassium current ik, n contributes to maturation of mouse outer hair cells.

Maricich, S. M., & Herrup, K. (1999). Pax-2 expression defines a subset of gabaergic interneurons and their precursors in the developing murine cerebellum. Journal of Neurobiology, 41(2), 281–294.

Marin, O. (2012). Interneuron dysfunction in psychiatric disorders. Nature Reviews Neuroscience, 13(2), 107–120.

Marin, O., & Rubenstein, J. L. (2001). A long, remarkable journey: Tangential migration in the telencephalon. Nature Reviews Neuroscience, 2(11), 780–790.

Markl, H., & Ehret, G. (2009). Die hörschwelle der maus (mus musculus)-eine kritische wertung der methoden zur bestimmung der hörschwelle eines säugetiers.

Matt, L., Eckert, P., Panford-Walsh, R., Geisler, H.-S., Bausch, A. E., Manthey, M., Müller, N. I., Harasztosi, C., Rohbock, K., Ruth, P., Friauf, E., Ott, T., Zimmermann, U., Rüttiger, L., Schimmang, T., Knipper, M., & Singer, W. (2018). Visualizing bdnf transcript usage during sound-induced memory linked plasticity. Frontiers in Molecular Neuroscience, 11, 260.

Maxwell, C. R., Ehrlichman, R. S., Liang, Y., Gettes, D. R., Evans, D. L., Kanes, S. J., Abel, T., Karp, J., & Siegel, S. J. (2006). Corticosterone modulates auditory gating in mouse. Neuropsychopharmacology, 31(5), 897–903.

Mazurek, B., Szczepek, A., & Hebert, S. (2015). Stress and tinnitus. HNO, 63(4), 258–265.

McCann, K. E., Lustberg, D. J., Shaughnessy, E. K., Carstens, K. E., Farris, S., Alexander, G. M., Radzicki, D., Zhao, M., & Dudek, S. M. (2021). Novel role for mineralocorticoid receptors in control of a neuronal phenotype. Molecular Psychiatry, 26(1), 350–364.

Meddis, R. (2006). Auditory-nerve first-spike latency and auditory absolute threshold: A computer model. The Journal of the Acoustical Society of America, 119(1), 406–417.

Meese, S., Cepeda, A. P., Gahlen, F., Adams, C. M., Ficner, R., Ricci, A. J., Heller, S., Reisinger, E., & Herget, M. (2017). Activity-dependent phosphorylation by camkiiδ alters the ca2+ affinity of the multi-c2-domain protein otoferlin. Frontiers in Synaptic Neuroscience, 9, 13.

Meis, S., Endres, T., Munsch, T., & Lessmann, V. (2019). Impact of chronic bdnf depletion on gabaergic synaptic transmission in the lateral amygdala. International Journal of Molecular Sciences, 20(17), 4310.

Meltser, I., & Canlon, B. (2011). Protecting the auditory system with glucocorticoids. Hearing Research, 281(1-2), 47–55.

Merchan-Perez, A., & Liberman, M. C. (1996). Ultrastructural differences among afferent synapses on cochlear hair cells: Correlations with spontaneous discharge rate. Journal of Comparative Neurology, 371(2), 208–221.

Micheyl, C., Delhommeau, K., Perrot, X., & Oxenham, A. J. (2006). Influence of musical and psychoacoustical training on pitch discrimination. Hearing Research, 219(1-2), 36–47.

Michie, P. T., Malmierca, M. S., Harms, L., & Todd, J. (2016). The neurobiology of mmn and implications for schizophrenia. Biological Psychology, 116, 90–97.

Mifsud, K. R., & Reul, J. M. (2016). Acute stress enhances heterodimerization and binding of corticosteroid receptors at glucocorticoid target genes in the hippocampus. Proceedings of the National Academy of Sciences, 113(40), 11336–11341.

Miller, E. K., & Buschman, T. J. (2013). Cortical circuits for the control of attention. Current Opinion in Neurobiology, 23(2), 216–222.

Moeller, M. P., Tomblin, J. B., Yoshinaga-Itano, C., Connor, C. M., & Jerger, S. (2007). Current state of knowledge: Language and literacy of children with hearing impairment. Ear and Hearing, 28(6), 740–753.

Mohn, J., Alexander, J., Pirone, A., Palka, C., Lee, S., Mebane, L., Haydon, P., & Jacob, M. (2014). Adenomatous polyposis coli protein deletion leads to cognitive and autism-like disabilities. Molecular Psychiatry, 19(10), 1133–1142.

Möhrle, D., Ni, K., Varakina, K., Bing, D., Lee, S. C., Zimmermann, U., Knipper, M., & Rüttiger, L. (2016). Loss of auditory sensitivity from inner hair cell synaptopathy can be centrally compensated in the young but not old brain. Neurobiology of Aging, 44, 173–184.

Möhrle, D., Reimann, K., Wolter, S., Wolters, M., Varakina, K., Mergia, E., Eichert, N., Geisler, H.-S., Sandner, P., Ruth, P., Friebe, A., Feil, R., Zimmermann, U., Koesling, D., Knipper, M., & Rüttiger, L. (2017). No-sensitive guanylate cyclase isoforms no-gc1 and no-gc2 contribute to noise-induced inner hair cell synaptopathy. Molecular Pharmacology, 92(4), 375–388.

Moita, M. A., Rosis, S., Zhou, Y., LeDoux, J. E., & Blair, H. T. (2003). Hippocampal place cells acquire location-specific responses to the conditioned stimulus during auditory fear conditioning. Neuron, 37(3), 485–497.

Montero-Odasso, M., Ismail, Z., & Livingston, G. (2020). One third of dementia cases can be prevented within the next 25 years by tackling risk factors. the case "for" and "against". Alzheimer's research & therapy, 12(1), 1–5.

Moore, D. R., Zobay, O., & Ferguson, M. A. (2020). Minimal and mild hearing loss in children: Association with auditory perception, cognition, and communication problems. Ear and Hearing, 41(4), 720–732.

Moser, T., Neef, A., & Khimich, D. (2006). Mechanisms underlying the temporal precision of sound coding at the inner hair cell ribbon synapse. The Journal of Physiology, 576(1), 55–62.

Muller, D., Hida, B., Guidone, G., Speth, R. C., Michurina, T. V., Enikolopov, G., & Middendorff, R. (2009). Expression of guanylyl cyclase (gc)-a and gc-b during brain development: Evidence for a role of gc-b in perinatal neurogenesis. Endocrinology, 150(12), 5520–5529.

Musacchia, G., Sams, M., Skoe, E., & Kraus, N. (2007). Musicians have enhanced subcortical auditory and audiovisual processing of speech and music. Proceedings of the National Academy of Sciences, 104(40), 15894–15898.

Nagy, D., Tingley III, F. D., Stoiljkovic, M., & Hajós, M. (2015). Application of neurophysiological biomarkers for huntington's disease: Evaluating a phosphodiesterase 9a inhibitor. Experimental Neurology, 263, 122–131.

Nakahara, H., Zhang, L. I., & Merzenich, M. M. (2004). Specialization of primary auditory cortex processing by sound exposure in the "critical period". Proceedings of the National Academy of Sciences, 101(18), 7170–7174.

Neef, J., Gehrt, A., Bulankina, A. V., Meyer, A. C., Riedel, D., Gregg, R. G., Strenzke, N., & Moser, T. (2009). The ca2+ channel subunit β2 regulates ca2+ channel abundance and function in inner hair cells and is required for hearing. Journal of Neuroscience, 29(34), 10730–10740.

Nehlig, A., de Vasconcelos, A. P., & Boyet, S. (1989). Postnatal changes in local cerebral blood flow measured by the quantitative autoradiographic [14c] iodoantipyrine technique in freely moving rats. Journal of Cerebral Blood Flow & Metabolism, 9(5), 579–588.

Nicholas, J. G., & Geers, A. E. (2006). Effects of early auditory experience on the spoken language of deaf children at 3 years of age. Ear and Hearing, 27(3), 286.

Noben-Trauth, K., Zheng, Q. Y., & Johnson, K. R. (2003). Association of cadherin 23 with polygenic inheritance and genetic modification of sensorineural hearing loss. Nature Genetics, 35(1), 21–23.

Nornes, H., Dressler, G., Knapik, E., Deutsch, U., & Gruss, P. (1990). Spatially and temporally restricted expression of pax2 during murine neurogenesis. Development, 109(4), 797–809.

Nouvian, R., Beutner, D., Parsons, T. D., & Moser, T. (2006). Structure and function of the hair cell ribbon synapse. The Journal of Membrane Biology, 209(2), 153–165.

Nunez, A., & Malmierca, E. (2007). Corticofugal modulation of sensory information.

Nyhus, E., & Curran, T. (2010). Functional role of gamma and theta oscillations in episodic memory. Neuroscience & Biobehavioral Reviews, 34(7), 1023–1035.

Oikkonen, J., Onkamo, P., Järvelä, I., & Kanduri, C. (2016). Convergent evidence for the molecular basis of musical traits. Scientific Reports, 6(1), 1–10.

O'Keefe, J., & Nadel, L. (1978). The hippocampus as a cognitive map. Oxford University Press.

Olthof, B. M., Gartside, S. E., & Rees, A. (2019). Puncta of neuronal nitric oxide synthase (nnos) mediate nmda receptor signaling in the auditory midbrain. Journal of Neuroscience, 39(5), 876–887.

Omichi, R., Shibata, S. B., Morton, C. C., & Smith, R. J. (2019). Gene therapy for hearing loss. Human Molecular Genetics, 28(R1), R65–R79.

Ostrovskaya, O. I., Cao, G., Eroglu, C., & Harris, K. M. (2020). Developmental onset of enduring long-term potentiation in mouse hippocampus. Hippocampus, 30(12), 1298–1312.

Ouda, L., Profant, O., & Syka, J. (2015). Age-related changes in the central auditory system. Cell and Tissue Research, 361(1), 337–358.

Pantev, C., Oostenveld, R., Engelien, A., Ross, B., Roberts, L. E., & Hoke, M. (1998). Increased auditory cortical representation in musicians. Nature, 392(6678), 811–814.

Panza, F., Lozupone, M., Sardone, R., Battista, P., Piccininni, M., Dibello, V., La Montagna, M., Stallone, R., Venezia, P., Liguori, A., et al. (2019). Sensorial frailty:

Age-related hearing loss and the risk of cognitive impairment and dementia in later life. Therapeutic Advances in Chronic Disease, 10, 2040622318811000.

Paquet-Durand, F., Silva, J., Talukdar, T., Johnson, L. E., Azadi, S., van Veen, T., Ueffing, M., Hauck, S. M., & Ekström, P. A. (2007). Excessive activation of poly (adp-ribose) polymerase contributes to inherited photoreceptor degeneration in the retinal degeneration 1 mouse. Journal of Neuroscience, 27(38), 10311–10319.

Park, E., Kim, H., Choi, I. H., Han, H. M., Han, K., Jung, H. H., & Im, G. J. (2020). Psychiatric distress as a common risk factor for tinnitus and joint pain: A national population-based survey. Clinical and Experimental Otorhinolaryngology, 13(3), 234.

Parthasarathy, A., & Kujawa, S. G. (2018). Synaptopathy in the aging cochlea: Characterizing early-neural deficits in auditory temporal envelope processing. Journal of Neuroscience, 38(32), 7108–7119.

Patel, N., Crider, A., Pandya, C. D., Ahmed, A. O., & Pillai, A. (2016). Altered mrna levels of glucocorticoid receptor, mineralocorticoid receptor, and co-chaperones (fkbp5 and ptges3) in the middle frontal gyrus of autism spectrum disorder subjects. Molecular Neurobiology, 53(4), 2090–2099.

Peixoto Pinheiro, B., Vona, B., Löwenheim, H., Rüttiger, L., Knipper, M., & Adel, Y. (2021). Age-related hearing loss pertaining to potassium ion channels in the cochlea and auditory pathway. Pflügers Archiv-European Journal of Physiology, 473(5), 823–840.

Penhune, V. B. (2011). Sensitive periods in human development: Evidence from musical training. Cortex, 47(9), 1126–1137.

Penrod, R. D., Kumar, J., Smith, L. N., McCalley, D., Nentwig, T. B., Hughes, B. W., Barry, G. M., Glover, K., Taniguchi, M., & Cowan, C. W. (2019). Activity-regulated cytoskeleton-associated protein (arc/arg3. 1) regulates anxiety-and novelty-related behaviors. Genes, Brain and Behavior, 18(7), e12561.

Pérez-González, D., & Malmierca, M. S. (2014). Adaptation in the auditory system: An overview. Frontiers in Integrative Neuroscience, 8, 19.

Perez-Valenzuela, C., Terreros, G., & Dagnino-Subiabre, A. (2019). Effects of stress on the auditory system: An approach to study a common origin for mood disorders and dementia. Reviews in the Neurosciences, 30(3), 317–324.

Persic, D., Thomas, M. E., Pelekanos, V., Ryugo, D. K., Takesian, A. E., Krumbholz, K., & Pyott, S. J. (2020). Regulation of auditory plasticity during critical periods and following hearing loss. Hearing Research, 397, 107976.

Picton, T. W., & Hillyard, S. A. (1974). Human auditory evoked potentials. ii: Effects of attention. Electroencephalography and Clinical Neurophysiology, 36, 191–200.

Pillsbury, H. C., Grose, J. H., & Hall, J. W. (1991). Otitis media with effusion in children: Binaural hearing before and after corrective surgery. Archives of Otolaryngology–Head & Neck Surgery, 117(7), 718–723.

Pirone, A., Alexander, J. M., Koenig, J. B., Cook-Snyder, D. R., Palnati, M., Wickham, R. J., Eden, L., Shrestha, N., Reijmers, L., Biederer, T., et al. (2018). Social stimulus causes aberrant activation of the medial prefrontal cortex in a mouse model with autism-like behaviors. Frontiers in Synaptic Neuroscience, 10, 35.

Poldrack, R. A., Temple, E., Protopapas, A., Nagarajan, S., Tallal, P., Merzenich, M., & Gabrieli, J. D. (2001). Relations between the neural bases of dynamic auditory processing and phonological processing: Evidence from fmri. Journal of Cognitive Neuroscience, 13(5), 687–697.

Polley, D. B., Thompson, J. H., & Guo, W. (2013). Brief hearing loss disrupts binaural integration during two early critical periods of auditory cortex development. Nature Communications, 4(1), 1–13.

Potter, L. R. (2011). Guanylyl cyclase structure, function and regulation. Cellular Signalling, 23(12), 1921–1926.

Pouille, F., & Scanziani, M. (2001). Enforcement of temporal fidelity in pyramidal cells by somatic feed-forward inhibition. Science, 293(5532), 1159–1163.

Pressnitzer, D., Sayles, M., Micheyl, C., & Winter, I. M. (2008). Perceptual organization of sound begins in the auditory periphery. Current Biology, 18(15), 1124–1128.

Prieto, G. A., Trieu, B. H., Dang, C. T., Bilousova, T., Gylys, K. H., Berchtold, N. C., Lynch, G., & Cotman, C. W. (2017). Pharmacological rescue of long-term potentiation in alzheimer diseased synapses. Journal of Neuroscience, 37(5), 1197–1212.

Pujol, R., & Puel, J.-L. (1999). Excitotoxicity, synaptic repair, and functional recovery in the mammalian cochlea: A review of recent findings. Annals of the New York Academy of Sciences, 884(1), 249–254.

Rankin, J., & Rinzel, J. (2022). Attentional control via synaptic gain mechanisms in auditory streaming. Brain Research, 1778, 147720.

Rao, Y. L., Ganaraja, B., Murlimanju, B., Joy, T., Krishnamurthy, A., & Agrawal, A. (2022). Hippocampus and its involvement in alzheimer's disease: A review. 3 Biotech, 12(2), 1–10.

Reim, D., & Schmeisser, M. J. (2017). Neurotrophic factors in mouse models of autism spectrum disorder: Focus on bdnf and igf-1. Translational Anatomy and Cell Biology of Autism Spectrum Disorder, 121–134.

Rendall, A. R., Ford, A. L., Perrino, P. A., & Holly Fitch, R. (2017). Auditory processing enhancements in the ts2-neo mouse model of timothy syndrome, a rare genetic disorder associated with autism spectrum disorders. Advances in Neurodevelopmental Disorders, 1(3), 176–189.

Reul, J., & Kloet, E. d. (1985). Two receptor systems for corticosterone in rat brain: Microdistribution and differential occupation. Endocrinology, 117(6), 2505–2511.

Rhode, W. S., & Smith, P. H. (1986). Encoding timing and intensity in the ventral cochlear nucleus of the cat. Journal of Neurophysiology, 56(2), 261–286.

Richard, D., & Lopez, C. (2013). Crh. Handbook of biologically active peptides (pp. 1084–1088). Elsevier.

Rinne, T., Balk, M. H., Koistinen, S., Autti, T., Alho, K., & Sams, M. (2008). Auditory selective attention modulates activation of human inferior colliculus. Journal of Neurophysiology, 100(6), 3323–3327.

Roth, R. H., Cudmore, R. H., Tan, H. L., Hong, I., Zhang, Y., & Huganir, R. L. (2020). Cortical synaptic ampa receptor plasticity during motor learning. Neuron, 105(5), 895–908.

Rowitch, D. H., Kispert, A., & McMahon, A. P. (1999). Pax-2 regulatory sequences that direct transgene expression in the developing neural plate and external granule cell layer of the cerebellum. Developmental Brain Research, 117(1), 99–108.

Ruel, J., Chabbert, C., Nouvian, R., Bendris, R., Eybalin, M., Leger, C. L., Bourien, J., Mersel, M., & Puel, J.-L. (2008). Salicylate enables cochlear arachidonic-acid-sensitive nmda receptor responses. Journal of Neuroscience, 28(29), 7313–7323.

Ruel, J., Nouvian, R., d'Aldin, C. G., Pujol, R., Eybalin, M., & Puel, J.-L. (2001). Dopamine inhibition of auditory nerve activity in the adult mammalian cochlea. European Journal of Neuroscience, 14(6), 977–986.

Russwurm, M., Russwurm, C., Koesling, D., & Mergia, E. (2013). No/cgmp: The past, the present, and the future. Guanylate Cyclase and Cyclic GMP, 1–16.

Rutherford, B. R., Brewster, K., Golub, J. S., Kim, A. H., & Roose, S. P. (2018). Sensation and psychiatry: Linking age-related hearing loss to late-life depression and cognitive decline. American Journal of Psychiatry, 175(3), 215–224.

Rutherford, M. A., von Gersdorff, H., & Goutman, J. D. (2021). Encoding sound in the cochlea: From receptor potential to afferent discharge. The Journal of Physiology, 599(10), 2527–2557.

Rüttiger, L., Sausbier, M., Zimmermann, U., Winter, H., Braig, C., Engel, J., Knirsch, M., Arntz, C., Langer, P., Hirt, B., Müller, M., Köpschall, I., Pfister, M., Münkner, S., Rohbock, K., Pfaff, I., Rüsch, A., Ruth, P., & Knipper, M. (2004). Deletion of the ca2+-activated potassium (bk) α-subunit but not the bkβ1-subunit leads to progressive hearing loss. Proceedings of the National Academy of Sciences, 101(35), 12922–12927.

Rüttiger, L., Zimmermann, U., & Knipper, M. (2017). Biomarkers for hearing dysfunction: Facts and outlook. ORL, 79(1-2), 93–111.

Ryan, A. F., Kujawa, S. G., Hammill, T., Le Prell, C., & Kil, J. (2016). Temporary and permanent noise-induced threshold shifts: A review of basic and clinical observations. Otology & Neurotology: official publication of the American Otological Society, American Neurotology Society [and] European Academy of Otology and Neurotology, 37(8), e271.

Sachs, M. B., & Abbas, P. J. (1974). Rate versus level functions for auditory-nerve fibers in cats: Tone-burst stimuli. The Journal of the Acoustical Society of America, 56(6), 1835–1847.

Sahaboglu, A., Tanimoto, N., Kaur, J., Sancho-Pelluz, J., Huber, G., Fahl, E., Arango-Gonzalez, B., Zrenner, E., Ekström, P., Löwenheim, H., et al. (2010). Parp1 gene knock-out increases resistance to retinal degeneration without affecting retinal function. PloS One, 5(11), e15495.

Sakurai, Y. (1990). Hippocampal cells have behavioral correlates during the performance of an auditory working memory task in the rat. Behavioral Neuroscience, 104(2), 253.

Salvi, R. J., Wang, J., & Ding, D. (2000). Auditory plasticity and hyperactivity following cochlear damage. Hearing Research, 147(1-2), 261–274.

Sanes, D. H. (2013). Synaptic and cellular consequences of hearing loss. Deafness (pp. 129–149). Springer.

Sanes, D. H. (2016). Mild hearing loss can impair brain function. Perspectives of the ASHA Special Interest Groups, 1(6), 4–16.

Sanes, D. H., & Woolley, S. M. (2011). A behavioral framework to guide research on central auditory development and plasticity. Neuron, 72(6), 912–929.

Sapolsky, R. M. (2015). Stress and the brain: Individual variability and the inverted-u. Nature Neuroscience, 18(10), 1344–1346.

Sapolsky, R. M., Romero, L. M., & Munck, A. U. (2000). How do glucocorticoids influence stress responses? integrating permissive, suppressive, stimulatory, and preparative actions. Endocrine Reviews, 21(1), 55–89.

Saunders, G., Field, D., & Haggard, M. (1992). A clinical test battery for obscure auditory dysfunction (oad): Development, selection and use of tests. British Journal of Audiology, 26(1), 33–42.

Schaette, R., & Kempter, R. (2009). Predicting tinnitus pitch from patients' audiograms with a computational model for the development of neuronal hyperactivity. Journal of Neurophysiology, 101(6), 3042–3052.

Schaette, R., & Kempter, R. (2012). Computational models of neurophysiological correlates of tinnitus. Frontiers in Systems Neuroscience, 6, 34.

Schaffert, N., Janzen, T. B., Mattes, K., & Thaut, M. H. (2019). A review on the relationship between sound and movement in sports and rehabilitation. Frontiers in Psychology, 10, 244.

Schimmang, T., Tan, J., Müller, M., Zimmermann, U., Rohbock, K., Köpschall, I., Limberger, A., Minichiello, L., & Knipper, M. (2003). Lack of bdnf and trkb signalling in the postnatal cochlea leads to a spatial reshaping of innervation along the tonotopic axis and hearing loss.

Schloesser, R. J., Martinowich, K., & Manji, H. K. (2012). Mood-stabilizing drugs: Mechanisms of action. Trends in Neurosciences, 35(1), 36–46.

Schmidt, H., Stonkute, A., Jüttner, R., Schäffer, S., Buttgereit, J., Feil, R., Hofmann, F., & Rathjen, F. G. (2007). The receptor guanylyl cyclase npr2 is essential for sensory axon bifurcation within the spinal cord. The Journal of Cell Biology, 179(2), 331–340.

Schönwiesner, M., Novitski, N., Pakarinen, S., Carlson, S., Tervaniemi, M., & Naatanen, R. (2007). Heschl's gyrus, posterior superior temporal gyrus, and mid-ventrolateral prefrontal cortex have different roles in the detection of acoustic changes. Journal of Neurophysiology, 97(3), 2075–2082.

Schultz, C., & Engelhardt, M. (2014). Anatomy of the hippocampal formation. The Hippocampus in Clinical Neuroscience, 34, 6–17.

Schulz, S. (2005). C-type natriuretic peptide and guanylyl cyclase b receptor. Peptides, 26(6), 1024–1034.

Sergeyenko, Y., Lall, K., Liberman, M. C., & Kujawa, S. G. (2013). Age-related cochlear synaptopathy: An early-onset contributor to auditory functional decline. Journal of Neuroscience, 33(34), 13686–13694.

Sharma, M., Bist, S. S., & Kumar, S. (2016). Age-related maturation of wave v latency of auditory brainstem response in children. Journal of Audiology & Otology, 20(2), 97.

Shi, Y., Thrippleton, M. J., Makin, S. D., Marshall, I., Geerlings, M. I., de Craen, A. J., Van Buchem, M. A., & Wardlaw, J. M. (2016). Cerebral blood flow in small vessel disease: A systematic review and meta-analysis. Journal of Cerebral Blood Flow & Metabolism, 36(10), 1653–1667.

Shibata, S., Kakazu, Y., Okabe, A., Fukuda, A., & Nabekura, J. (2004). Experience-dependent changes in intracellular cl- regulation in developing auditory neurons. Neuroscience Research, 48(2), 211–220.

Siemens, J., Lillo, C., Dumont, R. A., Reynolds, A., Williams, D. S., Gillespie, P. G., & Müller, U. (2004). Cadherin 23 is a component of the tip link in hair-cell stereocilia. Nature, 428(6986), 950–955.

Sihvonen, A. J., Särkämö, T., Leo, V., Tervaniemi, M., Altenmüller, E., & Soinila, S. (2017). Music-based interventions in neurological rehabilitation. The Lancet Neurology, 16(8), 648–660.

Silverman, J. L., Yang, M., Lord, C., & Crawley, J. N. (2010). Behavioural phenotyping assays for mouse models of autism. Nature Reviews Neuroscience, 11(7), 490–502.

Singer, W., Kasini, K., Manthey, M., Eckert, P., Armbruster, P., Vogt, M. A., Jaumann, M., Dotta, M., Yamahara, K., Harasztosi, C., Zimmermann, U., Knipper, M., & Rüttiger, L. (2018). The glucocorticoid antagonist mifepristone attenuates sound-induced long-term deficits in auditory nerve response and central auditory processing in female rats. The FASEB Journal, 32(6), 3005–3019.

Singer, W., Manthey, M., Panford-Walsh, R., Matt, L., Geisler, H.-S., Passeri, E., Baj, G., Tongiorgi, E., Leal, G., Duarte, C. B., Salazar, I. L., Eckert, P., Rohbock, K., Hu, J., Strotmann, J., Ruth, P., Zimmermann, U., Rüttiger, L., Ott, T., ... Knipper,

M. (2018). Bdnf-live-exon-visualization (blev) allows differential detection of bdnf transcripts in vitro and in vivo. Frontiers in Molecular Neuroscience, 325.

Sinha, Y., Silove, N., Hayen, A., & Williams, K. (2011). Auditory integration training and other sound therapies for autism spectrum disorders (asd). Cochrane Database of Systematic Reviews, (12).

Snyder, G. L., & Vanover, K. E. (2017). Pde inhibitors for the treatment of schizophrenia. Phosphodiesterases: CNS Functions and Diseases, 385–409.

Sobkowicz, H. M., August, B. K., & Slapnick, S. M. (2002). Influence of neurotrophins on the synaptogenesis of inner hair cells in the deaf bronx waltzer (bv) mouse organ of corti in culture. International Journal of Developmental Neuroscience, 20(7), 537–554.

Sohal, V. S., Zhang, F., Yizhar, O., & Deisseroth, K. (2009). Parvalbumin neurons and gamma rhythms enhance cortical circuit performance. Nature, 459(7247), 698–702.

Spirou, G. A., Davis, K. A., Nelken, I., & Young, E. D. (1999). Spectral integration by type ii interneurons in dorsal cochlear nucleus. Journal of Neurophysiology, 82(2), 648–663.

Stevens, K. E., Bullock, A. E., & Collins, A. C. (2001). Chronic corticosterone treatment alters sensory gating in c3h mice. Pharmacology Biochemistry and Behavior, 69(3-4), 359–366.

Steward, O., & Scoville, S. A. (1976). Cells of origin of entorhinal cortical afferents to the hippocampus and fascia dentata of the rat. Journal of Comparative Neurology, 169(3), 347–370.

Sugawara, M., Corfas, G., & Liberman, M. C. (2005). Influence of supporting cells on neuronal degeneration after hair cell loss. Journal of the Association for Research in Otolaryngology, 6(2), 136–147.

Sun, F., Zhou, K., Tian, K.-y., Zhang, X.-y., Liu, W., Wang, J., Zhong, C.-p., Qiu, J.-h., & Zha, D.-j. (2021). Atrial natriuretic peptide promotes neurite outgrowth and survival of cochlear spiral ganglion neurons in vitro through npr-a/cgmp/pkg signaling. Frontiers in Cell and Developmental Biology, 9, 1407.

Svirsky, M. A., Teoh, S.-W., & Neuburger, H. (2004). Development of language and speech perception in congenitally, profoundly deaf children as a function of age at cochlear implantation. Audiology and Neurotology, 9(4), 224–233.

Szeszko, P. R., Lehrner, A., & Yehuda, R. (2018). Glucocorticoids and hippocampal structure and function in ptsd. Harvard Review of Psychiatry, 26(3), 142–157.

Taberner, A. M., & Liberman, M. C. (2005). Response properties of single auditory nerve fibers in the mouse. Journal of Neurophysiology, 93(1), 557–569.

Takano, T. (2015). Interneuron dysfunction in syndromic autism: Recent advances. Developmental Neuroscience, 37(6), 467–475.

Tallal, P. (1980). Auditory temporal perception, phonics, and reading disabilities in children. Brain and Language, 9(2), 182–198.

Taoro-Gonzalez, L., Cabrera-Pastor, A., Sancho-Alonso, M., & Felipo, V. (2022). Intracellular and extracelluar cyclic gmp in the brain and the hippocampus. Vitamins and Hormones, 118, 247–288.

ten Cate, W.-J., Curtis, L., Rarey, K., & Small, G. (1993). Localization of glucocorticoid receptors and glucocorticoid receptor mrnas in the rat cochlea. The Laryngoscope, 103(8), 865–871.

ten Cate, W. J., Curtis, L. M., & Rarey, K. E. (1992). Immunochemical detection of glucocorticoid receptors within rat cochlear and vestibular tissues. Hearing Research, 60(2), 199–204.

Terakado, M., Kumagami, H., & Takahashi, H. (2011). Distribution of glucocorticoid receptors and 11 beta-hydroxysteroid dehydrogenase isoforms in the rat inner ear. Hearing Research, 280(1-2), 148–156.

Terreros, G., & Delano, P. H. (2015). Corticofugal modulation of peripheral auditory responses. Frontiers in Systems Neuroscience, 9, 134.

Tomas, F. J. B., Turko, P., Heilmann, H., Trimbuch, T., Yanagawa, Y., Vida, I., & Münster-Wandowski, A. (2020). Bdnf expression in cortical gabaergic interneurons. International Journal of Molecular Sciences, 21(5), 1567.

Tritsch, N. X., & Bergles, D. E. (2010). Developmental regulation of spontaneous activity in the mammalian cochlea. Journal of Neuroscience, 30(4), 1539–1550.

Tucsek, Z., Noa Valcarcel-Ares, M., Tarantini, S., Yabluchanskiy, A., Fülöp, G., Gautam, T., Orock, A., Csiszar, A., Deak, F., & Ungvari, Z. (2017). Hypertension-induced synapse loss and impairment in synaptic plasticity in the mouse hippocampus mimics the aging phenotype: Implications for the pathogenesis of vascular cognitive impairment. Geroscience, 39(4), 385–406.

Turner, H. A., Mitchell, K. J., Jones, L. M., Hamby, S., Wade Jr, R., & Beseler, C. L. (2019). Gun violence exposure and posttraumatic symptoms among children and youth. Journal of Traumatic Stress, 32(6), 881–889.

Tzingounis, A. V., & Nicoll, R. A. (2006). Arc/arg3. 1: Linking gene expression to synaptic plasticity and memory. Neuron, 52(3), 403–407.

Uran, S. L., Caceres, L. G., & Guelman, L. R. (2010). Effects of loud noise on hippocampal and cerebellar-related behaviors.: Role of oxidative state. Brain Research, 1361, 102–114.

Valero, M., Burton, J., Hauser, S., Hackett, T., Ramachandran, R., & Liberman, M. (2017). Noise-induced cochlear synaptopathy in rhesus monkeys (macaca mulatta). Hearing Research, 353, 213–223.

Van Eyken, E., Van Laer, L., Fransen, E., Topsakal, V., Lemkens, N., Laureys, W., Nelissen, N., Vandevelde, A., Wienker, T., Van De Heyning, P., et al. (2006). Kcnq4: A gene for age-related hearing impairment? Human Mutation, 27(10), 1007–1016.

Van Munster, J. J., Van der Valk, W. H., Stegeman, I., Lieftink, A. F., & Smit, A. L. (2020). The relationship of tinnitus distress with personality traits: A systematic review. Frontiers in Neurology, 11, 225.

Vazdarjanova, A., Ramirez-Amaya, V., Insel, N., Plummer, T. K., Rosi, S., Chowdhury, S., Mikhael, D., Worley, P. F., Guzowski, J. F., & Barnes, C. A. (2006). Spatial exploration induces arc, a plasticity-related immediate-early gene, only in calcium/calmodulin-dependent protein kinase ii-positive principal excitatory and inhibitory neurons of the rat forebrain. Journal of Comparative Neurology, 498(3), 317–329.

Vetter, D. E. (2015). Cellular signaling protective against noise-induced hearing loss–a role for novel intrinsic cochlear signaling involving corticotropin-releasing factor? Biochemical Pharmacology, 97(1), 1–15.

Viho, E. M., Buurstede, J. C., Mahfouz, A., Koorneef, L. L., Van Weert, L. T., Houtman, R., Hunt, H. J., Kroon, J., & Meijer, O. C. (2019). Corticosteroid action in the brain: The potential of selective receptor modulation. Neuroendocrinology, 109(3), 266–276.

Vinnik, E., Antopolskiy, S., Itskov, P. M., & Diamond, M. E. (2012). Auditory stimuli elicit hippocampal neuronal responses during sleep. Frontiers in Systems Neuroscience, 6, 49.

Vinogradova, O. (1975). Functional organization of the limbic system in the process of registration of information: Facts and hypotheses. The hippocampus (pp. 3–69). Springer.

Vogler, D. P., Robertson, D., & Mulders, W. H. (2011). Hyperactivity in the ventral cochlear nucleus after cochlear trauma. Journal of Neuroscience, 31(18), 6639–6645.

Von Bekesy, G., & Wever, E. G. (1960). Experiments in hearing (Vol. 195). McGraw-Hill New York.

Wan, G., Gomez-Casati, M. E., Gigliello, A. R., Liberman, M. C., & Corfas, G. (2014). Neurotrophin-3 regulates ribbon synapse density in the cochlea and induces synapse regeneration after acoustic trauma. eLife, 3, e03564.

Wang, Y., Fallah, E., & Olson, E. S. (2019). Adaptation of cochlear amplification to low endocochlear potential. Biophysical Journal, 116(9), 1769–1786.

Wang, Y., & Liberman, M. C. (2002). Restraint stress and protection from acoustic injury in mice. Hearing Research, 165(1-2), 96–102.

Wardle, R. A., & Poo, M.-m. (2003). Brain-derived neurotrophic factor modulation of gabaergic synapses by postsynaptic regulation of chloride transport. Journal of Neuroscience, 23(25), 8722–8732.

Waung, M. W., Pfeiffer, B. E., Nosyreva, E. D., Ronesi, J. A., & Huber, K. M. (2008). Rapid translation of arc/arg3. 1 selectively mediates mglur-dependent ltd through persistent increases in ampar endocytosis rate. Neuron, 59(1), 84–97.

Weinberger, N. M. (2015). New perspectives on the auditory cortex: Learning and memory. Handbook of Clinical Neurology, 129, 117–147.

Werker, J. F., & Hensch, T. K. (2015). Critical periods in speech perception: New directions. Annual Review of Psychology, 66, 173–196.

White, P. M., Kanazawa, A., & Yee, C. M. (2005). Gender and suppression of mid-latency erp components during stress. Psychophysiology, 42(6), 720–725.

Whitton, J. P., & Polley, D. B. (2011). Evaluating the perceptual and pathophysiological consequences of auditory deprivation in early postnatal life: A comparison of basic and clinical studies. Journal of the Association for Research in Otolaryngology, 12(5), 535–547.

Wiechers, B., Gestwa, G., Mack, A., Carroll, P., Zenner, H.-P., & Knipper, M. (1999). A changing pattern of brain-derived neurotrophic factor expression correlates with the rearrangement of fibers during cochlear development of rats and mice. Journal of Neuroscience, 19(8), 3033–3042.

Williamson, T. T., Zhu, X., Pineros, J., Ding, B., & Frisina, R. D. (2020). Understanding hormone and hormone therapies' impact on the auditory system. Journal of Neuroscience Research, 98(9), 1721–1730.

Williamson, T. T., Zhu, X., Walton, J. P., & Frisina, R. D. (2015). Auditory brainstem gap responses start to decline in mice in middle age: A novel physiological biomarker for age-related hearing loss. Cell and Tissue Research, 361(1), 359–369.

Wilson, B. S., Tucci, D. L., Merson, M. H., & O'Donoghue, G. M. (2017). Global hearing health care: New findings and perspectives. The Lancet, 390(10111), 2503–2515.

Wilson, B. S., Tucci, D. L., O'Donoghue, G. M., Merson, M. H., & Frankish, H. (2019). A lancet commission to address the global burden of hearing loss. The Lancet, 393(10186), 2106–2108.

Wittekindt, A., Kaiser, J., & Abel, C. (2014). Attentional modulation of the inner ear: A combined otoacoustic emission and eeg study. Journal of Neuroscience, 34(30), 9995–10002.

Witter, M. (2012). Hippocampus. The mouse nervous system (pp. 112–139). Elsevier.

Wollet, M., & Kim, J. H. (2022). Brain-derived neurotrophic factor is involved in activity-dependent tonotopic refinement of mntb neurons. Frontiers in Neural Circuits, 16.

Wolter, S., Möhrle, D., Schmidt, H., Pfeiffer, S., Zelle, D., Eckert, P., Krämer, M., Feil, R., Pilz, P. K., Knipper, M., & Rüttiger, L. (2018). Gc-b deficient mice with axon bifurcation loss exhibit compromised auditory processing. Frontiers in Neural Circuits, 12, 65.

Won, C., Lin, Z., Kumar T, P., Li, S., Ding, L., Elkhal, A., Szabo, G., & Vasudevan, A. (2013). Autonomous vascular networks synchronize gaba neuron migration in the embryonic forebrain. Nature Communications, 4(1), 1–14.

Wong, A. B., Jing, Z., Rutherford, M. A., Frank, T., Strenzke, N., & Moser, T. (2013). Concurrent maturation of inner hair cell synaptic ca2+ influx and auditory nerve spontaneous activity around hearing onset in mice. Journal of Neuroscience, 33(26), 10661–10666.

Wu, L.-G., Hamid, E., Shin, W., & Chiang, H.-C. (2014). Exocytosis and endocytosis: Modes, functions, and coupling mechanisms. Annual Review of Physiology, 76, 301–331.

Wu, P., Liberman, L., Bennett, K., De Gruttola, V., O'malley, J., & Liberman, M. (2019). Primary neural degeneration in the human cochlea: Evidence for hidden hearing loss in the aging ear. Neuroscience, 407, 8–20.

Xiong, Y., Mahmood, A., & Chopp, M. (2010). Angiogenesis, neurogenesis and brain recovery of function following injury. Current Opinion in Investigational Drugs (London, England: 2000), 11(3), 298.

Xu, H., Kotak, V. C., & Sanes, D. H. (2010). Normal hearing is required for the emergence of long-lasting inhibitory potentiation in cortex. Journal of Neuroscience, 30(1), 331–341.

Yao, X., & Rarey, K. E. (1996). Localization of the mineralocorticoid receptor in rat cochlear tissue. Acta Oto-Laryngologica, 116(3), 493–496.

Yates, G. K. (1991). Auditory-nerve spontaneous rates vary predictably with threshold. Hearing Research, 57(1), 57–62.

Yizhar, O., Fenno, L. E., Prigge, M., Schneider, F., Davidson, T. J., O'shea, D. J., Sohal, V. S., Goshen, I., Finkelstein, J., Paz, J. T., et al. (2011). Neocortical excitation/inhibition balance in information processing and social dysfunction. Nature, 477(7363), 171–178.

Yoon, Y. J., Lee, E. J., Hellstrom, S., & Kim, J. S. (2015). Atrial natriuretic peptide modulates auditory brainstem response of rat. Acta Oto-Laryngologica, 135(12), 1293–1297.

Young, E. D. (2012). Neural coding of sound with cochlear damage. Noise-induced hearing loss (pp. 87–135). Springer.

Yu, Y.-F., Zhai, F., Dai, C.-F., & Hu, J.-J. (2011). The relationship between age-related hearing loss and synaptic changes in the hippocampus of c57bl/6j mice. Experimental Gerontology, 46(9), 716–722.

Zahnert, T. (2011). The differential diagnosis of hearing loss. Deutsches Ärzteblatt International, 108(25), 433.

Zhang, H., Lin, S.-C., & Nicolelis, M. A. (2011). A distinctive subpopulation of medial septal slow-firing neurons promote hippocampal activation and theta oscillations. Journal of Neurophysiology, 106(5), 2749–2763.

Zhang, L., Wu, C., Martel, D. T., West, M., Sutton, M. A., & Shore, S. E. (2019). Remodeling of cholinergic input to the hippocampus after noise exposure and tinnitus induction in guinea pigs. Hippocampus, 29(8), 669–682.

Zhang, L., Wu, C., Martel, D. T., West, M., Sutton, M. A., & Shore, S. E. (2021). Noise exposure alters glutamatergic and gabaergic synaptic connectivity in the hippocampus and its relevance to tinnitus. Neural Plasticity, 2021.

Zhang, Y., Zhu, M., Sun, Y., Tang, B., Zhang, G., An, P., Cheng, Y., Shan, Y., Merzenich, M. M., & Zhou, X. (2021). Environmental noise degrades hippocampus-related learning and memory. Proceedings of the National Academy of Sciences, 118(1).

Zhao, T. C., & Kuhl, P. K. (2016). Effects of enriched auditory experience on infants' speech perception during the first year of life. Prospects, 46(2), 235–247.

Zheng, Y., Meng, M., Zhao, C., Liao, W., Zhang, Y., Wang, L., & Wen, E. (2014). Impact of environmental noise on growth and neuropsychological development of newborn rats. The Anatomical Record, 297(5), 949–954.

Zhou, X.-B., Wulfsen, I., Utku, E., Sausbier, U., Sausbier, M., Wieland, T., Ruth, P., & Korth, M. (2010). Dual role of protein kinase c on bk channel regulation. Proceedings of the National Academy of Sciences, 107(17), 8005–8010.

Zidanic, M., & Fuchs, P. A. (1995). Kinetic analysis of barium currents in chick cochlear hair cells. Biophysical Journal, 68(4), 1323–1336.

Zuccotti, A., Kuhn, S., Johnson, S. L., Franz, C., Singer, W., Hecker, D., Geisler, H.-S., Köpschall, I., Rohbock, K., Gutsche, K., Dlugaiczyk, J., Schick, Marcotti, W., Rüttiger, L., Schimmang, T., & Knipper, M. (2012). Lack of brain-derived neurotrophic factor hampers inner hair cell synapse physiology, but protects against noise-induced hearing loss. Journal of Neuroscience, 32(25), 8545–8553.

zum Gottesberge, A. M., Gagelmann, M., & Forssmann, W. (1991). Atrial natriuretic peptide-like immunoreactive cells in the guinea pig inner ear. Hearing Research, 56(1-2), 86–92.

frontiers in Molecular Neuroscience

ORIGINAL RESEARCH
published: 26 March 2021
doi: 10.3389/fnmol.2021.642679

Deletion of BDNF in Pax2 Lineage-Derived Interneuron Precursors in the Hindbrain Hampers the Proportion of Excitation/Inhibition, Learning, and Behavior

*Philipp Eckert[1†], Philine Marchetta[1†], Marie K. Manthey[1,2†], Michael H. Walter[3], Sasa Jovanovic[4], Daria Savitska[1], Wibke Singer[1], Michele H. Jacob[2], Lukas Rüttiger[1], Thomas Schimmang[5], Ivan Milenkovic[4], Peter K. D. Pilz[3] and Marlies Knipper[1]**

[1] Department of Otolaryngology, Head and Neck Surgery, Tübingen Hearing Research Centre, Molecular Physiology of Hearing, University of Tübingen, Tübingen, Germany, [2] Department of Neuroscience, Sackler School of Biomedical Sciences, Tufts University School of Medicine, Boston, MA, United States, [3] Department for Animal Physiology, Institute of Neurobiology, University of Tübingen, Tübingen, Germany, [4] School of Medicine and Health Sciences, Carl von Ossietzky University Oldenburg, Oldenburg, Germany, [5] Instituto de Biología y Genética Molecular, Consejo Superior de Investigaciones Científicas, Universidad de Valladolid, Valladolid, Spain

OPEN ACCESS

Edited by:
Xiao-Dong Wang, Zhejiang University, China

Reviewed by:
Yun-Ai Su, Peking University Sixth Hospital, China
Qi Zhang, Shanghai Jiao Tong University, China

***Correspondence:**
Marlies Knipper
marlies.knipper@uni-tuebingen.de

[†]These authors have contributed equally to this work

Received: *16 December 2020*
Accepted: *26 February 2021*
Published: *26 March 2021*

Citation:
Eckert P, Marchetta P, Manthey MK, Walter MH, Jovanovic S, Savitska D, Singer W, Jacob MH, Rüttiger L, Schimmang T, Milenkovic I, Pilz PKD and Knipper M (2021) Deletion of BDNF in Pax2 Lineage-Derived Interneuron Precursors in the Hindbrain Hampers the Proportion of Excitation/Inhibition, Learning, and Behavior. Front. Mol. Neurosci. 14:642679. doi: 10.3389/fnmol.2021.642679

Numerous studies indicate that deficits in the proper integration or migration of specific GABAergic precursor cells from the subpallium to the cortex can lead to severe cognitive dysfunctions and neurodevelopmental pathogenesis linked to intellectual disabilities. A different set of GABAergic precursors cells that express Pax2 migrate to hindbrain regions, targeting, for example auditory or somatosensory brainstem regions. We demonstrate that the absence of BDNF in Pax2-lineage descendants of *Bdnf*^{Pax2}KOs causes severe cognitive disabilities. In *Bdnf*^{Pax2}KOs, a normal number of parvalbumin-positive interneurons (**PV-IN**s) was found in the auditory cortex (**AC**) and hippocampal regions, which went hand in hand with reduced PV-labeling in neuropil domains and elevated activity-regulated cytoskeleton-associated protein (**Arc/Arg3.1**; here: **Arc**) levels in pyramidal neurons in these same regions. This immaturity in the inhibitory/excitatory balance of the AC and hippocampus was accompanied by elevated LTP, reduced (sound-induced) LTP/LTD adjustment, impaired learning, elevated anxiety, and deficits in social behavior, overall representing an autistic-like phenotype. Reduced tonic inhibitory strength and elevated spontaneous firing rates in dorsal cochlear nucleus (**DCN**) brainstem neurons in otherwise nearly normal hearing *Bdnf*^{Pax2}KOs suggests that diminished fine-grained auditory-specific brainstem activity has hampered activity-driven integration of inhibitory networks of the AC in functional (hippocampal) circuits. This leads to an inability to scale hippocampal post-synapses during LTP/LTD plasticity. BDNF in Pax2-lineage descendants in lower brain regions should thus be considered as a novel candidate for contributing to the development of brain disorders, including autism.

Keywords: BDNF, Pax2, Arc/Arg3.1, GABAergic interneuron, parvalbumin interneuron, autism spectrum disorder

INTRODUCTION

Current views suggest that γ-aminobutyric acid (**GABA**) interneurons (**INs**) that populate the cerebral cortex, striatum, hippocampus, or olfactory bulb, mainly derive from progenitor cells in the subpallium, from where they migrate in multiple streams to reach their destinations (Guo and Anton, 2014). Numerous studies suggest that dysfunctions of cortical GABAergic INs are linked with various neurodevelopmental disorders (Marin, 2012; Gao and Penzes, 2015; Uehara et al., 2015; Canetta et al., 2016; Ferguson and Gao, 2018; Lim et al., 2018; Skene et al., 2018; Lunden et al., 2019; Miyoshi, 2019; Wei et al., 2020).

Whereas the intrinsic migratory fate of subpallium-derived GABAergic IN precursors is characterized by the expression of the transcription factors Pax6 (Guo and Anton, 2014), Pax2-expressing (**Pax2+**) GABAergic IN precursors migrate from the ventricular zones to lower brain levels, such as the cerebellum (**Cb**), hindbrain and spinal cord, which are posterior to midbrain regions (Nornes et al., 1990; Maricich and Herrup, 1999; Rowitch et al., 1999; Larsson, 2017), and to a few thalamic frontal brain regions (Maricich and Herrup, 1999; Fotaki et al., 2008).

The role of Pax2-lineage descendants in brain function, particularly for higher brain function or neurodevelopmental disorders, is elusive. We have previously observed that a deletion of brain-derived nerve growth factor (**BDNF**) under the Pax2 promoter in *Bdnf*^{Pax2}KOs leads to circling behavior and does not profoundly alter basal auditory function, but diminishes fast auditory processing (Zuccotti et al., 2012; Chumak et al., 2016).

With sensory experience, fast auditory processing matures after hearing onset by the maturation of improved receptive fields following integration of inhibitory cortical networks into functional fronto-striatal circuits (Xu et al., 2010). Proper integration of inhibitory networks in functional fronto-striatal circuits is a predicted prerequisite for improved auditory perception and memory-dependent signal amplification processes (Kraus and White-Schwoch, 2015; Weinberger, 2015; Irvine, 2018; Knipper et al., 2020). Fast auditory processing is also suggested to be essential for memory-dependent central auditory adjustment processes following enriching sound exposure (**SE**) or auditory deprivation (Matt et al., 2018; Knipper et al., 2020). Accordingly, long-term plasticity changes following SE or auditory deprivation can be monitored through altered levels of activity-regulated cytoskeleton-associated protein (**Arc/Arg3.1**; here: **Arc**) and parvalbumin (**PV**) in the AC and hippocampus and through correlating changes in long-term potentiation (**LTP**) in hippocampal CA1 pyramidal neurons (Matt et al., 2018; Marchetta et al., 2020). Therefore, sound-induced adjustment processes are likely to be reflected by altered plasticity changes in the AC and hippocampus.

We here demonstrate that BDNF deletion in Pax2-lineage descendants in hindbrain regions of *Bdnf*^{Pax2}KO mice leads to elevated thresholds, lower dynamic range and diminished inhibitory strength of auditory brainstem responses in the DCN. *Bdnf*^{Pax2}KO mice moreover exhibit reduced PV-IN and elevated Arc labeling in the AC and hippocampus, suggesting that diminished auditory brainstem output activity has hampered activity-dependent integration of cortical GABAergic INs into functional hippocampal circuits. Accordingly, *Bdnf*^{Pax2}KOs developed elevated hippocampal LTP, deficits in LTP and long-term depression (**LTD**) adjustment to SE, and deficits in learning, social behavior, or anxiety control, altogether resembling an autistic-like phenotype. The role of BDNF in Pax2-lineage descendants in lower hindbrain regions thus needs to be revisited in the context of neurodevelopmental disorders, such as autism spectrum disorder (**ASD**).

RESULTS

BDNF Is Present in Pax2-Lineage Descendants in Brainstem and Hypothalamic Regions but Not in Cortical and Hippocampal Regions

The use of Rosa^{tdTomato} reporter mice (Madisen et al., 2010) crossed with Pax2-Cre mice, here called Pax2-CRE-Rosa^{tdTomato} mice, allowed us to efficiently visualize Cre-directed gene expression through native red fluorescence simultaneously with BDNF mRNA. We combined labeling for BDNF mRNA and PV-protein with tdTomato fluorescence to specify presumptive BDNF-expressing (**BDNF+**) Pax2-Cre descendent neurons during the maturation process of PV-INs throughout the critical developmental time period after hearing onset between P10-P14. This is the time period when cortical PV-IN networks are integrated in functional fronto-striatal circuits after tangential migrating GABAergic INs have reached their final destination (Kimura and Itami, 2019). We found that BDNF was expressed in Pax2-lineage descendants during the critical developmental time period and in adults in neuronal cells of the auditory brainstem but not in frontal brain regions. Representative images are shown for distinct regions between P10 and P14 or at the adult stage, such as the DCN (**Figure 1A**, left panel P14; right panel adult), inferior colliculus (**IC**; **Figure 1B**, left panel P10; right panel adult) and the anterior hypothalamic area (**AHA**; **Figure 1C**, P12). No labeling was observed in thalamic and frontal regions such as the hippocampus (**Figure 1D**, left panel P14; right panel adult), the AC (**Figure 1E**, left panel P14; right panel adult), superior colliculus (**SC**; **Figure 1F**, adult), visual cortex (**V1**; **Figure 1G**, adult), or somatosensory cortex (not shown). In the Cb an overlap of BDNF mRNA and tdTomato expression was only seen at P10 but not beyond this stage (**Figure 1H**, left panel P10; right panel adult).

In conclusion, BDNF is found in Pax2-lineage descendants in lower brainstem regions and AHA, but not in the thalamus, Cb, or frontal cortical regions including the hippocampus, visual and somatosensory systems.

Bdnf^{Pax2}KOs Exhibit Reduced PV-IN Labeling in Neuropil Regions and Elevated Levels of Arc in the AC and Hippocampus

Given that *Bdnf*^{Pax2}KO mice show diminished auditory processing (Zuccotti et al., 2012; Chumak et al., 2016) which

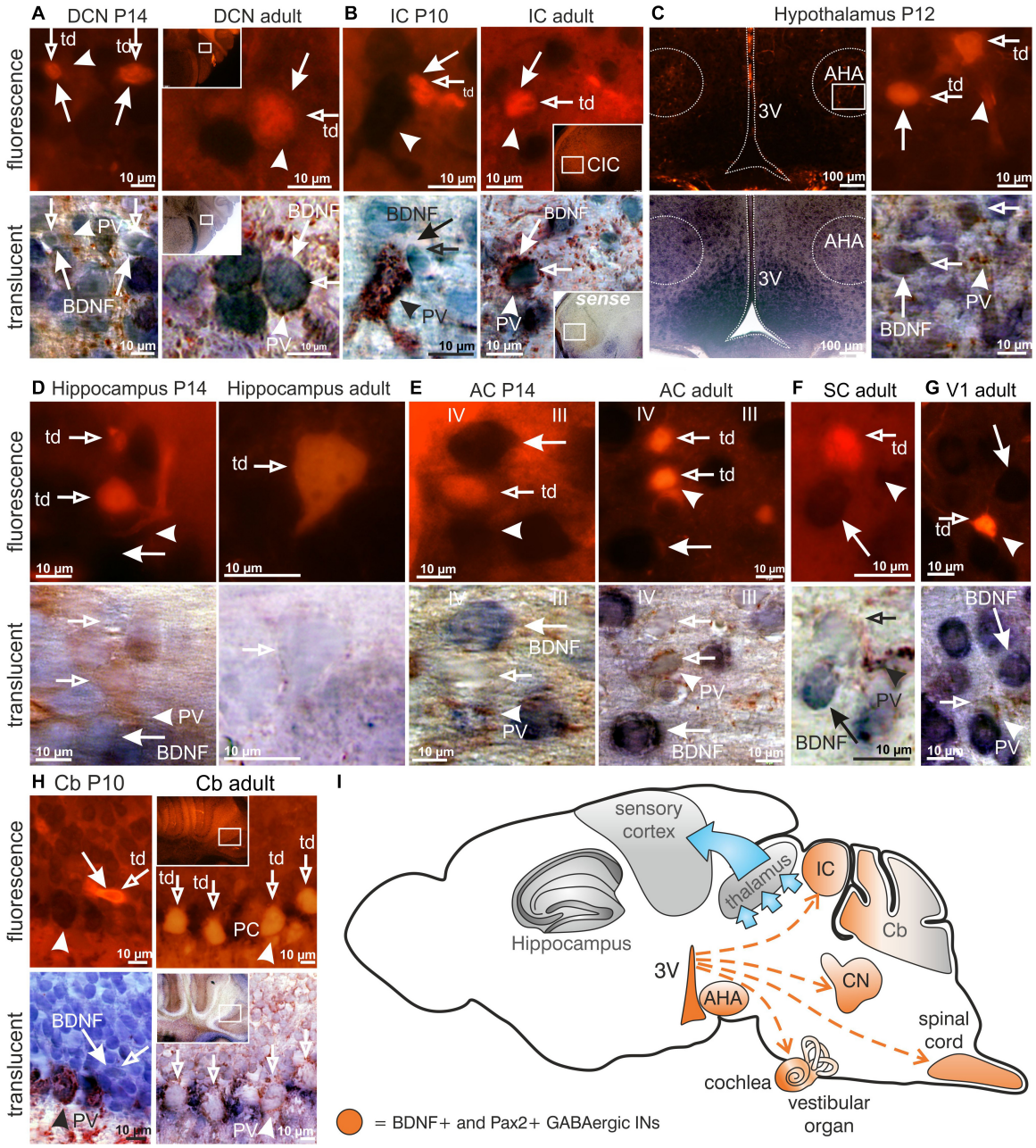

FIGURE 1 | Brain-derived nerve growth factor expression in Pax2-CRE-Rosa^{tdTomato} reporter mice. **(A)** In P14 and adult Pax2-CRE-Rosa^{tdTomato} mice Pax2-Cre (⇀) in the DCN, **(B)** as well as in the P10 and adult IC was co-localized with BDNF mRNA (⇀) and PV (▶). **(C)** In Pax2-CRE-Rosa^{tdTomato} reporter mice at the age of P12, Pax2 (⇀) in the anterior hypothalamic area (APA) was co-localized with BDNF mRNA (⇀), as well as with PV (▶). **(D,E)** Pax2-CRE-Rosa^{tdTomato} reporter mice showed neither co-localization of Pax2+ cells (⇀) with BDNF mRNA (⇀) in between layer III and IV in the AC at the age of P14, nor did adult animals. They also did not show co-localization of Pax2+ cells (⇀) with BDNF mRNA (⇀) in the CA1 region at the age of P14 or in adult animals. **(F)** Adult Pax2-CRE-Rosa^{tdTomato} reporter mice showed no co-localization of Pax2-Cre (⇀) with BDNF mRNA (⇀) in the superior colliculus, **(G)** visual cortex, **(H)**, as well as in the adult Cb. The Purkinje cells were surrounded by PV (⇀). At P10, some fusiform-shaped Pax2+ cells (⇀) overlapped with BDNF mRNA (⇀). **(I)** Scheme of BDNF+ Pax2-lineage descendants migration (red dashed arrows) to the cochlea, DCN, IC and AHA starting in the third ventricle (3V). Scale bar = 10 µM with the exception of **(E)** left panel, where it is 100 µm.

has been shown to influence plasticity genes and LTP in hippocampal circuits (Matt et al., 2018), we considered an impact of BDNF+ Pax2-lineage descendants in lower brainstem regions on higher brain functions. To test this hypothesis we analyzed PV immunostaining as a marker for fast-spiking, GABAergic INs (Cardin et al., 2009; Hu et al., 2014; Kim et al., 2016). As a marker for excitatory neurons, we analyzed the expression of Arc, which is preferentially

expressed in these neurons (Tzingounis and Nicoll, 2006; Bramham et al., 2008).

Neuronal cell counts of PV-INs in *Bdnf*^{Pax2}KO mice revealed no differences compared to controls as shown for the AC in layer III/IV [**Figures 2A,B**; unpaired two-tailed student's *t*-test, $t(14) = 0.4877$, $P = 0.6333$, $n = 8$ mice each] and the hippocampus [**Figures 2B,C**; unpaired two-tailed student's *t*-test, $t(14) = 0.7959$, $P = 0.4377$, $n = 8$ mice each]. This observation indicates that in *Bdnf*^{Pax2}KO mice, GABAergic INs of cortical and hippocampal regions have successfully reached their destination.

Next, we focused on PV-IN labeling in neuropil domains which are enriched in dendritic synapses and filopodia as for instance in layer III/IV of the AC, or the stratum radiatum and stratum lucidum of hippocampal CA1/CA3 regions, respectively. Quantification of PV-IN, and Arc mRNA levels revealed a strikingly reduced staining of PV-IN, parallel to the elevated Arc mRNA levels in *Bdnf*^{Pax2}KOs, as compared to controls (**Figure 2**). This was shown for layer III/IV in the AC [**Figures 2A,D**; unpaired two-tailed student's *t*-test, PV: $t(8) = 9.482$, $P < 0.0001$, Arc: $t(8) = 2.686$, $P = 0.0277$, $n = 5$ mice each] and for the hippocampus in the stratum pyramidale and stratum radiatum of the CA1 region [**Figures 2C,E**; unpaired two-tailed student's *t*-test, PV: $t(6) = 7.816$, $P = 0.0002$, Arc: $t(6) = 2.586$, $P = 0.0415$, $n = 4$ mice each] as well as for the CA3 region [**Figure 2H**; unpaired two-tailed student's *t*-test, PV: $t(8) = 2.718$, $P = 0.0263$, Arc: $t(6) = 3.501$, $P = 0.0128$, $n = 4$ mice each]. The levels of BDNF mRNA were not different between *Bdnf*^{Pax2}KOs and controls [**Figures 2F,G,I**; unpaired two-tailed student's *t*-test, AC: $t(8) = 1.262$, $P = 0.2426$, $n = 5$ mice each, CA1: $t(6) = 0.07922$, $P = 0.9394$, $n = 4$ mice each, CA3: $t(8) = 0.2594$, $P = 0.8019$, $n = 4$ mice each]. In the same sections in which no difference of BDNF mRNA levels was observed, elevated levels of Arc protein were visible; this was shown for the AC [**Figure 2F**; unpaired two-tailed student's *t*-test, $t(6) = 2.519$, $P = 0.0453$], and for the hippocampus in CA1 [**Figure 2G**; unpaired two-tailed student's *t*-test, $t(6) = 6.526$, $P = 0.0006$] and CA3 regions [**Figure 2I**; unpaired two-tailed student's *t*-test, $t(8) = 3.762$, $P = 0.0055$].

Therefore, although normal numbers of PV-INs were observed in *Bdnf*^{Pax2}KOs they showed reduced staining in their dendrites parallel to increased Arc levels. To explore to what extent this imbalance in inhibitory/excitatory markers may be the result of disturbed sculpting of PV-IN neurons by sensory experience, we analyzed the labeling of PV-INs prior to the critical plasticity period – between P6-P10, when in rodents sensory functions are still immature (de Villers-Sidani et al., 2007) – and toward its end (P14), as well as in adults (**Figure 3**).

In controls, between P6-P10 and at P14, we observed a significant elevation of PV protein staining in hippocampal regions, as shown for CA1 [**Figure 3A**; 2-way ANOVA, Genotype: $F(1,26) = 27.10$, $P < 0.0001$, Age: $F(2,26) = 17.45$, $P < 0.0001$, n = 4-7 mice] and CA3 regions [**Figure 3B**; 2-way ANOVA, Genotype: $F(1,28) = 80.16$, $P < 0.0001$, Age: $F(2,28) = 5.049$, $P < 0.05$, Interaction: $F(2,28) = 11.76$, $P = 0.0002$, n = 4-7 mice]. In *Bdnf*^{Pax2}KOs, at P6-P10, the level of PV protein staining was not different from controls (**Figures 3A,B**; Bonferroni's *post hoc* test: CA1: $P > 0.05$, CA3: $P > 0.05$, $n = 7$ mice each). However, at P14 and in adults, the levels of PV protein in *Bdnf*^{Pax2}KOs remained low [**Figures 3A,B**; lower panels; Bonferroni's *post hoc* test: P14: CA1: $P < 0.05$, CA3: $P < 0.0001$, $n = 4$ mice each, adult: CA1: $P < 0.05$, CA3: $P < 0.0001$, $n = 4$ (control) or 5 (*Bdnf*^{Pax2}KO) each]. These observations indicate a significantly attenuated maturation of dendritic outgrowth of PV-INs in *Bdnf*^{Pax2}KOs. This was also shown for the AC at P14 [**Figures 3C,D** left panel; unpaired two-tailed student's *t*-test, $t(6) = 6.229$, $P = 0.0008$, $n = 4$ mice each] and in adults [**Figures 3C,D**, right panel; unpaired two-tailed student's *t*-test, $t(8) = 6.165$, $P = 0.0003$, $n = 4$ mice each].

In order to explore if lower PV-IN labeling in the AC and hippocampus of *Bdnf*^{Pax2}KOs may be associated with specific sensory modalities, PV labeling was also analyzed in the somatosensory cortex (**Figure 3E**) and Cb (**Figure 3F**). At P14, a time point for specific refinement of sensory coding in the barrel cortex (van der Bourg et al., 2017), sections were co-labeled for PV (**Figure 3E**, red) and the vesicular glutamate receptor 2 (**vGluT2**; **Figure 3E**, green), used to follow proper column formation (Sun, 2009). No difference between PV-IN levels was observed between controls and *Bdnf*^{Pax2}KOs (**Figure 3E**). Also for the Cb, staining for PV-INs was not significantly different between controls and *Bdnf*^{Pax2}KO mice [**Figure 3F**; unpaired two-tailed student's *t*-test, $t(4) = 1.104$, $P = 0.3314$, $n = 3$ mice each]. This result suggests that the reduced PV-IN labeling intensity in *Bdnf*^{Pax2}KOs may not be a common feature of all sensory cortices.

In conclusion, deletion of BDNF in Pax2-lineage descendants in brainstem regions results in diminished PV-IN labeling independently from the number of PV-INs in the AC and in the hippocampus from the end of the critical period at P14 onward. From P14 onward, reduced dendritic PV-IN labeling and elevated Arc levels are observed.

Bdnf^{Pax2}KOs Exhibit Elevated LTP and Reduced LTD

Reduced labeling of dendrites in PV-INs linked to elevated Arc levels may indicate impaired integration of inhibitory PV-INs of the AC into functional hippocampal circuits. To test proper hippocampal function of *Bdnf*^{Pax2}KOs, we first analyzed LTP by recording field excitatory postsynaptic potentials (**fEPSP**s) from acute forebrain slices at the CA3 to CA1 Schaffer's collateral in the stratum radiatum. Interestingly, compared to controls, in *Bdnf*^{Pax2}KOs the elevated Arc levels were linked to significantly higher fEPSP amplitudes, observed after high-frequency stimulation (1 s, 100 Hz) of the Schaffer's collateral over the entire recording time period of 60 min (**Figure 4A**, left panel). Calculation of the mean of the last 10 min showed significantly higher LTP in *Bdnf*^{Pax2}KOs [**Figure 4A**, right panel, white vs. red bar; 1-way ANOVA, $F(5,62) = 42.81$, $P < 0.0001$, control: $n = 9/14$, *Bdnf*^{Pax2}KO: $n = 9/13$, P6-P10 controls: $n = 6/7$ mice/slices, Bonferroni's *post hoc* test: $P < 0.001$]. To examine whether elevated fEPSP amplitudes in *Bdnf*^{Pax2}KOs may be linked to the prevailing immaturity of the hippocampal PV-IN network (**Figure 3**), fEPSP slopes were also determined in acute brain slices from P6-P10 mice prior to the

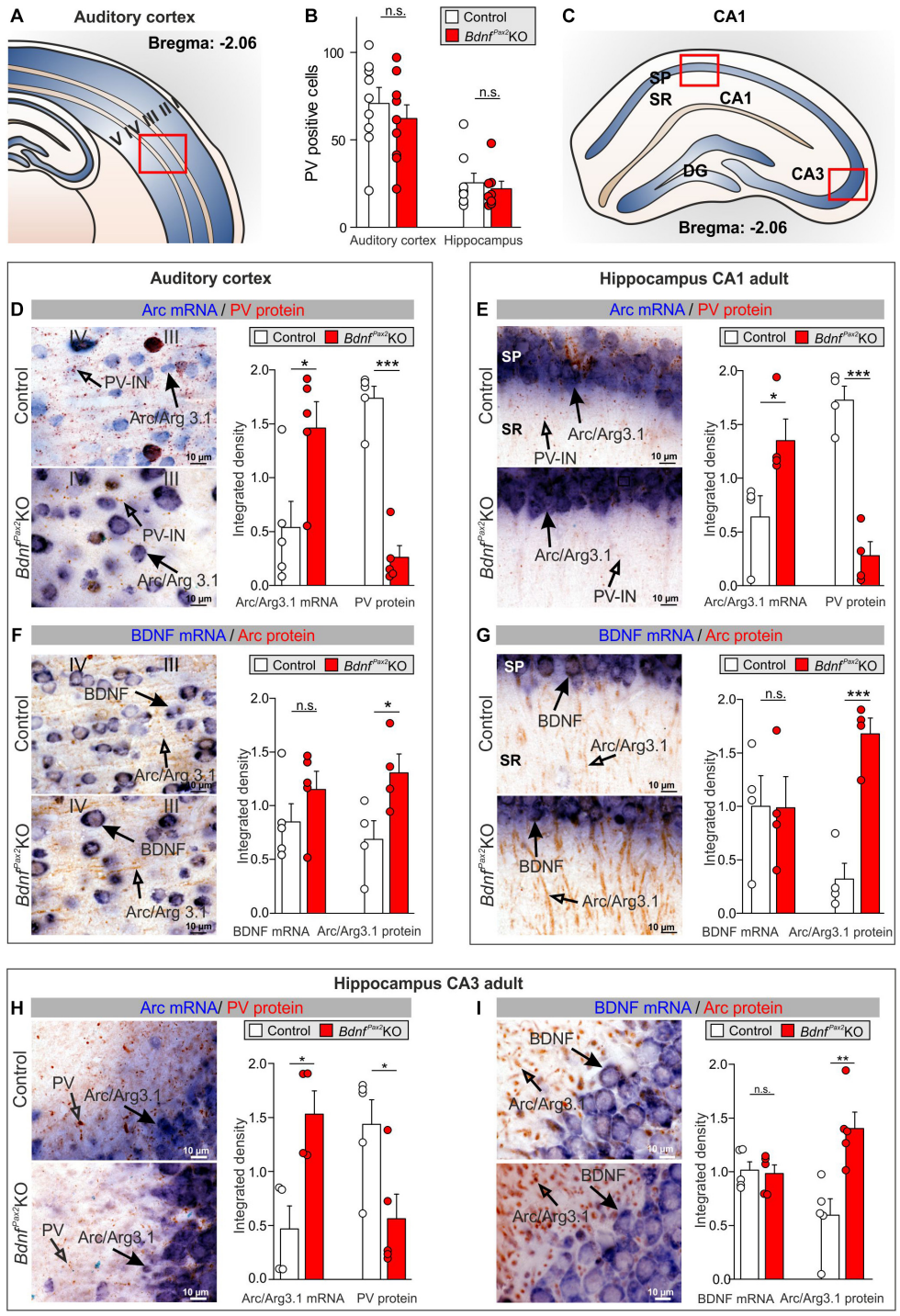

FIGURE 2 | Parvalbumin immunostaining and Arc/BDNF expression in *Bdnf*^{Pax2}KOs. **(A)** Scheme of the AC with layers I to V. **(B)** No difference in number of PV+ cells in the AC and hippocampus between *Bdnf*^{Pax2}KOs and controls (n = 8 each; $P > 0.05$). **(C)** Scheme of the hippocampus with CA1 and CA3 region and DG. **(D)** *Bdnf*^{Pax2}KOs showed increased Arc mRNA (→, n = 5 each; $P = 0.028$) and decreased PV protein levels (↠, n = 5 each; $P < 0.0001$) in the AC in comparison to controls, as well as **(E)** increased Arc mRNA (→, n = 4 each; $P = 0.042$) and decreased perisomatic and dendritic PV protein levels (↠, n = 4 each; $P < 0.001$) in the hippocampal CA1 region. **(F)** *Bdnf*^{Pax2}KOs revealed similar levels of BDNF mRNA in the AC (→, n = 5 each; $P = 0.243$), but increased Arc protein (↠, n = 4 each; $P = 0.0453$) compared to controls. **(G)** BDNF mRNA (→, n = 4 each; $P = 0.979$) remained unaltered in *Bdnf*^{Pax2}KOs, while Arc protein (↠, n = 4 each; $P < 0.001$) was increased in hippocampal CA1 regions in comparison to controls. Scale bar **(C–F)** = 10 µm, **(G)** = 100 µm. Mean ± S.E.M. **(H)** *Bdnf*^{Pax2}KOs showed increased Arc mRNA (→, n = 4 each; $P = 0.013$) and decreased perisomatic and dendritic PV protein levels (↠, n = 4 each; $P = 0.026$) in the hippocampal CA3 region in comparison to controls. **(I)** BDNF mRNA (→, n = 4 each; $P = 0.90$) remained unaltered in *Bdnf*^{Pax2}KOs, while Arc protein (↠, n = 4 each; $P = 0.006$) was increased in hippocampal CA3 regions, in comparison to controls. n.s. = $P > 0.05$, * = $P < 0.05$, ** = $P < 0.01$, *** = $P < 0.001$.

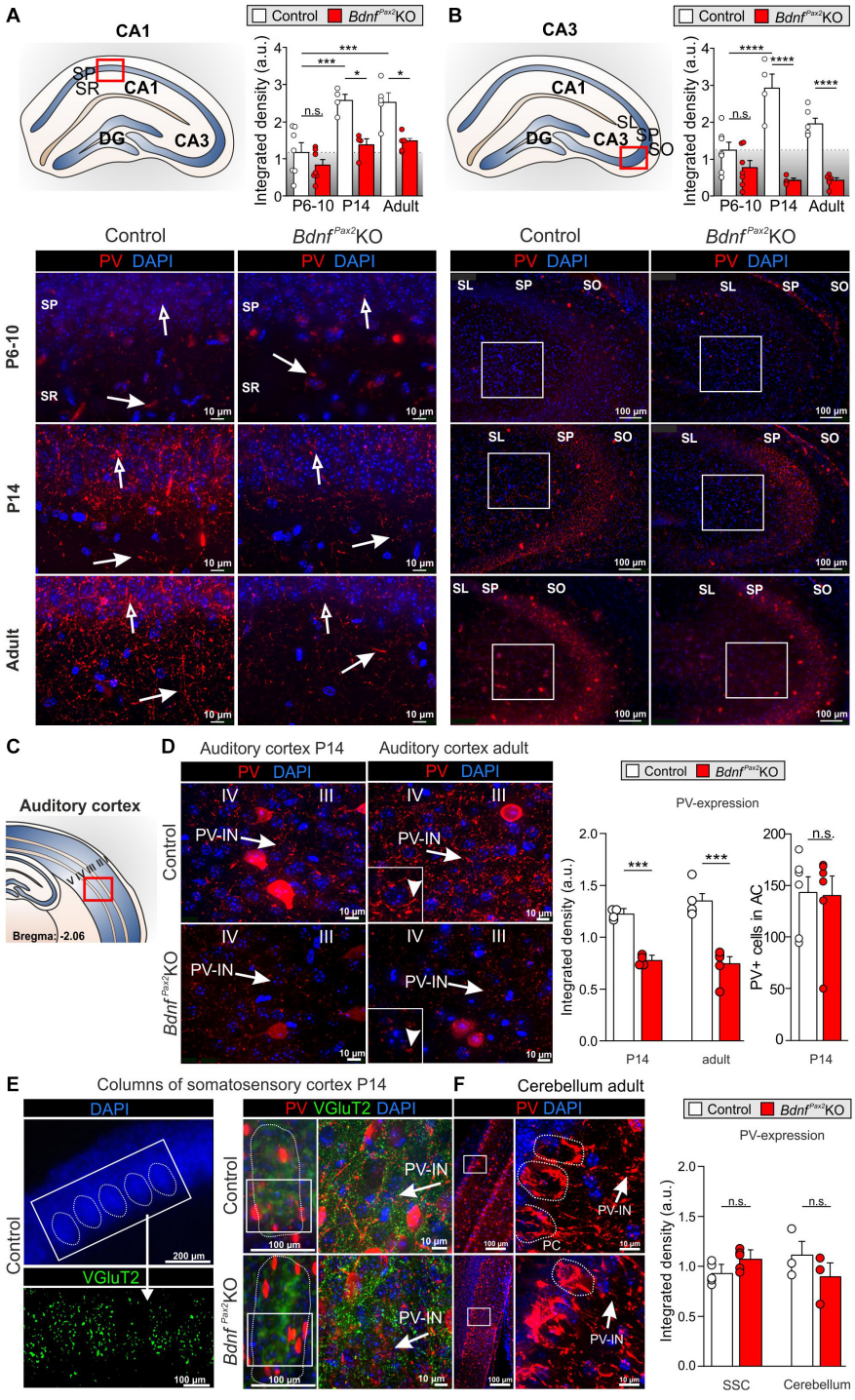

FIGURE 3 | Parvalbumin immunostaining in *Bdnf*^{Pax2}KOs during hearing onset. **(A)** Immunostaining of perisomatic PV (→) and dendritic PV (⊳) in the CA1 region during development. Scale bar = 10 µm. Right panel: Quantification of PV-IN fluorescence intensity in the CA1 region during development (n = 4-7 each, Genotype: $P < 0.0001$; Age: $P < 0.0001$). **(B)** Immunostaining of perisomatic PV (→) in the CA3 of adult *Bdnf*^{Pax2}KOs and controls. Right panel: Quantification of the PV expression in the CA3 region (see white squares; n = 4-7 each, Genotype: $P < 0.0001$; Age: $P < 0.05$; Interaction: $P < 0.001$). **(C)** Scheme of the hippocampus, with CA1 and CA3 region and dentate gyrus (DG), and the AC with layers I to V. **(D)** Decreased expression of perisomatic (→) and dendritic (▶) PV-IN in the AC of adult *Bdnf*^{Pax2}KOs (n = 5 each; $P < 0.001$) and P14 *Bdnf*^{Pax2}KOs (n = 4 each; $P < 0.001$), in comparison to controls, while no difference in number of PV + cells in the adult AC was seen (n = 6 each; $P > 0.05$). **(E)** Left panel, exemplary picture for SSC columns. Middle panel: Normal development of columns in the SSC of P14 *Bdnf*^{Pax2}KOs (red: PV; green: vGluT2). Left panel: Similar PV expression in SSC of P14 *Bdnf*^{Pax2}KOs (n = 5 each; P = 0.303), compared to controls. **(F)** Normal PV expression was observed in the Cb of *Bdnf*^{Pax2}KOs (n = 3 each; P = 0.331). Nuclear staining DAPI (blue). Scale bar **(A,B,D–F)** right panels: 10 µm; **(E)** lower left and middle panels, **(F)** left panel: 100 µm; **(E)** upper panel: 200 µm. Mean ± S.E.M. n.s. = $P > 0.05$, * = $P < 0.05$, *** = $P < 0.001$, **** = $P < 0.0001$.

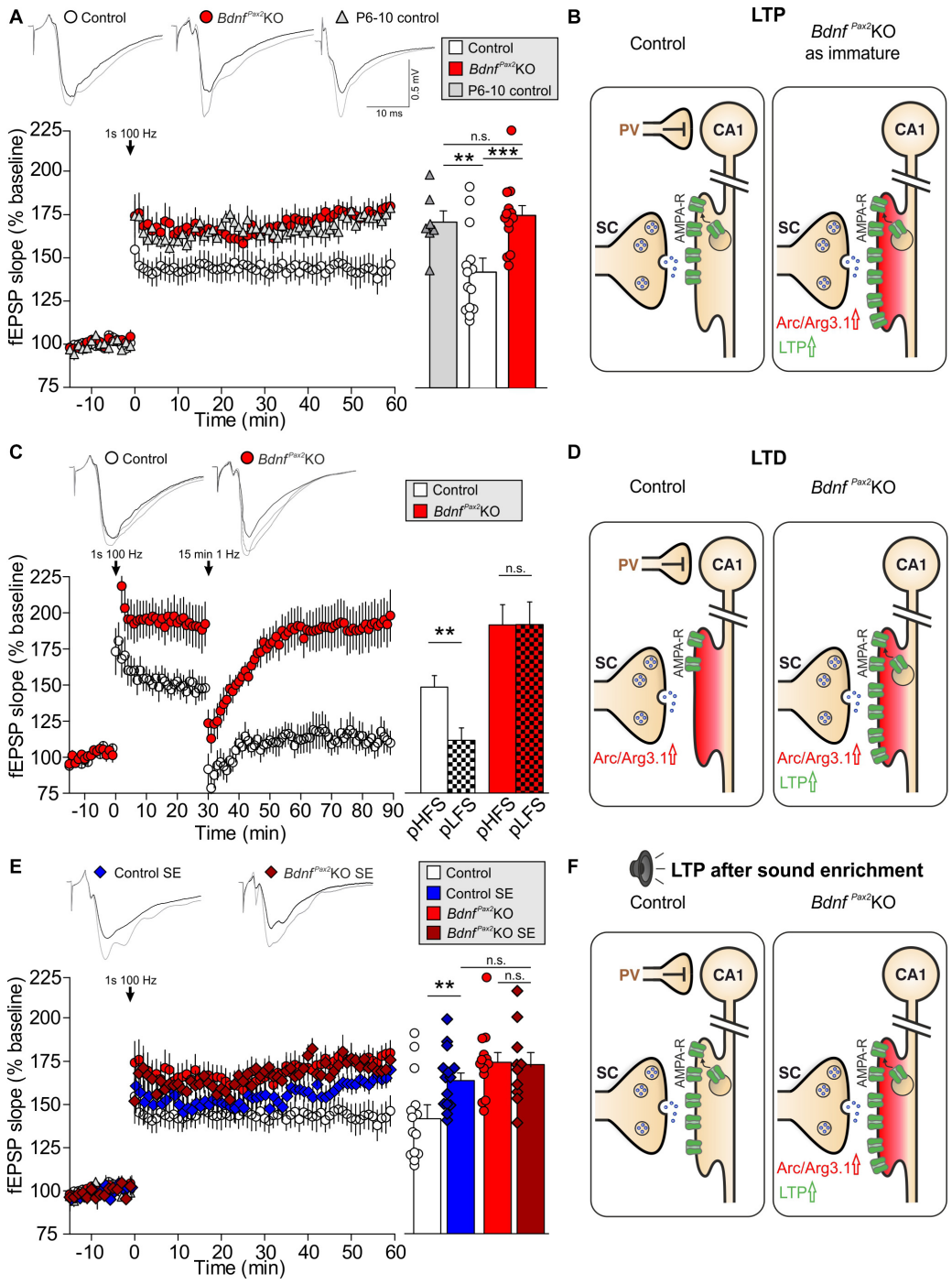

FIGURE 4 | Hippocampal LTP/LTD adjustment in *Bdnf*^{Pax2}KOs. **(A,C,E)** Upper panels, Averaged time courses of fEPSP slopes in acute brain slices from controls, *Bdnf*^{Pax2}KOs, P6-10 controls, sound-exposed (SE) controls, and *Bdnf*^{Pax2}KOs. Representative traces before (black) and after (gray) induction of LTP and after LTD induction (dotted black line) are shown. **(A)** Right panel: Higher LTP in adult *Bdnf*^{Pax2}KOs (n = 9/13 animals/slices; 175.5 ± 5.7%) and P6-10 controls (n = 6/7 animals/slices; 171.6 ± 6.5%) compared with adult controls (n = 9/14 animals/slices; 142.4 ± 8.2%; $P < 0.0001$). **(B)** *Bdnf*^{Pax2}KOs exhibit increased LTP due to reduced tonic PV inhibition. SC = Schaffer's collateral. **(C)** Right panel: Successful LTP (n = 6/8 animals/slices; 148.9 ± 8.0%) and LTD (n = 6/8 animals/slices; 111.8 ± 8.6%) was observed for controls. *Bdnf*^{Pax2}KOs had a significantly increased LTP (n = 6/10 animals/slices; 192.2 ± 14.1%) but did not show LTD maintenance (n = 6/10 animals/slices; 192.4 ± 15.7%) (control: $P < 0.0001$, *Bdnf*^{Pax2}KO: $P < 0.001$). **(D)** *Bdnf*^{Pax2}KOs exhibit impaired homeostatic plasticity to reduce synaptic strength. **(E)** Right panel: increased LTP was observed after SE (80-100 dB) controls (n = 4/11 animals/slices; 164.9 ± 5.9%) compared to unexposed controls (n = 9/14 animals/slices; 142.4 ± 8.2%) but not in SE *Bdnf*^{Pax2}KOs (n = 3/5 animals/slices; 172.9 ± 12.9%) compared to unexposed *Bdnf*^{Pax2}KOs (n = 9/14 animals/slices; 175.5 ± 5.7%; $P < 0.0001$). **(F)** *Bdnf*^{Pax2}KOs exhibit impaired synaptic scaling properties and are not able to increase LTP after SE. Mean ± S.E.M. n.s. = $P > 0.05$, ** = $P < 0.01$, *** = $P < 0.001$.

critical period when major sensory functions develop in rodents (de Villers-Sidani et al., 2007). We found that LTP levels were significantly higher in young (P6-P10) animals relative to adult controls (**Figure 4A**, left panel, gray bar; Bonferroni's *post hoc* test: $P < 0.01$). In fact, the LTP levels of P6-P10 animals were comparable to the levels observed in adult $Bdnf^{Pax2}$KO mice (Bonferroni's *post hoc* test: $P > 0.05$), suggesting that immaturity of hippocampal PV-INs is reflected by elevated LTP.

It is conceivable that the elevated Arc levels in $Bdnf^{Pax2}$KO mice may be due to insufficient shaping of synaptic contacts between PV-INs and pyramidal neurons through persistent (tonic) inhibition (**Figure 4B**). Since stimulus-induced endocytosis of postsynaptic AMPA receptors is required for the weakening of synapses during LTD (Jakkamsetti et al., 2013; Okuno et al., 2018), we next analyzed LTD responses in $Bdnf^{Pax2}$KOs. In controls, high-frequency stimulation (1s, 100 Hz) led to elevated fEPSPs (LTP) [**Figure 4C**, white clear bar; 1-way ANOVA, $F(2,21) = 13.59$, $P < 0.0001$, $n = 6/8$ mice/slices, Bonferroni's *post hoc* test: baseline/tetanized: $P < 0.001$] and subsequent low-frequency stimulation (15 min, 1 Hz) caused a reduction of fEPSP levels (LTD) back to baseline (**Figure 4C**, white patterned bar; Bonferroni's *post hoc* test: tetanized/LFS: $P < 0.01$). In contrast, in $Bdnf^{Pax2}$KOs, high-frequency stimulation led to even higher fEPSPs [**Figure 4C**, red clear bar; 1-way ANOVA, $F(2,27) = 18.44$, $P < 0.001$, $n = 6/10$ mice/slices, Bonferroni's *post hoc* test: baseline/tetanized: $P < 0.001$] but a subsequent low-frequency stimulation (15 min, 1Hz) did not cause a reduction to baseline levels (**Figure 4C**, red patterned bar; Bonferroni's *post hoc* test: tetanized/LFS: $P > 0.05$). These results suggest that the high levels of Arc in $Bdnf^{Pax2}$KOs may have prevented a weakening of synapses and thus counteracted the generation of LTD (**Figure 4D**).

To get a first insight into whether these LTP/LTD changes in hippocampal slices have an impact on sensory function, we tested whether enriching sensory stimulation would enhance LTP in $Bdnf^{Pax2}$KOs, as previously shown to occur in control mice 14 days after 40 min of SE at 80 dB SPL (Matt et al., 2018). Analysis of any LTP adjustment following SE at 80 dB SPL revealed significantly elevated LTP in the CA1 region of control animals [**Figure 4E**, blue bar; 1-way ANOVA; $F(7,78) = 37.24$, $P < 0.0001$, control: $n = 9/14$, control SE: $n = 4/11$, $Bdnf^{Pax2}$KO: $n = 9/14$, $Bdnf^{Pax2}$KO SE: $n = 3/5$ mice/slices; Bonferroni's *post hoc* test: control/control SE: $P < 0.05$]. In contrast, in $Bdnf^{Pax2}$KOs, the initial LTP responses were maintained (**Figure 4E**, red bar) and were not further elevated following SE (**Figure 4E**, dark red bar; Bonferroni's *post hoc* test: control/control SE: $P > 0.05$). This finding is best explained by the inability of $Bdnf^{Pax2}$KOs to adjust Arc levels in the postsynaptic spines of hippocampal pyramidal CA1 neurons, caused by impaired AMPA receptor trafficking (Diering and Huganir, 2018; Park, 2018; **Figure 4F**). Importantly, in response to a range of input strengths, $Bdnf^{Pax2}$KOs and controls displayed similar levels of fEPSP amplitudes [**Supplementary Figure 1A**; 1-way ANOVA, $F(4,25) = 0.80$, $P = 0.54$, control: $n = 9/14$, control SE: $n = 4/11$ mice/slices, $Bdnf^{Pax2}$KO SE: $n = 3/5$, $Bdnf^{Pax2}$KO: $n = 9/13$, P6-P10 control: $n = 6/7$ mice/slices], and paired-pulse facilitation [**Supplementary Figure 1B**; 1-way ANOVA, $F(4,25) = 0.49$, $P = 0.75$, control: $n = 9/14$, control SE: $n = 4/11$ mice/slice, $Bdnf^{Pax2}$KO SE: $n = 3/5$, $Bdnf^{Pax2}$KO: $n = 9/13$, P6-P10 control: $n = 6/7$ mice/slices]. This indicates that the observed differences are not due to changes in presynaptic function, and suggests a normal activity of pre-synaptic Schaffer's collaterals in $Bdnf^{Pax2}$KOs.

In conclusion, the levels of hippocampal fEPSPs were elevated in $Bdnf^{Pax2}$KOs, resembling the levels that were observed in controls prior to the critical developmental period of sensory onset between P10-P14. In adult $Bdnf^{Pax2}$KOs the increased hippocampal fEPSPs is linked with elevated Arc and LTP levels, diminished LTD and deficits in LTP/LTD adjustment to enriching SE.

$Bdnf^{Pax2}$KOs Exhibit Diminished Learning, Reduced Exploratory Activity, and Enhanced Anxiety

Reduced dendritic labeling of PV-INs linked to elevated Arc levels and impaired LTP/LTD adjustment in $Bdnf^{Pax2}$KOs may influence learning and behavioral processes. To approach this issue, a learning paradigm was used in which adult mice were trained to complete a maze in order to get a reward (access to their own mouse house). During this process, the mice had to find their way through the maze, memorizing 7 decision points in a multiple T-maze (**Figure 5A**). After completion of a successful run, the learning performance was analyzed by determining errors at the decision points of the maze. As shown in **Figure 5B**, in the four runs analyzed, the $Bdnf^{Pax2}$KOs had a significantly higher error rate, making 1-67 errors at the end of the learning phase (run 7), while the controls made only 0-1 errors [Wilcoxon/Kruskal-Wallis-Tests, $X^2(1, n = 8/9) = 12.2753$, $P = 0.0005$, control: $n = 9$ mice, $Bdnf^{Pax2}$KO: $n = 8$ mice]. As most $Bdnf^{Pax2}$KOs displayed circling behavior (Zuccotti et al., 2012), the correlation between circling behavior and motor activity or errors in the T-maze was explicitly tested. The circling behavior had neither an effect on the number of errors during runs 2 and 7 in the T-maze (**Figure 5C**; linear regression; $R^2 = 0.039$, $n = 8$ mice), nor on the motor activity (**Figure 5D**; linear regression; control: $R^2 = 0.014$, $Bdnf^{Pax2}$KO: $R^2 = 0.054$, control: $n = 7$ mice, $Bdnf^{Pax2}$KO: $n = 9$ mice) that was significantly increased in $Bdnf^{Pax2}$KOs, as measured on a ballistic platform in the startle apparatus [**Figure 5E**; unpaired two-tailed student's *t*-test, $t(17) = 3.08$, $P = 0.007$, control: $n = 7$ mice, $Bdnf^{Pax2}$KO: $n = 9$ mice]. This indicates that the increased learning errors in $Bdnf^{Pax2}$KOs can be linked to neither circling behavior nor altered motor activity.

Altered Arc levels affecting AMPA receptor trafficking not only weaken preference and discrimination for novelty, but also affect anxiety and social behavior (Cheng et al., 2017; Penrod et al., 2019). To test for altered behavior, we used Crawley's sociability 3-chamber test (**Figure 6A**) to analyze the social and explorative behaviors of controls and $Bdnf^{Pax2}$KOs. The time of sniffing contacts toward an empty cage or a cage with an unknown ("stranger") mouse was monitored and normalized to the time spent in the respective chamber. Controls spent more time sniffing toward the stranger-mouse chamber than

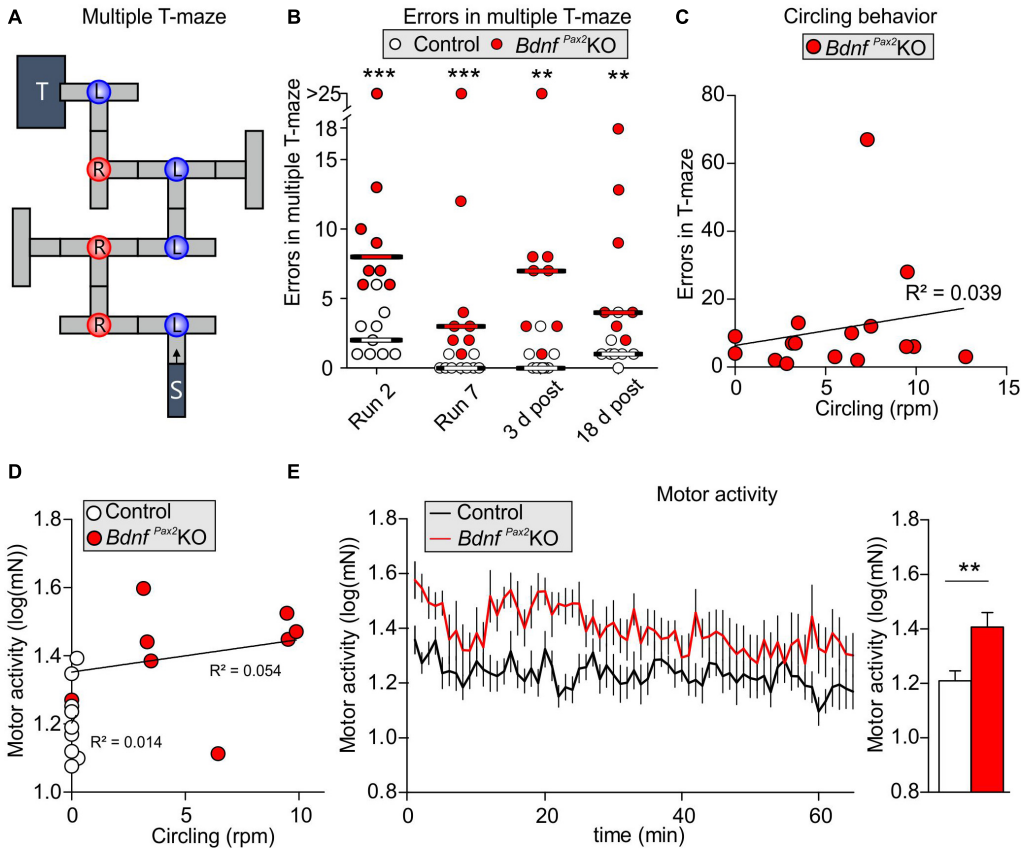

FIGURE 5 | Learning, circling behavior and motor activity in *Bdnf*^{Pax2}KOs. **(A)** The learning experiment was conducted in a multiple T-maze with 7 decision points (L, left turn correct; R, right turn correct). **(B)** *Bdnf*^{Pax2}KOs had a significantly higher median error rate in all evaluated runs (n = 8/9 mice; P = 0.002), but showed successful learning from run 2 to run 7. However, long-term memory 3 and 18 days after the last training run was impaired in *Bdnf*^{Pax2}KOs compared with controls. **(C)** Most *Bdnf*^{Pax2}KOs displayed circling behavior; this circling behavior was not significantly correlated with learning errors (*Bdnf*^{Pax2}KOs: n = 8; data shown for run 2 and 7). **(D)** While *Bdnf*^{Pax2}KOs displayed more circling as well as more motor activity than controls, there was no significant correlation between these two measures within the two genotypic groups (n = 8/9 each). **(E)** Motor activity, measured on a ballistic platform during a startle measurement (n = 7-9 each; P = 0.007), was increased in *Bdnf*^{Pax2}KOs. ** = $P < 0.01$, *** = $P < 0.001$.

toward the empty chamber, while *Bdnf*^{Pax2}KOs showed no preference between the two [**Figure 6B**; control: unpaired two-tailed student's t-test, $t(38) = 2.29$, $P = 0.027$, *Bdnf*^{Pax2}KO: unpaired two-tailed student's t-test, $t(18) = 0.11$, $P = 0.916$, $n = 20$ mice each]. Furthermore, *Bdnf*^{Pax2}KOs differed from controls in showing significantly reduced sniffing contacts toward both cages [**Figure 6D**; empty: unpaired two-tailed student's t-test, $t(38) = 5.84$, $P = 0.0278$, stranger: unpaired two-tailed student's t-test, $t(38) = 5.84$, $P < 0.0001$, $n = 20$ mice each], although the average latency for the first entry into the empty chamber or chamber with a stranger was not different between controls and *Bdnf*^{Pax2}KOs [**Figure 6C**; empty: unpaired two-tailed student's t-test, $t(30) = 1.68$, $P = 0.0205$, stranger: unpaired two-tailed student's t-test, $t(36) = 0.70$, $P = 0.486$, $n = 20$ mice each]. Moreover, in comparison to controls, *Bdnf*^{Pax2}KOs exhibited significantly fewer entries into both chambers [**Figure 6F**; empty: unpaired two-tailed student's t-test, $t(30) = 2.08$, $P = 0.0462$, stranger: unpaired two-tailed student's t-test, $t(36) = 2.59$, $P = 0.0138$, $n = 20$ mice each]. This suggests that *Bdnf*^{Pax2}KOs either show an altered behavioral reactivity during a novel situation, or develop diminished consolidation of newly learned information, both of which crucially influence stress and anxiety responses (de Kloet et al., 1999). Anxiety can be assessed through altered grooming or corticosterone levels (Kromer et al., 2005). When analyzing freezing or self-grooming behaviors, *Bdnf*^{Pax2}KOs showed a significant increase in spontaneous freezing [**Figure 6G**, left side; Chi-square test for trend, $X^2(1, n = 20 \text{ each}) = 199.8$, $P < 0.0001$] and self-grooming behaviors [**Figure 6G**, right side; Chi-square test for trend, $X^2(1, n = 20$ mice each$) = 24.5$, $P < 0.0001$].

The next measure was of the ultrasound vocalization (**USV**) of nursing infants at P7. This revealed significant differences in the vocalization patterns between control and *Bdnf*^{Pax2}KO pups, as depicted in **Figures 6F,G**. USV with multiple frequency jumps were more frequent in *Bdnf*^{Pax2}KO pups (**Figure 6F**, $n = 8$ mice each, Genotype: $P = 0.004$). Additionally, isolated *Bdnf*^{Pax2}KO pups showed increased numbers of all USV calls during a 5 min period (**Figure 6H**, $n = 8$ mice each; $P < 0.0001$),

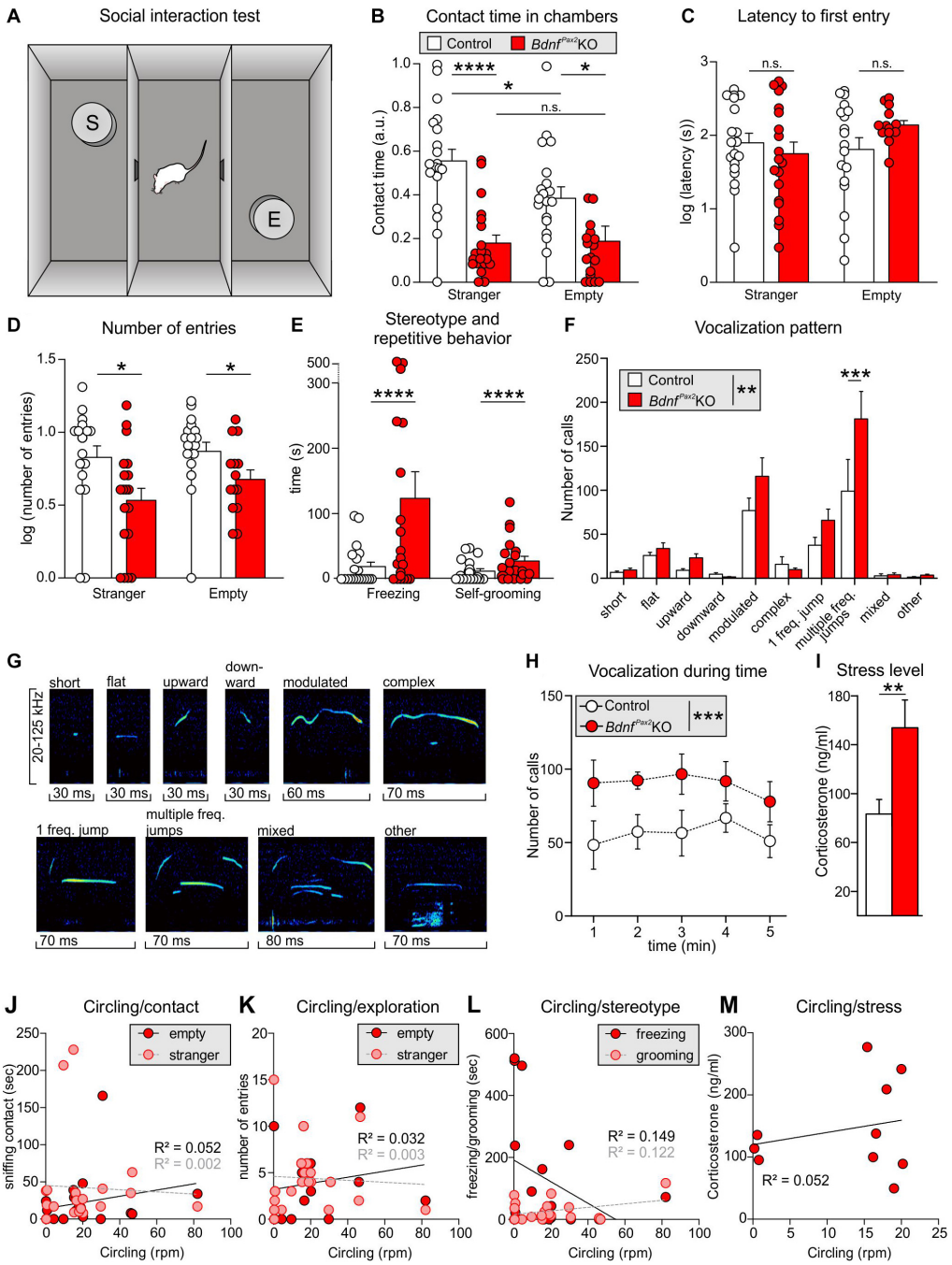

FIGURE 6 | Social behavior and anxiety studies in *Bdnf*^{Pax2}KOs. **(A)** Scheme of Crawley's sociability apparatus with three chambers. In one of the outer chambers, a stranger mouse (S) was placed below the container while the other chamber was equipped with an empty (E) container. **(B)** *Bdnf*^{Pax2}KOs spent less time with sniffing contacts toward both containers (n = 20 each, stranger: $P < 0.0001$; empty: $P = 0.0278$). Controls show a preference for the stranger which was not seen in *Bdnf*^{Pax2}KOs (n = 20 each, control: $P = 0.027$; *Bdnf*^{Pax2}KOs: $P = 0.916$). **(C)** The latency to the first entry of either outer compartment was similar for both genotypes [n = 14-19 each, stranger: $t(36) = 0.70$, $P = 0.486$; empty: $t(30) = 1.68$, $P = 0.104$]. **(D)** The number of entries into both chambers was decreased in *Bdnf*^{Pax2}KOs (n = 14-19 each, stranger: $P = 0.0138$; empty: $P = 0.0462$). **(E)** *Bdnf*^{Pax2}KOs revealed an increased stereotypic behavior shown by freezing (n = 20 each, $P < 0.0001$) and self-grooming (n = 20 each, $P < 0.0001$). **(F)** Differences in the vocalization pattern (shown in **G**) between *Bdnf*^{Pax2}KO and control pups with increased multiple frequency jumps in *Bdnf*^{Pax2}KOs (n = 8 each, Genotype: $P = 0.004$; Pattern: $P < 0.0001$; Interaction: $P = 0.027$). **(G)** Typical examples of vocalization patterns in mouse pups. **(H)** Ultrasonic call rate recorded in short-term isolated pups was increased in *Bdnf*^{Pax2}KOs (n = 8 each; $P < 0.001$]. **(I)** Blood corticosterone level was increased in *Bdnf*^{Pax2}KOs (n = 13 each, $P = 0.048$). **(J)** While *Bdnf*^{Pax2}KOs displayed more circling as well as sniffing contact to any chamber than controls, there was no significant correlation between these two measures (n = 20). **(K)** Also no significant correlation between circling and exploration in both chambers, **(L)** their stereotypic behavior, namely freezing and grooming (n = 20), **(M)** or their endogenous stress level could be observed in *Bdnf*^{Pax2}KOs (n = 8). **(C–H)** Mean ± S.E.M. n.s. = $P > 0.05$, * = $P < 0.05$, ** = $P < 0.01$, *** = $P < 0.001$, **** = $P < 0.0001$.

which indicated a higher index of anxiety (Kromer et al., 2005; Groenink et al., 2008). In adult $Bdnf^{Pax2}$KOs, basal corticosterone levels were significantly elevated compared to controls [**Figure 6I**; unpaired two-tailed student's *t*-test, $t(24) = 2.082$, $P = 0.0482$, $n = 13$ mice each], also indicating increased anxiety behavior, a hallmark of stress.

With regard to $Bdnf^{Pax2}$KOs displaying circling behavior (Chumak et al., 2016) and to suggest that specific vestibular dysfunction can cause learning and behavior deficits (Smith, 2019), we correlated circling with behavioral deficits in $Bdnf^{Pax2}$KOs. Although $Bdnf^{Pax2}$KOs displayed more circling and less sniffing contact to any chamber than controls, there was no significant correlation between these two measures in any chamber (**Figure 6J**; linear regression; empty: $R^2 = 0.052$, stranger: $R^2 = 0.0022$; $n = 20$ mice). There was also no significant correlation observed between circling and exploration in both chambers (**Figure 6K**; linear regression; empty: $R^2 = 0.0326$, stranger: $R^2 = 0.0032$; $n = 20$ mice), the circling and stereotypic behavior of freezing and grooming (**Figure 6L**; linear regression; freezing: $R^2 = 0.1491$, grooming: $R^2 = 0.1218$; $n = 20$ mice), or circling and the endogenous stress levels (**Figure 6M**; linear regression; $R^2 = 0.0521$; $n = 10$ mice).

Conclusion: In $Bdnf^{Pax2}$KOs reduced dendritic labeling of PV-INs and elevated Arc levels in the AC and hippocampus are associated with impaired LTP/LTD adjustment. How the attenuated capacity to memorize novel T-maze cues, the elevated anxiety, and the reduced social behavior, found in $Bdnf^{Pax2}$KOs are causally linked with impaired LTP/LTD adjustment and imbalanced PV-IN and Arc levels remains to be determined.

BDNF Deletion in Pax2-Lineage Descendants Led to Reduced Fine-Grained Auditory Brainstem Output Activity

The reduced dendritic PV-IN labeling in the AC and hippocampus of $Bdnf^{Pax2}$KOs from P10 onward (**Figure 3**) may suggest that BDNF in Pax2-lineage descendants in brainstem regions may be required to shape auditory brainstem activity in order to generate a proper auditory-specific driving force for thalamo-cortical integration of the GABAergic PV-IN network into functional fronto-striatal circuits (Wehr and Zador, 2003; Gabernet et al., 2005). Before testing for proper auditory brainstem responses (**ABR**), we confirmed near-normal hearing thresholds in $Bdnf^{Pax2}$KOs (Zuccotti et al., 2012). Normal electromechanical response properties of OHCs and slightly diminished IHC exocytosis in high-frequency cochlear regions (Zuccotti et al., 2012) led only to a mild threshold elevation and reduced response amplitude of responses to clicks, noise bursts or pure tone stimuli [**Supplementary Figure 2A**; click: unpaired two-tailed student's *t*-test, $t(47) = 3.224$, $P = 0.0023$, control: $n = 26$ mice, $Bdnf^{Pax2}$KO: 23 mice, noise: unpaired two-tailed student's *t*-test, $t(47) = 2.306$, $P = 0.0256$, control: $n = 26$ mice, $Bdnf^{Pax2}$KO: 23 mice, f-ABR: 2-way ANOVA, Genotype: $F(1,9) = 59.72$, $P < 0.0001$, $n = 16/32$ mice/ears each]. Next, the sensitivity for auditory-specific stimuli was determined by analyzing brainstem neurons in the cochlear nucleus (**CN**) that are targeted by auditory nerve **(AN)** fibers (**Figure 7A**). Fusiform/pyramidal neurons in the DCN receive direct excitatory inputs onto their basal dendrites from the descending branch of the AN (Palombi et al., 1994; Zhou et al., 2015). AN inputs also activate inhibitory GABAergic vertical cells that project to the soma of the fusiform/pyramidal DCN neurons (Spirou et al., 1999; **Figure 7A**, left panel). Recordings from DCN neurons of adult $Bdnf^{Pax2}$KO mice revealed elevated tone-evoked thresholds compared to control (**Figure 7B**; Mann-Whitney rank sum test, $U = 11$, $P < 0.001$, controls: $n = 14$ mice, $Bdnf^{Pax2}$KO: 10 mice). Moreover, a broader tuning in frequency bandwidth, measured as a reduced quality factor (Q_{10}) [**Figure 7C**; unpaired two-tailed student's *t*-test, $t(22) = 2.1$, $P = 0.048$, control: $n = 14$ mice, $Bdnf^{Pax2}$KO: 10 mice], and a decreased dynamic range (**Figure 7D**; Mann-Whitney rank sum test, $U = 34$, $P = 0.038$, control: $n = 14$ mice, $Bdnf^{Pax2}$KO: 10 mice) were observed. While the maximal firing rate was not different between the two genotypes (**Figure 7E**; Mann-Whitney rank sum test, $U = 66.5$, $P = 0.86$, control: $n = 14$ mice, $Bdnf^{Pax2}$KO: 10 mice), the spontaneous firing rate (**SFR**) was strongly increased in $Bdnf^{Pax2}$KOs (**Figure 7F**; Mann-Whitney rank sum test, $U = 1$, $P < 0.001$, control: $n = 14$ mice, $Bdnf^{Pax2}$KO: 10 mice). Furthermore, in $Bdnf^{Pax2}$KOs, the inhibitory strength was reduced within high-frequency sidebands (**Figure 7G** right panel; Mann-Whitney rank sum test, $U = 19$, $P = 0.021$, control: $n = 14$ mice, $Bdnf^{Pax2}$KO: 10 mice), but not within low frequency sidebands (**Figure 7G** left panel; Mann-Whitney rank sum test, $U = 15$, $P = 0.057$, control: $n = 14$ mice, $Bdnf^{Pax2}$KO: 10 mice). Action-potential firing rates were similar for excitatory frequency response areas [**Figure 7H** left panel; unpaired two-tailed student's *t*-test, $t(18) = 0.053$, $P = 0.958$, control: $n = 14$ mice, $Bdnf^{Pax2}$KO: 10 mice]. In contrast, $Bdnf^{Pax2}$KOs had strongly increased firing rates in non-inhibitory areas, i.e., outside of the excitatory area and the inhibitory sidebands [**Figure 7H** right panel; unpaired two-tailed student's *t*-test, $t(18) = 5.04$, $P < 0.001$, control: $n = 14$ mice, $Bdnf^{Pax2}$KO: 10 mice]. Comparison of the action-potential firing rates between excitatory and non-inhibitory areas of DCN neurons revealed a reduced ratio in $Bdnf^{Pax2}$KOs (**Figure 7I**; Mann-Whitney rank sum test, $U = 0$, $P < 0.001$, control: $n = 14$ mice, $Bdnf^{Pax2}$KO: 10 mice), indicating a tonically diminished inhibitory strength.

Elevated thresholds linked with elevated SFR, reduced inhibitory strength, and reduced dynamic range of sound-induced DCN responses identified a significantly diminished resolution of AN input. Altered summed AN activity, previously observed in $Bdnf^{Pax2}$KOs (Chumak et al., 2016), was confirmed, demonstrating a reduced supra-threshold summation of ABR wave I [**Supplementary Figure 2B**; 2-way ANOVA; Genotype: $F(1,18) = 199.0$, $P < 0.0001$, control: $n = 14/28$ mice/ears, $Bdnf^{Pax2}$KO: $n = 12/24$ mice/ears]. ABR wave I response patterns were found to be shortened in time [**Supplementary Figure 2B**, 2-way ANOVA; Genotype: $F(1,17) = 187.50$, $P < 0.0001$, control: $n = 14/28$ mice/ears, $Bdnf^{Pax2}$KO: $n = 12/24$ mice/ears], possibly resulting from a degraded spike precision, a reduced reliability or a diminished synchronicity of AN responses. Whereas DCN first spike latencies were not altered [unpaired

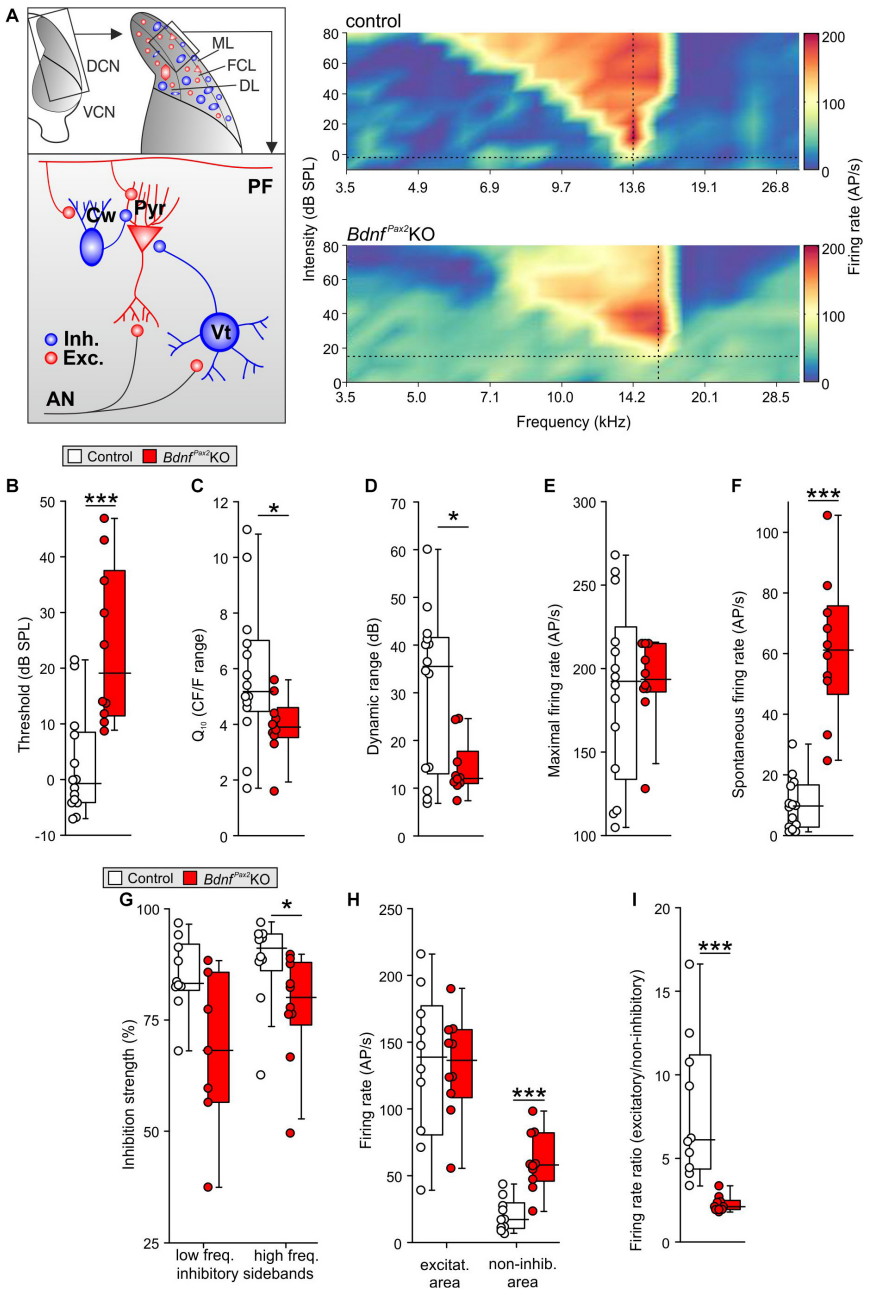

FIGURE 7 | *In vivo* recordings in the dorsal cochlear nucleus of *Bdnf*^{Pax2}KO. **(A)** Left: schematic drawing of neurons in the fusiform layer of the DCN. Right: Example for frequency response areas in DCN fusiform cells of controls (upper panel) and *Bdnf*^{Pax2}KOs (lower panel) representing the neuronal AP discharge rate evoked by 100ms pure-tone stimulation with varying frequency-level combinations. Color scale indicates firing rate between 0 (dark blue) and 205 (dark red) APs per second. Dotted vertical lines = units' characteristic frequency (CF), dotted horizontal lines = threshold levels. The frequency-level combinations evoking significant increase in firing rates form a characteristic V-shaped excitatory area (yellow to red). The regions with decreased activity form low- and high-frequency inhibitory sidebands (dark blue). Note the increased activity outside of the excitatory and inhibitory areas in *Bdnf*^{Pax2}KOs. **(B)** Elevated thresholds of tone-evoked responses in *Bdnf*^{Pax2}KOs in comparison to controls (n = 10-14; $P < 0.001$). **(C)** Quality factor (Q_{10}), representing the relative bandwidth of the excitatory field 10 dB above threshold, revealed sharper frequency selectivity in controls compared to *Bdnf*^{Pax2}KOs (n = 10-14; $P = 0.048$). **(D)** Dynamic ranges of rate-level function at units' CF were significantly smaller in *Bdnf*^{Pax2}KOs than in controls (n = 10-14; $P = 0.038$). **(E)** Maximal firing rates evoked by acoustic stimulation were comparable between the groups (n = 10-14; $P = 0.86$). **(F)** Spontaneous neuronal firing in *Bdnf*^{Pax2}KOs was significantly increased compared to controls (n = 10-14; $P < 0.001$). **(G)** Inhibitory strength in low-frequency inhibitory sidebands (left) was similar, while high-frequency inhibitory sidebands (right) showed reduced inhibitory strength in *Bdnf*^{Pax2}KOs (n = 10 each; low-frequency sidebands: $P = 0.057$, high-frequency sidebands: $P = 0.021$). **(H)** Action potential firing rates within units' excitatory areas (left) were similar. Non-inhibitory areas, i.e., outside of excitatory area and inhibitory sidebands (right), displayed markedly increased firing rates in *Bdnf*^{Pax2}KOs (n = 10 each; excitatory: $P = 0.958$, non-inhibitory: $P < 0.001$). **(I)** Ratios of AP firing rates between excitatory and non-inhibitory areas were smaller in *Bdnf*^{Pax2}KOs than in controls (n = 10 each, $P < 0.001$). Box plots show medians, the 25 and 75 percentiles, and the interdecile ranges. Dots show values for individual cells.
* = $P < 0.05$, *** = $P < 0.001$.

two-tailed student's *t*-test, $t(21) = 0.183$, $P = 0.857$, control: $n = 14$ mice, $Bdnf^{Pax2}$KO: 10 mice; data not shown], ABR wave IV was significantly delayed and reduced in amplitude in $Bdnf^{Pax2}$KOs [**Supplementary Figure 2C**; amplitude: 2-way ANOVA; Genotype: $F(1,18) = 15.76$, $P < 0.0001$, latency: 2-way ANOVA; Genotype: $F(1,17) = 78.96$, $P < 0.0001$, control: $n = 14/28$ mice/ears, $Bdnf^{Pax2}$KO: $n = 12/24$ mice/ears], confirming previous results (Chumak et al., 2016).

To explore possible temporal auditory processing deficits, we analyzed the coding of amplitude-modulated tones in auditory steady-state responses (**ASSR**s) by measuring the response to differently modulated stimuli. Compared to controls, we detected significantly reduced ASSRs at a modulation depth of more than 10% in $Bdnf^{Pax2}$KOs [**Supplementary Figure 2D**, left panel; 2-way ANOVA; Genotype: $F(1,15) = 10.92$, $P = 0.0011$, $n = 10$ mice each], indicating severe deficits in temporal resolution. When these ASSRs were analyzed as a function of the stimulus level in a phase-locked manner, responses in $Bdnf^{Pax2}$KO mice remained reduced, particularly for low sound pressure levels close to threshold [**Supplementary Figure 2D**, right panel; 2-way ANOVA; Genotype: $F(1,14) = 28.15$, $P < 0.0001$, $n = 10$ mice each], suggesting profound deficits in the fast temporal processing of sound signals near hearing threshold.

In conclusion: The absence of BDNF in Pax2-lineage descendants in $Bdnf^{Pax2}$KOs leads to elevated thresholds and reduced sound-evoked ABR amplitudes, linked with an increased SFR and a reduction of tonic inhibitory strength and dynamic range of sound-induced DCN responses (**Figures 8A,B**). Diminished fine-grained auditory input in $Bdnf^{Pax2}$KO mice (**Figure 8C**) is associated with elevated baseline levels of Arc and reduced labeling of PV-INs, particularly in dendritic regions of the AC and hippocampus, while leaving the number of PV-INs unchanged (**Figure 8D**). The subsequent inability to adjust LTP/LTD may be causally linked with the attenuated capacity to memorize novel T-maze cues, elevated anxiety, and reduced social behavior, all of which are characteristic features of an autistic-like phenotype (**Figure 8D**).

DISCUSSION

The results of the present study suggest that the absence of BDNF in Pax2-lineage descendants in hindbrain regions in $Bdnf^{Pax2}$KO mice may have an impact on learning and behavior through impaired activity-driven integration of the GABAergic PV-IN network of the AC into functional hippocampal circuits. As a result the observed deficits in stimulus-induced hippocampal LTP/LTD adjustments (social) learning, and anxiety control in $Bdnf^{Pax2}$KOs may be caused by an inability to scale hippocampal synapses.

BDNF Expression in Pax2-Lineage Descendants in Lower Auditory Hindbrain Regions

Here, BDNF mRNA was found to be present in Pax2-lineage descendants within brainstem regions, as well as the AHA area, but not in Pax2+ septo-hippocampal projection neurons, which modulate brain plasticity through AHA regions (Bakos et al., 2016), or in the Cb (**Figure 1**). Moreover, no overlap between tdTomato fluorescence and BDNF mRNA was found in any thalamic or cortical frontal brain region. The latter was expected, since GABAergic IN precursors, derived from Pax2-lineage descendants, are supposed to migrate mainly from ventricular zones to lower brain levels that are posterior to midbrain regions, including the Cb, spinal cord, and inner-ear regions (Nornes et al., 1990; Maricich and Herrup, 1999; Rowitch et al., 1999; Fotaki et al., 2008).

We did not observe BDNF expression in all Pax2-lineage descendants in brainstem/hindbrain regions between P10 and adults (**Figure 1**). However, BDNF may be transiently expressed in Pax2-lineage descendants before this stage. We thus cannot exclude that the early expression of BDNF in Pax2-lineage descendants in for instance the Cb may participate in inhibitory circuit formation at the level of basket, granule, and stellate cells (Collin et al., 2005) and thereby contributes to the elevated motor activity observed in $Bdnf^{Pax2}$KOs. More detailed analysis should also focus on the spinal cord and vestibular nucleus, particularly regarding numerous studies that demonstrate dysfunctions of both may possibly have the potential to lead to spatial memory deficits and cognitive decline in humans (Smith, 2019). Finally, we cannot entirely exclude that, in addition to the deficits in fast auditory processing, subtle functional deficits may also exist in the somatosensory or visual system of $Bdnf^{Pax2}$KOs, although we observed no apparent changes in inhibitory/excitatory balance within these systems. Here, more specific fine-structured testing would be required to further validate this aspect. In this context, tracing of BDNF+ cells in Pax2-lineage descendants may be required. While it is generally believed that BDNF mRNA transcripts are absent from inhibitory INs (Canals et al., 2001; Cohen-Cory et al., 2010; Andreska et al., 2014), the few studies that have observed BDNF in GABAergic IN precursors in hindbrain or cortical neurons (Jungbluth et al., 1997; Huang et al., 1999; Barreda Tomas et al., 2020) may be reconsidered in the light of the present data.

Reduced Dendritic Outgrowth of PV-INs in Frontal Brain Regions in $Bdnf^{Pax2}$KOs

Here, we demonstrated that PV-INs in $Bdnf^{Pax2}$KOs were unaffected up to P10, at which point their numbers reached normal levels in cortical and hippocampal regions (**Figure 2**). This indicates that subpallium-derived GABAergic neurons have most likely reached their cortical and hippocampal target regions in $Bdnf^{Pax2}$KOs, a process shown to be accomplished by the 2nd postnatal week in rodents (Marin and Rubenstein, 2001). Between P10 and P14, however, dendritic growth of PV-INs in the AC and hippocampus remained significantly diminished in $Bdnf^{Pax2}$KO mice, although BDNF mRNA expression was maintained at levels comparable to those of control mice (**Figure 3**).

During the critical period of sensory system maturation, neuronal activity (due to sensory experience) is likely to be important, not only for the termination of the migration of

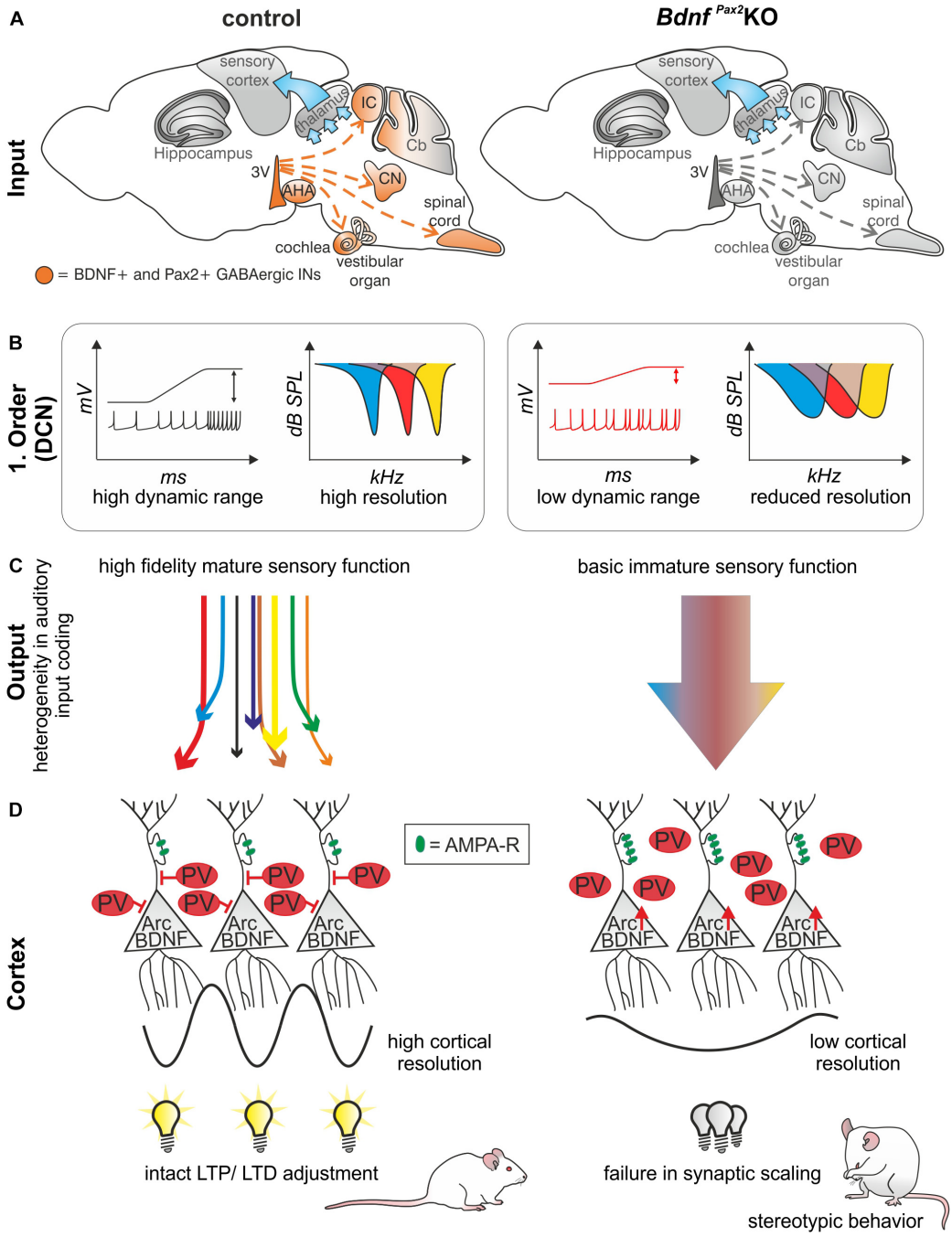

FIGURE 8 | Schematic how BDNF in GABAergic IN precursors shapes sensory memory. **(A)** In *Bdnf*^{Pax2}KOs, BDNF is deleted in Pax2-lineage descendants in the sensory periphery. **(B)** This leads to reduced dynamic range and reduced resolution in the first order neurons of *Bdnf*^{Pax2}KOs. **(C)** Mature sensory systems develops only if BDNF is expressed in GABAergic IN precursors. **(D)** *Bdnf*^{Pax2}KOs fail to mature dendritic outgrowth of PV-INs in the AC and hippocampus, resulting in impaired synaptic scaling in LTP and LTD and increased stereotypic behavior. AMPA-R = AMPA receptor.

cortical INs, but also for their proper integration into functional circuits (de Villers-Sidani et al., 2007; Lim et al., 2018). There is agreement that an activity-dependent release of BDNF from pyramidal neurons is required to sculpt the integration of the cortical PV-IN network in nearly all sensory cortices, probably by driving cortical tonic inhibition through synaptogenesis of peri-somatic PV-INs with pyramidal neurons (Hong et al., 2008; Xu et al., 2010; Griffen and Maffei, 2014; Lim et al., 2018; Meis et al., 2019). The proper integration of GABAergic INs into higher cortical sensory regions is essential for proper feed-forward inhibition, the sharpening of receptive fields, and pattern separation (Pouille and Scanziani, 2001; Leutgeb et al.,

2007). Only recently, it was shown that the process of GABA-IN dendritic synaptogenesis with pyramidal neurons during network integration may be linked with an upregulation of the potassium chloride cotransporter 2 (**KCC2**) in INs, which halts the motility of INs by gradual reduction of the frequency of spontaneous intracellular calcium transients in response to GABA (Bortone and Polleux, 2009), causing an excitatory-to-inhibitory switch in GABAergic signaling (Marin and Rubenstein, 2001; Ben-Ari, 2002). In the auditory system, the GABAergic excitatory-to-inhibitory switch occurs in a region-specific pattern after hearing onset (Kandler and Friauf, 1995; Friauf et al., 2011), possibly driven by sensory experience (Shibata et al., 2004). Previous findings suggest a crucial temporally and spatially heterogeneous role of KCC2 and BDNF for filopodia extensions of GABAergic INs during cortical maturation (Awad et al., 2018). When for example KCC2 is removed in immature cortical neurons spine maturation was prevented altogether, leading to an increase of filopodia protrusions (Li et al., 2007). BDNF is one of the strongest modulators of KCC2 activity (Wardle and Poo, 2003; De Koninck, 2007; Kaila et al., 2014). Likewise, BDNF is an activity-driven gene (West et al., 2001, 2014) that was previously suggested to require fast auditory processing in order to be recruited for memory-dependent adjustments of LTP following SE (Matt et al., 2018). Nearly normal basal hearing thresholds of *Bdnf*^{Pax2}KOs (Zuccotti et al., 2012; Chumak et al., 2016) which are also observed in the present study (**Figure 7**), along with reduced and delayed ABR wave IV responses indicate that basic sound processing through auditory fibers with a low spontaneous firing rate (**SR**) and high activation thresholds (Merchan-Perez and Liberman, 1996) that develop early at hearing onset (Glowatzki and Fuchs, 2002; Grant et al., 2010) is intact in *Bdnf*^{Pax2}KOs. On the other hand, our results strongly suggest that high-SR auditory fibers with low activation thresholds that develop only after hearing onset (Glowatzki and Fuchs, 2002; Grant et al., 2010) are underdeveloped in *Bdnf*^{Pax2}KOs. These fibers define the detection thresholds for sounds and the shortest latencies at any given characteristic frequency (Meddis, 2006; Heil et al., 2008; Bourien et al., 2014). Diminished fast (high-SR) auditory processing would best explain not only the reduced and delayed ABR wave IV responses, but also the reduced activation of fusiform/pyramidal DCN neurons in *Bdnf*^{Pax2}KOs. DCN neurons are directly activated through AN fibers (Palombi et al., 1994; Zhou et al., 2015). The diminished high-SR AN activity may thus explain elevated thresholds, broadened bandwidth, reduced high-frequency sideband inhibition, and elevated spontaneous firing rates of DCN neurons in *Bdnf*^{Pax2}KOs. Accordingly, less inhibitory shaping of AN responses or attenuated shaping of inhibitory GABAergic vertical cells that contact the soma of DCN neurons (Spirou et al., 1999) may explain the phenotype of DCN neurons in *Bdnf*^{Pax2}KOs. Regarding the previously observed diminished filopodia extensions of GABAergic INs observed upon KCC2 deletion (Awad et al., 2018), we may consider diminished filopodia extension of GABAergic IN during development to occur when driving force for KCC2 upregulation is too low. Therefore, if fast auditory-specific processing is too low or unspecific to promote activity-dependent BDNF-driven KCC2 upregulation in ascending auditory and associated fronto-striatal networks, it is likely that PV-IN filopodia extensions of GABAergic INs would not mature properly, as observed here in the AC and hippocampus of *Bdnf*^{Pax2}KO mice (**Figures 2**, **3**).

The crucial requirement for the proper integration of GABAergic INs into functional circuits is best documented by studies that demonstrated a dysfunction in subpallium-derived GABAergic migration processes that are suggested to lead to neurodevelopmental disorders, including ASD (Marin, 2012; Canetta et al., 2016; Skene et al., 2018).

The present study indicates that not only the dysfunction of subpallium-derived GABAergic migration processes, but also defects in GABAergic IN precursors migrating to lower hindbrain regions, can lead to neurodevelopmental disorders, including ASD. The latter process may provide the proper driving force for the former one, a dependency the brain cannot compensate for when deficient.

Bdnf^{Pax2}KOs Exhibit Diminished PV-IN Dendritic Outgrowth Linked With Impaired Executive Functions

Reduced PV-IN dendrites in *Bdnf*^{Pax2}KOs in cortical and hippocampal regions, coinciding with elevated levels of Arc mRNA and protein (**Figures 2**, **3**), suggest that the synaptic activity of PV-IN contacts with pyramidal neurons may lower the baseline of Arc levels in pyramidal neurons. The expression of Arc varies with brain regions. While Arc is present in excitatory neurons in the hippocampus and the primary cortex, in for example the dorsal striatum Arc can also be found in projection GABAergic medial septal neurons (Vazdarjanova et al., 2006; Gong et al., 2020). The preferential expression in glutamatergic excitatory neurons in the hippocampus and the change in number of Arc+ neurons and expression level with strength of stimuli in the hippocampus (Link et al., 1995; Guzowski et al., 2006; Vazdarjanova et al., 2006; Bramham et al., 2008; Zhang and Bramham, 2020) are consistent with the observations that **(i)** Upon glutamate-induced stimulation of projection neurons, expression of Arc is initiated remarkably quickly (∼15 s), leading to an elevation of its levels, which in turn induces a rapid removal of postsynaptic AMPA receptors and thereby weakens the synapse (Waung et al., 2008). If Arc baseline levels persist in a saturated stage because the resting potential of pyramidal neurons is not shaped through PV-IN inhibition, as hypothesized here for *Bdnf*^{Pax2}KOs (**Figures 2D,F**), postsynaptic spines of CA1 pyramidal neurons respond to high-frequency stimulation with elevated fEPSP levels as observed in the present study and also prior to hearing onset (**Figure 6A**). **(ii)** Moreover, consecutive stimulations at low-frequencies in *Bdnf*^{Pax2}KOs did not bring fEPSP levels back to baseline through LTD (**Figure 6C**), suggesting its incapacity to further elevate Arc levels and weaken synapses (Waung et al., 2008). **(iii)** SE at 80dB SPL typically leads to continuously elevated LTP in control animals (Matt et al., 2018), but not in *Bdnf*^{Pax2}KOs (**Figure 6E**), suggesting that the positive-feedback cycle predicted to be required to amplify specific sensory stimuli during improved task-performance (Irvine, 2018) does not work properly. **(iv)**

Based on the concept that novelty discrimination crucially depends on proper AMPA receptor trafficking in postsynaptic spines, which leads to the rapid weakening of synapses and LTD formation (Waung et al., 2008), the cognitive deficits of $Bdnf^{Pax2}$KOs in the multiple T-maze (**Figures 5A,B**) may be a consequence of inappropriate AMPA receptor trafficking in the postsynaptic spines of pyramidal neurons. This is due to saturated Arc baseline levels that, before lower baseline levels have been set, cannot be stimulated further to lower AMPA receptors in membranes. **(v)** The reduced explorative behavior (**Figure 6D**), enhanced stereotypic self-grooming (**Figure 6E**), and motor activity (**Figure 5E**), as well as the elevated corticosterone levels (**Figure 6I**) of $Bdnf^{Pax2}$KOs, reveal deficits in social learning and increased anxiety that may occur as a result of impaired stress control and novelty discrimination. Both stress control and novelty discrimination require proper AMPA receptor trafficking (Derkach et al., 2007; Blair et al., 2019; Penrod et al., 2019; Roth et al., 2020). **(vi)** Finally, various phenotypic characteristics of $Bdnf^{Pax2}$KO mice are reminiscent of mouse models relevant to neurodevelopmental disorders, such as ASD. These include reduced PV-IN labeling (Takano, 2015; Pirone et al., 2018; Goel et al., 2019), elevation of Arc levels (Korb and Finkbeiner, 2011; Goel et al., 2019), increased fEPSPs (Mohn et al., 2014), as well as elevated corticosterone levels (Das et al., 2019). Also, a mouse line deficient in adenomatous polyposis coli protein, a key regulator of synapse maturation (Hickman et al., 2015), also developed an autistic phenotype (Mohn et al., 2014; Alexander et al., 2020). These mice showed a reduced dynamic range of hearing and deficits in IHC synapses linked to altered high-SR and low threshold characteristics (Hickman et al., 2015), features similar to those observed in $Bdnf^{Pax2}$KO mice.

Fast inhibitory PV-INs are known to be important for gamma- (feed-forward inhibition) and beta-oscillations (feedback inhibition) (Sohal et al., 2009). A diminished activity in tonic fast-spiking PV-IN networks in rodent animal models for ASD was linked to enhanced baseline spontaneous gamma-band power and reduced beta oscillations (Gill and Grace, 2014). Interestingly, in children with fast auditory processing deficits and ASD, elevated and spontaneous baseline gamma-band power was recently found to be linked to reduced evoked gamma power (Foss-Feig et al., 2017; Mamashli et al., 2017; McCullagh et al., 2020).

In Conclusion: We propose that BDNF in GABAergic IN precursors contributes to the shaping of the tonic inhibitory conductance of hindbrain neurons through sensory experience. As shown here for auditory DCN brainstem neurons, tonic inhibitory strength is reduced in $Bdnf^{Pax2}$KOs and linked to elevated SFR and thresholds. Proper tonic inhibitory shaping is required to decrease the membrane time constant of sensory neurons in order to narrow the temporal window for synaptic integration by affecting background spontaneous firing rates (Kopp-Scheinpflug et al., 2011). This ensures a high signal-to-noise ratio for the transfer of specific, sensory-evoked information and filters signals that are not associated with the sensory stimuli, as previously also shown for sound-induced brainstem responses (Kopp-Scheinpflug et al., 2011). The findings in the present study may indicate that BDNF in Pax2-lineage descendent cells influences fast auditory processing. Fast auditory processing deficits following for example early brainstem injuries in children have been associated with cognitive deficits, including the failure to properly process rapidly changing acoustic information, a prerequisite during the acquisition of language and social learning (Fitch et al., 1997; Fitch and Tallal, 2003; Ramus, 2003; Rendall et al., 2017). Heterozygous Pax2 mice (Wei et al., 2020), exhibited an autistic-like pattern, evidenced through increased self-grooming and anxiety, although normal social behavior and working memory (Wei et al., 2020). It may be interesting to consider defects in BDNF expression in Pax2-deficient cells in future studies.

Numerous studies that predicted that abnormalities in the migration of GABAergic INs from subpallium areas to the cortex are a key factor underlying etiologies of various neurodevelopmental disorders including ASD, epilepsy, schizophrenia, anxiety, and depression (Levitt et al., 2004; Lewis et al., 2005; Marin, 2012; Kiss et al., 2014; Southwell et al., 2014; Takano, 2015; Shetty and Bates, 2016; Su et al., 2016; Reim and Schmeisser, 2017; Rendall et al., 2017; Li et al., 2018; Malhi and Mann, 2018; Peng et al., 2018), may now consider that, in addition, defects in targeting of GABAergic INs to lower hindbrain regions may contribute to neurodevelopmental problems, such as ASD.

MATERIALS AND METHODS

Animals

$Bdnf^{Pax2}$KO and control mice were obtained by crossing a Cre line, in which Cre is expressed under the promoter of the *Pax2* gene and a mouse line in which the protein coding *Bdnf-exon IX* is flanked by *loxP* sites. Both lines were obtained from the Mutant Mouse Regional Research Center, MMRRC (Rios et al., 2001; Ohyama and Groves, 2004; Zuccotti et al., 2012). To verify the deletion pattern of *Bdnf*, *Pax2*-Cre mice were crossed with $Rosa^{tdTomato}$ reporter mice (Madisen et al., 2010). Deletion of the *Bdnf* gene in distinct brain areas of $Bdnf^{Pax2}$KO was verified by Northern and Western blots. Genotyping of the mouse lines was performed as described (Rios et al., 2001). For all experiments, mice of either sex were used. The ages of adult animals were between 2 and 6 months, while for juveniles, the age is given in the respective results section. The sample size was chosen with the experience of previous publications, recommendations in literature, and on the basis of the expected effect size *n* calculated with G power. The care and use of mice and the experimental protocol were reviewed and approved by the University of Tübingen, Veterinary Care Unit, and by the Animal Care and Ethics Committee of the Regional Board of the Federal State Government of Baden-Württemberg, Germany, and followed the guidelines of the European Union Directive 2010/63/EU for animal experiments.

Co-localization of mRNA and Protein in Brain Sections

Animals were deeply anesthetized with CO_2 and then sacrificed by decapitation. Brain tissue was prepared and

sectioned with a vibratome at 60 μm, as previously described (Singer et al., 2016). mRNA and protein were co-localized on free-floating brain sections as previously described (Singer et al., 2014). In brief, following prehybridization for 1 h at 37°C, sections were incubated overnight with BDNF or Arc riboprobes at 56°C, incubated with anti-digoxigenin antibody conjugated to alkaline phosphatase (anti-Dig-AP, Roche, Germany, 11093274910), and developed as previously described (Singer et al., 2013). For protein detection, streptavidin–biotin was blocked according to the manufacturer's instructions (Streptavidin–Biotin Blocking Kit, Vector Laboratories, United States) after blocking endogenous peroxidase. Sections were incubated overnight at 4°C with the primary antibodies against Arc/Arg3.1 (Synaptic Systems, Germany, anti-rabbit, 1:200, 156003) (Nikolaienko et al., 2018) or parvalbumin (Abcam, United Kingdom, anti-rabbit, 1:500, ab11427), followed by incubation with the secondary antibody (biotinylated goat anti-rabbit, Vector Laboratories, BA-1000) and chromogenic detection (AEC, 3-amino-9-ethylcarbazole, Vector Laboratories, SK-4200). For co-labeling of BDNF mRNA and tdTomato, brain slices of Pax2-CRE-Rosa^{tdTomato} reporter mice were taken. For BX61 microscopy (Olympus, Japan) evaluation photographs were taken with a florescence camera (XM 10, Olympus, Japan) for detection of tdTomato florescence, and with a bright-field camera (DP 71, Olympus, Japan) for detection of mRNA and protein, without adjusting the picture frame or the plane of focus. As confocal microscopy is not possible, the resolution at higher magnification was limited.

Immunohistochemistry

Animals were deeply anesthetized with CO_2 and then sacrificed by decapitation. Brain tissue for fluorescence-immunohistochemistry was prepared and sectioned with a vibratome at 60 μm, as previously described (Singer et al., 2016). The sections of mouse brains were stained as described (Tan et al., 2007; Singer et al., 2016). Antibodies directed against parvalbumin (Abcam, United Kingdom, anti-rabbit, 1:2000, ab11427) and vGluT2 (Synaptic Systems, Germany, anti-mouse, 1:500, 135421) were detected using appropriate Alexa 488 (Molecular Probes, Germany, 1:500, A11001) and Cy3 (Jackson Immuno Research Europe, United Kingdom, 1:500, 711-166-152) conjugated secondary antibodies. Sections were viewed using a BX61 microscope (Olympus, Japan), as previously described (Zampini et al., 2010).

Field Excitatory Postsynaptic Potential (fEPSP) Recordings in Hippocampal Slices

Animals were deeply anesthetized with CO_2 and then sacrificed by decapitation. Extracellular fEPSP recordings were performed according to standard methods, as previously described (Matt et al., 2011; Ngodup et al., 2015; Chenaux et al., 2016). In brief, stimulation (TM53CCINS, WPI) and recording (ACSF-filled glass pipettes, 2–3 MΩ) electrodes were positioned in the stratum radiatum (SR) to record Schaffer collateral field excitatory postsynaptic potentials (fEPSPs). The same stimulus intensity was applied during baseline recording (0.067 Hz, 20–30 min) and induction of LTP using 100 Hz stimulation for 1 sec or LTD using 1 Hz stimulation for 15 min. The baseline was determined by averaging fEPSP initial slopes from the period before the LTP or LTD stimulation. The level of LTP/LTD was determined by averaging fEPSP slopes from the period between 50 and 60 min after the high-frequency/low-frequency stimulation. Before the LTP/LTD stimulation, each slice was used to record input-output relationship (25–150 μA in 25 μA steps) and paired-pulse facilitation (10–20–50–100–200–500 ms interpulse interval at the same stimulation strength as LTP/LTD recordings). For IOR changes in fEPSP slope were averaged for each group and plotted against the stimulus intensity. For PPF paired-pulse ratio of EPSP2/EPSP1 slope at each interstimulus interval were defined per slice and mean values per group were plotted. EPSP1 was calculated as an average of EPSP1s from all interstimulus intervals for each single slice. Four traces were averaged (WinWCP V5.5.3) for each single analyzed data point.

Multiple T-Maze

The maze consisted of nine equally sized T-elements (8 × 4.5 × 0.4 cm, Lange-Asschenfeldt et al., 2007) made of PVC. The maze also included a start element (14 × 4.5 cm) and a target platform (19 × 12.6 cm). Each element was mounted on a stand; the total element height was 23 cm. To reach the target platform 7 decision points needed to be passed (order: LRRLLRL). The individual mouse house (Tecniplast, Italy) from the home cage was placed on the target platform. Mice were trained on the maze for three consecutive days. On day 1 and 2, each mouse had three runs. If a mouse reached the target platform within the time limit of 10 min, it was scored as a successful run; if not, the trial was terminated. On day 3, each mouse had to perform as many runs as necessary to reach 7 successful training runs. Mice were re-tested twice after a break of 3 and 18 days following their last training run. The sequence in which the mice were placed on the maze was pseudorandomized and then maintained throughout the experiment. Experiments were performed between 10 am and 6 pm. After each run, the maze was cleaned with 70% ethanol. The average light intensity in the maze was 75 lux.

Motor Activity

The force of the mouse movement was measured during acoustic startle experiments (not shown). Motor activity was measured in the 50 ms time window before the stimulus was presented with a piezoelectric force transducer situated inside a sound-attenuated chamber by calculation of the peak-to-peak force. The apparatus consisted of a measuring platform with a wire mesh test cage with a metal floor plate (5 × 9 × 5 cm). The output of the transducer was amplified and filtered from 2 to 150 Hz (University of Tuebingen, Piezo-Amp-System, Tuebingen, Germany). The resulting voltage was sampled (1 kHz) by an analog-to-digital converter located within a computer (Microstar DAP 1200, Washington, DC), results are given in mN (milli-Newton).

Social-Interaction Test

The apparatus for Crawley's sociability test (Silverman et al., 2010) consisted of a rectangular three-chamber PVC box in which each compartment had an area of 19 × 45 cm. In the outer chambers, two identical wired cup-like containers were placed. In one of them, a "stranger" (mouse of the same background, age and gender but without prior contact to the subject mouse) was placed. In the other chamber, an empty container worked as a novel object. The experimental mouse was placed in the center compartment for 5 minutes to adapt, while the lateral compartments were isolated by dividing walls. The walls were then removed and the experimental mouse was allowed to discover all three chambers for 10 minutes. The behavioral testing was performed between 9 am and 5 pm. After each trial, the chambers were cleaned with 70% ethanol.

Ultrasonic Vocalization

Ultrasonic vocalizations of P7 pups were recorded to analyze the reaction of short (5 min) separation from the parental cage as described in Kromer et al. (2005) and Groenink et al. (2008). The pups were randomly selected, the body weight was measured and the single animal was placed on a fresh paper towel in the middle of a plastic box (13 × 13 cm) in a soundproofed chamber with constant temperature of 23 ± 1°C. An ultrasonic microphone (Neutrix), connected with a preamplifier (Avisoft UltraSoundGate416) was fixed with a distance of 12 cm from the middle of the experimental box. For recording, Avisoft (Avisoft Bioacoustic RECORDER Version 4.2.29) was used with a sampling rate of 250 kHz which allows a frequency range from 0 to 125 kHz. With SASlab (Avisoft-SASLabPro Version 5.2.13) a spectrogram of the recordings was calculated and the number of calls was counted manually.

Blood Corticosterone Level Analysis

Blood was collected from the tail vein of anesthetized mice (anesthesia see section *Hearing Measurements and Sound Exposure*) within 5 min after injection, centrifuged, and stored at −80°C. The corticosterone concentration in the blood was measured using a Corticosterone ELISA Kit (Enzo Life Sciences, Farmingdale, NY, United States). The optical density of the samples was finally read at 405 nm in the FLUOstar Optima (BMG LABTECH GmbH, Ortenberg, Version 2.20). To rule out major influences of the circadian rhythm, all blood was taken in the afternoon (between 3 and 5 pm).

In vivo Recordings in the Dorsal Cochlear Nucleus (DCN)

Juxtacellular single-unit recordings were performed in adult controls and in $Bdnf^{Pax2}$KOs. The experimental protocol for such recordings was described previously (Müller et al., 2019). Animals were intraperitoneally anesthetized with a mixture of ketamine hydrochloride (0.1 mg/g bodyweight; Ketamin-Ratiopharm, Ratiopharm) and xylazine hydrochloride (5 μg/g bodyweight; Rompun, Bayer). Throughout recording sessions, anesthesia was maintained by additional subcutaneous application of one-third of the initial dose approximately every 60 min. Briefly, recordings were performed in a sound-attenuating chamber (Type 400, Industrial Acoustic Company) with the animal stabilized in a custom-made stereotaxic apparatus. Acoustic stimuli were digitally generated using custom-written Matlab functions (version 7.5, The MathWorks Inc, Natick, United States, RRID:SCR_001622). The stimuli were transferred to a D/A converter (RP2.1 real-time processor, 97.7 kHz sampling rate, Tucker-Davis Technologies) and delivered through custom-made earphones (acoustic transducer: DT 770 pro, Beyer Dynamics). Juxtacellular recordings of DCN single-units were performed with glass micropipettes (GB150F-10, Science Products, 5-10 MΩ) filled with 3M KCl. The DCN was approached dorsally, and reached at penetrations depths of 3500-4000 μm. Fusiform cells were identified based on the biphasic waveform, V-shaped FRA, and pauser/build-up PSTH (Rhode et al., 1983; Rhode and Smith, 1986; Felix et al., 2017). Subsequently, the mouse was perfused transcardially with 0.9% NaCl solution followed by 5% PFA. Coronal slices containing the cochlear nucleus were cut on a vibratome (HM 650V, Microm), and the tissue sections were visualized under a fluorescent microscope (Zeiss Axioskop 2). The recording sites were histologically verified by iontophoretic injection of Flurogold (+5 μA, 5 min).

Hearing Measurements and Sound Exposure

The hearing function of adult $Bdnf^{Pax2}$KO and controls was studied by measuring and analyzing auditory brainstem responses (**ABR**) and auditory steady-state responses (**ASSR**), as previously described (Zuccotti et al., 2012; Rüttiger et al., 2013; Wolter et al., 2018). Animals were exposed to enriching sound as described (Matt et al., 2018). Animals were anesthetized with intraperitoneal injections of fentanyl (0.05 mg/kg bodyweight, Fentadon; Albrecht GmbH, Aulendorf, Germany), midazolam (2.5 mg/kg body weight, Midazolam-hameln; Hameln Pharma plus GmbH, Hameln, Germany), medetomidin (0.5 mg/kg bodyweight, Sedator; Albrecht GmbH, Aulendorf, Germany) and atropine sulfate (0.2 mg/kg body weight, B. Braun, Melsungen, Germany). Additional doses of anesthetics were administered if needed.

Quantification and Statistical Analysis

Statistics and Numbers

All statistical information, including the statistical tests and *post hoc* tests used, the exact value of *n*, what n represents and the precision documentation of statistical outcome, can be found in **Supplementary Table 1**. Basic statistical information, such as *P*-values and *n,* can be found in the figure legends. In the figures, significance is indicated by asterisks ($^{*}P < 0.05$, $^{**}P < 0.01$, $^{***}P < 0.001$, and $^{****}P < 0.0001$). n.s. denotes non-significant results ($P > 0.05$). A trend is indicated by asterisk in brackets [$(^{*})$ $P < 0.1$].

Colocalization of mRNA and Protein and Immunohistochemistry in Brain Sections

Brain sections were quantified by integrating density values of color pixels for each single specimen using ImageJ software. The density values of all specimens stained within the same

experiment were then normalized to the group mean (i.e., all hippocampal brain sections stained in the same experiment gave an average value of 1.0) or, in the case of development studies, they were normalized to all animals in the age range of P6 to P10. This correction allowed compensating for the high inter-trial variation of staining intensity. All sections from one mouse were then averaged and entered the statistical evaluation as $n = 1$.

fEPSP Recordings in Hippocampal Slices

Data was processed and analyzed using WinWCP V5.5.3, Clampfit 10.7 (Molecular Devices), Microsoft Excel and GraphPad Prism 8. The data presented per experimental group/condition contained (additionally to mean ± SEM) single dots which showed the fEPSP slope values for each individual brain slice. The *n* indicates the number of slices and animals (slices/animals) used in the analysis.

Multiple T-Maze

Each trial was video-recorded with a webcam (Logitech c920). If a mouse fell from the maze, it was immediately placed back on the same spot. Errors were counted offline using the software BORIS (Friard and Gamba, 2016). An error was counted when a mouse deviated from the correct path to the target with all four paws. Consecutive errors made at the same decision point were counted as one error. Statistics was calculated with JMP 14 (SAS Institute Inc., United States). The circling behavior was measured by counting the number of full 360° rotations during the time in the maze. Data from two mice, which failed to find the target platform during the first 5 training runs, were excluded from further analysis. Time measurement was stopped when a mouse reached the mouse house with all four paws.

Social-Interaction Test

The duration of sniffing contact of the mouse at the stranger- and the empty container were normalized to the time spent in the respective compartment, and the number of entries the mouse made in each of the compartments, the latency to the first entry into each chamber, as well as the time the experimental mouse spent with freezing or grooming during the 10 min period was analyzed. The circling behavior was measured by counting the number of full 360° rotations during the habituation time.

Blood Corticosterone Level Analysis

The values measured for optical density were exported to Excel (Microsoft, 2016) and analyzed according to manufacturer's instructions found online at myassays.com.

In vivo Recordings in the Dorsal Cochlear Nucleus (DCN)

Response threshold (the lowest stimulus level resulting in an increase of spiking), characteristic frequency (**CF**, the sound frequency causing increased firing at the lowest sound level), and maximum discharge rate were analyzed as described (Müller et al., 2019). The quality factor (Q_{10}) was calculated as the ratio between the unit's CF and the frequency bandwidth (CF/BW) at 10 dB above threshold. The dB range between 10 and 90% of the rising slope of the rate-level function at CF was defined as the dynamic range. For units with prominent inhibitory sidebands, indicated by a significant decrease in firing below the spontaneous rate, inhibitory strength was calculated as the relative reduction of the firing rate within the inhibitory sideband with respect to the rate outside of excitatory receptive field ("non-inhibitory area") (Chumak et al., 2016). In addition, the ratio between AP discharge rates in excitatory and non-inhibitory areas was calculated (Chumak et al., 2016). Peri-stimulus time histograms were used to determine the first spike latency (**FSL**), calculated as the time between stimulus onset and the peak of a kernel density function (Botev et al., 2010) fitted over the AP spike times.

ABR Wave Form Analysis

Auditory brainstem responses waveforms were analyzed for consecutive amplitude deflections (waves), with each wave consisting of a starting negative (n) peak and the following positive (p) peak. Wave latencies were defined by the onset timing (negative peak) of each corresponding wave. Peak amplitudes and latencies of ABR waves I and IV were extracted and defined as wave I: I_n - I_p (0.85-1.9 ms); wave IV: IV_n – IV_p (3.15-6.05 ms). A customized computer program (Peak, University of Tübingen) was used to extract ABR peak amplitudes and latencies based on these definitions. From the extracted peaks, ABR peak-to-peak (wave) amplitude and latency growth functions (Burkard and Don, 2007) were calculated for individual ears for increasing stimulus levels. All ABR wave amplitude and latency growth functions were normalized with reference to the ABR thresholds (from -10 dB to a maximum of 90 dB relative to threshold for wave amplitudes and from 0 dB to a maximum of 90 dB above threshold for wave latencies).

SIGNIFICANCE STATEMENT

The present findings demonstrate a requirement for BDNF in Pax2-lineage descendants (GABAergic precursors) in hindbrain regions for the development of proper cognitive abilities. *Bdnf*^{Pax2}KO mice lack proper maturation of fine-grained resolution of auditory brainstem output activity, maturation of dendritic outgrowth of PV–INs and scaled Arc levels in the auditory cortex and hippocampus, required for LTP/LTD adjustments, learning, and control of anxiety and social behavior. BDNF in Pax2-lineage descendants in lower brainstem regions may thus be involved in the disturbed migration of GABAergic INs which may contribute to the pathophysiology of multiple psychiatric disorders, including autism.

DATA AVAILABILITY STATEMENT

The raw data supporting the conclusions of this article will be made available by the authors, without undue reservation.

ETHICS STATEMENT

The animal study was reviewed and approved by the Animal Care and Ethics Committee of the Regional Board of the Federal State Government of Baden-Württemberg, Germany.

AUTHOR CONTRIBUTIONS

PE, PM, LR, and MK designed the research. PE, PM, MM, MW, SJ, DS, LR, IM, PP, and MK performed the research. PE, PM, MM, MW, SJ, DS, WS, LR, and PP contributed to unpublished reagents and analytic tools and analyzed the data. PE and MK wrote the first draft of the manuscript. MJ, TS, PP, and MK edited the manuscript. PE, PM, LR, and MK wrote the manuscript. All authors contributed to the article and approved the submitted version.

FUNDING

We acknowledge grants from the Deutsche Forschungsgemeinschaft FOR 2060 project RU 713/3-2 (WS and LR), GRK 2381 (PM), SPP 1608 RU 316/12-1 (PE and LR), MI 954/3-1 (IM and SJ), KN 316/12-1 (MM and MK), BFU2016-76580-P (TS), and NIH NIMH 1R01MH106623 (MJ).

ACKNOWLEDGMENTS

We thank Hyun-Soon Geisler, Karin Rohbock, and Iris Köpschall for their excellent technical assistance, Morgan Hess and stels-ol.de for English-language services.

SUPPLEMENTARY MATERIAL

The Supplementary Material for this article can be found online at: https://www.frontiersin.org/articles/10.3389/fnmol.2021.642679/full#supplementary-material

Supplementary Figure 1 | Hippocampal fEPSP slope in *Bdnf*^{Pax2}KOs. **(A)** Averaged fEPSP slope was plotted as a function of stimulus intensity. No difference was observed between slices from controls, *Bdnf*^{Pax2}KOs, P6-10 controls and enriching sound-exposed (SE) controls and *Bdnf*^{Pax2}KOs. Traces from representative recordings are shown on the right (control: n = 9/14 animals/slices, *Bdnf*^{Pax2}KOs: n = 9/10 animals/slices, P6-10 controls n = 6/7 animals/slices, controls exposed n = 4/11 animals/slices, *Bdnf*^{Pax2}KOs exposed n = 3/5 animals/slices; P = 0.54). **(B)** Paired pulse facilitation was not different between slices from controls, *Bdnf*^{Pax2}KOs, P6-10 controls and sound-exposed controls and *Bdnf*^{Pax2}KOs for all inter-stimulus intervals. Traces from representative recordings are shown on the right (controls: n = 9/14 animals/slices, *Bdnf*^{Pax2}KOs: n = 9/10 animals/slices, P6-10 controls n = 6/7 animals/slices, controls exposed n = 4/11 animals/slices, *Bdnf*^{Pax2}KOs exposed n = 3/5 animals/slices; P = 0.75). Mean ± S.E.M.

Supplementary Figure 2 | Hearing function of *Bdnf*^{Pax2}KOs. **(A)** Click evoked (n = 23-26/46-52 mice/ears; P = 0.002), noise burst (P = 0.026) and frequency-specific ABR thresholds (n = 16/32 mice/ears each; $P < 0.0001$). Schematic ABR waveform of controls (black) and *Bdnf*^{Pax2}KOs (red) in relation to the corresponding auditory nuclei in the ascending auditory pathway. **(B)** Noise stimulus-evoked amplitude of AN activity (left panel) and latency (right panel) (amplitude: n = 12-14/24-28 mice/ears; $P < 0.0001$; latency: n = 12-14/24-28 mice/ears; $P < 0.0001$). **(C)** Noise stimulus-evoked amplitude of midbrain activity (left panel) and latency (right panel) (Amplitude: n = 12-14/24-28 mice/ears; $P < 0.0001$; latency: n = 12-14/24-28 mice/ears; $P < 0.0001$). **(D)** The signal to noise ratio (SNR) of modulation depth response (left panel; n = 10/10 mice/ears each; P = 0.001) and SNR modulation I-O function of an amplitude-modulated tone (right panel; n = 10/10 mice/ears each; $P < 0.0001$) was reduced in *Bdnf*^{Pax2}KOs. Mean ± S.E.M.

Supplementary Table 1 | Detailed statistical information.

REFERENCES

Alexander, J. M., Pirone, A., and Jacob, M. H. (2020). Excessive beta-catenin in excitatory neurons results in reduced social and increased repetitive behaviors and altered expression of multiple genes linked to human autism. *Front. Synaptic Neurosci.* 12:14. doi: 10.3389/fnsyn.2020.00014

Andreska, T., Aufmkolk, S., Sauer, M., and Blum, R. (2014). High abundance of BDNF within glutamatergic presynapses of cultured hippocampal neurons. *Front. Cell. Neurosci.* 8:107. doi: 10.3389/fncel.2014.00107

Awad, P. N., Amegandjin, C. A., Szczurkowska, J., Carrico, J. N., Fernandes do Nascimento, A. S., Baho, E., et al. (2018). KCC2 regulates dendritic spine formation in a brain-region specific and BDNF dependent manner. *Cereb. Cortex* 28, 4049–4062. doi: 10.1093/cercor/bhy198

Bakos, J., Zatkova, M., Bacova, Z., and Ostatnikova, D. (2016). The role of hypothalamic neuropeptides in neurogenesis and neuritogenesis. *Neural Plast.* 2016:3276383.

Barreda Tomas, F. J., Turko, P., Heilmann, H., Trimbuch, T., Yanagawa, Y., Vida, I., et al. (2020). BDNF expression in cortical GABAergic interneurons. *Int. J. Mol. Sci.* 21:1567. doi: 10.3390/ijms21051567

Ben-Ari, Y. (2002). Excitatory actions of gaba during development:the nature of the nurture. *Nat. Rev. Neurosci.* 3, 728–739. doi: 10.1038/nrn920

Blair, L. J., Criado-Marrero, M., Zheng, D., Wang, X., Kamath, S., Nordhues, B. A., et al. (2019). The disease-associated chaperone FKBP51 impairs cognitive function by accelerating AMPA receptor recycling. *eNeuro* 6:ENEURO.242-18.2019.

Bortone, D., and Polleux, F. (2009). KCC2 expression promotes the termination of cortical interneuron migration in a voltage-sensitive calcium-dependent manner. *Neuron* 62, 53–71. doi: 10.1016/j.neuron.2009.01.034

Botev, Z. I., Grotowski, J. F., and Kroese, D. P. (2010). Kernel density estimation via diffusion. *Ann. Stat.* 38, 2916–2957. doi: 10.1214/10-aos799

Bourien, J., Tang, Y., Batrel, C., Huet, A., Lenoir, M., Ladrech, S., et al. (2014). Contribution of auditory nerve fibers to compound action potential of the auditory nerve. *J. Neurophysiol.* 112, 1025–1039. doi: 10.1152/jn.00738.2013

Bramham, C. R., Worley, P. F., Moore, M. J., and Guzowski, J. F. (2008). The immediate early gene arc/arg3.1: regulation, mechanisms, and function. *J. Neurosci.* 28, 11760–11767. doi: 10.1523/jneurosci.3864-08.2008

Burkard, R. F., and Don, M. (2007). "The auditory brainstem response," in *Auditory Evoked Potentials: Basic Principles and Clinical Application*, eds R. F. Burkard, J. J. Eggermont, and M. Don (Philadelphia, PA: Lippincott Williams and Wilkins).

Canals, J. M., Checa, N., Marco, S., Akerud, P., Michels, A., Perez-Navarro, E., et al. (2001). Expression of brain-derived neurotrophic factor in cortical neurons is regulated by striatal target area. *J. Neurosci.* 21, 117–124. doi: 10.1523/jneurosci.21-01-00117.2001

Canetta, S., Bolkan, S., Padilla-Coreano, N., Song, L. J., Sahn, R., Harrison, N. L., et al. (2016). Maternal immune activation leads to selective functional deficits in offspring parvalbumin interneurons. *Mol. Psychiatry* 21, 956–968. doi: 10.1038/mp.2015.222

Cardin, J. A., Carlen, M., Meletis, K., Knoblich, U., Zhang, F., Deisseroth, K., et al. (2009). Driving fast-spiking cells induces gamma rhythm and controls sensory responses. *Nature* 459, 663–667. doi: 10.1038/nature08002

Chenaux, G., Matt, L., Hill, T. C., Kaur, I., Liu, X.-B., and Kirk, L. M. (2016). Loss of SynDIG1 reduces excitatory synapse maturation but not formation *in vivo*. *eNeuro* 3:ENEURO.0130-16.2016. doi: 10.1523/ENEURO.0130-16.2016

Cheng, G. R., Li, X. Y., Xiang, Y. D., Liu, D., McClintock, S. M., and Zeng, Y. (2017). The implication of AMPA receptor in synaptic plasticity impairment

and intellectual disability in fragile X syndrome. *Physiol. Res.* 66, 715–727. doi: 10.33549/physiolres.933473

Chumak, T., Rüttiger, L., Lee, S. C., Campanelli, D., Zuccotti, A., Singer, W., et al. (2016). BDNF in lower brain parts modifies auditory fiber activity to gain fidelity but increases the risk for generation of central noise after injury. *Mol. Neurobiol.* 53, 5607–5627. doi: 10.1007/s12035-015-9474-x

Cohen-Cory, S., Kidane, A. H., Shirkey, N. J., and Marshak, S. (2010). Brain-derived neurotrophic factor and the development of structural neuronal connectivity. *Dev. Neurobiol.* 70, 271–288.

Collin, T., Chat, M., Lucas, M. G., Moreno, H., Racay, P., Schwaller, B., et al. (2005). Developmental changes in parvalbumin regulate presynaptic Ca2+ signaling. *J. Neurosci.* 25, 96–107. doi: 10.1523/jneurosci.3748-04.2005

Das, I., Estevez, M. A., Sarkar, A. A., and Banerjee-Basu, S. (2019). A multifaceted approach for analyzing complex phenotypic data in rodent models of autism. *Mol. Autism* 10:11.

de Kloet, E. R., Oitzl, M. S., and Joels, M. (1999). Stress and cognition:are corticosteroids good or bad guys? *Trends Neurosci.* 22, 422–426. doi: 10.1016/s0166-2236(99)01438-1

De Koninck, Y. (2007). Altered chloride homeostasis in neurological disorders:a new target. *Curr. Opin. Pharmacol.* 7, 93–99. doi: 10.1016/j.coph.2006.11.005

de Villers-Sidani, E., Chang, E. F., Bao, S., and Merzenich, M. M. (2007). Critical period window for spectral tuning defined in the primary auditory cortex (A1) in the rat. *J. Neurosci.* 27, 180–189. doi: 10.1523/jneurosci.3227-06.2007

Derkach, V. A., Oh, M. C., Guire, E. S., and Soderling, T. R. (2007). Regulatory mechanisms of AMPA receptors in synaptic plasticity. *Nat. Rev. Neurosci.* 8, 101–113. doi: 10.1038/nrn2055

Diering, G. H., and Huganir, R. L. (2018). The AMPA receptor code of synaptic plasticity. *Neuron* 100, 314–329. doi: 10.1016/j.neuron.2018.10.018

Felix, R. A. II, Elde, C. J., Nevue, A. A., and Portfors, C. V. (2017). Serotonin modulates response properties of neurons in the dorsal cochlear nucleus of the mouse. *Hear. Res.* 344, 13–23. doi: 10.1016/j.heares.2016.10.017

Ferguson, B. R., and Gao, W. J. (2018). PV interneurons:critical regulators of E/I balance for prefrontal cortex-dependent behavior and psychiatric disorders. *Front. Neural Circuits* 12:37. doi: 10.3389/fncir.2018.00037

Fitch, R. H., Miller, S., and Tallal, P. (1997). Neurobiology of speech perception. *Annu. Rev. Neurosci.* 20, 331–353. doi: 10.1146/annurev.neuro.20.1.331

Fitch, R. H., and Tallal, P. (2003). Neural mechanisms of language-based learning impairments:insights from human populations and animal models. *Behav. Cogn. Neurosci. Rev.* 2, 155–178. doi: 10.1177/1534582303258736

Foss-Feig, J. H., Schauder, K. B., Key, A. P., Wallace, M. T., and Stone, W. L. (2017). Audition-specific temporal processing deficits associated with language function in children with autism spectrum disorder. *Autism Res.* 10, 1845–1856. doi: 10.1002/aur.1820

Fotaki, V., Price, D. J., and Mason, J. O. (2008). Newly identified patterns of Pax2 expression in the developing mouse forebrain. *BMC Dev. Biol.* 8:79. doi: 10.1186/1471-213X-8-79

Friard, O., and Gamba, M. (2016). BORIS:a free, versatile open-source event-logging software for video/audio coding and live observations. *Methods Ecol. Evol.* 7, 1325–1330. doi: 10.1111/2041-210x.12584

Friauf, E., Rust, M. B., Schulenborg, T., and Hirtz, J. J. (2011). Chloride cotransporters, chloride homeostasis, and synaptic inhibition in the developing auditory system. *Hear. Res.* 279, 96–110. doi: 10.1016/j.heares.2011.05.012

Gabernet, L., Jadhav, S. P., Feldman, D. E., Carandini, M., and Scanziani, M. (2005). Somatosensory integration controlled by dynamic thalamocortical feed-forward inhibition. *Neuron* 48, 315–327. doi: 10.1016/j.neuron.2005.09.022

Gao, R., and Penzes, P. (2015). Common mechanisms of excitatory and inhibitory imbalance in schizophrenia and autism spectrum disorders. *Curr. Mol. Med.* 15, 146–167. doi: 10.2174/1566524015666150303003028

Gill, K. M., and Grace, A. A. (2014). The role of α5 $GABA_A$ receptor agonists in the treatment of cognitive deficits in schizophrenia. *Curr. Pharm. Des.* 20, 5069–5076. doi: 10.2174/1381612819666131216114612

Glowatzki, E., and Fuchs, P. A. (2002). Transmitter release at the hair cell ribbon synapse. *Nat. Neurosci.* 5, 147–154. doi: 10.1038/nn796

Goel, A., Cantu, D. A., Guilfoyle, J., Chaudhari, G. R., Newadkar, A., Todisco, B., et al. (2019). Author Correction: impaired perceptual learning in a mouse model of Fragile X syndrome is mediated by parvalbumin neuron dysfunction and is reversible. *Nat. Neurosci.* 22:143. doi: 10.1038/s41593-018-0273-3

Gong, W. K., Ni, J., Yu, L. F., Wang, L., and Huang, Z. L. (2020). Temporal dynamics of Arc/Arg3.1 expression in the dorsal striatum during acquisition and consolidation of a motor skill in mice. *Neurobiol. Learn. Mem.* 168:107156. doi: 10.1016/j.nlm.2019.107156

Grant, L., Yi, E., and Glowatzki, E. (2010). Two modes of release shape the postsynaptic response at the inner hair cell ribbon synapse. *J. Neurosci.* 30, 4210–4220. doi: 10.1523/jneurosci.4439-09.2010

Griffen, T. C., and Maffei, A. (2014). GABAergic synapses:their plasticity and role in sensory cortex. *Front. Cell. Neurosci.* 8:91. doi: 10.3389/fncel.2014.00091

Groenink, L., Verdouw, P. M., van Oorschot, R., and Olivier, B. (2008). Models of anxiety:ultrasonic vocalizations of isolated rat pups. *Curr. Protoc. Pharmacol* Chapter 5:Unit5.18.

Guo, J., and Anton, E. S. (2014). Decision making during interneuron migration in the developing cerebral cortex. *Trends Cell Biol.* 24, 342–351. doi: 10.1016/j.tcb.2013.12.001

Guzowski, J. F., Miyashita, T., Chawla, M. K., Sanderson, J., Maes, L. I., Houston, F. P., et al. (2006). Recent behavioral history modifies coupling between cell activity and Arc gene transcription in hippocampal CA1 neurons. *Proc. Natl. Acad. Sci. U.S.A.* 103, 1077–1082. doi: 10.1073/pnas.0505519103

Heil, P., Neubauer, H., Brown, M., and Irvine, D. R. (2008). Towards a unifying basis of auditory thresholds: distributions of the first-spike latencies of auditory-nerve fibers. *Hear. Res.* 238, 25–38. doi: 10.1016/j.heares.2007.09.014

Hickman, T. T., Liberman, M. C., and Jacob, M. H. (2015). Adenomatous polyposis coli protein deletion in efferent olivocochlear neurons perturbs afferent synaptic maturation and reduces the dynamic range of hearing. *J. Neurosci.* 35, 9236–9245. doi: 10.1523/jneurosci.4384-14.2015

Hong, E. J., McCord, A. E., and Greenberg, M. E. (2008). A biological function for the neuronal activity-dependent component of Bdnf transcription in the development of cortical inhibition. *Neuron* 60, 610–624. doi: 10.1016/j.neuron.2008.09.024

Hu, H., Gan, J., and Jonas, P. (2014). Interneurons. Fast-spiking, parvalbumin+ GABAergic interneurons: from cellular design to microcircuit function. *Science* 345:1255263. doi: 10.1126/science.1255263

Huang, Z. J., Kirkwood, A., Pizzorusso, T., Porciatti, V., Morales, B., Bear, M. F., et al. (1999). BDNF regulates the maturation of inhibition and the critical period of plasticity in mouse visual cortex. *Cell* 98, 739–755.

Irvine, D. R. F. (2018). Auditory perceptual learning and changes in the conceptualization of auditory cortex. *Hear. Res.* 366, 3–16. doi: 10.1016/j.heares.2018.03.011

Jakkamsetti, V., Tsai, N. P., Gross, C., Molinaro, G., Collins, K. A., Nicoletti, F., et al. (2013). Experience-induced Arc/Arg3.1 *primes CA*1 pyramidal neurons for metabotropic glutamate receptor-dependent long-term synaptic depression. *Neuron* 80, 72–79. doi: 10.1016/j.neuron.2013.07.020

Jungbluth, S., Koentges, G., and Lumsden, A. (1997). Coordination of early neural tube development by BDNF/trkB. *Development* 124, 1877–1885.

Kaila, K., Price, T. J., Payne, J. A., Puskarjov, M., and Voipio, J. (2014). Cation-chloride cotransporters in neuronal development, plasticity and disease. *Nat. Rev. Neurosci.* 15, 637–654. doi: 10.1038/nrn3819

Kandler, K., and Friauf, E. (1995). Development of glycinergic and glutamatergic synaptic transmission in the auditory brainstem of perinatal rats. *J. Neurosci.* 15, 6890–6904. doi: 10.1523/jneurosci.15-10-06890.1995

Kim, H., Ahrlund-Richter, S., Wang, X., Deisseroth, K., and Carlen, M. (2016). Prefrontal parvalbumin neurons in control of attention. *Cell* 164, 208–218. doi: 10.1016/j.cell.2015.11.038

Kimura, K., and Itami, C. (2019). A hypothetical model concerning how spike-timing-dependent plasticity contributes to neural circuit formation and initiation of the critical period in barrel cortex. *J. Neurosci.* 39, 3784–3791. doi: 10.1523/JNEUROSCI.1684-18.2019

Kiss, J. Z., Vasung, L., and Petrenko, V. (2014). Process of cortical network formation and impact of early brain damage. *Curr. Opin. Neurol.* 27, 133–141. doi: 10.1097/wco.0000000000000068

Knipper, M., van Dijk, P., Schulze, H., Mazurek, B., Krauss, P., Scheper, V., et al. (2020). The neural bases of tinnitus: lessons from deafness and cochlear implants. *J. Neurosci.* 40, 7190–7202. doi: 10.1523/jneurosci.1314-19.2020

Kopp-Scheinpflug, C., Tozer, A. J., Robinson, S. W., Tempel, B. L., Hennig, M. H., and Forsythe, I. D. (2011). The sound of silence: ionic mechanisms encoding sound termination. *Neuron* 71, 911–925. doi: 10.1016/j.neuron.2011.06.028

Korb, E., and Finkbeiner, S. (2011). Arc in synaptic plasticity: from gene to behavior. *Trends Neurosci.* 34, 591–598. doi: 10.1016/j.tins.2011.08.007

Kraus, N., and White-Schwoch, T. (2015). Unraveling the biology of auditory learning: a cognitive-sensorimotor-reward framework. *Trends Cogn. Sci.* 19, 642–654. doi: 10.1016/j.tics.2015.08.017

Kromer, S. A., Kessler, M. S., Milfay, D., Birg, I. N., Bunck, M., Czibere, L., et al. (2005). Identification of glyoxalase-I as a protein marker in a mouse model of extremes in trait anxiety. *J. Neurosci.* 25, 4375–4384. doi: 10.1523/jneurosci.0115-05.2005

Lange-Asschenfeldt, C., Lohmann, P., and Riepe, M. W. (2007). Spatial performance in a complex maze is associated with persistent long-term potentiation enhancement in mouse hippocampal slices at early training stages. *Neuroscience* 147, 318–324. doi: 10.1016/j.neuroscience.2007.04.020

Larsson, M. (2017). Pax2 is persistently expressed by GABAergic neurons throughout the adult rat dorsal horn. *Neurosci. Lett.* 638, 96–101. doi: 10.1016/j.neulet.2016.12.015

Leutgeb, J. K., Leutgeb, S., Moser, M. B., and Moser, E. I. (2007). Pattern separation in the dentate gyrus and CA3 of the hippocampus. *Science* 315, 961–966. doi: 10.1126/science.1135801

Levitt, P., Eagleson, K. L., and Powell, E. M. (2004). Regulation of neocortical interneuron development and the implications for neurodevelopmental disorders. *Trends Neurosci.* 27, 400–406. doi: 10.1016/j.tins.2004.05.008

Lewis, D. A., Hashimoto, T., and Volk, D. W. (2005). Cortical inhibitory neurons and schizophrenia. *Nat. Rev. Neurosci.* 6, 312–324. doi: 10.1038/nrn1648

Li, H., Khirug, S., Cai, C., Ludwig, A., Blaesse, P., Kolikova, J., et al. (2007). KCC2 interacts with the dendritic cytoskeleton to promote spine development. *Neuron* 56, 1019–1033. doi: 10.1016/j.neuron.2007.10.039

Li, S., Kumar, T. P., Joshee, S., Kirschstein, T., Subburaju, S., Khalili, J. S., et al. (2018). Endothelial cell-derived GABA signaling modulates neuronal migration and postnatal behavior. *Cell Res.* 28, 221–248. doi: 10.1038/cr.2017.135

Lim, L., Mi, D., Llorca, A., and Marin, O. (2018). Development and functional diversification of cortical interneurons. *Neuron* 100, 294–313. doi: 10.1016/j.neuron.2018.10.009

Link, W., Konietzko, U., Kauselmann, G., Krug, M., Schwanke, B., Frey, U., et al. (1995). Somatodendritic expression of an immediate early gene is regulated by synaptic activity. *Proc. Natl. Acad. Sci. U.S.A.* 92, 5734–5738. doi: 10.1073/pnas.92.12.5734

Lunden, J. W., Durens, M., Phillips, A. W., and Nestor, M. W. (2019). Cortical interneuron function in autism spectrum condition. *Pediatr. Res.* 85, 146–154. doi: 10.1038/s41390-018-0214-6

Madisen, L., Zwingman, T. A., Sunkin, S. M., Oh, S. W., Zariwala, H. A., Gu, H., et al. (2010). A robust and high-throughput Cre reporting and characterization system for the whole mouse brain. *Nat. Neurosci.* 13, 133–140. doi: 10.1038/nn.2467

Malhi, G. S., and Mann, J. J. (2018). Depression. *Lancet* 392, 2299–2312.

Mamashli, F., Khan, S., Bharadwaj, H., Michmizos, K., Ganesan, S., Garel, K. A., et al. (2017). Auditory processing in noise is associated with complex patterns of disrupted functional connectivity in autism spectrum disorder. *Autism Res.* 10, 631–647. doi: 10.1002/aur.1714

Marchetta, P., Savitska, D., Kubler, A., Asola, G., Manthey, M., Mohrle, D., et al. (2020). Age-dependent auditory processing deficits after cochlear synaptopathy depend on auditory nerve latency and the ability of the brain to recruit LTP/BDNF. *Brain Sci.* 10:710. doi: 10.3390/brainsci10100710

Maricich, S. M., and Herrup, K. (1999). Pax-2 expression defines a subset of GABAergic interneurons and their precursors in the developing murine cerebellum. *J. Neurobiol.* 41, 281–294. doi: 10.1002/(sici)1097-4695(19991105)41:2<281::aid-neu10>3.0.co;2-5

Marin, O. (2012). Interneuron dysfunction in psychiatric disorders. *Nat. Rev. Neurosci.* 13, 107–120. doi: 10.1038/nrn3155

Marin, O., and Rubenstein, J. L. (2001). A long, remarkable journey: tangential migration in the telencephalon. *Nat. Rev. Neurosci.* 2, 780–790. doi: 10.1038/35097509

Matt, L., Eckert, P., Panford-Walsh, R., Geisler, H. S., Bausch, A. E., Manthey, M., et al. (2018). Visualizing BDNF transcript usage during sound-induced memory linked plasticity. *Front. Mol. Neurosci.* 11:260. doi: 10.3389/fnmol.2018.00260

Matt, L., Michalakis, S., Hofmann, F., Hammelmann, V., Ludwig, A., Biel, M., et al. (2011). HCN2 channels in local inhibitory interneurons constrain LTP in the hippocampal direct perforant path. *Cell. Mol. Life Sci.* 68, 125–137. doi: 10.1007/s00018-010-0446-z

McCullagh, E. A., Rotschafer, S. E., Auerbach, B. D., Klug, A., Kaczmarek, L. K., Cramer, K. S., et al. (2020). Mechanisms underlying auditory processing deficits in Fragile X syndrome. *FASEB J.* 34, 3501–3518. doi: 10.1096/fj.201902435r

Meddis, R. (2006). Auditory-nerve first-spike latency and auditory absolute threshold: a computer model. *J. Acoust. Soc. Am.* 119, 406–417. doi: 10.1121/1.2139628

Meis, S., Endres, T., Munsch, T., and Lessmann, V. (2019). Impact of chronic BDNF depletion on GABAergic synaptic transmission in the lateral amygdala. *Int. J. Mol. Sci.* 20:4310. doi: 10.3390/ijms20174310

Merchan-Perez, A., and Liberman, M. C. (1996). Ultrastructural differences among afferent synapses on cochlear hair cells: correlations with spontaneous discharge rate. *J. Comp. Neurol.* 371, 208–221. doi: 10.1002/(sici)1096-9861(19960722)371:2<208::aid-cne2>3.0.co;2-6

Miyoshi, G. (2019). Elucidating the developmental trajectories of GABAergic cortical interneuron subtypes. *Neurosci. Res.* 138, 26–32. doi: 10.1016/j.neures.2018.09.012

Mohn, J. L., Alexander, J., Pirone, A., Palka, C. D., Lee, S. Y., Mebane, L., et al. (2014). Adenomatous polyposis coli protein deletion leads to cognitive and autism-like disabilities. *Mol. Psychiatry* 19, 1133–1142. doi: 10.1038/mp.2014.61

Müller, M. K., Jovanovic, S., Keine, C., Radulovic, T., Rubsamen, R., and Milenkovic, I. (2019). Functional development of principal neurons in the anteroventral cochlear nucleus extends beyond hearing onset. *Front. Cell. Neurosci.* 13:119.

Ngodup, T., Goetz, J. A., McGuire, B. C., Sun, W., Lauer, A. M., and Xu-Friedman, M. A. (2015). Activity-dependent, homeostatic regulation of neurotransmitter release from auditory nerve fibers. *Proc. Natl. Acad. Sci. U.S.A.* 112, 6479–6484. doi: 10.1073/pnas.1420885112

Nikolaienko, O., Patil, S., Eriksen, M. S., and Bramham, C. R. (2018). Arc protein: a flexible hub for synaptic plasticity and cognition. *Semin. Cell Dev. Biol.* 77, 33–42. doi: 10.1016/j.semcdb.2017.09.006

Nornes, H. O., Dressler, G. R., Knapik, E. W., Deutsch, U., and Gruss, P. (1990). Spatially and temporally restricted expression of Pax2 during murine neurogenesis. *Development* 109, 797–809.

Ohyama, T., and Groves, A. K. (2004). Generation of Pax2-Cre mice by modification of a Pax2 bacterial artificial chromosome. *Genesis* 38, 195–199. doi: 10.1002/gene.20017

Okuno, H., Minatohara, K., and Bito, H. (2018). Inverse synaptic tagging: An inactive synapse-specific mechanism to capture activity-induced Arc/arg3.1 and to locally regulate spatial distribution of synaptic weights. *Semin. Cell Dev. Biol.* 77, 43–50. doi: 10.1016/j.semcdb.2017.09.025

Palombi, P. S., Backoff, P. M., and Caspary, D. M. (1994). Paired tone facilitation in dorsal cochlear nucleus neurons: a short-term potentiation model testable *in vivo*. *Hear. Res.* 75, 175–183. doi: 10.1016/0378-5955(94)90068-x

Park, M. (2018). AMPA receptor trafficking for postsynaptic potentiation. *Front. Cell. Neurosci.* 12:361. doi: 10.3389/fncel.2018.00361

Peng, S., Li, W., Lv, L., Zhang, Z., and Zhan, X. (2018). BDNF as a biomarker in diagnosis and evaluation of treatment for schizophrenia and depression. *Discov Med* 26, 127–136.

Penrod, R. D., Kumar, J., Smith, L. N., McCalley, D., Nentwig, T. B., Hughes, B. W., et al. (2019). Activity-regulated cytoskeleton-associated protein (Arc/Arg3.1) regulates anxiety- and novelty-related behaviors. *Genes Brain Behav.* 18:e12561.

Pirone, A., Alexander, J. M., Koenig, J. B., Cook-Snyder, D. R., Palnati, M., Wickham, R. J., et al. (2018). Social stimulus causes aberrant activation of the medial prefrontal cortex in a mouse model with autism-like behaviors. *Front. Synaptic Neurosci.* 10:35. doi: 10.3389/fnsyn.2018.00035

Pouille, F., and Scanziani, M. (2001). Enforcement of temporal fidelity in pyramidal cells by somatic feed-forward inhibition. *Science* 293, 1159–1163. doi: 10.1126/science.1060342

Ramus, F. (2003). Developmental dyslexia: specific phonological deficit or general sensorimotor dysfunction? *Curr. Opin. Neurobiol.* 13, 212–218. doi: 10.1016/s0959-4388(03)00035-7

Reim, D., and Schmeisser, M. J. (2017). Neurotrophic Factors in Mouse Models of Autism Spectrum Disorder: Focus on BDNF and IGF-1. *Adv. Anat. Embryol. Cell Biol.* 224, 121–134. doi: 10.1007/978-3-319-52498-6_7

Rendall, A. R., Ford, A. L., Perrino, P. A., and Holly Fitch, R. (2017). Auditory processing enhancements in the TS2-neo mouse model of Timothy Syndrome, a rare genetic disorder associated with autism spectrum disorders. *Adv. Neurodev. Disord.* 1, 176–189. doi: 10.1007/s41252-017-0029-1

Rhode, W. S., and Smith, P. H. (1986). Physiological studies on neurons in the dorsal cochlear nucleus of cat. *J. Neurophysiol.* 56, 287–307. doi: 10.1152/jn.1986.56.2.287

Rhode, W. S., Smith, P. H., and Oertel, D. (1983). Physiological response properties of cells labeled intracellularly with horseradish peroxidase in cat dorsal cochlear nucleus. *J. Comp. Neurol.* 213, 426–447. doi: 10.1002/cne.902130407

Rios, M., Fan, G., Fekete, C., Kelly, J., Bates, B., Kuehn, R., et al. (2001). Conditional deletion of brain-derived neurotrophic factor in the postnatal brain leads to obesity and hyperactivity. *Mol. Endocrinol.* 15, 1748–1757. doi: 10.1210/mend.15.10.0706

Roth, R. H., Cudmore, R. H., Tan, H. L., Hong, I., Zhang, Y., and Huganir, R. L. (2020). Cortical synaptic AMPA receptor plasticity during motor learning. *Neuron* 105, 895–908.e5.

Rowitch, D. H., Kispert, A., and McMahon, A. P. (1999). Pax-2 regulatory sequences that direct transgene expression in the developing neural plate and external granule cell layer of the cerebellum. *Brain Res. Dev. Brain Res.* 117, 99–108. doi: 10.1016/s0165-3806(99)00104-2

Rüttiger, L., Singer, W., Panford-Walsh, R., Matsumoto, M., Lee, S. C., Zuccotti, A., et al. (2013). The reduced cochlear output and the failure to adapt the central auditory response causes tinnitus in noise exposed rats. *PLoS One* 8:e57247. doi: 10.1371/journal.pone.0057247

Shetty, A. K., and Bates, A. (2016). Potential of GABA-ergic cell therapy for schizophrenia, neuropathic pain, and Alzheimer's and Parkinson's diseases. *Brain Res.* 1638(Pt A), 74–87. doi: 10.1016/j.brainres.2015.09.019

Shibata, S., Kakazu, Y., Okabe, A., Fukuda, A., and Nabekura, J. (2004). Experience-dependent changes in intracellular Cl- regulation in developing auditory neurons. *Neurosci. Res.* 48, 211–220. doi: 10.1016/j.neures.2003.10.011

Silverman, J. L., Yang, M., Lord, C., and Crawley, J. N. (2010). Behavioural phenotyping assays for mouse models of autism. *Nat. Rev. Neurosci.* 11, 490–502. doi: 10.1038/nrn2851

Singer, W., Geisler, H. S., and Knipper, M. (2013). The Geisler method: tracing activity-dependent cGMP plasticity changes upon double detection of mRNA and protein on brain slices. *Methods Mol. Biol.* 1020, 223–233. doi: 10.1007/978-1-62703-459-3_15

Singer, W., Geisler, H. S., Panford-Walsh, R., and Knipper, M. (2016). Detection of excitatory and inhibitory synapses in the auditory system using fluorescence immunohistochemistry and high-resolution fluorescence microscopy. *Methods Mol. Biol.* 1427, 263–276. doi: 10.1007/978-1-4939-3615-1_15

Singer, W., Panford-Walsh, R., and Knipper, M. (2014). The function of BDNF in the adult auditory system. *Neuropharmacology* 76(Pt C), 719–728. doi: 10.1016/j.neuropharm.2013.05.008

Skene, N. G., Bryois, J., Bakken, T. E., Breen, G., Crowley, J. J., Gaspar, H. A., et al. (2018). Genetic identification of brain cell types underlying schizophrenia. *Nat. Genet.* 50, 825–833.

Smith, P. F. (2019). The growing evidence for the importance of the otoliths in spatial memory. *Front. Neural Circuits* 13:66. doi: 10.3389/fncir.2019.00066

Sohal, V. S., Zhang, F., Yizhar, O., and Deisseroth, K. (2009). Parvalbumin neurons and gamma rhythms enhance cortical circuit performance. *Nature* 459, 698–702. doi: 10.1038/nature07991

Southwell, D. G., Nicholas, C. R., Basbaum, A. I., Stryker, M. P., Kriegstein, A. R., Rubenstein, J. L., et al. (2014). Interneurons from embryonic development to cell-based therapy. *Science* 344:1240622. doi: 10.1126/science.1240622

Spirou, G. A., Davis, K. A., Nelken, I., and Young, E. D. (1999). Spectral integration by type II interneurons in dorsal cochlear nucleus. *J. Neurophysiol.* 82, 648–663. doi: 10.1152/jn.1999.82.2.648

Su, P., Liu, Y. C., and Lin, H. C. (2016). Risk factors for the recurrence of post-semicircular canal benign paroxysmal positional vertigo after canalith repositioning. *J. Neurol.* 263, 45–51. doi: 10.1007/s00415-015-7931-0

Sun, Q. Q. (2009). Experience-dependent intrinsic plasticity in interneurons of barrel cortex layer IV. *J. Neurophysiol.* 102, 2955–2973. doi: 10.1152/jn.00562.2009

Takano, T. (2015). Interneuron dysfunction in syndromic autism: recent advances. *Dev. Neurosci.* 37, 467–475. doi: 10.1159/000434638

Tan, J., Rüttiger, L., Panford-Walsh, R., Singer, W., Schulze, H., Kilian, S. B., et al. (2007). Tinnitus behavior and hearing function correlate with the reciprocal expression patterns of BDNF and Arg3.1/arc in auditory neurons following acoustic trauma. *Neuroscience* 145, 715–726. doi: 10.1016/j.neuroscience.2006.11.067

Tzingounis, A. V., and Nicoll, R. A. (2006). Arc/Arg3.1:linking gene expression to synaptic plasticity and memory. *Neuron* 52, 403–407. doi: 10.1016/j.neuron.2006.10.016

Uehara, T., Sumiyoshi, T., and Kurachi, M. (2015). New pharmacotherapy targeting cognitive dysfunction of schizophrenia via modulation of GABA neuronal function. *Curr. Neuropharmacol.* 13, 793–801. doi: 10.2174/1570159x13666151009120153

van der Bourg, A., Yang, J. W., Reyes-Puerta, V., Laurenczy, B., Wieckhorst, M., Stuttgen, M. C., et al. (2017). Layer-specific refinement of sensory coding in developing mouse barrel cortex. *Cereb. Cortex* 27, 4835–4850.

Vazdarjanova, A., Ramirez-Amaya, V., Insel, N., Plummer, T. K., Rosi, S., Chowdhury, S., et al. (2006). Spatial exploration induces ARC, a plasticity-related immediate-early gene, only in calcium/calmodulin-dependent protein kinase II-positive principal excitatory and inhibitory neurons of the rat forebrain. *J. Comp. Neurol.* 498, 317–329. doi: 10.1002/cne.21003

Wardle, R. A., and Poo, M. M. (2003). Brain-derived neurotrophic factor modulation of GABAergic synapses by postsynaptic regulation of chloride transport. *J. Neurosci.* 23, 8722–8732. doi: 10.1523/jneurosci.23-25-08722.2003

Waung, M. W., Pfeiffer, B. E., Nosyreva, E. D., Ronesi, J. A., and Huber, K. M. (2008). Rapid translation of Arc/Arg3.1 selectively mediates mGluR-dependent LTD through persistent increases in AMPAR endocytosis rate. *Neuron* 59, 84–97. doi: 10.1016/j.neuron.2008.05.014

Wehr, M., and Zador, A. M. (2003). Balanced inhibition underlies tuning and sharpens spike timing in auditory cortex. *Nature* 426, 442–446. doi: 10.1038/nature02116

Wei, H., Wang, M., Lv, N., Yang, H., Zhao, M., Huang, B., et al. (2020). Increased repetitive self-grooming occurs in Pax2 mutant mice generated using CRISPR/Cas9. *Behav. Brain Res.* 393:112803. doi: 10.1016/j.bbr.2020.112803

Weinberger, N. M. (2015). New perspectives on the auditory cortex: learning and memory. *Handb. Clin. Neurol.* 129, 117–147.

West, A. E., Chen, W. G., Dalva, M. B., Dolmetsch, R. E., Kornhauser, J. M., Shaywitz, A. J., et al. (2001). Calcium regulation of neuronal gene expression. *Proc. Natl. Acad. Sci. U.S.A.* 98, 11024–11031.

West, A. E., Pruunsild, P., and Timmusk, T. (2014). Neurotrophins: transcription and translation. *Handb. Exp. Pharmacol.* 220, 67–100. doi: 10.1007/978-3-642-45106-5_4

Wolter, S., Mohrle, D., Schmidt, H., Pfeiffer, S., Zelle, D., Eckert, P., et al. (2018). GC-B deficient mice with axon bifurcation loss exhibit compromised auditory processing. *Front. Neural Circuits* 12:65. doi: 10.3389/fncir.2018.00065

Xu, H., Kotak, V. C., and Sanes, D. H. (2010). Normal hearing is required for the emergence of long-lasting inhibitory potentiation in cortex. *J. Neurosci.* 30, 331–341. doi: 10.1523/jneurosci.4554-09.2010

Zampini, V., Johnson, S. L., Franz, C., Lawrence, N. D., Munkner, S., Engel, J., et al. (2010). Elementary properties of CaV1.3 Ca(2+) channels expressed in mouse cochlear inner hair cells. *J. Physiol.* 588(Pt 1), 187–199. doi: 10.1113/jphysiol.2009.181917

Zhang, H., and Bramham, C. R. (2020). Arc/Arg3.1 function in long-term synaptic plasticity: Emerging mechanisms and unresolved issues. *Eur. J. Neurosci.* doi: 10.1111/ejn.14958 [Epub ahead of print].

Zhou, M., Li, Y. T., Yuan, W., Tao, H. W., and Zhang, L. I. (2015). Synaptic mechanisms for generating temporal diversity of auditory representation in the dorsal cochlear nucleus. *J. Neurophysiol.* 113, 1358–1368. doi: 10.1152/jn.00573.2014

Zuccotti, A., Kuhn, S., Johnson, S. L., Franz, C., Singer, W., Hecker, D., et al. (2012). Lack of brain-derived neurotrophic factor hampers inner hair cell synapse physiology, but protects against noise-induced hearing loss. *J. Neurosci.* 32, 8545–8553. doi: 10.1523/jneurosci.1247-12.2012

Conflict of Interest: The authors declare that the research was conducted in the absence of any commercial or financial relationships that could be construed as a potential conflict of interest.

brain sciences

MDPI

Article

Age-Dependent Auditory Processing Deficits after Cochlear Synaptopathy Depend on Auditory Nerve Latency and the Ability of the Brain to Recruit LTP/BDNF

Philine Marchetta [1,†], Daria Savitska [1,†], Angelika Kübler [1], Giulia Asola [1], Marie Manthey [1], Dorit Möhrle [1], Thomas Schimmang [2], Lukas Rüttiger [1], Marlies Knipper [1,*] and Wibke Singer [1]

1 Department of Otolaryngology, Head & Neck Surgery, Tübingen Hearing Research Centre (THRC), Molecular Physiology of Hearing, University of Tübingen, Elfriede-Aulhorn-Straße 5, 72076 Tübingen, Germany; philine.marchetta@uni-tuebingen.de (P.M.); daria.savitska@uni-tuebingen.de (D.S.); kuebler.angelika@gmail.com (A.K.); guiliaasola@hotmail.it (G.A.); marie.manthey@tufts.edu (M.M.); dorit.moehrle@googlemail.com (D.M.); lukas.ruettiger@uni-tuebingen.de (L.R.); wibke.singer@uni-tuebingen.de (W.S.)

2 Instituto de Biologíay Genética Molecular, Universidad de Valladolid y Consejo Superior de Investigaciones Científicas, E-47003 Valladolid, Spain; schimman@ibgm.uva.es

* Correspondence: marlies.knipper@uni-tuebingen.de; Tel.: +49-(0)7071-2988194; Fax: +49-(0)7071-294950

† These authors contributed equally.

Received: 27 August 2020; Accepted: 2 October 2020; Published: 6 October 2020

Abstract: Age-related decoupling of auditory nerve fibers from hair cells (cochlear synaptopathy) has been linked to temporal processing deficits and impaired speech recognition performance. The link between both is elusive. We have previously demonstrated that cochlear synaptopathy, if centrally compensated through enhanced input/output function (neural gain), can prevent age-dependent temporal discrimination loss. It was also found that central neural gain after acoustic trauma was linked to hippocampal long-term potentiation (LTP) and upregulation of brain-derived neurotrophic factor (BDNF). Using middle-aged and old BDNF-live-exon-visualization (BLEV) reporter mice we analyzed the specific recruitment of LTP and the activity-dependent usage of *Bdnf* exon-IV and -VI promoters relative to cochlear synaptopathy and central (temporal) processing. For both groups, specimens with higher or lower ability to centrally compensate diminished auditory nerve activity were found. Strikingly, *low compensating* mouse groups differed from *high compensators* by prolonged auditory nerve latency. Moreover, low compensators exhibited attenuated responses to amplitude-modulated tones, and a reduction of hippocampal LTP and *Bdnf* transcript levels in comparison to high compensators. These results suggest that latency of auditory nerve processing, recruitment of hippocampal LTP, and *Bdnf* transcription, are key factors for age-dependent auditory processing deficits, rather than cochlear synaptopathy or aging per se.

Keywords: central compensation; cochlear synaptopathy; auditory nerve latency; age-related hearing loss; activity dependent BDNF; long term potentiation

1. Introduction

Aging people often experience difficulties in perceiving speech in a noisy environment, even without elevated audiometric thresholds [1]. The development of poor supra-threshold speech processing during aging in humans was attributed to progressive cochlear synaptopathy, similarly to phenomena observed in aging animals [2,3]. In rodents [4–6] and humans [7] it was recently shown that loss of afferent auditory fibers (cochlear synaptopathy) can progress over aging or following

'non-traumatic' loud sound. This can coincide with hearing deficits even when audiometric thresholds are normal and independently from the loss of outer hair cells. In humans, older people who have maintained good hearing sensitivity, nevertheless frequently report difficulties in acoustically complex environments. This general profile of auditory deficiency, which can occur in individuals with a normal audiogram, is supposed to reflect impaired processing of acoustic temporal cues due to cochlear synaptopathy [8,9]. It was hypothesized that a reduction in the viable population of auditory nerve fibers over age [5,10], particularly of the subpopulation of fibers with a low spontaneous firing rate (low-SR) and a high threshold, might lead to auditory deficits at supra-threshold levels and in challenging listening situations such as in the presence of background noise [2,5,6,11–13]. In accord, these fibers with a low SR and a high threshold, that account for 40% of the total amount of fibers, have a high vulnerability to noise and aging [10,14–16]. Unlike fibers with a high spontaneous firing rate (high-SR) and a low threshold, low-SR fibers do not contribute to auditory threshold sensitivity [4,5,10]. Therefore, the loss of low-SR fibers would provide a rationale for the numerous studies that report listening deficits in humans despite normal hearing thresholds, e.g., [5,10,17–19].

We have previously observed that temporal processing loss was not necessarily attenuated as a consequence of cochlear deafferentation, if reduced auditory input was centrally compensated [6]. In this study [6], stimulus-driven auditory steady state responses (ASSR) were determined, which reflect attention-driven responses in the central auditory pathway to amplitude-modulated tones [20–22]. The results demonstrated that only animals with a reduced neural gain over age showed a loss of temporal resolution in auditory processing [6], suggesting neural gain and not cochlear synaptopathy per se as a key factor for temporal processing. This notion is supported by a recent study on the detection abilities for temporally and spectrally modulated stimuli in aging listeners. This study could not confirm a causal link between compromised supra-threshold auditory nerve amplitudes and reduced temporal processing [23].

We also observed that central auditory compensation after acoustic trauma-induced cochlear deafferentation was linked to increased hippocampal long-term potentiation (LTP), and recruitment of activity-dependent *Bdnf* exon-IV and -VI transcription [24], providing a mechanistic explanation for the idea that temporal auditory processing abilities are related to each individual's cognitive skills [25].

Here we asked how, during aging, cochlear synaptopathy is linked to a central compensation via neural gain, hippocampal LTP and BDNF recruitment.

BDNF-live-exon-visualization (BLEV) reporter mice [26] were used to determine the activity-dependent usage of *Bdnf* exon-IV and -VI promoters through bi-cistronic coexpression of cyan- and yellow-fluorescent-protein (CFP/YFP), respectively [24,26]. Importantly, BLEV mice allow the visualization of *Bdnf* exon-IV-CFP and *Bdnf* exon-VI-YFP transcripts at their sites of translation [26].

We compared young (2.9–6.6 months old), middle-aged (9.4–14.3 months old), and old (15.3–22.5 months old) BLEV mice to uncover differences in central responsiveness at defined states of age-related cochlear synaptopathy. We measured auditory brainstem responses (ABR) to determine wave amplitudes corresponding to the auditory nerve (wave I) and inferior colliculus (IC, wave IV) [27], and examined ASSR, offering an insight in temporal resolution of auditory processing [6]. In addition, we have determined hippocampal LTP and *Bdnf* transcripts to find a correlation between the central auditory adjustment and a memory-dependent facilitation process [24,26]. Strikingly, we found that independently of age and reduced amplitude of the ABR wave I animals with a lower central auditory compensation capacity exhibited a prolonged auditory nerve latency and reduced sensitivity to follow amplitude-modulated tones. These low-compensating groups exhibited reduced LTP after stimulation of the hippocampal Schaffer's collaterals and attenuated *Bdnf* exon-IV and -VI expression in and around hippocampal capillaries, compared to animals with a higher central capacity to compensate. Prevailed fast auditory nerve processing and the ability of the brain to recruit a LTP/BDNF-dependent facilitation path may therefore play a key role for preventing age-related hearing difficulties caused by cochlear synaptopathy.

2. Materials and Methods

2.1. Animals

Animal care, procedure, and experimental protocols correspond to national and institutional guidelines and were reviewed and approved by University of Tübingen, Veterinary Care Unit, and the Animal Care and Ethics Committee of the regional board of the Federal State Government of Baden-Württemberg, Germany. All experiments were performed according to the European Union Directive 2010/63/EU for the protection of animals used for experimental and other scientific purposes. In-house bred mice were kept according to the national guidelines for animal care in a specific pathogen free animal facility at 25 °C on a 12 h/12 h light/dark cycle with average noise levels of around 50–60 dB SPL_{RMS}.

Female and male homozygous BLEV mice were used and categorized into different age groups. Young animals were between 2.9 and 6.6 months, middle-aged between 9.4 and 14.3 months, and old between 15.3 and 22.5 months old.

The mouse model was generated as described [26]. Briefly, the *Bdnf* exon-IV and -VI sequences, both including the corresponding promoter sequences, were extended by CFP or YFP, respectively, both containing a stop codon. A HA-tag was added to *Bdnf* exon-IV-CFP and a cMyc-tag to *Bdnf* exon-VI-YFP. The translation of the protein-coding *Bdnf* exon-IX was enabled by an internal ribosomal entry site sequence, which keeps the mRNA at the ribosome, despite the presence of a stop codon. Additionally, the growth-associated protein 43, was added to anchor the fluorescent proteins at the site of translation. This allows differential monitoring of the noncoding *Bdnf* exon-IV and *Bdnf* exon-VI by the fluorescent proteins CFP and YFP without interfering with *Bdnf* exon-IX.

2.2. Hearing Measurements

Hearing measurements were done under anesthesia 75 mg/kg ketamine hydrochloride (Ketavet®, Zoetis GmbH, Berlin, Germany), 5 mg/kg xylazine hydrochloride (Rompun®, Bayer Vital GmbH, Leverkusen, Germany), and 0.2 mg/kg atropine (Atropinsulfat B.Braun, Melsungen, Germany) in a soundproof chamber (IAC, Niederkrüchten, Germany), as previously described [28].

The ABR, evoked by short duration sound stimuli, represents the summed activity of neurons in distinct anatomical structures along the ascending auditory pathway [29] and was measured by averaging the evoked electrical response recorded via subcutaneous cranial electrodes. In short, ABR thresholds were elicited with click (100 ms), noise-burst (1 ms duration), or pure-tone stimuli (3 ms, including 1 ms cosine squared rise and fall envelope, 2–45.2 kHz).

ASSRs were measured with amplitude modulated sinusoidal stimuli (carrier frequency 11.31 kHz). The stimuli were presented between −10 and 60 dB in 5 dB steps relative to threshold (re thr). Stimuli were amplitude modulated with 100% modulation depth and 512 Hz modulation frequency. A modulation index was calculated for individual animals by building the ratio between the maximal signal and the baseline (defined as the average of all points except the maximum and the neighboring points). Even if measured threshold normalized, the data were not normalized by threshold for analysis.

2.3. Field Excitatory Postsynaptic Potential (fEPSP) Recordings in Hippocampal Slices

Extracellular fEPSP recordings were performed according to standard methods as previously described [30,31].

In brief, 400 µm thick coronal brain slices were cut on a vibratome (Leica VT 1000S) in ice-cold dissection buffer (mM): 127 NaCl, 1.9 KCl, 1.2 KH_2PO_4, 26 $NaHCO_3$, 10 D-glucose, 2 $MgSO_4$, and 1.1 $CaCl_2$, constantly saturated with 5% CO_2 and 95% O_2 (pH 7.4). Slices were incubated in oxygenated artificial cerebrospinal fluid (ACSF, in mM: 127 NaCl, 1.9 KCl, 1.2 KH_2PO_4, 26 $NaHCO_3$, 10 D-glucose, 1 $MgSO_4$, 2.2 $CaCl_2$; pH 7.4) for 1 h at 30 °C and afterwards stored at room temperature. Recordings were performed in a submerged-type recording chamber (Warner Instruments). Stimulation (TM53CCINS, WPI) and recording (ACSF-filled glass pipettes, 2–3 MΩ) electrodes were positioned in the stratum

radiatum (SR) to record Schaffer collateral field excitatory postsynaptic potentials (fEPSPs). Signals were amplified with an Axopatch 200B (Molecular Devices), digitized at 5 kHz with an ITC-16 (HEKA) and recorded using WinWCP from the Strathclyde Electrophysiology Suite. Stimuli (100 µs) were delivered through a stimulus isolator (WPI). For each individual slice the strength of the stimulation (typically between 30–125 µA) was chosen to evoke 40–60% of the maximal response, defined by initial fEPSP slope. Only slices that showed stable fiber volley and fEPSP were used for further recording. The same stimulus intensity was applied during baseline recording (0.067 Hz, 20–30 min) and induction of LTP using 100 stimuli during 1 s (100 Hz, 1 s). The baseline was determined by averaging fEPSP initial slopes from the period before the tetanic stimulation (at least 15 min of stable recording). The level of LTP was determined by averaging fEPSP slopes from the period between 50 and 60 min after the high-frequency stimulation. Before the tetanic stimulation, each slice was used to record input–output relationship (IOR, 25–150 µA in 25 µA steps) and paired-pulse facilitation (PPF, 10–20–50–100–200–500 ms interpulse interval at the same stimulation strength as LTP recordings). IOR changes in fEPSP slope and fiber volley amplitude were normalized within each slice (% from the maximal response at the highest stimulus strength was calculated) and averaged values for each group were plotted against the stimulus intensity. For PPF paired-pulse ratio of EPSP2/EPSP1 slope and amplitude at each interstimulus interval were defined per slice and mean values per group were plotted. EPSP1 was calculated as an average of EPSP1s from all interstimulus intervals for each single slice.

Four traces were averaged for each single data point analyzed.

2.4. Tissue Preparation

Tissue preparation was carried out as described in detail previously [32]. In brief, for cochlear cross-section immunohistochemistry, cochleae were isolated, fixed by immersion in 2% paraformaldehyde, 125 mM sucrose in 100 mM phosphate buffered saline (pH 7.4) for 2 h and then decalcified for 45 min in RDO rapid decalcifier (Apex Engineering Products Corporation, Aurora, IL, USA). Cochleae were stored in Sucrose-Hank's solution rotated at 4 °C overnight before they were embedded in Tissue-tek and cryosectioned in slices of 10 µm, and mounted on SuperFrost*/plus microscope slides before storage at −20 °C.

Brains were fixed by immersion for 48 h in 2% paraformaldehyde (exchange of fixative solution after 24 h) and then stored in 0.4% paraformaldehyde until embedded in 4% agarose. Brains were cut in 60 µm slices with a vibratome (Leica VT 1000S) and stored at −20 °C in cryoprotectant (mix 150 g of sucrose in 200 mL 1× phosphate buffer saline and 150 mL ethylene glycol) until used for immunohistochemistry.

2.5. Immunohistochemistry

Immunohistochemistry was carried out as described in detail previously [32]. Antibodies against C-terminal-binding protein 2 (CtBP2)/RIBEYE (rabbit, diluted 1:1500; ARP American Research Products, Inc.™, Waltham, MA, USA) or parvalbumin (PV, rabbit, diluted 1:8000; Abcam, Cambridge, UK #ab11427) were used. Primary antibodies were detected using appropriate Cy3 secondary antibodies (1:1500, Jackson Immuno Research Laboratories, West Grove PA, USA #AB_2338006).

All samples were viewed as previously described [33] using an Olympus BX61 microscope (Olympus, Hamburg, Germany) equipped with epifluorescence illumination and analyzed with CellSens Dimension software (OSIS GmbH, Münster, Germany). To increase spatial resolution, slices were imaged over a distance of 15 µm within an image-stack along the *z*-axis (z-stack), followed by 3-dimensional deconvolution using CellSens Dimension's built-in algorithm.

2.6. Data Analyses

2.6.1. Statistics and Numbers

Unless otherwise stated, all data were presented as group mean with standard deviation (SD) or with standard error of the mean (SEM) for *n* animals per experimental group. Data were tested for normal distribution (Shapiro–Wilk Normality Test, $\alpha = 0.05$). Differences of the means were compared for statistical significance either by ungrouped two-tailed Student's *t*-test (parametric)/Mann–Whitney U test (nonparametric), 1-way, or 2-way analysis of variance (ANOVA, parametric)/Kruskal–Wallis test (nonparametric) with $\alpha = 0.05$ and correction for type 1 error after Tukey-test/Bonferroni's multiple comparisons test (parametric) or two-stage linear step-up procedure of Benjamini, Krieger, and Yekutieli (nonparametric). In figures, significance is indicated by asterisks (* $p < 0.05$, ** $p < 0.01$, *** $p < 0.001$, **** $p < 0.0001$). n.s. denotes nonsignificant results ($p > 0.05$). All statistical information and *n* numbers can be found in Section 3 and in Table 1. Statistical calculations and visualizations were done with GraphPad Prism.

Table 1. Statistical information of the results.

Figure	Comparison	Statistical Test	Test Value	*p*-Value	Post-Hoc Test with *p*-Value		*n*—Number
					Tukey´s multiple comp. Test		
Fig. 1a	Click-ABR	1-way ANOVA	F (2, 157) = 39.70	$p < 0.0001$	Y vs. M-A Y vs. O MA vs. O	$p > 0.05$ $p < 0.0001$ $p < 0.0001$	Y $n = 27$ animals M-A $n = 14$ animals O $n = 27$ animals
Fig. 1b	Noise-ABR	1-way ANOVA	F (2, 157) = 27.23	$p < 0.0001$	Y vs. M-A Y vs. O M-A vs. O	$p > 0.05$ $p < 0.0001$ $p < 0.0001$	
Fig. 1c	f-ABR	2-way ANOVA	F (2, 741) = 73.33	$p < 0.0001$	Y vs. M-A Y vs. O M-A vs. O	$p < 0.05$ for all freq > 22.6 kHz $p < 0.05$ for all freq shown $p < 0.05$ for all freq shown except 22.6 kHz	
					Tukey´s multiple comp. Test		
Fig. 2b	ABR wave I ampl.	2-way ANOVA	F (2, 2214) = 236.1	$p < 0.0001$	Y vs. M-A Y vs. O M-A vs. O	$p < 0.05$ for all SPL > 20 dB re Thr $p < 0.05$ for SPL between 15 and 85 dB re Thr $p > 0.05$	Y $n = 24$ animals M-A $n = 25$ animals O $n = 22$ animals
Fig. 2c	ABR wave IV ampl.	2-way ANOVA	F (2, 2025) = 414.7	$p < 0.0001$	Y vs. M-A Y vs. O M-A vs. O	$p < 0.05$ for all SPL > 15 dB re Thr $p < 0.05$ for all SPL > 20 dB re Thr $p < 0.05$ for SPL between 50 and 75 dB re Thr	
Fig. 2e	IHC ribbons apical	1-way ANOVA	F (2, 85) = 11.34	$p < 0.0001$	Y vs. M-A Y vs.O M-A vs. O	$p < 0.01$ $p < 0.001$ $p > 0.05$	Y $n = 7$ animals M-A $n = 8$ animals O $n = 7$ animals
	IHC ribbons medial	1-way ANOVA	F (2, 88) = 4.61	$p = 0.0125$	Y vs. M-A Y vs. O M-A vs. O	$p > 0.05$ $p < 0.05$ $p > 0.05$	
	IHC ribbons midbasal	1-way ANOVA	F (2, 85) = 11.34	$p < 0.0001$	Y vs. M-A Y vs. O M-A vs. O	$p < 0.01$ $p < 0.001$ $p > 0.05$	

Table 1. *Cont.*

Figure	Comparison	Statistical Test	Test Value	*p*-Value	Post-Hoc Test with *p*-Value		*n*—Number
Fig. 3b	Amplification Y	Regression	$y = 0.9322x + 1.7392$	$R^2 = 0.6005$			Y $n = 34$ animals M-A $n = 29$ animals O $n = 29$ animals
	Amplification M-A		$y = 0.9081x + 1.1758$	$R^2 = 0.7313$			
	Amplification O		$y = 0.8248x + 0.6833$	$R^2 = 0.5378$			
	Comparison between ages	Steepness of regression lines	F (2, 86) = 0.12	$p = 0.883$			
		Are regression lines different?	F (2, 88) = 20.79	$p < 0.0001$			
Fig. 3c	Compensation Y	Regression	$y = 2.2714x^{-0.277}$	$R^2 = 0.2768$			
	Compensation M-A		$y = 2.3313x^{-0.532}$	$R^2 = 0.3446$			
	Compensation O		$y = 2.6943x^{-0.502}$	$R^2 = 0.2068$			
	Compensation all		$y = 2.4733x^{-0.405}$	$R^2 = 0.2815$			
					Bonferroni's multiple comp. test		
Fig. 4a	ABR wave I strength	1-way ANOVA	F (2, 35) = 21.98	$p < 0.0001$	HC vs. LC	$p > 0.05$	LC $n = 5$ HC $n = 7$ Y $n = 26$ animals mean of both ears
					Y vs. HC	$p < 0.001$	
					Y vs. LC	$p < 0.001$	
	ABR wave IV strength	1-way ANOVA	F (2, 35) = 41.15	$p < 0.0001$	HC vs. LC	$p < 0.1$	
					Y vs. HC	$p < 0.001$	
					Y vs. LC	$p < 0.001$	
Fig. 4b	ABR wave I latency	1-way ANOVA	F (2, 36) = 12.55	$p < 0.0001$	HC vs. LC	$p < 0.001$	
					Y vs. HC	$p < 0.001$	
					Y vs. LC	$p > 0.05$	
	ABR wave IV latency	1-way ANOVA	F (2, 35) = 4.592	$p = 0.0169$	HC vs. LC	$p < 0.1$	
					Y vs. HC	$p < 0.05$	
					Y vs. LC	$p > 0.05$	
Fig. 4c	Central conductance	1-way ANOVA	F (1, 34) = 4.045	$p = 0.0266$	HC vs. LC	$p > 0.05$	HC $n = 7$ LC $n = 6$
					Y vs. HC	$p > 0.05$	
					Y vs. LC	$p < 0.05$	
Fig. 4d	IHC ribbons apical	1-way ANOVA	F (2, 34) = 9.1	$p < 0.001$	HC vs. LC	$p > 0.05$	Y $n = 7$ animals M-A $n = 8$ animals O $n = 7$ animals
					Y vs. HC	$p < 0.05$	
					Y vs. LC	$p < 0.001$	
	IHC ribbons medial	1-way ANOVA	F (2, 35) = 9.72	$p < 0.001$	HC vs. LC	$p < 0.05$	
					Y vs. HC	$p > 0.05$	
					Y vs. LC	$p < 0.001$	
	IHC ribbons midbasal	1-way ANOVA	F (2, 35) = 41.93	$p < 0.0001$	HC vs. LC	$p < 0.001$	
					Y vs. HC	$p < 0.01$	
					Y vs. LC	$p < 0.001$	
Fig. 4e	ASSR input–output function	2-way ANOVA	F (1, 106) = 7.52	$p = 0.0072$	HC vs. LC	$p > 0.05$	HC $n = 7$ LC $n = 6$
Fig. 5b	HC baseline vs. post HFS	Mann–Whitney U	U (21) = 0	$p < 0.0001$			n = animals/slices Y $n = 7/21$ HC $n = 7/21$ LC $n = 5/15$
	LC baseline vs. post HFS		U (15) = 0	$p < 0.0001$			
Fig. 5c	LTP HC vs. LC	Mann–Whitney U	U (21, 15) = 74	$p = 0.0066$			
					Two-stage linear step-up procedure of Benjamini, Krieger, and Yekutieli		
Fig. 5d	LTP high and LC dependent on age and Y control group	1-way nonparametric ANOVA on ranks (Kruskal–Wallis test)	H (5) = 20.18, $p = 0.0005$	$p < 0.001$	HC M-A vs. O	$p < 0.01$	
					low comp. M-A vs. O	$p > 0.05$	
					Y vs. M-A HC	$p > 0.05$	
					Y vs. M-A LC	$p > 0.05$	
					Y vs. O HC	$p > 0.05$	
					Y vs. O LC	$p < 0.01$	
					M-A HC vs. LC	$p < 0.01$	
					O HC vs. LC	$p > 0.05$	

Table 1. *Cont.*

Figure	Comparison	Statistical Test	Test Value	*p*-Value	Post-Hoc Test with *p*-Value		*n*—Number
Fig. 6c	*Bdnf* exon-IV-CFP	Mann–Whitney U	U (4) = 24.31	$p < 0.0001$			
	Bdnf exon-IV-YFP		U (4) = 4.994	$p = 0.0075$			
	Parvalbumin		U (4) = 2.127	$p = 0.1005$			
Fig. S1b	IOR fEPSP slope	2-way ANOVA	F (2, 300) = 1.446	$p = 0.2371$			
Fig. S1c	IOR fiber volley amplitude	2-way ANOVA	F (2, 300) = 4.127	$p = 0.0171$	**Two-stage linear step-up procedure of Benjamini, Krieger, and Yekutieli** HC vs. LC Y vs. HC Y vs. LC	 $p > 0.05$ $p > 0.05$ $p > 0.05$	*n* = animals/slices Y *n* = 7/21 HC *n* = 7/20 LC *n* = 5/12
Fig. S1d	fEPSP slope vs. fiber volley amplitude	Difference between regression lines (slopes)	F (2, 323) = 0.69	$p = 0.5023$			
Fig. S2b	Paired-pulse ratio EPSP2/EPSP1 (slope)	2-way ANOVA	F (2, 330) = 0.9445	$p = 0.3899$			*n* = animals/slices Y *n* = 7/21 HC *n* = 7/20 LC *n* = 5/16
Fig. S2c	Paired-pulse ratio EPSP2/EPSP1 (amplitude)	2-way ANOVA	F (2, 330) = 4.487	$p = 0.0120$	**Two-stage linear step-up procedure of Benjamini, Krieger, and Yekutieli** HC vs. LC Y vs. HC Y vs. LC (only at 10 ms interpulse interval)	 $p > 0.05$ $p > 0.05$ $p < 0.01$	

Y = young, M-A = middle-aged, O = old, HC = high compensator, LC = low compensator.

2.6.2. ABR Analysis

For each individual ear, the peak input–output function and the latency (averaged for intensities between 0 and 30 dB re thr) of the noise-ABR measurements were analyzed as previously described [34].

Two peak classes were selected: (1) early peaks (at 1.2–1.8 ms, wave I) interpreted as the sum of the first stimulus-related action potential within the auditory nerve, and (2) delayed peaks (at 4.1–4.9 ms, wave IV), the response from the auditory midbrain.

For further analysis, the *strength* of the ABR growth function was determined. Therefore the mean of the three values within the supra-threshold growth function with the highest wave amplitude was calculated (more detailed described in [26]) with Excel (Microsoft Excel 2016).

Wave VI/I ratio was calculated by dividing for individual animals at all intensities relative to threshold (re thr) the ABR wave VI amplitude by ABR wave I amplitude. For further analyses, the mean between 20 and 80 dB (re thr) was calculated.

To determine the level of central compensation for individual animals, wave IV/I ratio was plotted against wave I strength. The power function (y = a*x^b) was inserted as a regression line for each group. Only animals with wave I strength smaller than 1.9 µV (which is the mean of all ears in all groups) were subdivided along the black regression line (all ears of all groups). Animals below the line were *low compensators*, while animals above were *high compensators*.

2.6.3. fEPSP Recordings in Hippocampal Slices

Data were analyzed and processed using Clampfit 10 (Molecular Devices) and Microsoft Excel. The data presented per experimental group/condition contained (additionally to mean ± SEM) single dots which showed the fEPSP slope values for each individual brain slice. The *n* indicates the number of slices and animals (slices/animals) used in the analysis.

2.6.4. Fluorescence Analysis of Immunohistochemistry

Pictures acquired from brain sections stained for PV, were analyzed using the free Image J software (NIH, Bethesda, MD, USA). For each section, pictures for each single channel (YFP, CFP, PV) were saved and analyzed independently. For the 10× magnified pictures, after conversion to an 8-bit image, background was reduced using the rolling bar algorithm (available as a tool for Image J) with standard parameters in each single channel picture. Afterwards the integrated density of the fluorescence of CFP and YFP within the picture was calculated. For analysis, data were normalized between both groups. For each individual animal two pictures from duplicate immunostainings were taken and finally the results were averaged to include each animal only once in statistics.

For IHC ribbon counting, pictures were taken from all turns of both ears from duplicate immunohistochemical stainings.

2.6.5. Data Availability

The datasets generated and/or analyzed during the current study are available from the corresponding author upon request.

3. Results

3.1. Auditory Brainstem Response-Evoked Thresholds Are Elevated in Old but Not Middle-Aged Animals

To study the compensation mechanisms underlying age-related synaptopathy, we first compared the hearing thresholds between young (2.9–6.6 months, *n* = 54/27 ears/animals), middle-aged (9.4–14.3 months, *n* = 28/14 ears/animals), and old (15.3–22.5 months, 54/27 ears/animals) BLEV reporter mice. The ABR evoked by low frequency-containing (click), high frequency-containing (noise burst), and pure tone frequency-specific auditory stimuli were tested as described [35]. Old BLEV mice showed a significant increase in threshold compared with young and middle-aged animals measured by click-evoked ABR (Figure 1a; all statistical findings and details of the tests can be found in the figure legends and in Table 1), noise-burst stimuli (Figure 1b), and pure tone frequencies (Figure 1c). Middle-aged BLEV animals showed no different results compared to young BLEV animals upon click and noise stimuli but revealed an increased threshold for frequencies higher than 16 kHz (Figure 1c).

In conclusion, BLEV reporter mice showed an increase of auditory thresholds mainly in the last third of their life span (old animals). This threshold increase started at high frequencies in middle-aged animals but finally all frequencies were affected in old animals.

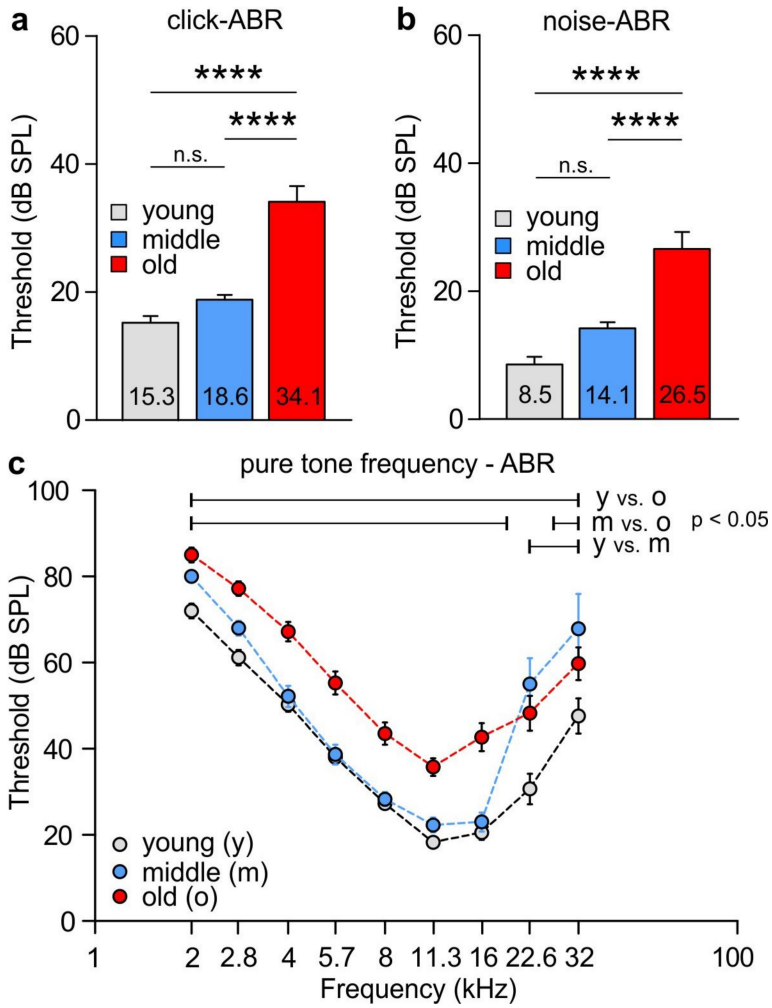

Figure 1. Analysis of the hearing threshold over age. In old animals, hearing thresholds became significantly worse. This was shown for (**a**) click stimuli (1-way ANOVA, F (2, 157) = 39.70, $p < 0.0001$, Tukey's post hoc test: young vs. middle-aged $p > 0.05$, young vs. old $p < 0.0001$, middle-aged vs. old $p < 0.0001$) and (**b**) noise stimuli (1-way ANOVA, F (2, 157) = 27.23, $p < 0.0001$, Tukey´s post hoc test: young vs. middle-aged $p > 0.05$, young vs. old $p < 0.0001$, middle-aged vs. old $p < 0.0001$). (**c**) With pure-tone frequency-specific auditory stimuli, specifically for high frequencies already middle-aged animals showed increased thresholds compared to young BLEV mice (2-way ANOVA, F (2, 625) = 70.73, $p < 0.0001$, Tukey's post hoc test: bars indicate significant differences between respective groups in the shown range). n for all comparisons: young n = 54/27; middle-aged n = 28/14; old n = 54/27 (ears/animals). **** $p < 0.0001$. Mean ± SEM.

3.2. Late Supra-Threshold ABR Wave Varies in Middle-Aged and Old Animals

Aging and acoustic trauma have been shown to induce degeneration of auditory fibers (auditory neuropathy) which damages nerve terminals of the inner hair cell (IHC) (synaptopathy) in mice, non-human primates, and humans [36–38]. Auditory-nerve degeneration may occur independently of outer hair cell loss and is called hidden hearing loss [4,10]. To investigate the impact of age on the vulnerability of pre- and post-synaptic structures of the IHC, we analyzed a potential neuropathy by comparing supra-threshold ABR wave amplitudes (Figure 2a) in BLEV mice at different ages. Supra-threshold ABR wave amplitudes change proportionally with discharge rates and the number of synchronously firing auditory fibers [39], the latter of which is defined by the number of IHC synaptic ribbons [40]. Therefore, auditory neuropathy and IHC synaptopathy is well reflected by changes in supra-threshold ABR wave amplitudes, and IHC ribbon numbers, respectively [4,6,34,41].

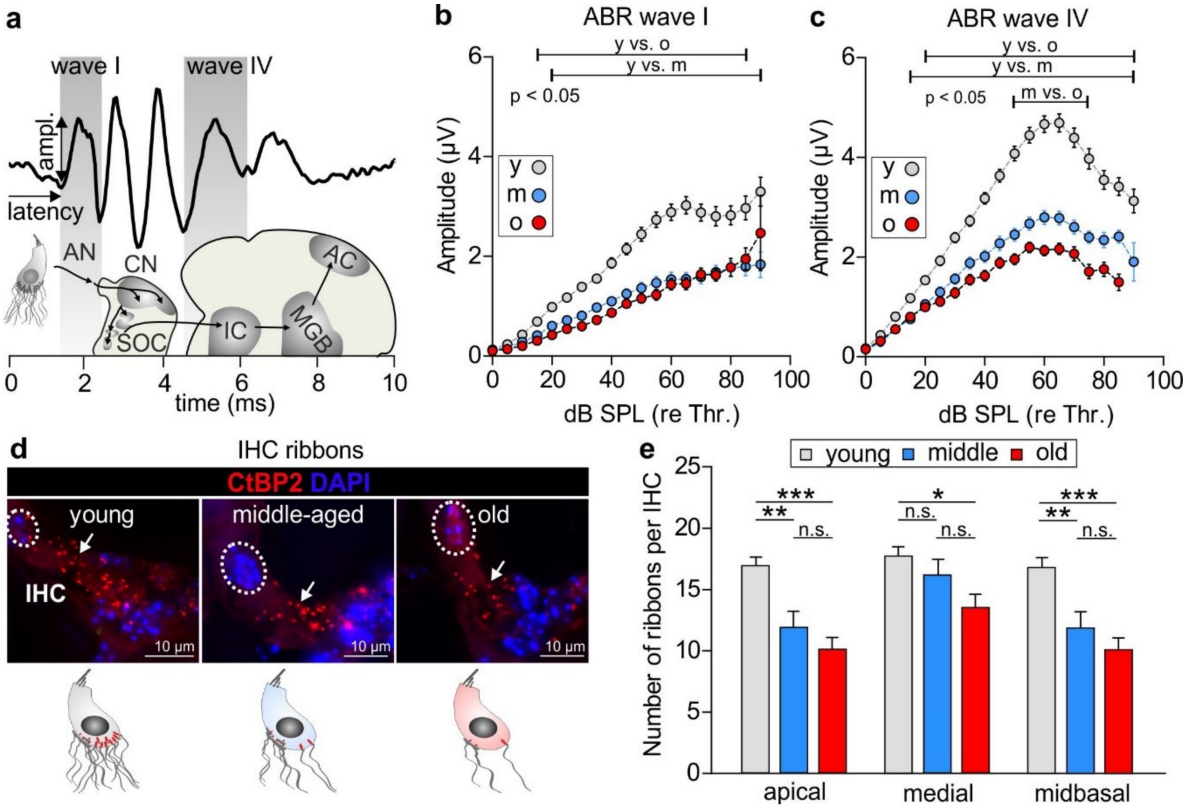

Figure 2. Supra-threshold analyses of auditory brainstem response (ABR) waves I and IV and inner hair cell (IHC) function. (**a**) Schematic drawing of the auditory pathway and correlated stimulus-evoked deflections of ABR waves. AN = auditory nerve, CN = cochlear nucleus, SOC = superior olivary complex, IC = inferior colliculus, MGB = medial geniculate body, AC = auditory cortex. (**b**) ABR wave I amplitude was significantly reduced over age in comparison to young animals (2-way repeated measurements ANOVA, F (2, 2214) = 236.1, $p < 0.0001$, Tukey's post hoc test: bars indicate significant differences between respective groups in the shown range). (**c**) ABR wave IV amplitude was also significantly reduced over age (2-way repeated measurements ANOVA, F (2, 2025) = 414.7, $p < 0.0001$, Tukey's post hoc test: bars indicate significant differences between respective groups in the shown range). The middle-aged group had a significantly higher ABR wave IV amplitude between 50 and 75 dB (re thr) than the old animals. For (**b**,**c**): young $n = 54/27$; middle-aged $n = 28/14$; old $n = 54/27$ (ears/animals). Mean ± SEM. (**d**) Antibody against CtBP2/RIBEYE was used as marker for IHC ribbon synapses with afferent auditory neurons. Nuclei were stained with DAPI (blue). Scale bars: 10 µm. (**e**) Immunopositive dots were counted to estimate the number of auditory nerve fiber synapses per IHC, which decreased over age. Arrows indicate a reduced number of CtBP2/RIBEYE-positive dots at the base of IHCs (apical: 1-way ANOVA, F(2, 85) = 11.34; $p < 0.0001$; Bonferroni's multiple comparisons test: young vs. middle-aged $p < 0.01$; young vs. old $p < 0.001$; middle-aged vs. old $p > 0.05$; medial: 1-way ANOVA, F(2, 88) = 4.61; $p < 0.05$; Bonferroni's multiple comparisons test: young vs. middle-aged $p > 0.05$; young vs. old $p < 0.05$; middle-aged vs. old $p > 0.05$; midbasal: 1-way ANOVA, F(2, 85) = 11.34; $p < 0.0001$; Bonferroni's multiple comparisons test: young vs. middle-aged $p < 0.01$; young vs. old $p < 0.001$; middle-aged vs. old $p > 0.05$). Young $n = 7$ mice; middle-aged $n = 8$ mice; old $n = 7$ mice. * $p < 0.05$; ** $p < 0.01$; *** $p < 0.001$. Mean ± SEM.

The auditory stimulus-evoked ABR wave I (Figure 2a,b) reflects the summed activity of the auditory nerve fibers [27] and is a useful functional biomarker of auditory-nerve degeneration after noise exposure [42]. ABR wave IV, on the other hand (Figure 2a,c), reflects the sound-induced activity generated at the level of the IC and lateral lemniscus [27]. The analysis of supra-threshold ABR wave I (Figure 2b) and IV (Figure 2c) revealed a significant reduction of both waves in middle-aged and old BLEV mice compared with young BLEV mice. Although the averaged ABR wave I amplitude of

middle-aged BLEV mice was similar to that of old BLEV mice, the ABR wave IV of the former showed a larger amplitude between 50 and 75 dB (re thr) in comparison to old animals, indicating that these animals may compensate a reduced ABR wave I amplitude through a disproportionally enhanced ABR wave IV amplitude.

In young, middle-aged, and old animals we quantified the number of CtBP2/RIBEYE-immuno-positive dots as indicators for ribbon synapses derived from dendrites from spiral ganglion neurons [43] and as an estimation for deafferentation [4] (Figure 2d,e). As especially shown by quantifications of the midbasal cochlear regions (midbasal: >17 kHz [28]) (Figure 2d, right panel) numbers of ribbons in IHCs from young mice were higher than those counted in middle-aged and old mice. This analysis confirmed that the number of CtBP2/RIBEYE-stained ribbon synapses tends to decrease over age (Figure 2e), as also previously observed for aging rats [6].

In conclusion, the auditory input was significantly reduced during the last two thirds of the lifespan of BLEV mice and central output activity varied in middle-aged and old animals.

3.3. Central Compensation and Auditory Processing Following Age-Related Reduced Auditory Nerve Activity Differs Depending on Prevailed Latency of Auditory Nerve Response

ABR wave amplitudes and latencies corresponding to click-evoked neuronal activity in the auditory nerve (wave I) and lateral lemiscus and IC (wave IV) were analyzed [27] for increasing stimulus levels. We were interested to what extent the age of animals contributes to the individual's ability to centrally compensate for reduced auditory nerve activity. We therefore tested the correlation between wave I and wave IV in all age groups. We calculated the *strength* of wave amplitudes in each individual by averaging the three highest amplitude values (Figure 3a). Upon plotting the strength of wave I against the strength of wave IV, we observed a linear correlation between them in all three age groups (Figure 3b). The steepness of regression lines, that represents the degree of wave IV amplification depending on the strength of wave I, was similar in young, middle-aged, and old animals. This indicated that the aging process per se does not affect the physiological amplification mechanism in the ascending auditory pathway. However, the general sensitivity for stimuli, which is determined by *y*-axis intercepts, is decreasing over age (Figure 3b). These results mirror the analysis of ABR waves I and IV amplitude growth functions (Figure 2), which were decreased over age.

To test whether age causes a disproportionally increasing wave IV/I ratio (neural gain), this ratio was calculated for all age groups and the average value between 20 and 80 dB (re thr) was used to plot wave I strength against the wave IV/I ratio (Figure 3c). The power function (y = a*xˆb) was inserted as a regression line for each age group and additionally another regression line was plotted for all ears of all groups (black) (Figure 3c). While young animals exhibited a rather flat curve at relatively high values of wave I (Figure 3c, grey), both middle-aged (blue) and old animals (red) showed a wide spreading in the wave IV/I ratio (Figure 3c, *y*-axis) at rather constantly low values of wave I (Figure 3c, *x*-axis). In a subgroup of animals later used for LTP measurements (see below), we also noticed that middle-aged and old animals could be subdivided into two groups (Figure 3d): animals characterized by dots lying below the black regression line were defined by exhibiting a small neuronal gain, which from now on will be called *low compensators*. In contrast, animals reflected by dots above the black trend line exhibited a large neuronal gain, indicating a high central compensation (*high compensators*). Interestingly, individual animals defined as either high (Figure 3d, green arrow) or low compensators (Figure 3d, dark grey arrow), were present in both middle-aged and old mice (Figure 3d, red and blue dots).

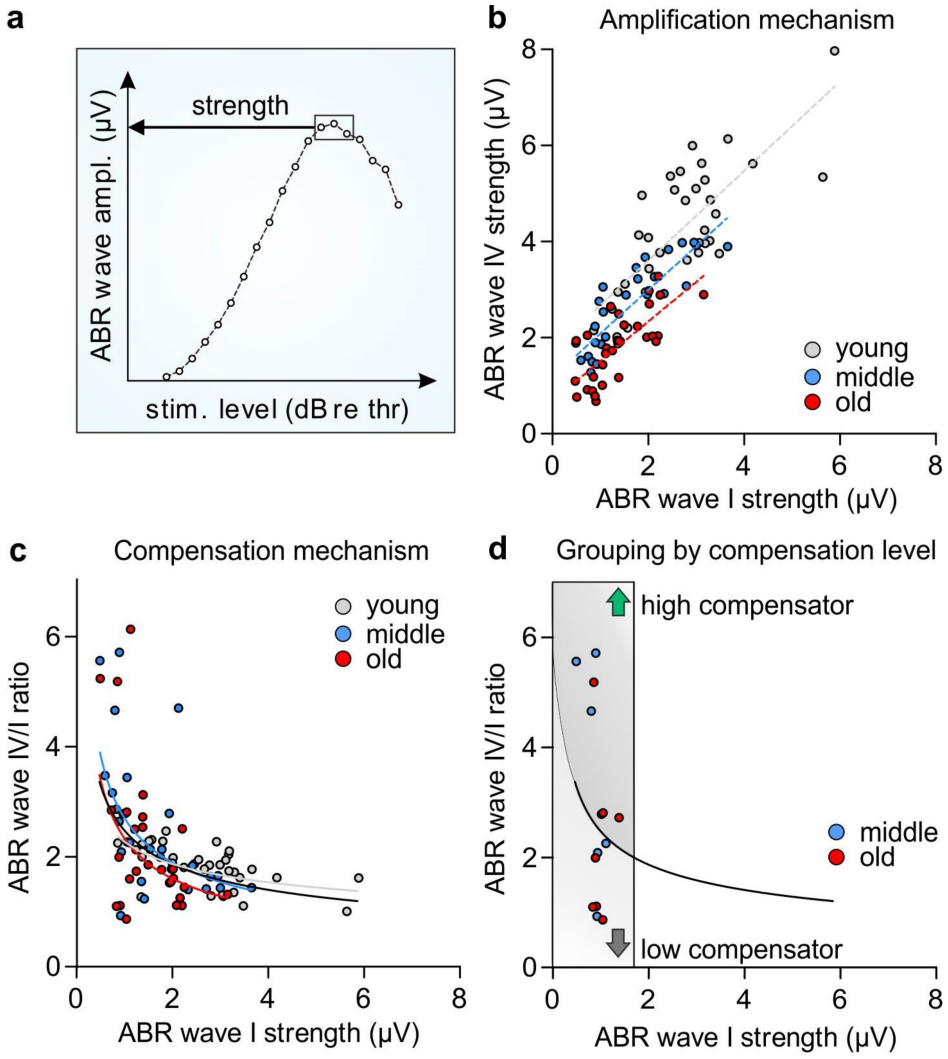

Figure 3. Neural gain mechanisms over age and temporal auditory processing in high and low compensators. (**a**) The ABR wave strength was calculated by averaging the three largest values of wave amplitudes in the I/O function. (**b**) Similar waves I–IV amplification mechanisms (steepness of lines; 2-way ANOVA, F (2, 86) = 0.12, $p > 0.05$, young $n = 34$ animals, middle-aged $n = 29$ animals, old $n = 29$ animals) but decreasing sensitivity over age (y-axis intercept; 2-way ANOVA, F (2, 88) = 20.79, $p < 0.0001$). (**c**) Wave IV/I ratio dependent on the wave I amplitude was plotted to picture the central compensation in animals. Regression lines were fitted by power function (y = a*xˆb). (**d**) Middle-aged and old animals with reduced wave I (inside grey box; ABR wave I < 1.9 µV) were subdivided along the black regression line (regression of all three groups) into low compensators (dark grey arrow) and high compensators (green arrow). In both groups of age high and low compensators were found.

High and low compensators did not differ in the strength of ABR wave I which was reduced in both of these groups compared to young animals (Figure 4a, left panel).

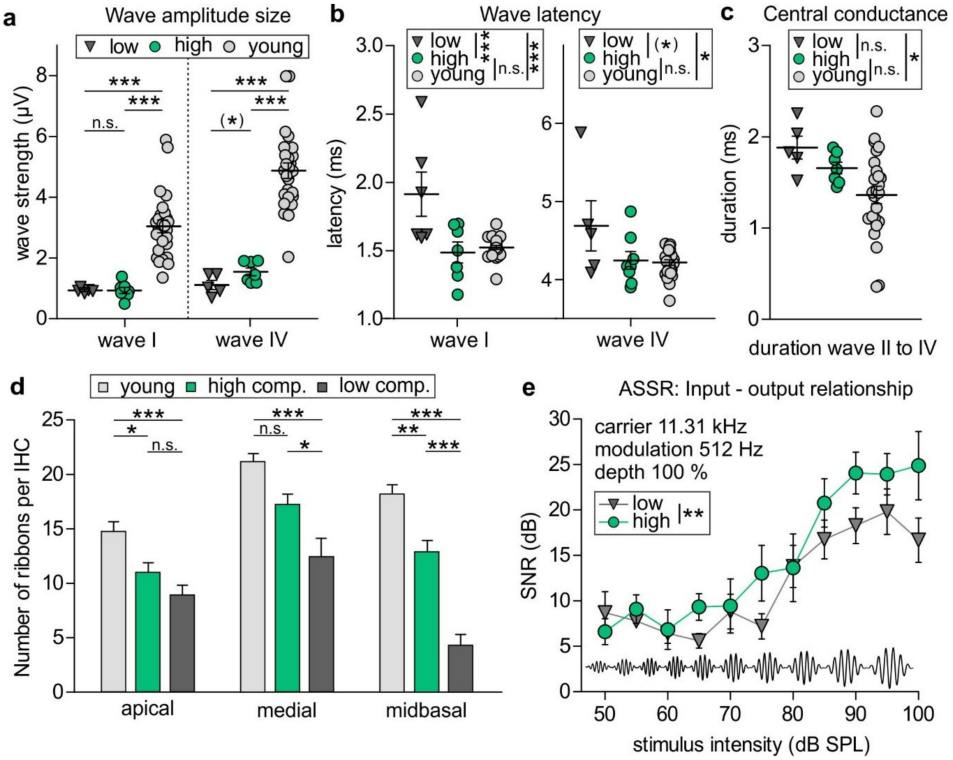

Figure 4. Auditory fine structure analysis and IHC ribbons in high and low compensators. (**a**) ABR wave I strength was similar for high and low compensators and reduced compared with young animals (1-way ANOVA; $F(2, 35) = 21.98$; $p < 0.0001$; Bonferroni's multiple comparisons test: high vs. low compensator $p > 0.05$; young vs. high compensator $p < 0.001$; young vs. low compensator $p < 0.001$). ABR wave IV strength was reduced in both ages groups compared to young animals, but high compensators had a trend for a higher ABR wave IV strength compared to low compensators (1-way ANOVA; $F(2, 35) = 41.15$; $p < 0.0001$; Bonferroni's multiple comparisons test: high vs. low compensator $p < 0.1$; young vs. high compensator $p < 0.001$; young vs. low compensator $p < 0.001$). (**b**) The latency of both, ABR waves I and IV was similar for high compensators and young animals, while low compensators had a prolonged latency (ABR wave I: 1-way ANOVA; $F(2, 36) = 12.55$; $p < 0.0001$; Bonferroni's multiple comparisons test: high vs. low compensator $p < 0.001$; young vs. high compensator $p < 0.001$; young vs. low compensator $p > 0.05$; ABR wave IV: 1-way ANOVA; $F(2, 35) = 4.592$; $p < 0.05$; Bonferroni's multiple comparisons test: high vs. low compensator $p < 0.1$; young vs. high compensator $p < 0.05$; young vs. low compensator $p > 0.05$). (**c**) Low, but not high compensators had a prolonged conduction of central processing, measured by duration between ABR waves II and IV (1-way ANOVA, $F(2, 34) = 4.045$; $p < 0.05$; Bonferroni's multiple comparisons test: high vs. low compensator $p > 0.05$; young vs. high compensator $p > 0.05$; young vs. low compensator $p < 0.05$). For (**a**–**c**): Low compensators $n = 5$; high compensators $n = 7$; young $n = 26$ animals. (**d**) While high compensators showed only moderate reduction of IHC ribbons in the apical and midbasal turns when compared to young animals, low compensators showed a highly significant reduction of ribbons in all three cochlear turns in comparison with young animals, which was most prominent for high-frequency cochlear regions (apical: 1-way ANOVA, $F(2, 34) = 9.1$; $p < 0.001$; Bonferroni's multiple comparisons test: high vs. low compensator $p > 0.05$; young vs. high compensator $p < 0.05$; young vs. low compensator $p < 0.001$; medial: 1-way ANOVA, $F(2, 35) = 9.72$; $p < 0.001$; Bonferroni's multiple comparisons test: high vs. low compensator $p < 0.05$; young vs. high compensator $p > 0.05$; young vs. low compensator $p < 0.001$; midbasal: 1-way ANOVA, $F(2, 35) = 41.93$; $p < 0.0001$; Bonferroni's multiple comparisons test: high vs. low compensator $p < 0.001$; young vs. high compensator $p < 0.01$; young vs. low compensator $p < 0.001$). Young $n = 4$ mice; low compensators $n = 5$ mice; high compensators $n = 5$ mice. (**e**) Input–output relationship of auditory steady state responses with a carrier frequency of 11.32 kHz, a modulation frequency of 512 Hz, and a modulation depth of 100% showed a reduction of temporal auditory resolution in low compensators (2-way ANOVA, $F(1, 106) = 7.52$, $p < 0.01$; Bonferroni's multiple comparisons test for all stimulus intensities: $p > 0.05$). Low compensators $n = 5$; high compensators $n = 7$. (*) $p < 0.1$; * $p < 0.05$; ** $p < 0.01$; *** $p < 0.001$. Mean ± SEM.

In contrast, the strength of ABR wave IV in high compensators had a trend for a higher level compared to low compensators, while both were significantly reduced in comparison to young animals (Figure 4a, right panel), indicating that high and low compensators differed in central compensation rather than in the size of the auditory nerve amplitude. Strikingly, however, the latency of ABR waves I and IV was significantly prolonged in low compensators in comparison to high compensators and young animals (Figure 4b). Taking into account that, at any given characteristic frequency in the auditory system, high-SR fibers with low thresholds have the shortest latencies in comparison to fibers with low-spontaneous firing rates and high thresholds [44,45], our findings suggest that low compensators exhibit compromised high-SR auditory fiber processing.

Additional to prolonged latency of ABR wave I in low compensators, the duration from ABR wave II to ABR wave IV was longer in low compensators compared to young BLEV mice (Figure 4c), indicating that not only the auditory nerve response is delayed but also the central conductance is prolonged in these animals.

Next, we were interested if high and low compensators also differ in their number of IHC ribbons. Both high and low compensators had reduced numbers of IHC ribbons (Figure 4d). However, the decline was much higher in low compensators (Figure 4d). Especially in high-frequency cochlear regions the difference between high and low compensators was most prominent and ribbon loss in low compensators exceeded > 50% reduction, indicating a significant contribution of high-SR auditory fibers (Figure 4d, midbasal).

We finally searched for a difference in temporal processing between high and low compensators using ASSR as described [6], using the amplitude of a carrier frequency of 11.32 kHz that was modulated by a second, slower frequency of 512 Hz with a modulation depth of 100%. Especially for high SPLs > 60 dB a significant attenuated temporal resolution of auditory stimuli was observed in low compensators in comparison to high compensators (Figure 4e). This suggests that the reduced strength of ABR wave IV (Figure 4a, right panel) and the prolonged latency of ABR wave I and ABR wave IV in low compensators (Figure 4b), as well as reduced number of IHC ribbons (Figure 3d) may be linked to a lower temporal auditory resolution in this group.

Conclusion: We observed that both middle-aged and old animals could be subdivided in groups with a lower and higher ability to centrally compensate reduced cochlear synaptopathy. Auditory nerve activity (ABR wave I), although not different in ABR wave size, was prolonged in latency and central conduction time in low compensators in comparison to high compensators and young animals. Furthermore, compared with high compensators, the number of IHC ribbons was strongly reduced in high-frequency regions of low compensators. All of these findings were linked to an attenuated ASSR to follow amplitude-modulated tones in low compensators. This suggests that over age the ability of the brain to disproportionally elevate output activity relative to cochlear input activity (neural gain) and temporal auditory processing is compromised when fast auditory processing is diminished.

3.4. Delayed Auditory Nerve Response and Attenuated Central Auditory Processing Due to Age-Dependent Reduced Auditory Nerve Activity Is Linked with Lower Hippocampal Long-Term Potentiation

We previously observed that central compensation of cochlear synaptopathy is compromised when a critical diminution of auditory input, encompassing high-SR auditory fibers, hampers hippocampal field excitatory postsynaptic potentials (fEPSPs) [24]. Hypothesizing differences in memory-linked facilitation pathways between low and high compensating groups, LTP was measured as described [24]. The recording electrode was placed in the stratum radiatum (SR) of the CA1 region, while stimulating the CA3 Schaffer's collateral axons which have synaptic contacts to CA1 pyramidal cells [24]. LTP was induced in acute coronal brain slices of young, middle-aged, and old BLEV mice. LTP recordings from middle-aged and old animals were then subdivided according to high and low compensators, regardless of their age.

LTP was induced by high-frequency stimulation (HFS; 1s, 100 Hz) and the mean of the last 10 min from the 60 min recording showed that the post HFS fEPSPs were significantly different from the baseline in both low and highly compensating animals (Figure 5a,b).

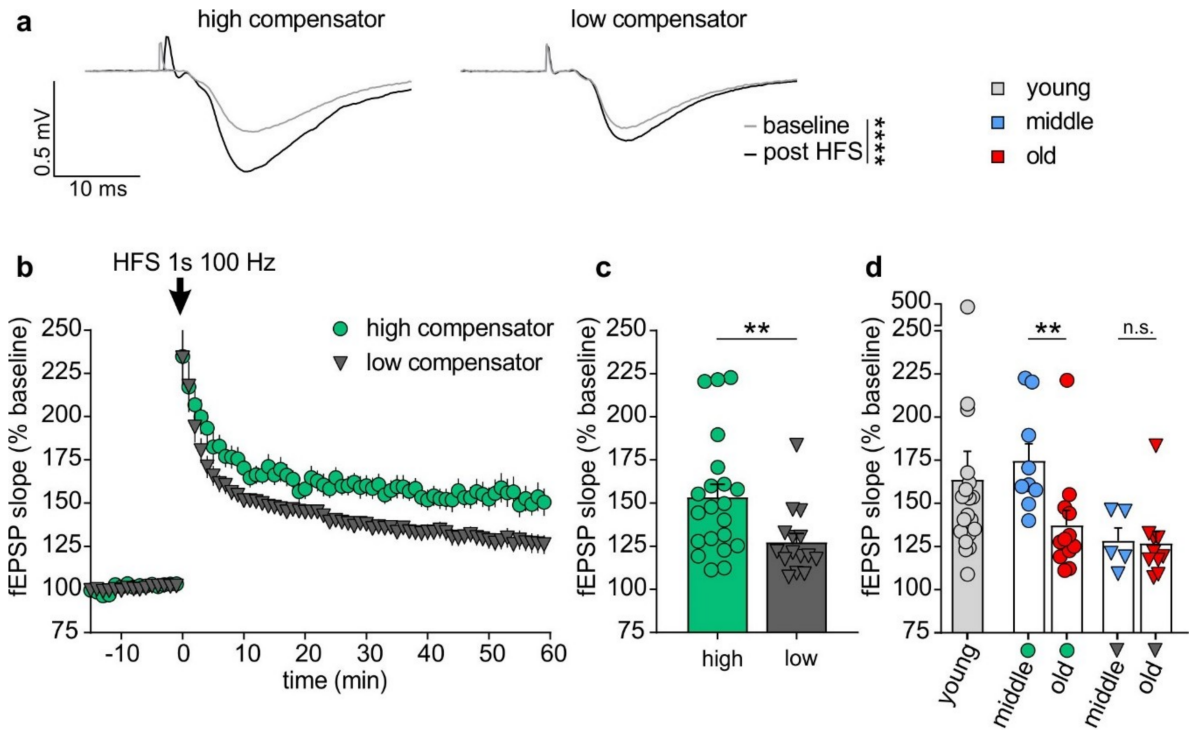

Figure 5. Long-term potentiation (LTP)-induced changes of field excitatory postsynaptic potentials (fEPSPs) in low and high compensators. (**a**) Representative traces before (baseline) and after (post high frequency stimulation) LTP induction as well as (**b**) averaged time courses of fEPSP slopes in acute coronal brain slices displayed prominent LTP in all groups of animals (baseline vs. post HFS; high compensators: Mann–Whitney U test, U (21) = 0, $p < 0.0001$; low compensators: Mann–Whitney U test, U (15) = 0, $p < 0.0001$). (**c**) Highly compensating BLEV mice (153.38% ± 7.56%; n = 7/21 animals/slices) showed significantly elevated LTP in comparison to low compensating (127.39% ± 5.05%; n = 5/15 animals/slices) BLEV mice (Mann–Whitney U test, U (21, 15) = 74, $p < 0.01$). (**d**) Highly compensating animals are present in both, middle-aged (174.69% ± 9.96%; n = 4/9 animals/slices) and old (137.39% ± 11.08%; n = 3/9 animals/slices) groups and do not differ significantly from young animals (163.84% ± 16.31%; n = 7/21 animals/slices; Kruskal–Wallis test with two-stage linear step-up procedure of Benjamini, Krieger, and Yekutieli: young vs. middle-aged high compensator, $p > 0.05$; young vs. old high compensator, $p > 0.05$). At the same time, we observed significant differences between highly compensating middle-aged (174.69% ± 9.96%; n = 4/9 animals/slices) and highly compensating old animals (137.39% ± 11.08%; n = 3/9 animals/slices), but no prominent difference between low compensating middle-aged (128.35% ± 7.46%; n = 2/5 animals/slices) and low compensating old animals (126.90% ± 6.86%; n = 3/10 animals/slices; Kruskal–Wallis test with two-stage linear step-up procedure of Benjamini, Krieger, and Yekutieli: highly compensating middle-aged vs. highly compensating old, $p < 0.01$; low compensating middle-aged vs. low compensating old, $p > 0.05$). ** $p < 0.01$; *** $p < 0.001$. Mean ± SEM. In (**c**,**d**) each dot represents fEPSP slope (average of last 10 min post HFS) of a single coronal brain slice.

However, animals that showed poor central compensation of cochlear synaptopathy (Figure 4d), had significantly reduced hippocampal LTP maintenance compared to animals with a higher capacity for central compensation (Figure 5c). Subdivision of high and low compensators according to age (Figure 5d) revealed that for high compensators age still plays a role, as middle-aged high compensators (blue circles) had a significantly higher LTP than old high compensators (Figure 5d; red circles). In

contrast, for low compensators no difference between middle-aged (Figure 5d; blue triangles) and old animals (Figure 5d; red triangles) could be observed (Figure 5d). Interestingly, the LTP in middle-aged high compensators was not different from that of young control animals (Figure 5d; light grey).

Importantly, neither high nor low compensators exhibited changes in basal synaptic transmission compared to young animals (Figure S1a) as both highly and low compensating groups displayed a similar growth of fEPSP slopes (Figure S1b), but shifted slightly in fiber volley amplitude changes (Figure S1c). However, a regression between both (fEPSP slopes and fiber volley amplitudes) was not different (Figure S1d). This indicates that no changes in presynaptic function occurred which could have caused the observed differences, and thus point to normal activity in pre-synaptic Schaffer's collaterals in both highly and low compensating groups. Moreover, paired-pulse facilitation (PPF) was similar between both groups of animals (Figure S2a–c). Additionally, both high and low compensators' PPF was similar to that of young animals at almost every interpulse interval applied (Figure S2b,c) with the exception of the paired-pulse ratio of the EPSP2/EPSP1 amplitude observed at 10 ms (Figure S2c). This implies that rather than diminished presynaptic fEPSPs and deficient short-term plasticity, attenuated postsynaptic fEPSPs and LTP is linked to reduced central compensation in low compensating groups in comparison to high compensators.

Conclusively, this finding suggests that low compensators with delayed and reduced auditory nerve response and attenuated ability to respond with central compensation and temporal precision exhibit a less pronounced ability to recruit hippocampal LTP in comparison to high compensators with an auditory nerve response which is not delayed.

3.5. Delayed Auditory Nerve Response and Attenuated Central Auditory Processing Due to Age-Dependent Reduced Auditory Nerve Activity Is Linked to Lower Levels of Hippocampal BDNF

Attenuated central compensation following crucial diminution of auditory input was previously shown not only to hamper LTP, but was also linked to diminished recruitment of *Bdnf* exon-IV-CFP and exon-VI-YFP transcripts in the hippocampus [24]. To test if low and high compensators differ in recruitment of activity-dependent *Bdnf* transcripts, we analyzed activity-dependent changes of CFP and YFP, tagged via bi-cistronic expression to translational sites of *Bdnf* exon-IV and -VI mRNAs in BLEV reporter mice, as described previously (see introduction, Figure 6a, [26]).

We examined *Bdnf* exon-IV-CFP and exon-VI-YFP in deconvoluted high resolution fluorescence stacks in the hippocampus (red framed schematic view in Figure 6b). Stacks were costained with parvalbumin (PV) used to identify changes in fast-spiking GABAergic interneurons [24,46]. Among one pair of middle-aged high and low compensators and two pairs of old high and low compensators tested, all high compensators expressed significantly higher levels of *Bdnf* exon-IV-CFP and exon-VI-YFP (Figure 6c, averaged for both age groups, each performed in duplicates). At low magnification of the hippocampal CA3 region, higher *Bdnf* exon-IV-CFP and exon-VI-YFP expression could be observed in high compensators (Figure 6d) compared to low compensators (Figure 6e). Higher magnification revealed the presence of more abundantly overlapping CFP and YFP puncta in the stratum lucidum (SL) of high compensators in comparison to low compensators (Figure 6d, lower panel). For the SL, between the CA1 region and dentate gyrus (DG) (Figure 6b, frame around SL), numerous YFP-positive *Bdnf* exon-VI transcripts were translated in nerve terminals [26] close to CFP-positive *Bdnf* exon-IV transcripts expressed in capillaries [26], particularly in high compensators (Figure 6f) in comparison to low compensators (Figure 6g). So far, no differences in the levels of PV labeling were seen between low and high compensators at any age. Further quantifications of higher magnification images may be required to elucidate if more subtle differences in labeling of PV-positive staining may be identified at perisomatic or axo-dendritic positions between low and highly compensating groups.

Conclusively, in both, middle-aged and old animals, *Bdnf* transcript-IV/VI levels were diminished in low compensating groups in comparison to high compensators (Figure 6).

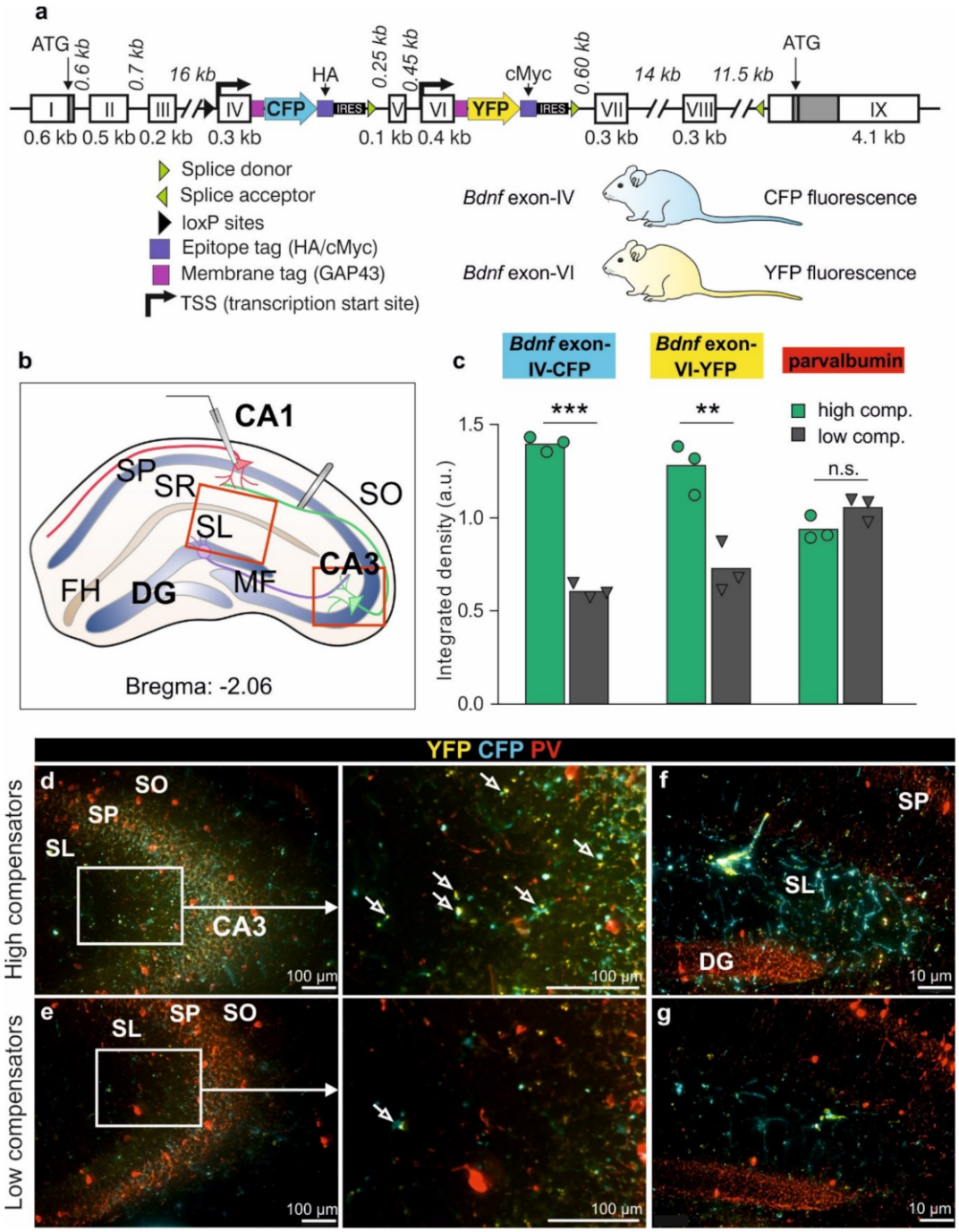

Figure 6. *Bdnf* exon IV/VI and PV expression in the hippocampus of low and high compensators. (**a**) *Bdnf* gene construct depicting insertion sites of the BLEV construct. (**b**) Abstract scheme of hippocampal coronal section. Red boxes indicate the inset seen in d/e (CA3 region) or f/g (SL/DG). SL = stratum lucidum; DG = dentate gyrus; SP = stratum pyramidale; SO = stratum oriens; FH = fissura hippocampalis; SR = stratum radiatum; MF = mossy fiber. (**c**) Quantification of SL/DG region shows larger CFP (Mann–Whitney U test; U(4) = 24.31; $p < 0.0001$) and YFP (Mann–Whitney U test; U(4) = 4.994; $p = 0.0075$) expression in high compensators but no difference of PV in both groups (Mann–Whitney U test; U(4) = 2.127; $p > 0.05$). High compensator n = 3/6; low compensator n = 3/6 (animals/hippocampal hemispheres). ** $p < 0.01$; *** $p < 0.001$. Bars represent Mean. (**d**) Highly compensating animal showing strong expression of *Bdnf* exon IV (CFP) and *Bdnf* exon VI (YFP) in the hippocampal CA3 region (upper panel). With higher magnification, a colocalization of CFP and YFP could be observed (middle panel). (**e**) A low compensating animal showed reduced expression of CFP and YFP in the hippocampal CA3 region (upper and middle panel) compared to high compensators. (**f**) In the SL, a prominent CFP and YFP expression could also be observed in the high compensators, (**g**) which was reduced in the low compensator animals.

Overall the findings suggest that independently from an animal being middle-aged or old, some animals with a delayed and reduced auditory nerve response exhibited a lower central neural gain (Figure 7, right panel, ABR wave, low compensators) in comparison to those with a response that was not delayed and a higher central neural gain (Figure 7, left panel, ABR wave, high compensators). These low compensators exhibited an attenuated sensitivity to follow amplitude-modulated tones (Figure 7, ABR wave, minus), generated less pronounced LTP response (Figure 7, hippocampus, minus) and diminished levels of *Bdnf* exon-VI-YFP and *Bdnf* exon-IV-CFP transcripts close to capillaries in hippocampal regions (Figure 7, yellow, cyan hippocampus and inset).

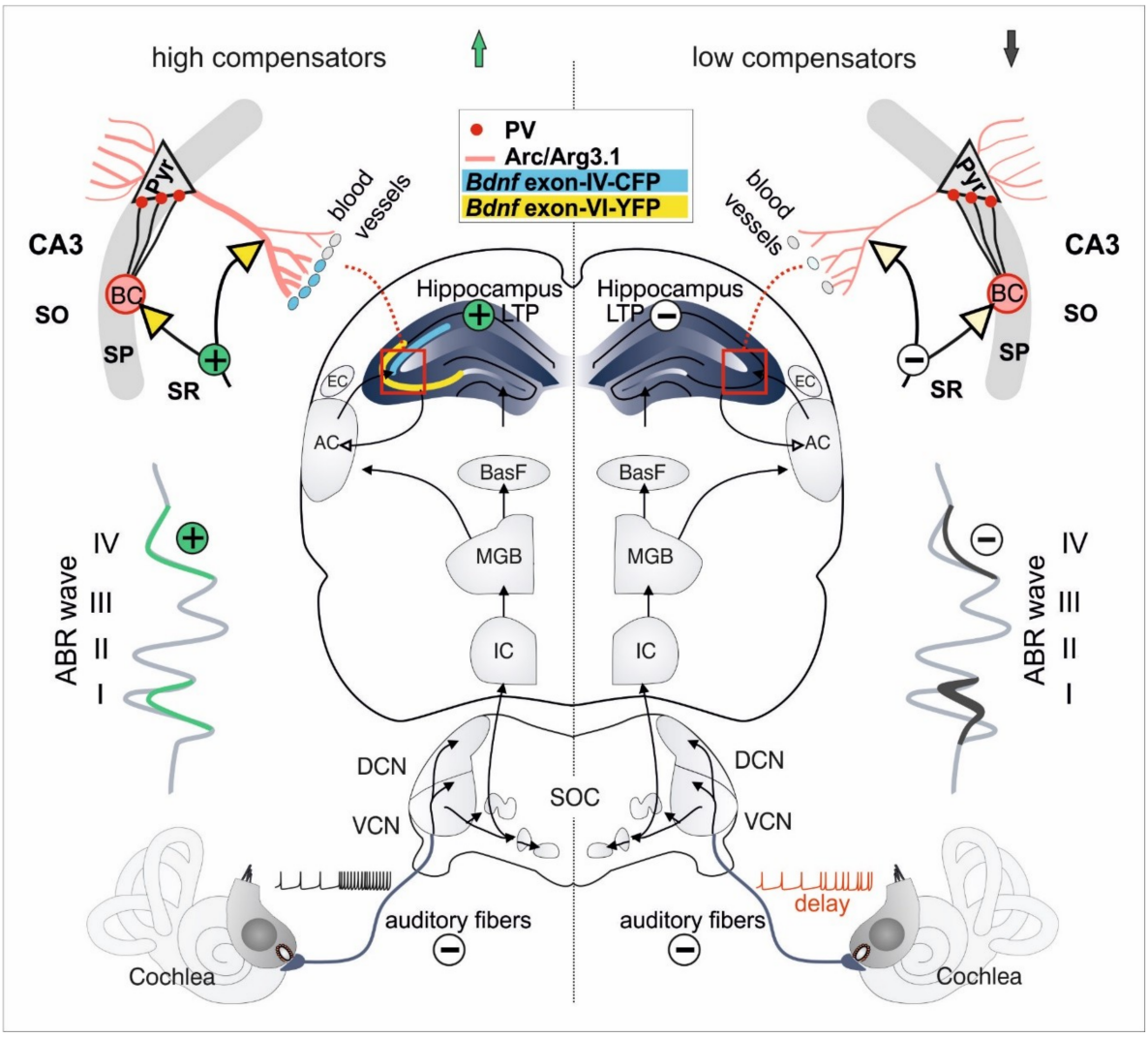

Figure 7. Abstract scheme of mechanisms in the auditory pathway caused by central compensation. High compensators (left side) show disproportionally increased ABR wave IV despite reduced ABR wave I. This is reflected by intact LTP and prominent expression of CFP (*Bdnf* exon-IV) and YFP (*Bdnf* exon-VI). Low compensators (right side) cannot overcome the reduced ABR wave I and therefore have also a reduction in ABR wave IV. Furthermore, LTP is decreased, and CFP and YFP expression is diminished. The black arrows represent the ascending auditory pathway, beginning in the cochlea, from where the signal is sent via auditory fibers to the auditory brainstem (DCN, VCN), midbrain (IC) and the medial geniculate body (MGB), from where it is directly sent to the cortex (AC) and indirectly via the basal forebrain (BasF) to the hippocampus.

4. Discussion

We here describe that independently from being middle-aged or old and unrelated to an overall reduced maximal auditory nerve amplitude size, delayed auditory nerve activity is linked to a lower central compensation and temporal coding capacity and a reduced ability to recruit LTP and hippocampal *Bdnf* transcripts. This indicates that not age-dependent cochlear synaptopathy per se, but attenuation of fast (high-SR) auditory processing, may limit memory-dependent temporal auditory precision and thereby contribute to age-dependent deficits in speech understanding in the presence of noise.

4.1. Auditory (Temporal) Processing Deficits Due to Age-Dependent Cochlear Synaptopathy Differ Depending on Prevailed Latency of Auditory Nerve Response

Age-related hearing loss has long been discussed in the context of problems of understanding speech in the presence of background noise (see [47–49] for a review). Even when elderly listeners retained near-normal audiometric thresholds, hearing difficulties in acoustically complex environments have been reported (e.g., [17–19,49]). Moreover, recent studies suggest that already before hearing loss is measurable in a standard clinical audiogram, a reduction of supra-threshold stimuli encoding precision can be observed that may be linked to a cochlear neuropathy [8,9,50] and may cause poor speech discrimination [2]. Until now fibers with a low SR and a high threshold were suggested to be responsible for temporal processing deficits [5,10], as (i) they emerge perceptually at supra-threshold levels and in challenging listening situations such as in the presence of background noise [51], providing a rationale for the numerous studies that report listening deficits in humans despite normal hearing thresholds (e.g., [5,10,17–19]). High-SR auditory fibers would be driven to saturation under these conditions [2,12,13], as envelope cues that are important for speech-on-speech masking release rely particularly on low-SR supra-threshold coding [52], and (ii) low-SR fibers were also shown to have a high vulnerability to noise and aging [10,14–16]. However, recently some conflicting findings which debate the hypothesis that low-SR linked cochlear synaptopathy is the main source of temporal auditory resolution were reported. Thus, despite similar peripheral sensitivity between young and middle-aged groups a loss of temporal resolving power with reduced speech understanding was found starting from middle-age [48]. In line with this observation various studies could not find a direct association between a potential substrate of cochlear synaptopathy and deficits in the detection of proper envelope time cues in humans [23,53–55].

The delay in auditory nerve response in the group of low compensating animals observed in the present study that is linked with a significantly increased ribbon loss in high-frequency cochlear turns compared to high compensators (Figure 4), suggests that a critical proportion of high-SR auditory fibers, shown to account > 60% of auditory fibers [56], may be affected. High-SR auditory fibers are known to be responsible for the shortest latencies of auditory responses at any given characteristic frequency [44]. This, therefore, may best explain the delayed auditory nerve response and prolonged central conductance (Figure 3) observed in low compensators in comparison to high compensators. High-SR auditory fibers mature after hearing onset with fast auditory processing by developing active feedforward and feedback PV+ interneuron microcircuits providing thereby the basis of auditory-specific connectivity to fronto-striatal brain regions responsible for contrast-amplification and neural gain (see [57] for a review). This suggests that a crucial attenuation of high-SR auditory fiber activity, as here suggested for low-compensating groups, might be functionally linked to the reduced central compensation in these groups (Figure 4). Indirectly the requirement for sustained numbers of high-SR fibers with low thresholds for central compensation of synaptopathy was already predictable from a computerized model that argued that the persistence of a crucial level of high-SR fibers with low thresholds after acoustic noise trauma is a prerequisite for the generation of a sufficient homeostatic increase in discharge rate in auditory brainstem neurons that are targeted by auditory fibers [58]. Within this view a crucial level of maintained spike trains in auditory fibers is essential to drive compensating increases in spike trains in target neurons after deprived auditory input [58,59]. Regarding this

scenario, the higher firing rates in auditory brainstem regions following deafferentation may be driven by a homeostatic decrease in inhibition, as shown to occur in numerous studies following hearing loss [60–63]. This enhanced neural activity is likely to be amplified through cholinergic memory-dependent facilitation circuit (see below). Only previously these central compensation circuits that are generated through neural gain were suggested as a prerequisite for sustained temporal auditory processing following cochlear synaptopathy over age [6].

Conclusively, independently from age and size of the auditory nerve amplitude, lower and higher central compensation (with a correspondingly lower or higher temporal resolution) is linked to delayed or normal auditory nerve response and more or less IHC ribbon loss, respectively. Different kinds of cochlear synaptopathy linked to differential power of the brain to centrally compensate for auditory deprivation, must, therefore, be interpreted in the context of proper central auditory processing over age.

4.2. Auditory (Temporal) Processing Deficits Due to Age-Dependent Cochlear Synaptopathy Differ Depending on Hippocampal LTP and Bdnf Transcript Recruitment

We here report that independently of being middle-aged or old, animals with prolonged auditory nerve latencies exhibit reduced central auditory compensation, lower hippocampal LTP levels and lower recruitment of *Bdnf* transcripts in hippocampal regions in comparison to animals with prevailed auditory nerve activity. Central auditory compensation is a complex process that, similar to the attention-driven contrast amplification of auditory responses, has only previously been suggested to involve coactivation of auditory and fronto-striatal regions such as (i) the basal forebrain to accentuate particular auditory stimuli [64–66], (ii) the inferior frontal gyrus activity, to distinguish new or deviant signals from previous ones [67,68], (iii) the hippocampus to extract and memorize the behaviorally relevant signal and to adjust synaptic strength [64,65,69], and (iv) prefrontal cortex regions to balance attention-driven plasticity responses [70–72].

During this process, auditory information, processed in the medial geniculate body, can activate the network of fronto-striatal brain areas [65,66,71]. Although not explicitly shown for age-dependent hearing loss, previous and present studies demonstrating central neural gain following age-dependent cochlear synaptopathy ([6], present study), may suggest that increased spontaneous and evoked activity in the cochlear nucleus, as shown to occur after acoustic trauma [24,63,73–78], can be amplified through an attention- and learning-dependent circuit. Central neural gain thus likely requires critical high-SR auditory fiber power that maintains a proper baseline of PV+ interneuron-dependent microcircuits (review [57]), on the basis of which central compensating adjustment and contrast-amplification processes occur, the latter of which are crucial for listeners to properly attend to relevant stimuli, while ignoring irrelevant ones [57,79–83].

As shown for contrast amplification pathways [71], these central amplification processes following auditory deprivation are suggested to require a context-specific signal, to assure that synchronized output responses (neural gain) occur specifically in the frequency-deprived regions [24]. Thus, activity-dependent activation of *Bdnf* transcripts was previously suggested as a context-specific carrier [24]. Accordingly, following mild acoustic trauma or sound enrichment, increased levels of *Bdnf* exon-IV-CFP and -VI-YFP were observed in the auditory brainstem and hippocampus that correlated with enhanced or compensated central neural gain and enhanced hippocampal LTP levels [24,84]. In contrast, upon a trauma-induced reduction of auditory input that comprised critical high-SR auditory fiber contribution, hippocampal LTP and *Bdnf* transcript recruitment was diminished similar to central neural gain [24].

In line with this, in the present study a crucial reduction of auditory input in low compensating aged groups was accompanied by lower hippocampal LTP levels and lower recruitment of *Bdnf* transcripts in hippocampal regions compared to same aged high compensators.

Interestingly, this effect was not only independent of age (Figure 3c,d) but also independent of short term plasticity changes, measured by PPF (Figure S2). This may suggest that the long-term

consolidation process of memory that e.g., requires activity-dependent BDNF and glucocorticoid receptor-triggered spine formation to form and maintain learning-dependent synapses [85], rather is a part of a central neural gain processes and subsequent to prevailed fast (high-SR) temporal coding.

Considering how *Bdnf* transcript recruitment may act during facilitation circuits, it is interesting to take into account that the increased levels of *Bdnf* exon-VI-YFP fluorescence in high-compensator groups (Figure 6) were most likely observed in presynaptic nerve endings. This is concluded from studies that showed that BDNF was targeted via anterograde transport in an activity-dependent way to mossy fiber nerve terminals [86] and from colocalization of *Bdnf* exon-VI-YFP with vesicular glutamate transporters in nerve terminals of pyramidal neurons [26]. Low compensating groups showed less *Bdnf* exon-IV-CFP expression in capillary vessels within the highly vascularized fissura hippocampalis region (Figure 6). *Bdnf* exon-IV was traced in these regions to platelets [26], where it was suggested to respond to the activity of store-operated calcium channels [87]. Regarding that specific neuronal activity may tightly regulate blood flow [88], we may hypothesize that the link between reduced recruitment of activity-driven *Bdnf* exon-VI transcripts in nerve endings and of *Bdnf* exon-IV-CFP expression in capillary vessels in low compensators in comparison to high compensators (Figure 6), may reflect a lower ability of neuro-vascular coupling, a feature that requires more extensive future studies. It is also important to point out that temporal auditory processing was not only shown to rely on speed and working memory [25,55,89,90], but also that hypertension-linked memory-deficits over age were linked with lower BDNF levels [91] and that attention- and memory-linked accentuation processes can fail due to deficits in age-dependent circulation of blood flow [92].

Within this context, hearing loss, which is linked to an increased risk of cognitive decline in epidemiological studies [93–95], may reflect the fragility of an individual's neural substrates, particularly of those that control fast (high-SR) auditory processing and auditory-modality specific recruitment of LTP-BDNF-dependent processing, rather than hearing loss, cochlear synaptopathy or age per se.

Supplementary Materials: The following are available online at http://www.mdpi.com/2076-3425/10/10/710/s1, Figure S1: Input-output relationship between fEPSP slope, fiber volley amplitude and stimulus intensity, Figure S2: Paired-pulse facilitation (PPF) as an indicator of short-term plasticity.

Author Contributions: Conceptualization, W.S., M.K.; methodology, L.R.; software, L.R.; validation, W.S., M.K., L.R.; formal analysis, P.M., D.S., A.K., G.A., W.S., M.K., M.M., D.M.; investigation, P.M., D.S., A.K., M.M., D.M., G.A.; data curation, W.S., M.K., L.R.; writing—original draft preparation, P.M., D.S., M.K., W.S.; writing—review and editing, P.M., D.S., T.S., M.K., L.R., W.S.; visualization, W.S., P.M., D.S.; supervision, W.S., M.K., L.R.; project administration, W.S., M.K., L.R.; funding acquisition, M.K. All authors have read and agreed to the published version of the manuscript.

Funding: We acknowledge grants from the Deutsche Forschungsgemeinschaft FOR 2060 project RU 713/3-2 (W.S., L.R., D.M.), Projektnummer 335549539/GRK 2381 (P.M.), SPP 1608 RU 316/12-1 (L.R.), and KN 316/12-1 (M.M, M.K.), Siegmund Kiener Stiftung (D.S.) and BFU2016-76580-P (T.S).

Acknowledgments: We thank Hyun-Soon Geisler, Karin Rohbock, and Iris Köpschall for excellent technical assistance.

Conflicts of Interest: The authors declare no conflict of interest.

Abbreviations

Auditory brainstem responses (ABR); artificial cerebrospinal fluid (ACSF); analysis of variance (ANOVA); auditory steady state responses (ASSR); BDNF-live-exon-visualization (BLEV); cyan- and yellow-fluorescent-protein (CFP/YFP); C terminal-binding protein 2 (CtBP2); dentate gyrus (DG); field excitatory postsynaptic potentials (fEPSPs); high-frequency stimulation (HFS); high spontaneous firing rate (high-SR); inferior colliculus (IC); inner hair cell (IHC); input–output relationship (IOR); low spontaneous firing rate (low-SR); long-term potentiation (LTP); paired-pulse facilitation (PPF); parvalbumin (PV); relative to threshold (re thr); standard error of the mean (SEM); standard deviation (SD); stratum lucidum (SL); stratum radiatum (SR).

References

1. Fullgrabe, C.; Moore, B.C. Effects of age and hearing loss on stream segregation based on interaural time differences. *J. Acoust. Soc. Am.* **2014**, *136*, EL185–EL191. [CrossRef]

2. Bharadwaj, H.M.; Verhulst, S.; Shaheen, L.; Liberman, M.C.; Shinn-Cunningham, B.G. Cochlear neuropathy and the coding of supra-threshold sound. *Front. Syst. Neurosci.* **2014**, *8*, 26. [CrossRef]
3. Bramhall, N.; Ong, B.; Ko, J.; Parker, M. Speech perception ability in noise is correlated with auditory brainstem response wave I amplitude. *J. Am. Acad. Audiol.* **2015**, *26*, 509–517. [CrossRef]
4. Kujawa, S.G.; Liberman, M.C. Adding insult to injury: Cochlear nerve degeneration after "temporary" noise-induced hearing loss. *J. Neurosci.* **2009**, *29*, 14077–14085. [CrossRef]
5. Sergeyenko, Y.; Lall, K.; Liberman, M.C.; Kujawa, S.G. Age-related cochlear synaptopathy: An early-onset contributor to auditory functional decline. *J. Neurosci.* **2013**, *33*, 13686–13694. [CrossRef]
6. Möhrle, D.; Ni, K.; Varakina, K.; Bing, D.; Lee, S.C.; Zimmermann, U.; Knipper, M.; Rüttiger, L. Loss of auditory sensitivity from inner hair cell synaptopathy can be centrally compensated in the young but not old brain. *Neurobiol. Aging* **2016**, *44*, 173–184. [CrossRef]
7. Viana, L.M.; O'Malley, J.T.; Burgess, B.J.; Jones, D.D.; Oliveira, C.A.; Santos, F.; Merchant, S.N.; Liberman, L.D.; Liberman, M.C. Cochlear neuropathy in human presbycusis: Confocal analysis of hidden hearing loss in post-mortem tissue. *Hear. Res.* **2015**, *327*, 78–88. [CrossRef] [PubMed]
8. Liberman, M.C.; Kujawa, S.G. Cochlear synaptopathy in acquired sensorineural hearing loss: Manifestations and mechanisms. *Hear. Res.* **2017**, *349*, 138–147. [CrossRef]
9. Kobel, M.; Le Prell, C.G.; Liu, J.; Hawks, J.W.; Bao, J. Noise-induced cochlear synaptopathy: Past findings and future studies. *Hear. Res.* **2017**, *349*, 148–154. [CrossRef]
10. Furman, A.C.; Kujawa, S.G.; Liberman, M.C. Noise-induced cochlear neuropathy is selective for fibers with low spontaneous rates. *J. Neurophysiol.* **2013**, *110*, 577–586. [CrossRef]
11. Schmiedt, R.A.; Mills, J.H.; Boettcher, F.A. Age-related loss of activity of auditory-nerve fibers. *J. Neurophysiol.* **1996**, *76*, 2799–2803. [PubMed]
12. Parthasarathy, A.; Kujawa, S.G. Synaptopathy in the aging cochlea: Characterizing early-neural deficits in auditory temporal envelope processing. *J. Neurosci.* **2018**, *38*, 7108–7119. [CrossRef]
13. Ridley, C.L.; Kopun, J.G.; Neely, S.T.; Gorga, M.P.; Rasetshwane, D.M. Using thresholds in noise to identify hidden hearing loss in humans. *Ear Hear.* **2018**, *39*, 829–844. [CrossRef]
14. Heinz, M.G.; Young, E.D. Response growth with sound level in auditory-nerve fibers after noise-induced hearing loss. *J. Neurophysiol.* **2004**, *91*, 784–795.
15. Heinz, M.G.; Issa, J.B.; Young, E.D. Auditory-nerve rate responses are inconsistent with common hypotheses for the neural correlates of loudness recruitment. *J. Assoc. Res. Otolaryngol.* **2005**, *6*, 91–105. [CrossRef]
16. Ruel, J.; Chabbert, C.; Nouvian, R.; Bendris, R.; Eybalin, M.; Leger, C.L.; Bourien, J.; Mersel, M.; Puel, J.L. Salicylate enables cochlear arachidonic-acid-sensitive NMDA receptor responses. *J. Neurosci.* **2008**, *28*, 7313–7323. [CrossRef]
17. King, K.; Stephens, D. Auditory and psychological factors in 'auditory disability with normal hearing'. *Scand. Audiol.* **1992**, *21*, 109–114. [CrossRef]
18. Saunders, G.H.; Field, D.L.; Haggard, M.P. A clinical test battery for obscure auditory dysfunction (OAD): Development, selection and use of tests. *Br. J. Audiol.* **1992**, *26*, 33–42. [CrossRef]
19. Stephens, D.; Zhao, F. The role of a family history in king kopetzky syndrome (obscure auditory dysfunction). *Acta Otolaryngol.* **2000**, *120*, 197–200. [CrossRef]
20. Kuwada, S.; Anderson, J.S.; Batra, R.; Fitzpatrick, D.C.; Teissier, N.; D'Angelo, W.R. Sources of the scalp-recorded amplitude-modulation following response. *J. Am. Acad. Audiol.* **2002**, *13*, 188–204. [CrossRef] [PubMed]
21. Bidet-Caulet, A.; Fischer, C.; Besle, J.; Aguera, P.E.; Giard, M.H.; Bertrand, O. Effects of selective attention on the electrophysiological representation of concurrent sounds in the human auditory cortex. *J. Neurosci.* **2007**, *27*, 9252–9261. [CrossRef]
22. Brugge, J.F.; Nourski, K.V.; Oya, H.; Reale, R.A.; Kawasaki, H.; Steinschneider, M.; Howard, M.A., 3rd. Coding of repetitive transients by auditory cortex on Heschl's gyrus. *J. Neurophysiol.* **2009**, *102*, 2358–2374. [CrossRef]
23. Grose, J.H.; Buss, E.; Elmore, H. Age-related changes in the auditory brainstem response and suprathreshold processing of temporal and spectral modulation. *Trends Hear.* **2019**, *23*. [CrossRef]
24. Matt, L.; Eckert, P.; Panford-Walsh, R.; Geisler, H.S.; Bausch, A.E.; Manthey, M.; Muller, N.I.C.; Harasztosi, C.; Rohbock, K.; Ruth, P.; et al. Visualizing BDNF transcript usage during sound-induced memory linked plasticity. *Front. Mol. Neurosci.* **2018**, *11*, 260. [CrossRef]

25. Kamerer, A.M.; AuBuchon, A.; Fultz, S.E.; Kopun, J.G.; Neely, S.T.; Rasetshwane, D.M. The role of cognition in common measures of peripheral synaptopathy and hidden hearing loss. *Am. J. Audiol.* **2019**, *28*, 843–856. [CrossRef]
26. Singer, W.; Manthey, M.; Panford-Walsh, R.; Matt, L.; Geisler, H.S.; Passeri, E.; Baj, G.; Tongiorgi, E.; Leal, G.; Duarte, C.B.; et al. BDNF-live-exon-visualization (BLEV) allows differential detection of BDNF transcripts in vitro and in vivo. *Front. Mol. Neurosci.* **2018**, *11*, 325. [CrossRef] [PubMed]
27. Melcher, J.R.; Kiang, N.Y. Generators of the brainstem auditory evoked potential in cat. III: Identified cell populations. *Hear. Res.* **1996**, *93*, 52–71.
28. Engel, J.; Braig, C.; Rüttiger, L.; Kuhn, S.; Zimmermann, U.; Blin, N.; Sausbier, M.; Kalbacher, H.; Münkner, S.; Rohbock, K.; et al. Two classes of outer hair cells along the tonotopic axis of the cochlea. *Neuroscience* **2006**, *143*, 837–849.
29. Burkard, R.F.; Don, M. The auditory brainstem response. In *Auditory Evoked Potentials: Basic Principles and Clinical Application*; Burkard, R.F., Eggermont, J.J., Don, M., Eds.; Lippincott Williams and Wilkins: Philadelphia, PA, USA, 2007.
30. Matt, L.; Michalakis, S.; Hofmann, F.; Hammelmann, V.; Ludwig, A.; Biel, M.; Kleppisch, T. HCN2 channels in local inhibitory interneurons constrain LTP in the hippocampal direct perforant path. *Cell. Mol. Life Sci.* **2011**, *68*, 125–137. [CrossRef]
31. Chenaux, G.; Matt, L.; Hill, T.C.; Kaur, I.; Liu, X.-B.; Kirk, L.M.; Speca, D.J.; McMahon, S.A.; Zito, K.; Hell, J.W.; et al. Loss of SynDIG1 reduces excitatory synapse maturation but not formation in vivo. SynDIG1 regulates excitatory synapse maturation. *ENeuro* **2016**, *3*. [CrossRef]
32. Singer, W.; Geisler, H.S.; Panford-Walsh, R.; Knipper, M. Detection of excitatory and inhibitory synapses in the auditory system using fluorescence immunohistochemistry and high-resolution fluorescence microscopy. *Methods Mol. Biol.* **2016**, *1427*, 263–276. [CrossRef]
33. Zampini, V.; Johnson, S.L.; Franz, C.; Lawrence, N.D.; Munkner, S.; Engel, J.; Knipper, M.; Magistretti, J.; Masetto, S.; Marcotti, W. Elementary properties of CaV1.3 Ca(2+) channels expressed in mouse cochlear inner hair cells. *J. Physiol.* **2010**, *588*, 187–199. [CrossRef]
34. Chumak, T.; Rüttiger, L.; Lee, S.C.; Campanelli, D.; Zuccotti, A.; Singer, W.; Popelar, J.; Gutsche, K.; Geisler, H.S.; Schraven, S.P.; et al. BDNF in lower brain parts modifies auditory fiber activity to gain fidelity but increases the risk for generation of central noise after injury. *Mol. Neurobiol.* **2016**, *53*, 5607–5627. [CrossRef]
35. Marchetta, P.; Mohrle, D.; Eckert, P.; Reimann, K.; Wolter, S.; Tolone, A.; Lang, I.; Wolters, M.; Feil, R.; Engel, J.; et al. Guanylyl cyclase A/cGMP signaling slows hidden, age- and acoustic trauma-induced hearing loss. *Front. Aging Neurosci.* **2020**, *12*, 83. [CrossRef]
36. Gleich, O.; Semmler, P.; Strutz, J. Behavioral auditory thresholds and loss of ribbon synapses at inner hair cells in aged gerbils. *Exp. Gerontol.* **2016**, *84*, 61–70. [CrossRef] [PubMed]
37. Valero, M.D.; Burton, J.A.; Hauser, S.N.; Hackett, T.A.; Ramachandran, R.; Liberman, M.C. Noise-induced cochlear synaptopathy in rhesus monkeys (Macaca mulatta). *Hear. Res.* **2017**, *353*, 213–223. [CrossRef]
38. Wu, P.Z.; Liberman, L.D.; Bennett, K.; de Gruttola, V.; O'Malley, J.T.; Liberman, M.C. Primary neural degeneration in the human cochlea: Evidence for hidden hearing loss in the aging ear. *Neuroscience* **2019**, *407*, 8–20. [CrossRef]
39. Johnson, D.H.; Kiang, N.Y. Analysis of discharges recorded simultaneously from pairs of auditory nerve fibers. *Biophys. J.* **1976**, *16*, 719–734. [PubMed]
40. Buran, B.N.; Strenzke, N.; Neef, A.; Gundelfinger, E.D.; Moser, T.; Liberman, M.C. Onset coding is degraded in auditory nerve fibers from mutant mice lacking synaptic ribbons. *J. Neurosci.* **2010**, *30*, 7587–7597. [CrossRef]
41. Jaumann, M.; Dettling, J.; Gubelt, M.; Zimmermann, U.; Gerling, A.; Paquet-Durand, F.; Feil, S.; Wolpert, S.; Franz, C.; Varakina, K.; et al. cGMP-Prkg1 signaling and Pde5 inhibition shelter cochlear hair cells and hearing function. *Nat. Med.* **2012**, *18*, 252–259. [CrossRef] [PubMed]
42. Rüttiger, L.; Zimmermann, U.; Knipper, M. Biomarkers for hearing dysfunction: facts and outlook. *ORL* **2017**, *79*, 93–111. [CrossRef]
43. Khimich, D.; Nouvian, R.; Pujol, R.; Tom Dieck, S.; Egner, A.; Gundelfinger, E.D.; Moser, T. Hair cell synaptic ribbons are essential for synchronous auditory signalling. *Nature* **2005**, *434*, 889–894.
44. Rhode, W.S.; Smith, P.H. Encoding timing and intensity in the ventral cochlear nucleus of the cat. *J. Neurophysiol.* **1986**, *56*, 261–286. [CrossRef] [PubMed]

45. Rhode, W.S.; Smith, P.H. Physiological studies on neurons in the dorsal cochlear nucleus of cat. *J. Neurophysiol.* **1986**, *56*, 287–307. [CrossRef]
46. Hu, H.; Gan, J.; Jonas, P. Interneurons. Fast-spiking, parvalbumin^{+} GABAergic interneurons: From cellular design to microcircuit function. *Science* **2014**, *345*, 1255263. [CrossRef] [PubMed]
47. Ouda, L.; Profant, O.; Syka, J. Age-related changes in the central auditory system. *Cell Tissue Res.* **2015**, *361*, 337–358. [CrossRef]
48. Williamson, T.T.; Zhu, X.; Walton, J.P.; Frisina, R.D. Auditory brainstem gap responses start to decline in mice in middle age: A novel physiological biomarker for age-related hearing loss. *Cell Tissue Res.* **2015**, *361*, 359–369. [CrossRef]
49. Frisina, D.R.; Frisina, R.D. Speech recognition in noise and presbycusis: Relations to possible neural mechanisms. *Hear. Res.* **1997**, *106*, 95–104. [CrossRef] [PubMed]
50. Kujawa, S.G.; Liberman, M.C. Synaptopathy in the noise-exposed and aging cochlea: Primary neural degeneration in acquired sensorineural hearing loss. *Hear. Res.* **2015**, *330*, 191–199. [CrossRef]
51. Bourien, J.; Tang, Y.; Batrel, C.; Huet, A.; Lenoir, M.; Ladrech, S.; Desmadryl, G.; Nouvian, R.; Puel, J.L.; Wang, J. Contribution of auditory nerve fibers to compound action potential of the auditory nerve. *J. Neurophysiol.* **2014**, *112*, 1025–1039. [CrossRef]
52. Frisina, R.D.; Karcich, K.J.; Tracy, T.C.; Sullivan, D.M.; Walton, J.P.; Colombo, J. Preservation of amplitude modulation coding in the presence of background noise by chinchilla auditory-nerve fibers. *J. Acoust. Soc. Am.* **1996**, *99*, 475–490. [CrossRef] [PubMed]
53. Grose, J.H.; Buss, E.; Hall, J.W., 3rd. Loud music exposure and cochlear synaptopathy in young adults: Isolated auditory brainstem response effects but no perceptual consequences. *Trends Hear.* **2017**, *21*, 2331216517737417. [CrossRef]
54. Prendergast, G.; Guest, H.; Munro, K.J.; Kluk, K.; Leger, A.; Hall, D.A.; Heinz, M.G.; Plack, C.J. Effects of noise exposure on young adults with normal audiograms I: Electrophysiology. *Hear. Res.* **2017**, *344*, 68–81. [CrossRef] [PubMed]
55. Yeend, I.; Beach, E.F.; Sharma, M.; Dillon, H. The effects of noise exposure and musical training on suprathreshold auditory processing and speech perception in noise. *Hear. Res.* **2017**, *353*, 224–236. [CrossRef] [PubMed]
56. Yates, G.K. Auditory-nerve spontaneous rates vary predictably with threshold. *Hear. Res.* **1991**, *57*, 57–62. [PubMed]
57. Knipper, M.; van Dijk, P.; Schulze, H.; Mazurek, B.; Krauss, P.; Scheper, V.; Warnecke, A.; Schlee, W.; Schwabe, k.; Singer, W.; et al. The neural bases of tinnitus: Lessons from deafness and cochlear implants. *J. Neurosci.* **2020**, *40*, 7190–7202.
58. Schaette, R.; Kempter, R. Predicting tinnitus pitch from patients' audiograms with a computational model for the development of neuronal hyperactivity. *J. Neurophysiol.* **2009**, *101*, 3042–3052. [CrossRef] [PubMed]
59. Schaette, R.; Kempter, R. Computational models of neurophysiological correlates of tinnitus. *Front. Syst. Neurosci.* **2012**, *6*, 34. [CrossRef]
60. Caspary, D.M.; Milbrandt, J.C.; Helfert, R.H. Central auditory aging: GABA changes in the inferior colliculus. *Exp. Gerontol.* **1995**, *30*, 349–360. [CrossRef] [PubMed]
61. Levakova, M.; Tamborrino, M.; Ditlevsen, S.; Lansky, P. A review of the methods for neuronal response latency estimation. *Biosystems* **2015**, *136*, 23–34. [CrossRef]
62. Heeringa, A.N.; van Dijk, P. The dissimilar time course of temporary threshold shifts and reduction of inhibition in the inferior colliculus following intense sound exposure. *Hear. Res.* **2014**, *312*, 38–47. [CrossRef]
63. Cai, S.; Ma, W.L.; Young, E.D. Encoding intensity in ventral cochlear nucleus following acoustic trauma: Implications for loudness recruitment. *J. Assoc. Res. Otolaryngol.* **2009**, *10*, 5–22. [CrossRef] [PubMed]
64. Irvine, D.R.F. Plasticity in the auditory system. *Hear. Res.* **2018**, *362*, 61–73. [CrossRef]
65. Kraus, N.; White-Schwoch, T. Unraveling the biology of auditory learning: A cognitive-sensorimotor-reward framework. *Trends Cogn. Sci.* **2015**, *19*, 642–654. [CrossRef]
66. Kilgard, M.P.; Pandya, P.K.; Engineer, N.D.; Moucha, R. Cortical network reorganization guided by sensory input features. *Biol. Cybern.* **2002**, *87*, 333–343. [CrossRef] [PubMed]
67. Schonwiesner, M.; Novitski, N.; Pakarinen, S.; Carlson, S.; Tervaniemi, M.; Naatanen, R. Heschl's gyrus, posterior superior temporal gyrus, and mid-ventrolateral prefrontal cortex have different roles in the detection of acoustic changes. *J. Neurophysiol.* **2007**, *97*, 2075–2082. [CrossRef]

68. Malmierca, M.S.; Sanchez-Vives, M.V.; Escera, C.; Bendixen, A. Neuronal adaptation, novelty detection and regularity encoding in audition. *Front. Syst. Neurosci.* **2014**, *8*, 111. [CrossRef]
69. Weinberger, N.M. New perspectives on the auditory cortex: Learning and memory. *Handb. Clin. Neurol.* **2015**, *129*, 117–147. [CrossRef]
70. de Kloet, E.R. From receptor balance to rational glucocorticoid therapy. *Endocrinology* **2014**, *155*, 2754–2769. [CrossRef]
71. Irvine, D.R.F. Auditory perceptual learning and changes in the conceptualization of auditory cortex. *Hear. Res.* **2018**, *366*, 3–16. [CrossRef]
72. Viho, E.M.G.; Buurstede, J.C.; Mahfouz, A.; Koorneef, L.L.; van Weert, L.; Houtman, R.; Hunt, H.J.; Kroon, J.; Meijer, O.C. Corticosteroid action in the brain: The potential of selective receptor modulation. *Neuroendocrinology* **2019**, *109*, 266–276. [CrossRef]
73. Kaltenbach, J.A.; Zhang, J. Intense sound-induced plasticity in the dorsal cochlear nucleus of rats: Evidence for cholinergic receptor upregulation. *Hear. Res.* **2007**, *226*, 232–243. [PubMed]
74. Salvi, R.J.; Wang, J.; Ding, D. Auditory plasticity and hyperactivity following cochlear damage. *Hear. Res.* **2000**, *147*, 261–274.
75. Wang, H.; Brozoski, T.J.; Turner, J.G.; Ling, L.; Parrish, J.L.; Hughes, L.F.; Caspary, D.M. Plasticity at glycinergic synapses in dorsal cochlear nucleus of rats with behavioral evidence of tinnitus. *Neuroscience* **2009**, *164*, 747–759.
76. Dehmel, S.; Pradhan, S.; Koehler, S.; Bledsoe, S.; Shore, S. Noise overexposure alters long-term somatosensory-auditory processing in the dorsal cochlear nucleus—Possible basis for tinnitus-related hyperactivity? *J. Neurosci.* **2012**, *32*, 1660–1671. [CrossRef]
77. Groschel, M.; Ryll, J.; Gotze, R.; Ernst, A.; Basta, D. Acute and long-term effects of noise exposure on the neuronal spontaneous activity in cochlear nucleus and inferior colliculus brain slices. *Biomed. Res. Int.* **2014**, *2014*, 909260. [CrossRef]
78. Vogler, D.P.; Robertson, D.; Mulders, W.H. Hyperactivity in the ventral cochlear nucleus after cochlear trauma. *J. Neurosci.* **2011**, *31*, 6639–6645. [CrossRef]
79. Sowell, E.R.; Delis, D.; Stiles, J.; Jernigan, T.L. Improved memory functioning and frontal lobe maturation between childhood and adolescence: A structural MRI study. *J. Int. Neuropsychol. Soc.* **2001**, *7*, 312–322.
80. Nunez, A.; Malmierca, E. Corticofugal modulation of sensory information. *Adv. Anat. Embryol. Cell Biol.* **2007**, *187*, 1–74. [PubMed]
81. Wittekindt, A.; Kaiser, J.; Abel, C. Attentional modulation of the inner ear: A combined otoacoustic emission and EEG study. *J. Neurosci.* **2014**, *34*, 9995–10002. [CrossRef] [PubMed]
82. Dragicevic, C.D.; Marcenaro, B.; Navarrete, M.; Robles, L.; Delano, P.H. Oscillatory infrasonic modulation of the cochlear amplifier by selective attention. *PLoS ONE* **2019**, *14*, e0208939. [CrossRef]
83. Miller, E.K.; Buschman, T.J. Cortical circuits for the control of attention. *Curr. Opin. Neurobiol.* **2013**, *23*, 216–222. [CrossRef]
84. Singer, W.; Gröschel, M.; Zuccotti, A.; Mueller, S.; Ernst, A.; Basta, D.; Knipper, M.; Rüttiger, L. The aftermath of tinnitus-inducing inner ear damage for auditory brainstem responses and MEMR imaging of central brain activity in the rat. *Hear. Balance Commun. Artic.* **2020**, 1–9. [CrossRef]
85. Arango-Lievano, M.; Borie, A.M.; Dromard, Y.; Murat, M.; Desarmenien, M.G.; Garabedian, M.J.; Jeanneteau, F. Persistence of learning-induced synapses depends on neurotrophic priming of glucocorticoid receptors. *Proc. Natl. Acad. Sci. USA* **2019**, *116*, 13097–13106. [CrossRef] [PubMed]
86. Dieni, S.; Matsumoto, T.; Dekkers, M.; Rauskolb, S.; Ionescu, M.S.; Deogracias, R.; Gundelfinger, E.D.; Kojima, M.; Nestel, S.; Frotscher, M.; et al. BDNF and its pro-peptide are stored in presynaptic dense core vesicles in brain neurons. *J. Cell Biol.* **2012**, *196*, 775–788. [CrossRef]
87. Chacon-Fernandez, P.; Sauberli, K.; Colzani, M.; Moreau, T.; Ghevaert, C.; Barde, Y.A. Brain-derived neurotrophic factor in megakaryocytes. *J. Biol. Chem.* **2016**, *291*, 9872–9881. [CrossRef]
88. Hillman, E.M. Coupling mechanism and significance of the BOLD signal: A status report. *Annu. Rev. Neurosci.* **2014**, *37*, 161–181. [CrossRef]
89. Broadway, J.M.; Engle, R.W. Lapsed attention to elapsed time? Individual differences in working memory capacity and temporal reproduction. *Acta Psychol.* **2011**, *137*, 115–126. [CrossRef]

90. Fullgrabe, C.; Moore, B.C.; Stone, M.A. Age-group differences in speech identification despite matched audiometrically normal hearing: Contributions from auditory temporal processing and cognition. *Front. Aging Neurosci.* **2014**, *6*, 347. [CrossRef]
91. Tucsek, Z.; Valcarcel-Ares, M.N.; Tarantini, S.; Yabluchanskiy, A.; Fulop, G.; Gautam, T.; Orock, A.; Csiszar, A.; Deak, F.; Ungvari, Z. Hypertension-induced synapse loss and impairment in synaptic plasticity in the mouse hippocampus mimics the aging phenotype: Implications for the pathogenesis of vascular cognitive impairment. *Geroscience* **2017**, *39*, 385–406. [CrossRef]
92. Shi, Y.; Thrippleton, M.J.; Makin, S.D.; Marshall, I.; Geerlings, M.I.; de Craen, A.J.M.; van Buchem, M.A.; Wardlaw, J.M. Cerebral blood flow in small vessel disease: A systematic review and meta-analysis. *J. Cereb. Blood Flow Metab.* **2016**, *36*, 1653–1667. [CrossRef]
93. Lin, V.Y.; Chung, J.; Callahan, B.L.; Smith, L.; Gritters, N.; Chen, J.M.; Black, S.E.; Masellis, M. Development of cognitive screening test for the severely hearing impaired: Hearing-impaired MoCA. *Laryngoscope* **2017**, *127* (Suppl. 1), S4–S11. [CrossRef]
94. Livingston, G.; Frankish, H. A global perspective on dementia care: A lancet commission. *Lancet* **2015**, *386*, 933–934. [CrossRef]
95. Montero-Odasso, M.; Ismail, Z.; Livingston, G. One third of dementia cases can be prevented within the next 25 years by tackling risk factors. The case "for" and "against". *Alzheimer's Res. Ther.* **2020**, *12*, 81. [CrossRef]

iScience

CellPress
OPEN ACCESS

Article

Loss of central mineralocorticoid or glucocorticoid receptors impacts auditory nerve processing in the cochlea

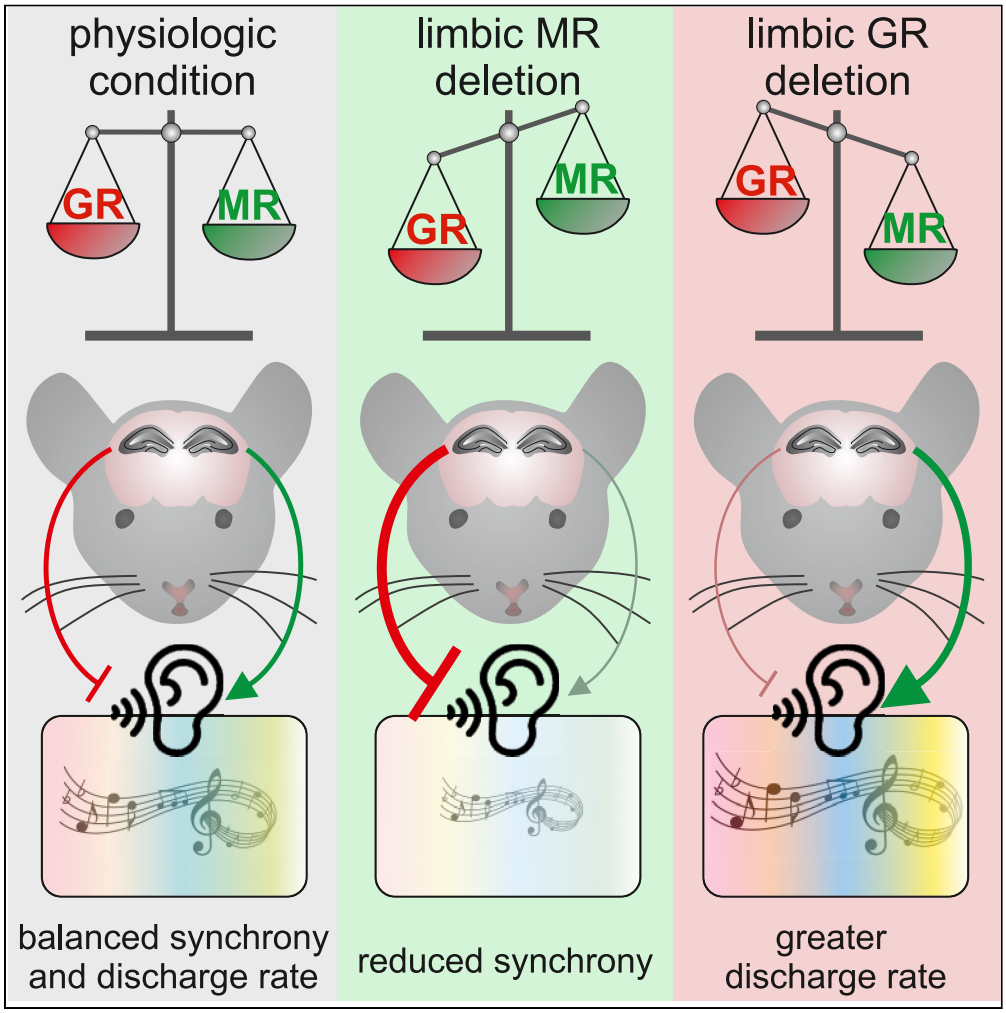

Philine Marchetta, Philipp Eckert, Robert Lukowski, Peter Ruth, Wibke Singer, Lukas Rüttiger, Marlies Knipper

marlies.knipper@uni-tuebingen.de

Highlights

Top-down MR/GR signaling differentially contributes to cochlear sound processing

Limbic MR stimulates auditory nerve fiber discharge rates

Central GR deteriorates auditory nerve fiber synchrony

Marchetta et al., iScience 25, 103981
March 18, 2022
https://doi.org/10.1016/j.isci.2022.103981

iScience

CellPress
OPEN ACCESS

Article

Loss of central mineralocorticoid or glucocorticoid receptors impacts auditory nerve processing in the cochlea

Philine Marchetta,[1] Philipp Eckert,[1] Robert Lukowski,[2] Peter Ruth,[2] Wibke Singer,[1] Lukas Rüttiger,[1] and Marlies Knipper[1,3,*]

SUMMARY

The key auditory signature that may associate peripheral hearing with central auditory cognitive defects remains elusive. Suggesting the involvement of stress receptors, we here deleted the mineralocorticoid and glucocorticoid receptors (MR and GR) using a CaMKIIα-based tamoxifen-inducible Cre^{ERT2}/*loxP* approach to generate mice with single or double deletion of central but not cochlear MR and GR. Hearing thresholds of MRGR$^{CaMKII\alpha CreERT2}$ conditional knockouts (cKO) were unchanged, whereas auditory nerve fiber (ANF) responses were larger and faster and auditory steady state responses were improved. Subsequent analysis of single MR or GR cKO revealed discrete roles for both, central MR and GR on cochlear functions. Limbic MR deletion reduced inner hair cell (IHC) ribbon numbers and ANF responses. In contrast, GR deletion shortened the latency and improved the synchronization to amplitude-modulated tones without affecting IHC ribbon numbers. These findings imply that stress hormone-dependent functions of central MR/GR contribute to "precognitive" sound processing in the cochlea.

INTRODUCTION

Hearing loss with age has recently been suggested to be an important modifying factor increasing the risk of dementia (Livingston et al., 2017; Montero-Odasso et al., 2020). The link between both pathologies is controversial. Until now, peripheral hearing and deficits in central cognitive processes, including cognitive decline and dementia, were predicted to be linked through limbic frontal brain dysfunction (Mudar and Husain, 2016), independent of cochlear functionality (Cope et al., 2015) and possibly disproportionate to peripheral hearing loss (Johnson et al., 2021). Among others, central hearing deficits include deficits in attention or executive function (Rutherford et al., 2018) that are also altered through chronic stress (Perez-Valenzuela et al., 2019; Panza et al., 2019; Canlon et al., 2013). Blockade of stress-hormone binding mineralocorticoid receptors (**MR**), for instance, impairs both memory tasks and selective attention (Wingenfeld and Otte, 2019; de Kloet et al., 2000, 2019). On the other hand, through neuronal atrophy and synaptic dysfunction, chronic stress can contribute to the degradation of synaptic plasticity and thereby influence cognitive functions (for review see Vyas et al., 2016). In the auditory system, numerous studies that analyzed stress-related hearing dysfunction in response to age, acoustic trauma (**AT**), or posttraumatic stress observed associated changes in cognitive functions (Jafari et al., 2019; Basner et al., 2014; Mazurek et al., 2019; Nadhimi and Llano, 2021; Johnson et al., 2021; Wang and Puel, 2020; Canlon et al., 2013; Meltser and Canlon, 2011). How stress-receptor activation links hearing and cognition is, however, currently elusive.

Glucocorticoid receptors (**GR**) and MR in the limbic system, including the prefrontal cortex and hippocampus, are suggested to mediate the top-down and bottom-up control of stress coping with environmental challenges through hypothalamic and extrahypothalamic prefrontal and hippocampal regions (de Kloet et al., 2000, 2019). Previous studies implied that pharmacological or acoustic trauma-induced stress affects central auditory processing through sensorineural cochlear responses (Singer et al., 2013, 2018). To examine whether the brain's ability to recognize and interpret sound depends on stress hormone receptors, we tested the effect of induced genetic disruption of central MR and GR on cochlear function. Employing the tissue-specific tamoxifen (**TMX**)-inducible Cre^{ERT2}/*loxP* system allowed for single and combined

[1]University of Tübingen, Department of Otolaryngology, Head and Neck Surgery, Tübingen Hearing Research Centre, Molecular Physiology of Hearing, Elfriede-Aulhorn-Straße 5, 72076 Tübingen, Germany

[2]University of Tübingen, Institute of Pharmacy, Pharmacology, Toxicology and Clinical Pharmacy, 72076 Tübingen, Germany

[3]Lead contact

*Correspondence: marlies.knipper@uni-tuebingen.de

https://doi.org/10.1016/j.isci.2022.103981

deletion of MR and GR in glutamatergic forebrain neurons under the promoter of CaMKIIα in adult mice (conditional MRGR$^{CaMKII\alpha CreERT2}$ knockout; **MRGR cKO**). This leads to deletion of MR and GR, mainly in the forebrain, with preference for the limbic system, as high levels of CaMKIIα can be found in the hippocampus, cortex, and amygdala; lower levels of CaMKIIα are expressed in striatum, thalamus, and hypothalamus, while CaMKIIα is not present in the cerebellum or outside of the brain (Erdmann et al., 2007). Given that GR are expressed in virtually all cell types in the rodent brain, and MR are expressed primarily in neurons of limbic regions such as the hippocampus, lateral septum, and amygdala (de Kloet et al., 2005; McEwen et al., 2016; Chao et al., 1989; Reul and de Kloet, 1985), while both MR and GR are expressed in cochlear hair cells, supporting cells, and spiral-ganglion neurons (Kil and Kalinec, 2013; Yao and Rarey, 1996; Erichsen et al., 2001; ten Cate et al., 1992, 1993; Zuo et al., 1995), this targeting strategy allowed us to test the specific influences of central stress receptors on peripheral cochlear function.

GR and MR differ in their glucocorticoid (**GC**) binding affinity (de Kloet et al., 2005). MR are highly affine for the endogenous GC cortisol and corticosterone (**CORT**; the latter is the predominant GC in mice), with an approximate Kd (dissociation constant) of 0.5 nM (Reul et al., 1990), which makes MR responsive to acute and mild stress events that are relevant for proper neural responses of learning, memory, and selective attention to novel situations (Joels and de Kloet, 2017; Wirz et al., 2017; Plieger et al., 2018). Compared to MR, GR have only a 10th of the affinity (Kd ≈ 5 nM) for GC. GR play an important role in memory consolidation and long-time adaptation to stressful situations (de Kloet et al., 2005); in addition, because of their widespread expression, are most reactive during chronic stress responses (Sapolsky, 2015; de Kloet et al., 1999, 2005). Thus, assessing specific single MR$^{CaMKII\alpha CreERT2}$ knockout (**MR cKO**) or GR$^{CaMKII\alpha CreERT2}$ knockout (**GR cKO**) mutant mice should give us insights into the common or distinct role of central MR and GR in peripheral cochlear function.

In the present study we observed that the double-deletion of MR and GR strikingly improved cochlear sensitivity, as measured by auditory brainstem response (**ABR**) wave amplitude, compound action-potential (**CAP**) threshold and latency, and neural temporal sound processing underlying auditory steady state responses (**ASSR**). This occurred independently of changes in the mechanics of cochlear outer hair cells (**OHC**) as measured via distortion-product otoacoustic emissions (**DPOAE**), reflecting a negative top-down action of limbic forebrain stress receptors on high-fidelity signal coding and fast auditory processing. The phenotype of MRGR cKO mice combined the unfavorable effects of MR deletion on inner hair cell (**IHC**) ribbon numbers that determine the discharge rate of auditory nerve fibers (**ANF**) on the one hand, with positive effects of GR deletion on CAP latencies and ASSR, influencing temporal auditory coding on the other. Apparently, limbic forebrain MR and GR activities can directly improve or weaken, respectively, the temporal power of sound processing at the level of the cochlea. We suggest that central, i.e., forebrain limbic MR and GR activity, can influence the cochlear sound processing through its top-down influence.

RESULTS

Deletion of MR and GR in CaMKIIα-expressing forebrain regions but not in the cochlea

The Cre^{ERT2}-dependent deletion of the stress receptors MR and GR was performed under control of the CaMKIIα promoter (Erdmann et al., 2007), which is expressed in the whole forebrain, but with highest density in the hippocampus (Dragatsis and Zeitlin, 2000; Wang et al., 2013). To validate the TMX-induced Cre^{ERT2}-directed recombination, the Rosa^{tdTomato} Cre-reporter strain (Madisen et al., 2010) was crossed with CaMKIIα-Cre^{ERT2} mice. Double-transgenic CaMKIIα-Rosa^{tdTomato} mice were examined for Cre^{ERT2}-mediated expression of endogenous red fluorescence in the hippocampus and the cochlea. Although staining was absent in Cre^{ERT2} negative mice (Figure S1A, left panel), strong endogenous red tdTomato fluorescence was found in the hippocampus of Cre^{ERT2} positive CaMKII-Rosa^{tdTomato} mice (Figure S1A, right panel). In neither Cre positive nor Cre negative Rosa^{tdTomato} mice was red fluorescence detectable in cochlear whole-mounts (Figure S1B), indicating that CaMKIIα-Cre^{ERT2} was not activated by TMX injection in the cochlea.

Next, we induced the deletion of MR and GR by TMX injection (5 days, twice daily 1 mg i.p.) in adult pre-mutants bearing floxed MRGR alleles (Figure 1A). In hippocampal pyramidal neurons of the CA1 region, anti-MR staining (Figure S1C, green), as well as anti-GR staining (Figure S1D, green), was only seen in control mice (left panel), but not in MRGR cKO mice (right panel) receiving TMX.

In contrast, MR expression at the level of OHC was found in both control and MRGR cKO mice (Figure S1E, green), whereas GR labeling was seen in the cochlea at the level of IHC and OHC. This labeling was again

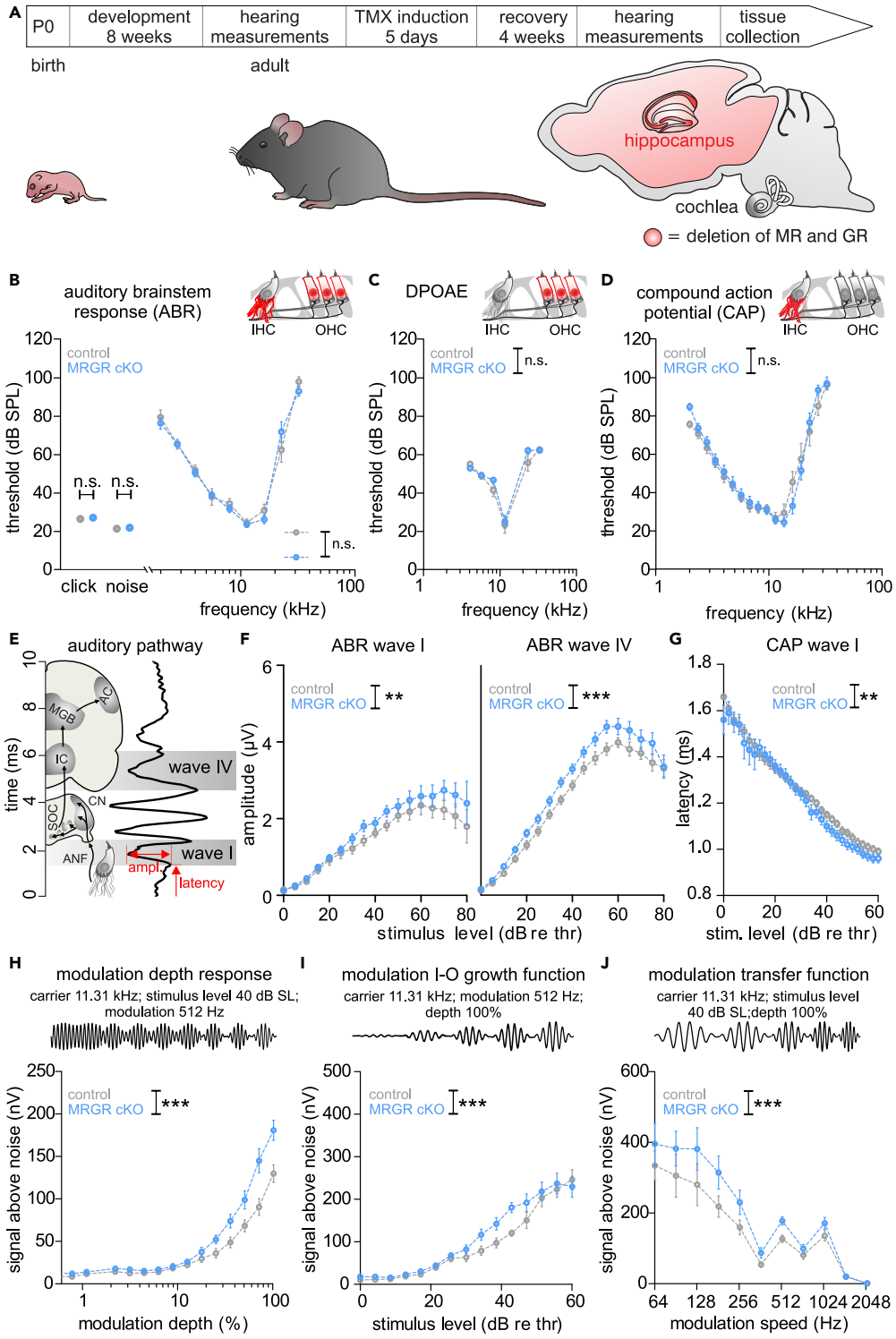

Figure 1. Improved suprathreshold hearing function in MRGR cKO

(A) Workflow of the experiment. 8 weeks after birth, adult, developed mice were checked for hearing function and injected with tamoxifen (TMX). After 4 weeks of recovery, the hearing was measured again and mice were sacrificed to collect brain and cochlea tissue. The TMX induction led to a tissue-specific deletion of MR and GR under the promoter of CaMKIIα, which is expressed in the forebrain, but not the cochlea.

Figure 1. *Continued*

(B) No difference between thresholds in MRGR cKO and control mice with click- (unpaired Student's *t* test, t(50) = 0.620, p = 0.538, WT: n = 12/24, KO: n = 14/28 mice/ears), noise-burst evoked auditory brainstem responses (**ABR**; t(50) = 0.451, p = 0.653, WT: n = 12/24, KO: n = 14/28 mice/ears), as well as pure tone ABR (two-way ANOVA, F(1,8) = 0.191, p = 0.663, WT: n = 10, KO: n = 11 mice/ears).

(C) No difference between thresholds in MRGR cKO and control mice in distortion-product otoacoustic emission (**DPOAE**) thresholds (two-way ANOVA, F(1,5) = 1.772, p = 0.186, WT: n = 5/10, KO: n = 8/16 mice/ears).

(D) No difference between CAP thresholds (two-way ANOVA, F(1,16) = 0.368, p = 0.5443, WT: n = 5/9, KO: n = 7/13 mice/ears) between MRGR cKO and control mice.

(E) Schematic drawing of the auditory pathway and correlated ABR waves.

(F) Left panel: Increased ABR wave I amplitude in MRGR cKO (two-way ANOVA, F(1,17) = 10.80, p = 0.0011, WT: n = 12/24, KO: n = 15/30 mice/ears) and (right panel) increased ABR wave IV amplitude (two-way ANOVA, F(1,17) = 31.62, p < 0.0001, WT: n = 12/24, KO: n = 14/28 mice/ears) compared to controls.

(G) Shortened CAP latency of wave I in MRGR cKO mice (two-way ANOVA, F(1,620) = 70.94, p = 0.0022, WT: n = 6/11, KO: n = 7/13 mice/ears) as compared to controls.

(H) Larger modulation depth function in MRGR cKO mice (two-way ANOVA, F(1,572) = 11.38, p = 0.0008, WT: n = 19, KO: n = 18 mice/ears).

(I) Increased growth function in MRGR cKO mice (two-way ANOVA, F(1,688) = 5.210, p = 0.023, WT: n = 18, KO: n = 20 mice/ears) compared to controls.

(J) Increased modulation transfer function in MRGR cKO mice (two-way ANOVA, F(1,473) = 14.37, p = 0.0002, n = 19 mice/ears) compared to WT mice.

Mean ± SEM. * = p < 0.05, ** = p < 0.01, *** = p < 0.001, n.s. = not significant (p > 0.05). AN = auditory nerve, CN = cochlear nucleus, SOC = superior olivary complex, IC = inferior colliculus, MGB = medial geniculate body, AC = auditory cortex.

not different between control and CaMKIIα-Cre^{ERT2}-mediated conditional MRGR mutants (Figure S1F, green).

We conclude that our TMX-induction protocol promotes the activation of CaMKIIα-Cre^{ERT2}, which leads to an efficient deletion of MR and GR specifically in limbic brain regions (hippocampus) (Erdmann et al., 2007), but that TMX injection did not delete these receptors in the auditory periphery, as schematically depicted in Figure 1A.

Deletion of MR and GR in MRGR cKO mice exposed a negative impact of stress receptors on auditory temporal processing, independently of OHC

We demonstrated that the hearing of Cre positive and Cre negative animals bearing floxed MRGR alleles was not different in the absence of TMX (data not shown). In addition, after TMX injection, ABR thresholds of control and MRGR cKO mice were not different, as shown for click-evoked and noise-evoked responses and for pure-tone stimuli between 2 and 32 kHz (Figure 1B). When DPOAE thresholds were analyzed, providing information about electromechanical properties of OHC function, no difference between the genotypes was observed (Figure 1C). Likewise, the population response thresholds to sound from ANF were not different between the two genotypes (Figure 1D). In contrast, suprathreshold click-evoked ABR that are calculated as peak-to-peak amplitude growth functions of ABR wave I (originating from the auditory nerve) and ABR wave IV (originating from the inferior colliculus) (Melcher et al., 1996), were significantly increased in MRGR cKO mice (Figures 1E and 1F, left and right panel). Thus the stimulus-level-dependent spreading of sound-response amplitudes was already elevated in the auditory periphery, where MR and GR levels were unaltered in MRGR cKO (Figure S1B).

The effects of simultaneous MR deletion and GR deletion on auditory-nerve processing were confirmed by the shorter CAP response latencies in MRGR cKO mice in comparison to control mice, especially at stimulus levels >30 dB above the threshold (Figure 1G). Moreover, stronger ASSR, used as a measure for temporal sound-coding capacity, as described in (Möhrle et al., 2016), was observed in MRGR cKO mice (Figures 1H–1J). ASSR are periodic electrical brain oscillations induced by acoustic stimuli and sinusoidally modulated in amplitude and frequency (Picton et al., 2003). They reflect the synchronous discharge of auditory neurons phase-locked to the modulation frequency of the stimulus (Brenner et al., 2009; Dolphin and Mountain, 1992; Kuwada et al., 2002; Parthasarathy and Bartlett, 2012). We used a carrier frequency of 11.32 kHz that was modulated by a second, slower frequency, ranging between 64 and 2048 Hz, with a modulation depth between 1 and 100% and a stimulus level ranging between 0 and 60 dB above ABR threshold. To this stimulus, MRGR cKO mice showed a significantly enhanced response compared with control mice

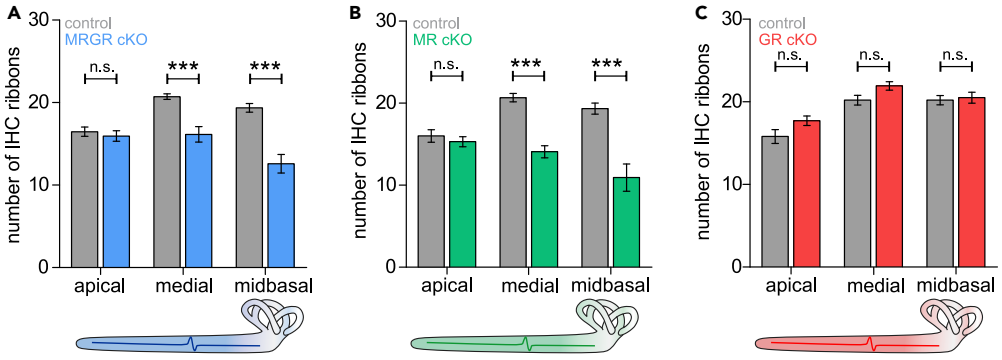

Figure 2. MRGR cKO mice and MR cKO mice, but not GR cKO mice, show reduced numbers of IHC ribbon synapses

(A) Reduced numbers of IHC ribbons in medial and midbasal turns of MRGR cKO mice (two-way ANOVA, $F(1,2) = 41.10$, $p < 0.0001$, WT vs. KO apical: $p > 0.05$, medial: $p < 0.001$, midbasal: $p < 0.001$, WT: n = 19/9, KO: n = 18/9 IHC/mice).

(B) Reduced numbers of IHC ribbons in medial and midbasal turns of MR cKO mice (two-way ANOVA, $F(1,2) = 44.25$, $p < 0.0001$, WT vs. KO apical: $p > 0.05$, medial: $p < 0.001$, midbasal: $p < 0.001$, WT: n = 12/5, KO: 14/5 IHC/mice).

(C) No difference in IHC ribbons numbers between GR cKO and control mice (two-way ANOVA, $F(1,2) = 6.603$, $p = 0.0125$, WT vs. KO apical: $p > 0.05$, medial: $p > 0.05$, midbasal: $p > 0.05$, WT: n = 10/5, KO: n = 14/6 IHCs/mice).

Mean ± SEM. *** = $p < 0.001$, n.s. = not significant ($p > 0.05$).

with regard to modulation depth (Figure 1H), growth rate with stimulus level (Figure 1I), and modulation speed (Figure 1J).

Together, these findings imply that the acute, combined deletion of MR and GR under the CaMKIIα promoter, while not influencing the electromechanical properties of OHC, leads to faster and more sensitive sensorineural cochlear processing, resulting in elevated brain responses to amplitude-modulated tones. This in turn suggests that the combined MR/GR activation during, e.g., elevated (chronic) stress might inhibit auditory neuronal synchronization and temporal auditory processing.

Differential influences of MR or GR on discharge rate and synchrony of auditory nerve responses contribute to the overall phenotype of MRGR cKO on auditory processing

As a possible rationale for the observed altered auditory responses in the MRGR cKO mice, we considered differences in the number of IHC ribbons, which influence auditory processing through defining an ANF's discharge rate (Kujawa and Liberman, 2009; Buran et al., 2010). To examine the ribbons, we used antibodies directed against the RIBEYE protein CtBP2 (Khimich et al., 2005). In MRGR cKO mice, IHC ribbon numbers were significantly reduced in high-frequency coding medial and midbasal cochlear turns (Figure 2A). It is assumed that IHC ribbons can be subdivided into modiolar-sided vs. pillar-sided ribbon synapses, which contact postsynapses that differ functionally in spontaneous firing rates (**SR**) and thresholds for sound coding. The large modiolar ribbon synapses are known to have contact with small postsynapses of low-SR, high-threshold ANF, which are recruited at higher SPL and show little or no saturation. The small pillar ribbon synapses have contact with large postsynapses of high-SR, low-threshold ANF, which are activated in response to lower SPL and rapidly saturate (Liberman, 1982; Liberman and Oliver, 1984; Merchan-Perez and Liberman, 1996; Winter et al., 1990). In C57BL/6 mice the ratio between modiolar-sided and pillar-sided IHC ribbons is around 50:50 (Reijntjes et al., 2020). The same proportion was confirmed in MRGR control mice when analyzing the modiolar/pillar gradient of IHC ribbons in the midbasal turn (Figure S2A). However, MRGR cKO had less ribbons located on the pillar side of the IHC in comparison to ribbons counted on the modiolar side (Figure S2B; left panel). This was contrary to assumptions, as typically, a larger ABR wave I is expected to correlate with a larger, and not a reduced, number of IHC ribbons (Buran et al., 2010; Kujawa and Liberman, 2009). These inconsistencies might have their rational in an overlap of contrasting MR-influences or GR-influences on sensorineural responses (see below).

We hypothesized that a combined MRGR cKO may uncover possible differential effects of the individual MR or GR functions on auditory processing. Indeed, examining TMX-inducible single MR cKO and GR cKO mice revealed that IHC ribbons in MR cKO mice were like in MRGR cKO mice numerically reduced (Figure 2B) and exhibited in high frequency cochlear regions a smaller number of IHC ribbons on the pillar

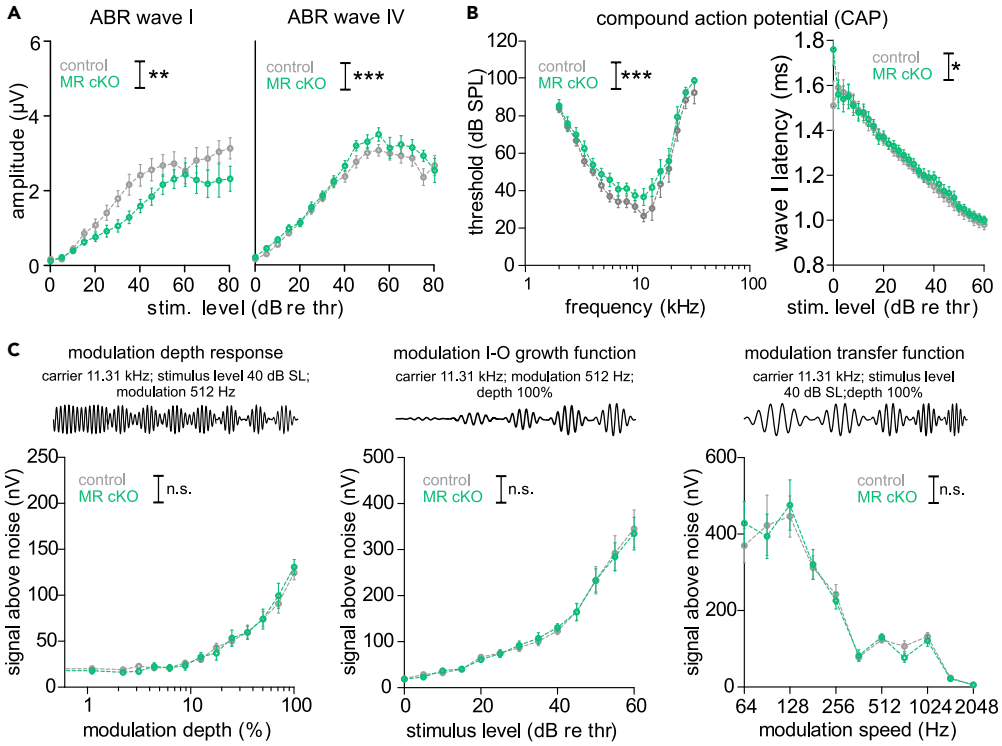

Figure 3. Reduced hearing function in MR cKO

(A) Reduced ABR wave I amplitude (left panel, two-way ANOVA, $F(1,18) = 19.40$, $p < 0.0001$, WT: n = 8/16, KO: n = 8/16 mice/ears), but increased ABR wave IV amplitude MR cKO compared with WT mice (right panel, two-way ANOVA, $F(1,17) = 6.991$, $p = 0.0085$, WT: n = 8/16, KO: n = 8/16 mice/ears).

(B) Left panel: Increased CAP pure tone-evoked threshold in MR cKO (two-way ANOVA, $F(1,16) = 14.92$, $p = 0.0001$, n = 7/14 mice/ears). Right panel: Extended CAP wave I latency in MR cKO (two-way ANOVA, $F(1,733) = 5.57$, $p = 0.0186$, WT: n = 7/14, KO: n = 6/11 mice/ears).

(C) No difference in modulation-depth function (two-way ANOVA, $F(1,701) = 0.14$, $p = 0.999$, WT: n = 24, KO: n = 21 mice/ears), stimulus growth function (two-way ANOVA, $F(1,955) = 0.01$, $p = 1.000$, WT: n = 24, KO: n = 22 mice/ears), and modulation transfer function (two-way ANOVA, $F(1,583) = 0.02$, $p = 0.8905$, WT: n = 24, KO: n = 22 mice/ears) between MR cKO and control mice.

Mean ± SEM. * = $p < 0.05$, ** = $p < 0.01$, *** = $p < 0.001$, n.s. = not significant ($p > 0.05$).

vs. the modiolar side (Figure S2B; middle panel). In contrast, in GR cKO mice, no changes of IHC ribbon numbers (Figure 2C) between controls and GR cKO mice were seen, and the percentage of IHC ribbons numbers on pillar vs. modiolar sides in midbasal turns were not different in WT and GR cKO mice (Figure S2B; right panel). This may suggest that the observed reduction of IHC ribbon numbers, seen in MRGR cKO mice, is rather linked to the deletion of central MR.

When putative effects of the distinct limbic MR and GR ablation on ABR and DPOAE thresholds were analyzed, the ABR hearing thresholds in response to click-tone, noise-tone, or pure-tone stimuli (Figures S3A and S3C), as well as DPOAE thresholds (Figures S3B and S3D), were not found to be different in MR cKO nor GR cKO compared to their respective controls. This supports the notion that neither the limbic MR nor GR affects basal hearing thresholds or electromechanical OHC response properties.

The reduction of IHC ribbons in MR cKO mice was linked to a reduction of the click-evoked ABR wave I amplitude when compared to controls (Figure 3A, left panel). This was, however, centrally compensated, as evident from the normal-sized or even larger ABR wave IV (right panel). The smaller ABR wave I response in MR cKO mice was functionally reflected in slightly, but significantly, higher CAP thresholds compared to control mice (Figure 3B, left panel), and in slightly prolonged CAP latencies (right panel). When ASSR were analyzed in MR cKO mice, we observed no difference to control mice in the modulation-depth function at 40 dB relative to threshold (Figure 3C, left panel), in modulation

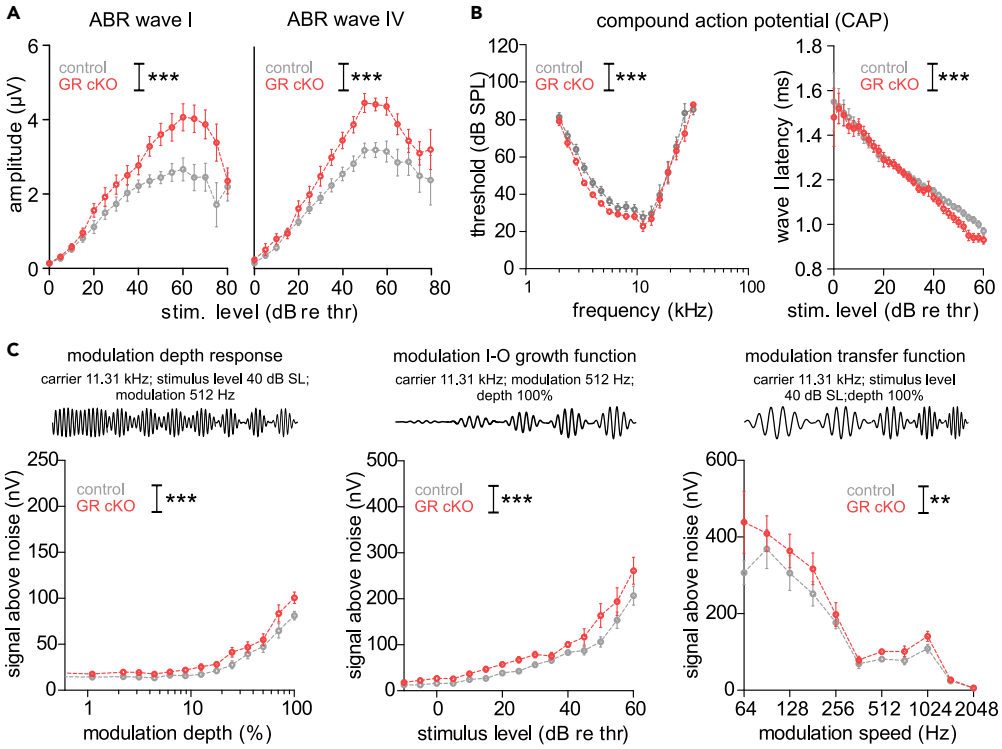

Figure 4. Improved hearing function in GR cKO

(A) Increased ABR wave I (left panel, two-way ANOVA, $F(1,17) = 45.83$, $p < 0.0001$, WT: n = 7/14, KO: n = 8/16 mice/ears) and ABR wave IV amplitudes (right panel, two-way ANOVA, $F(1,17) = 57.51$, $p < 0.0001$, WT: n = 7/14, KO: n = 8/16 mice/ears) in GR cKO compared with control mice.

(B) Left panel: Improved CAP threshold in GR cKO mice (two-way ANOVA, $F(1,16) = 14.60$, $p = 0.0001$, WT: n = 8/15, KO: n = 9/18 mice/ears). Right panel: Shortened CAP wave I latency in GR cKO mice (two-way ANOVA, $F(11,043) = 14.04$, $p = 0.0002$, WT: n = 10/20, KO: n = 10/19 mice/ears).

(C) Larger signal-to-noise ratio (two-way ANOVA, $F(1,780) = 15.56$, $p < 0.0001$, WT: n = 26, KO: n = 24 mice/ears), growth function (two-way ANOVA, $F(11,025) = 34.58$, $p < 0.0001$, WT: n = 30, KO: n = 28 mice/ears), and modulation transfer function (two-way ANOVA, $F(1,636) = 9.99$, $p = 0.0017$, WT: n = 26, KO: n = 24 mice/ears) in GR cKO mice compared with control mice.

Mean ± SEM. ** = $p < 0.01$, *** = $p < 0.001$.

growth functions (middle panel), or in the modulation transfer function (right panel). This together suggested that the influence of MR deletion on auditory processing is restricted to IHC ribbon numbers and ABR wave I amplitudes. In contrast, the deletion of limbic GR, while leaving IHC synapse ribbon numbers unaffected, led to higher click-evoked ABR wave I (Figure 4A, left panel) and wave IV amplitudes (right panel), as also observed in MRGR cKO mice (Figure 1F). Consistently, compared with control mice, GR cKO mice exhibited a significantly lower CAP threshold (Figure 4B, left panel), and shorter CAP wave I latency (right panel). The shorter CAP latency in GR cKO mice was coincident with stronger ASSR responses, evident in a larger signal than in controls when measuring responses to amplitude-modulated stimuli with variation in modulation depth (Figure 4C, left panel), modulated in stimulus level (Figure 4C, middle panel, or changes in modulation frequency (Figure 4C, right panel). Thus, GR deletion influences auditory processing through changes in spike timing and in the synchronization of neural auditory responses that were shown to be required for following amplitude-modulated stimuli (Johnson, 1980).

Overall, these findings in MRGR cKO mice suggested a negative influence of limbic MR deletion on auditory nerve responses, evidenced through reduced IHC ribbon numbers (Figure 2), reduced ABR wave amplitudes, elevated CAP thresholds, and prolonged CAP latencies in MR cKO mice (Figure 3). This negative effect was counterbalanced after central GR loss that – as shown in GR cKO mice – results in elevated ABR amplitudes, lower CAP thresholds, and shortened CAP latencies, as well as facilitated

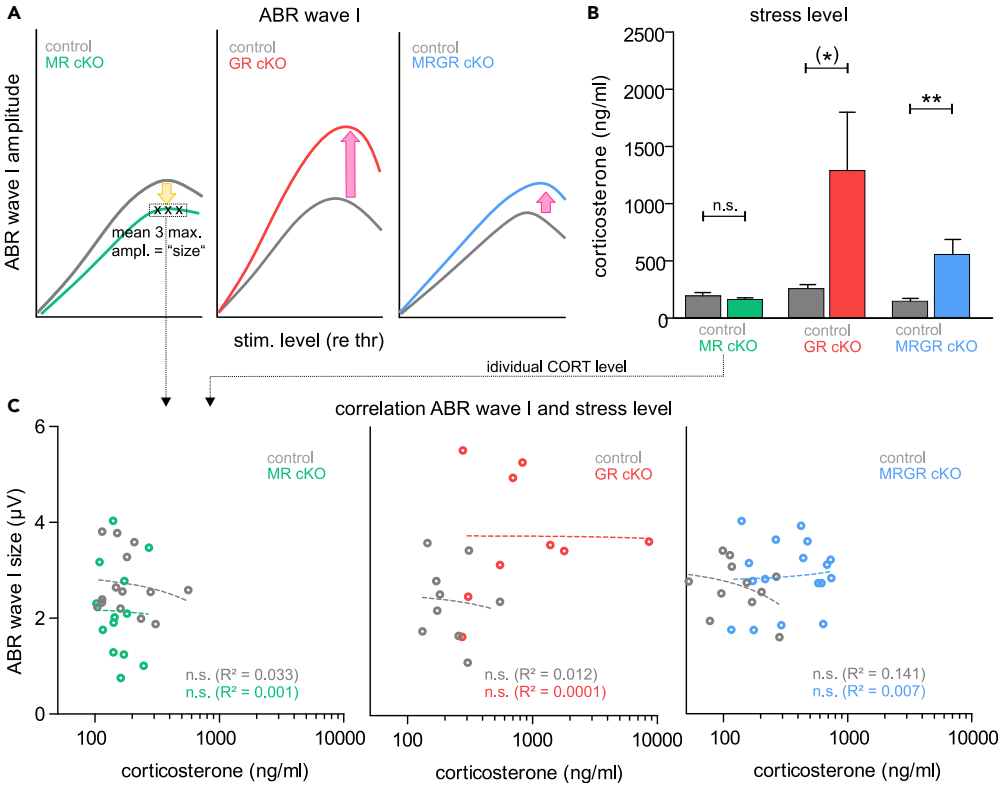

Figure 5. Corticosterone (CORT) levels do not correlate with wave I amplitude

(A) Schematic drawing of reduced ABR wave I amplitude in MR cKO (left panel), strongly increased ABR wave I amplitude in GR cKO (middle panel), and increased ABR wave I amplitude in MRGR cKO mice (left panel).

(B) Similar CORT levels in MR cKO and control mice (unpaired Student's *t* test, t(28) = 90.9285, p = 0.3611, WT: n = 16, KO: n = 14 mice). Increased CORT levels in GR cKO mice, compared with control mice (unpaired Student's *t* test, t(28) = 1.884, p = 0.070, WT: n = 14, KO: n = 16 mice). Increased CORT levels in MRGR cKO mice, compared with control mice (unpaired Student's *t* test, t(24) = 2.905, p = 0.0078, WT: n = 12, KO: n = 14 mice).

(C) Left panel: No correlation for MR cKO and control mice between ABR wave I amplitude and CORT level (linear regression; WT: R^2 = 0.033, p = 0.5329, KO: R^2 = 0.001, p = 0.9322, WT: n = 14, KO: n = 13 mice). Middle panel: No correlation for GR cKO and control mice between ABR wave I amplitude and CORT level (linear regression; WT: R^2 = 0.012, p = 0.7802, KO: R^2 = 0.0001, p = 0.9723, n = 9 mice). Right panel: No correlation for MRGR cKO and control mice between ABR wave I amplitude and CORT level (linear regression; WT: R^2 = 0.141, p = 0.2540, KO: R^2 = 0.007, p = 0.7574, WT: n = 11, KO: n = 17 mice).

Mean ± SEM. (*) = p < 0.1, ** = p < 0.01, n.s. = not significant (p > 0.05).

ASSR (Figure 4). Both phenotypes together, reduction of the peripheral auditory processing after MR deletion and stimulation after GR deletion, contribute to the complex phenotype of MRGR cKO mice (Figure 1).

Blood corticosterone levels do not account for the differential effects on peripheral hearing in MR cKO, GR cKO, and MRGR cKO mice

Previously, the spatiotemporal deletion of GR in limbic forebrain regions was shown to enhance blood CORT levels through an unbalanced autoregulation of hippocampal GR on the hypothalamus-pituitary-adrenal (**HPA**)-axis (Erdmann et al., 2007). To investigate to what extent TMX-induced deletion of MR/GR might also exhibit its influence through an unbalanced HPA-axis, we analyzed the CORT level from blood plasma in anesthetized MR cKO, GR cKO, MRGR cKO, and control mice during hearing measurements. In MR cKO mice that exhibited smaller ABR wave amplitudes (Figure 5A, left panel), the level of CORT was identical to that of controls (Figure 5B, left panel), and the ABR wave I amplitude size, which was the mean of the three maximal amplitude values of the individual ears' suprathreshold amplitude growth function, was not correlated with an individual animal's stress-hormone levels (Figure 5C, left

panel). In contrast, in GR cKO mice, characterized by an elevated ABR wave I (Figure 5A, middle panel), a tendency toward higher CORT levels was observed (Figure 5B, middle panel). Again, no direct correlation between ABR wave I amplitude size and an individual animal's stress levels was found (Figure 5C, middle panel). In MRGR cKO both ABR wave I (Figure 5A, right panel) and the CORT level were elevated (Figure 5B, right panel). However, no correlation between the ABR wave I amplitude size and an individual animal's stress hormone levels was found (Figure 5C, right panel). This may suggest that the GR-deletion-induced HPA-axis dysregulation is not the primary driver for the observed changes of MR/GR cKO on peripheral hearing.

In conclusion, GC activation works in a binary fashion on IHC synapses and auditory-nerve synchrony: by activation of either the stimulating limbic MR (Figure 6, green plus) on the one hand and by activation of the inhibiting GR (Figure 6, red minus) on the other hand. Signaling through these receptors thus provides a key auditory signature that may associate peripheral hearing with central auditory cognitive hearing defects (Figure 6).

DISCUSSION

Physical and psychological stressors are manifested through the activation of the HPA-axis, and the production of GC exerts profound effects on neuronal networks and sensory gating. Acutely elevated and chronically elevated GC levels are assumed to influence sensory gating at the cortical or hippocampal level, independent of peripheral sensory function (Johnson et al., 2021; Basner et al., 2014). By investigating TMX-induced conditional single or combined deletion of MR/GR in forebrain regions, we report functional roles of limbic MR and GR as peripheral modulators of the IHC synapse and in ANF processing. This provides a concept for limbic MR and GR activities during acute or chronic stress, which should be reconsidered as modulators for subcortical processing and filtering elements during auditory perception. In this context, either limbic MR or GR function contribute to the precision of auditory processing, thereby possibly influencing speech comprehension and cognitive hearing function.

Specificity of the TMX–induced limbic deletion of MR and GR

Homozygous global GR KO (Cole et al., 1995), as well as Cre-mediated early embryonic ablation of GR by a constitutively active Cre in $GR^{CaMKII\alpha}$ KO mice (Erdmann et al., 2008), are lethal. As early as P8, animals with germline inactivation of MR, as shown in the homozygous global MR KO, suffer from hyperkalemia, hyponatremia, weight loss, and a strong increase in renin, angiotensin II, and aldosterone plasma concentrations. Consequently, a global lack of MR induces early postnatal death because of bodily dehydration (exsiccosis) as a consequence of massive renal sodium and water loss (Berger et al., 1998). To overcome the lethal phenotype of global GR KO and cell-specific (non-inducible) $GR^{CaMKII\alpha}$ KO, and the severely diseased phenotype of young MR KO (Erdmann et al., 2007; Berger et al., 1998), we used TMX-inducible Cre driver lines (Berger et al., 2006; Erdmann et al., 2008) for the generation of adult MR cKO, GR cKO, and MRGR cKO mouse models. This enabled in parallel the extraction of specific roles of GR and MR in hearing in adulthood. As shown for MRGR cKO mice, both target genes were deleted in pyramidal cells of the forebrain (Figures S1C and S1D), but not in the cochlea (Figures S1E and S1F). The absence of CaMKIIα in the cochlea is in line with other studies (Meese et al., 2017). We observed high CORT levels in MRGR cKO mice, and partly also in the GR cKO, which corresponds well with an analogous $GR^{CaMKII\alpha}$ KO mouse line generated by Erdmann and coworkers, whereas no increase was seen in MR cKO mice (Figure 5A) (Erdmann et al., 2007). This suggests that the TMX-inducible double deletion and single deletion of MR and GR mirrors previous mouse models with respect to HPA-axis dysfunction. However, GR cKO and MR cKO mice presented with distinct hearing phenotypes, which is in line with predictions that GR and MR serve nonredundant functions in neurons to control distinct transcriptional networks (Mifsud and Reul, 2016; Obradovic et al., 2004; de Kloet et al., 2000; McCann et al., 2021; Reul and de Kloet, 1985). As both nuclear receptors recognize the same specific DNA promoter sequences, called GC response elements (Rupprecht et al., 1993; Mifsud and Reul, 2016), the differential effects of MR and GR may stem from the different MR/GR expression profiles. GR is expressed in virtually all cell types in the rodent brain, whereas MR is expressed primarily in neurons of limbic regions such as the hippocampus, lateral septum, and amygdala (de Kloet et al., 2000; Chao et al., 1989; Reul and de Kloet, 1985). Besides their individual expression profile across the brain, differential MR and GR effects derive from different affinities of the individual receptors, with MR having a 10-fold higher affinity for CORT than GR, being occupied by ligands even under baseline, low-stress conditions (Arriza et al., 1988; Gomez-Sanchez and Gomez-Sanchez, 2014). GR, in contrast, are activated when the animal

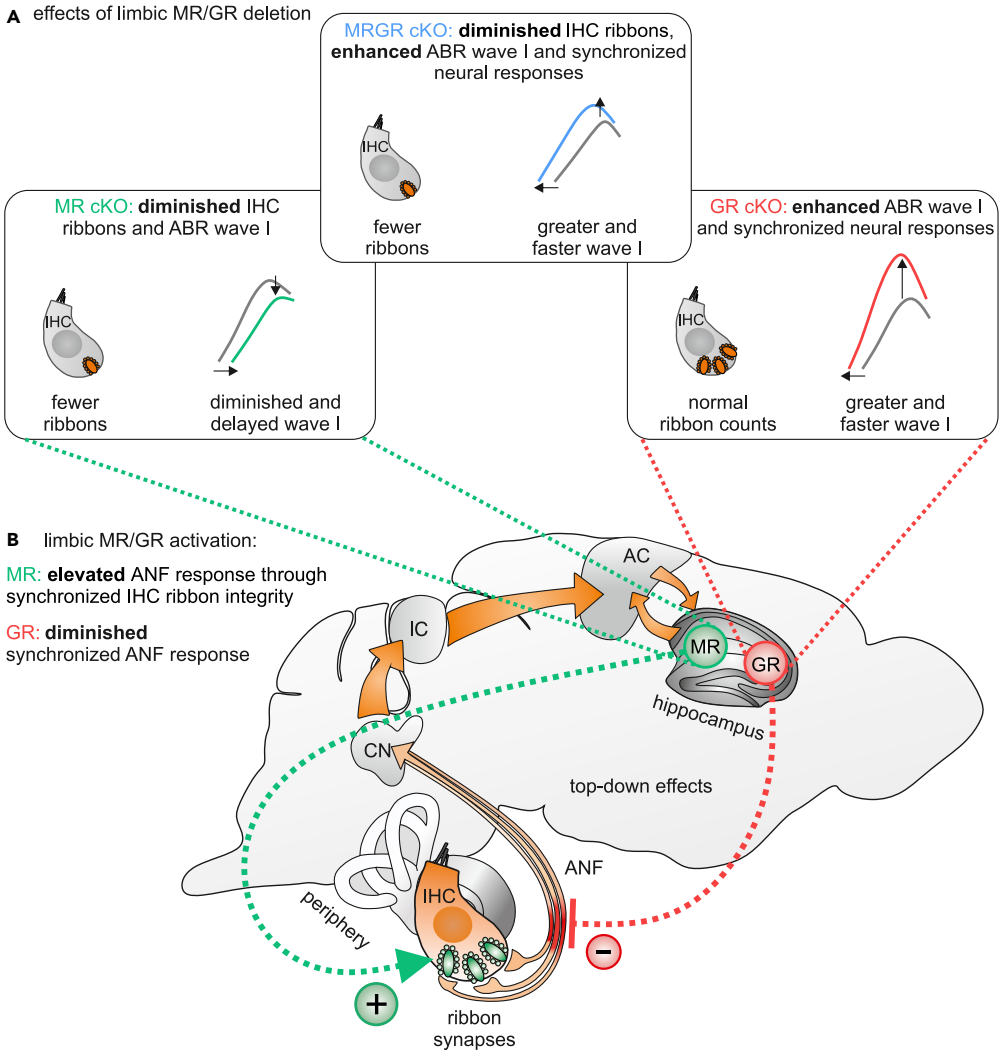

Figure 6. Hypothesized effect of limbic MR/GR activation on auditory processing in the cochlea

(A) Compound limbic deletion of MR and GR leads to reduced IHC ribbon numbers and enhanced auditory neural responses to modulated tones, indicating improved synchrony of neural responses. This phenotype is a mixture of MR cKO mice with reduced IHC ribbon numbers, reduced ABR wave I, but without effects on synchronized neural auditory responses, and GR cKO mice with normal IHC ribbon numbers and increased ANF synchrony.

(B) Hypothesized physiological effect of the activation of limbic MR, possibly contributing to discharge rate, stabilized presynaptic IHC elements, and thereby to an improved ASSR, whereas the activation of limbic GR leads to the inhibition of ANF synchrony, thereby diminishing temporal auditory coding through degradation of synchronized neural auditory responses

is stressed or during circadian periods when circulating CORT levels are naturally elevated (Mifsud and Reul, 2016; Joels et al., 2008; de Kloet et al., 1993).

Because MR has the same binding affinity for aldosterone, cortisol, and CORT (Gomez-Sanchez and Gomez-Sanchez, 2014), changes in presumptive aldosterone effects on hearing might contribute substantially to the MR cKO phenotype. Until now, only long-term effects of aldosterone on hearing have been described, acting through influences on the endocochlear potential (Bazard et al., 2020). The inactivation of cortisol and CORT by 11beta-hydroxysteroid dehydrogenase type 2 (**11beta-HSD2**) is, moreover, required to allow aldosterone to activate MR within aldosterone target cells (Gomez-Sanchez and Gomez-Sanchez, 2014). An immunoreactivity of 11beta-HSD2 has, however, not been detected in any inner ear tissues (Terakado et al., 2011).

Finally, regarding the prominent circadian activity exhibited by the HPA-axis, functional hearing experiments were conducted during the same time period of the day. We were thereby able to avoid dynamic changes in the intrinsic properties of these MR-positive and/or GR-positive neural populations, which may alter the function of neural circuits affecting central or peripheral auditory pathways.

Together, the distinct central and cochlear MR/GR expression profiles, MR/GR-dependent changes in blood CORT levels, as well as the apparently contrasting auditory functions of limbic MR and GR, mirror, at least partly, the respective phenotypes of global and conditional MR/GR KO (Cole et al., 1995; Erdmann et al., 2008). Combined, these findings substantiate the specific MR and GR deletion in limbic forebrain regions of these mouse models.

Differential impact of limbic MR and GR activation on auditory-nerve processing is independent of OHC

Activation of both MR and GR in frontal brain regions and the hippocampus has a direct and differential impact on peripheral auditory processing. This can be concluded from the observation that the induced, combined limbic deletion of MR and GR in adult animals significantly enhanced amplitudes and reduced delays in auditory-nerve responses, independently of OHC function, as no difference was found in the DPOAE measurements of control and MRGR cKO mice (Figure 1). The amplitude of the suprathreshold evoked ABR wave I (Kujawa and Liberman, 2009), the peripheral neural response that is affected in MR and GR cKO mice, is determined through discharge rate and synchrony changes of the auditory nerve (Johnson and Kiang, 1976; Kujawa and Liberman, 2009). ABR wave I spreads centrally to generate ABR wave IV at the level of the inferior colliculus (Melcher et al., 1996). At the cochlear level the effect of MR/GR deletion was quantified through the altered threshold and latency of acoustically-evoked CAP responses reflecting summed single-fiber action potentials of ANF (Earl and Chertoff, 2010; Rüttiger et al., 2017). These CAP measurements allow, moreover, a first estimate of possible distinct contributions of ANF types, which exhibit either high-SR, low-threshold ANF, which are activated in response to lower SPL and rapidly saturate, or low-SR, high-threshold ANF, which are recruited at higher SPL and show little or no saturation (Winter et al., 1990). CAP thresholds are insensitive to changes in low-SR ANF contributions, and only shift when high-SR ANF are affected (Bourien et al., 2014). As high-SR ANF are responsible for the shortest latencies of auditory responses at any given characteristic frequency and are suggested to define perception thresholds (Meddis, 2006; Heil et al., 2008), changes in the thresholds or latencies of an evoked CAP response might point to a contribution of such high-SR ANF.

The deletion of both MR and GR in MRGR cKO mice resulted in larger and faster ABR wave I and IV waves, with both changes occurring independently of any changes in DPOAE function. This improved neural auditory response in MRGR cKO mice was confirmed through shorter CAP latencies and improved ASSR resolution (Figure 1), indicating that compound limbic MR and GR activation might exhibit an overall negative impact on auditory temporal processing.

Interestingly, an analysis of induced, tissue-specific single MR or GR deletions revealed that the response pattern of MRGR cKO mice results from the contrasting effects of MR and GR on either auditory nerve activity and **discharge rates** (**MR cKO**) or on spike timing and **synchrony** (**GR cKO**). Thus, the lack of MR in the limbic system results in reduced IHC ribbon numbers, and specifically to a reduction of pillar-sided IHC ribbons, and reduced amplitudes of ABR wave I, while leaving ASSR responses intact (Figures 2B and 3; Figure S2B). IHC ribbons contribute through their influence on the readily-releasable vesicle pool at IHC synapses to spontaneous and evoked discharge rates of ANF, and when absent, lead to a severe reduction in ABR wave I amplitude and to deficits in onset responses and first-spike latencies (Buran et al., 2010). In the absence of IHC ribbons, the hearing threshold, dynamic range, and response precision to amplitude-modulated tones remain intact, and spreading auditory response amplitudes of ABR wave II, generated in the superior olivocochlear complex (Melcher et al., 1996), are centrally compensated (Buran et al., 2010). In MR cKO mice, the IHC ribbon numbers and ABR wave I amplitude are reduced, the ABR wave IV is enhanced, and ASSR are normal; from this we may conclude that the limbic MR affects the temporal resolving power of the auditory nerve responses through its influences on IHC ribbon integrity (Figure 6). The spatial gradient of IHC ribbon synapses provides information about postsynaptic ANF that functionally differ in SR and thresholds, if localized either on the pillar or modiolar side (Liberman, 1982; Liberman and Oliver, 1984; Merchan-Perez and Liberman, 1996). As our findings suggest a role of central MR on IHC ribbons at the pillar side, it is conceivable that under healthy conditions, central MR may improve presynaptic

contact stabilization to ANF with high-SR and low thresholds that dominate more on the pillar side. It is challenging to consider for future studies if retrocochlear influences of MR activities may be realized through stress-MR-mediated effects on efferent cochlear feedback control.

In contrast, GR cKO mice showed higher-amplitude ABR waves I and IV, a shorter CAP wave I latency, reduced CAP threshold, and a better ability to detect temporally challenging, frequency-modulated tones (Figure 4), while leaving IHC ribbon numbers intact (Figure 2C). Intact IHC ribbon numbers, but altered ASSR responses, suggest that limbic GR activation exerts a "negative" top-down effect on temporal auditory processing through influencing the synchronization of spike times. Precise spike synchronization is influenced through, e.g., the fast kinetics of voltage-gated calcium channels ($Ca_v1.3$) in IHC (Zidanic and Fuchs, 1995; Neef et al., 2009). These are required to ensure Ca^{2+}-binding during the docking of release-ready vesicles and exocytosis (Wong et al., 2013; Rutherford et al., 2021; Johnson et al., 2019). This process critically depends on the metabolically demanding and timely retrieval of vesicles through endocytosis (Wu et al., 2014). Although the underlying details need to be determined further, limbic GR activation may provide the proper metabolic supply for precise spike synchronization. This concept is strengthened through the profound influences of CAP threshold and latency shifts in GR cKO- and MRGR cKO mice (Figures 1 and 4), that may indicate a specific vulnerability of high-SR ANF responses to limbic GR activation, as only high-SR ANF alter CAP thresholds and latencies (Bourien et al., 2014).

In addition, previous findings indirectly pointed to a GR contribution to synchronization of ANF responses. Thus, AT-induced changes in the dynamic range of auditory nerve response were weakened by GR, but not MR antagonists (Singer et al., 2018). As described in Buran et al. (2010) the dynamic range of ANF, which is defined as the range of stimulus levels over which discharge rate increases, is unaffected upon a loss of synaptic ribbons, following Bassoon deletion. This would mean that the dynamic range of the auditory nerve response is strongly affected by synchronized spike responses, but less through altered discharge rates (Buran et al., 2010). In total, the findings in GR cKO and MRGR cKO mice suggest that limbic GR activation may influence temporal auditory processing independently of discharge-rate changes of ANF, but rather through its negative impact on spike timing and synchronization of neural responses by affecting high-SR ANF processing (Figure 6). Although further studies are required to confirm the differential effect of MR and GR on discharge rate and synchronization of ANF responses, it is a striking observation that the GR function in auditory nerve processing did not correlate with blood CORT level changes. Previous studies observed limbic MR/GR functions to be the result of locally synthesized CORT on MR and GR in hippocampal cells, independently of GC produced by adrenal glands (Croft et al., 2008; Taves et al., 2011; McCann et al., 2021). Such local MR effects have previously been shown to alter e.g., social behavior or behavioral responses to novelty (McCann et al., 2021). Further studies are required to elucidate the signaling cascade by which limbic MR and GR improve or degrade auditory neural responses.

Relation of the finding to corticosterone blood level changes

It was surprising that — despite obvious differences in the blood CORT level between GR cKO, MRGR cKO, and their littermate controls — we could not show a correlation between auditory nerve processing and the individual blood CORT level (Figure 5). As blood CORT is a central determinant of MR and GR function, we discuss reasons for this apparent disparity in depth as follows:

(i) Blood samples were taken under exactly the same conditions to avoid CORT changes. Thus, differences in GR and MR cKO CORT blood levels were not because of influences of, e.g., anesthesia level, which can dramatically change CORT (see Arnold and Langhans, 2010). We further made sure that samples were always collected by the same experimenter during the same time of the day, to minimize circadian variation of blood CORT (see Atkinson and Waddell, 1997).

(ii) Although effect sizes in male and female MR cKO, GR cKO, and MRGR cKO mice and their respective control groups were almost identical, we cannot exclude gender-related effects of blood CORT on auditory nerve function.

(iii) As differences in the blood CORT level were only observed in GR cKO and MRGR cKO, but not MR cKO mice, significant effects of central MR on auditory nerve responses are unlikely to be controlled by plasma CORT levels.

(iv) High levels of basal CORT reportedly impaired auditory nerve responses (Singer et al., 2018). In the present study, GR cKO mice had the largest auditory nerve responses, but at the same time the

highest levels of basal blood CORT. In this group of animals, we saw an opposite relation between mean CORT and ABR wave I amplitude, which is another hint that CORT itself is not responsible for the reduced inhibition of auditory nerve sensitivity.

However, in many disorders, HPA-axis activity abnormalities are not evident in baseline blood plasma CORT levels, but are observed in the presence of an acute stressor. Further studies are required to test the extent to which stress levels in MR, GR, or MRGR cKO are different under acute stress and if such changes affect the processing of sound. So far, our data allow us to conclude that the changes in peripheral auditory processing and IHC ribbon synapses in MR cKO, GR cKO, and MRGR cKO are not directly related to changes in the blood CORT level. Mechanisms underlying this top-down signaling from central MR/GR to the auditory periphery remain, however, unclear at present.

Besides CORT itself, other hormones influence the body's responses after exposure to stressful events. Corticotropin releasing hormone (**CRH**) is highly expressed and widely distributed in neurons of the CNS. A large amount of CRH is synthesized in the paraventricular nucleus, and its release stimulates the pituitary gland to produce and secrete adrenocorticotropin (Richard and Lopez, 2013). Beside its modulation of the HPA-axis, CRH is responsible for food intake and energy expenditure (Richard and Lopez, 2013), and in several species CRH also controls the HPA-axis by inducing the secretion of thyroid-stimulating hormone (De Groef et al., 2006) and thereby possibly plays a key role in the endocrine regulation of life-stage transitions. Effects of CRH on ABR wave I are unclear, although it has previously been shown that CRH plays a role in cochlear hearing sensitivity and noise vulnerability (Vetter, 2015; Graham et al., 2010, 2011) and is expressed during the development of hair-cell innervation (Graham and Vetter, 2011). Further quantification of CRH blood level and its local expression in the cochlea should help clarify the role of CRH in ANF signaling in MR cKO, GR cKO, and MRGR cKO mice.

Previous studies observed limbic MR/GR activation in response to locally synthesized CORT in hippocampal cells, independently of GC produced by adrenal glands (Croft et al., 2008; Taves et al., 2011; McCann et al., 2021). Moreover, local MR activation has previously been shown to alter, e.g., social behavior or behavioral responses to novelty (McCann et al., 2021). CA2 pyramidal cells are further distinguished from neighboring CA1 and CA3 pyramidal cells in that they exhibit a unique pattern of gene expression that permits tight regulation of synaptic plasticity of Schaffer's collateral synapses (McCann et al., 2021), and confers sensitivity to the social neuropeptides oxytocin and vasopressin (Pagani et al., 2015; Raam et al., 2017). Vasopressin and oxytocin are expressed not only in the limbic forebrain (Cilz et al., 2019) but also in the cochlea (Reuss et al., 2009). Oxytocin also stimulates soluble guanylate cyclase and increases intracellular cGMP (Porzionato et al., 2010; Conrad et al., 1993), the signaling cascade that was shown to act on auditory nerve processing (Chumak et al., 2016; Marchetta et al., 2020, 2021).

Alternatively, MR and GR forebrain activities may exhibit retrocochlear top-down effects to the periphery through e.g., the olivocochlear efferent feedback system, which has been shown to be activated by selective attention (for review see (Lopez-Poveda, 2018)). Here, one very important modulator is the lateral olivocochlear system (Guinan, 2006), where among other neurotransmitters dopamine plays a crucial role (for review see (Lopez-Poveda, 2018)). In the cochlea, dopamine acts at a postsynaptic level through axodendritic auditory nerve terminal, where it tonically decreased CAP wave I amplitude and prolonged latency when the cochlea was perfused with dopamine (Ruel et al., 2001). It is thus challenging to consider a contrasting modification of dopamine mediated tonic inhibition as a target of either GR or MR triggered retrocochlear feedback.

Role of central/limbic MR in perceptual auditory object formation

In conclusion, we suggest that MR in the limbic brain or GR in central brain regions, both shown to optimize stress-coping (de Kloet et al., 2019), control top-down signaling to the auditory system by improving or weakening IHC synapse processing.

Numerous studies that describe positive effects of acute or low CORT levels on hearing (Meltser and Canlon, 2011; Canlon et al., 2013) should be reconsidered in the light of our present findings on limbic MR activities. This includes the acute and subchronic administration of hydrocortisone, which was shown to transiently enhance the amplitude of auditory evoked potentials in normal subjects (Ashton et al., 2000; Born et al., 1989). It also

includes acute restraint stress, which was observed to improve sound-induced responses in the auditory cortex (Ma et al., 2015), and finally low-dose CORT effects that enhanced the amplitude of auditory evoked potentials recorded from electrodes placed in the CA3 region of the hippocampus (Maxwell et al., 2006). In all cases, limbic MR activation explains these findings because of its direct impact on peripheral auditory processing. Limbic MR activities might be a most attractive key top-down signature linking limbic and auditory neural circuits that are causatively involved in improved hearing, speech discrimination, or communications skills (Jauset-Berrocal and Soria-Urios, 2018; Sihvonen et al., 2017; Sinha et al., 2011; Schaffert et al., 2019; Micheyl et al., 2006). A reduced expression of MR could be linked to neurodevelopmental disorders, such as autism spectrum disorder (Patel et al., 2016) and a human genome mutation leading to a stop-gain alteration of MR protein was found in three brothers with autism (Cukier et al., 2020). Autism spectrum disorder has been hypothesized to be linked with auditory processing deficits in humans (Foss-Feig et al., 2017; Beers et al., 2014) and animal models (Eckert et al., 2021; Truong et al., 2015).

On the other hand, numerous studies point to high CORT or chronic stress as diminishing auditory gating (Maxwell et al., 2006; Stevens et al., 2001; Elling et al., 2011; White et al., 2005; Ma et al., 2017), or to reduced auditory responsiveness following acoustic trauma-induced stress (Ryan et al., 2016; Matt et al., 2018), post-traumatic stress, or chronic stress (MacGregor et al., 2020; Turner et al., 2019; Kreuzer et al., 2014; Mazurek et al., 2019). These studies may now be reconsidered in the context of a possibly direct impact of limbic GC/GR signaling on spike-timing precision and synchronization of neural auditory responses. The close relationship between distress and tinnitus (Boecking et al., 2021; Elarbed et al., 2021; Park et al., 2020; van Munster et al., 2020; Clifford et al., 2019), and the increasing evidence suggesting a role of high-SR ANF processing deficits in tinnitus (Knipper et al., 2013), must be adapted to reflect the herein described limbic GR effects on cochlear function. Interestingly it was shown that patients suffering from a hyperfunctioning pituitary tumor (Cushing Disease) have an increased risk for hearing impairments as comorbidities (Kuan et al., 2017). On the other hand, adrenal cortical insufficiency led to lower hearing thresholds and higher hearing sensitivity in patients, such as in our GR cKO mice (Henkin et al., 1967).

Within this context, the present findings should guide consideration of limbic MR and GR effects on auditory processing, possibly being one of the enigmatic contributors to perceptual auditory object recognition. Although all acoustic input in the environment is detected in multiple "streams," attention can be laid on each of the streams selectively and is used when a person follows e.g., a musical instrument in the middle of an orchestra (Pressnitzer et al., 2008). Such streaming allows the suppression of responses to unimportant auditory cues in a sound mixture, and thereby influences auditory perception, understanding, and behavioral responses in hearing function in an everyday setting. For object recognition, natural auditory environments or "scenes" require listening to sounds at different time points and frequencies to match the incoming auditory input with stored central information to, e.g., isolate and match voices in a crowded environment to previously memorized information and thus recognize the person (Cope et al., 2017). This process of auditory perception has been found to use "precognitive" subcortical processing information (Michie et al., 2016; Perez-Gonzalez and Malmierca, 2014; Antunes and Malmierca, 2021), possible tuned as low as the cochlea (Pressnitzer et al., 2008). The key signature that bridges the "central hearing" and the "peripheral hearing" to extract the information in "scenes" is currently missing (Johnson et al., 2021). As MR plays a role in selective attention (Cornelisse et al., 2011), we may hypothesize that recruitment of limbic MR activities could be a possible candidate mediator to bridge central processing with peripheral processing during the streaming process.

Overall, the roles that MR activation is predicted to play in attention, decision-making, and empathy (Wingenfeld and Otte, 2019; Joels, 2018; Chumak et al., 2016), and that GR activation is predicted to play in memory deficits, cognitive decline, and psychopathologies including Alzheimer's disease (Finsterwald and Alberini, 2014; Ouanes and Popp, 2019; Johnson et al., 2021), make MR and GR most attractive candidates for positive and negative "precognitive" cochlear processing during auditory perception and auditory cognitive dysfunction (Johnson et al., 2021).

Limitations of the study

The present study demonstrates that central/limbic deletion of MR and/or GR leads to changes in peripheral auditory processing and IHC ribbon synapses. This indicates a defective top-down signaling in the

auditory system of MR cKO, GR cKO, and MRGR cKO. With the experimental setting used in the present study, we found no correlation of blood CORT levels with the observed auditory phenotypes. Future studies thus might expose a possible spatiotemporal window of blood CORT not yet identified, through which MR/GR signaling activities alter cochlear nerve processing.

STAR★METHODS

Detailed methods are provided in the online version of this paper and include the following:

- KEY RESOURCES TABLE
- RESOURCE AVAILABILITY
  - Lead contact
  - Materials availability
  - Data and code availability
- EXPERIMENTAL MODEL AND SUBJECT DETAILS
- METHOD DETAILS
  - Hearing measurements
  - DPOAE
  - ABR
  - Auditory steady-state responses
  - Electrocochleographic recordings
  - Tissue preparation
  - Immunohistochemistry and ribbon counting
  - Corticosterone analysis
- QUANTIFICATION AND STATISTICAL ANALYSIS
  - Hearing measurements
  - Ribbon counting
  - Corticosterone analysis

SUPPLEMENTAL INFORMATION

Supplemental information can be found online at https://doi.org/10.1016/j.isci.2022.103981.

ACKNOWLEDGMENTS

This work was funded by the Deutsche Forschungsgemeinschaft – P.M., M.K., R.L., and P.R. are members of the Research Training Group [grant number 335549539/GRK 2381]; FOR 2060 project RU 713/3-2 (W.S. and L.R.), SPP 1608 RU 316/12-1 (P.E. and L.R.), KN 316/12-1 (M.K.), and the Sigmund Kiener Stiftung (P.E.). English language services were provided by stels-ol.de. We thank Karin Rohbock, Iris Köpschall, and Hyun-Soon Geisler for their technical support.

AUTHOR CONTRIBUTIONS

Conceptualization, M.K. and L.R.; Methodology, M.K. and L.R.; Software, L.R.; Formal Analysis, P.M. and L.R.; Investigation, P.M., P.E., and M.K.; Writing – Original Draft, P.M. and M.K.; Writing – Review & Editing, P.M., W.S., L.R., R.L., P.R., and M.K.; Visualization, P.M.; Supervision, W.S., L.R., and M.K.; Funding Acquisition, M.K., L.R., R.L., and P.R.

DECLARATION OF INTERESTS

The authors declare no competing interests.

Received: December 15, 2021
Revised: January 26, 2022
Accepted: February 21, 2022
Published: March 18, 2022

REFERENCES

Antunes, F.M., and Malmierca, M.S. (2021). Corticothalamic pathways in auditory processing: recent advances and insights from other sensory systems. Front. Neural Circuits *15*, 721186.

Arnold, M., and Langhans, W. (2010). Effects of anesthesia and blood sampling techniques on plasma metabolites and corticosterone in the rat. Physiol. Behav. *99*, 592–598.

Arriza, J.L., Simerly, R.B., Swanson, L.W., and Evans, R.M. (1988). The neuronal mineralocorticoid receptor as a mediator of glucocorticoid response. Neuron *1*, 887–900.

Ashton, C.H., Lunn, B., Marsh, V.R., and Young, A.H. (2000). Subchronic hydrocortisone treatment alters auditory evoked potentials in normal subjects. Psychopharmacology (Berl) *152*, 87–92.

Atkinson, H.C., and Waddell, B.J. (1997). Circadian variation in basal plasma corticosterone and adrenocorticotropin in the rat: sexual dimorphism and changes across the estrous cycle. Endocrinology *138*, 3842–3848.

Basner, M., Babisch, W., Davis, A., Brink, M., Clark, C., Janssen, S., and Stansfeld, S. (2014). Auditory and non-auditory effects of noise on health. Lancet *383*, 1325–1332.

Bazard, P., Ding, B., Chittam, H.K., Zhu, X., Parks, T.A., Taylor-Clark, T.E., Bhethanabotla, V.R., Frisina, R.D., and Walton, J.P. (2020). Aldosterone up-regulates voltage-gated potassium currents and NKCC1 protein membrane fractions. Sci. Rep. *10*, 15604.

Beers, A.N., Mcboyle, M., Kakande, E., Dar Santos, R.C., and Kozak, F.K. (2014). Autism and peripheral hearing loss: a systematic review. Int. J. Pediatr. Otorhinolaryngol. *78*, 96–101.

Berger, S., Bleich, M., Schmid, W., Cole, T.J., Peters, J., Watanabe, H., Kriz, W., Warth, R., Greger, R., and Schutz, G. (1998). Mineralocorticoid receptor knockout mice: pathophysiology of Na+ metabolism. Proc. Natl. Acad. Sci. U S A *95*, 9424–9429.

Berger, S., Wolfer, D.P., Selbach, O., Alter, H., Erdmann, G., Reichardt, H.M., Chepkova, A.N., Welzl, H., Haas, H.L., Lipp, H.P., et al. (2006). Loss of the limbic mineralocorticoid receptor impairs behavioral plasticity. Proc. Natl. Acad. Sci. U S A *103*, 195–200.

Boecking, B., Rose, M., Brueggemann, P., and Mazurek, B. (2021). Two birds with one stone. Addressing depressive symptoms, emotional tension and worry improves tinnitus-related distress and affective pain perceptions in patients with chronic tinnitus. PLoS One *16*, e0246747.

Born, J., Hitzler, V., Pietrowsky, R., Pauschinger, P., and Fehm, H.L. (1989). Influences of cortisol on auditory evoked potentials (AEPs) and mood in humans. Neuropsychobiology *20*, 145–151.

Bourien, J., Tang, Y., Batrel, C., Huet, A., Lenoir, M., Ladrech, S., Desmadryl, G., Nouvian, R., Puel, J.L., and Wang, J. (2014). Contribution of auditory nerve fibers to compound action potential of the auditory nerve. J. Neurophysiol. *112*, 1025–1039.

Brenner, C.A., Krishnan, G.P., Vohs, J.L., Ahn, W.Y., Hetrick, W.P., Morzorati, S.L., and O'donnell, B.F. (2009). Steady state responses: electrophysiological assessment of sensory function in schizophrenia. Schizophr. Bull. *35*, 1065–1077.

Buran, B.N., Strenzke, N., Neef, A., Gundelfinger, E.D., Moser, T., and Liberman, M.C. (2010). Onset coding is degraded in auditory nerve fibers from mutant mice lacking synaptic ribbons. J. Neurosci. *30*, 7587–7597.

Canlon, B., Theorell, T., and Hasson, D. (2013). Associations between stress and hearing problems in humans. Hear. Res. *295*, 9–15.

Chao, H.M., Choo, P.H., and Mcewen, B.S. (1989). Glucocorticoid and mineralocorticoid receptor mRNA expression in rat brain. Neuroendocrinology *50*, 365–371.

Chumak, T., Ruttiger, L., Lee, S.C., Campanelli, D., Zuccotti, A., Singer, W., Popelar, J., Gutsche, K., Geisler, H.S., Schraven, S.P., et al. (2016). BDNF in lower brain parts modifies auditory fiber activity to gain fidelity but increases the risk for generation of central noise after injury. Mol. Neurobiol. *53*, 5607–5627.

Cilz, N.I., Cymerblit-Sabba, A., and Young, W.S. (2019). Oxytocin and vasopressin in the rodent hippocampus. Genes Brain Behav. *18*, e12535.

Clifford, R.E., Baker, D., Risbrough, V.B., Huang, M., and Yurgil, K.A. (2019). Impact of TBI, PTSD, and hearing loss on tinnitus progression in a US marine cohort. Mil. Med. *184*, 839–846.

Cole, T.J., Blendy, J.A., Monaghan, A.P., Krieglstein, K., Schmid, W., Aguzzi, A., Fantuzzi, G., Hummler, E., Unsicker, K., and Schutz, G. (1995). Targeted disruption of the glucocorticoid receptor gene blocks adrenergic chromaffin cell development and severely retards lung maturation. Genes Dev. *9*, 1608–1621.

Conrad, K.P., Gellai, M., North, W.G., and Valtin, H. (1993). Influence of oxytocin on renal hemodynamics and sodium excretion. Ann. N Y Acad. Sci. *689*, 346–362.

Cope, T.E., Baguley, D.M., and Griffiths, T.D. (2015). The functional anatomy of central auditory processing. Pract. Neurol. *15*, 302–308.

Cope, T.E., Sohoglu, E., Sedley, W., Patterson, K., Jones, P.S., Wiggins, J., Dawson, C., Grube, M., Carlyon, R.P., Griffiths, T.D., et al. (2017). Evidence for causal top-down frontal contributions to predictive processes in speech perception. Nat. Commun. *8*, 2154.

Cornelisse, S., Joels, M., and Smeets, T. (2011). A randomized trial on mineralocorticoid receptor blockade in men: effects on stress responses, selective attention, and memory. Neuropsychopharmacology *36*, 2720–2728.

Croft, A.P., O'callaghan, M.J., Shaw, S.G., Connolly, G., Jacquot, C., and Little, H.J. (2008). Effects of minor laboratory procedures, adrenalectomy, social defeat or acute alcohol on regional brain concentrations of corticosterone. Brain Res. *1238*, 12–22.

Cukier, H.N., Griswold, A.J., Hofmann, N.K., Gomez, L., Whitehead, P.L., Abramson, R.K., Gilbert, J.R., Cuccaro, M.L., Dykxhoorn, D.M., and Pericak-Vance, M.A. (2020). Three brothers with autism carry a stop-gain mutation in the HPA-axis gene NR3C2. Autism Res. *13*, 523–531.

De Groef, B., Van der Geyten, S., Darras, V.M., and Kuhn, E.R. (2006). Role of corticotropin-releasing hormone as a thyrotropin-releasing factor in non-mammalian vertebrates. Gen. Comp. Endocrinol. *146*, 62–68.

de Kloet, E.R., Sutanto, W., Van Den Berg, D.T., Carey, M.P., Van Haarst, A.D., Hornsby, C.D., Meijer, O.C., Rots, N.Y., and Oitzl, M.S. (1993). Brain mineralocorticoid receptor diversity: functional implications. J. Steroid Biochem. Mol. Biol. *47*, 183–190.

de Kloet, E.R., Oitzl, M.S., and Joels, M. (1999). Stress and cognition: are corticosteroids good or bad guys? Trends Neurosci. *22*, 422–426.

de Kloet, E.R., Van Acker, S.A., Sibug, R.M., Oitzl, M.S., Meijer, O.C., Rahmouni, K., and De Jong, W. (2000). Brain mineralocorticoid receptors and centrally regulated functions. Kidney Int. *57*, 1329–1336.

de Kloet, E.R., Joels, M., and Holsboer, F. (2005). Stress and the brain: from adaptation to disease. Nat. Rev. Neurosci. *6*, 463–475.

de Kloet, E.R., de Kloet, S.F., de Kloet, C.S., and de Kloet, A.D. (2019). Top-down and bottom-up control of stress-coping. J. Neuroendocrinol. *31*, e12675.

Dolphin, W.F., and Mountain, D.C. (1992). The envelope following response: scalp potentials elicited in the Mongolian gerbil using sinusoidally AM acoustic signals. Hear. Res. *58*, 70–78.

Dragatsis, I., and Zeitlin, S. (2000). CaMKIIalpha-Cre transgene expression and recombination patterns in the mouse brain. Genesis *26*, 133–135.

Earl, B.R., and Chertoff, M.E. (2010). Predicting auditory nerve survival using the compound action potential. Ear Hear. *31*, 7–21.

Eckert, P., Marchetta, P., Manthey, M.K., Walter, M.H., Jovanovic, S., Savitska, D., Singer, W., Jacob, M.H., Ruttiger, L., Schimmang, T., et al. (2021). Deletion of BDNF in Pax2 lineage-derived interneuron precursors in the hindbrain hampers the proportion of excitation/inhibition, learning, and behavior. Front. Mol. Neurosci. *14*, 642679.

Elarbed, A., Fackrell, K., Baguley, D.M., and Hoare, D.J. (2021). Tinnitus and stress in adults: a scoping review. Int. J. Audiol. *60*, 171–182.

Elling, L., Steinberg, C., Brockelmann, A.K., Dobel, C., Bolte, J., and Junghofer, M. (2011). Acute stress alters auditory selective attention in humans independent of HPA: a study of evoked potentials. PLoS One *6*, e18009.

Erdmann, G., Schutz, G., and Berger, S. (2007). Inducible gene inactivation in neurons of the adult mouse forebrain. BMC Neurosci. *8*, 63.

Erdmann, G., Schutz, G., and Berger, S. (2008). Loss of glucocorticoid receptor function in the

pituitary results in early postnatal lethality. Endocrinology *149*, 3446–3451.

Erichsen, S., Mikkola, M., Sahlin, L., and Hultcrantz, M. (2001). Cochlear distribution of Na,K-ATPase and corticosteroid receptors in two mouse strains with congenital hearing disorders. Acta Otolaryngol. *121*, 794–802.

Finsterwald, C., and Alberini, C.M. (2014). Stress and glucocorticoid receptor-dependent mechanisms in long-term memory: from adaptive responses to psychopathologies. Neurobiol. Learn. Mem. *112*, 17–29.

Foss-Feig, J.H., Schauder, K.B., Key, A.P., Wallace, M.T., and Stone, W.L. (2017). Audition-specific temporal processing deficits associated with language function in children with autism spectrum disorder. Autism Res. *10*, 1845–1856.

Gomez-Sanchez, E., and Gomez-Sanchez, C.E. (2014). The multifaceted mineralocorticoid receptor. Compr. Physiol. *4*, 965–994.

Graham, C.E., Basappa, J., Turcan, S., and Vetter, D.E. (2011). The cochlear CRF signaling systems and their mechanisms of action in modulating cochlear sensitivity and protection against trauma. Mol. Neurobiol. *44*, 383–406.

Graham, C.E., Basappa, J., and Vetter, D.E. (2010). A corticotropin-releasing factor system expressed in the cochlea modulates hearing sensitivity and protects against noise-induced hearing loss. Neurobiol. Dis. *38*, 246–258.

Graham, C.E., and Vetter, D.E. (2011). The mouse cochlea expresses a local hypothalamic-pituitary-adrenal equivalent signaling system and requires corticotropin-releasing factor receptor 1 to establish normal hair cell innervation and cochlear sensitivity. J. Neurosci. *31*, 1267–1278.

Guinan, J.J., JR. (2006). Olivocochlear efferents: anatomy, physiology, function, and the measurement of efferent effects in humans. Ear Hear. *27*, 589–607.

Heil, P., Neubauer, H., Brown, M., and Irvine, D.R. (2008). Towards a unifying basis of auditory thresholds: distributions of the first-spike latencies of auditory-nerve fibers. Hear. Res. *238*, 25–38.

Henkin, R.I., Mcglone, R.E., Daly, R., and Bartter, F.C. (1967). Studies on auditory thresholds in normal man and in patients with adrenal cortical insufficiency: the role of adrenal cortical steroids. J. Clin. Invest. *46*, 429–435.

Jafari, Z., Kolb, B.E., and Mohajerani, M.H. (2019). Age-related hearing loss and tinnitus, dementia risk, and auditory amplification outcomes. Ageing Res. Rev. *56*, 100963.

Jauset-Berrocal, J.A., and Soria-Urios, G. (2018). [Cognitive neurorehabilitation: the foundations and applications of neurologic music therapy]. Rev. Neurol. *67*, 303–310.

Joels, M. (2018). Corticosteroids and the brain. J. Endocrinol. *238*, R121–R130.

Joels, M., and de Kloet, E.R. (2017). 30 Years of the mineralocorticoid receptor: the brain mineralocorticoid receptor: a saga in three episodes. J. Endocrinol. *234*, T49–T66.

Joels, M., Karst, H., Derijk, R., and de Kloet, E.R. (2008). The coming out of the brain mineralocorticoid receptor. Trends Neurosci. *31*, 1–7.

Johnson, D.H. (1980). The relationship between spike rate and synchrony in responses of auditory-nerve fibers to single tones. J. Acoust. Soc. Am. *68*, 1115–1122.

Johnson, D.H., and Kiang, N.Y. (1976). Analysis of discharges recorded simultaneously from pairs of auditory nerve fibers. Biophys. J. *16*, 719–734.

Johnson, J.C.S., Marshall, C.R., Weil, R.S., Bamiou, D.E., Hardy, C.J.D., and Warren, J.D. (2021). Hearing and dementia: from ears to brain. Brain *144*, 391–401.

Johnson, S.L., Safieddine, S., Mustapha, M., and Marcotti, W. (2019). Hair cell afferent synapses: function and dysfunction. Cold Spring Harb. Perspect. Med. *9*, a033175.

Khimich, D., Nouvian, R., Pujol, R., Tom Dieck, S., Egner, A., Gundelfinger, E.D., and Moser, T. (2005). Hair cell synaptic ribbons are essential for synchronous auditory signalling. Nature *434*, 889–894.

Kil, S.H., and Kalinec, F. (2013). Expression and dexamethasone-induced nuclear translocation of glucocorticoid and mineralocorticoid receptors in Guinea pig cochlear cells. Hear. Res. *299*, 63–78.

Knipper, M., Van Dijk, P., Nunes, I., Ruttiger, L., and Zimmermann, U. (2013). Advances in the neurobiology of hearing disorders: recent developments regarding the basis of tinnitus and hyperacusis. Prog. Neurobiol. *111*, 17–33.

Kreuzer, P.M., Landgrebe, M., Vielsmeier, V., Kleinjung, T., De Ridder, D., and Langguth, B. (2014). Trauma-associated tinnitus. J. Head Trauma Rehabil. *29*, 432–442.

Kuan, E.C., Peng, K.A., Suh, J.D., Bergsneider, M., and Wang, M.B. (2017). Otolaryngic manifestations of Cushing disease. Ear Nose Throat J. *96*, E28–E30.

Kujawa, S.G., and Liberman, M.C. (2009). Adding insult to injury: cochlear nerve degeneration after "temporary" noise-induced hearing loss. J. Neurosci. *29*, 14077–14085.

Kuwada, S., Anderson, J.S., Batra, R., Fitzpatrick, D.C., Teissier, N., and D'angelo, W.R. (2002). Sources of the scalp-recorded amplitude-modulation following response. J. Am. Acad. Audiol. *13*, 188–204.

Liberman, M.C. (1982). Single-neuron labeling in the cat auditory nerve. Science *216*, 1239–1241.

Liberman, M.C., and Oliver, M.E. (1984). Morphometry of intracellularly labeled neurons of the auditory nerve: correlations with functional properties. J. Comp. Neurol. *223*, 163–176.

Livingston, G., Sommerlad, A., Orgeta, V., Costafreda, S.G., Huntley, J., Ames, D., Ballard, C., Banerjee, S., Burns, A., Cohen-Mansfield, J., et al. (2017). Dementia prevention, intervention, and care. Lancet *390*, 2673–2734.

Lopez-Poveda, E.A. (2018). Olivocochlear efferents in animals and humans: from anatomy to clinical relevance. Front. Neurol. *9*, 197.

Ma, L., Li, W., Li, S., Wang, X., and Qin, L. (2017). Effect of chronic restraint stress on inhibitory gating in the auditory cortex of rats. Stress *20*, 312–319.

Ma, L., Zhang, J., Yang, P., Wang, E., and Qin, L. (2015). Acute restraint stress alters sound-evoked neural responses in the rat auditory cortex. Neuroscience *290*, 608–620.

MacGregor, A.J., Joseph, A.R., Walker, G.J., and Dougherty, A.L. (2020). Co-occurrence of hearing loss and posttraumatic stress disorder among injured military personnel: a retrospective study. BMC Public Health *20*, 1076.

Madisen, L., Zwingman, T.A., Sunkin, S.M., Oh, S.W., Zariwala, H.A., Gu, H., Ng, L.L., Palmiter, R.D., Hawrylycz, M.J., Jones, A.R., et al. (2010). A robust and high-throughput Cre reporting and characterization system for the whole mouse brain. Nat. Neurosci. *13*, 133–140.

Marchetta, P., Mohrle, D., Eckert, P., Reimann, K., Wolter, S., Tolone, A., Lang, I., Wolters, M., Feil, R., Engel, J., et al. (2020). Guanylyl cyclase A/cGMP signaling slows hidden, age- and acoustic trauma-induced hearing loss. Front. Aging Neurosci. *12*, 83.

Marchetta, P., Ruttiger, L., Hobbs, A.J., Singer, W., and Knipper, M. (2021). The role of cGMP signalling in auditory processing in health and disease. Br. J. Pharmacol. https://doi.org/10.1111/bph.15455.

Matt, L., Eckert, P., Panford-Walsh, R., Geisler, H.S., Bausch, A.E., Manthey, M., Muller, N.I.C., Harasztosi, C., Rohbock, K., Ruth, P., et al. (2018). Visualizing BDNF transcript usage during sound-induced memory linked plasticity. Front. Mol. Neurosci. *11*, 260.

Maxwell, C.R., Ehrlichman, R.S., Liang, Y., Gettes, D.R., Evans, D.L., Kanes, S.J., Abel, T., Karp, J., and Siegel, S.J. (2006). Corticosterone modulates auditory gating in mouse. Neuropsychopharmacology *31*, 897–903.

Mazurek, B., Boecking, B., and Brueggemann, P. (2019). Association between stress and tinnitus-new aspects. Otol. Neurotol. *40*, e467–e473.

McCann, K.E., Lustberg, D.J., Shaughnessy, E.K., Carstens, K.E., Farris, S., Alexander, G.M., Radzicki, D., Zhao, M., and Dudek, S.M. (2021). Novel role for mineralocorticoid receptors in control of a neuronal phenotype. Mol. Psychiatry *26*, 350–364.

McEwen, B.S., Nasca, C., and Gray, J.D. (2016). Stress effects on neuronal structure: hippocampus, amygdala, and prefrontal cortex. Neuropsychopharmacology *41*, 3–23.

Meddis, R. (2006). Auditory-nerve first-spike latency and auditory absolute threshold: a computer model. J. Acoust. Soc. Am. *119*, 406–417.

Meese, S., Cepeda, A.P., Gahlen, F., Adams, C.M., Ficner, R., Ricci, A.J., Heller, S., Reisinger, E., and Herget, M. (2017). Activity-dependent phosphorylation by CaMKIIdelta alters the Ca(2+)

affinity of the multi-C2-domain protein otoferlin. Front. Synaptic Neurosci. *9*, 13.

Melcher, J.R., Knudson, I.M., Fullerton, B.C., Guinan, J.J., Jr., Norris, B.E., and Kiang, N.Y. (1996). Generators of the brainstem auditory evoked potential in cat. I. An experimental approach to their identification. Hear. Res. *93*, 1–27.

Meltser, I., and Canlon, B. (2011). Protecting the auditory system with glucocorticoids. Hear. Res. *281*, 47–55.

Merchan-Perez, A., and Liberman, M.C. (1996). Ultrastructural differences among afferent synapses on cochlear hair cells: correlations with spontaneous discharge rate. J. Comp. Neurol. *371*, 208–221.

Micheyl, C., Delhommeau, K., Perrot, X., and Oxenham, A.J. (2006). Influence of musical and psychoacoustical training on pitch discrimination. Hear. Res. *219*, 36–47.

Michie, P.T., Malmierca, M.S., Harms, L., and Todd, J. (2016). The neurobiology of MMN and implications for schizophrenia. Biol. Psychol. *116*, 90–97.

Mifsud, K.R., and Reul, J.M. (2016). Acute stress enhances heterodimerization and binding of corticosteroid receptors at glucocorticoid target genes in the hippocampus. Proc. Natl. Acad. Sci. U S A *113*, 11336–11341.

Möhrle, D., Ni, K., Varakina, K., Bing, D., Lee, S.C., Zimmermann, U., Knipper, M., and Ruttiger, L. (2016). Loss of auditory sensitivity from inner hair cell synaptopathy can be centrally compensated in the young but not old brain. Neurobiol. Aging *44*, 173–184.

Montero-Odasso, M., Ismail, Z., and Camicioli, R. (2020). Alzheimer Disease, biomarkers, and clinical symptoms-quo vadis? JAMA Neurol. *77*, 393–394.

Mudar, R.A., and Husain, F.T. (2016). Neural alterations in acquired age-related hearing loss. Front. Psychol. *7*, 828.

Muller, M., Von Hunerbein, K., Hoidis, S., and Smolders, J.W. (2005). A physiological place-frequency map of the cochlea in the CBA/J mouse. Hear. Res. *202*, 63–73.

Nadhimi, Y., and Llano, D.A. (2021). Does hearing loss lead to dementia? A review of the literature. Hear. Res. *402*, 108038.

Neef, J., Gehrt, A., Bulankina, A.V., Meyer, A.C., Riedel, D., Gregg, R.G., Strenzke, N., and Moser, T. (2009). The Ca2+ channel subunit beta2 regulates Ca2+ channel abundance and function in inner hair cells and is required for hearing. J. Neurosci. *29*, 10730–10740.

Obradovic, D., Tirard, M., Nemethy, Z., Hirsch, O., Gronemeyer, H., and Almeida, O.F. (2004). DAXX, FLASH, and FAF-1 modulate mineralocorticoid and glucocorticoid receptor-mediated transcription in hippocampal cells–toward a basis for the opposite actions elicited by two nuclear receptors? Mol. Pharmacol. *65*, 761–769.

Ouanes, S., and Popp, J. (2019). High cortisol and the risk of dementia and alzheimer's disease: a review of the literature. Front. Aging Neurosci. *11*, 43.

Pagani, J.H., Zhao, M., Cui, Z., Avram, S.K., Caruana, D.A., Dudek, S.M., and Young, W.S. (2015). Role of the vasopressin 1b receptor in rodent aggressive behavior and synaptic plasticity in hippocampal area CA2. Mol. Psychiatry *20*, 490–499.

Panza, F., Lozupone, M., Sardone, R., Battista, P., Piccininni, M., Dibello, V., La Montagna, M., Stallone, R., Venezia, P., Liguori, A., et al. (2019). Sensorial frailty: age-related hearing loss and the risk of cognitive impairment and dementia in later life. Ther. Adv. Chronic Dis. *10*, 2040622318811000.

Park, E., Kim, H., Choi, I.H., Han, H.M., Han, K., Jung, H.H., and Im, G.J. (2020). Psychiatric distress as a common risk factor for tinnitus and joint pain: a national population-based survey. Clin. Exp. Otorhinolaryngol. *13*, 234–240.

Parthasarathy, A., and Bartlett, E. (2012). Two-channel recording of auditory-evoked potentials to detect age-related deficits in temporal processing. Hear. Res. *289*, 52–62.

Patel, N., Crider, A., Pandya, C.D., Ahmed, A.O., and Pillai, A. (2016). Altered mRNA levels of glucocorticoid receptor, mineralocorticoid receptor, and co-chaperones (FKBP5 and PTGES3) in the middle frontal gyrus of autism spectrum disorder subjects. Mol. Neurobiol. *53*, 2090–2099.

Perez-Gonzalez, D., and Malmierca, M.S. (2014). Adaptation in the auditory system: an overview. Front. Integr. Neurosci. *8*, 19.

Perez-Valenzuela, C., Terreros, G., and Dagnino-Subiabre, A. (2019). Effects of stress on the auditory system: an approach to study a common origin for mood disorders and dementia. Rev. Neurosci. *30*, 317–324.

Picton, T.W., John, M.S., Dimitrijevic, A., and Purcell, D. (2003). Human auditory steady-state responses. Int. J. Audiol. *42*, 177–219.

Plieger, T., Felten, A., Splittgerber, H., Duke, E., and Reuter, M. (2018). The role of genetic variation in the glucocorticoid receptor (NR3C1) and mineralocorticoid receptor (NR3C2) in the association between cortisol response and cognition under acute stress. Psychoneuroendocrinology *87*, 173–180.

Porzionato, A., Macchi, V., Rucinski, M., Malendowicz, L.K., and De Caro, R. (2010). Natriuretic peptides in the regulation of the hypothalamic-pituitary-adrenal axis. Int. Rev. Cell Mol. Biol. *280*, 1–39.

Pressnitzer, D., Sayles, M., Micheyl, C., and Winter, I.M. (2008). Perceptual organization of sound begins in the auditory periphery. Curr. Biol. *18*, 1124–1128.

Raam, T., Mcavoy, K.M., Besnard, A., Veenema, A.H., and Sahay, A. (2017). Hippocampal oxytocin receptors are necessary for discrimination of social stimuli. Nat. Commun. *8*, 2001.

Reijntjes, D.O.J., Koppl, C., and Pyott, S.J. (2020). Volume gradients in inner hair cell-auditory nerve fiber pre- and postsynaptic proteins differ across mouse strains. Hear. Res. *390*, 107933.

Reul, J.M., and de Kloet, E.R. (1985). Two receptor systems for corticosterone in rat brain: microdistribution and differential occupation. Endocrinology *117*, 2505–2511.

Reul, J.M., De Kloet, E.R., Van Sluijs, F.J., Rijnberk, A., and Rothuizen, J. (1990). Binding characteristics of mineralocorticoid and glucocorticoid receptors in dog brain and pituitary. Endocrinology *127*, 907–915.

Reuss, S., Disque-Kaiser, U., Antoniou-Lipfert, P., Gholi, M.N., Riemann, E., and Riemann, R. (2009). Neurochemistry of olivocochlear neurons in the hamster. Anat. Rec. (Hoboken) *292*, 461–471.

Richard, D., and Lopez, C. (2013). In Handbook of Biologically Active Peptides, A. Kastin, ed. (Academic Press).

Ruel, J., Nouvian, R., Gervais D'aldin, C., Pujol, R., Eybalin, M., and Puel, J.L. (2001). Dopamine inhibition of auditory nerve activity in the adult mammalian cochlea. Eur. J. Neurosci. *14*, 977–986.

Rupprecht, R., Arriza, J.L., Spengler, D., Reul, J.M., Evans, R.M., Holsboer, F., and Damm, K. (1993). Transactivation and synergistic properties of the mineralocorticoid receptor: relationship to the glucocorticoid receptor. Mol. Endocrinol. *7*, 597–603.

Rutherford, B.R., Brewster, K., Golub, J.S., Kim, A.H., and Roose, S.P. (2018). Sensation and psychiatry: linking age-related hearing loss to late-life depression and cognitive decline. Am. J. Psychiatry *175*, 215–224.

Rutherford, M.A., Von Gersdorff, H., and Goutman, J.D. (2021). Encoding sound in the cochlea: from receptor potential to afferent discharge. J. Physiol. *599*, 2527–2557.

Rüttiger, L., Zimmermann, U., and Knipper, M. (2017). Biomarkers for hearing dysfunction: facts and outlook. ORL J. Otorhinolaryngol. Relat. Spec. *79*, 93–111.

Ryan, A.F., Kujawa, S.G., Hammill, T., Le Prell, C., and Kil, J. (2016). Temporary and permanent noise-induced threshold shifts: a review of basic and clinical observations. Otol. Neurotol. *37*, e271–e275.

Sapolsky, R.M. (2015). Stress and the brain: individual variability and the inverted-U. Nat. Neurosci. *18*, 1344–1346.

Schaffert, N., Janzen, T.B., Mattes, K., and Thaut, M.H. (2019). A review on the relationship between sound and movement in sports and rehabilitation. Front. Psychol. *10*, 244.

Sihvonen, A.J., Sarkamo, T., Leo, V., Tervaniemi, M., Altenmuller, E., and Soinila, S. (2017). Music-based interventions in neurological rehabilitation. Lancet Neurol. *16*, 648–660.

Singer, W., Zuccotti, A., Jaumann, M., Lee, S.C., Panford-Walsh, R., Xiong, H., Zimmermann, U., Franz, C., Geisler, H.S., Kopschall, I., et al. (2013). Noise-induced inner hair cell ribbon loss disturbs central arc mobilization: a novel molecular paradigm for understanding tinnitus. Mol. Neurobiol. *47*, 261–279.

Singer, W., Kasini, K., Manthey, M., Eckert, P., Armbruster, P., Vogt, M.A., Jaumann, M., Dotta,

M., Yamahara, K., Harasztosi, C., et al. (2018). The glucocorticoid antagonist mifepristone attenuates sound-induced long-term deficits in auditory nerve response and central auditory processing in female rats. FASEB J. *32*, 3005–3019.

Sinha, Y., Silove, N., Hayen, A., and Williams, K. (2011). Auditory integration training and other sound therapies for autism spectrum disorders (ASD). Cochrane Database Syst. Rev. *2011*, CD003681.

Stevens, K.E., Bullock, A.E., and Collins, A.C. (2001). Chronic corticosterone treatment alters sensory gating in C3H mice. Pharmacol. Biochem. Behav. *69*, 359–366.

Taves, M.D., Gomez-Sanchez, C.E., and Soma, K.K. (2011). Extra-adrenal glucocorticoids and mineralocorticoids: evidence for local synthesis, regulation, and function. Am. J. Physiol. Endocrinol. Metab. *301*, E11–E24.

ten Cate, W.J., Curtis, L.M., and Rarey, K.E. (1992). Immunochemical detection of glucocorticoid receptors within rat cochlear and vestibular tissues. Hear. Res. *60*, 199–204.

ten Cate, W.J., Curtis, L.M., Small, G.M., and Rarey, K.E. (1993). Localization of glucocorticoid receptors and glucocorticoid receptor mRNAs in the rat cochlea. Laryngoscope *103*, 865–871.

Terakado, M., Kumagami, H., and Takahashi, H. (2011). Distribution of glucocorticoid receptors and 11 beta-hydroxysteroid dehydrogenase isoforms in the rat inner ear. Hear. Res. *280*, 148–156.

Truong, D.T., Rendall, A.R., Castelluccio, B.C., Eigsti, I.M., and Fitch, R.H. (2015). Auditory processing and morphological anomalies in medial geniculate nucleus of Cntnap2 mutant mice. Behav. Neurosci. *129*, 731–743.

Turner, H.A., Mitchell, K.J., Jones, L.M., Hamby, S., Wade, R., Jr., and Beseler, C.L. (2019). Gun violence exposure and posttraumatic symptoms among children and youth. J. Trauma. Stress *32*, 881–889.

van Munster, J., Van der Valk, W.H., Stegeman, I., Lieftink, A.F., and Smit, A.L. (2020). The relationship of tinnitus distress with personality traits: a systematic review. Front. Neurol. *11*, 225.

Vetter, D.E. (2015). Cellular signaling protective against noise-induced hearing loss - a role for novel intrinsic cochlear signaling involving corticotropin-releasing factor? Biochem. Pharmacol. *97*, 1–15.

Vyas, S., Rodrigues, A.J., Silva, J.M., Tronche, F., Almeida, O.F., Sousa, N., and Sotiropoulos, I. (2016). Chronic stress and glucocorticoids: from neuronal plasticity to neurodegeneration. Neural Plast. *2016*, 6391686.

Wang, J., and Puel, J.L. (2020). Presbycusis: an update on cochlear mechanisms and therapies. J. Clin. Med. *9*, 218.

Wang, X., Zhang, C., Szabo, G., and Sun, Q.Q. (2013). Distribution of CaMKIIalpha expression in the brain in vivo, studied by CaMKIIalpha-GFP mice. Brain Res. *1518*, 9–25.

White, P.M., Kanazawa, A., and Yee, C.M. (2005). Gender and suppression of mid-latency ERP components during stress. Psychophysiology *42*, 720–725.

Wingenfeld, K., and Otte, C. (2019). Mineralocorticoid receptor function and cognition in health and disease. Psychoneuroendocrinology *105*, 25–35.

Winter, I.M., Robertson, D., and Yates, G.K. (1990). Diversity of characteristic frequency rate-intensity functions in Guinea pig auditory nerve fibres. Hear. Res. *45*, 191–202.

Wirz, L., Reuter, M., Wacker, J., Felten, A., and Schwabe, L. (2017). A haplotype associated with enhanced mineralocorticoid receptor expression facilitates the stress-induced shift from "cognitive" to "habit" learning. eNeuro *4*. https://doi.org/10.1523/ENEURO.0359-17.2017.

Wong, A.B., Jing, Z., Rutherford, M.A., Frank, T., Strenzke, N., and Moser, T. (2013). Concurrent maturation of inner hair cell synaptic Ca2+ influx and auditory nerve spontaneous activity around hearing onset in mice. J. Neurosci. *33*, 10661–10666.

Wu, L.G., Hamid, E., Shin, W., and Chiang, H.C. (2014). Exocytosis and endocytosis: modes, functions, and coupling mechanisms. Annu. Rev. Physiol. *76*, 301–331.

Yao, X., and Rarey, K.E. (1996). Localization of the mineralocorticoid receptor in rat cochlear tissue. Acta Otolaryngol. *116*, 493–496.

Zidanic, M., and Fuchs, P.A. (1995). Kinetic analysis of barium currents in chick cochlear hair cells. Biophys. J. *68*, 1323–1336.

Zuo, J., Curtis, L.M., Yao, X., Ten Cate, W.J., Bagger-Sjoback, D., Hultcrantz, M., and Rarey, K.E. (1995). Glucocorticoid receptor expression in the postnatal rat cochlea. Hear. Res. *87*, 220–227.

STAR★METHODS

KEY RESOURCES TABLE

REAGENT or RESOURCE	SOURCE	IDENTIFIER
Antibodies		
Rabbit Polyclonal C-terminal-binding protein 2 (CtBP2)/RIBEYE	ARP American Research Products, Inc™, Waltham, MA, USA	Cat#10-P1554
Rabbit Polyclonal Vesicular Glutamate Transporter 3	Synaptic Systems, Göttingen, Germany	Cat#135203 RRID:AB_887886
Mouse Monoclonal Mineralocorticoid Receptor	Thermo Fisher, Rockford, IL, USA	Cat#H10E4C9F/MA1-620 RRID:AB_2298880
Mouse Monoclonal Glucocorticoid Receptor	Thermo Fisher, Rockford, IL, USA	Cat#BUGR2/MA1-510 RRID:AB_2811764
Secondary Antibody Cy3	Jackson Immuno Research Laboratories, West Grove PA, USA	Cat#111-166-046 RRID:AB_2338009
Secondary Antibody Alexa 488	Molecular Probes , Eugene, OR, USA	Cat#A11001
Chemicals, peptides, and recombinant proteins		
Tamoxifen	Sigma-Aldrich	SKU#T5648-1G
Fentanyl	Fentanyl-Hameln, Hameln Pharma plus, Hameln, Germany	PZN#06143427
Midazolam	Midazolam-hameln®; Hameln Pharma plus, Hameln, Germany	PZN#4467367
Medetomidin	Sedator®; Albrecht, Aulendorf, Germany	PZN#1901022
Atropine sulphate	B. Braun, Melsungen, Germany	PZN#00648037
Ampuwa	Fresenius KABI, Bad Homburg, Germany	PZN#10333435
Naloxon	Naloxon-hameln®; Hameln Pharma plus, Hameln, Germany	PZN#04464535
Flumazenil	Flumazenil®; Fresenius KABI, Bad Homburg, Germany	PZN#04952364
Atipazemol	Antisedan®; VETOQUINOL GmbH, Ravensburg, Germany	GTIN#05012674902110
Xylocain 2%	AstraZeneca, Wedel, Germany	PZN# 01138002
sunflower oil	Sigma-Aldrich	SKU# S5007-250ML
Critical commercial assays		
CORT ELISA kit	Enzo Life Sciences Inc., Farmingdale, NY, USA	Cat#ADI-901-097
Deposited data		
Raw and analyzed data	This paper	N/A
Experimental models: Organisms/strains		
CaMKIIαCre^{ERT2} mice: C57BL6/N-TgN(CaMKIIaERT2-cre)1743/2Gsc	Prof. Günther Schütz (DKFZ, Molecular Biology of the Cell I, Heidelberg, Germany)	N/A
MR cKO mice: C57BL6/N-TgH(MRflox)1101/2Gsc x TgN(CaMKIIaERT2-cre)1743/2Gsc	Prof. Günther Schütz (DKFZ, Molecular Biology of the Cell I, Heidelberg, Germany)	N/A
GR cKO mice: C57BL6/N-TgH(GRflox)1103/2Gsc x TgN(CaMKIIaERT2-cre)1743/2Gsc	Prof. Günther Schütz (DKFZ, Molecular Biology of the Cell I, Heidelberg, Germany)	N/A
MRGR cKO mice: C57BL6/N-TgH(GRflox)1103/2Gsc x TgH(MRflox)1101/2Gsc x TgN(CaMKIIaERT2-cre)1743/2Gsc	Prof. Günther Schütz (DKFZ, Molecular Biology of the Cell I, Heidelberg, Germany)	N/A
Rosa^{tdTomato} reporter mouse	Prof. Hubert Löwenheim from the Tübingen Hearing Research Centre (THRC)	N/A

(*Continued on next page*)

Continued

REAGENT or RESOURCE	SOURCE	IDENTIFIER
Software and algorithms		
GraphPad PRISM Version 5.01	GraphPad Software, Inc.	www.graphpad.com
CorelDRAW Version 15.2.0.695	Corel Corporation	www.corel.com
Microsoft Excel	Microsoft Corporation	www.microsoft.com
PEAK.exe	University of Tübingen	N/A
CAP.exe	University of Tübingen	N/A

RESOURCE AVAILABILITY

Lead contact

Further information and requests for resources and reagents should be directed to and will be fulfilled by the lead contact, Marlies Knipper (marlies.knipper@uni-tuebingen.de).

Materials availability

This study did not generate new, unique reagents.

Data and code availability

All data reported in this paper will be shared by the lead contact upon request.

This paper does not report original code.

Any additional information required to reanalyze the data reported in this paper is available from the lead contact upon request.

EXPERIMENTAL MODEL AND SUBJECT DETAILS

In the present study, three tamoxifen-inducible conditional knock-out mouse lines were studied, in which MR and GR or either MR or GR are deleted, mainly in the forebrain. To generate the MRGR cKO, MR cKO and GR cKO mice and corresponding control animals, three different mouse lines were used. We received from Prof. Günther Schütz (DKFZ, Molecular Biology of the Cell I, Heidelberg, Germany) homozygous floxed MR and GR mouse lines (Berger et al., 2006; Erdmann et al., 2007), in which the exon 3 of either *Mr* or *Gr* is flanked by loxP sites. These lines were crossed in our laboratory to obtain a homozygous MRGRflox line. These three lines were than bred with a CaMKIIα Cre^{ERT2} line (Erdmann et al., 2007) (kindly provided by Prof. Günther Schütz) in which the Cre-Recombinase is expressed under the CaMKIIα promoter after Tamoxifen (**TMX**) injection. In brief, after confirmation of a normal hearing function, mice received an intraperitoneal injection of 1 mg TMX in 100 µl TMX-solution (Sigma-Aldrich, T-5648, Munich) twice a day on 5 consecutive days at the age of approximately 8 weeks. For the solution, 50 mg TMX was dissolved in 500 µl Ethanol abs. (Merck, Darmstadt) and mixed with 4.5 ml sunflower oil (Sigma-Aldrich, S-5007). After the last injection, the animals were allowed to recover in their home cages for four weeks before the experiments started. The Cre-recombinase leads to the excision of exon 3 of *Mr* and *Gr* or either *Mr* or *Gr* in cells where CaMKIIα is expressed. To verify the deletion pattern of MR and GR, CaMKIIαCre^{ERT2} transgenic mice (Erdmann et al., 2007), were crossed with a $Rosa^{tdTomato}$ reporter mouse line (Madisen et al., 2010), kindly provided by Prof. Hubert Löwenheim from the Tübingen Hearing Research Centre (THRC). For all transgenic mouse lines, homozygous floxed Cre-negative littermates that also received TMX were used as controls. For all lines, mice of both sexes aged between 1.8 and 8.4 months were used. The genetic status of all mouse lines was confirmed by genotyping using gene-specific PCR protocols.

Mice were housed in the animal facility of the ENT University Hospital of Tübingen and had access to water and food pellets *ad libitum*. They were housed alone or in groups of 2 to 5. Females and single males had a wooden house or tunnel in their cages. The dark-light cycle was 12-12 h, with a light period from 6 am to 6 pm summer time. Humidity was 55 (±5) % and temperature 21.5 (±1)°C. The weight of the animals was

controlled on every experimental day. The average noise level in the animal facility was below 50 – 60 dB SPL.

Animal care, procedures, and experimental protocols corresponded to national and institutional guidelines and were reviewed and approved by the University of Tübingen Veterinary Care Unit and the Animal Care and Ethics Committee of the regional board of the Federal State Government of Baden-Württemberg, Germany. All experiments were performed according to the European Union Directive for the protection of animals used for experimental and other scientific purposes (2010/63/EU). Mice were kept according to the national guidelines for animal care in a specifically pathogen-free animal facility.

METHOD DETAILS

Hearing measurements

Hearing function was studied before and after TMX-induction by measuring Distortion Product Otoacoustic Emission (**DPOAE**), Auditory Brainstem Responses (**ABR**) and Elelctrocochleographic Recordings in a soundproof chamber (IAC 400-A, Industrial Acoustics Company GmbH, Niederkrüchten).

Mice were anesthetized with an intraperitoneal injection of a mixture of Fentanyl (Fentanyl-Hameln, Hameln Pharma plus, Hameln, Germany), Midazolam (Midazolam-hameln®; Hameln Pharma plus, Hameln, Germany), Medetomidin (Sedator®; Albrecht, Aulendorf, Germany) and atropine sulfate (B. Braun, Melsungen, Germany) diluted with water ad. inj. (Ampuwa, Fresenius KABI, Bad Homburg, Germany) to an injection volume of 10 ml per kg bodyweight. Additional doses of anesthetics were administered if needed. The anesthesia was antagonized after the measurements by a subcutaneously administered mixture of Naloxon (Naloxon-hameln®; Hameln Pharma plus, Hameln, Germany), Flumazenil (Flumazenil®; Fresenius KABI, Bad Homburg, Germany), and Atipazemol (Antisedan®; VETOQUINOL GmbH, Ravensburg, Germany) diluted with water ad. inj. (Ampuwa, Fresenius KABI, Bad Homburg, Germany) to an injection volume of 10 ml/kg.

DPOAE

For DPOAE measurements, the anaesthetized mice lay on a pre-warmed resting pad (37°C) in the soundproof chamber and an acoustic coupler was carefully placed in the ear canal. The cubic 2f1 - f2 DPOAE was measured for frequencies (f) f2 = 1.24 × f1 and levels (L) L2 = L1 - 10 dB using a sensitive microphone inside the coupler (MK231, Microtech Gefell, Gefell, Germany, Preamplifier B&K 2669C, Bruel & Kjaer, Naerum, Denmark). Stimuli pair presented contained frequencies between f2 = 4.0 to 32.0 kHz with L2 either constantly at 50 dB SPL (DP-gram) or increasing from -5 to 65 dB SPL in 5 dB steps (I/O growth function).

ABR

The anaesthetized mice lay on a pre-warmed resting pad (37°C) in the soundproof chamber. ABR in anesthetized mice were evoked by short-duration sound stimuli with the same stimulus parameters for all groups of KO and control animals. They represent the summed activity of neurons in distinct anatomical structures along the ascending auditory pathway recorded from subcutaneous cranial electrodes. A microphone (Bruel & Kjaer 4191, Naerum, Denmark) was used to calibrate and record the acoustic stimuli. ABR thresholds were elicited with click (100 microsecond duration with an FFT mean of 5.4 kHz), noise-burst (1 ms duration, FFT mean of 7.9 kHz), or pure-tone stimuli (3 ms duration, including 1 ms cosine squared rise and fall envelope, 2–32 kHz). The stimulus level was increased stepwise from 10 to 100 dB SPL in 5 dB steps. Stimuli were generated with an I-O-card (PCI-6052E, PCI-6251, or PCIe-6259, National Instruments, Austin, Texas, USA) in an IBM compatible computer. The SPL of the stimuli was modulated by custom-made amplifier and attenuator systems (Wulf Elektronik, Frankfurt). The measured signals were band-pass filtered from 200 Hz to 5 kHz (F1, 6-pole Butterworth hardware Filter, Wulf Elektronik, Frankfurt) and amplified by 100,000. The analog/digital **(A/D)** rate was 20 kHz. Each stimulus had a recording interval of 16 ms and was directly repeated and averaged up to 512 times (256 for pure-tone stimuli).

Auditory steady-state responses

The response on amplitude modulation was tested on the ear with the lower click- and noise-evoked threshold directly after finishing the standard ABR protocol, with similar electrode positions. Auditory steady-state responses (**ASSR**) were measured with amplitude-modulated sinusoidal stimuli (carrier frequency 11.31 kHz). For the modulation depth function, stimuli were amplitude modulated with modulation

depth varying from 0% (unmodulated) to 100% (maximal modulation) and 512 Hz modulation frequency, at 40 dB relative to threshold. For the growth function, the stimuli, modulated 100% with 512 Hz, were presented between 0 and 60 dB relative to threshold in 5 dB steps. For the transfer function, stimuli were modulated with a frequency between 64 and 2048 Hz at 100% modulation depth and 40 dB relative to threshold.

Electrocochleographic recordings

We studied electrical potentials of auditory nerve fibers (**ANF**) by electrocochleography in living anaesthetized mice. The mice were anesthetized as described above, 20-40 µl Xylocain 2% (AstraZeneca, Wedel, Germany) was applied subcutaneously at sites of surgical incisions and the mice were laid on a pre-warmed resting pad (37°C). The bony auditory bulla was exposed by cutting the skin behind the ear and carefully moving muscles, nerves, and connective tissues beside. A small hole (0.6 mm diameter) was drilled into the bulla, and the round-window niche of the cochlea visualized. A silver wire electrode insulated by varnish and silicone and ending in a small silver bead was placed within the niche. The skin above the ear was closed and the mouse placed in the sound-attenuating booth in front of a loudspeaker for recording. Compound action potential (**CAP**) threshold responses from the auditory nerves were measured by stimulation with short tone pips (3 ms duration including 1 ms on- and off-ramp cos-square shaped, 32-96 repetitions with stimulus interval 16 ms and alternating polarity) presented with 5 dB 12 incremental steps from 0-100 between 2 and 34 kHz. Electrical potentials were amplified (80 dB) and filtered between 0.2 and 5 kHz before being sampled at 20 kHz A/D rate, averaged, and saved to file. Thresholds were determined from individual ears from averaged waveform responses as the lowest SPL, resulting in a signal visually distinguishable from noise.

For the CAP latency, electrical responses were recorded for 100 µs click stimuli of 0 to 100 dB SPL. Responses were amplified, filtered (DC, 50 kHz low pass), sampled at 100 kHz A/D rate, and averaged for 64 repetitions (ISI 50 ms). For CAP input-output analysis, the averaged waveform was manually inspected for the first negative amplitude deflection after stimulus onset. The latency of the CAP is registered for each stimulus intensity for each individual ear and the resulting growth function averaged and presented as the mean and SEM.

Tissue preparation

The mice were euthanized by exposure to CO_2. After decapitation the skull was opened and the complete brain was removed. The residual skull was cut in half and the cochleae were removed from the temporal bone under the microscope.

For cochlear whole-mounts the cochleae were isolated, fixed by immersion in 4% paraformaldehyde, 125 mM sucrose in 100 mM phosphate buffered saline (pH 7.4) for 15 min on ice and then dissected for whole-mounts. For cochlear cross-sections, the cochleae were fixated in 2% paraformaldehyde for 2h at 4°C on a rotating wheel, decalcified until the bone was soft and stored in Sucrose-Hank's solution (4°C) over night. Afterwards the cochleae were embedded in Tissue-Tek, frozen at -80°C and sliced in 10 µm sections, using a Cryostat (Leica Cryostat 1720 Digital Leica, Wetzlar, Germany).

Brains were fixed by immersion for 48 h in 2 % paraformaldehyde (exchange of fixative solution after 24 h) and then stored in 0.4 % paraformaldehyde until embedded in 4% agarose. Brains were cut in 60 µm slices with a vibratome (Leica VT 1000S) and stored at -20°C in cryoprotectant (mix 150 g of sucrose in 200 ml 1× phosphate buffer saline (**PBS**) and 150 ml ethylene glycol) until used for immunohistochemistry.

Immunohistochemistry and ribbon counting

Object slides with cochlear sections or whole-mount preparations were thaw at room temperature for 30 min. After permeabilization for 10 min, the tissue was rinsed with PBS and blocking solution was given to each slice for 30 min. The primary antibody was diluted in reaction buffer and applied to the object slides. After incubation overnight at 4°C and 3x washing in PBS, the secondary antibody, which was diluted in reaction buffer was pipet and incubated for 1h at room temperature. After 3x rinsing in PBS, the cochlear tissue was covered using Vectashield mounting medium with DAPI.

For free-floating brain immunohistochemistry, brain slices were taken out of the cryosolution and transferred into 1× PBS. After 2x washing with PBS for 15 min, the tissue was permeabilized and blocked for

30 min in 3 % BSA containing 0.2 % Triton-X 100. Primary antibodies were diluted in 0.5–1.5 % BSA, containing 0.1 % Triton-X 100 for incubation at 4°C overnight. The slices were washed 3x for 15 min in 1× PBS before 1h incubation at room temperature with secondary antibodies (diluted in 0.5–1.5 % BSA, containing 0.1 % Triton-X 100). The slices were washed 3x for 15 min in 1× PBS, transferred to object slides and mounted with Vectashield mounting medium with DAPI.

Antibodies against C-terminal-binding protein 2 (CtBP2)/RIBEYE (rabbit, diluted 1:1500; ARP American Research Products, Inc™, Waltham, MA, USA), VGlut3, (rabbit, diluted 1:1500; Synaptic Systems, Göttingen, Germany), MR (mouse, diluted 1:500; Thermo Fisher, Rockford, IL, USA) or GR (mouse, diluted 1:500; Thermo Fisher, Rockford, IL, USA) were used. Primary antibodies were detected using appropriate secondary antibodies Cy3 (1:1500, Jackson Immuno Research Laboratories, West Grove PA, USA) and Alexa 488 (1:500, Molecular Probes, Eugene, OR, USA).

All samples were viewed using an Olympus BX61 microscope (Olympus, Hamburg, Germany) equipped with an X-Cite epifluorescence illumination. Images were acquired using an Olympus XM10 CCD monochrome camera and analyzed with CellSens Dimension software (OSIS GmbH, Münster, Germany). To increase spatial resolution, slices were imaged over a distance of ~15 µm within an image-stack along the z-axis (z-stack), followed by 3-dimensional deconvolution using CellSens Dimension's built-in algorithm.

Cross-sections from the apical, medial, mid-basal and basal half-turn of the mouse organ of Corti correspond to frequency ranges of 2–7 kHz (apical), 7–16 kHz (medial), 16 –36 kHz (mid-basal) and 36 –70 kHz (basal) as estimated from place frequency maps (Muller et al., 2005).

For the ribbon gradient analysis, at least two deconvoluted pictures of a z-stack, rotated to a proper orientation for pillar vs. modiolar IHC sides were analyzed per animal. A line was drawn through the center of the IHC by two blinded persons and modiolar and pillar ribbons were counted. The amount of pillar/modiolar ribbons was calculated in %, averaged from all pictures per animal and both person's judgements. and presented as the mean and SD and analyzed by unpaired Student's t-test with $\alpha = 0.05$ (GraphPad Prism).

Corticosterone analysis

Corticosterone (**CORT**) concentration was measured in venous blood samples that were collected into heparin-coatedmicrovettes (Sarsted) directly after the onset of anesthesia for hearing measurements (i.e. < 5 min after handling and injection) in the time window between 9 and 12 am. Each blood sample was around 50 - 70µl. After collection, the sample was centrifuged at 1800 x *g* for 5 min and the plasma was pipetted to 1.5 ml Eppendorf tubes and stored at – 80°C. The analysis was assessed by using CORT ELISA kit (Catalog Nr. ADI-901-097) from Enzo Life Sciences Inc. (Farmingdale, NY, USA), following the manufacturers protocol. The plates were read with an optima FLUOstar microplate reader at 405 nm.

QUANTIFICATION AND STATISTICAL ANALYSIS

All statistical information and n numbers can be found in the results section and in Table 1. In figures, significance and a trend for significance is indicated by asterisks ((*) $p < 0.1$, * $p < 0.05$, ** $p < 0.01$, *** $p < 0.001$). n.s. denotes non-significant results ($p \geq 0.05$). The p-values of the 2-way ANOVAs refer to the main effect of the genotype.

Hearing measurements

DPOAE

For analysis, the respective thresholds for the single frequencies were identified. The criteria for reaching the threshold, were a signal level above -15 dB SPL, 5 dB above noise level, and as part of an increasing function. Data were presented as the mean and SEM and analyzed by 2-way ANOVA with $\alpha = 0.05$, followed by Bonferroni *post hoc* test (GraphPad Prism).

ABR

The threshold for all click, noise, and pure-tone ABR measurements were manually defined as the lowest sound level at which a clear signal could be discriminated from the baseline. Data are shown as the mean ± SEM. Click- and noise-evoked ABR measurements were compared between genotypes by an

Table 1. Detailed statistical information

Fig. No	Context	Statistical test	Test value	p value	Bonferroni *post hoc* test with p value		*n*-number
1B	Click	unpaired two-tailed Student's *t* test	t(50) = 0.620	p = 0.538	-	-	WT: n = 12/24, KO: n = 14/28 mice/ears
	Noise		t(50) = 0.451	p = 0.653			
	f-ABR	two-way ANOVA	F(1,5) = 1.772	p = 0.186	-	-	WT: n = 10, KO: n = 11 mice/ears
1C	DPOAE	two-way ANOVA	F(1,5) = 1.772	p = 0.186	-	-	WT: n = 5/10, KO: n = 8/16 mice/ears
1D	CAP	two-way ANOVA	F(1,16) = 0.368	p = 0.5443	-	-	WT: n = 5/9, KO: n = 7/13 mice/ears
1F	ABR wave I	two-way ANOVA	F(1,17) = 10.80	p = 0.0011	-	-	WT: n = 12/24, KO: n = 15/30 mice/ears
	ABR wave IV		F(1,17) = 31.62	p < 0.0001	-	-	WT: n = 12/24, KO: n = 14/28 mice/ears
1G	Latency	two-way ANOVA	F(1,620) = 70.94	p = 0.0022	-	-	WT: n = 6/11, KO: n = 7/13 mice/ears
1H	AMD	two-way ANOVA	F(1,572) = 11.38	p = 0.0008			WT: n = 19, KO: n = 18 mice/ears
1I	AMG		F(1,688) = 5.210	p = 0.023			WT: n = 18, KO: n = 20 mice/ears
1J	AMT		F(1,473) = 14.37	p = 0.0002	-	-	n = 19 mice/ears
2A	MRGR ribbons	two-way ANOVA	F(1,2) = 41.10	p < 0.0001	apical	p > 0.05	WT: n = 19/9, KO: n = 18/9 IHC/mice
					medial	p < 0.001	
					mid-basal	p < 0.001	
2B	MR ribbons	two-way ANOVA	F(1,2) = 44.25	p < 0.0001	apical	p > 0.05	WT: n = 12/5, KO: 14/5 IHC/mice
					medial	p < 0.001	
					mid-basal	p < 0.001	
2C	GR ribbons	two-way ANOVA	F(1,2) = 6.603	p = *0.0125*	apical	p > 0.05	WT: n = 10/5, KO: n = 14/6 IHCs/mice
					medial	p > 0.05	
					mid-basal	p > 0.05	
3A	ABR wave I	two-way ANOVA	F(1,18) = 19.40	p < 0.0001	-	-	WT: n = 8/16, KO: n = 8/16 mice/ears
	ABR wave IV		F(1,17) = 6.991	p = 0.0085	-	-	WT: n = 8/16, KO: n = 8/16 mice/ears
3B	CAP	two-way ANOVA	F(1,16) = 14.92	p = 0.0001	-	-	n = 7/14 mice/ears
	Latency	two-way ANOVA	F(1,733) = 5.57	p = 0.0186	-	-	WT: n = 7/14, KO: n = 6/11 mice/ears
3C	AMD	two-way ANOVA	F(1,701) = 0.14	p = 0.999	-	-	WT: n = 24, KO: n = 21 mice/ears
	AMG		F(1,955) = 0.01	p = 1.000			WT: n = 24, KO: n = 22 mice/ears
	AMT		F(1,583) = 0.02	p = 0.8905	-	-	WT: n = 24, KO: n = 22 mice/ears
4A	ABR wave I	two-way ANOVA	F(1,17) = 45.83	p < 0.0001	-	-	WT: n = 7/14, KO: n = 8/16 mice/ears
	ABR wave IV		F(1,17) = 57.51	p < 0.0001	-	-	WT: n = 7/14, KO: n = 8/16 mice/ears

(*Continued on next page*)

Table 1. *Continued*

Fig. No	Context	Statistical test	Test value	p value	Bonferroni *post hoc* test with p value		*n*-number
4B	CAP	two-way ANOVA	F(1,16) = 14.60	p = 0.0001	-	-	WT: n = 8/15, KO: n = 9/18 mice/ears
	Latency	two-way ANOVA	F(11,043) = 14.04	p = 0.0002	-	-	WT: n = 10/20, KO: n = 10/19 mice/ears
4C	AMD	two-way ANOVA	F(1,780) = 15.56	p < 0.0001	-	-	WT: n = 26, KO: n = 24 mice/ears
	AMG		F(11,025) = 34.58	p < 0.0001			WT: n = 30, KO: n = 28 mice/ears
	AMT		F(1,636) = 9.99	p = 0.0017	-	-	WT: n = 26, KO: n = 24 mice/ears
5B	CORT MR	unpaired two-tailed Student's *t* test	t(28) = 90.9285	p = 0.3611	-	-	WT: n = 16, KO: n = 14 mice
	CORT GR		t(28) = 1.884	p = 0.070			WT: n = 14, KO: n = 16 mice
	CORT MRGR		t(24) = 2.905	p = 0.0078	-	-	WT: n = 12, KO: n = 14 mice
5C	corr. MR	linear regression	WT: R^2 = 0.033	p = 0.5329	-	-	WT: n = 14, KO: n = 13 mice
			KO: R^2 = 0.001	p = 0.9322			
	corr. GR		WT: R^2 = 0.012	p = 0.7802			n = 9 mice
			KO: R^2 = 0.0001	p = 0.9723			
	corr. MRGR		WT: R^2 = 0.141	p = 0.2540			WT: n = 11, KO: n = 17 mice
			KO: R^2 = 0.007	p = 0.7574	-	-	
S2B	MRGR	unpaired two-tailed Student's *t* test	t(15) = 3.57	p = 0.0028			WT: n = 9, KO: n = 8 mice
	MR		t(10) = 2.38	p = 0.0387			n = 6 mice
	GR		t(8) = 0.79	p = 0.4551			n = 5 mice
S3A	Click	unpaired two-tailed Student's *t* test	t(56) = 0.07	p = 0.944			WT: n = 14/28, KO: n = 15/30 mice/ears
	Noise		t(56) = 0.64	p = 0.519	-	-	
	f-ABR	two-way ANOVA	F(1,8) = 0.045	p = 0.832			WT: n = 14, KO: n = 15 mice
S3B	DPOAE	two-way ANOVA	F(1,5) = 4.030	p = 0.455	-	-	WT: n = 5/10, KO: n = 8/16 mice/ears
S3C	Click	unpaired two-tailed Student's *t* test	t(58) = 1.398	p = 0.168	-	-	WT: n = 14/28, KO: n = 16/32 mice/ears
	Noise		t(58) = 0.124	p = 0.902			
	f-ABR	two-way ANOVA	F(1,8) = 0.078	p = 0.781	-	-	WT: n = 13, KO: n = 16 mice
S3D	DPOAE	two-way ANOVA	F(1,5) = 0.182	p = 0.670	-	-	WT: n = 14/28, KO: n = 16/32 mice/ears

unpaired Student's t-test with $\alpha = 0.05$. F-ABR measurements were group analyzed by 2-way ANOVA with $\alpha = 0.05$ followed by Bonferroni *post hoc* test (GraphPad Prism).

Supra-threshold click-evoked ABR waveforms were analyzed for consecutive amplitude deflections (waves), with each wave consisting of a starting negative (n) peak and the following positive (p) peak. Two peak classes were selected: (1) early peaks (wave I: In – Ip at 1.2-1.8 ms) interpreted as the sum of the first stimulus-related action potential within the auditory nerve, and (2) late peaks (wave IV: IVn – IVp at 4.1-4.9 ms), the response from the auditory midbrain. All ABR wave supra-threshold amplitude growth functions were calculated for increasing stimulus levels with reference to the ABR thresholds (from 0 to a maximum of 80 dB above threshold). For Figure 5 the ABR response amplitude size was calculated by averaging the three maximal amplitude values of the individual ears' supra-threshold amplitude growth

function. In Figure 5 for each animal the mean of both ears' ABR wave I size was correlated with the CORT level of the animal. Data were shown as the mean ± SEM and analyzed by 2-way ANOVA with $\alpha = 0.05$ followed by Bonferroni *post hoc* test (GraphPad Prism).

ASSR

For analysis, a fast Fourier transform (FFT) of the response was calculated. From the FFT, the spectral amplitude at the modulation frequency was extracted, along with the first five harmonics. Additionally, from the FFT, the noise level from the neighboring frequency spectral amplitude (± 4 Hz) was extracted. From this, the signal above noise (μV) was calculated. Data were shown as the mean ± SEM and analyzed by 2-way ANOVA with $\alpha = 0.05$ followed by Bonferroni *post hoc* test (GraphPad Prism).

Electrocochleographic recordings

Thresholds were determined from individual ears from averaged waveform responses as the lowest SPL resulting in a signal visually distinguishable from noise. Data were analyzed by 2-way ANOVA with $\alpha = 0.05$ (GraphPad Prism). For CAP input-output analysis, the averaged waveform was manually inspected for the first negative amplitude deflection after stimulus onset. The latency of the CAP was registered for each stimulus intensity for each individual ear, and the resulting growth function averaged and presented as the mean and SEM. Data were analyzed by 2-way ANOVA with $\alpha = 0.05$ followed by Bonferroni *post hoc* test (GraphPad Prism).

Ribbon counting

Ribbons are shown as average ribbon number per IHC ± SEM. Statistical analysis was performed using 2-way ANOVA with $\alpha = 0.05$ followed by Bonferroni *post hoc* test (GraphPad Prism). The amount of pillar/modiolar ribbons was presented as the mean and SD and analyzed by unpaired Student's t-test with $\alpha = 0.05$ (GraphPad Prism).

Corticosterone analysis

Calculation of the CORT levels were performed using an online data analysis tool (myassays.com). Finally, CORT levels were averaged per genotype and presented as the mean ± SEM. Statistical analysis was performed by unpaired Student's t-test with $\alpha = 0.05$ (GraphPad Prism).

frontiers in Aging Neuroscience

ORIGINAL RESEARCH
published: 09 April 2020
doi: 10.3389/fnagi.2020.00083

Guanylyl Cyclase A/cGMP Signaling Slows Hidden, Age- and Acoustic Trauma-Induced Hearing Loss

Philine Marchetta[1†], Dorit Möhrle[1,2†], Philipp Eckert[1], Katrin Reimann[1], Steffen Wolter[1], Arianna Tolone[3], Isabelle Lang[4], Markus Wolters[5], Robert Feil[5], Jutta Engel[4], François Paquet-Durand[3], Michaela Kuhn[6], Marlies Knipper[1] and Lukas Rüttiger[1]**

[1] Molecular Physiology of Hearing, Tübingen Hearing Research Centre, Department of Otolaryngology, University of Tübingen, Tübingen, Germany, [2] Department of Anatomy and Cell Biology, Schulich School of Medicine and Dentistry, University of Western Ontario, London, ON, Canada, [3] Cell Death Mechanisms Group, Institute for Ophthalmic Research, Centre for Ophthalmology, University of Tübingen, Tübingen, Germany, [4] Department of Biophysics, Center for Integrative Physiology and Molecular Medicine, Hearing Research, Saarland University, Homburg, Germany, [5] Signal Transduction and Transgenic Models, Interfaculty Institute of Biochemistry, University of Tübingen, Tübingen, Germany, [6] Institute of Physiology, University of Würzburg, Würzburg, Germany

OPEN ACCESS

Edited by:
Tobias Kleinjung,
University of Zurich, Switzerland

Reviewed by:
Agnieszka J. Szczepek,
Charité – Universitätsmedizin Berlin, Germany
Christopher R. Cederroth,
Karolinska Institutet (KI), Sweden

***Correspondence:**
Marlies Knipper
marlies.knipper@uni-tuebingen.de
Lukas Rüttiger
lukas.ruettiger@uni-tuebingen.de

† These authors have contributed equally to this work

Received: 18 November 2019
Accepted: 10 March 2020
Published: 09 April 2020

Citation:
Marchetta P, Möhrle D, Eckert P, Reimann K, Wolter S, Tolone A, Lang I, Wolters M, Feil R, Engel J, Paquet-Durand F, Kuhn M, Knipper M and Rüttiger L (2020) Guanylyl Cyclase A/cGMP Signaling Slows Hidden, Age- and Acoustic Trauma-Induced Hearing Loss. Front. Aging Neurosci. 12:83. doi: 10.3389/fnagi.2020.00083

In the inner ear, cyclic guanosine monophosphate (cGMP) signaling has been described as facilitating otoprotection, which was previously observed through elevated cGMP levels achieved by phosphodiesterase 5 inhibition. However, to date, the upstream guanylyl cyclase (GC) subtype eliciting cGMP production is unknown. Here, we show that mice with a genetic disruption of the gene encoding the cGMP generator GC-A, the receptor for atrial and B-type natriuretic peptides, display a greater vulnerability of hair cells to hidden hearing loss and noise- and age-dependent hearing loss. This vulnerability was associated with GC-A expression in spiral ganglia and outer hair cells (OHCs) but not in inner hair cells (IHCs). GC-A knockout mice exhibited elevated hearing thresholds, most pronounced for the detection of high-frequency tones. Deficits in OHC input–output functions in high-frequency regions were already present in young GC-A-deficient mice, with no signs of an accelerated progression of age-related hearing loss or higher vulnerability to acoustic trauma. OHCs in these frequency regions in young GC-A knockout mice exhibited diminished levels of KCNQ4 expression, which is the dominant K^+ channel in OHCs, and decreased activation of poly (ADP-ribose) polymerase-1, an enzyme involved in DNA repair. Further, GC-A knockout mice had IHC synapse impairments and reduced amplitudes of auditory brainstem responses that progressed with age and with acoustic trauma, in contrast to OHCs, when compared to GC-A wild-type littermates. We conclude that GC-A/cGMP-dependent signaling pathways have otoprotective functions and GC-A gene disruption differentially contributes to hair-cell damage in a healthy, aged, or injured system. Thus, augmentation of natriuretic peptide GC-A signaling likely has potential to overcome hidden and noise-induced hearing loss, as well as presbycusis.

Keywords: inner ear, cGMP, otoprotection, guanylyl cyclase A, aging, hidden hearing loss, PARP-1, KCNQ4

INTRODUCTION

Hearing loss is considered the fourth leading cause of disability worldwide and is one of the most common conditions affecting older people. Peripheral age-dependent hearing loss has recently been defined as a severe but amendable risk factor for the development of dementia. Thus, treatment of hearing deficits can be important for cognitive health[1] (Livingston and Frankish, 2015; Fitzakerley and Trachte, 2018).

As we age, hearing sensitivity gradually and progressively declines. The presbycusis refers to a progressive, age-dependent hearing loss that results from loss of outer hair cell (OHC) function. This decline in OHC function typically begins in regions that respond to high-frequency sounds (Frisina, 2009; Frisina and Frisina, 2013; Lee, 2015). The majority of the aging population experiences difficulties in perceiving speech in noise, even if audiometric thresholds are still normal or at least appear to be within the normal range, a phenomenon called hidden hearing loss (Füllgrabe et al., 2014). As demonstrated in rodents (Kujawa and Liberman, 2009; Rüttiger et al., 2013; Sergeyenko et al., 2013; Möhrle et al., 2019) and humans (Viana et al., 2015; Wu et al., 2019), hidden hearing loss is linked to a synaptopathy of the inner hair cell (IHC) synapse, the first synapse in the auditory system between the sensory cell and the afferent axon of the spiral ganglion neuron (SGN). IHC synaptopathy and auditory neuropathy precede presbycusis and progress with age (Sergeyenko et al., 2013; Möhrle et al., 2016). The protection of IHC and OHC function and therapeutic counteraction of noise-induced or age-dependent hearing loss may therefore be vital for maintaining speech comprehension and for the preservation of central auditory, or even cognitive, functions (Livingston et al., 2017). Accordingly, there is an urgent need for new pharmacological prevention strategies that have the potential to preserve cochlear hair cells and auditory fibers during aging and in response to the daily noise burden.

There is evidence that the genetics and function of cochlear cyclic guanosine monophosphate (cGMP)-forming guanylyl cyclases (GCs) play a fundamental role in normal hearing and cochlear pathophysiology (Fitzakerley and Trachte, 2018). A protective role of the cGMP-dependent protein kinase I (cGKI) signaling cascade for IHC synapses and OHCs was shown in rodent models of noise-induced damage (Jaumann et al., 2012). However, the upstream signaling pathways driving cGMP/cGKI signaling could not be sufficiently linked neither with the soluble GC (sGC) activated by nitric oxide (NO) (Möhrle et al., 2017), nor with the transmembrane, particulate GC-B, also named natriuretic peptide (NP) receptor NPR-B, activated by C-type NP (CNP) (Wolter et al., 2018). Using reverse transcription PCR analysis of cochlear tissue, the transmembrane, particulate GC-A, also named NPR-A, and its peptide ligand atrial NP (ANP) have been shown to be expressed in cochlear hair cells, supporting cells, and SGN (Krause et al., 1997; Suzuki et al., 1998; Dornhoffer et al., 2002; Qiao et al., 2011; Möhrle et al., 2017). The second specific GC-A ligand, B-type NP (BNP), was suggested to be absent from the inner ear (Suzuki et al., 1998; Shen et al., 2015).

GC-A is also expressed in various organs, such as the kidney, lung, adrenal gland, vasculature, brain, liver, endothelial and adipose tissues, or heart, and its fundamental role in cardiorenal biology is well known (reviewed in Potter, 2011). Thus, GC-A null mice exhibit cardiac hypertrophy, high blood pressure, and ventricular fibrosis (reviewed in Kuhn, 2016; Pandey, 2019). Also, GC-A activators have emerged as potential renal protective therapies, most importantly for the prevention and treatment of acute kidney injury (Chen and Burnett, 2018). The protective function of GC-A is based on the activation by the GC-A ligands ANP and BNP — both of these NPs bind to GC-A. These peptides have emerged as key regulators for energy consumption and metabolism, since they promote lipid oxidation and mitochondrial respiration (Kuhn, 2016).

Whether GC-A displays a protective role for hearing by stimulating the cGMP/cGKI signaling cascade remains elusive. Because ANP and BNP have emerged as key regulators of energy consumption and metabolism (Ramos et al., 2015), we suggest that GC-A signaling in the inner ear is important for metabolic supply as well. Several findings indicate that under conditions of acoustic trauma (AT), aging, metabolic demand, mitochondrial dysfunction, oxidative stress (Fujimoto and Yamasoba, 2019), or activation of hormonal stress responses (Singer et al., 2013, 2018; Fetoni et al., 2019; Möhrle et al., 2019; Prasad and Bondy, 2020) particularly the cochlear partitions corresponding to high-frequency sound processing are affected. If GC-A and activation by its ligands ANP and BNP shall have a protective role for IHC synapses and OHC function to prevent loss of hearing after loud sound exposure or aging, we hypothesize that GC-A gene disruption will negatively influence hearing function with stronger effects in the cochlear regions that are most sensitive to damage. We therefore focused our study on high-frequency representing cochlear partitions (mid-basal and basal cochlear turns) and analyzed the impact of a genetic GC-A (*Npr1*) disruption in GC-A knockout (KO) mice of different ages on hearing and hearing loss after noise exposure.

We included the analysis of the characteristic features of OHC and IHC phenotypes. Both types of sensory hair cells respond to cGMP upregulation through phosphodiesterase (PDE) 5 inhibitors (Jaumann et al., 2012). This encompasses the analysis of the membrane-bound potassium channel KCNQ4, a member of the voltage-gated channel subfamily (KQT member 4) that mediates the dominating K^+ current in OHCs, $I_{K,n}$ (Marcotti and Kros, 1999). Furthermore, we quantified poly (ADP-ribose) (PAR) polymers, products of PAR polymerase (PARP) activity and abundance (Paquet-Durand et al., 2007), and CtBP2/RIBEYE immunoreactivity at the basal IHC pole, where it labels the ribbon structures associated with synaptic vesicles (Kujawa and Liberman, 2009). Both KCNQ4 and PAR were shown to be linked with cGMP signaling in a previous study where PDE 5 inhibition by vardenafil led to increased PAR concentrations. The increased PAR concentrations were suggested to be responsible for persistent KCNQ4 staining after acoustic overexposure, due to DNA repair mechanisms (Jaumann et al., 2012). In that previous study, the vardenafil-induced elevation of PAR concentrations was accompanied by a healthy, "rescued" phenotype, as shown by persistent KCNQ4 staining in the OHCs and the maintenance

[1]https://www.nia.nih.gov/health/hearing-loss-common-problem-older-adults

of ribbons in the IHC synapses (Jaumann et al., 2012). To underscore a possible role of GC-A in the inner ear, we examined GC-A ligand ANP and BNP expression in specific cell types of the cochlea [IHC, OHC, spiral ganglia (SG)].

While we found hearing thresholds in young GC-A KO mice to be normal, a systematic longitudinal investigation of hearing function in young, middle-aged, and old GC-A KO mice with either sham exposure or AT revealed an earlier age-dependent hearing loss in comparison to wild-type (WT) littermates. The fine-structure analysis [auditory brainstem response (ABR) wave amplitude] of hearing function in GC-A KO mice, compared to GC-A WT mice, identified for the first time a differential contribution of GC-A to OHC and IHC damage in response to aging and AT. These findings may prompt future preclinical tests to assess the use of ANP/GC-A/cGMP signaling augmentation as an intervention strategy to counteract age- and noise-induced hearing loss (NIHL).

MATERIALS AND METHODS

Generation of GC-A KO Mice

Mice with global gene disruption of GC-A (GC-A KO, 129-Npr1$^{tm1Gar/J}$) were generated on a genetic background of C57BL/6 as previously described (Lopez et al., 1995). The mice were taken from the colony of Prof. Michaela Kuhn (Würzburg, Germany) and bred in the animal facility of the institute in Tübingen. Adult female and male GC-A KO mice and their WT littermates, as controls, were studied. Animals were bred by crossing heterozygous GC-A parental animals. They were housed in the animal care facility of the Department of Otolaryngology, University of Tübingen (Germany), where noise levels did not exceed 50–60 dB sound pressure level $(SPL)_{rms}$. Animals from three different age groups [2–4 months (young), 7–12 months (middle-age), and 16–18 months (old)] were studied. Mice were held in groups of one (only fighting males) to five mice in standard Macrolon polycarbonate cages containing nesting material, food (Altromin, 1324 BEST), and water *ad libitum* under a 12 h light–dark schedule (daylight period from 6 am to 6 pm). Animal care, procedures, and treatments were performed in accordance with institutional and national guidelines following approval by the University of Tübingen, Veterinary Care Unit, and the Animal Care and Ethics Committee of the regional board of the State Government of Baden-Württemberg, Germany, and followed the guidelines of the EU Directive 2010/63/EU for animal experiments (number: HN3/14).

Hearing Measurements: Auditory Brainstem Response (ABR) and Distortion Product Otoacoustic Emission (DPOAE)

The auditory brainstem response (ABR) evoked by short-duration sound stimuli represents the summed activity of neurons in distinct anatomical structures along the ascending auditory pathway (Burkard and Don, 2007) and is measured by averaging the evoked electrical response recorded via subcutaneous cranial electrodes. ABR to click and noise-burst stimuli and the distortion product otoacoustic emission (DPOAE) for f2 = 1.24*f1 kHz and L2 = L1-10 dB were recorded under anesthesia [0.05 mg/kg Fentanyl (Fentanyl-ratiopharm® ratiopharm GmbH, Ulm, Germany), 0.5 mg/kg Medetomidin hydrochloride (Sedator, Eurovet Animal Health B.V., Bladel, Netherlands), 2.5 mg/kg Midazolam (Midazolam-hameln®; Hameln Pharma plus GmbH, Hameln, Germany), 0.2 mg/kg atropine (Atropinsulfat B.Braun, Melsungen, Germany)] in a soundproof chamber (IAC, Niederkrüchten, Germany), as previously described (Engel et al., 2006). In short, ABR thresholds were elicited with click (100 μs), noise-burst (1 ms duration), or pure-tone stimuli (3 ms, including 1 ms cosine squared rise and fall envelope, 2–45.2 kHz). OHC function was assessed by the DP-gram and growth function of the 2f1-f2 DPOAE (Knipper et al., 2000; Engel et al., 2006). Sound from two loudspeakers (Beyerdynamic DT-911, Heilbronn, Germany), and a probe microphone (Brüel & Kjaer 4135; preamplifier Brüel & Kjaer 2670, Naerum, Denmark) were directly channeled into the ear canal. Distortion product emission signals were recorded during a 260 ms sound presentation and averaged four times for each combination of sound pressure and frequency. The 2f1-f2 distortion product amplitude was measured for L1 ranging from 0 to 60 dB SPL at frequencies of f2 between 4 and 32 kHz. The frequencies f1 and f2 differ by a defined octave distance (f2/f1 = 1.24) and sound pressure (L1 = L2 + 10 dB). For the growth function at f2 = 5.6 or 11.3 kHz, only the OHC responses up to stimulus levels of 45 dB SPL were considered. Above 50 dB SPL stimulus level (L1), response compression by stereocilial non-linearity [saturation of mechanoelectrical transducer (MET) channels] and efferent feedback must be considered. We therefore limited the analysis to within the range up to 45 dB SPL, at which stimulus level the maximum contribution of OHC motility to the amplification of the basilar membrane movement is expected.

Noise Exposure

Acoustic trauma was induced by exposing mice to broadband noise (8–16 kHz, 120 dB SPL_{rms} for 40 min) under anesthesia (see above), as previously described (Jaumann et al., 2012). The degree of the ABR threshold shift was measured approximately 30 min after sham or noise exposure to estimate temporary threshold shifts, and again after 7 days when noise-induced permanent threshold shifts had settled and further recovery from damage would no longer be expected (Liberman, 1980). Sham-exposed animals were anesthetized and placed in the chamber, but not exposed to the acoustic stimulus.

Tissue Preparation

For cochlear cross-section immunohistochemistry, cochleae were isolated, fixed by immersion in 2% paraformaldehyde, 125 mM sucrose in 100 mM phosphate buffered saline, pH 7.4, for 2 h, and then decalcified for 45 min in RDO rapid decalcifier (Apex Engineering Products Corporation, Aurora, IL, United States) as previously described (Knipper et al., 1999; Zuccotti et al., 2012; Duncker et al., 2013; Singer et al., 2013),

cryosectioned at 10 μm, and mounted on SuperFrost*/plus microscope slides before storage at –20°C. For whole-mount immunohistochemistry, temporal bones of mature mice were dissected on ice and fixed using Zamboni's fixative as described (Duncker et al., 2013).

Immunohistochemistry

For immunohistochemistry, mouse cochlear sections were stained as previously described (Tan et al., 2007; Zuccotti et al., 2012; Duncker et al., 2013; Singer et al., 2013). Antibodies against prestin (rabbit, diluted 1:3000, for antibodies see **Table 3**) (Weber et al., 2002), potassium voltage-gated channel subfamily KQT member 4 (mouse, diluted 1:50) (StressMarq, Victoria, BC, Canada; Kharkovets et al., 2006), and C-terminal-binding protein 2 (CtBP2)/RIBEYE (rabbit, diluted 1:1500; ARP American Research Products, Inc.^{TM}, Waltham, MA, United States; Uthaiah and Hudspeth, 2010) were used. Primary antibodies were detected using appropriate Cy3- (1:1500, Jackson Immuno Research Laboratories, West Grove PA, United States) or Alexa488-conjugated secondary antibodies (1:500, Invitrogen Molecular Probes, Paisley, United Kingdom). For double-labeling studies, both antibodies were simultaneously incubated for identical time periods. Sections and whole-mount preparations were viewed as previously described (Zampini et al., 2010) using an Olympus BX61 microscope (Olympus, Hamburg, Germany) equipped with epifluorescence illumination and analyzed with CellSens Dimension software (OSIS GmbH, Münster, Germany). To increase spatial resolution, slices were imaged over a distance of 15 μm within an image-stack along the *z*-axis (*z*-stack), followed by three-dimensional deconvolution using cellSens Dimension's built-in algorithm.

Colocalization of mRNA and Protein in Cochlea Whole-Mounts

mRNA (GC-A) and protein (Tuj-1) were colocalized on cochlear whole-mounts, as previously described (Singer et al., 2014). In brief, following prehybridization for 1 h at 37°C, sections were incubated overnight with GC-A riboprobes (for: 5′-TGT GAA ACG TGT GAA CCG GA-3′ and rev: 5′-AGG CGG ATC GTT GAA AGG G-3′) at 56°C, incubated with anti-digoxigenin antibody conjugated to alkaline phosphatase (anti-Dig-AP, Roche, Germany, 11093274910), and developed as previously described (Singer et al., 2013). For protein detection, streptavidin–biotin was blocked according to the manufacturer's instructions (Streptavidin–Biotin Blocking Kit, Vector Laboratories, United States). Sections were incubated overnight at 4°C with the primary antibodies against Tuj-1 (1:500; monoclonal mouse Biozol MMS-435P), followed by incubation with the secondary antibody (1:500; biotinylated goat anti-rabbit, Vector Laboratories, BA-1000), streptavidin–horseradish peroxidase (1:300 in 1% BSA; Vector Laboratories, Burlingame, CA, United States), and chromogenic detection (AEC, 3-amino-9-ethylcarbazole, Vector Laboratories, SK-4200). Sections were cover slipped with gelatin, and analyzed using a BX61 microscope (Olympus, Hamburg, Germany).

ABC/DAB Immunostaining in Cochlear Sections

The DAB staining was performed as described (Paquet-Durand et al., 2007). In short, the cochlear sections were put in a quenching solution containing H_2O_2, Methanol and PBST (0.1% Triton). To block endogenous peroxidase, the slices were treated with 10% normal goat serum (NGS) in 0.1% PBST. Sections were incubated over night at 4°C with a primary antibody against PAR (Abcam #ab14460; diluted 1:200), as a marker for PARP activity. For detection, an appropriate biotinylated secondary antibody (mouse, diluted 1:150) and an ABC kit (Vector, Burlingame, CA, United States), including avidin and biotinylated horseradish peroxidase, were used according to the manufacturer's instructions (dilution 1:150 each). For chromogenic detection, the slices were finally placed for 2 min in a DAB-solution that contained phosphate buffer (0.1 M), glucose (20%), NH_4Cl (0.4%), nickel ammonium sulfate (1%), glucoseoxidase, and DAB. Sections were cover slipped with Aquatex (Aquatex, Merck, Darmstadt) and analyzed using a BX61 microscope (Olympus, Hamburg, Germany).

RNA Isolation and Reverse Transcription-PCR

For RNA isolation, apical and medial turns of the organ of Corti from 28-day-old mice were dissected and placed on a coverslip. Hensen's and Claudius' cells were removed with cleaning pipettes. 30–60 OHCs were harvested with micropipettes under flow of Tris-Cl solution (0.7 ml/min). Subsequently, outer pillar cells were removed and 30 IHCs were harvested with their adjacent supporting cells (inner phalangeal and border cells). For SG dissection, the cochleae were opened, the stria vascularis and organ of Corti were removed, and the modiolus with SG was used. For cochlea dissection, the bone was removed and the whole remaining tissue was used. The used tissue was frozen in liquid nitrogen. For each age and species, experiments were repeated at least three times.

For isolated OHCs and IHCs, cell lysis and reverse transcription into cDNA was started directly by sampling from the micropipette into the tube (final volume 20 μl). Always, for RT-PCR 5 μl cDNA was used. The first PCR reaction of the nested PCR approach contained enough PCR product for detection in the second PCR reaction. From SG of four cochleae, about 270 ng RNA was isolated. From two mice, total cochleae about 480 ng was isolated. The amount and quality of the RNA were analyzed photometrically. The resulting 260/280 ratio of about 2 (regularly 1.9–2.1 in our hands) was considered as pure.

The PCR program, according to the manufacturer's instructions, included an initial activation step at 95°C for 3 min, followed by 35 cycles of a 30 s denaturing step at 95°C, a 30 s combined annealing/extension step at 55°C, and 25 s at 72°C; ending with 5 min at 72°C. For nested RT-PCR, the PCR program included an initial activation step at 95°C for 3 min, followed by 35 cycles of a 30 s denaturing step at 95°C, a 30 s combined annealing/extension step at 58°C, and 30 s at 72°C; ending with 5 min at 72°C. All PCR fragments were

extracted (QIAGEN Gel Extraction Kit) and sequenced to confirm product specificity.

Data Analysis

ABR Fine-Structure Analysis

ABR functions were analyzed for consecutive amplitude deflections (waves), each wave consisting of a starting negative peak and the following positive peak. Peak amplitudes of noise-burst, stimulus-evoked ABR (noise-ABR) wave I were extracted with customized computer programs, as previously described (Rüttiger et al., 2013). ABR peak-to-peak (wave) amplitude input–output (I/O) growth functions were constructed for each individual ear and increasing stimulus levels with reference to the ABR thresholds using Excel (Microsoft Excel 2016, Redmond, United States).

Calculation of Hearing Loss Over Age

For the calculation of DPOAE amplitude loss over age (in dB), the mean value between f1 = 30–45 dB SPL (f1 = 5.6 kHz) or between f1 = 0–65 dB SPL (f1 = 11.3 kHz) was calculated. For the calculation of ABR wave amplitude loss over age (in μV), the mean value between 20 and 65 dB SPL stimulation was calculated. The means of middle-aged and old animals were each normalized to the mean of the young animals.

PAR Quantification

The intensity of PAR staining (as a surrogate marker for PARP activity) was quantified by asking six "blinded" volunteers to choose the darker staining of a GC-A WT and KO pair of either IHC, OHC, or SG. This procedure was repeated for $n = 3$ mice with both ears, taking pictures of at least two slices on each slide on both basal and midbasal turns. The pictures were shown in direct comparison on PowerPoint slides (Microsoft PowerPoint 2016, Redmond, United States), with arrows marking the cell nuclei of interest. During analysis, the judgment of the volunteers was evaluated by counting the number of cases for which they choose the WT as exhibiting a darker staining in the nuclei, in comparison to the KO and a relation $[(n_{\text{cases with judgment WT darker}}/n_{\text{all}})^*1]$ was calculated.

Statistical Analysis

Results for ABR thresholds, DPOAE thresholds and ABR fine structure analysis from the two individual ears of each animal were averaged and the statistical analysis run based on the number of animals. Statistical significance of PARP activity was tested with a z-test to compare the mean of the decisions against chance level (0.5). Unless otherwise stated, all data are presented as group mean, with standard error of the mean (SEM). Differences of the means were compared for statistical significance either by a Student's t-test, two-way ANOVA, or regression tests using Excel (Microsoft Excel 2016, Redmond, United States), or GraphPad Prism 5.01 (La Jolla, CA, United States). Two-way ANOVA tests were followed by multiple comparison tests with correction for type 1 error after Bonferroni. The chosen statistical significance level was $\alpha = 0.05$, and resulting p-values are reported in the legends using $(^*)P < 0.1$; $^*P < 0.05$; $^{**}P < 0.01$; $^{***}P < 0.001$; n.s., not significant.

RESULTS

GC-A, ANP, BNP, and PDE9a Expression in Cochlear Cells

To study differential compartment- or cell-specific GC-A expression, GC-A-specific riboprobes were generated (see section "Materials and Methods") and colocalized on free-floating whole-mount cochleae with mouse monoclonal neuron-specific class III β-tubulin antibody. Tuj-1 is a marker of neural cochlear fibers (Molea et al., 1999; Liu et al., 2009). Double detection of mRNA and protein in whole-mount cochlear preparations was performed as previously described for analysis of brain vibratome sections (Singer et al., 2014; see section "Materials and Methods"). Whole-mount cochlear preparations were dissected separately for apical, medial, and midbasal cochlear regions and mounted before visualization. We observed strong GC-A staining in OHCs (**Figure 1A**) and no staining in sense controls (**Figure 1A**). With higher magnification, GC-A staining in OHCs (**Figure 1B**, closed arrow) and absence of GC-A in IHCs (**Figure 1B**, open arrow), close to Tuj-1-positive afferent terminals at the IHC level (**Figure 1B**, stars), became evident. Many, but not all, SGNs also strongly expressed GC-A (**Figure 1C**, short arrows).

With the aim of strengthening understanding of the regulatory role of GC-A and its ligands in possible hair-cell-specific effects, we investigated ANP, BNP, and GC-A mRNA expression in isolated hair cells. IHCs and OHCs were dissected from adult mice as described in section "Materials and Methods," and mRNA was isolated as described (Engel et al., 2006; Möhrle et al., 2017). All PCR fragments were extracted and sequenced as described in the methods to confirm product specificity. As shown by mRNA analyses, nested primers amplified a GC-A-specific fragment in OHCs and SG but not in IHCs, while ANP and BNP mRNA was detected in IHCs, OHCs, and SG (**Figure 1D**).

Because the cGMP-degrading enzyme PDE9a might be a target accessible to drug influence to increase cGMP pools that are predominantly controlled by ANP/GC-A (Lee et al., 2015), we also explicitly searched for PDE9a expression in the cochlea. PDE9a was expressed in the cochlea and in the auditory cortex (AC) (**Figure 1E**).

Accelerated Progression of Age-Related Hearing Loss in GC-A KO Mice

To study the effect of GC-A gene disruption on hearing, we first compared the hearing thresholds of age-matched young (2–4 months), middle-aged (7–12 months), and old (16–18 months) unexposed GC-A WT and KO mice. The ABR evoked by low frequency-containing (click), high frequency-containing (noise-burst), and pure tone frequency-specific auditory stimuli were tested as described (Jaumann et al., 2012; Möhrle et al., 2016). As shown in **Figure 2A**, young GC-A WT and KO mice did not differ in hearing thresholds for click- or for noise-burst stimuli (**Figure 2A**, left panel and **Table 2A**). An elevation in hearing threshold to pure tone auditory stimuli > 22 kHz in GC-A KO mice compared to GC-A WT mice is apparent (**Figure 2B**, left panel), but this difference did not reach statistical significance. In contrast, both middle-aged (**Figure 2A**, middle

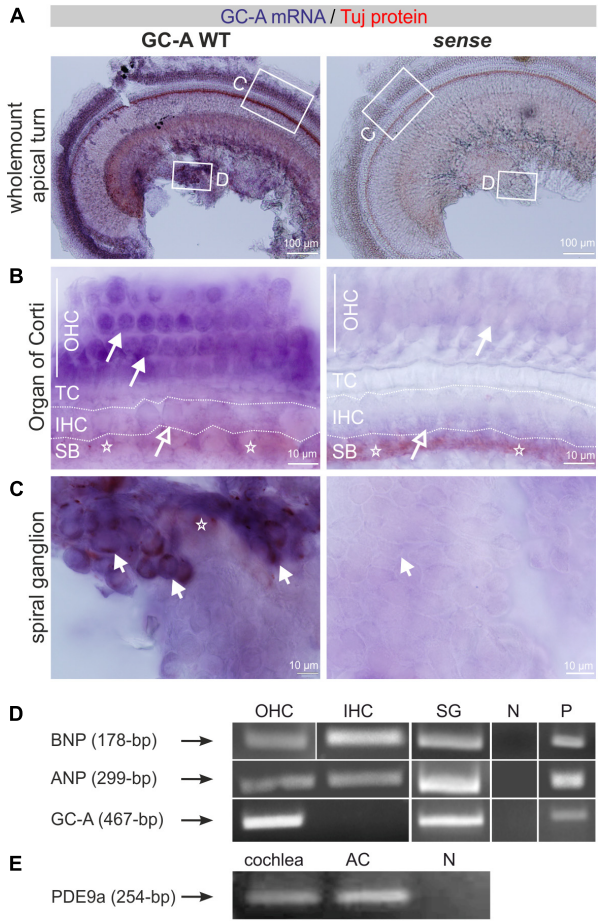

FIGURE 1 | Expression of GC-A, its ligands, and PDE9a in the cochlea. **(A)** GC-A mRNA and Tuj-1 protein staining in GC-A WT antisense and sense whole-mount cochlear preparations. Scale bars: 100 µm. **(B)** GC-A mRNA staining was shown in GC-A WT OHC (closed arrows), but not IHC (open arrows). Tuj-1 staining (stars) in the spiral bundle (SB) in both WT and KO. TC = tunnel of Corti. Scale bars: 10 µm. **(C)** GC-A mRNA staining was shown in GC-A WT SGN (short arrows) but not in GC-A KO. Tuj-1 staining (stars) in the SGN. Scale bars: 10 µm. **(D)** Reverse transcription-PCR of WT IHC and OHC cDNA shows a fragment of ANP (299-bp) and BNP (178-bp) expressed in isolated OHCs, IHCs, and SG. GC-A at 467-bp was only found in OHCs, but not IHCs. **(E)** PDE9a was expressed in both cochlear and auditory-cortex (AC) tissue samples. Abbreviations: N, negative control; P, positive control (heart).

panel) and old GC-A animals (**Figure 2A**, right panel) exhibited elevated thresholds for click, noise-burst, and frequency-specific stimuli, and the changes were most pronounced at middle ages. The typically-occurring, profound age-dependent elevation in hearing thresholds in the last third of life (**Figures 2A,B** and **Table 1**) partially abolished the differences in ABR thresholds between old GC-A WT and KO mice. This was confirmed when frequency-specific ABR thresholds were compared in GC-A WT and KO mice. A threshold elevation became particularly evident in middle-aged GC-A KO mice (**Figure 2B**, middle panel), but not in old GC-A KO mice compared to GC-A WT mice (**Figure 2B**, right panel).

It was shown that during the last two-thirds of life, GC-A KO mice developed elevated hearing thresholds relative to GC-A WT mice.

GC-A KO Mice Exhibit Early Dysfunction of OHCs Independent of Age

To assign the hearing threshold elevation in GC-A KO mice to specific cochlear compartments, we first analyzed electromotile properties of OHCs that form the basis of sound-evoked neural potentials at threshold (Marcon and Patuzzi, 2008). Electromotile properties of OHCs can be assessed by recording ear-canal sound-pressure changes induced by DPOAEs (Shera and Guinan, 1999) that are specifically generated by electromechanical responses of OHCs (El-Badry and McFadden, 2007; Rüttiger et al., 2017). Frequency-specific thresholds of DPOAE signals from amplitude I/O functions were analyzed by presenting pure-tone sounds from f2 = 4–32 kHz and increasing sound level (L2 = −10 to 45 dB SPL) in young, middle-aged, and old GC-A WT and GC-A KO mice (**Figure 3** and **Table 2B**). Despite differences in ABR thresholds in response to click, noise-burst, and frequency-specific stimuli (**Figure 2**), DPOAE thresholds were similar between WT and GC-A KO mice for all ages tested (**Figure 3A**). However, when the I/O functions of DPOAEs for f1 = 5.6 and 11.3 kHz were compared between GC-A WT and KO mice at different ages, it became evident that DPOAE I/O responses to f1 = 5.6 kHz remained similar between GC-A KO and WT mice across the different age groups (**Figure 3B**). In contrast, OHC-specific responses at higher frequencies (f1 = 11.3 kHz) were already reduced in young GC-A KO mice (**Figure 3C**). Interestingly, the difference in DPOAE I/O responses between GC-A KO mice and WT mice remained constant throughout all ages, in line with a typically occurring, age-dependent hearing loss that progresses independently of GC-A signaling in the last third of life.

Previously, increased cGMP levels have been shown to protect against noise-induced loss of the membranous potassium voltage-gated channel subfamily KQT member 4 (KCNQ4) in OHCs. KCNQ4 is the voltage-dependent K^+ channel that maintains the OHC resting potential and is vital for OHC survival (Marcotti and Kros, 1999). Therefore, we further investigated the impact of GC-A gene disruption on the expression pattern of KCNQ4 in OHCs from young, middle-aged, and old mice. Using high-resolution confocal microscopy, KCNQ4 was co-stained with the OHC motor protein prestin, which is encoded by the *Slc26a5* gene and responsible for the electromechanical properties of OHCs (Zheng et al., 2000) (**Figure 3**). KCNQ4 surface expression at the base of OHCs was reduced in high-frequency cochlear regions of GC-A KO mice of all ages compared to GC-A WT mice (**Figure 3D**, mid-basal turn, yellow stars), as shown by $n = 3$ independent repetitions. In contrast, membrane staining of the OHC motor protein prestin was preserved in the lateral walls of OHCs across age, although the intensity of prestin staining in OHCs from GC-A KO mice appeared to be slightly reduced in aged animals (**Figure 3D**) because of degeneration of cell membrane in which prestin is placed.

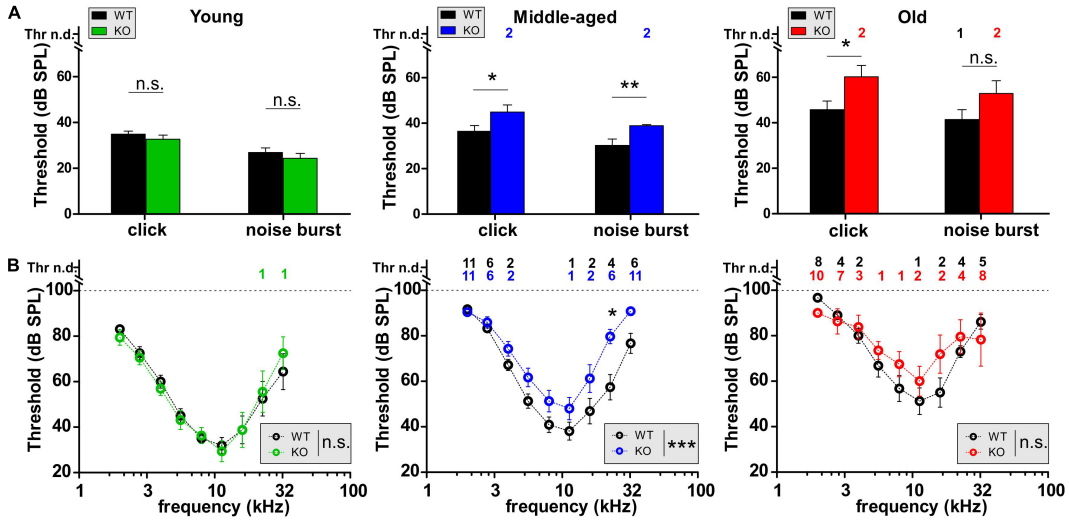

FIGURE 2 | Auditory brainstem responses (ABRs) in GC-A WT and KO mice over age. **(A,B)** Hearing thresholds of WT and GC-A KO littermates assessed from auditory brainstem response (ABR) potentials in response to low-frequency-containing (click), high-frequency containing (noise burst), and pure-tone frequency-specific auditory stimuli. **(A)** Click-evoked ABR thresholds were not affected in young GC-A KO animals [green, unpaired two-tailed student's *t*-test: $t(30) = 0.9870$, $P = 0.3315$, $n = 8/16$ mice/ears each], but elevated in middle-aged [blue, unpaired two-tailed student's *t*-test: $t(100) = 2.125$, $P = 0.0361$, WT $n = 27/54$ mice/ears; KO $n = 48/24$ mice/ears] and old [red, unpaired two-tailed student's *t*-test: $t(47) = 2.350$, $P = 0.0230$, WT $n = 14/28$ mice/ears; KO $n = 11/21$ mice/ears] GC-A KOs compared to WTs. Also, noise-burst evoked ABR thresholds were elevated in middle-aged GC-A KOs [blue, unpaired two-tailed student's *t*-test: $t(100) = 2.890$, $P = 0.0047$, WT $n = 27/54$ mice/ears; KO $n = 24/48$ mice/ears]. Young and old animals did not show differences in noise-burst evoked ABR thresholds [young: unpaired two-tailed student's *t*-test: $t(30) = 0.8649$, $P = 0.3940$, $n = 8/16$ mice/ears each; old: unpaired two-tailed student's *t*-test: $t(47) = 1.648$, $P = 0.1509$, WT $n = 14/28$ mice/ears; KO $n = 10/21$ mice/ears]. **(B)** With pure-tone frequency-specific stimuli in the range between 2 and 32 kHz, middle-aged GC-A KOs (blue) had increased ABR thresholds compared to WTs [two-way ANOVA: $F(1,8) = 26.54$, $P < 0.0001$, WT $n = 27/27$ mice/ears; KO $n = 23/23$ mice/ears]. Young and old animals did not show differences [young: two-way ANOVA: $F(1,126) = 0.00$, $P = 0.9781$, $n = 8/8$ mice/ears each; old: two-way ANOVA: $F(1,142) = 1.43$ $P = 0.2235$, WT $n = 14/14$ mice/ears; KO $n = 10/10$ mice/ears]. Thr n.d. = Threshold not detectable. Mean ± SEM. $^*P < 0.05$; $^{**}P < 0.01$; $^{***}P < 0.001$.

TABLE 1 | Primer sequences and information used for PCR.

	Position and length	Forward	Reverse
ANP	Accession number BC089615, position 194-609, 416-bp	5′-GTA CAG TGC GGT GTC CAA CA-3′ (Zhang et al., 2017)	5′-GCT CAA GCA GAA TCG ACT GC-3′ (Nie et al., 2018)
ANP nested	Position 204-502, 299-bp	5′-TTC AAG AAC CTG CTA GAC CAC C-3′ Self-designed	5′-CCA ATC CTG TCA ATC CTA CCC C-3′ Self-designed
BNP	Accession number BC061165, position 202-424, 222-bp	5′-AAG CTG CTG GAG CTG ATA AGA-3′ (Kuhn et al., 2009)	5′-GTT ACA GCC CAA ACG ACT GAC-3′ (Kuhn et al., 2009)
BNP nested	Position 224-401, 178-bp	5′-GAA AAG TCG GAG GAA ATG GCC C-3′ Self-designed	5′-ATC CGA TCC GGT CTA TCT TGT GC-3′ Self-designed
GC-A	Accession number BC110659, position 1927-2599, 702-bp	5′-TGT GAA ACG TGT GAA CCG GA-3′ Self-designed	5′-AGG CGG ATC GTT GAA AGG G-3′ Self-designed
GC-A nested	Position 1998-2464, 467-bp	5′-TGT GCA GAA TGA GCA CTT GAC C-3′ Self-designed	5′-CCA AAC CTT CCA CAT AGA AGA CCC-3′ Self-designed
PDE9a	Accession number NM_008804, position 199-452, 254-bp	5′-ACC ACC ATC TCC CTT TTA ACC-3′ Self-designed	5′-AGT CCT TCC AAT TCC ACC C-3′ Self-designed

GC-A KO mice already showed impaired OHC function compared to GC-A WT mice at a young age.

GC-A KO Mice Exhibit Early Dysfunction of OHCs Independent of Acoustic Trauma

Noise exposure is a major cause of age-dependent hearing loss, because it can induce sensory-cell degeneration, especially in the OHCs at the high-frequency end of the cochlea (Keithley, 2019). To study whether GC-A/cGMP signaling attenuates NIHL, young GC-A WT and KO mice received an AT induced by exposure to 8–16 kHz, 120 dB SPL_{rms} sound for 40 min (see section "Materials and Methods"). Hearing loss, evident through threshold shifts, was analyzed using frequency-specific ABRs 7 days after acoustic-trauma induction. Young GC-A WT and KO mice did not differ in their degree of hearing loss in response to the traumatizing noise. This was

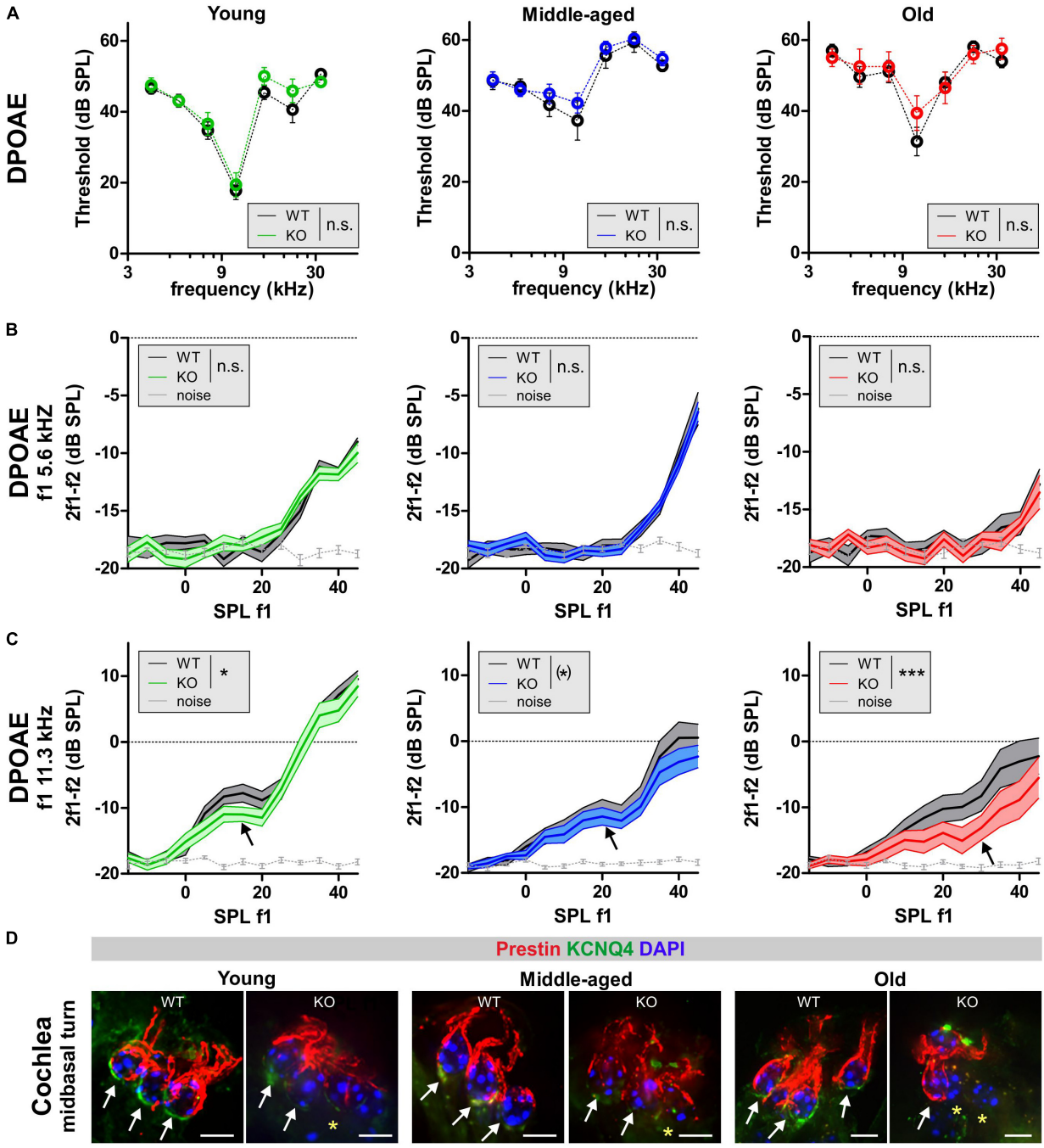

FIGURE 3 | DPOAEs and expression of KCNQ4 in GC-A WT and GC-A KO mice at different ages. **(A–C)** OHC function assessed from distortion-product otoacoustic emissions (DPOAEs) that are generated by electromechanical responses of OHCs. **(A)** Frequency-specific thresholds of DPOAE signals for pure-tone sounds from f2 = 4–32 kHz did not differ between GC-A KO and WT mice [young: two-way ANOVA, $F(1,84) = 0.04$, $P = 0.8510$, $n = 8/16$ mice/ears each; middle-aged: two-way ANOVA, $F(1,132) = 1.54$, $P = 0.2157$, WT $n = 6/12$ mice/ears KO $n = 8/16$ mice/ears; old: two-way ANOVA, $F(1,247) = 0.52$, $P = 0.4697$, WT $n = 14/27$ mice/ears KO $n = 10/20$ mice/ears]. **(B)** DPOAE growth function in response to pure-tone sounds at f1 = 5.6 kHz were similar between GC-A KO and WT mice in all three age groups [young: two-way ANOVA, $F(1,382) = 0.17$, $P = 0.679$, $n = 8/16$ mice/ears each; middle-aged: two-way ANOVA, $F(1,577) = 0.00$, $P = 0.9879$, WT $n = 10/20$ mice/ears KO $n = 14/28$ mice/ears; old: two-way ANOVA, $F(1,382) = 0.59$, $P = 0.4439$, $n = 8/16$ mice/ears each]. **(C)** DPOAE growth function in response to pure-tone sounds at f1 = 11.3 kHz were reduced in GC-A KO compared to WT mice in all three age groups [young: two-way ANOVA, $F(1,382) = 4.40$, $P = 0.0367$, $n = 8/16$ mice/ears each; middle-aged: two-way ANOVA, $F(1,577) = 3.34$, $P = 0.0681$, WT $n = 10/20$ mice/ears KO $n = 14/28$ mice/ears; old: two-way ANOVA, $F(1,382) = 14.01$, $P = 0.0002$, $n = 8/16$ mice/ears each]. Mean ± SEM. $^*P < 0.1$; $^*P < 0.05$; $^{***}P < 0.001$. **(D)** The intactness of the OHC phenotype was investigated by immunohistochemical staining for KCNQ4 (green) and the motor protein prestin (red) as markers for OHC viability and their capacity for electromechanical responses. Staining for KCNQ4 in cochlear OHCs of GC-A mice was reduced in OHCs (upper panel) in comparison to WT mice, while prestin seems to be only slightly reduced due to degeneration of membrane. Nuclei were stained with 4',6-diamidin-2-phenylindol (DAPI, blue). Yellow asterisk shows absence of KCNQ4 in OHCs. Scale bars: 5 μm.

TABLE 2 | Table of statistics.

(A) Click, noise-burst, and frequency-specific ABR thresholds in GC-A WT and KO mice as a function of age.

	Young	Middle-aged	Old
Click	Unpaired two-tailed student's *t*-test: t(30) = 0.9870 *P* = 0.3315, *n* = 8/16 mice/ears each	Unpaired two-tailed student's *t*-test: *t*(100) = 2.125 *P* = 0.0361, WT *n* = 27/54 mice/ears; KO *n* = 48/24 mice/ears	Unpaired two-tailed student's *t*-test: *t*(47) = 2.350 *P* = 0.0230, WT *n* = 14/28 mice/ears; KO *n* = 11/21 mice/ears
Noise burst	Unpaired two-tailed student's *t*-test: *t*(30) = 0.8649 *P* = 0.3940, *n* = 8/16 mice/ears each	Unpaired two-tailed student's *t*-test: *t*(100) = 2.890 *P* = 0.0047, WT *n* = 27/54 mice/ears; KO *n* = 24/48 mice/ears	Unpaired two-tailed student's *t*-test: *t*(47) = 1.648 *P* = 0.1509, WT *n* = 14/28 mice/ears; KO *n* = 10/21 mice/ears
Frequency	Two-way ANOVA: *F*(1,126) = 0.00 *P* = 0.9781, *n* = 8/8 mice/ears each	Two-way ANOVA: *F*(1,8) = 26.54 *P* < 0.0001, WT *n* = 27/27 mice/ears; KO *n* = 23/23 mice/ears	Two-way ANOVA: *F*(1,142) = 1.43 *P* = 0.2235, WT *n* = 14/14 mice/ears; KO *n* = 10/10 mice/ears

(B) Thresholds and input/output function of DPOAEs at different f1 frequencies in GC-A WT and KO mice as a function of age.

	Young	Middle-aged	Old
Threshold	Two-way ANOVA, *F*(1,84) = 0.04, *P* = 0.8510, *n* = 8/16 mice/ears each	Two-way ANOVA, *F*(1,132) = 1.54, *P* = 0.2157, WT *n* = 6/12 mice/ears KO *n* = 8/16 mice/ears	Two-way ANOVA, *F*(1,247) = 0.52, *P* = 0.4697, WT *n* = 14/27 mice/ears KO *n* = 10/20 mice/ears
5.6 kHz	Two-way ANOVA, *F*(1,382) = 0.17, *P* = 0.679, *n* = 8/16 mice/ears each	Two-way ANOVA, *F*(1,577) = 0.00, *P* = 0.9879, WT *n* = 10/20 mice/ears KO *n* = 14/28 mice/ears	Two-way ANOVA, *F*(1,382) = 0.59, *P* = 0.4439, *n* = 8/16 mice/ears each
11.3 kHz	Two-way ANOVA, *F*(1,382) = 4.40, *P* = 0.0367, *n* = 8/16 mice/ears each;	Two-way ANOVA, *F*(1,577) = 3.34, *P* = 0.0681, WT *n* = 10/20 mice/ears KO *n* = 14/28 mice/ears	Two-way ANOVA, *F*(1,382) = 14.01, *P* = 0.0002, *n* = 8/16 mice/ears each

(C) OHC function after acoustic trauma in young GC-A WT and KO mice.

Delta ABR threshold		**Delta DPOAE threshold**
Two-way ANOVA, *F*(1,44) = 3.11, *P* = 0.0845, WT *n* = 3/3 mice/ears KO *n* = 4/4 mice/ears		Two-way ANOVA, *F*(1,84) = 1.43, *P* = 0.2344, WT *n* = 3/6 mice/ears KO *n* = 4/8 mice/ears
	5.6 kHz	**11.3 kHz**
Post I/O	Two-way ANOVA, *F*(1,147) = 2.31, *P* > 0.05, WT *n* = 3/6 mice/ears KO *n* = 4/8 mice/ears	Two-way ANOVA, *F*(1,147) = 1.46, *P* > 0.05, WT *n* = 3/6 mice/ears KO *n* = 4/8 mice/ears
	5.6 kHz	**11.3 kHz**
Delta I/O	Two-way ANOVA, *F*(1,121) = 0.03, *P* = 0.8693, WT *n* = 3/6 mice/ears KO *n* = 4/7 mice/ears	Two-way ANOVA, *F*(1,180) = 6.06, *P* = 0.0148, WT *n* = 3/6 mice/ears KO *n* = 4/8 mice/ears
Regression	*t*(183) = 0.226, *P* = 0.98, WT *n* = 85 KO *n* = 102	*t*(69) = 0.027, *P* = 0.98, WT *n* = 28 KO *n* = 45

(D) Supra-threshold ABR wave I and IV amplitudes in GC-A WT and KO mice as a function of age and before and after acoustic trauma.

	Young	Middle-aged	Old
ABR wave I	Two-way ANOVA, *F*(1,374) = 10.57, *P* = 0.0013, *n* = 8/16 mice/ears each	Two-way ANOVA, *F*(1,247) = 5.38, *P* = 0.0212, WT *n* = 6/12 mice/ears KO *n* = 5/10 mice/ears	Two-way ANOVA, *F*(1,255) = 82.55, *P* < 0.0001, WT *n* = 7/14 mice/ears KO *n* = 5/10 mice/ears
ABR wave IV	Two-way ANOVA, *F*(1,362) = 0.00, *P* = 0.9568, *n* = 8/16 mice/ears each	Two-way ANOVA, *F*(1,462) = 32.21, *P* < 0.0001, WT *n* = 11/21 mice/ears KO *n* = 10/20 mice/ears	Two-way ANOVA, *F*(1,269) = 43.28, *P* < 0.0001, WT *n* = 7/14 mice/ears each
ABR wave I post acoustic trauma	Two-way ANOVA, *F*(1,117) = 36.46, *P* < 0.0001, WT *n* = 3/6 mice/ears KO *n* = 4/8 mice/ears	Two-way ANOVA, *F*(1,105) = 4.84, *P* = 0.0300, *n* = 5/10 mice/ears each	
ABR wave IV post acoustic trauma	Two-way ANOVA, *F*(1,113) = 17.20, *P* < 0.0001, WT *n* = 3/6 mice/ears KO *n* = 4/8 mice/ears	Two-way ANOVA, *F*(1,108) = 17.58, *P* < 0.0001, WT *n* = 5/10 mice/ears KO *n* = 6/12 mice/ears	

(Continued)

TABLE 2 | Continued

(E) IHC ribbon numbers in GC-A WT and KO mice as a function of age and before and after acoustic trauma (AT).

	Young	Middle-aged	Old
Basal turn	Two-way ANOVA, Genotype: $F(1,20) = 65.9$, $P < 0.0001$, $n = 6/3$ samples/mice each; AT: $F(1,20) = 185.69$, $P < 0.0001$, $n = 6/3$ samples/mice each, *post hoc* test: sham WT vs. sham KO $P < 0.001$, sham KO vs. AT WT $P < 0.001$, AT WT vs. AT KO $P < 0.0001$	Two-way ANOVA, Genotype: $F(1,23) = 15.40$, $P = 0.0007$, WT $n = 8/4$ samples/mice KO $n = 7/4$ samples/mice; AT: $F(1,23) = 14.96$, $P = 0.0008$, WT $n = 6/4$ samples/mice KO $n = 6/4$ samples/mice, *post hoc* test: sham WT vs. sham KO $P < 0.05$, sham KO vs. AT WT $P > 0.05$, AT WT vs. AT KO $P > 0.05$	Unpaired two-tailed student's *t*-test, $t(5) = 5.811$ $P < 0.0002$, $n = 6/3$ samples/mice each
Midbasal turn	Two-way ANOVA, Genotype: $F(1,21) = 74.62$, $P < 0.0001$, $n = 6/3$ samples/mice each; AT: $F(1,21) = 41.97$, $P < 0.0001$, $n = 6/3$ samples/mice each, *post hoc* test: sham WT vs. sham KO $P < 0.01$, sham KO vs. AT WT $P > 0.05$, AT WT vs. AT KO $P < 0.0001$	Two-way ANOVA, Genotype: $F(1,25) = 47.12$, $P < 0.0001$ WT $n = 7/4$ samples/mice KO $n = 6/4$ samples/mice; AT: $F(1,25) = 37.21$, $P < 0.0001$, Interaction: $F(1,25) = 6.926$, $P = 0.0143$, WT $n = 8/4$ samples/mice KO $n = 7/4$ samples/mice, *post hoc* test: sham WT vs. sham KO $P < 0.0001$, sham KO vs. AT WT $P > 0.05$, AT WT vs. AT KO $P > 0.05$	Unpaired two-tailed student's *t*-test, $t(10) = 5.580$ $P < 0.0002$, $n = 6/3$ samples/mice each
Apical turn	Two-way ANOVA, Genotype: $F(1,20) = 19.49$, $P = 0.0003$; $n = 6/3$ samples/mice each, AT: $F(1,20) = 6.307$, $P = 0.0207$, $n = 6/3$ samples/mice each, Interaction: $F(1,20) = 7.510$, $P = 0.0126$, *post hoc* test: sham WT vs. sham KO $P < 0.01$, sham KO vs. AT WT $P < 0.001$, AT WT vs. AT KO $P > 0.05$	Two-way ANOVA, Genotype: $F(1,24) = 11.41$, $P = 0.0025$ WT $n = 7/4$ samples/mice KO $n = 6/4$ samples/mice; $F(1,24) = 2.740$, $P = 0.1109$ WT $n = 8/4$ samples/mice KO $n = 7/4$ samples/mice, *post hoc* test: sham WT vs. sham KO $P > 0.05$, sham KO vs. AT WT $P < 0.01$, AT WT vs. AT KO $P > 0.05$	Unpaired two-tailed student's *t*-test, $t(10) = 2.789$ $P = 0.0192$, $n = 6/3$ samples/mice each

(F) Aging progress in OHC function and auditory nerve responses.

	DPOAE 5.6 kHz	DPOAE 11.3 kHz	Noise burst ABR wave I
Loss of amplitude	Two-way ANOVA, $F(1,106) = 0.01$, $P = 0.928$, n = 8–14/16–28 mice/ears each	Two-way ANOVA, $F(1,106) = 0.00$, $P = 0.951$, n = 8–14/16–28 mice/ears each	Two-way ANOVA, $F(1,71) = 4.72$, $P = 0.0033$, n = 5–8/10–16 mice/ears each

TABLE 3 | Antibodies for immunostaining.

	Host organism	Dilution	Company
Prestin	Rabbit	1:3000	Squarix, Berlin, Germany #976102#5
KCNQ4	Mouse	1:50	Stress marq, British Columbia, United Kingdom SMC-309D
CtBP2/RIBEYE	Rabbit	1:1500	American Research Products, Waltham, United States #10-P1554
Tuj1	Mouse	1:500	BioLegend/Biozol, Eching, Germany #801201
PAR	Chicken	1:200	Abcam, Cambridge, United Kingdom #ab14460
Digoxigenin	Sheep	1:750	Anti-Dig-AP, Roche, Germany, 11093274910
Biotinylated IgG	Goat	1:500/1:150	Vector Laboratories, BA-1000
Cy3	Goat	1:1500	Jackson Immuno Research Laboratories, West Grove PA, United States
Alexa488	Goat	1:500	Invitrogen Molecular Probes, Paisley, United Kingdom

evident by comparison of frequency-specific ABRs (**Figure 4A** and **Table 2C**) and DPOAEs (**Figure 4B**). In addition, the threshold shift in GC-A WT and KO mice in response to AT did not differ when analyzing DPOAE I/O responses to f1 = 5.6 kHz and 11.3 kHz stimuli (**Figure 4C**), although the 11.3 kHz I/O functions showed stronger loss of DPOAE signal in GC-A WT mice than in KO mice (**Supplementary Figure S1A**). To clarify a possible alteration in the decline of OHC motility (DPOAEs) in GC-A KO mice, the regression line between the measured DPOAE signal (in dB SPL) after AT and the loss of DPOAE signal (in dB SPL) was calculated, but not found to be different between GC-A WT and KO mice with f1 = 5.6 kHz or with f1 = 11.3 kHz stimulus (**Supplementary Figure S1C**). This suggests that the relative loss of DPOAE I/O function after AT is comparable in GC-A WT and KO mice.

It was shown that GC-A KO mice already have deficits in OHC function in higher frequency regions at f1 = 11.3 kHz at a young age. Moreover, this GC-A-dependent loss in OHC function is not further worsened by aging or AT.

GC-A KO Mice Exhibit Early, Age- and Acoustic Trauma-Induced Neuropathy and Synaptopathy

Aging and AT have been shown to induce auditory nerve-fiber degeneration (auditory neuropathy) related to IHC nerve terminal damage (synaptopathy) in mice, non-human primates,

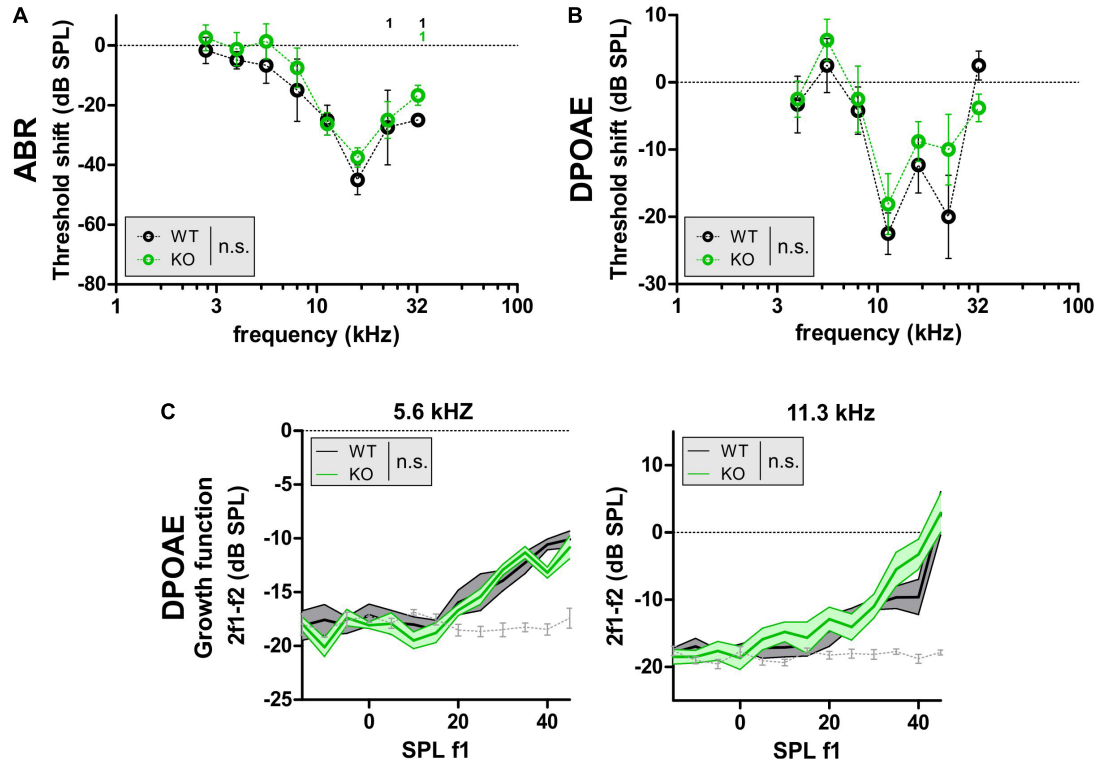

FIGURE 4 | DPOAE signals in GC-A WT and GC-A KO mice after acoustic trauma. **(A–C)** ABR threshold and OHC function, assessed by DPOAE measurements 7 days after acoustic trauma induction in young GC-A WT and KO mice. **(A,B)** Shift of frequency-specific ABR thresholds and DPOAE thresholds, when compared before and 7 days after acoustic trauma, did not show differences between WT and KO mice [f-ABR: two-way ANOVA, $F(1,44) = 3.11$, $P = 0.0845$, WT $n = 3/3$ mice/ears KO $n = 4/4$ mice/ears; DPOAE: two-way ANOVA, $F(1,84) = 1.43$, $P = 0.2344$, WT $n = 3/6$ mice/ears KO $n = 4/8$ mice/ears]. **(C)** DPOAE signal growth function in response to pure tones at f1 = 5.6 and 11.3 kHz were similar between GC-A KO and WT mice after acoustic trauma [5 kHz: two-way ANOVA, $F(1,147) = 2.31$, $P > 0.05$, WT $n = 3/6$ mice/ears KO $n = 4/8$ mice/ears; 11 kHz: two-way ANOVA, $F(1,147) = 1.46$, $P > 0.05$, WT $n = 3/6$ mice/ears KO $n = 4/8$ mice/ears]. DPOAE signal growth function in response to pure tone sounds at f1 = 22 kHz were also smaller in GC-A KO than WT mice after acoustic trauma [two-way ANOVA, $F(1,147) = 11.51$, $P = 0.0009$, WT $n = 3/6$ mice/ears KO $n = 4/8$ mice/ears].

and humans (Gleich et al., 2016; Valero et al., 2017; Wu et al., 2019). Auditory-nerve degeneration can occur independently of OHC loss and is called hidden hearing loss (Kujawa and Liberman, 2009; Furman et al., 2013). It has been shown that elevated cGMP levels can prevent AT-induced damage of IHC nerve terminals (Jaumann et al., 2012). To investigate the impact of GC-A-induced cGMP generation on the vulnerability of pre- and postsynaptic structures of IHCs, we analyzed a possible GC-A-induced neuropathy by comparing supra-threshold ABR wave amplitudes in GC-A WT and KO mice prior to and after AT and at different ages. Supra-threshold ABR wave amplitudes change proportionally with discharge rates and the number of synchronously firing auditory nerve fibers (Johnson and Kiang, 1976), the latter defined by IHC synaptic ribbons (Buran et al., 2010). Therefore, auditory neuropathy or IHC synaptopathy is well reflected by changes in supra-threshold ABR amplitudes and IHC ribbon numbers, respectively (Kujawa and Liberman, 2009; Jaumann et al., 2012; Chumak et al., 2016; Möhrle et al., 2016). The auditory stimulus-evoked ABR wave I (**Figure 5A**, wave I and **Table 2D**) reflects the summed activity of the auditory nerve fibers (Melcher and Kiang, 1996) and is a useful functional biomarker of auditory-nerve degeneration after noise exposure (Rüttiger et al., 2017), while ABR wave IV (**Figure 5A**, wave I) reflects the sound-induced activity generated at the level of the inferior colliculus and lateral lemniscus (Melcher and Kiang, 1996).

The analysis of supra-threshold ABR wave I (**Figure 5B**) and IV (**Figure 5C**) revealed a reduction in ABR amplitude I and ABR amplitude IV in middle-aged and old GC-A KO mice, but not in young GC-A KO mice compared to GC-A WT mice. This indicates that unlike the effect of GC-A inactivation on OHCs (which was already apparent in young KO mice), auditory-nerve responses declined in GC-A KO mice as they aged. A slight augmentation of the ABR wave I amplitudes in young GC-A KO mice (**Figure 5B**) was not evident in the more centrally generated ABR wave IV, suggesting that the putatively higher auditory input from the cochlea is centrally adapted or compensated (**Figure 5C**).

To validate the impact of GC-A on AT-induced auditory-nerve responses, young and middle-aged GC-A WT and KO mice were exposed to 8–16 kHz broad band noise (120 dB SPL_{rms} for 40 min), and ABR wave I and IV amplitudes were

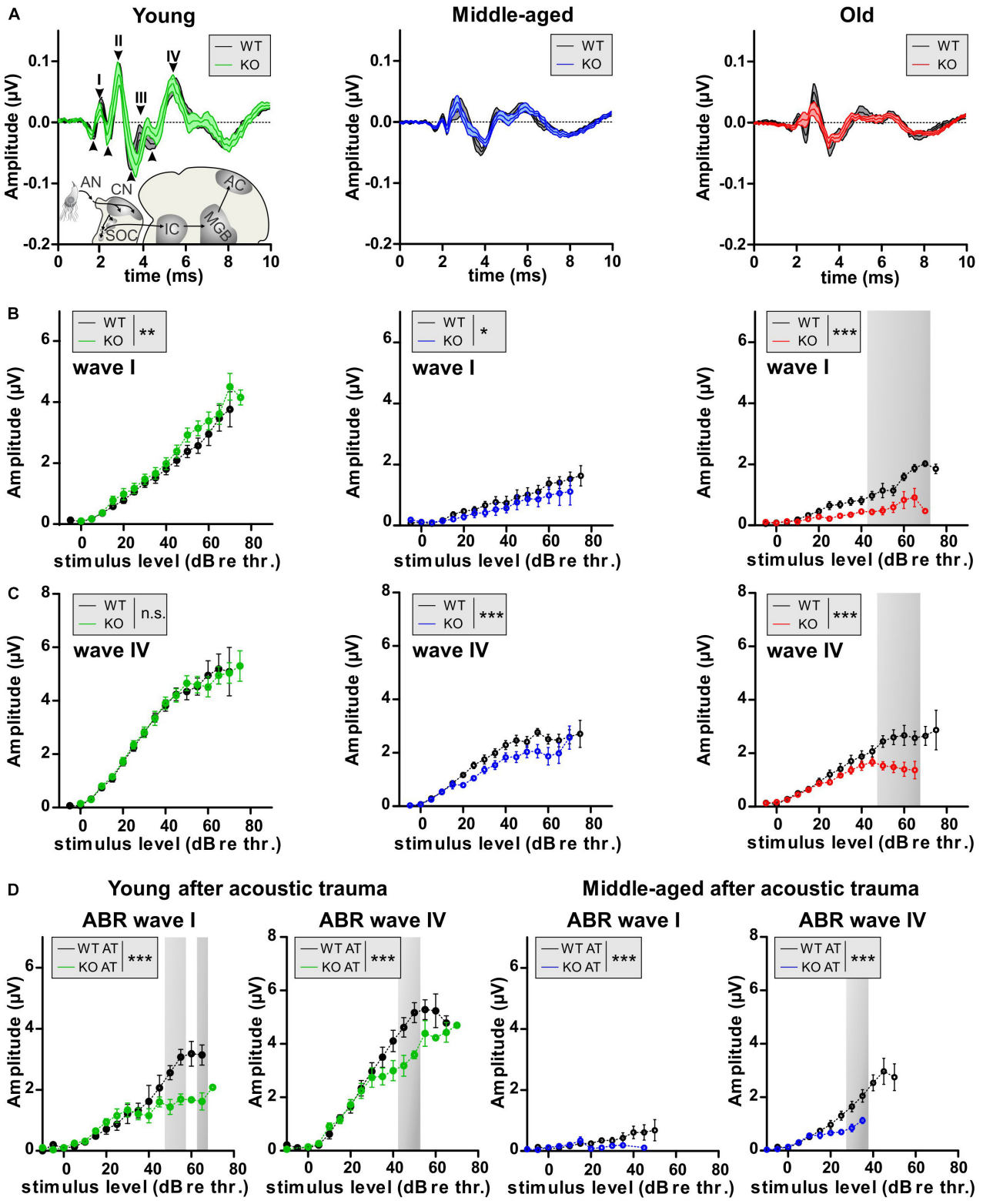

FIGURE 5 | Auditory nerve and brainstem response amplitudes in GC-A WT and KO mice. **(A)** ABR waveform, indicating ABR wave I peak-to-peak amplitude 40 dB above the hearing threshold. Mean ± SEM. **(B)** The noise-burst evoked ABR wave I as a measure of the summed activity of auditory-nerve fibers assessed to investigate the effect of GC-A gene disruption on auditory-nerve responses in mice before noise exposure. Noise-burst-evoked ABR wave I amplitude growth functions were affected in GC-A KO mice (young: green, middle-aged: blue, old: red) in all three age groups compared with WT mice (all ages: black) before noise

(Continued)

FIGURE 5 | Continued
exposure [young: two-way ANOVA, $F(1,374) = 10.57$, $P = 0.0013$, $n = 8/16$ mice/ears each; middle-aged: two-way ANOVA, $F(1,247) = 5.38$, $P = 0.0212$, WT $n = 6/12$ mice/ears KO $n = 5/10$ mice/ears, old: two-way ANOVA, $F(1,255) = 82.55$, $P < 0.0001$, WT $n = 7/14$ mice/ears KO $n = 5/10$ mice/ears]. **(C)** Noise-burst-evoked ABR wave IV amplitude growth functions were decreased in middle-aged and old GC-A KO mice, but not young GC-A KO mice compared to WT mice before noise exposure [young: two-way ANOVA, $F(1,362) = 0.00$, $P = 0.9568$, $n = 8/16$ mice/ears each; middle-aged: two-way ANOVA, $F(1,462) = 32.21$, $P < 0.0001$, WT $n = 11/21$ mice/ears KO $n = 10/20$ mice/ears, old: two-way ANOVA, $F(1,269) = 43.28$, $P < 0.0001$, WT $n = 7/14$ mice/ears each]. **(D)** 7 days after acoustic trauma, noise-burst-evoked ABR wave I amplitude growth functions were more decreased in young and middle-aged GC-A KO mice than in WT mice [young: two-way ANOVA, $F(1,117) = 36.46$, $P < 0.0001$, WT $n = 3/6$ mice/ears KO $n = 4/8$ mice/ears; middle-aged: two-way ANOVA, $F(1,105) = 4.84$, $P = 0.0300$, $n = 5/10$ mice/ears each]. **(E)** ABR wave IV amplitudes were also more decreased in young and middle-aged GC-A KO mice compared to WT mice 7 days after noise exposure [young: two-way ANOVA, $F(1,113) = 17.20$, $P < 0.0001$, WT $n = 3/6$ mice/ears KO $n = 4/8$ mice/ears; middle-aged: two-way ANOVA, $F(1,108) = 17.58$, $P < 0.0001$, WT $n = 5/10$ mice/ears KO $n = 6/12$ mice/ears]. Mean ± SEM. $^{*}P < 0.05$; $^{**}P < 0.01$; $^{***}P < 0.001$.

analyzed 7 days post AT-induction. In young and middle-aged GC-A KO mice, the AT-induced reduction in ABR wave I and IV amplitudes was more pronounced than in WT littermates (**Figure 5D**).

Overall, this indicated that, unlike effects on OHCs (**Figures 3**, **4** and **Supplementary Figure S1**), GC-A gene disruption accelerated age-dependent auditory-nerve vulnerability and aggravated the effect of AT.

The GC-A effect on IHC synaptopathy was analyzed through staining of IHC ribbons with antibodies directed against the RIBEYE protein CtBP2. Its numbers at IHC presynaptic sides can be used as an approximate metric for the number of IHC afferent synapses (Kujawa and Liberman, 2009; Buran et al., 2010). IHC ribbon numbers in $n = 3$ or 4 animals ($n = 6$ or 8 ears) from each group were quantified in individual cochlear turns as described (Möhrle et al., 2016, 2017). The IHC ribbons in basal/midbasal turns declined with advancement in age in GC-A WT mice (**Figure 6**, basal turn, black bars), which has also been observed in previous studies (Kujawa and Liberman, 2009; Sergeyenko et al., 2013; Möhrle et al., 2016). The IHC ribbon numbers in basal and mid-basal cochlear turns of middle-aged and old GC-A KO mice was reduced in comparison to those in WT mice (**Figures 6A,B** and **Table 2E**). Already in young GC-A KO mice, a reduction in IHC ribbons was seen in mid-basal and basal cochlear turns (**Figures 6A,B**), although at that age, the IHC ribbon numbers in apical cochlear turns of GC-A KO mice were augmented (**Figure 6C**). Consistently, ABR wave I was not yet reduced at that age but even slightly enhanced (**Figure 5B**), suggesting that lower frequency cochlear regions might contribute to ABR wave I generation in response to noise-burst stimuli. In the apical cochlear turn, the GC-A KO mice still had an equal number of synaptic ribbons when compared to the WT (**Figure 6C**), even though the amplitudes of the ABR wave I were smaller than in the GC-A WT mice. This indicated that IHC ribbons cease to function properly before the reduction of CtBP2 protein becomes obvious from histology. Expression studies on postsynaptic markers should be considered in future experiments. In GC-A KO mice, AT led to a further loss in IHC ribbon number in these turns. For example, this is illustrated for CtBP2 immunostained IHCs in basal cochlear turns from middle-aged GC-A WT mice and GC-A KO mice, with or without AT (**Figure 6D**).

Looking on IHC and auditory fibers, GC-A KO mice exhibit IHC synaptopathy and auditory neuropathy that is most pronounced for higher-frequency regions and that progresses over age and with AT.

GC-A Mediated Poly (ADP-Ribose) Polymerase (PARP) Activity in the Organ of Corti and SG

To link the damaging effects of GC-A gene disruption on hair cell function with potential downstream effectors of the cGKI pathway, we studied the presence of PAR polymers, which were previously shown to be activated by elevated cGMP in cochlear hair cells (Jaumann et al., 2012). Cochleae of young GC-A WT and KO animals were analyzed before and after AT for possible differences in intracellular accumulation of PAR, with six ears from three animals judged by six persons in blind evaluations, and PAR was found to be either elevated or reduced in GC-A KO mice relative to GC-A WT mice (**Figure 7E**). In GC-A WT mice, a ubiquitous basal level of PAR was observed in nuclei of OHCs and IHCs, supporting the presence of Deiters' cells (DCs) (**Figure 7A**, left panel) and SGN or satellite cells (SCs), respectively (**Figure 7C**, left panel). In OHCs, sham GC-A KO mice exhibited a decline in PARP activity in mid-basal and basal cochlear turns compared with GC-A WT mice (**Figures 7A,E**, left panel) but not in apical turns (not shown). After AT, the PAR accumulation in OHCs of GC-A KO mice was only reduced in the mid-basal turn compared to that in GC-A WT mice (**Figures 7B,E**, right panel). Reduced PARP activity, reduced DPOAE I/O, and reduced KCNQ4 surface expression were observed in young GC-A KO mice and may thus be regarded as an endogenous convergent downstream target of the GC-A-induced cGMP signaling pathway in OHCs. In IHCs or SGN/SCs from GC-A KO mice, a decline in PAR staining intensity was observed in mid-frequency cochlear turns as shown for IHCs in mid-basal turns (**Figures 7A,E**, left panel) or SGN/SCs in basal and mid-basal turns (**Figures 7C,E**, left panel).

However, in contrast to PAR in OHCs, at the IHC/SGN level, PAR staining decreased in GC-A KO mice compared with WT mice after AT, as shown for IHCs in basal and mid-basal cochlear turns (**Figures 7B,E**, right panel) and SGNs/SCs in mid-basal turns after trauma (**Figures 7D,E**).

The experiment could confirm that GC-A KO mice exhibit a differential reduction in PAR staining, likely caused by a decrease in PARP activity in OHCs and at the IHC, SGN, and SC level. The PARP-1 decline at the IHC/SGN level in GC-A KO mice may be

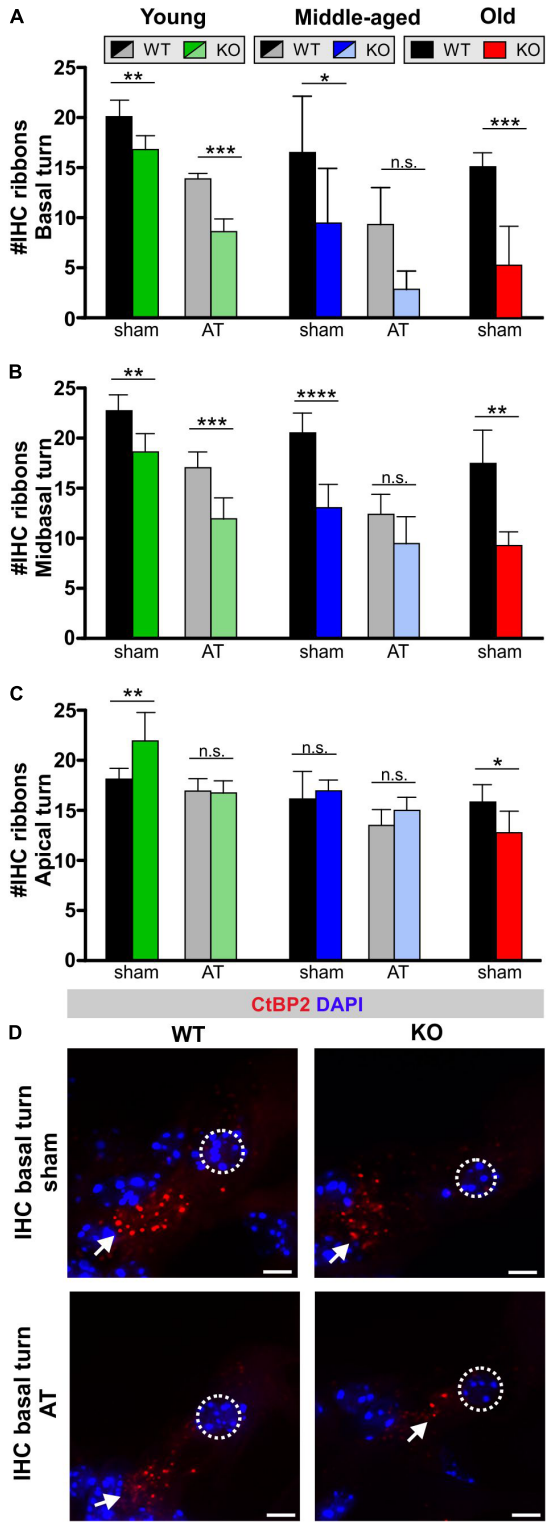

FIGURE 6 | Inner hair cell ribbons in GC-A WT and KO mice 7 days after sham treatment or acoustic trauma. **(A)** Ribbon-synapse numbers of IHCs in the basal cochlear turn after sham exposure and acoustic trauma [young: two-way ANOVA, Genotype: $F(1,20) = 65.9$, $P < 0.0001$; AT: $F(1,20) = 185.69$, $P < 0.0001$, *post hoc* test: sham WT vs. sham KO

(Continued)

FIGURE 6 | Continued

$P < 0.001$, AT WT vs. AT KO $P < 0.0001$; middle-aged: two-way ANOVA, Genotype: $F(1,23) = 15.40$, $P = 0.0007$; AT: $F(1,23) = 14.96$, $P = 0.0008$, *post hoc* test: sham WT vs. sham KO $P < 0.05$, AT WT vs. AT KO $P > 0.05$; old: unpaired two-tailed student's *t*-test, $t(5) = 5.811$, $P < 0.0002$]. **(B)** Ribbon-synapse numbers of IHCs in the mid-basal cochlear turn after sham exposure and acoustic trauma [young: two-way ANOVA, Genotype: $F(1,21) = 74.62$, $P < 0.0001$; AT: $F(1,21) = 41.97$, $P < 0.0001$, *post hoc* test: sham WT vs. sham KO $P < 0.01$, AT WT vs. AT KO $P < 0.0001$; middle-aged: two-way ANOVA, Genotype: $F(1,25) = 47.12$, $P < 0.0001$; AT: $F(1,25) = 37.21$, $P < 0.0001$, Interaction: $F(1,25) = 6.926$, $P = 0.0143$, *post hoc* test: sham WT vs. sham KO $P < 0.0001$, AT WT vs. AT KO $P > 0.05$; old: unpaired two-tailed student's *t*-test, $t(10) = 5.580$, $P < 0.0002$]. **(C)** Ribbon-synapse numbers of IHCs in the apical cochlear turn after sham exposure and acoustic trauma [young: two-way ANOVA, Genotype: $F(1,20) = 19.49$, $P = 0.0003$; AT: $F(1,20) = 6.307$, $P = 0.0207$, Interaction: $F(1,20) = 7.510$, $P = 0.0126$, *post hoc* test: sham WT vs. sham KO $P < 0.01$, AT WT vs. AT KO $P > 0.05$; middle-aged: two-way ANOVA, Genotype: $F(1,24) = 11.41$, $P = 0.0025$; $F(1,24) = 2.740$, $P = 0.1109$, *post hoc* test: sham WT vs. sham KO $P > 0.05$, AT WT vs. AT KO $P > 0.05$; old: unpaired two-tailed student's *t*-test, $t(10) = 2.791$, $P = 0.0191$]. Mean ± SD. $^*P < 0.05$; $^{**}P < 0.01$; $^{***}P < 0.001$; $^{****}P < 0.0001$. **(D)** IHC ribbon synapses with afferent auditory neurons were stained by antibodies against CtBP2/RIBEYE. Immunopositive dots were counted to estimate the number of auditory nerve fiber synapses per IHC. The effect of GC-A gene disruption on IHC ribbon counts was analyzed in young, middle-aged and old mice. Arrows indicate a reduced number of CtBP2/RIBEYE-positive dots at the basal pole of IHCs. Nuclei were stained with DAPI (blue). Scale bars: 5 μm.

part of the observed functional changes in GC-A KO mice at the auditory-nerve and IHC ribbon-synapse level.

Thus far, the overall conclusion relies on GC-A-induced protective activities at the OHC level being independent of aging (and AT), while the GC-A-induced protective activities at the IHC/SGN level, reflected in ABR wave I changes, show evidence of being reinforced with age (or AT). To validate this idea, we analyzed the progression of age-related hearing loss in GC-A WT and KO mice for OHC function measured as DPOAE (**Figures 8A,B** and **Table 2F**) or IHC function measured as ABR wave I (**Figure 8C**). While GC-A KO mice exhibit the same aging process regarding OHC function measured with DPOAE I/O function in response to pure-tone sounds at f1 = 5.6 and 11.3 kHz (**Figures 8A,B**), the reduction in auditory-nerve responses was greater in GC-A KO mice as age increased (**Figure 8C**).

In summary, these findings point to hair-cell-specific GC-A expression and function acting differentially in OHCs and IHCs during aging. OHC electromechanical properties in high-frequency cochlear turns are already diminished at a young age in the absence of GC-A, when KCNQ4 surface expression or PARP-1 levels are also reduced. Thereby, ANP and BNP, both expressed in OHCs, can act on GC-A in OHCs in an autocrine or paracrine manner. The data demonstrate that GC-A possibly maintains basic OHC function through cGMP/cGKI/cyclic AMP response-element binding (CREB), or PARP signaling independent of aging or AT (**Figure 9**). In contrast, at the IHC level, paracrine activation of GC-A signaling, possibly also through cGMP/cGKI/PARP, in SG feed-back to IHC nerve terminals and summed auditory nerve (ABR wave I) responses protects against noise/age-dependent hearing loss (**Figure 9**, IHC and SGN).

DISCUSSION

In the present study, we identified the particulate GC-A receptor (also named NPR-A) as an upstream regulator of otoprotective cGMP activities. We recognized hair-cell-specific differences in GC-A function in IHCs and OHCs with respect to normal hearing, aging, and AT-induced injury. In line with our hypothesis, we present clear evidence that GC-A receptor ligands have a crucial function for maintaining OHC's and IHC's pre-postsynaptic integrity, particularly in high-frequency cochlear turns. The therapeutic value of these findings is significant, since neprilysin-inhibitors (the peptidase responsible for degrading ANP and BNP, which are ligands for GC-A) are safe and well-tolerated drugs already used for chronic therapy in heart-failure patients (Feygina et al., 2019).

Expression of GC-A and Its Ligands in the Cochlea

Using isolated hair cells and SG of the mature cochlea, we identified the NPs ANP and BNP as well as GC-A in OHCs and SG and confirmed the presence of NPs in IHCs, corroborating previous studies (Meyer zum Gottesberge et al., 1991; Yoon and Anniko, 1994; Suzuki et al., 1998, 2000; Kuhn, 2003, 2009; Schulz, 2005; Kemp-Harper and Feil, 2008; Kleppisch and Feil, 2009; Alexander et al., 2011; Qiao et al., 2011; Sun et al., 2013, 2014; Shen et al., 2015; Möhrle et al., 2017; Fitzakerley and Trachte, 2018). We could not detect GC-A in IHCs. This suggests a possible autocrine or paracrine NP/GC-A effect on OHCs and SG, whereas GC-A affects IHC synapses, likely indirectly through retrograde signaling from SGNs on IHCs. Retrograde signaling between the IHC presynapse and auditory nerve postsynapse (Kujawa and Liberman, 2009) is suggested from AT-induced damage of IHC pre- and postsynapses, possibly including signaling cascades from SCs (Sugawara et al., 2005; Wan et al., 2014).

GC-A KO Mice Exhibit OHC Impairment Independent of Acoustic Trauma and Aging

In the present study, GC-A KO mice were shown to exhibit a normal hearing threshold, reflected through normal thresholds of DPOAEs. However, already at young ages, the shallow growth of the DPOAE I/O function (**Figure 3**) indicated a loss of OHC electromotility in response to higher frequency (11.3 kHz) stimuli. This phenotype of GC-A KO mice was not aggravated after AT (**Figure 4**) or with aging (**Figure 8**). This suggests that GC-A in OHCs exhibits endogenous, basal otoprotective activity. If this is lost, OHCs lose their proper functional phenotype. GC-A/cGMP signaling may maintain the functional OHC phenotype through different downstream cascades:

(i) Already at a young age, GC-A KO mice had developed diminished electromechanical properties of OHCs; not, however, at threshold, but at higher sound levels in high-frequency cochlear regions, where a stronger K^+ influx through the stereocilial MET-channels needs to be managed. This was associated with a visible loss of KCNQ4 type K^+ channels on

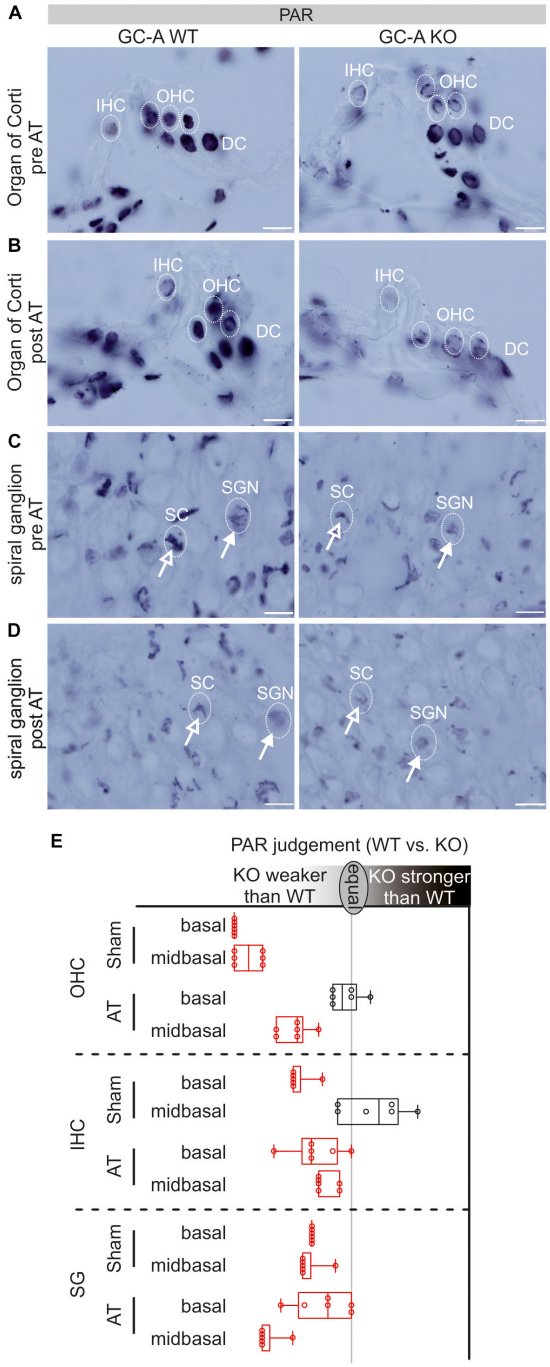

FIGURE 7 | PAR-staining in organ of Corti and SG in GC-A WT and KO mice pre and post acoustic trauma. **(A)** Reduced PAR-staining of OHC nuclei but not DCs in the GC-A KO mouse. No difference was found for IHC in mid-basal turns. **(B)** After acoustic trauma, a reduction of PAR (not significant) was shown for IHC and OHCs in the GC-A KO mice, compared to WT. **(C)** PAR-staining in SG of SGNs (closed arrow) and satellite cells (SCs, open arrow) in sham-exposed GC-A WT and KO mice. **(D)** After acoustic trauma, GC-A KO animals had weaker PAR-staining of SCs and SGNs than WT mice. Scale bars: 10 μm. **(E)** Quantification of PAR-staining in OHC, IHC, and SG as evaluated by six independent referees; red colors indicate a reduction of PAR in GC-A. Boxplot shows median ± quartiles; whiskers mark the whole range.

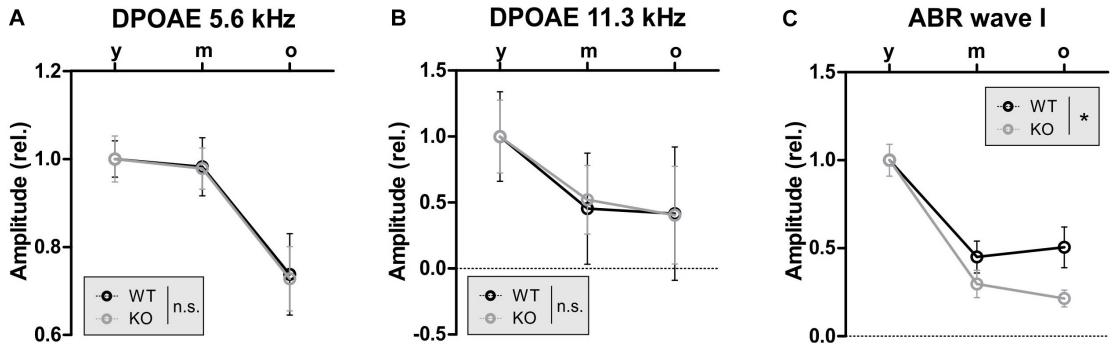

FIGURE 8 | GC-A KO exhibit the same aging progress in OHC function as GC-A WT but accelerated reduction of auditory nerve responses over age. **(A,B)** DPOAE signal growth function in response to pure-tone sounds at f1 = 5.6 and 11.3 kHz were similarly reduced over age in GC-A KO and WT mice [5 kHz: two-way ANOVA, $F(1,106) = 0.01$, $P = 0.928$, n = 8–14/16–28 mice/ears each, 11 kHz: two-way ANOVA, $F(1,106) = 0.00$, $P = 0.951$, n = 8–14/16–28 mice/ears each]. **(C)** Noise-burst-evoked ABR wave I amplitude growth functions were more strongly reduced over age in GC-A KO than in WT mice [two-way ANOVA, $F(1,71) = 4.72$, $P = 0.0033$, n = 5–8/10–16 mice/ears each]. Mean ± SEM. $^*P < 0.05$.

the surface OHC membranes. KCNQ4 channels mediate the major OHC K^+ current $I_{K,n}$ at rest and thus determine the membrane potential and time constant (Housley and Ashmore, 1992; Marcotti and Kros, 1999; Kharkovets et al., 2000, 2006). When KCNQ4 is not functional in OHCs, e.g., in non-syndromic autosomal dominant (DFNA2) patients or mouse models with mutation of KCNQ4 (Jentsch, 2000; Kharkovets et al., 2000; Gao et al., 2013), progressive high-frequency hearing loss linked to OHC loss develops. Furthermore, dysfunction of KCNQ4 contributes to noise- and age-dependent high-frequency hearing loss (Van Eyken et al., 2006). Questioning how GC-A may influence KCNQ4 surface expression, the obvious need for fast repolarization of OHCs following intense and high-frequency stimulation, to keep KCNQ4 proteins in place, should be considered. The function of the big potassium (BK) channel is known to be associated with maintenance of KCNQ4 channel expression (Rüttiger et al., 2004). BK is typically activated through efferent inhibition of OHCs that works via the unusual combination of Ca^{2+} influx through the acetylcholine receptor AChRa9/10 (Weisstaub et al., 2002). AChRa9/10 mediates Ca^{2+} influx that leads to BK activation, which triggers K^+ conductance (Oliver et al., 2000; Maison et al., 2013). Indeed, large-conductance BK channels can be activated through cGMP/cGKI-induced phosphorylation (Zhou et al., 2010; Kyle et al., 2013), providing a mechanism by which endogenous GC-A/cGMP activities might contribute to maintaining stable OHC function in high-frequency regions under high sound intensities (**Figure 9**) (Rüttiger et al., 2004; Beisel et al., 2005; Engel et al., 2006). As posttraumatic loss of KCNQ4 in OHCs was prevented by elevation of cGMP levels through PDE5 inhibition with vardenafil (Jaumann et al., 2012), cGMP was predicted to rescue OHCs by maintaining OHC membrane potential and membrane time constants in high-frequency regions during exposure to traumatic sound intensities (Jaumann et al., 2012). However, here, we observed a GC-A effect independent of AT and age in OHCs, suggesting that a GC-A-independent cGMP generator pathway, in addition to GC-A/cGMP/cGKI signaling, may contribute to aging and AT vulnerability in OHCs.

(ii) Alternatively, GC-A/cGMP/cGKI-induced signaling may positively influence OHC stability through phosphorylation of the transcription factor CREB as previously described (Fiscus, 2002). A well-known downstream target of CREB is PARP-1, a polymerase mediating PolyADP-ribosylation. PAR polymers are products of PARP activity, which has been shown to be involved in DNA repair and transcriptional activity in a cGMP- and cGKI-dependent manner, independent of CREB (Kim et al., 1999; Paquet-Durand et al., 2007). PARP was also shown to be directly activated by cGMP (Paquet-Durand et al., 2007; Sahaboglu et al., 2010). CREB and cGMP-induced activation of PARP is suggested to exhibit survival and anti-aging potential (Beneke and Burkle, 2007). During this process, enhanced cell stability or survival induced by activated PARP was suggested to be based on the counteracting of ongoing cellular DNA breaks by PARP, which facilitates transcription, replication, and DNA base-excision repair (Yu et al., 2006).

In conclusion, a reduction in KCNQ4 and PARP in OHCs was observed in young GC-A KO mice in comparison to GC-A WT mice. Both KCNQ4, via BK activation, and PARP-1 activity may be part of endogenous GC-A/cGMP-induced protective signaling cascades that help maintain the basal OHC phenotype and function following AT during metabolically demanding conditions.

GC-A KO Mice Exhibit Enhanced IHC Synaptopathy and Auditory Neuropathy in Response to Acoustic Trauma and Aging

In contrast to OHCs, where the negative effect of GC-A gene disruption is not reinforced by AT or aging, the impact of GC-A inactivation on IHC synapses and SGN integrity was more pronounced following AT and over the lifespan. The absence of GC-A expression in isolated IHCs suggests that the observed age- and AT-induced reductions in ribbon numbers in IHC

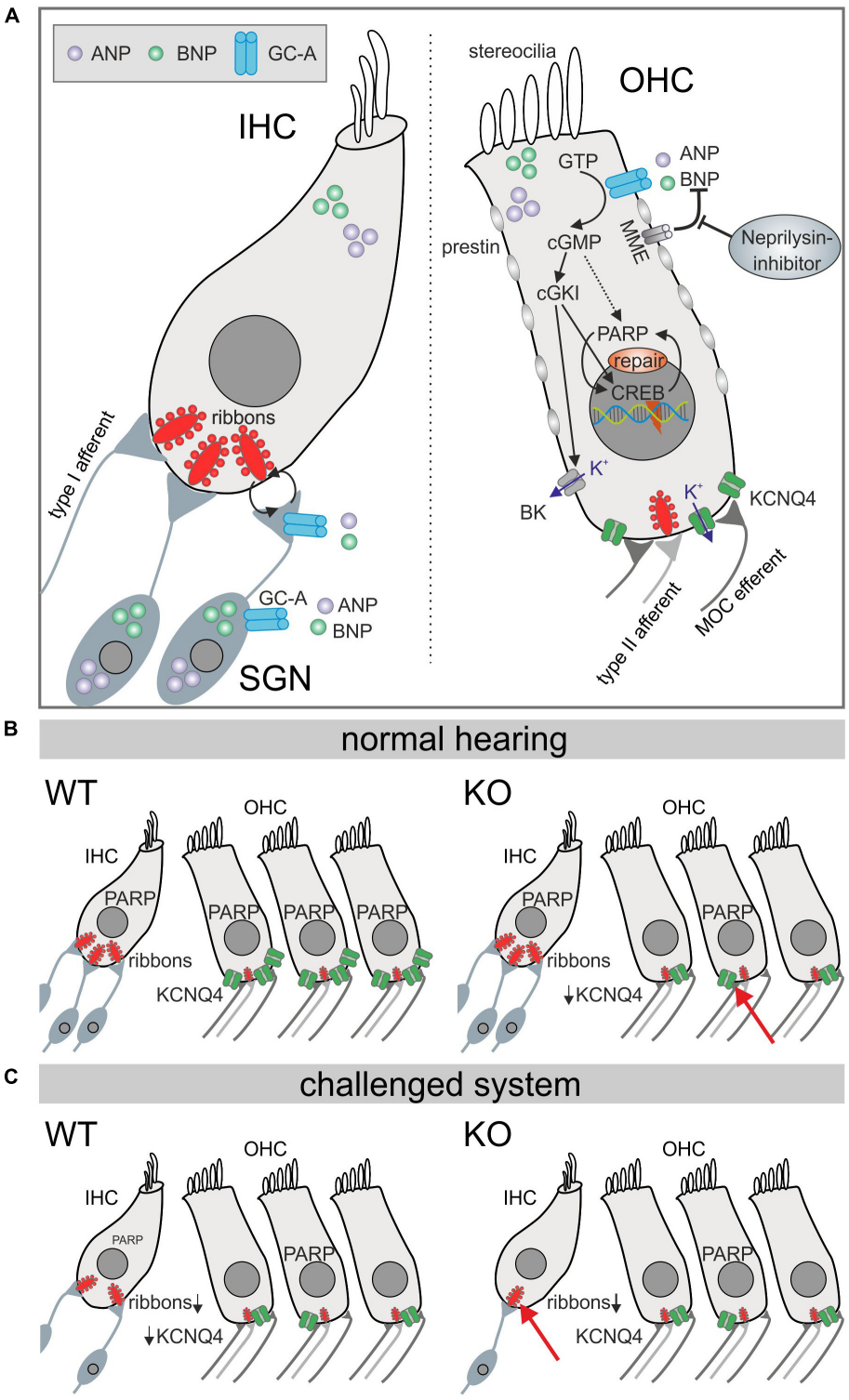

FIGURE 9 | Diagram illustrating GC-A/cGMP signaling mechanisms in auditory hair cells. **(A)** Summery of GC-A dependent intercellular signaling in IHC, OHC, and SGNs. The natriuretic peptides ANP (violet) and BNP (bright green) both bind to the membrane bound GC-A (blue) in OHCs or the SGN and activate a cGMP dependent cascade that ends in PARP increase. The effects in IHCs are due to pre- and postsynaptic integrity. **(B)** In the basic hearing situation, the number of IHC ribbons is not reduced in GC-A KOs, but in OHCs, KCNQ4 is impaired which leads to a functional phenotype measureable in DPOAE growth functions. **(C)** However, in the challenged system after acoustic overexposure or in aged animals, the number of IHC ribbons is more reduced in GC-A KO mice compared with WT which is correlated with a decreased ABR wave I amplitude, while OHCs are unaffected.

synapses in GC-A KO mice occur secondarily through damage of SGNs. Postsynaptic excitotoxicity events are suggested to lead to deafferentation during age- and NIHL (Pujol and Puel, 1999; Kujawa and Liberman, 2009). SC signaling (Sugawara et al., 2005) may secondarily affect IHC synapses in a similar manner, as we predicted here for IHC synapse damage in GC-A KO mice. Although we cannot exclude subthreshold expression of GC-A that remained undetected in IHCs, the present study argues on the assumption that IHC synapse damage in GC-A KO mice is the result of a GC-A/cGMP/cGKI/PARP cascade in SG.

In GC-A KO mice, auditory neuropathy is reflected as a loss of IHC ribbons in higher-frequency cochlear turns. This loss is associated with a reduction in the summed response of the auditory nerve (ABR wave I amplitude), indicating an auditory neuropathy in GC-A KO mice that is most pronounced in middle-aged and old mice and after AT. In young GC-A KO mice, the number of IHC synaptic ribbons in high-frequency cochlear regions was already reduced. This decline was not yet translated to reduced auditory-nerve responses, but was already accompanied by reduced PAR in the SG in these regions (**Figure 8**). If the observed worsening and acceleration of IHC synapse damage and loss of ABR wave I amplitude after AT and during aging in GC-A KO mice is reflected in altered PAR accumulation, this would need further inspection.

In conclusion, this finding reveals a clear role for GC-A ligands in maintaining basic IHC synapse function and pre- and postsynaptic integrity of IHC in high-frequency cochlear regions during aging and AT. The metabolic sensitivity of IHC synapses and their contribution to hidden and age-dependent hearing loss is thereby confirmed (Keithley, 2019; Lee et al., 2019). This also confirms our initial hypothesis that GC-A ligands act as possible key regulators of energy consumption and metabolism to maintain hearing function.

Considerations of the Therapeutic Value of GC-A Signaling

Based on these results, future studies should focus on the potential of enhancing ANP/GC-A/cGMP signaling for restoration of normal hearing to counteract hidden hearing loss and IHC synaptopathy, as well as age-related hearing loss or NIHL. Here, efforts to stimulate GC-A through the ligand ANP may be particularly promising because (i) ANP levels in endolymph are two orders of magnitude higher than in plasma (Yoon et al., 2012); (ii) the ANP-producing serine protease corin is expressed in the cochlea, indicating that cochlear cells are capable of converting proANP to ANP (Labine et al., 2015; Fitzakerley and Trachte, 2018); and (iii) preliminary studies pointed to a transient improvement in hearing thresholds following systemic ANP administration (Yoon et al., 2015).

Alternatively, stimulation with the GC-A ligand BNP may be considered. While BNP was not found to be expressed in the cochlea (Fitzakerley and Trachte, 2018), the present study clearly indicates BNP expression in hair cells and SG of the adult murine cochlea. Interestingly, in this context, BNP has been shown to increase the open probability of BK channels and to suppress the membrane excitability of small-sized dorsal-root-ganglion neurons (Li et al., 2016). As BK is stimulated through cGKI signaling (Zhou et al., 1998; Frankenreiter et al., 2017) and BK channel activation is predicted to possibly counteract excitotoxic events in hair cells (Rüttiger et al., 2004; Engel et al., 2006, see above), a BNP/GC-A/cGMP/cGKI/BK cascade may also contribute to the observed GC-A otoprotective functions.

Moreover, because the cGMP-degrading enzyme PDE9a might be a target for drugs that increase cGMP pools that are predominantly controlled by ANP/GC-A (Lee et al., 2015), we searched for and found PDE9a expression in the cochlea. Therefore, PDE9a inhibitors should be included as potential pharmaceutical drug candidates for the inner ear in future studies.

Finally, inhibition of the NP-degrading enzymes, e.g., membrane metalloendopeptidase (MME) (also called neprilysin or neutral endopeptidase), that typically reduce cGMP production through GC-A should be considered. Indeed, MME mRNA was found to be expressed in hair cells and possibly in SG (Shen et al., 2015; Fitzakerley and Trachte, 2018), but the protective potential of MME inhibition against AT or age-dependent hearing loss has not yet been tested.

Hypertension in GC-A KO Mice

GC-A KO mice develop arterial hypertension (Kuhn, 2005). Whether arterial hypertension itself may contribute to age-related hearing loss is still controversial (Przewozny et al., 2015; Soares et al., 2016; Reed et al., 2019). Although we cannot exclude the possibility that glucose metabolism may be altered in the GC-A KO mice, and consequently affect hearing, other mouse mutants with hypertension (NO-GC KO mice) have normal and persisting hearing function (Friebe et al., 2007; Möhrle et al., 2017). However, it is advisable to consider whether proper blood flow and glucose metabolism participates in the age- and AT-related pre- and postsynaptic deficits observed here in GC-A KO mice. A normal metabolic supply is required for sustained and untiring vesicle release, particularly in high-frequency cochlear regions. The use of tissue-specific KO mouse mutants may help to avoid the hypertensive phenotype in future studies.

CONCLUSION

The present longitudinal study of GC-A KO mice strongly supports our initial hypothesis that GC-A signaling may contribute to the metabolic supply of OHCs. Thus, we could demonstrate that GC-A maintains endogenous OHC stability, and contributes to AT- and age vulnerability of IHC and auditory-nerve function. The protective GC-A effect on hearing thereby differs profoundly from that of GC-B and NO-GC. The deletion of GC-B leads to diminished temporal auditory processing likely through affecting efferent feedback loops (Wolter et al., 2018). In contrast, the loss of NO-GC may have positive effects: The deletion of NO-GC subtype 1 and 2 leads to slight protection of OHCs, IHCs, and auditory nerve function after noise damage (Möhrle et al., 2017). In conclusion, the observed otoprotective functions of elevated cGMP levels previously achieved through PDE 5 inhibition (Jaumann et al., 2012) may have a major

GC-A contribution. Augmenting NP/GC-A signaling should be considered as a protective therapy for hearing preservation.

DATA AVAILABILITY STATEMENT

The raw data supporting the conclusions of this article will be made available by the authors, without undue reservation, to any qualified researcher.

ETHICS STATEMENT

Animal care, procedures, and treatments were performed in accordance with institutional and national guidelines following approval by the University of Tübingen, Veterinary Care Unit, and the Animal Care and Ethics Committee of the regional board of the Federal State Government of Baden-Württemberg, Germany, and followed the guidelines of the EU Directive 2010/63/EU for animal experiments.

AUTHOR CONTRIBUTIONS

PM, DM, MaK, and LR contributed to conceptualization and writing. PM, DM, and LR contributed to analysis. PM, DM, PE, KR, SW, AT, IL, and MW contributed to investigation. MaK and LR contributed to supervision. RF, JE, FP-D, MiK, LR, and MaK contributed to review and editing.

FUNDING

This work was funded by the Deutsche Forschungsgemeinschaft [DFG, German Research Foundation; FOR 2060 project RU 713/3-2 (PE, KR, and SW), project FE 438/6-1 (MW), Projektnummer 335549539/GRK2381 (PM), and PP1608 project En194/5-6,7 (IL)], transmed H2020-MSCA-765441 (AT), Fortüne 2339-0-0 (University of Tübingen, Tübingen, Germany; KR).

ACKNOWLEDGMENTS

We thank Hyun-Soon Geisler, Karin Rohbock, and Iris Köpschall for excellent technical assistance and Frank Schweda and Karina Gültig for kindly providing their mouse lines. Language services were provided by stels-ol.de.

SUPPLEMENTARY MATERIAL

The Supplementary Material for this article can be found online at: https://www.frontiersin.org/articles/10.3389/fnagi.2020.00083/full#supplementary-material

FIGURE S1 | Slopes of growth functions of DPOAE signals and regressions on DPOAEs loss in GC-A WT and GC-A KO mice. **(A)** Shifts of DPOAE signal growth functions in response to pure-tone sounds at f1 = 5.6 kHz (left panel) were similar between GC-A KO and WT mice [two-way ANOVA, $F(1,121) = 0.03$, $P = 0.8693$, WT $n = 3/6$ mice/ears KO $n = 4/7$ mice/ears], while GC-A KO mice had smaller shifts after acoustic trauma for pure-tone sounds with f1 = 11.3 kHz [middle panel, two-way ANOVA, $F(1,180) = 6.06$, $P = 0.0148$, WT $n = 3/6$ mice/ears KO $n = 4/8$ mice/ears]. **(B)** To normalize the DPOAE I/O shift for respective frequencies, and to account for genotype differences preceding acoustic trauma induction, the regression between the measured DPOAE signal (in dB SPL) after acoustic trauma and the loss of DPOAE signal (in dB SPL) was calculated. The regression lines were not different between GC-A WT and KO mice with f1 = 5.6 kHz [left panel: unpaired two-tailed student's *t*-test $t(183) = 0.226$, $P = 0.98$, WT $n = 85$ KO $n = 102$] and 11.3 kHz [middle panel: unpaired two-tailed student's *t*-test $t(69) = 0.027$, $P = 0.98$, WT $n = 28$ KO $n = 45$], indicating similar relative loss of slope of the DPOAE I/O function. Mean ± SEM.

REFERENCES

Alexander, S. P., Mathie, A., and Peters, J. A. (2011). Guide to receptors and channels (GRAC), 5th edition. *Br. J. Pharmacol.* 164(Suppl. 1), S1–S324. doi: 10.1111/j.1476-5381.2011.01649_1.x

Beisel, K. W., Rocha-Sanchez, S. M., Morris, K. A., Nie, L., Feng, F., Kachar, B., et al. (2005). Differential expression of KCNQ4 in inner hair cells and sensory neurons is the basis of progressive high-frequency hearing loss. *J. Neurosci.* 25, 9285–9293. doi: 10.1523/jneurosci.2110-05.2005

Beneke, S., and Burkle, A. (2007). Poly(ADP-ribosyl)ation in mammalian ageing. *Nucleic Acids Res.* 35, 7456–7465. doi: 10.1093/nar/gkm735

Buran, B. N., Strenzke, N., Neef, A., Gundelfinger, E. D., Moser, T., and Liberman, M. C. (2010). Onset coding is degraded in auditory nerve fibers from mutant mice lacking synaptic ribbons. *J. Neurosci.* 30, 7587–7597. doi: 10.1523/JNEUROSCI.0389-10.2010

Burkard, R. F., and Don, M. (2007). "The auditory brainstem response," in *Auditory Evoked Potentials: Basic Principles and Clinical Application*, eds R. F. Burkard, M. Don, and J. J. Eggermont, (Baltimore, MD: Lippincott Williams & Wilkins), 229–250.

Chen, Y., and Burnett, J. C. (2018). Particulate Guanylyl Cyclase A/cGMP signaling pathway in the kidney: physiologic and therapeutic indications. *Int. J. Mol. Sci.* 19, E1006. doi: 10.3390/ijms19041006

Chumak, T., Rüttiger, L., Lee, S. C., Campanelli, D., Zuccotti, A., Singer, W., et al. (2016). BDNF in lower brain parts modifies auditory fiber activity to gain fidelity but increases the risk for generation of central noise after injury. *Mol. Neurobiol.* 53, 5607–5627. doi: 10.1007/s12035-015-9474-x

Dornhoffer, J. L., Danner, C., Zhou, L., and Li, S. (2002). Atrial natriuretic peptide receptor upregulation in the rat inner ear. *Ann. Otol. Rhinol. Laryngol.* 111, 1040–1044. doi: 10.1177/000348940211101116

Duncker, S. V., Franz, C., Kuhn, S., Schulte, U., Campanelli, D., Brandt, N., et al. (2013). Otoferlin couples to clathrin-mediated endocytosis in mature cochlear inner hair cells. *J. Neurosci.* 33, 9508–9519. doi: 10.1523/JNEUROSCI.5689-12.2013

El-Badry, M. M., and McFadden, S. L. (2007). Electrophysiological correlates of progressive sensorineural pathology in carboplatin-treated chinchillas. *Brain Res.* 1134, 122–130. doi: 10.1016/j.brainres.2006.11.078

Engel, J., Braig, C., Rüttiger, L., Kuhn, S., Zimmermann, U., Blin, N., et al. (2006). Two classes of outer hair cells along the tonotopic axis of the cochlea. *Neuroscience* 143, 837–849. doi: 10.1016/j.neuroscience.2006.08.060

Fetoni, A. R., Paciello, F., Rolesi, R., Paludetti, G., and Troiani, D. (2019). Targeting dysregulation of redox homeostasis in noise-induced hearing loss: oxidative stress and ROS signaling. *Free Radic. Biol. Med.* 135, 46–59. doi: 10.1016/j.freeradbiomed.2019.02.022

Feygina, E. E., Artemieva, M. M., Postnikov, A. B., Tamm, N. N., Bloshchitsyna, M. N., Medvedeva, N. A., et al. (2019). Detection of Neprilysin-Derived BNP fragments in the circulation: possible insights for targeted neprilysin inhibition therapy for heart failure. *Clin. Chem.* 65, 1239–1247. doi: 10.1373/clinchem.2019.303438

Fiscus, R. R. (2002). Involvement of cyclic GMP and protein kinase G in the regulation of apoptosis and survival in neural cells. *Neurosignals* 11, 175–190. doi: 10.1159/000065431

Fitzakerley, J. L., and Trachte, G. J. (2018). Genetics of guanylyl cyclase pathways in the cochlea and their influence on hearing. *Physiol. Genomics* 50, 780–806. doi: 10.1152/physiolgenomics.00056.2018

Frankenreiter, S., Bednarczyk, P., Kniess, A., Bork, N. I., Straubinger, J., Koprowski, P., et al. (2017). cGMP-elevating compounds and ischemic conditioning provide cardioprotection against ischemia and reperfusion injury via cardiomyocyte-specific BK channels. *Circulation* 136, 2337–2355. doi: 10.1161/CIRCULATIONAHA.117.028723

Friebe, A., Mergia, E., Dangel, O., Lange, A., and Koesling, D. (2007). Fatal gastrointestinal obstruction and hypertension in mice lacking nitric oxide-sensitive guanylyl cyclase. *Proc. Natl. Acad. Sci. U.S.A.* 104, 7699–7704. doi: 10.1073/pnas.0609778104

Frisina, R. D. (2009). Age-related hearing loss: ear and brain mechanisms. *Ann. N. Y. Acad. Sci.* 1170, 708–717. doi: 10.1111/j.1749-6632.2009.03931.x

Frisina, R. D., and Frisina, D. R. (2013). Physiological and neurobiological bases of age-related hearing loss: biotherapeutic implications. *Am. J. Audiol.* 22, 299–302. doi: 10.1044/1059-0889(2013/13-0003)

Fujimoto, C., and Yamasoba, T. (2019). Mitochondria-targeted antioxidants for treatment of hearing loss: a systematic review. *Antioxidants* 8:E109. doi: 10.3390/antiox8040109

Füllgrabe, C., Moore, B. C., and Stone, M. A. (2014). Age-group differences in speech identification despite matched audiometrically normal hearing: contributions from auditory temporal processing and cognition. *Front. Aging Neurosci.* 6:347. doi: 10.3389/fnagi.2014.00347

Furman, A. C., Kujawa, S. G., and Liberman, M. C. (2013). Noise-induced cochlear neuropathy is selective for fibers with low spontaneous rates. *J. Neurophysiol.* 110, 577–586. doi: 10.1152/jn.00164.2013

Gao, Y., Yechikov, S., Vazquez, A. E., Chen, D., and Nie, L. (2013). Impaired surface expression and conductance of the KCNQ4 channel lead to sensorineural hearing loss. *J. Cell Mol. Med.* 17, 889–900. doi: 10.1111/jcmm.12080

Gleich, O., Semmler, P., and Strutz, J. (2016). Behavioral auditory thresholds and loss of ribbon synapses at inner hair cells in aged gerbils. *Exp. Gerontol.* 84, 61–70. doi: 10.1016/j.exger.2016.08.011

Housley, G. D., and Ashmore, J. F. (1992). Ionic currents of outer hair cells isolated from the guinea-pig cochlea. *J. Physiol.* 448, 73–98. doi: 10.1113/jphysiol.1992.sp019030

Jaumann, M., Dettling, J., Gubelt, M., Zimmermann, U., Gerling, A., Paquet-Durand, F., et al. (2012). cGMP-Prkg1 signaling and Pde5 inhibition shelter cochlear hair cells and hearing function. *Nat. Med.* 18, 252–259. doi: 10.1038/nm.2634

Jentsch, T. J. (2000). Neuronal KCNQ potassium channels: physiology and role in disease. *Nat. Rev. Neurosci.* 1, 21–30. doi: 10.1038/35036198

Johnson, D. H., and Kiang, N. Y. (1976). Analysis of discharges recorded simultaneously from pairs of auditory nerve fibers. *Biophys. J.* 16, 719–734. doi: 10.1016/s0006-3495(76)85724-4

Keithley, E. M. (2019). Pathology and mechanisms of cochlear aging. *J. Neurosci. Res.* doi: 10.1002/jnr.24439 [Epub ahead of print].

Kemp-Harper, B., and Feil, R. (2008). Meeting report: cGMP matters. *Sci. Signal.* 1:pe12. doi: 10.1126/stke.19pe12

Kharkovets, T., Dedek, K., Maier, H., Schweizer, M., Khimich, D., Nouvian, R., et al. (2006). Mice with altered KCNQ4 K+ channels implicate sensory outer hair cells in human progressive deafness. *EMBO J.* 25, 642–652. doi: 10.1038/sj.emboj.7600951

Kharkovets, T., Hardelin, J. P., Safieddine, S., Schweizer, M., El-Amraoui, A., Petit, C., et al. (2000). KCNQ4, a K+ channel mutated in a form of dominant deafness, is expressed in the inner ear and the central auditory pathway. *Proc. Natl. Acad. Sci. U.S.A.* 97, 4333–4338. doi: 10.1073/pnas.97.8.4333

Kim, Y. M., Chung, H. T., Kim, S. S., Han, J. A., Yoo, Y. M., Kim, K. M., et al. (1999). Nitric oxide protects PC12 cells from serum deprivation-induced apoptosis by cGMP-dependent inhibition of caspase signaling. *J. Neurosci.* 19, 6740–6747. doi: 10.1523/jneurosci.19-16-06740.1999

Kleppisch, T., and Feil, R. (2009). ""cGMP signalling in the mammalian brain: role in synaptic plasticity and behaviour," in *cGMP: Generators, Effectors and Therapeutic Implications. Handbook of Experimental Pharmacology*, Vol. 191, eds H. H. H. W. Schmidt, F. Hofmann, and J. P. Stasch, (Berlin: Springer), 549–579. doi: 10.1007/978-3-540-68964-5_24

Knipper, M., Gestwa, L., Ten Cate, W. J., Lautermann, J., Brugger, H., Maier, H., et al. (1999). Distinct thyroid hormone-dependent expression of TrKB and p75NGFR in nonneuronal cells during the critical TH-dependent period of the cochlea. *J. Neurobiol.* 38, 338–356. doi: 10.1002/(sici)1097-4695(19990215)38:3<338::aid-neu4>3.0.co;2-1

Knipper, M., Zinn, C., Maier, H., Praetorius, M., Rohbock, K., Köpschall, I., et al. (2000). Thyroid hormone deficiency before the onset of hearing causes irreversible damage to peripheral and central auditory systems. *J. Neurophysiol.* 83, 3101–3112. doi: 10.1152/jn.2000.83.5.3101

Krause, G., Meyer Zum Gottesberge, A. M., Wolfram, G., and Gerzer, R. (1997). Transcripts encoding three types of guanylyl-cyclase-coupled trans-membrane receptors in inner ear tissues of guinea pigs. *Hear. Res.* 110, 95–106. doi: 10.1016/s0378-5955(97)00064-6

Kuhn, M. (2003). Structure, regulation, and function of mammalian membrane guanylyl cyclase receptors, with a focus on guanylyl cyclase-A. *Circ. Res.* 93, 700–709. doi: 10.1161/01.res.0000094745.28948.4d

Kuhn, M. (2005). Cardiac and intestinal natriuretic peptides: insights from genetically modified mice. *Peptides* 26, 1078–1085. doi: 10.1016/j.peptides.2004.08.031

Kuhn, M. (2009). "Function and dysfunction of mammalian membrane guanylyl cyclase receptors: lessons from genetic mouse models and implications for human diseases," in *cGMP: Generators, Effectors and Therapeutic Implications. Handbook of Experimental Pharmacology*, eds H. H. H. W. Schmidt, F. Hofmann, and J. Stasch, (Berlin: Springer), 47–69. doi: 10.1007/978-3-540-68964-5_4

Kuhn, M. (2016). Molecular physiology of membrane guanylyl cyclase receptors. *Physiol. Rev.* 96, 751–804. doi: 10.1152/physrev.00022.2015

Kuhn, M., Volker, K., Schwarz, K., Carbajo-Lozoya, J., Flogel, U., Jacoby, C., et al. (2009). The natriuretic peptide/guanylyl cyclase–a system functions as a stress-responsive regulator of angiogenesis in mice. *J. Clin. Invest.* 119, 2019–2030. doi: 10.1172/JCI37430

Kujawa, S. G., and Liberman, M. C. (2009). Adding insult to injury: cochlear nerve degeneration after "temporary" noise-induced hearing loss. *J. Neurosci.* 29, 14077–14085. doi: 10.1523/JNEUROSCI.2845-09.2009

Kyle, B. D., Hurst, S., Swayze, R. D., Sheng, J., and Braun, A. P. (2013). Specific phosphorylation sites underlie the stimulation of a large conductance, Ca^{2+}-activated K^+ channel by cGMP-dependent protein kinase. *FASEB J.* 27, 2027–2038. doi: 10.1096/fj.12-223669

Labine, J., Prince, S. C., Fitzakerley, J. L., and Trachte, G. J. (2015). Colocalization of the atrial natriuretic peptide synthesizing enzyme corin and natriureticpeptide receptor A in the cochlea. *ARO Midwinter Meet Abstr.* 38:PS-59.

Lee, D. I., Zhu, G., Sasaki, T., Cho, G.-S., Hamdani, N., Holewinski, R., et al. (2015). Phosphodiesterase 9A controls nitric-oxide-independent cGMP and hypertrophic heart disease. *Nature* 519, 472–476. doi: 10.1038/nature14332

Lee, J. H., Kang, M., Park, S., Perez-Flores, M. C., Zhang, X. D., Wang, W., et al. (2019). The local translation of KNa in dendritic projections of auditory neurons and the roles of KNa in the transition from hidden to overt hearing loss. *Aging* 11, 11541–11564. doi: 10.18632/aging.102553

Lee, J. Y. (2015). Aging and Speech Understanding. *J Audiol Otol* 19, 7–13. doi: 10.7874/jao.2015.19.1.7

Li, Z. W., Wu, B., Ye, P., Tan, Z. Y., and Ji, Y. H. (2016). Brain natriuretic peptide suppresses pain induced by BmK I, a sodium channel-specific modulator, in rats. *J. Headache Pain* 17:90.

Liberman, M. C. (1980). Morphological differences among radial afferent fibers in the cat cochlea: an electron-microscopic study of serial sections. *Hear. Res.* 3, 45–63. doi: 10.1016/0378-5955(80)90007-6

Liu, W., Bostrom, M., and Rask-Andersen, H. (2009). Expression of peripherin in the pig spiral ganglion–aspects of nerve injury and regeneration. *Acta Otolaryngol.* 129, 608–614. doi: 10.1080/00016480802369294

Livingston, G., and Frankish, H. (2015). A global perspective on dementia care: a Lancet Commission. *Lancet* 386, 933–934. doi: 10.1016/s0140-6736(15)00078-1

Livingston, G., Sommerlad, A., Orgeta, V., Costafreda, S. G., Huntley, J., Ames, D., et al. (2017). Dementia prevention, intervention, and care. *Lancet* 390, 2673–2734.

Lopez, M. J., Wong, S. K. F., Kishimoto, I., Dubois, S., Mach, V., Friesen, J., et al. (1995). Salt-resistant hypertension in mice lacking the guanylyl cyclase-A receptor for atrial natriuretic peptide. *Nature* 378, 65–68. doi: 10.1038/378065a0

Maison, S. F., Pyott, S. J., Meredith, A. L., and Liberman, M. C. (2013). Olivocochlear suppression of outer hair cells in vivo: evidence for combined action of BK and SK2 channels throughout the cochlea. *J. Neurophysiol.* 109, 1525–1534. doi: 10.1152/jn.00924.2012

Marcon, S., and Patuzzi, R. (2008). Changes in cochlear responses in guinea pig with changes in perilymphatic K^+. Part I: summating potentials, compound action potentials and DPOAEs. *Hear. Res.* 237, 76–89. doi: 10.1016/j.heares.2007.12.011

Marcotti, W., and Kros, C. J. (1999). Developmental expression of the potassium current IK,n contributes to maturation of mouse outer hair cells. *J. Physiol.* 520(Pt 3), 653–660. doi: 10.1111/j.1469-7793.1999.00653.x

Melcher, J. R., and Kiang, N. Y. (1996). Generators of the brainstem auditory evoked potential in cat. III: identified cell populations. *Hear. Res.* 93, 52–71. doi: 10.1016/0378-5955(95)00200-6

Meyer zum Gottesberge, A. M., Gagelmann, M., and Forssmann, W. G. (1991). Atrial natriuretic peptide-like immunoreactive cells in the guinea pig inner ear. *Hear. Res.* 56, 86–92. doi: 10.1016/0378-5955(91)90157-5

Möhrle, D., Hofmeier, B., Amend, M., Wolpert, S., Ni, K., Bing, D., et al. (2019). Enhanced Central Neural Gain Compensates Acoustic Trauma-induced Cochlear Impairment, but Unlikely Correlates with Tinnitus and Hyperacusis. *Neuroscience* 407, 146–169. doi: 10.1016/j.neuroscience.2018.12.038

Möhrle, D., Ni, K., Varakina, K., Bing, D., Lee, S. C., Zimmermann, U., et al. (2016). Loss of auditory sensitivity from inner hair cell synaptopathy can be centrally compensated in the young but not old brain. *Neurobiol. Aging* 44, 173–184. doi: 10.1016/j.neurobiolaging.2016.05.001

Möhrle, D., Reimann, K., Wolter, S., Wolters, M., Varakina, K., Mergia, E., et al. (2017). NO-sensitive guanylate cyclase isoforms NO-GC1 and NO-GC2 contribute to noise-induced inner hair cell synaptopathy. *Mol. Pharmacol.* 92, 375–388. doi: 10.1124/mol.117.108548

Molea, D., Stone, J. S., and Rubel, E. W. (1999). Class III beta-tubulin expression in sensory and nonsensory regions of the developing avian inner ear. *J. Comp. Neurol.* 406, 183–198. doi: 10.1002/(sici)1096-9861(19990405)406:2<183::aid-cne4>3.0.co;2-k

Nie, X., Fan, J., Li, H., Yin, Z., Zhao, Y., Dai, B., et al. (2018). miR-217 promotes cardiac hypertrophy and dysfunction by targeting PTEN. *Mol. Ther. Nucleic Acids* 12, 254–266. doi: 10.1016/j.omtn.2018.05.013

Oliver, D., Klocker, N., Schuck, J., Baukrowitz, T., Ruppersberg, J. P., and Fakler, B. (2000). Gating of Ca^{2+}-activated K^+ channels controls fast inhibitory synaptic transmission at auditory outer hair cells. *Neuron* 26, 595–601. doi: 10.1016/s0896-6273(00)81197-6

Pandey, K. N. (2019). Genetic ablation and guanylyl cyclase/natriuretic peptide receptor-A: impact on the pathophysiology of cardiovascular dysfunction. *Int. J. Mol. Sci.* 20:3946. doi: 10.3390/ijms20163946

Paquet-Durand, F., Silva, J., Talukdar, T., Johnson, L. E., Azadi, S., Van Veen, T., et al. (2007). Excessive activation of poly(ADP-ribose) polymerase contributes to inherited photoreceptor degeneration in the retinal degeneration 1 mouse. *J. Neurosci.* 27, 10311–10319. doi: 10.1523/jneurosci.1514-07.2007

Potter, L. R. (2011). Guanylyl cyclase structure, function and regulation. *Cell. Signal.* 23, 1921–1926. doi: 10.1016/j.cellsig.2011.09.001

Prasad, K. N., and Bondy, S. C. (2020). Increased oxidative stress, inflammation, and glutamate: potential preventive and therapeutic targets for hearing disorders. *Mech. Ageing Dev.* 185:111191. doi: 10.1016/j.mad.2019.111191

Przewozny, T., Gojska-Grymajlo, A., Kwarciany, M., Gasecki, D., and Narkiewicz, K. (2015). Hypertension and cochlear hearing loss. *Blood Press.* 24, 199–205. doi: 10.3109/08037051.2015.1049466

Pujol, R., and Puel, J. L. (1999). Excitotoxicity, synaptic repair, and functional recovery in the mammalian cochlea: a review of recent findings. *Ann. N. Y. Acad. Sci.* 884, 249–254. doi: 10.1111/j.1749-6632.1999.tb08646.x

Qiao, L., Han, Y., Zhang, P., Cao, Z., and Qiu, J. (2011). Detection of atrial natriuretic peptide and its receptor in marginal cells and cochlea tissues from the developing rats. *Neuro Endocrinol. Lett.* 32, 187–192.

Ramos, H. R., Birkenfeld, A. L., and De Bold, A. J. (2015). INTERACTING DISCIPLINES: cardiac natriuretic peptides and obesity: perspectives from an endocrinologist and a cardiologist. *Endocr. Connect.* 4, R25–R36. doi: 10.1530/EC-15-0018

Reed, N. S., Huddle, M. G., Betz, J., Power, M. C., Pankow, J. S., Gottesman, R., et al. (2019). Association of midlife hypertension with late-life hearing loss. *Otolaryngol. Head Neck Surg.* 161, 996–1003. doi: 10.1177/0194599819868145

Rüttiger, L., Sausbier, M., Zimmermann, U., Winter, H., Braig, C., Engel, J., et al. (2004). Deletion of the Ca^{2+}-activated potassium (BK) alpha-subunit but not the BKbeta1-subunit leads to progressive hearing loss. *Proc. Natl. Acad. Sci. U.S.A.* 101, 12922–12927. doi: 10.1073/pnas.0402660101

Rüttiger, L., Singer, W., Panford-Walsh, R., Matsumoto, M., Lee, S. C., Zuccotti, A., et al. (2013). The reduced cochlear output and the failure to adapt the central auditory response causes tinnitus in noise exposed rats. *PLoS One* 8:e57247. doi: 10.1371/journal.pone.0057247

Rüttiger, L., Zimmermann, U., and Knipper, M. (2017). Biomarkers for hearing dysfunction: facts and outlook. *ORL J. Otorhinolaryngol. Relat. Spec.* 79, 93–111. doi: 10.1159/000455705

Sahaboglu, A., Tanimoto, N., Kaur, J., Sancho-Pelluz, J., Huber, G., Fahl, E., et al. (2010). PARP1 gene knock-out increases resistance to retinal degeneration without affecting retinal function. *PLoS One* 5:e15495. doi: 10.1371/journal.pone.0015495

Schulz, S. (2005). C-type natriuretic peptide and guanylyl cyclase B receptor. *Peptides* 26, 1024–1034. doi: 10.1016/j.peptides.2004.08.027

Sergeyenko, Y., Lall, K., Liberman, M. C., and Kujawa, S. G. (2013). Age-related cochlear synaptopathy: an early-onset contributor to auditory functional decline. *J. Neurosci.* 33, 13686–13694. doi: 10.1523/JNEUROSCI.1783-13.2013

Shen, J., Scheffer, D. I., Kwan, K. Y., and Corey, D. P. (2015). SHIELD: an integrative gene expression database for inner ear research. *Database* 2015:bav071. doi: 10.1093/database/bav071

Shera, C. A., and Guinan, J. J. Jr. (1999). Evoked otoacoustic emissions arise by two fundamentally different mechanisms: a taxonomy for mammalian OAEs. *J. Acoust. Soc. Am.* 105, 782–798. doi: 10.1121/1.426948

Singer, W., Kasini, K., Manthey, M., Eckert, P., Armbruster, P., Vogt, M. A., et al. (2018). The glucocorticoid antagonist mifepristone attenuates sound-induced long-term deficits in auditory nerve response and central auditory processing in female rats. *FASEB J.* 32, 3005–3019. doi: 10.1096/fj.201701041RRR

Singer, W., Panford-Walsh, R., and Knipper, M. (2014). The function of BDNF in the adult auditory system. *Neuropharmacology* 76(Pt C), 719–728. doi: 10.1016/j.neuropharm.2013.05.008

Singer, W., Zuccotti, A., Jaumann, M., Lee, S. C., Panford-Walsh, R., Xiong, H., et al. (2013). Noise-induced inner hair cell ribbon loss disturbs central arc mobilization: a novel molecular paradigm for understanding tinnitus. *Mol. Neurobiol.* 47, 261–279. doi: 10.1007/s12035-012-8372-8

Soares, M. A., Sanches, S. G., Matas, C. G., and Samelli, A. G. (2016). The audiological profile of adults with and without hypertension. *Clinics* 71, 187–192. doi: 10.6061/clinics/2016(04)02

Sugawara, M., Corfas, G., and Liberman, M. C. (2005). Influence of supporting cells on neuronal degeneration after hair cell loss. *J. Assoc. Res. Otolaryngol.* 6, 136–147. doi: 10.1007/s10162-004-5050-1

Sun, F., Zhou, K., Wang, S. J., Liang, P. F., Wu, Y. X., Zhu, G. X., et al. (2013). Expression and localization of atrial natriuretic peptide and its receptors in rat spiral ganglion neurons. *Brain Res. Bull.* 95, 28–32. doi: 10.1016/j.brainresbull.2013.04.001

Sun, F., Zhou, K., Wang, S. J., Liang, P. F., Zhu, M. Z., and Qiu, J. H. (2014). Expression patterns of atrial natriuretic peptide and its receptors within the cochlear spiral ganglion of the postnatal rat. *Hear. Res.* 309, 103–112. doi: 10.1016/j.heares.2013.11.010

Suzuki, M., Kitanishi, T., Kitano, H., Yazawa, Y., Kitajima, K., Takeda, T., et al. (2000). C-type natriuretic peptide-like immunoreactivity in the rat inner ear. *Hear. Res.* 139, 51–58. doi: 10.1016/s0378-5955(99)00173-2

Suzuki, M., Kitano, H., Kitanishi, T., Yazawa, Y., Kitajima, K., Takeda, T., et al. (1998). RT-PCR analysis of mRNA expression of natriuretic peptide family and their receptors in rat inner ear. *Brain Res. Mol. Brain Res.* 55, 165–168. doi: 10.1016/s0169-328x(98)00016-3

Tan, J., Rüttiger, L., Panford-Walsh, R., Singer, W., Schulze, H., Kilian, S. B., et al. (2007). Tinnitus behavior and hearing function correlate with the reciprocal expression patterns of BDNF and Arg3.1/arc in auditory neurons following acoustic trauma. *Neuroscience* 145, 715–726. doi: 10.1016/j.neuroscience.2006.11.067

Uthaiah, R. C., and Hudspeth, A. J. (2010). Molecular anatomy of the hair cell's ribbon synapse. *J. Neurosci.* 30, 12387–12399. doi: 10.1523/JNEUROSCI.1014-10.2010

Valero, M. D., Burton, J. A., Hauser, S. N., Hackett, T. A., Ramachandran, R., and Liberman, M. C. (2017). Noise-induced cochlear synaptopathy in rhesus monkeys (*Macaca mulatta*). *Hear. Res.* 353, 213–223. doi: 10.1016/j.heares.2017.07.003

Van Eyken, E., Van Laer, L., Fransen, E., Topsakal, V., Lemkens, N., Laureys, W., et al. (2006). KCNQ4: a gene for age-related hearing impairment? *Hum. Mutat.* 27, 1007–1016. doi: 10.1002/humu.20375

Viana, L. M., O'Malley, J. T., Burgess, B. J., Jones, D. D., Oliveira, C. A., Santos, F., et al. (2015). Cochlear neuropathy in human presbycusis: confocal analysis of hidden hearing loss in post-mortem tissue. *Hear. Res.* 327, 78–88. doi: 10.1016/j.heares.2015.04.014

Wan, G., Gomez-Casati, M. E., Gigliello, A. R., Liberman, M. C., and Corfas, G. (2014). Neurotrophin-3 regulates ribbon synapse density in the cochlea and induces synapse regeneration after acoustic trauma. *eLife* 3:e03564. doi: 10.7554/eLife.03564

Weber, T., Zimmermann, U., Winter, H., Mack, A., Köpschall, I., Rohbock, K., et al. (2002). Thyroid hormone is a critical determinant for the regulation of the cochlear motor protein prestin. *Proc. Natl. Acad. Sci. U.S.A.* 99, 2901–2906. doi: 10.1073/pnas.052609899

Weisstaub, N., Vetter, D. E., Elgoyhen, A. B., and Katz, E. (2002). The alpha9alpha10 nicotinic acetylcholine receptor is permeable to and is modulated by divalent cations. *Hear. Res.* 167, 122–135. doi: 10.1016/s0378-5955(02)00380-5

Wolter, S., Möhrle, D., Schmidt, H., Pfeiffer, S., Zelle, D., Eckert, P., et al. (2018). GC-B deficient mice with axon bifurcation loss exhibit compromised auditory processing. *Front. Neural Circuits* 12:65. doi: 10.3389/fncir.2018.00065

Wu, P. Z., Liberman, L. D., Bennett, K., De Gruttola, V., O'Malley, J. T., and Liberman, M. C. (2019). Primary neural degeneration in the human cochlea: evidence for hidden hearing loss in the aging ear. *Neuroscience* 407, 8–20. doi: 10.1016/j.neuroscience.2018.07.053

Yoon, Y. J., and Anniko, M. (1994). Distribution of alpha-ANP in the cochlea and the vestibular organs. *ORL J. Otorhinolaryngol. Relat. Spec.* 56, 73–77. doi: 10.1159/000276613

Yoon, Y. J., Lee, E. J., Hellstrom, S., and Kim, J. S. (2015). Atrial natriuretic peptide modulates auditory brainstem response of rat. *Acta Otolaryngol.* 135, 1293–1297. doi: 10.3109/00016489.2015.1073354

Yoon, Y. J., Lee, E. J., and Kim, S. H. (2012). Synthesis of atrial natriuretic peptide in the rabbit inner ear. *Laryngoscope* 122, 1605–1608. doi: 10.1002/lary.23235

Yu, Z., Kuncewicz, T., Dubinsky, W. P., and Kone, B. C. (2006). Nitric oxide-dependent negative feedback of PARP-1 trans-activation of the inducible nitric-oxide synthase gene. *J. Biol. Chem.* 281, 9101–9109. doi: 10.1074/jbc.m511049200

Zampini, V., Johnson, S. L., Franz, C., Lawrence, N. D., Münkner, S., Engel, J., et al. (2010). Elementary properties of CaV1.3 Ca^{2+} channels expressed in mouse cochlear inner hair cells. *J. Physiol.* 588, 187–199. doi: 10.1113/jphysiol.2009.181917

Zhang, S., Lin, X., Li, G., Shen, X., Niu, D., Lu, G., et al. (2017). Knockout of Eva1a leads to rapid development of heart failure by impairing autophagy. *Cell Death Dis.* 8:e2586. doi: 10.1038/cddis.2017.17

Zheng, J., Shen, W., He, D. Z., Long, K. B., Madison, L. D., and Dallos, P. (2000). Prestin is the motor protein of cochlear outer hair cells. *Nature* 405, 149–155. doi: 10.1038/35012009

Zhou, X. B., Schlossmann, J., Hofmann, F., Ruth, P., and Korth, M. (1998). Regulation of stably expressed and native BK channels from human myometrium by cGMP- and cAMP-dependent protein kinase. *Pflugers Arch.* 436, 725–734. doi: 10.1007/s004240050695

Zhou, X. B., Wulfsen, I., Utku, E., Sausbier, U., Sausbier, M., Wieland, T., et al. (2010). Dual role of protein kinase C on BK channel regulation. *Proc. Natl. Acad. Sci. U.S.A.* 107, 8005–8010. doi: 10.1073/pnas.0912029107

Zuccotti, A., Kuhn, S., Johnson, S. L., Franz, C., Singer, W., Hecker, D., et al. (2012). Lack of brain-derived neurotrophic factor hampers inner hair cell synapse physiology, but protects against noise-induced hearing loss. *J. Neurosci.* 32, 8545–8553. doi: 10.1523/JNEUROSCI.1247-12.2012

Conflict of Interest: The authors declare that the research was conducted in the absence of any commercial or financial relationships that could be construed as a potential conflict of interest.

Philine Silja Marchetta

Education

Eberhard-Karls-University, Tübingen
Bachelor of Science in Biology
10/2013 - 09/2016
Thesis:*"The influence of noise prepulses as variable stimuli in comparison to tonal prepulses in prepulse-facilitation"*

Philipps-University, Marburg
Master of Sciences in Molecular and Cellular Neuroscience
10/2016 - 12/2018
Thesis: *"Stress receptors in the forebrain influence auditory nerve and brainstem responses"*

University Hospital Tübingen
PhD in Pharmacy
GRK 2381 "cGMP: From Bedside to Bench"
04/2019 - 07/2022
Thesis: *"cGMP pathways as novel molecular targets in the brain for fast auditory processing and cognitive function"*

Publications & Manuscripts

Engelhardt, K.-A., **Marchetta, P.**, Schwarting, R., Melo-Thomas, L. (2018): Haloperidol-induced catalepsy is ameliorated by deep brain stimulation of the inferior colliculus. *Scientific Reports*, 8(1), 2216.

Marchetta P*, Möhrle D*, Eckert P, Reimann K, Wolter S, Tolone A, Lang I, Wolters M, Feil R, Engel J, Paquet-Durand F, Kuhn M, Knipper M, Rüttiger L. (2020): Guanylyl Cyclase A/cGMP Signaling Slows Hidden, Age- and Acoustic Trauma-Induced Hearing Loss. *Frontiers in Aging Neuroscience*

Marchetta P*, Savitska D*, Kübler A, Asola G, Manthey M, Möhrle D, Schimmang T, Rüttiger L, Knipper M, Singer W (2020): Age-Dependent Auditory Processing Deficits after Cochlear Synaptopathy Depend on Auditory Nerve Latency and the Ability of the Brain to Recruit LTP/BDNF. *Brain Sci.*

Eckert P*, **Marchetta P***, Manthey MK*, Walter MH, Jovanovic S, Savitska D, Singer W, Jacob MH, Rüttiger L, Schimmang T, Milenkovic I, Pilz PKD, Knipper M (2021): Deletion of BDNF in Pax2 Lineage-Derived Interneuron Precursors in the Hindbrain Hampers the Proportion of Excitation/Inhibition, Learning, and Behavior. *Front Mol Neurosci.*

Marchetta P, Rüttiger L, Hobbs A, Singer W, Knipper M (2021): The role of cGMP signalling in auditory processing in health and disease. *Br J Pharmacol.*

Jeng J-Y, Harasztosi C, Carlton A J, Corns L F, **Marchetta P**, Johnson S L, Goodyear R J, Legan K P, Rüttiger L, Richardson G P, Marcotti W (2021): MET currents and otoacoustic emissions from mice with a detached tectorial membrane indicate the extracellular matrix regulates Ca2+ near stereocilia. *Journal of Physiology*

Marchetta P, Eckert P, Lukowski R, Ruth P, Singer W, Rüttiger L, Knipper M (2022): Loss of central mineralocorticoid or glucocorticoid receptors impacts auditory nerve processing in the cochlea. *iScience*

Savitska D, Hess M, Calis D, **Marchetta P**, Harasztosi C, Fink S, Eckert P, Ruth P, Rüttiger L, Knipper M, Singer W (2022): Stress affects central compensation of neural responses to cochlear synaptopathy in a cGMP-dependent way. *Frontiers in Neuroscience*

Calis D, Hess M, **Marchetta P**, Singer W, Lukowski R, Ruth P, Knipper M, Rüttiger L (in preparation): Specific function of membrane-bound cGMP generator GC-A for LTP-dependent central auditory adaptation processes

Doll J*, **Marchetta P***, Peixoto Pinheiro B, Vallian S, Müller M, Gültig K, Rohbock K, Refa M, Aboulfazl R, Hofrichter MAH, Dittrich M, Müller T, Mack TGA, Löwenheim H, Eickholt BJ, Rüttiger L, Haaf T, Knipper M, Vona B (in preparation): Loss of drebrin affects the central auditory pathway in mice and is responsible for hearing loss and delayed speech understanding in an Iranian family

(*equal contribution)

Acknowledgements

Ich bin sehr dankbar für die vielen Menschen, die mich während meiner Doktorarbeit begleitet und unterstützt haben.

Vielen, vielen Dank an Prof. Dr. Marlies Knipper für dieses vielfältige und spannende Thema! Und natürlich für alle Hilfe, Unterstützung und Inspiration. Ich durfte sehr viel bei und von ihr lernen.

Vielen Dank an Prof. Dr. Robert Lukowski, für die großartige Betreuung dieser Arbeit. An dieser Stelle möchte ich darüber hinaus für alle Unterstützung des GRK2381 "cGMP: From bedside to bench" danken.

Thank you to my Boston supervisor Prof. Dr. Michele Jacob for giving me continuously great support and bringing up new ideas.

Vielen Dank an Prof. Dr. Peter Ruth und Prof. Dr. Kerstin Schwabe, die ganz spontan als Berichterstatter eingesprungen sind und apl. Prof. Dr. Peter Pilz für die Teilhabe am Prüfungskommitee.

Sehr großer Dank geht auch an apl. Prof. Dr. Lukas Rüttiger für seine nie endende Geduld, mit der er sich Zeit für alle Fragen und Probleme genommen hat und für die bereitwillige Teilhabe an seinem riesigen Wissensschatz.

Merci au Dr. Jérôme Bourien, au Prof. Dr. Jean-Luc Puel, et à tout le laboratoire auditif de INM. J'ai apprécié ce séjour à Montpellier.

Was wäre meine Doktorandenzeit nur ohne meine wunderbaren Kolleginnen und Kollegen gewesen? Herzlichen Dank besonders an Wibke, Philipp, Benedikt, Dorit, Marie, Barbara, Dila und Morgan für die vielen "Wall-of-Fame"-Momente.

Vielen Dank auch an Karin, Iris und Hyun-Soon, die nicht nur mit ihrer hervorragenden Arbeit einen Beitrag zu allen Publikationen geliefert, sondern immer ein offenes Ohr und Schokolade für mich gehabt haben. Vielen Dank auch den Bufdis und Tierpflegern und natürlich an Kerstin, für die administrative Hilfe, aber auch unsere gemeinsamen Läufer-Erlebnisse!

Einen weiteren Dank möchte ich den vielen Kooperationspartnern aussprechen, die mit ihren Ideen und Methoden die Publikationen sehr bereichert haben.

Zuletzt noch herzlichen Dank an meine Liebsten außerhalb der Arbeit, die hinnehmen mussten, dass ich nicht selten mal wieder "kurz ins Labor" musste. Danke für alle Unterstützung und viel Verständis.